The Special Role of SLR for Inter-Technique Combinations

Markus Rothacher

Forschungseinrichtung Satellitengeodäsie, TU München (FESG)

ILRS Workshop 2003

October 28-31, 2003
Koetzting, Germany

Content

- Introduction
- S&S: **S**olutions and **S**tatistics
- W&W: **W**avelength and **W**ater Vapor
- C&C: **C**locks and **C**orrelations
- A&A: **A**ntennas and **A**bsolute Scale
- G&G: **G**eometry and **G**ravity
- O&O: **O**rbits and "**O**-C"
- Conclusions

Introduction: Vision of a Rigorous Combination

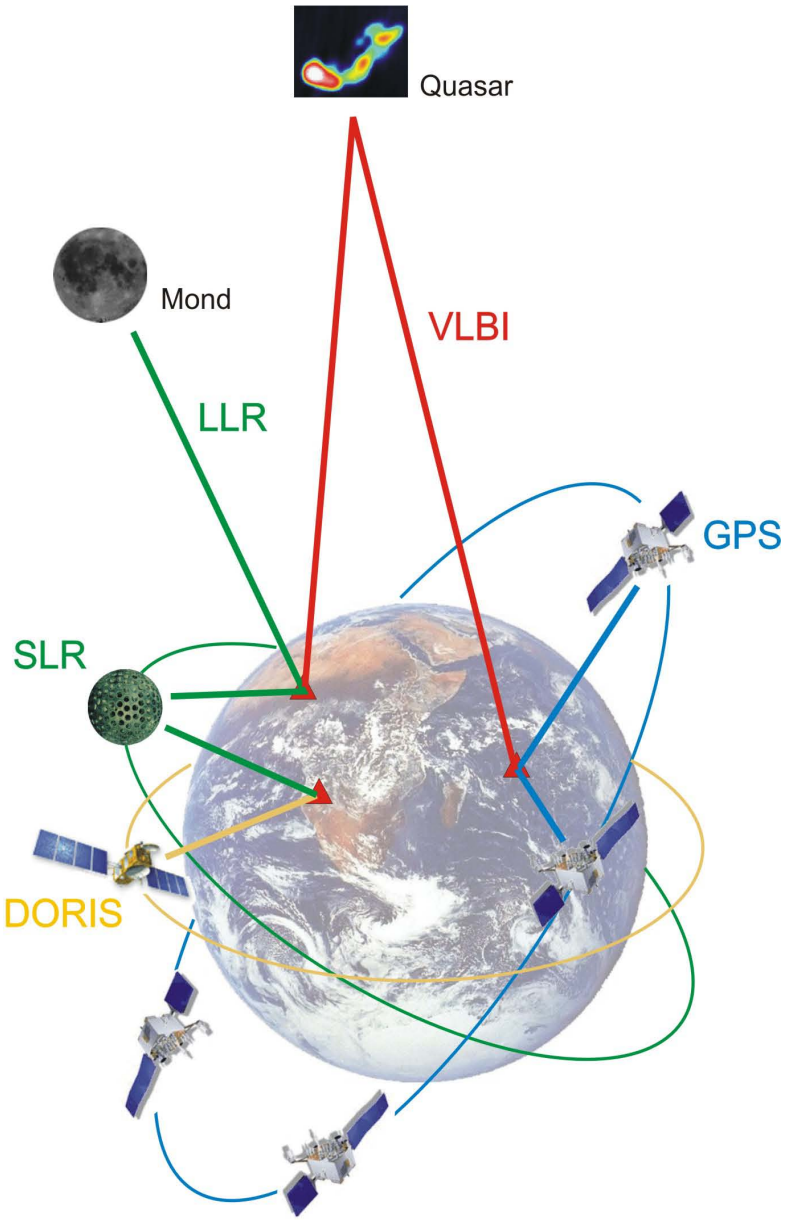

- Make use of the **strengths** of the individual observation techniques
- Profit from **co-location** of instruments (sites and satellites)
- Ensure **consistency** between all techniques
- Differ between technique-specific systematic **biases** and genuine geodetic/geophysical **signals**
- **Final goal**: All common parameters of all observing techniques are rigorously combined as consistent input to the IGGOS project

Parameter Space for Combination

Parameter Type	VLBI	GPS/ GLON.	DORIS/ PRARE	SLR	LLR	Alti- metry
Quasar Coord. (ICRF)	X					
Nutation	X	(X)		(X)	X	
Polar Motion	X	X	X	X	X	
UT1	X					
Length of Day (LOD)		X	X	X	X	
Sub-Daily ERPs	X	X				
ERP Ocean Tide Amplitudes	X	X		X		X
Coord.+Veloc.(ITRF)	X	X	X	X	X	(X)
Geocenter		X	X	X		X
Gravity Field		X	X	X	(X)	X
Orbits		X	X	X	X	X
LEO Orbits		X	X	X		X
Ionosphere	X	X	X			X
Troposphere	X	X	X			X
Time/Freq. Transfer	(X)	X		(X)		

Major SLR Contributions

Solutions and Statistics (S&S)

CONT‘02 VLBI Campaign

- DGFI: **VLBI** solutions
- TUM : **GPS** solutions
- TUM : **SLR** solutions (L1+L2)

October 17-30, 2003, continuous VLBI

SLR: few observations but also few parameters (no clocks, no troposphere, no ambiguities,…)

CONT‘02	SLR	VLBI	GPS
# Obs.	5’195	46’682	5’935’760
# Coord.	81	24	459
# EOP	75	75	75
# Tropos.	0	1’554	26’726
# Orbits	30	0	3’770
# Ambig.	0	0	43’238
# Clocks	0	1’164	---
# Param.	186	2’817	74’268

Wavelength and Water Vapor (W&W)

SLR is the only technique observing at optical wavelengths:

- SLR is in a **unique situation** concerning atmospheric refraction
- Troposphere **dispersive** for SLR, but not for microwaves
- Two-frequency laser ranging (mainly **validation tool** ?)
- Dry delay can be modeled with pressure data at the site
- Wet delay is quite small

All other techniques (GPS, VLBI, DORIS, altimetry, InSAR, …):

- Suffer from the **same tropospheric refraction effects**
- Suffer from **similar ionospheric refraction effects**
- Have tropospheric refraction as the or a **major error source**

Only SLR can help to detect biases (e.g. due to atmosphere mismodeling) common to all other techniques

Wavelength and Water Vapor (W&W)

Influence of water vapor e on SLR/LLR (Marini-Murray):

$$\delta\rho^{SLR}_{trp,wet}(z=0) \approx 0.000141 \cdot e$$

Influence of water vapor on GPS/VLBI/DORIS (Saastamoinen):

$$\delta\rho^{Micro}_{trp,wet}(z=0) \approx 0.002277 \cdot \left(\frac{1225}{T} + 0.05\right) \cdot e \approx 0.0096 \cdot e$$

Ratio of Microwave/SLR:

$$\frac{\delta\rho^{Micro}_{trp,wet}(z=0)}{\delta\rho^{SLR}_{trp,wet}(z=0)} \approx 68$$

Wet delay: GPS/VLBI/DORIS up to 40 cm; SLR up to 6 mm

Troposphere zenith delay parameters — weakening the solutions — have to be estimated for microwave techniques, but not for SLR

Clocks and Correlations (C&C)

Estimation of clock parameters:

- **SLR**: the only technique, where in general **no clock corrections** have to be estimated
- **GPS**: receiver and satellite clock parameters for every epoch
- **VLBI**: receiver clock corrections about every hour (between stations)
- **DORIS**: clock biases have to be estimated too

Estimation of clock parameters degrades the height quality

Exceptions for SLR:

- Estimation of a **range bias** for an SLR station: corresponds to a **receiver clock correction** in GPS/VLBI/DORIS
- Estimation of a **time biases** for an SLR station

Estimation of range biases should be avoided to the extent possible

Parameter Zenith-Dependence

Station Height

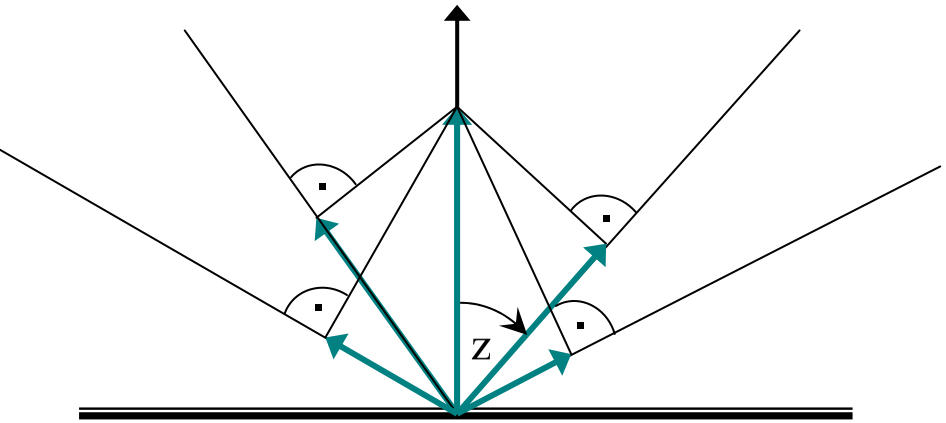

$$\delta\rho_h(z) = \cos(z) \cdot \delta\rho_h(0)$$

Zenith Troposphere Delay

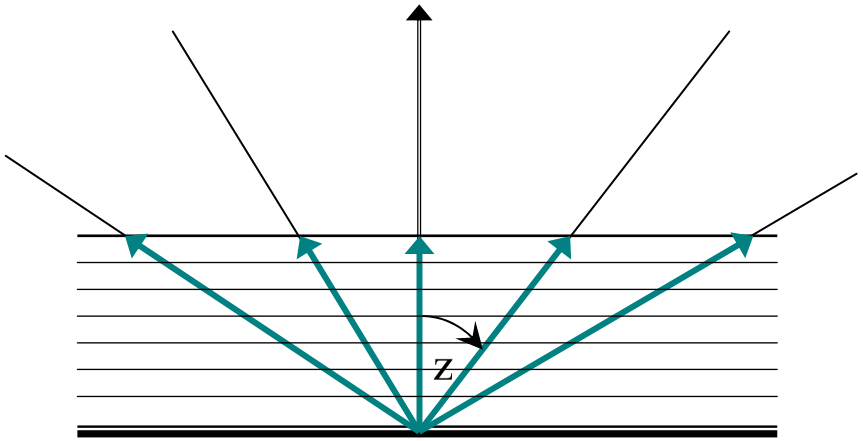

$$\delta\rho_{trp}(z) = \frac{1}{\cos(z)} \cdot \delta\rho_{trp}(0)$$

Clock Correction

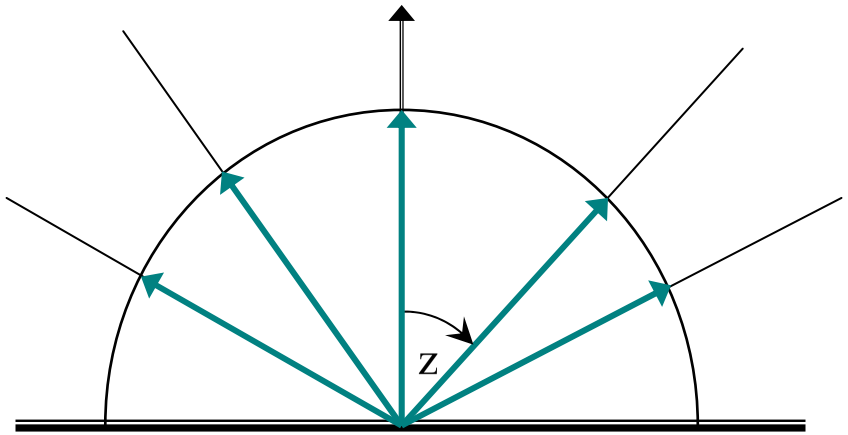

$$\delta\rho_{clk}(z) = \delta\rho_{clk}(0) = c \cdot \delta t_R$$

Correlation: Height, Clocks, Troposphere

Coord. + Clock **Coord. only** **Coord.+Tropo.**

10°	station coord. & clock	station coordinates	station coord. & tropo. delay
Equatorial site	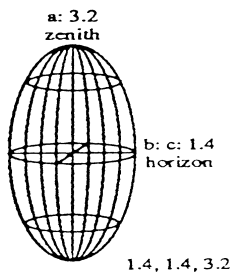 1.4, 1.4, 3.2 σx, σy, σz	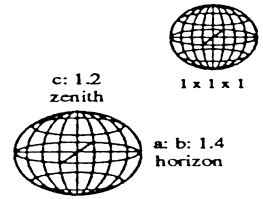 1.4, 1.4, 1.2 σx, σy, σz	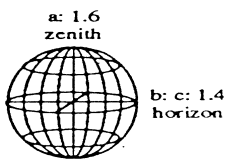 1.4, 1.4, 1.6 σx, σy, σz
Mid-latitude site	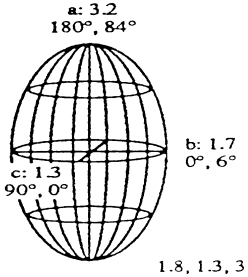 1.8, 1.3, 3.2 σx, σy, σz	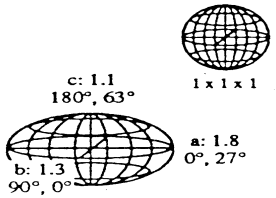 1.7, 1.3, 1.3 σx, σy, σz	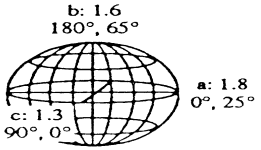 1.8, 1.3, 1.6 σx, σy, σz
Polar site	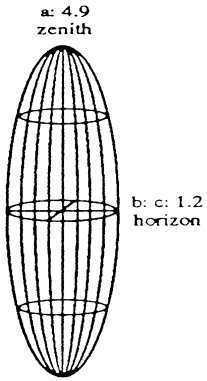 1.2, 1.2, 4.9 σx, σy, σz	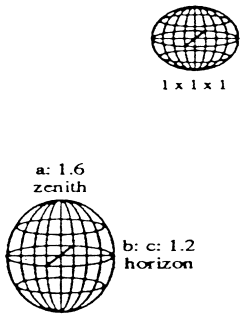 1.2, 1.2, 1.6 σx, σy, σz	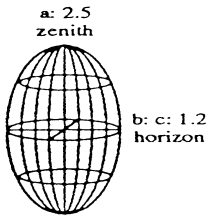 1.2, 1.2, 2.5 σx, σy, σz

- Influence of clock and troposphere estimation on station height (Santerre)
- Extreme correlations between height, clock, and troposphere zenith delay
- No problem for SLR: heights should be perfect

z_{max}	$\sigma 1_h/\sigma 0_h$	Cor(h,trp)
70	13.78	-0.964
75	9.23	-0.943
80	6.13	-0.907
85	3.94	-0.830

Observation Geometry

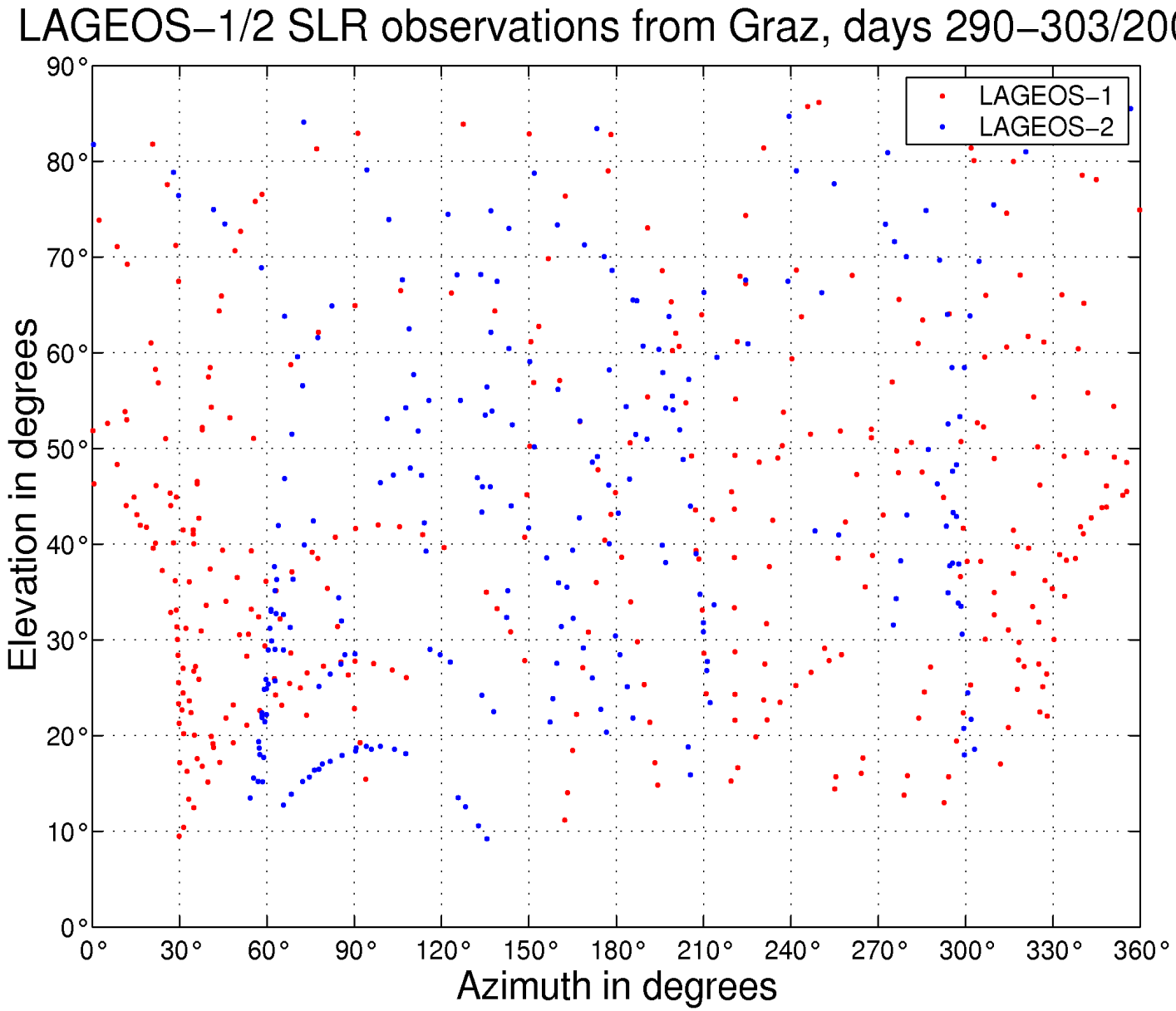

Nice observation geometry for good stations (14 days)

Well-suited for height determination

SLR very important for absolute height estimation

Estimation of range biases should be avoided to the extent possible

Antennas and Absolute Scale (A&A)

Characteristics of GPS receiver and satellite antennas:

- Not accurately known, changing with elevation and azimuth
- GPS results dependent on **elevation cut-off**
- Large systematic effects due to **antenna phase center** corrections (receiver and satellite antennas)
- Many changes of GPS receiver/antenna equipment (jumps in height)
- GPS is too much affected by systematic effects to allow accurate **absolute height** and **absolute scale** determination in the global network and for ITRF.

VLBI telescopes:

- VLBI telescopes are huge and heavy structures
- VLBI **telescope deformation** may bias results (elevation dependence?)

SLR: no such antenna problems (deformation should be small, no phase center variations): well-suited to define scale of ITRF; but calibration has to be very accurate and reliable.

Antenna Phase Center Corrections

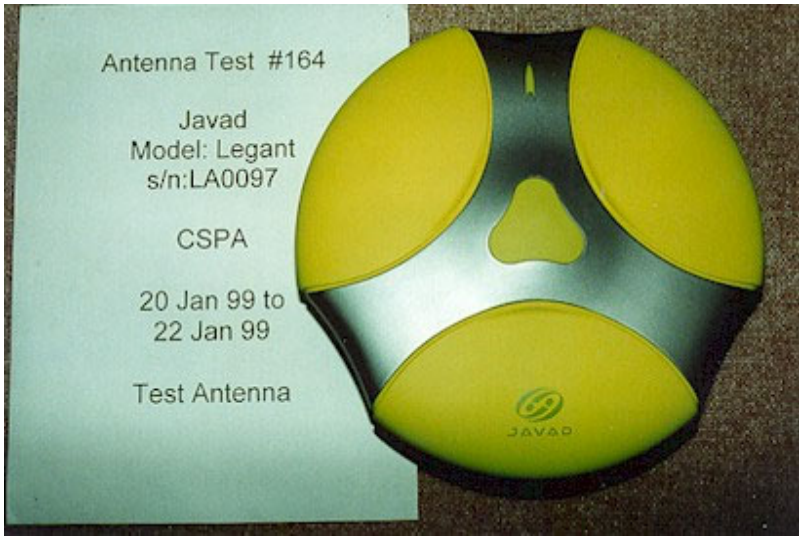

Antenna phase center variations:

- GPS receiver antenna
- GPS satellite antenna

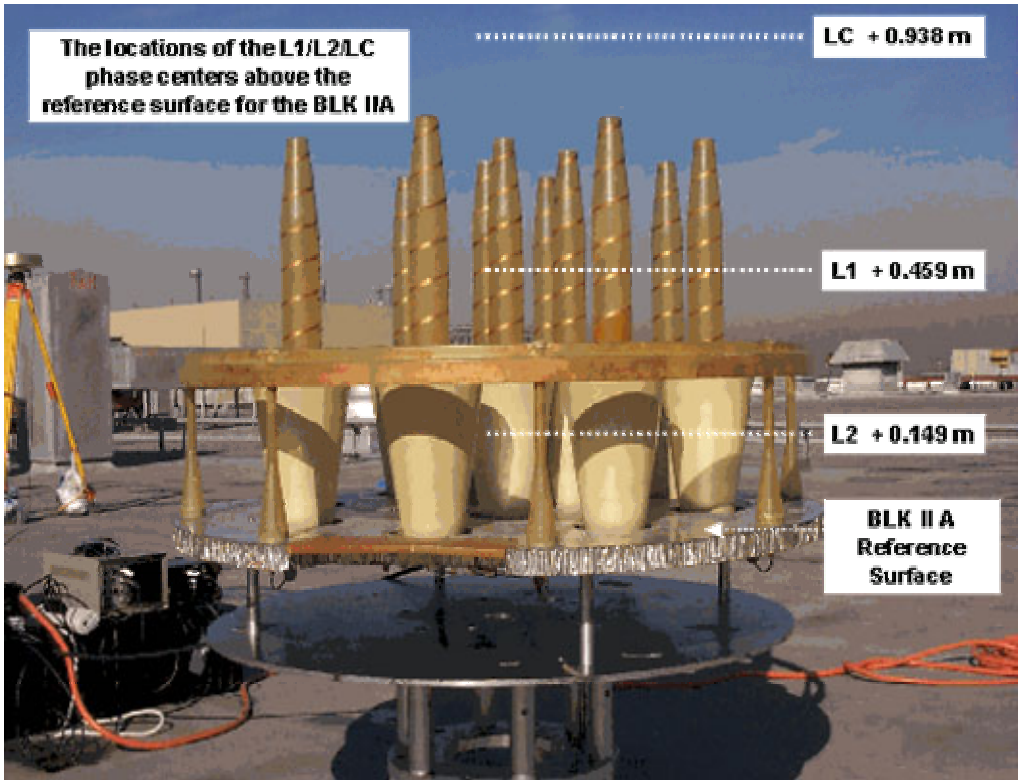

GPS: Elevation Cut-Off Effect

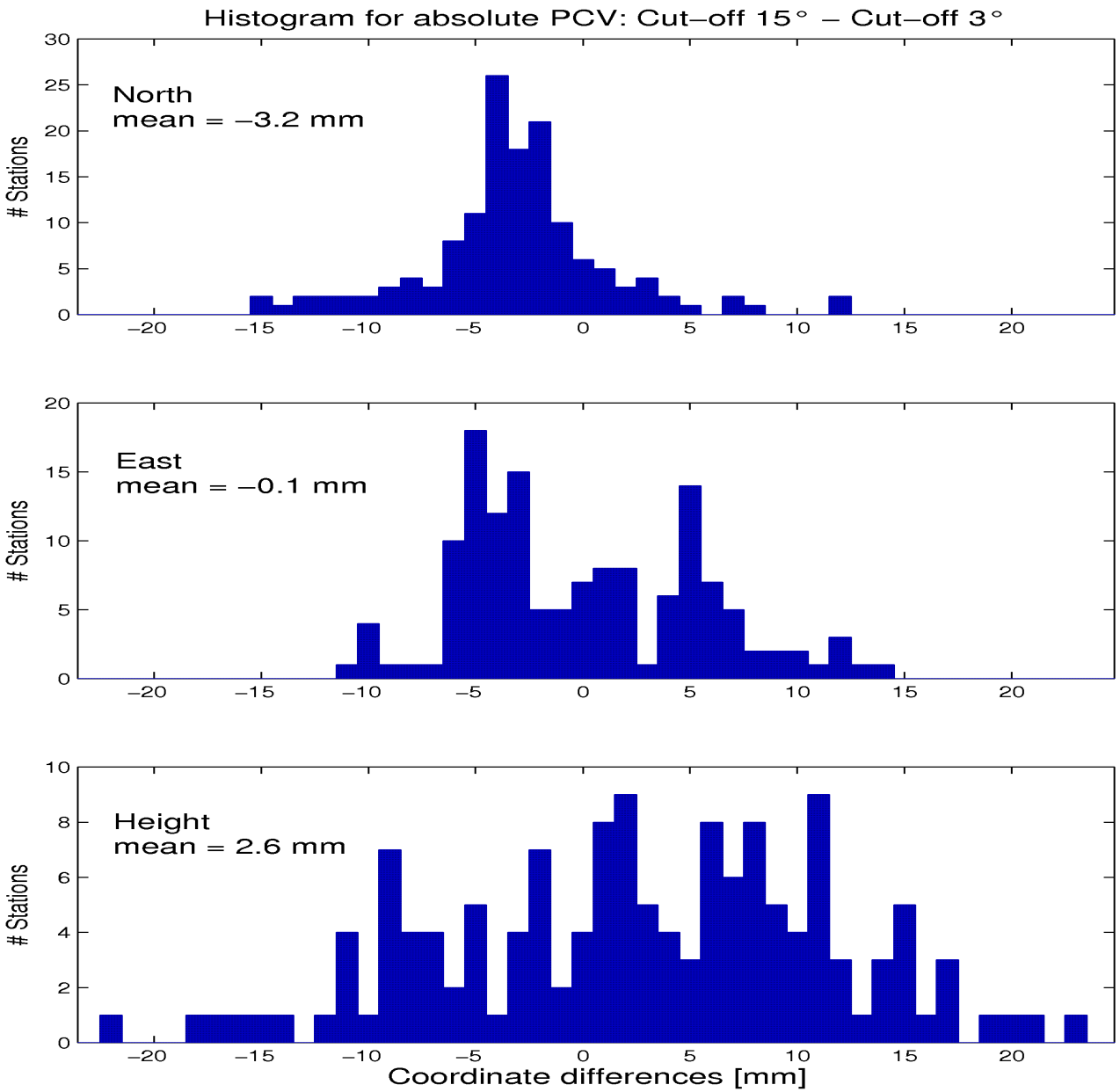

- Change of station coordinates due to a change in **elevation cut-off angle**
- Most up-to-date **absolute phase center variations** used for receivers (robot measurements) and satellites (global estimation)
- **Antennas are a critical error source !**

GPS: Absolute-Relative Antenna Patterns

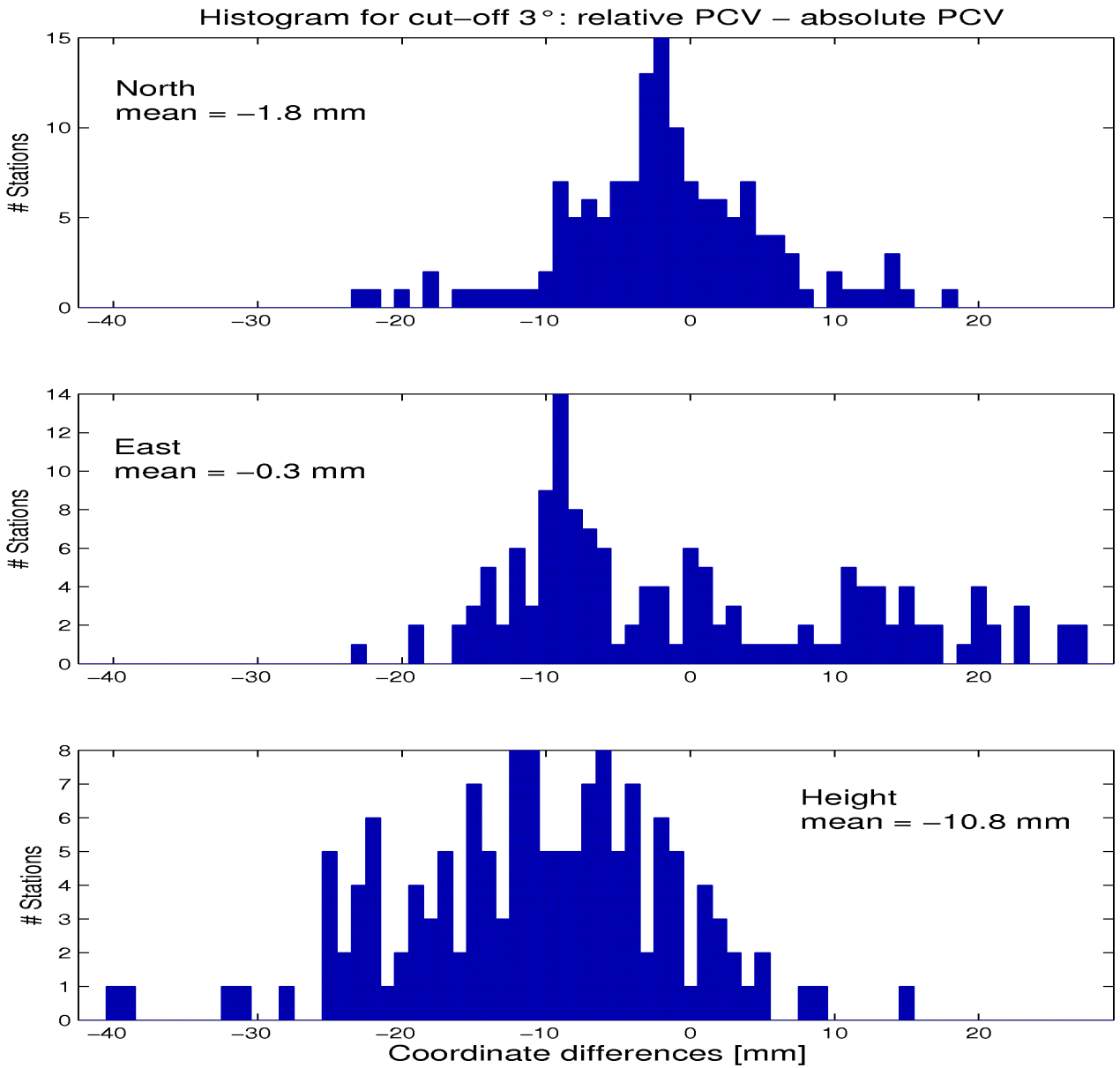

- Change from **relative** (now in use) to **absolute** antenna information (to be used by IGS in future)
- Absolute phase center variations only derivable with fixed ITRF scale.
- Systematic change in scale to ITRF (several mm)

Comparison of GPS & VLBI Troposphere

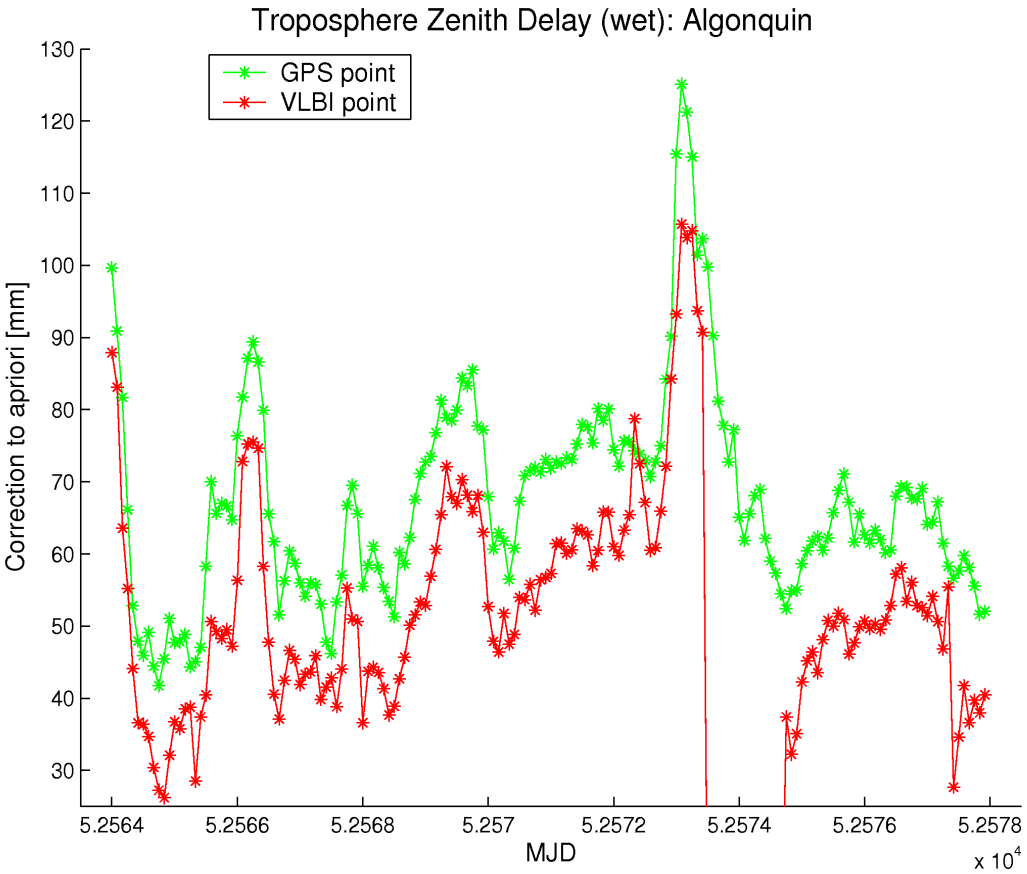

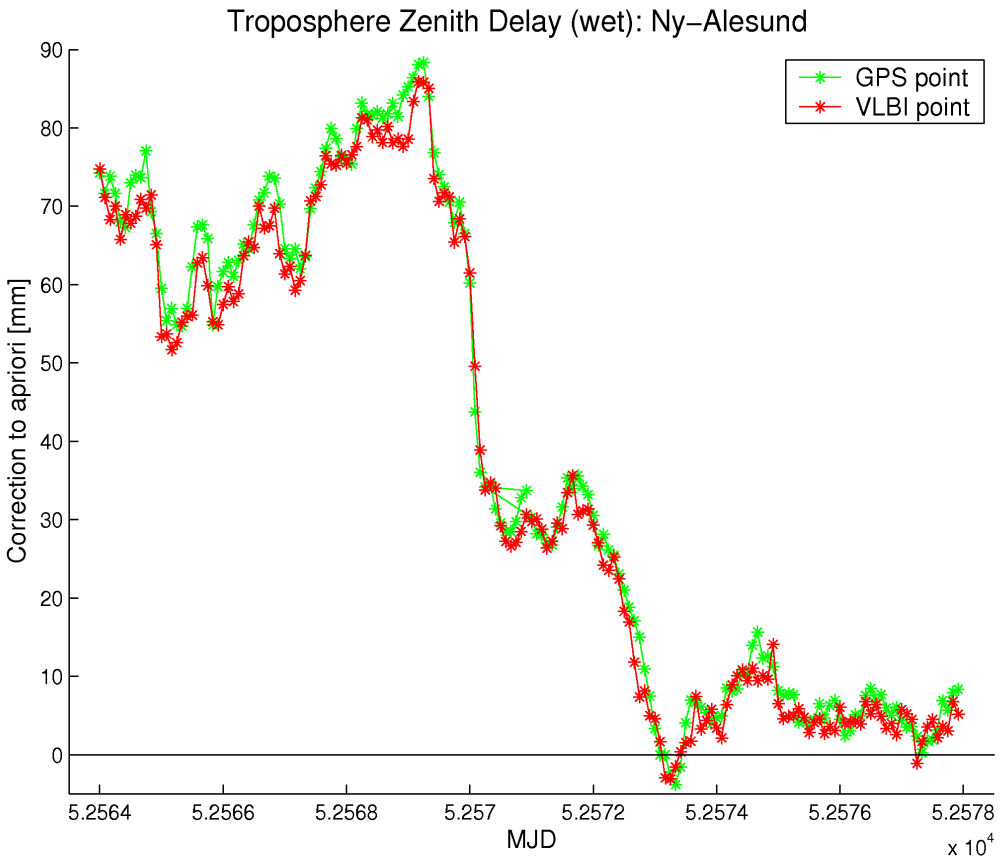

- CONT'02 Campaign (14 days)
- Very nice agreement in temporal variations, but **large systematic biases** between VLBI and GPS, indicating some unmodeled effects

Comparison of GPS & VLBI Troposphere

Station	ΔHeight (local tie) [m]	ΔZTD Theory [mm]	ΔZTD Estim. [mm]
ALGO	23.11	6.9	14.0
FAIR	13.08	3.9	6.8
HRAO	1.54	0.5	7.8
KOKB	9.24	2.8	14.2
NYA1	3.07	0.9	1.7
ONSA	13.71	4.1	5.1
WES2	1.75	0.5	11.7
WTZR	3.10	0.9	4.5

ΔHeight = 10m → ΔZD ≈ 3mm

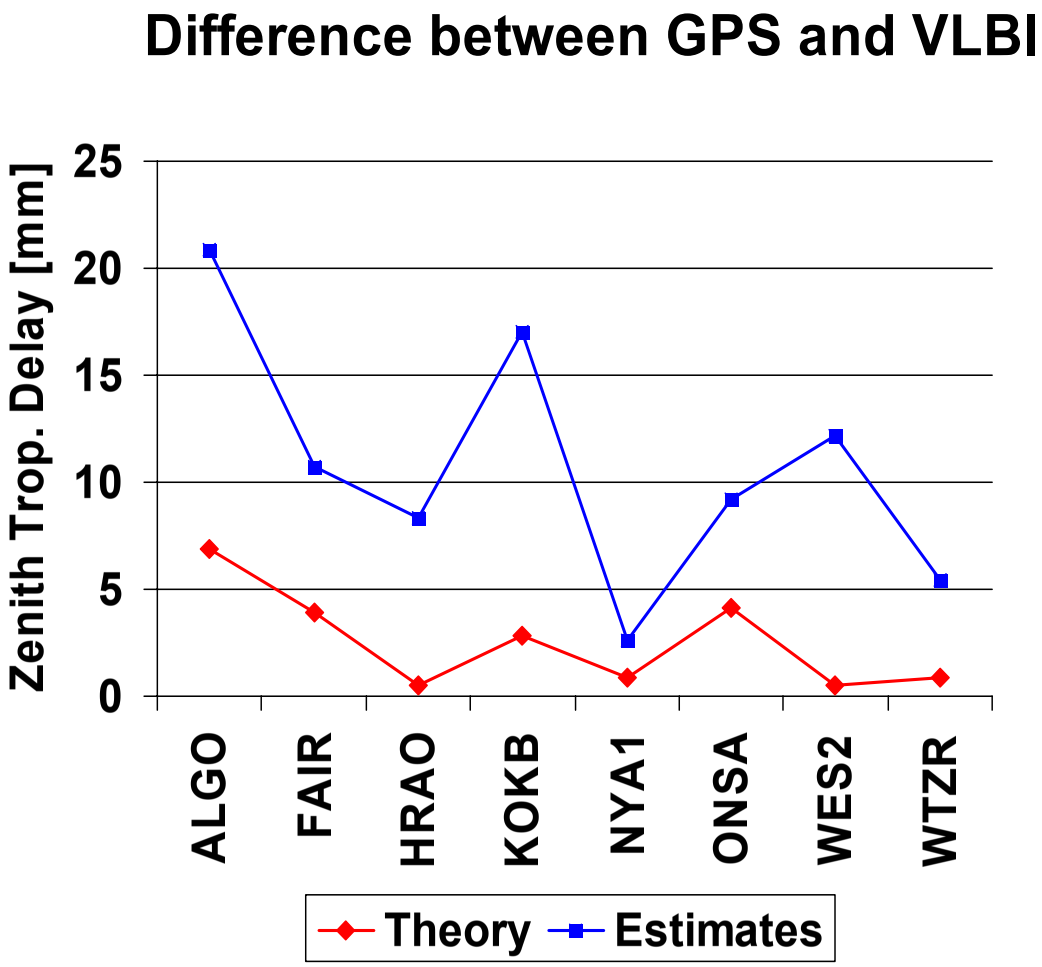

Rotation and Rotation Rates (R&R)

One-to-one relation between changes in **UT1-UTC, Δε, Δψ** and changes in the orbital elements **Ω, i, u_0** (ρ=1.0027379):

$$\begin{aligned} \Delta(\mathrm{UT1\text{–}UTC}) &= -(\Delta\Omega + \cos i \cdot \Delta u_0)/\rho \\ \delta\Delta\epsilon &= \cos\Omega \cdot \Delta i + \sin i \sin\Omega \cdot \Delta u_0 \\ \delta\Delta\psi \cdot \sin\epsilon_0 &= -\sin\Omega \cdot \Delta i + \sin i \cos\Omega \cdot \Delta u_0 \end{aligned}$$

→ UT1-UTC and nutation offsets cannot be estimated together with orbital elements

$$\begin{aligned} \dot{(\mathrm{UT1\text{–}UTC})} &= -\mathrm{LOD} = -(\dot\Omega + \cos i \cdot \dot u_0)/\rho \\ \Delta\dot\epsilon &= \cos\Omega \cdot \dot i + \sin i \sin\Omega \cdot \dot u_0 \\ \Delta\dot\psi \cdot \sin\epsilon_0 &= -\sin\Omega \cdot \dot i + \sin i \cos\Omega \cdot \dot u_0 \end{aligned}$$

→ LOD and nutation rates can be estimated by satellite techniques; quality of orbit model is crucial (changes of elements with time)

UT1-UTC and Nutation from SLR

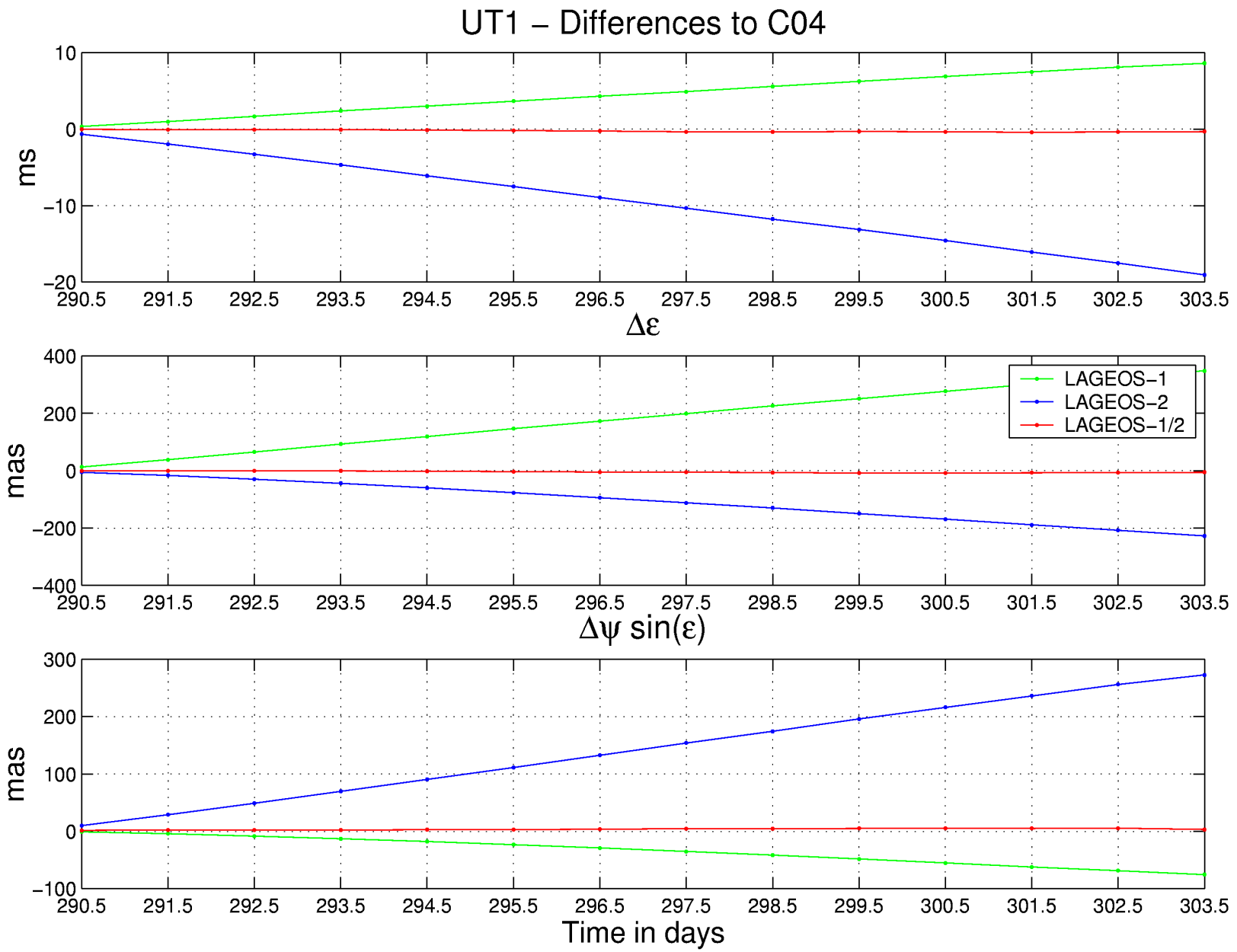

LOD and Nutation Rates from SLR

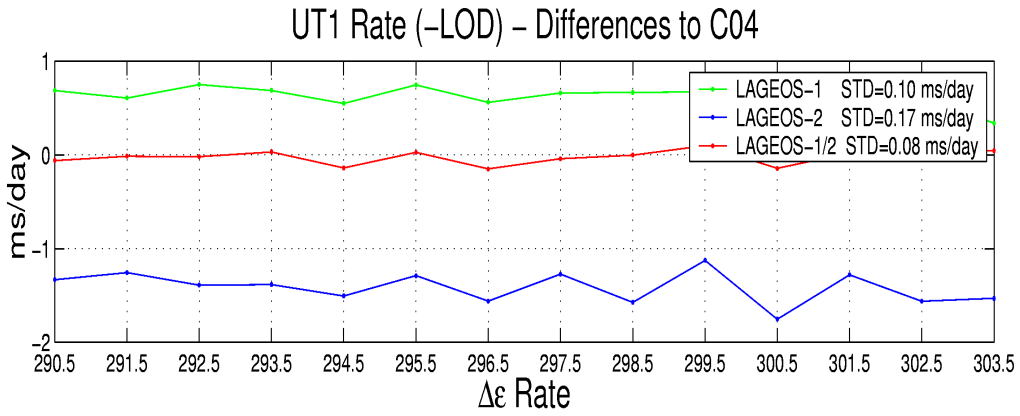

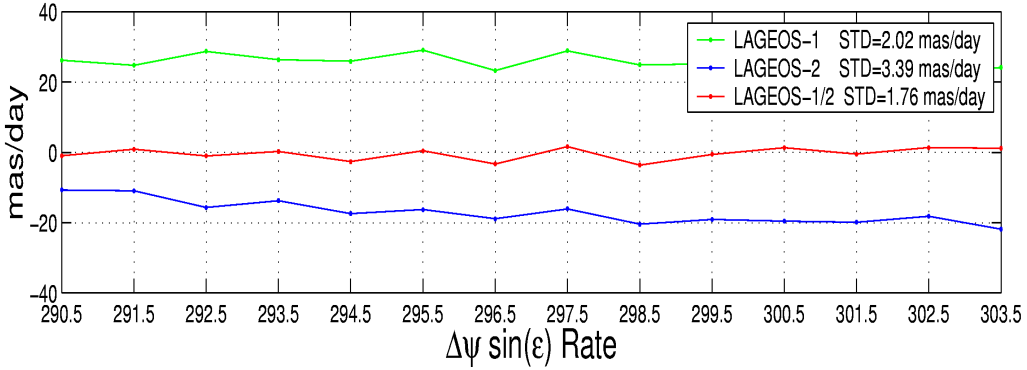

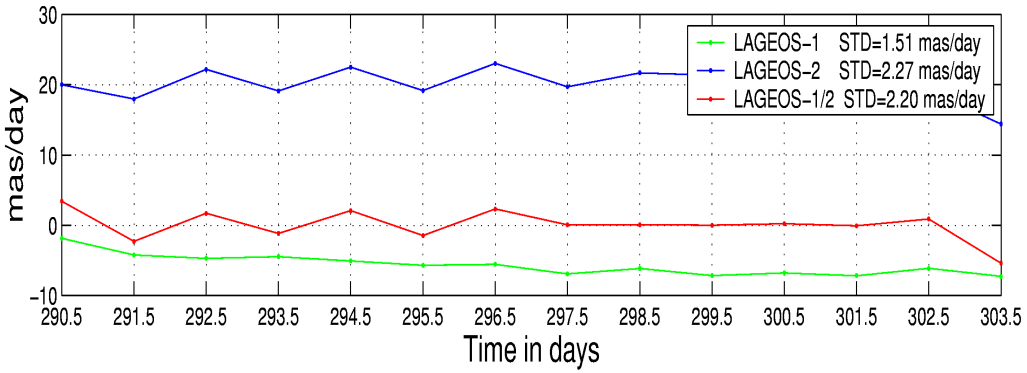

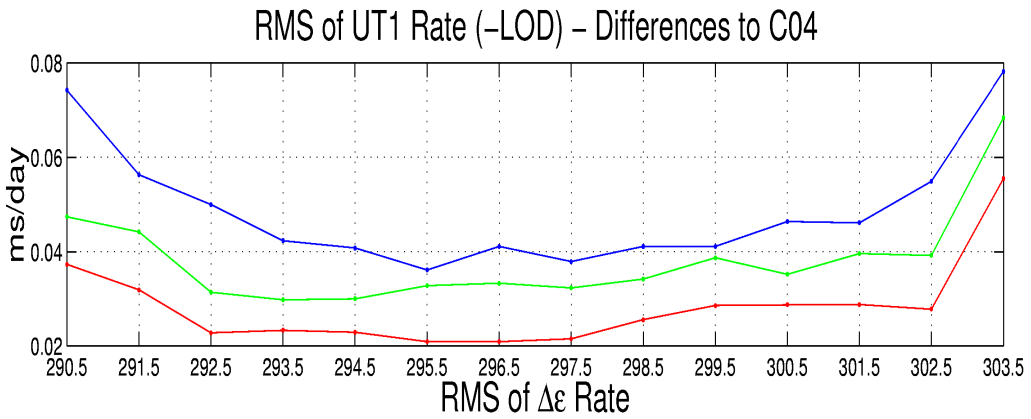

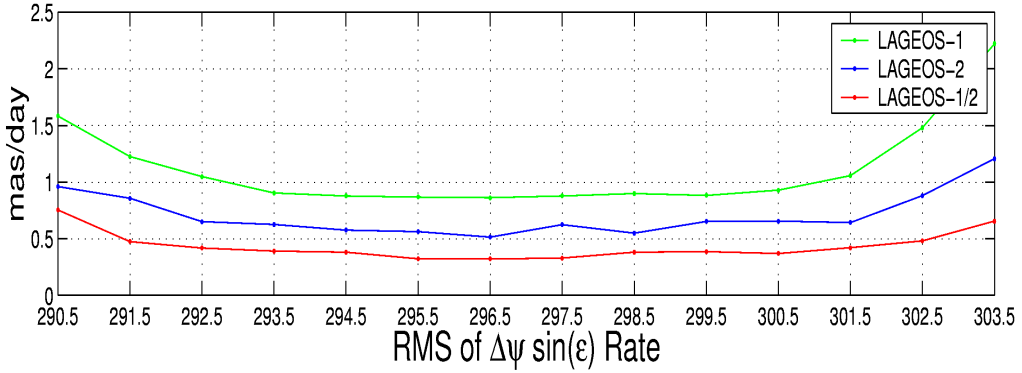

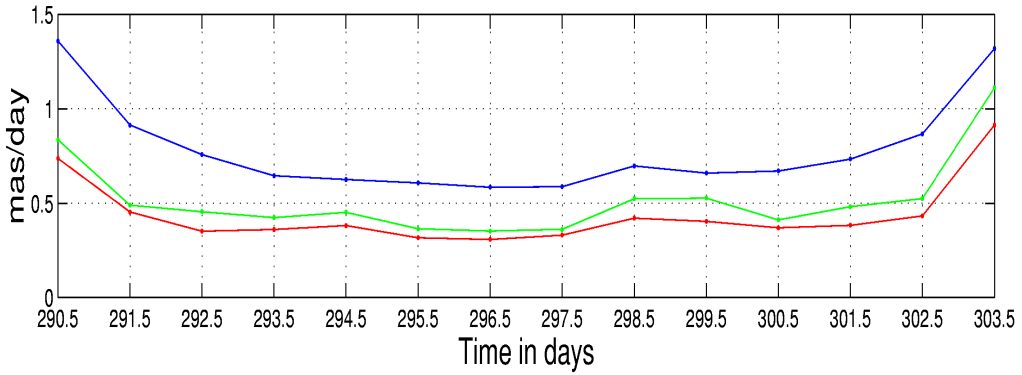

Nutation from SLR, GPS, and VLBI

- Comparison of nutation during the CONT'02 Campaign (14 days)
- SLR results similar to those of GPS (at least in obliquity)

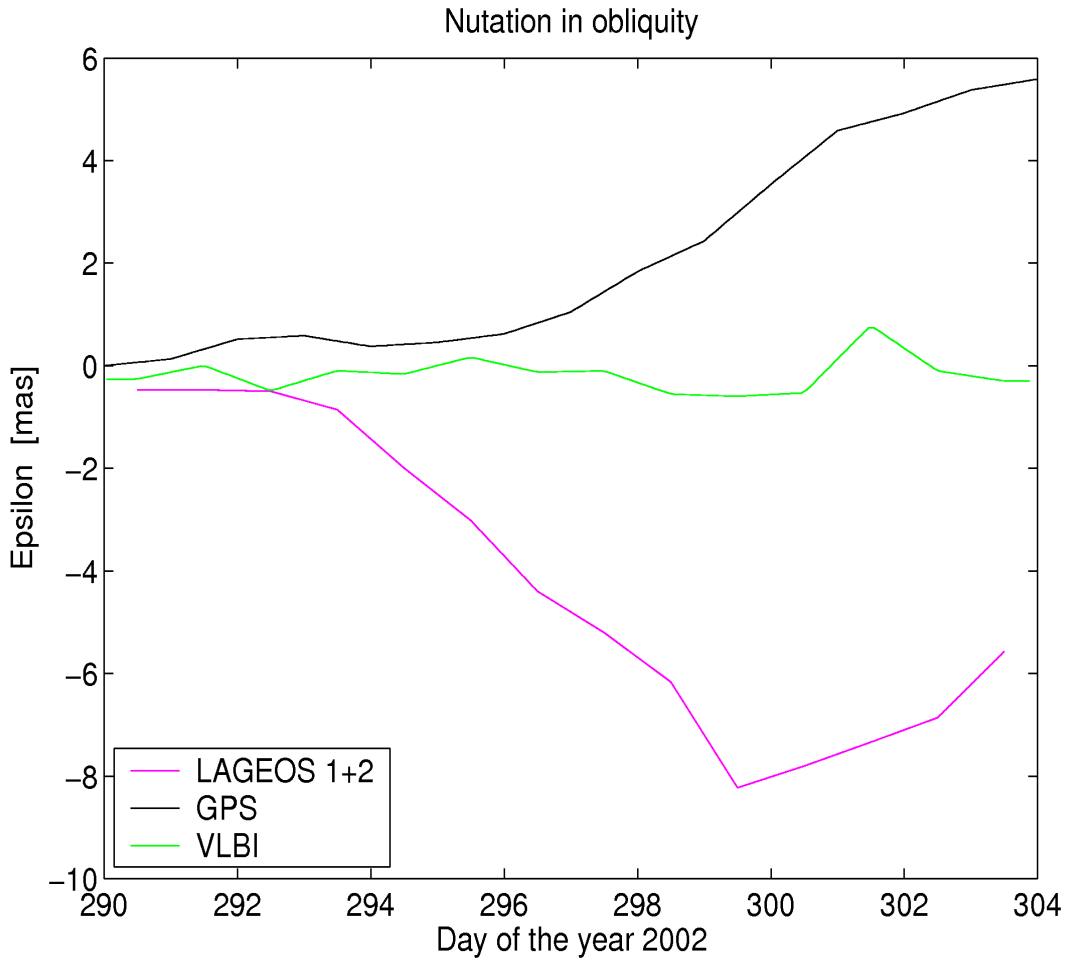

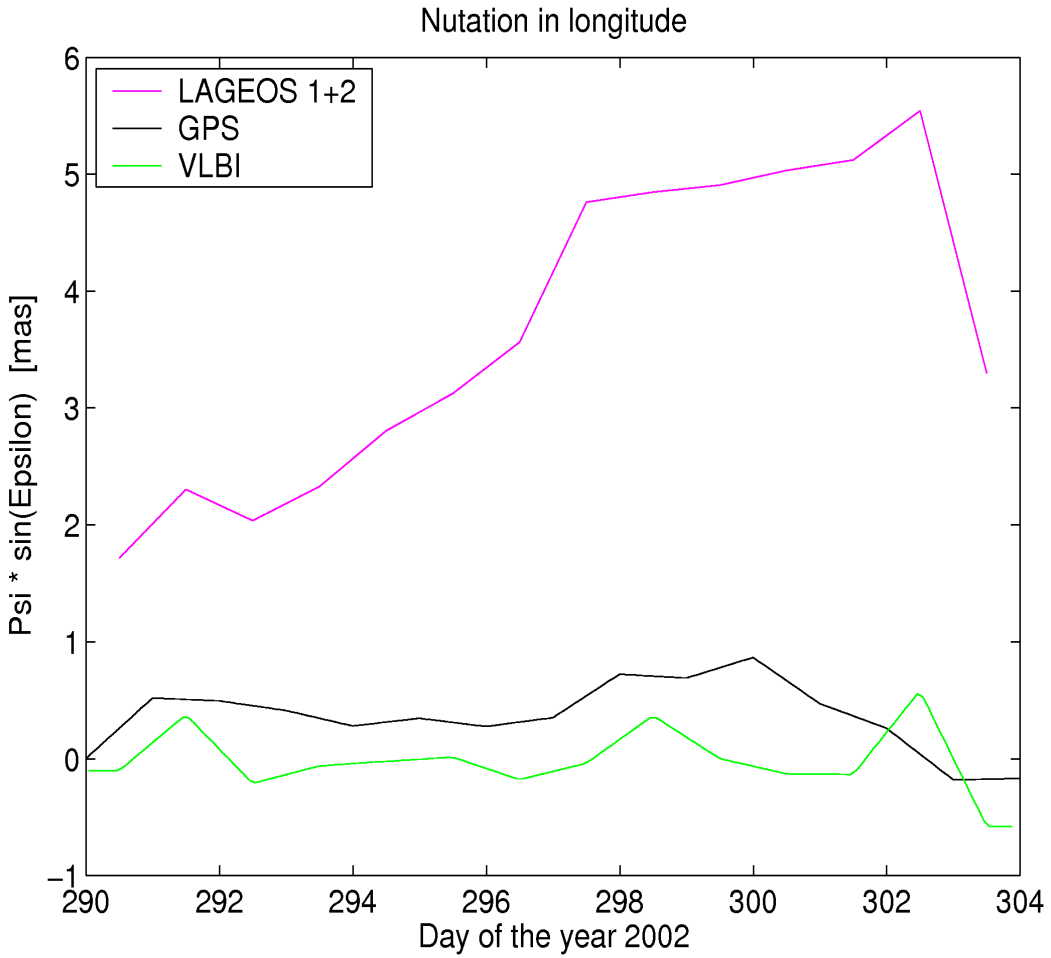

LOD from SLR, GPS, and VLBI

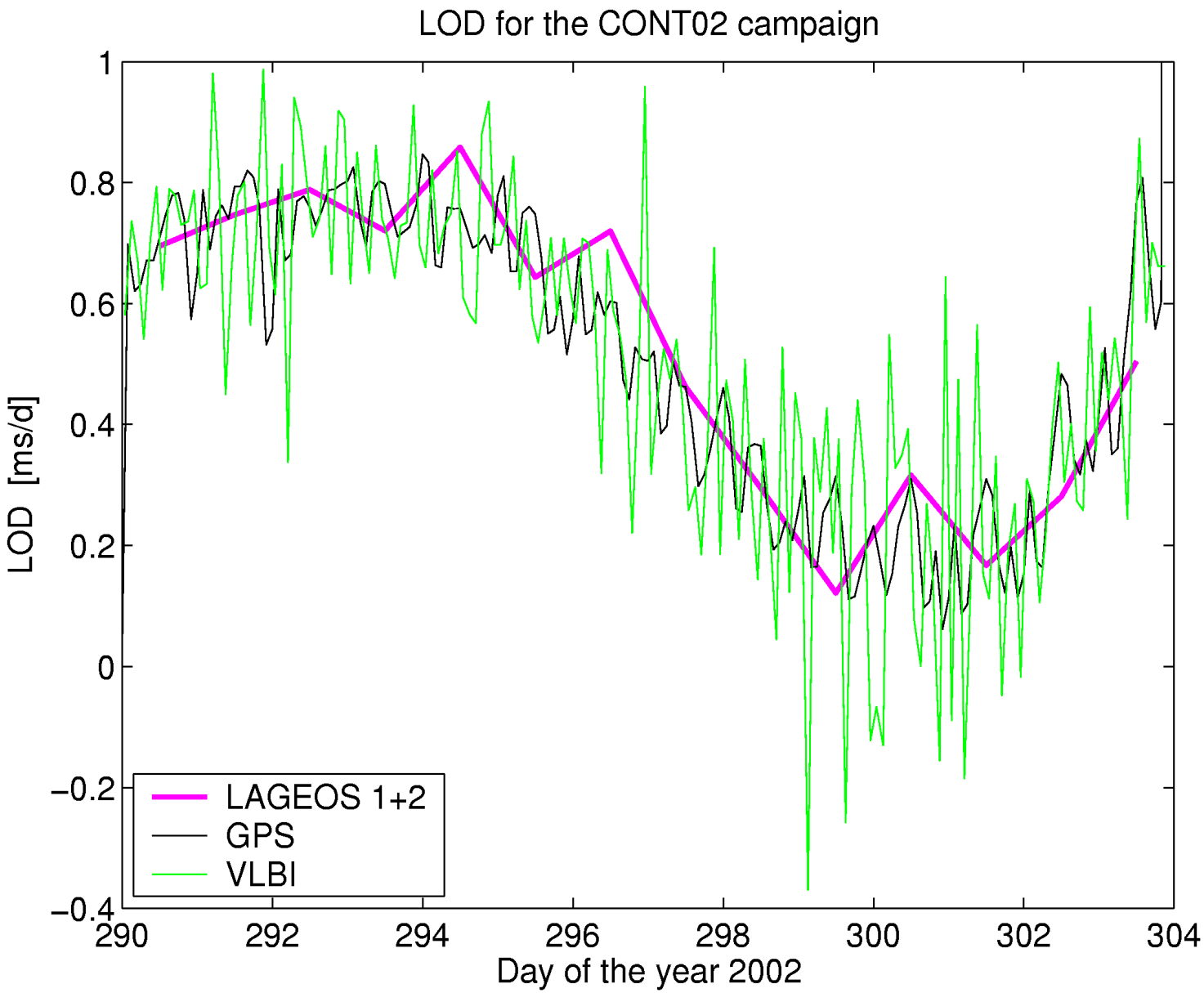

- CONT'02 Campaign (14 days)
- Subdaily LOD from GPS and VLBI
- Daily values from SLR (Lageos 1 + 2)

X- and Y-Pole from SLR

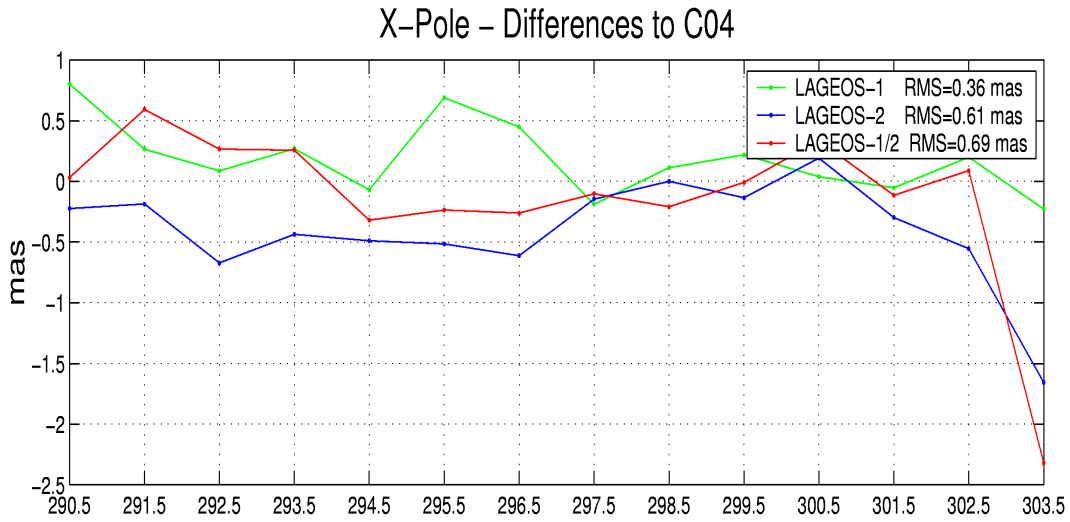

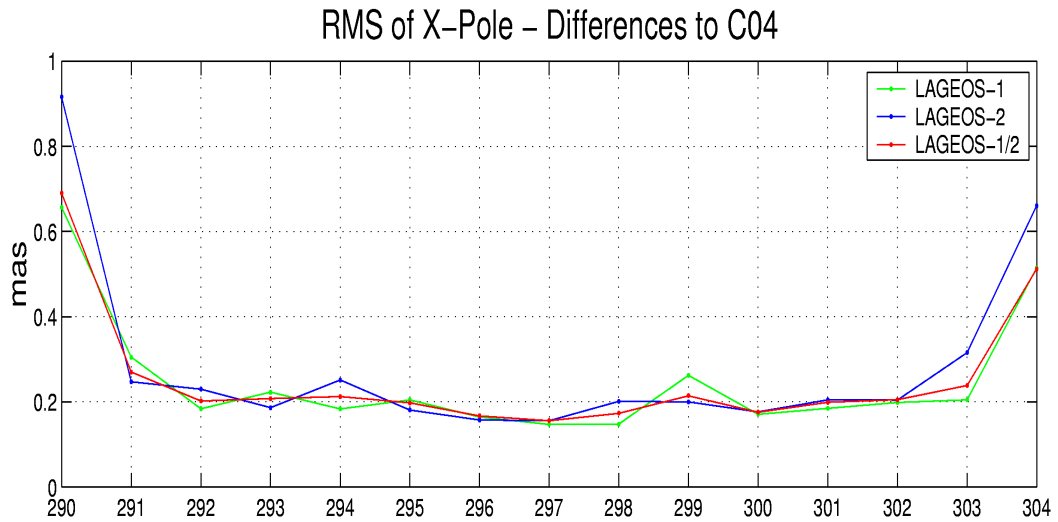

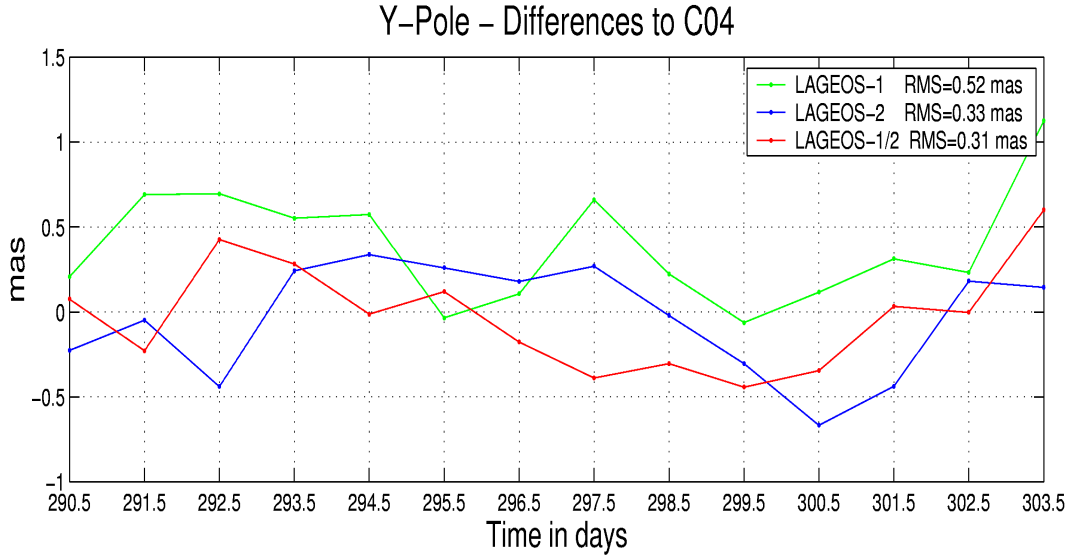

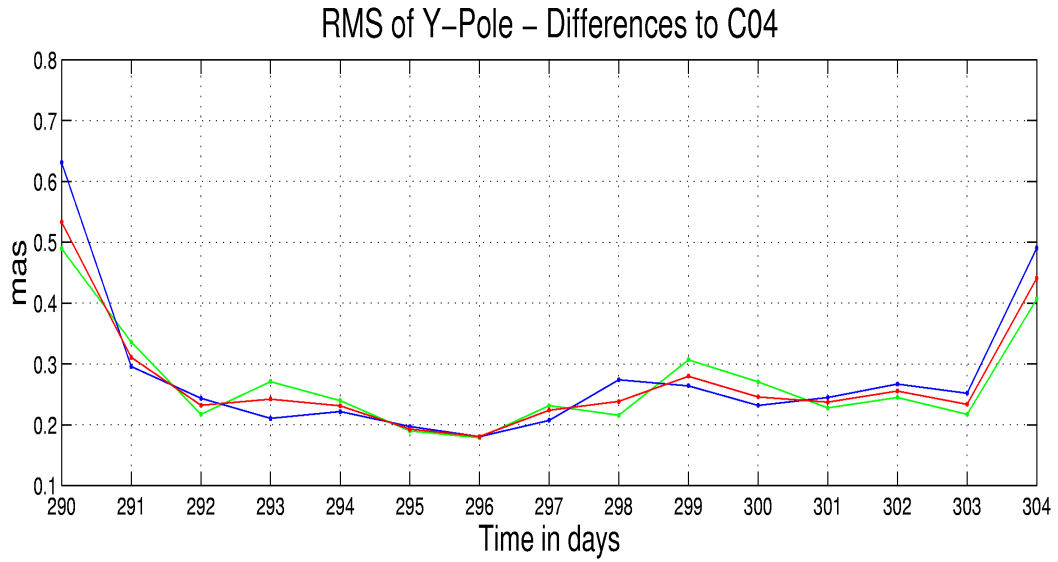

CONT'02 Campaign

Geometry and Gravity (G&G)

SLR is one of the major techniques to establish a link between geometry, Earth rotation, and gravity (three pillars of geodesy):

- Geocenter: relation between origin of ITRF and low order harmonics coefficient $\mathbf{C_{01}}$, $\mathbf{C_{11}}$, $\mathbf{S_{11}}$ of the Earth's gravity field
- Principle axes of inertia tensor: relation between Earth rotation, orientation of the gravity field ($\mathbf{C_{21}}$, $\mathbf{S_{21}}$, $\mathbf{S_{22}}$), and ITRF orientation
- Help to distinguish between "matter terms" and "motion terms" (gravity "feels" only "matter", Earth rotation "matter" and "motion")

SLR as a link between 3 pillars: very important for the IGGOS integration concept and for IERS reference frame definitions

Gravity field variations due to exactly the **same Earth processes** (e.g., from geophysical fluids) as Earth rotation and deformation (geometry)

Three Layers of Objects

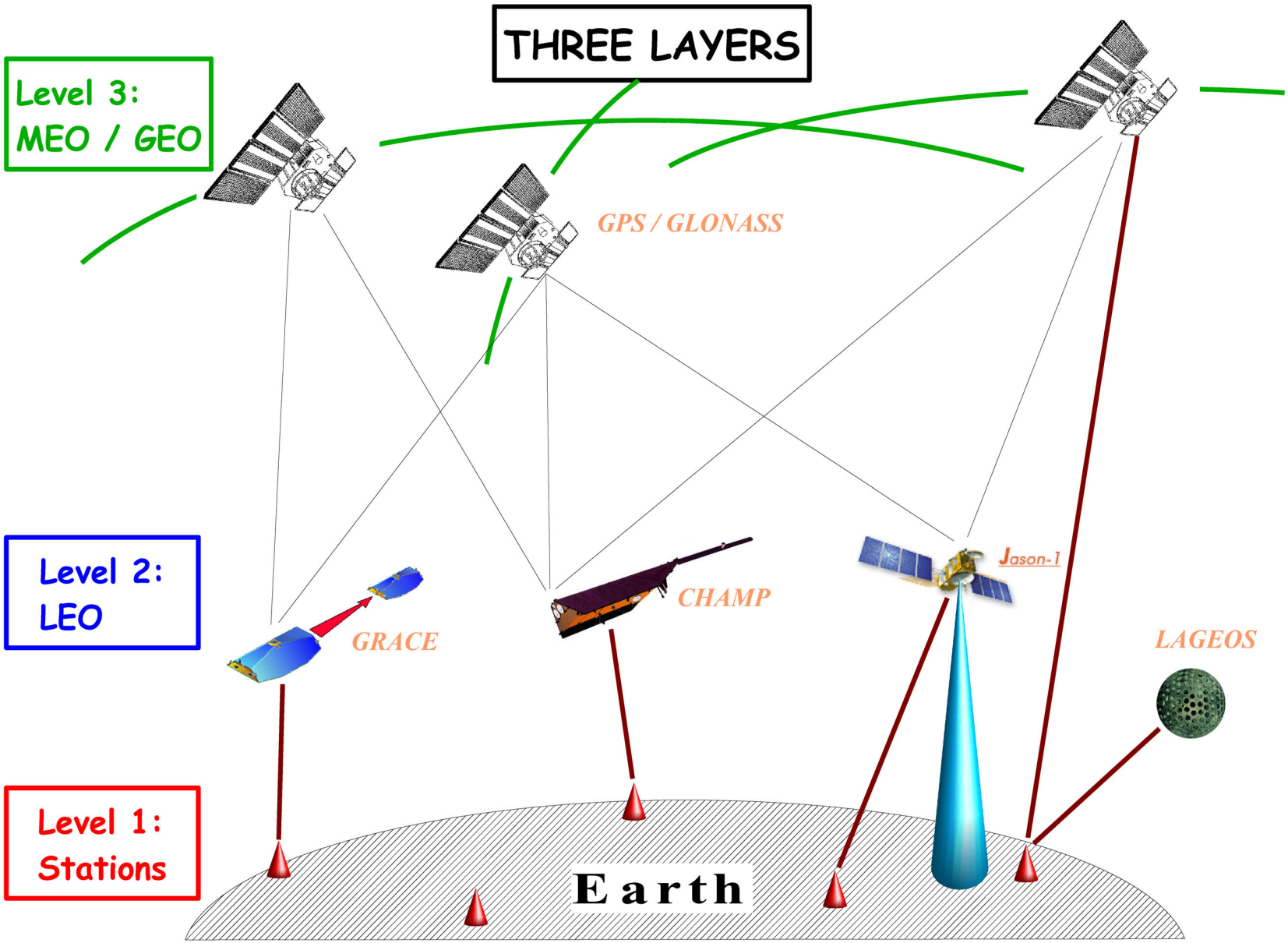

Orbits and „Observed-Computed“ (O&O)

Validation of GNSS orbits (GPS, Glonass, Galileo, …):

- SLR measurements are successfully used to validate GNSS orbits
- **Systematic bias** of about **4-5 cm** (!) between GPS orbits from microwave and SLR observations — reason still unclear
- May become important for **Galileo** satellites, too

Validation of Low Earth Orbiter (LEO) orbits:

- Much progress in **precise orbit determination** (POD) of **LEOs** thanks to validation with SLR “observed-computed” (O-C)
- Evaluation of different **strategies** (kinematic, reduced-dynamic, …) and **software packages** and **parameterizations**
- SLR “O-C” values allow detection of **systematic orbit errors**

SLR observations are extremely valuable for POD studies; POD becomes ever more crucial for new satellite missions

SLR Validation of CHAMP GPS Orbits

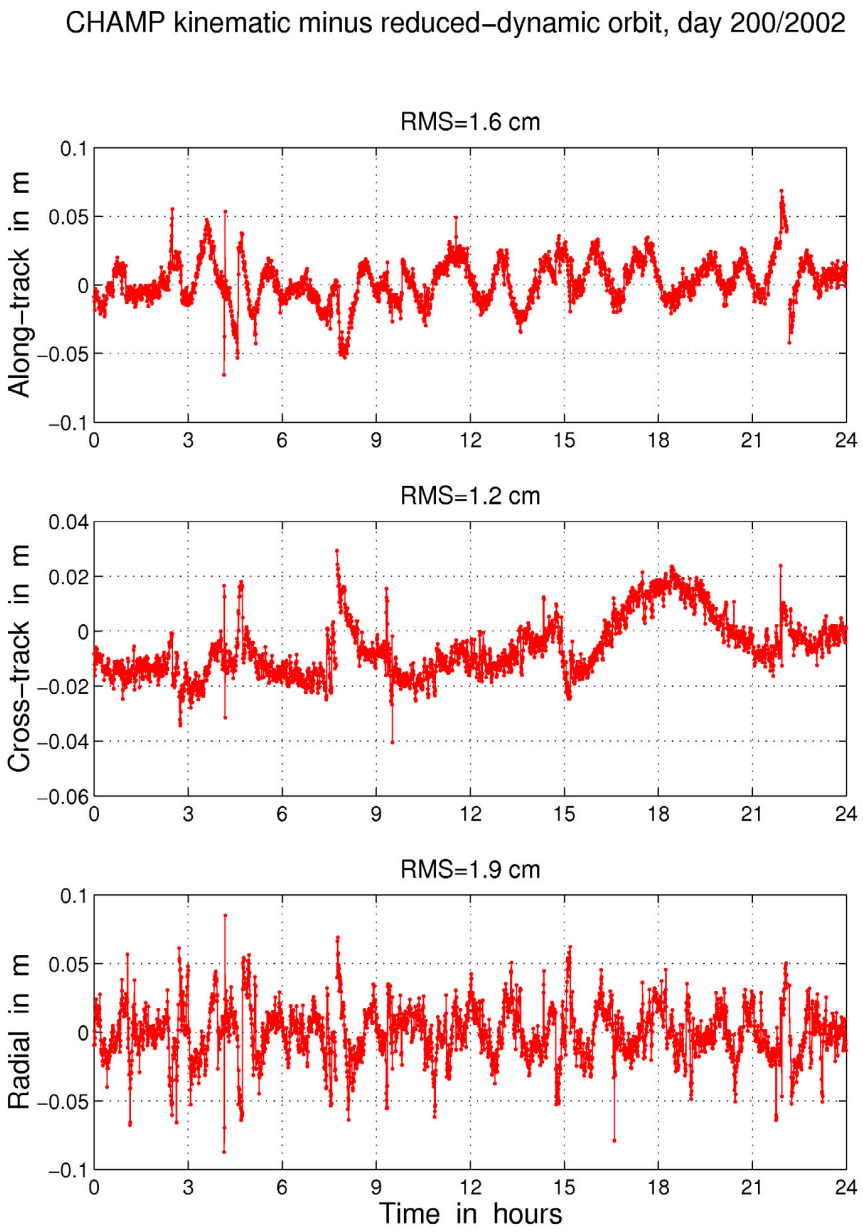

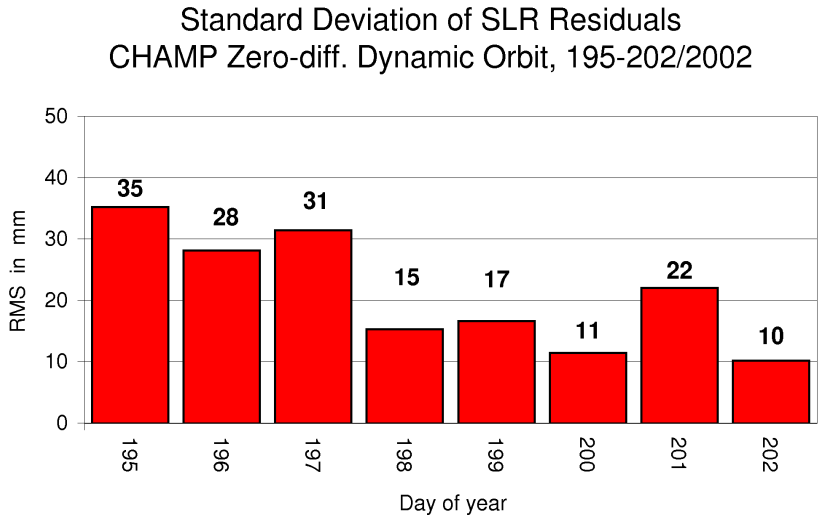

mean SLR STD = **21** mm

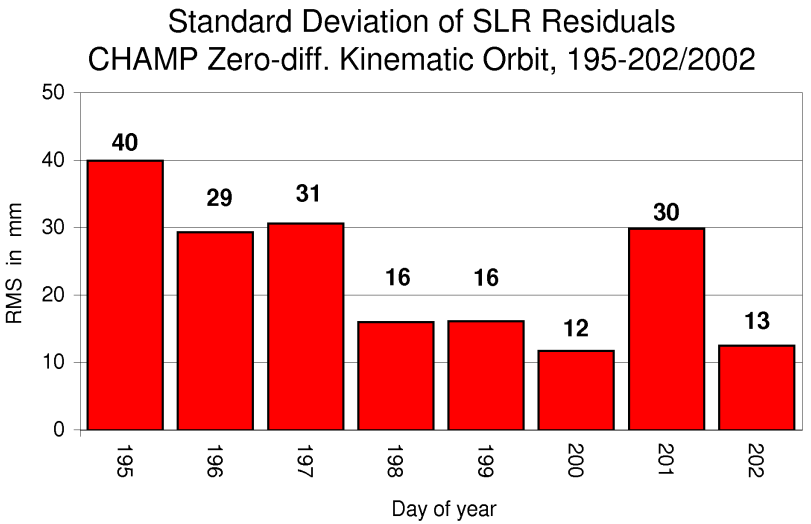

mean SLR STD = **23** mm

CHAMP Orbits: Observed-Computed

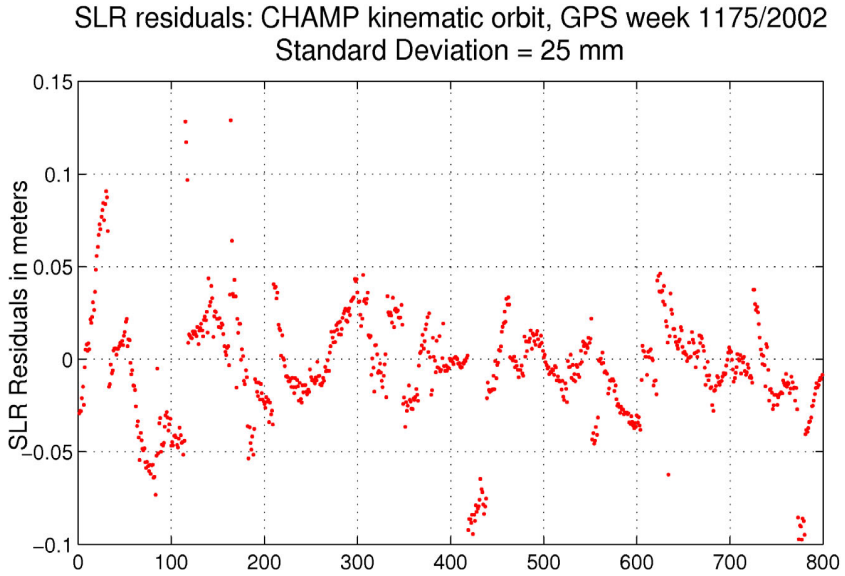

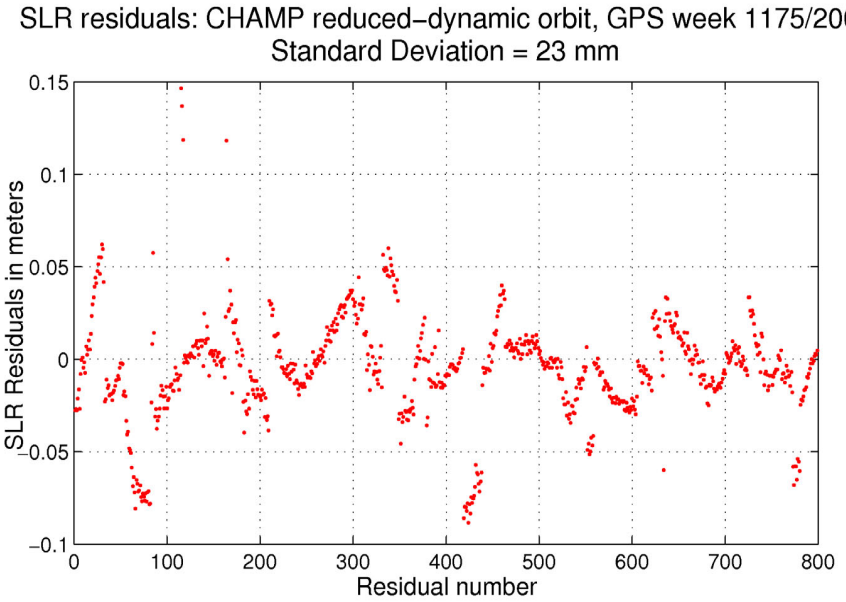

- SLR “O-C” values (or residuals) still show **significant systematic trends** for individual passes
- Similar behavior of **kinematic** and **reduced-dynamic** orbit residuals
- Detailed analysis of the residuals may give information on **model deficiences**, e.g.:
  - GPS polarization effect
  - Relativistic corrections
  - Higher order ionospheric corrections
  - Orbit parameterization …

Future Combination: "Weekly" SINEX Solutions

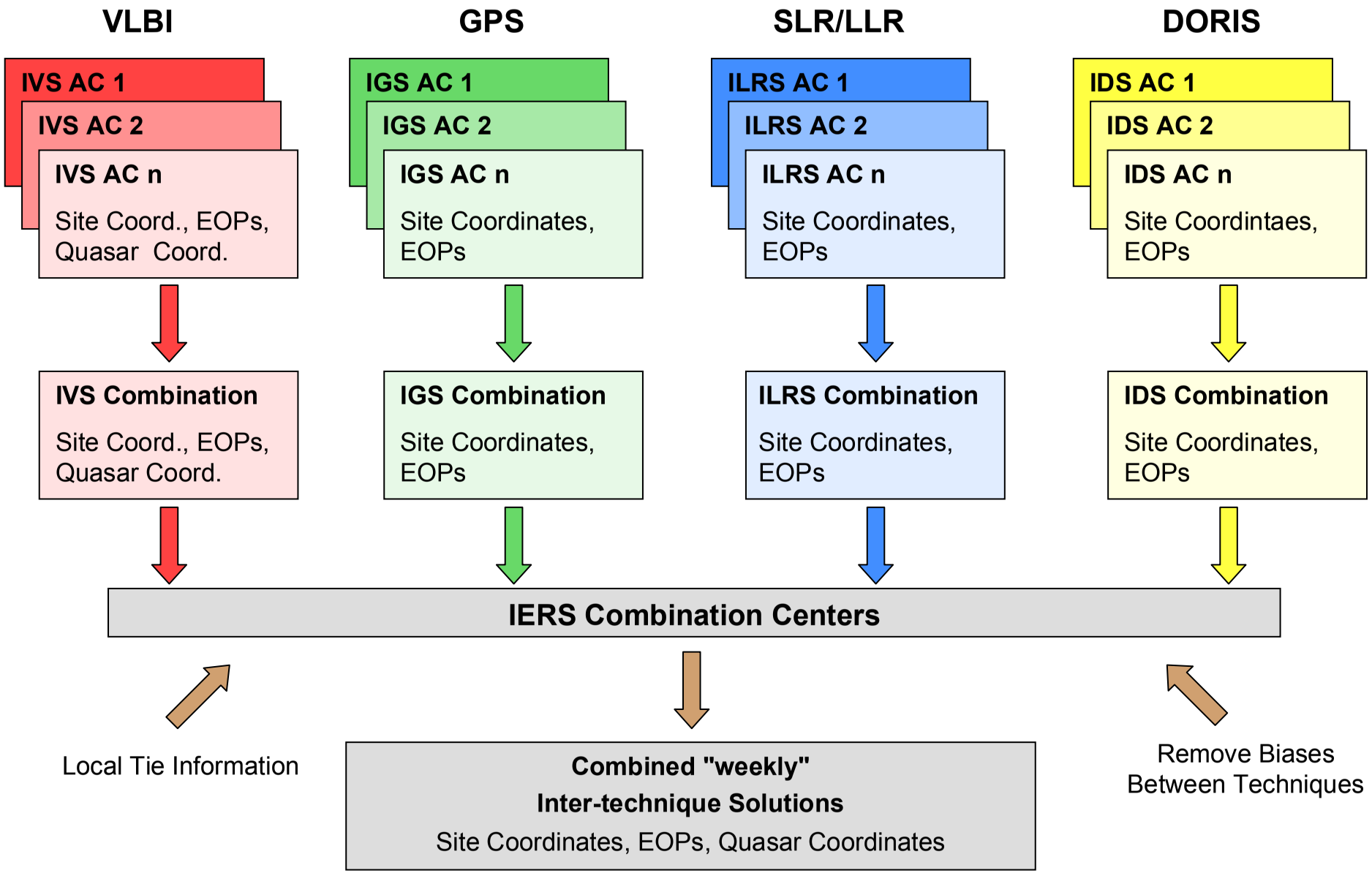

Future Combination: Multi-Year Solutions

(Fully Consistent Set of ITRF/EOPs/ICRF)

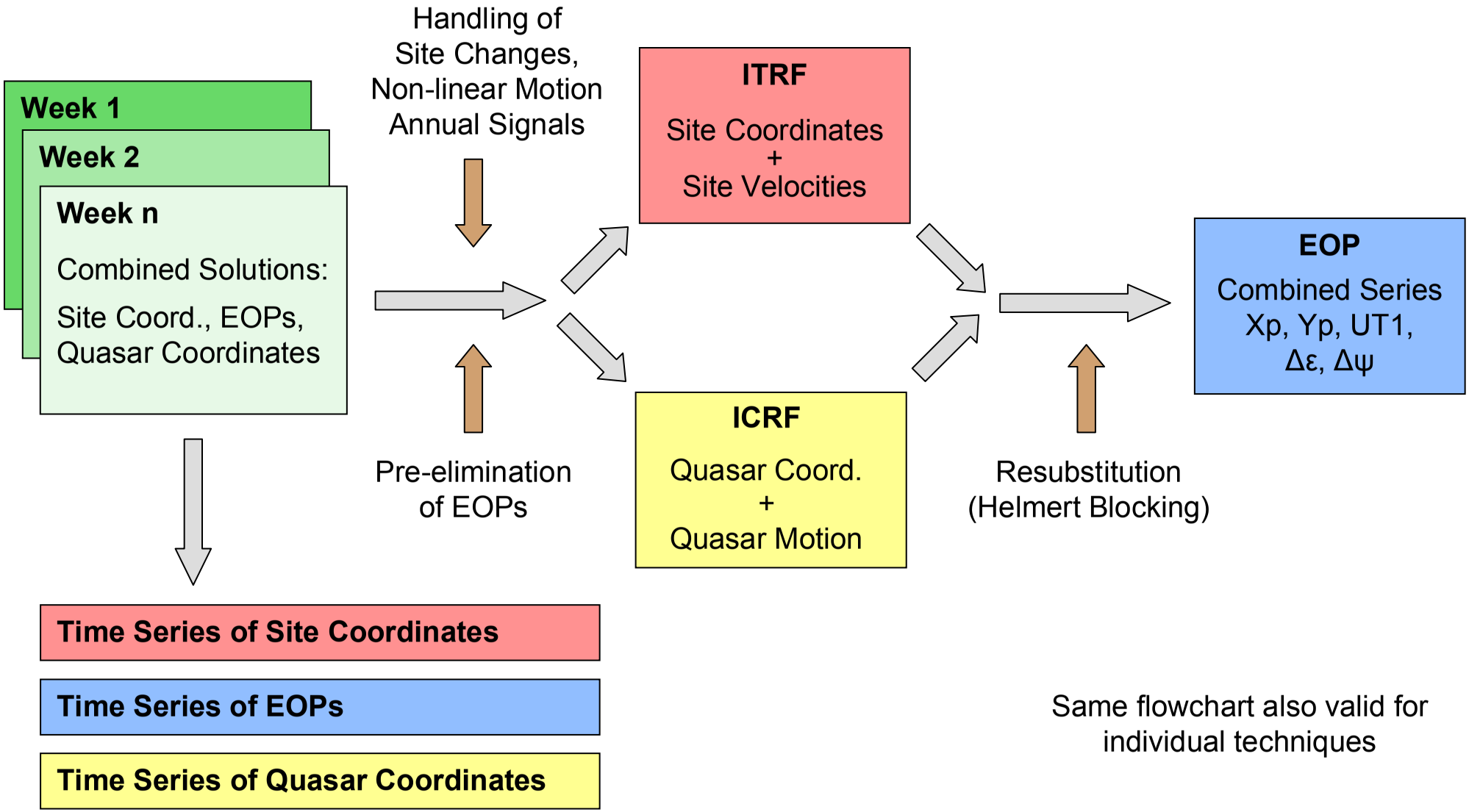

Same flowchart also valid for individual techniques

Measuring and Modeling the Earth System

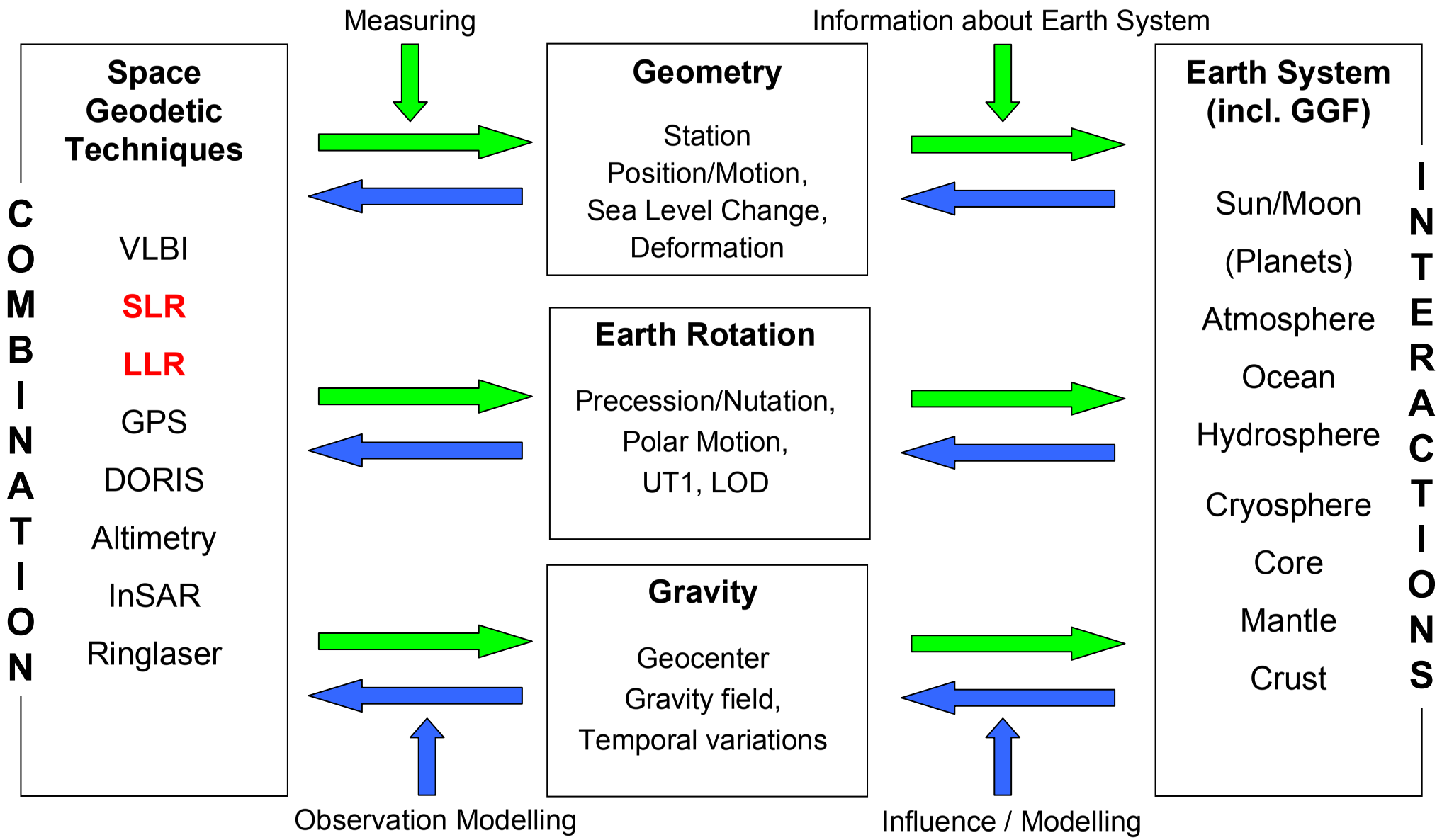

Conclusions

- SLR has few observations, but also few parameters to estimate
- SLR is the only optical technique (unique to assess atmosphere biases)
- No troposphere estimation necessary for SLR (correlations, biases)
- No clock correction estimation necessary for SLR (correlations, biases) → good heights
- No big antenna problems → absolute scale, heights
- Important link between gravity, Earth rotation, and geometry
- SLR O-C crucial for progress in POD

SLR is a unique partner in the goal of a rigorous combination of the space geodetic techniques (IERS and IGGOS)

The individual techniques should feel as a part of a larger whole with a common goal rather than working in competition

Interlinked, the techniques are much stronger and it is more difficult to isolate and cut individual techniques

Session 1

A Review of Station Performance and Data Throughput

Mike Pearlman, Van Husson

Station Qualification

- Begins Jan 1, 2004
- Requirements
  - **Data Quantity**
    - Within the past 12 months, ***50 LAGEOS*** passes within a ***consecutive 3 month*** period
  - **Data Quality**
    - ***NP RMS: 1 cm***
    - ***Short term stability: 4 cm***
    - ***Percentage of Good Data: 80%***
  - **Operational Compliance**
    - ***Completed Site Log***
    - ***Collocated with GPS*** (grace period July 1, 2004)

Station Qualification
as of 3rd Quarter 2003

EUROLAS		
Location	**CDP#**	**Status**
Borowiec	7811	Operational
Concepcion	7405	Operational
Grasse (LLR)	7845	Operational
Graz	7839	Operational
Herstmonceux	7840	Operational
Matera (MLRO)	7941	Operational
Potsdam	7836	Operational
San Fernando	7824	Operational
Wettzell	8834	Operational
Zimmerwald	7810	Operational
FTLRS at Chania	7830	Associate
Mendeleevo	1870	Associate
Metsahovi2	7806	Associate
Potsdam3	7841	Associate
Riga	1884	Associate
Grasse	7835	Closed

NASA		
Location	**CDP#**	**Status**
Arequipa	7403	Operational
Greenbelt	7105	Operational
Haleakala	7210	Operational
Hartebeesthoek	7501	Operational
McDonald	7080	Operational
Monument Peak	7110	Operational
Tahiti	7124	Operational

WPLTN		
Location	**CDP#**	**Status**
Changchun	7237	Operational
Koganei (CRL)	7308	Operational
Riyadh	7832	Operational
Shanghai	7837	Operational
Yarragadee	7090	Operational
Beijing	7249	Associate
BeijingA	7357	Associate
Golosiiv	1824	Associate
Katsively	1893	Associate
Komsomolsk	1868	Associate
Kunming	7820	Associate
Lviv	1831	Associate
Maidanak1	1864	Associate
Maidanak2	1863	Associate
Simeiz	1873	Associate
Simosato	7838	Associate
TROS at Urumqi	7355	Associate
Wuhan	7231	Associate
Mt. Stromlo	7849	Closed

Systems under Development	Operational
SLR2000 prototype, NASA	2004
Stromlo2, WPLTN	2004
Argentina, WPLTN	2004
GUTS - Japan, WPLTN	2004
Stafford(NRL), USA	
CTLRS-1, WPLTN	
Apache Point (LLR), USA	

Station Qualification

Location	CDP#	Status	LAGEOS Total	NP RMS	Bias Stability	% of Good NPs	Site Log	Collocated with GPS	Network
Borowiec	7811	Operational	yes	yes	yes	yes	yes	yes	EUROLAS
Concepcion	7405	Operational	yes	yes	yes	yes	yes	yes	EUROLAS
Grasse (LLR)	7845	Operational	yes	yes	yes	yes	yes	yes	EUROLAS
Graz	7839	Operational	yes	yes	yes	yes	yes	yes	EUROLAS
Herstmonceux	7840	Operational	yes	yes	yes	yes	yes	yes	EUROLAS
Matera (MLRO)	7941	Operational	yes	yes	yes	yes	yes	yes	EUROLAS
Potsdam	7836	Operational	yes	yes	yes	yes	yes	yes	EUROLAS
San Fernando	7824	Operational	yes	yes	yes	yes	yes	yes	EUROLAS
Wettzell	8834	Operational	yes	yes	yes	yes	yes	yes	EUROLAS
Zimmerwald	7810	Operational	yes	yes	yes	yes	yes	yes	EUROLAS
Grasse	7835	Closed	yes	N/A	N/A	N/A	yes	yes	EUROLAS
FTLRS at Chania	7830	Associate	no	N/A	N/A	N/A	yes	yes	EUROLAS
Mendeleevo	1870	Associate	no	N/A	N/A	N/A	yes	yes	EUROLAS
Metsahovi2	7806	Associate	no	yes	yes	yes	yes	yes	EUROLAS
Potsdam3	7841	Associate	no	yes	yes	yes	yes	yes	EUROLAS
Riga	1884	Associate	no	yes	yes	yes	yes	yes	EUROLAS
Arequipa	7403	Operational	yes	yes	yes	yes	yes	yes	NASA
Greenbelt	7105	Operational	yes	yes	yes	yes	yes	yes	NASA
Haleakala	7210	Operational	yes	yes	yes	yes	yes	yes	NASA
Hartebeesthoek	7501	Operational	yes	yes	yes	yes	yes	yes	NASA
McDonald	7080	Operational	yes	yes	yes	yes	yes	yes	NASA
Monument Peak	7110	Operational	yes	yes	yes	yes	yes	yes	NASA
Tahiti	7124	Operational	yes	yes	yes	yes	yes	yes	NASA
Changchun	7237	Operational	yes	yes	yes	yes	yes	no	WPLTN
Koganei (CRL)	7308	Operational	yes	yes	yes	yes	yes	yes	WPLTN
Riyadh	7832	Operational	yes	yes	yes	yes	yes	no	WPLTN
Shanghai	7837	Operational	yes	yes	yes	yes	yes	yes	WPLTN
Yarragadee	7090	Operational	yes	yes	yes	yes	yes	yes	WPLTN
Mt. Stromlo	7849	Closed	yes	N/A	N/A	N/A	yes	yes	WPLTN
Beijing	7249	Associate	no	yes	N/A	N/A	yes	yes	WPLTN
BeijingA	7357	Associate	no	yes	yes	yes	yes	yes	WPLTN
Golosiiv	1824	Associate	no	no	N/A	yes	yes	yes	WPLTN
Katsively	1893	Associate	no	N/A	N/A	N/A	yes	no	WPLTN
Komsomolsk	1868	Associate	no	N/A	N/A	no	no	no	WPLTN
Kunming	7820	Associate	no	N/A	N/A	N/A	yes	yes	WPLTN
Lviv	1831	Associate	no	N/A	N/A	N/A	yes	yes	WPLTN
Maidanak1	1864	Associate	yes	no	yes	yes	no	no	WPLTN
Maidanak2	1863	Associate	yes	yes	yes	yes	no	no	WPLTN
Simeiz	1873	Associate	yes	no	no	yes	yes	yes	WPLTN
Simosato	7838	Associate	yes	yes	no	yes	yes	yes	WPLTN
Urumqi	7355	Associate	yes	no	yes	yes	yes	yes	WPLTN
Wuhan	7231	Associate	no	yes	N/A	N/A	yes	yes	WPLTN

Station Qualification

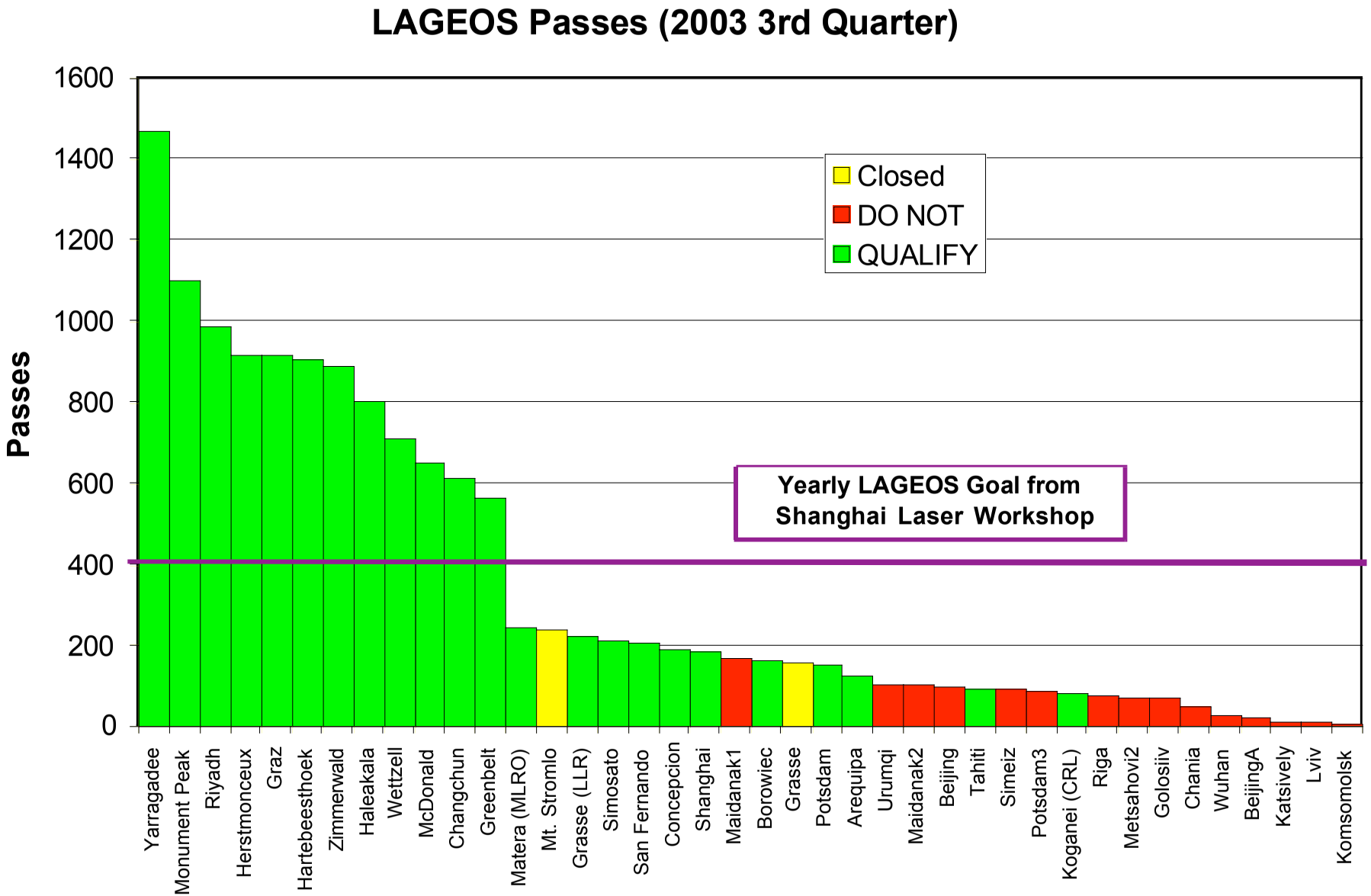

Session 2

Daylight Ranging

Werner Gurtner, Ulrich Schreiber

Daylight Tracking

Werner Gurtner
Ulrich Schreiber

ILRS Workshop
28-31 October 2003
Kötzting

Topics to Discuss

- Why is daylight ranging so important?
- Why is the daylight ranging so poor?
- What is the experience at the most successful stations?
- How do we improve it?
- What are the hardware issues?
- What are the software issues?
- Would better predictions help?
- What are the current limitations?

Why is daylight ranging so important?

- Number of observed passes
- Number of observations
- Longer gaps in orbit coverage
- Systematic errors in products

Percentage of Day Time Passes

- Stella, Starlette, Lageos-1, Topex, Ajisai — 40 %
- Jason, BE-C, GFO-1, Lageos-2, ERS-2, Envisat, Champ — 30 %
- Grace A/B — 25 %
- Glonass, Etalon — 10 %
- GPS — 5 %

Day and Night Time NP per Satellite

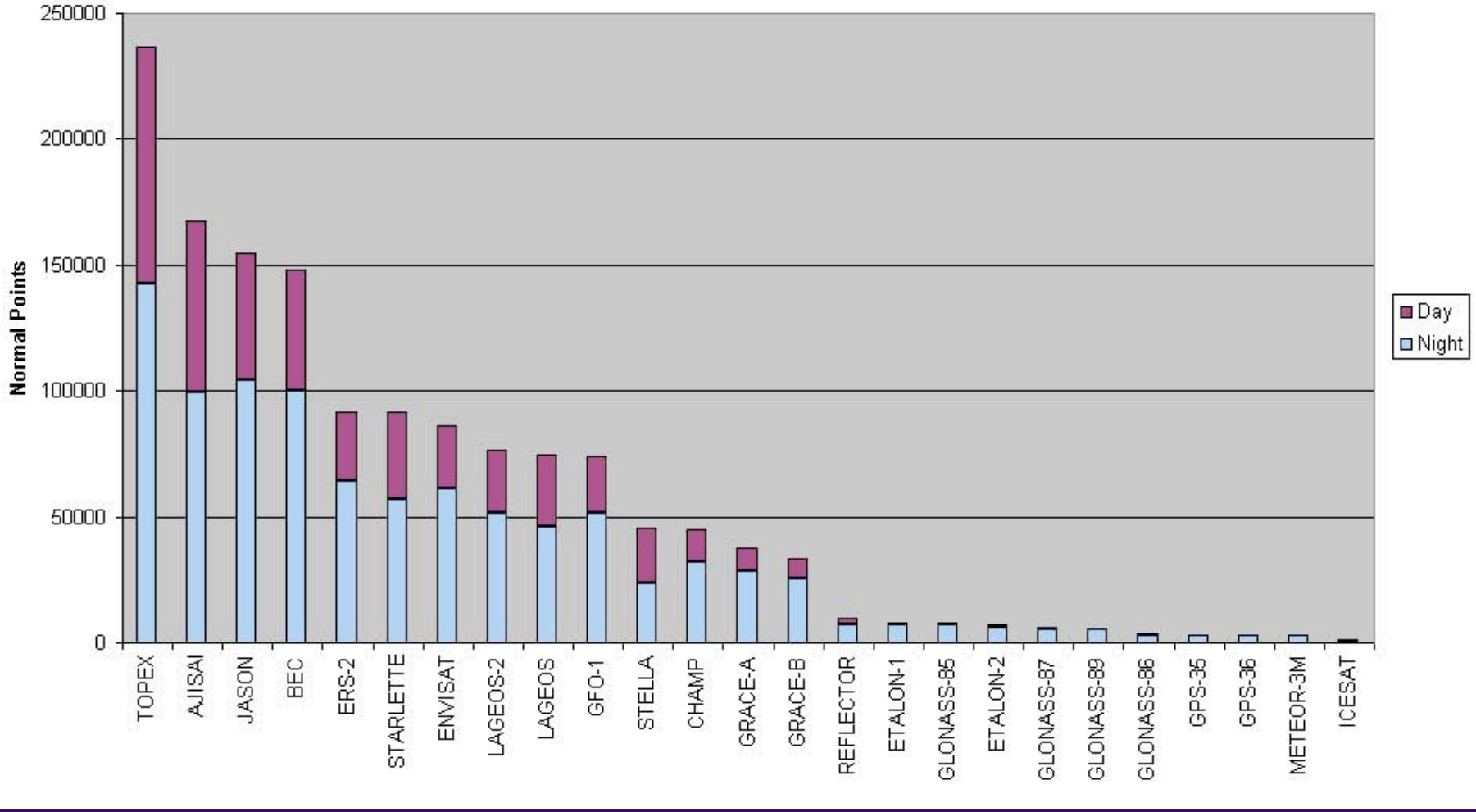

Percentage of Day Time Data (NP)

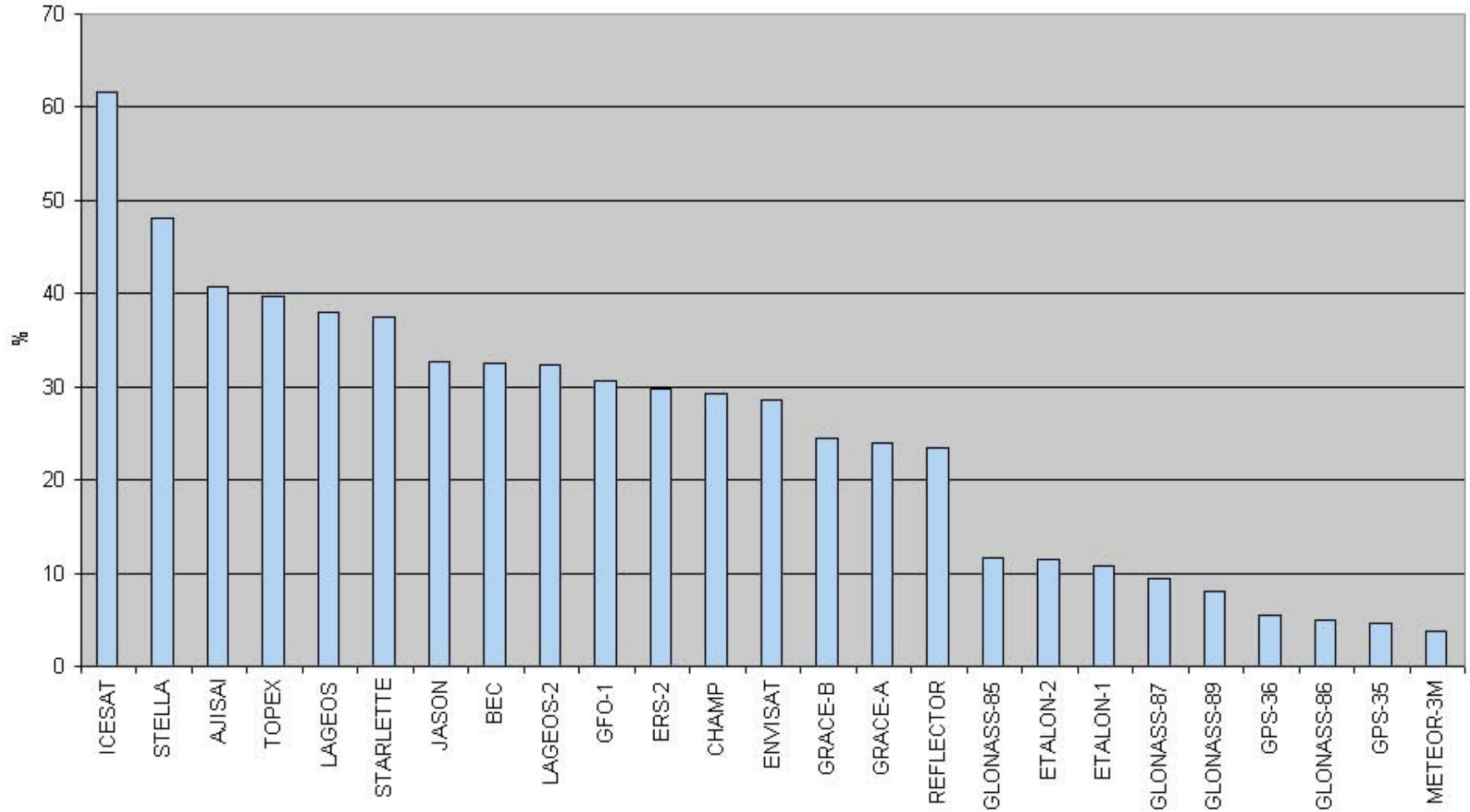

Day and Night Time Data per Station

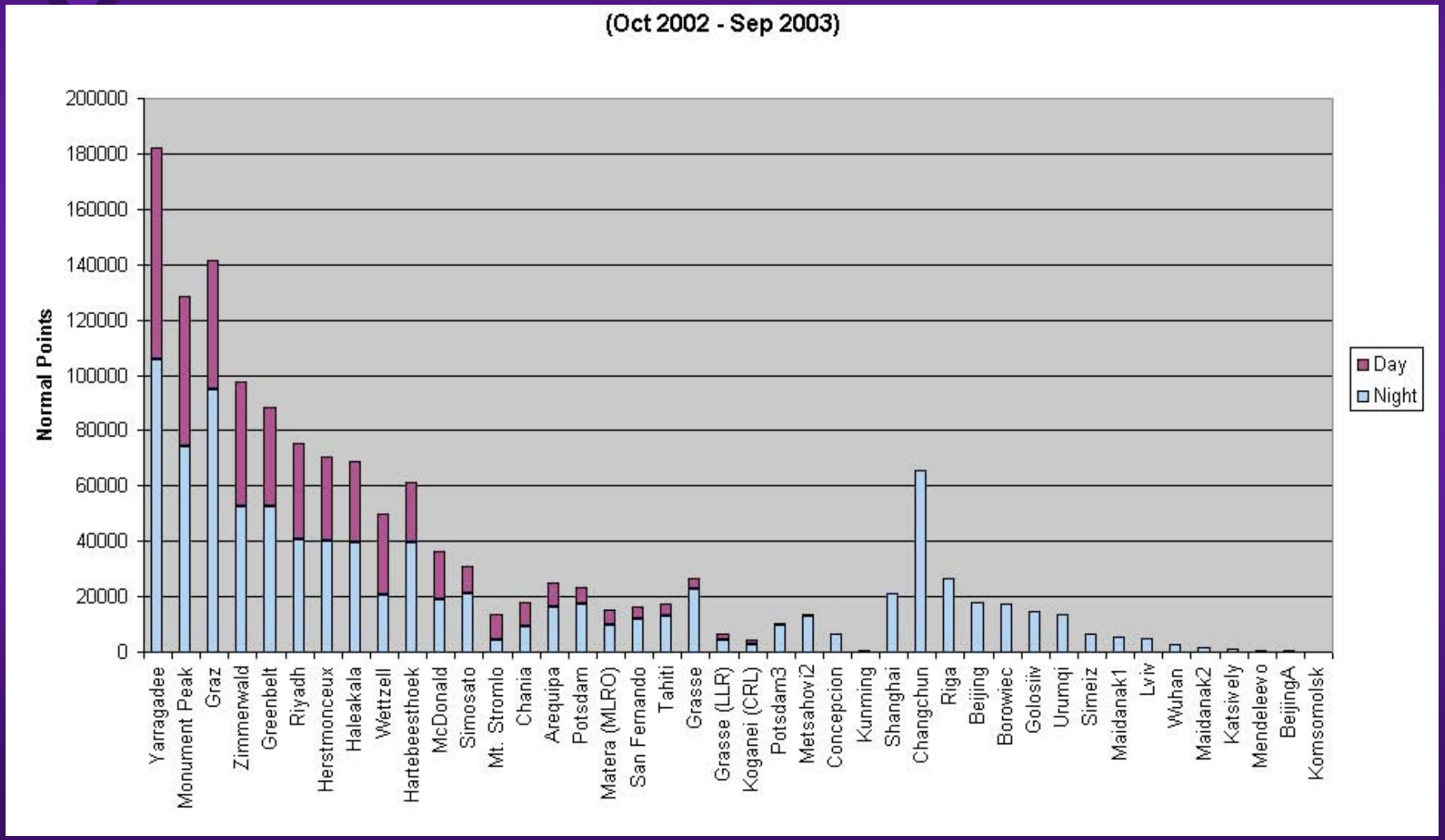

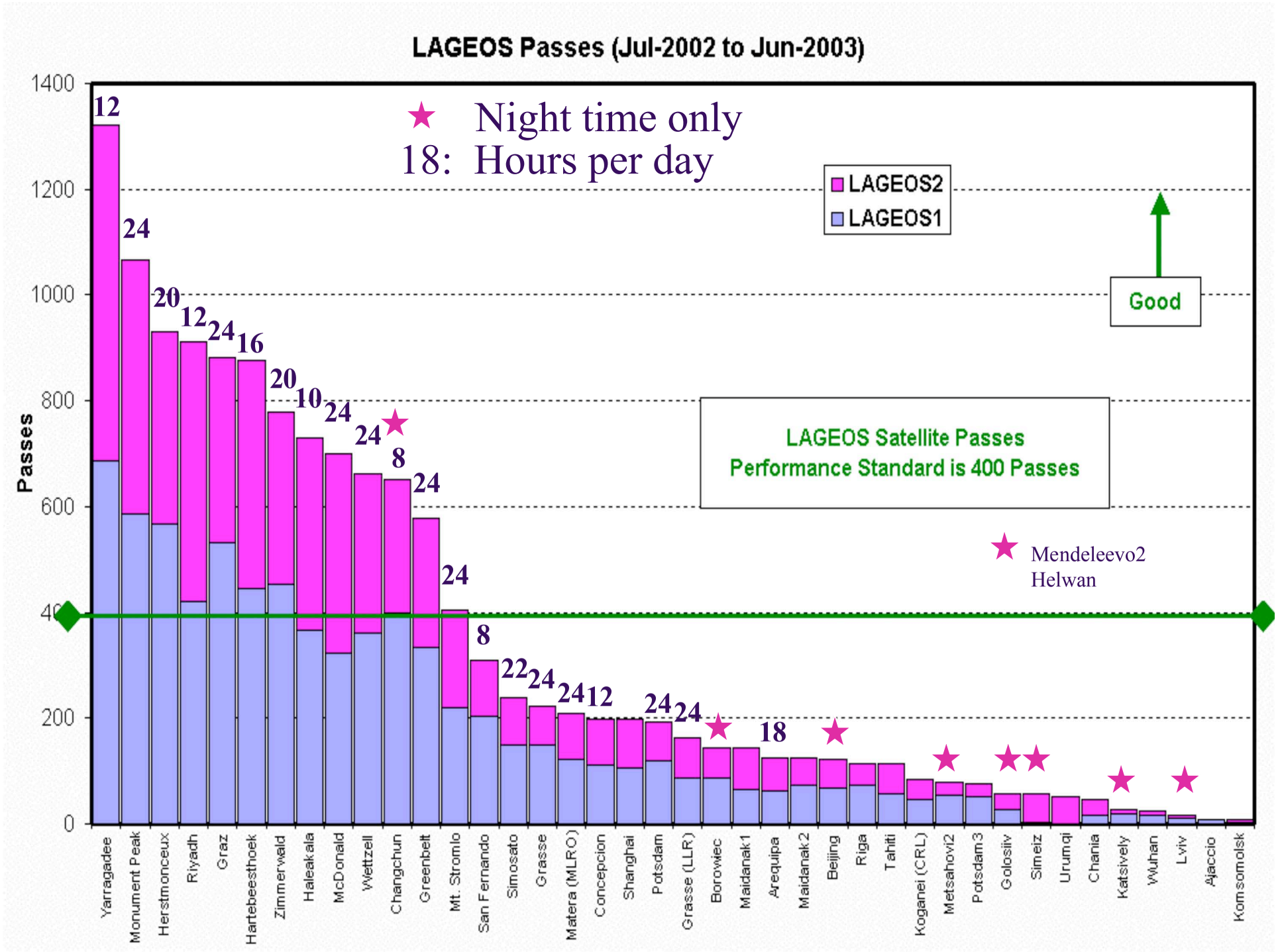
LAGEOS Passes (Jul-2002 to Jun-2003)
★ Night time only
18: Hours per day
LAGEOS2
LAGEOS1
Good
LAGEOS Satellite Passes
Performance Standard is 400 Passes
★ Mendeleevo2
Helwan
Passes
1400
1200
1000
800
600
400
200
0
12
24
20
12
24
16
20
10
24
24
8
24
24
8
22
24
24
12
24
24
18
Yarragadee
Monument Peak
Herstmonceux
Riyadh
Graz
Hartebeesthoek
Zimmerwald
Haleakala
McDonald
Wettzell
Changchun
Greenbelt
Mt. Stromlo
San Fernando
Simosato
Grasse
Matera (MLRO)
Concepcion
Shanghai
Potsdam
Grasse (LLR)
Borowiec
Maidanak1
Arequipa
Maidanak2
Beijing
Riga
Tahiti
Koganei (CRL)
Metsahovi2
Potsdam3
Golosiiv
Simeiz
Urumqi
Chania
Katsively
Wuhan
Lviv
Ajaccio
Komsomolsk

LAGEOS NP Data Yield

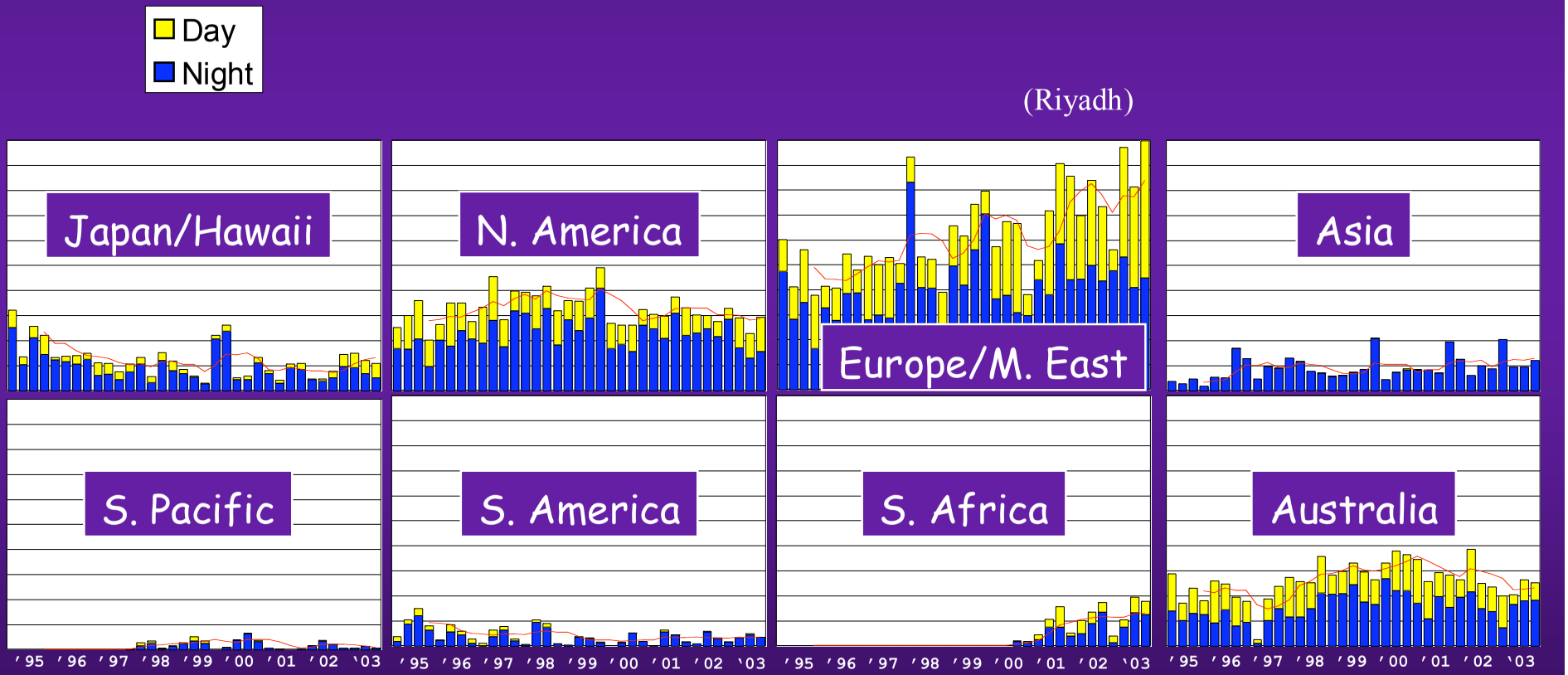

Etalon NP Data Yield

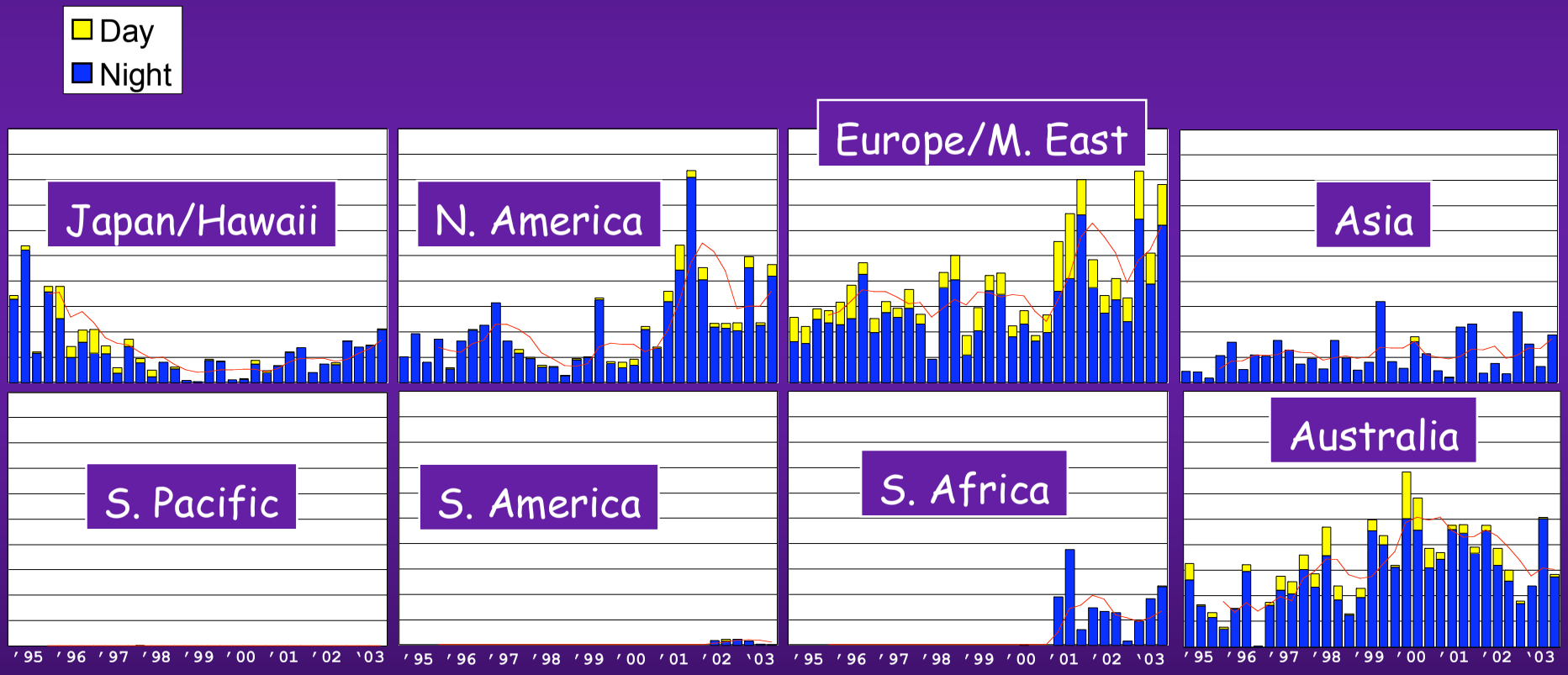

Problem: Bad Pointing

- Problem: Bad pointing accuracy, misalignments
  - Inherent precision of the telescope or the alignment procedures
  - Daytime degradation due to direct sun radiation → tens of arc seconds
- Impact
  - large field of view necessary
  - too much noise
- Possible actions
  - Protection/insulation → Herstmonceux, Potsdam, Zimmerwald
  - Daytime mount model (bright stars, red filters)

Problem: Sun Interference

- Problem: Possible damage by focussed sun light
- Solution:
  - Evasion routines: Maintain minimum distance to sun (e.g. 25 deg)
  - Emergency shutters
- Loss of a certain percentage of possible tracking coverage
  (e.g., 15 % when ranging down to 20 deg elevation)

Problem: Background Noise

- Problem: Too much background noise
- Absolut Limit: 100 percent noise returns before laser return arrives at the sensor
- Solutions
  - Narrower spectral filter
  - Smaller window ←→ prediction
  - Smaller field of view ←→ prediction, pointing
  - Neutral density filter for strong satellites
  - Window swaying

Problem: High Orbiting Satellites

- Low signal to noise ratio
- Acquisition of echoes is difficult in the presence of noise (**one has to wait longer on one spot**)
- Searching for a satellite on a collimated system is difficult in the presence of a small telescope pointing error (**larger spatial segment needs to be scanned**)

Search and Range Gate Width

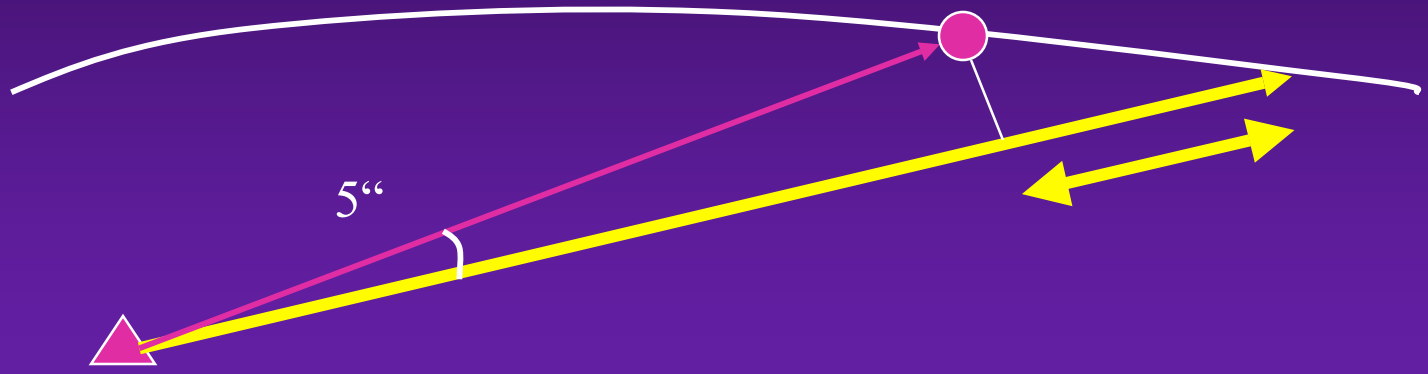

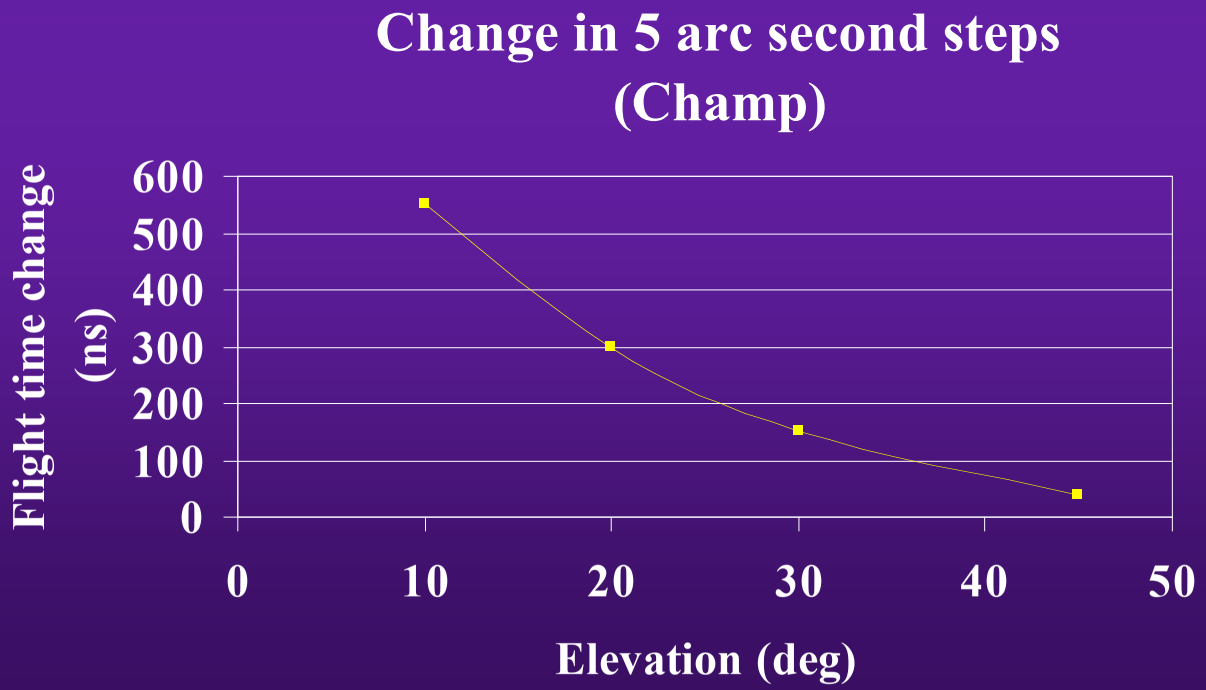

Delta range and pointing per ms along-track error

(Champ)

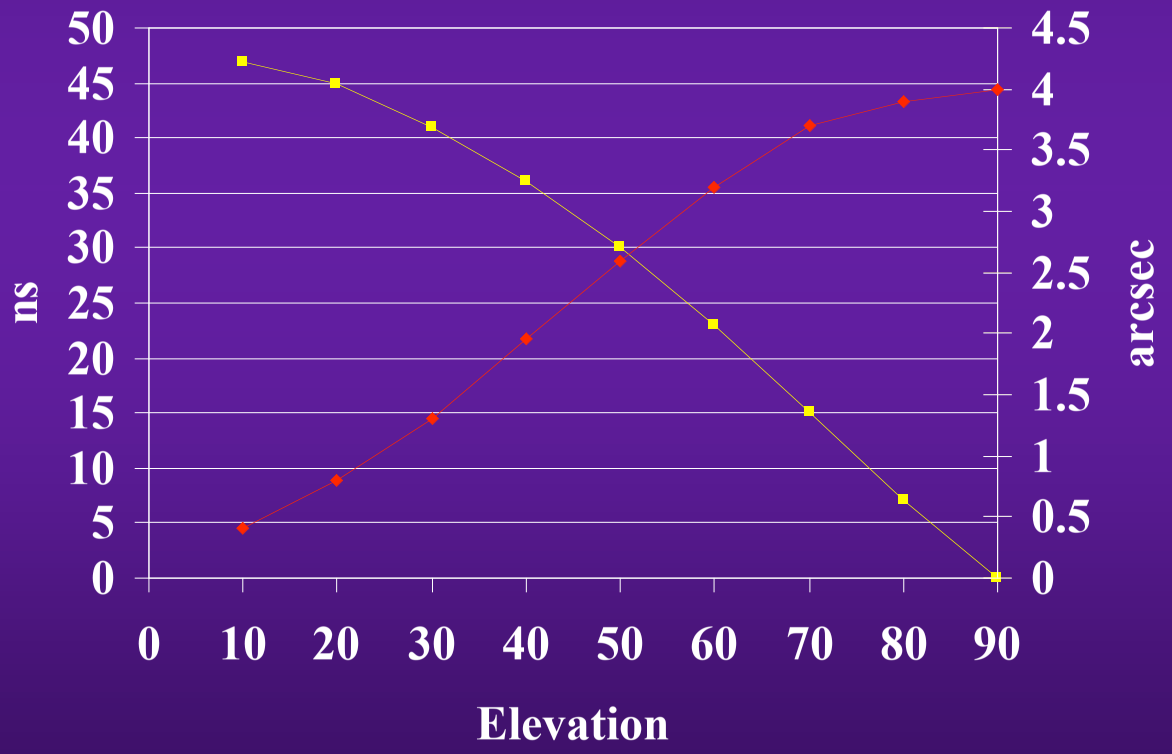

Maximum Prediction Errors

(Herstmonceux)

- High-orbiting satellites: No problem (?)
- Stella,Starlette,Ajisai,Topex and Jason: < 5 ms
- ERS2,Envisat and GFO : < 30 ms
- Champ and Grace: < 40 ms

- Time bias functions for Champ and Grace: Problem
- Best prediction sets
  - ERS-2: GFZ
  - Envisat: Not ESOC

Prediction Quality
(Grasse)

- Very good on Lageos and Etalon (?)
- Poor predictions on GPS and Etalon (?) for daylight tracking
- Generally sufficient for LEO except Envisat, Grace and Champ

Realtime noise rejection / data identification

- Visual inspection of observed – predicted
- Histogram within window
- Direct comparison of obs-pred
- Convert obs-pred into Δt, compare or form histogram (does not work well around C.A) (Grasse, Zimmerwald)

- Improve predictions with realtime Δt

Current limitations

- Pointing precision
- Noise
- Predictions
  - Range (time bias)
  - Position (?)
- Man power
- Schedule (high orbit satellites skipped when LEOs are around)

NASA SLR Daytime Tracking

Successful daytime tracking requires a system design approach concentrating on Signal-to-Noise ratio.

No one component will enable effective daytime operations unless the remaining system, both HW and SW, is capable.

- Experienced, well trained operators
- 10Å daylight filter (~ 65% transmission)
- Triple gated receive signal (+/- 40 nsec around signal)
- 532 nm “Peaked” transmit/receive optics
- Variable receive iris
- Telescope shroud to limit off axis light to 10 degrees
- Variable optical ND filter for receive signal amplitude control

International Laser Ranging Service

NASA SLR Daytime Tracking

- Precise satellite pointing vectors
- Precision transmit/receive boresight
- Calibrated Constant Fraction Discriminator
- Precision mount pointing performance (+/-2.0 arcsec)
- 30 arcsecond transmit beam divergence
- Precise star calibration
- Daytime to nighttime focus adjustment
- 0.76 meter Receive Telescope
- 100 millijoule, 200ps laser

International Laser Ranging Service

Honeywell

Session 3

Implementation of the New Engineering Data File

Georg Kirchner, Van Husson

Data Engineering File

(NASA systems stored info and measurements per pass)

Station info

- PAD (Station) ID
- Occupation Number
- Station Latitude
- Station Longitude
- Station Height

Satellite info

- Sat ID
- Sat # Obs, # Rejections
- Sat RMS
- Applied System Delay
- Sat A1 Mean, RMS
- Sat PMT Voltage Mean, RMS
- Sat Receive Energy Mean, RMS
- Sat Transmit Delay Mean, RMS
- Time Bias Correction
- Range Bias Correction
- ND Filter Correction
- IRV Time Bias
- IRV Range Bias
- # Normal Pt Bins
- # Normal Pt Bins with Sat data
- Sat Skew
- Sat Kurtosis

Calibration info

- Cal Target ID, Distance
- Cal # Obs, # Rejections
- Cal RMS
- Cal Shift (Pre - Post)
- System Delay
- Cal A1 Mean, RMS
- Cal PMT Voltage Mean, RMS
- Cal Transmit Energy Mean, RMS
- Cal Receive Energy Mean, RMS

Meteorological Data

- Sat Min, Max and Mean Temperatures
- Sat Min, Max and Mean Pressures
- Cal Mean Temperature
- Humidity
- Day/Night Pass

Session 4

Local Survey Monumentation and Eccentricity Measurement

Wolfgang Schlueter

Summary of the IERS workshop on site co-location surveys

- The International Earth rotation and Reference Systems Service (IERS) had organized a workshop devoted to „site co-location survey objectives, methods and issues“.
- It took place in Matera / Italy on October 23 / 24, 2003.
- Presently the quality of the station coordinates results from the various space techniques is in the order of a few millimetres in the horizontal and about 1 cm in the vertical component.

In view of this precision, one of the major limiting factors is the quality and the availability of accurate local tie information for all the co-located sites around the globe:

- to study the systematic errors going along with each space technique,
- to establish a unique, high-precision terrestrial reference frame
- to enable an analysis which rigorously combine all geodetic space observing techniques by their common parameters

In 5 sessions attention has been given to:

- Co-location sites and their importance for the ITRF
- Site surveys
- Analysis and SINEX
- Reporting and Archiving
- Planning for 2004

- More than 30 participants from Australia, South Africa, USA and Europe discussed various examples, analysis methods and survey strategies.
- Finally guidelines for co-location site surveys and report templates have been proposed.
- The potential availability of survey teams as well as the planning for surveys in 2004 have been investigated.

The important recommendations are the following:

- Local ties between co-located instruments should be determined with an accuracy of 1 mm, with full variance/covariance information, available in SINEX format.
- Local survey measurements should have the same importance as and should be treated like any of the space geodetic techniques
- Site coordinates (VLBI, GPS, SLR, DORIS) should be better tied to the ground. The Local ties quality should be such that they can be assumed true for the combination.
- A database will be established at IERS (ITRS PC and CB) for all information in connection with site co-location (list of co-location sites, local ties in SINEX, co-location instruments, site maps and pictures, survey reports, survey status, site events and history, etc…)

The workshop information (programme, presentations and recommendations) will be available at the IERS web-pages (www.iers.org) on November 4, 2003 and the proceedings will be published as IERS Technical Note No. 33.

Session 5

Improved Data QC at the Stations

Georg Kirchner, Van Husson

Background of Minimum Observation Per NP

- In 1999, a study group of analysts (the 'Jaguar' Team) was tasked by the Data Format & Procedures Working Group to investigate this issue
- In Sep 1999, the Jaguar Team concluded the minimum observations/NP should be 1, otherwise valid data would be lost
- EUROLAS Workshop Recommendation (Mar 2002)
  - Minimum is 3 observations/NP for NIGHT
  - Minimum is 6 observation/NP for DAY
  - Exceptions
    - Very Low LEOS
    - Systems with low laser repetition rates
  - EUROLAS recommended this action be sent to the AWG, but prior to this being done it was presented and approved by the ILRS Governing Board

Minimum Observation Per NP
(all satellites)

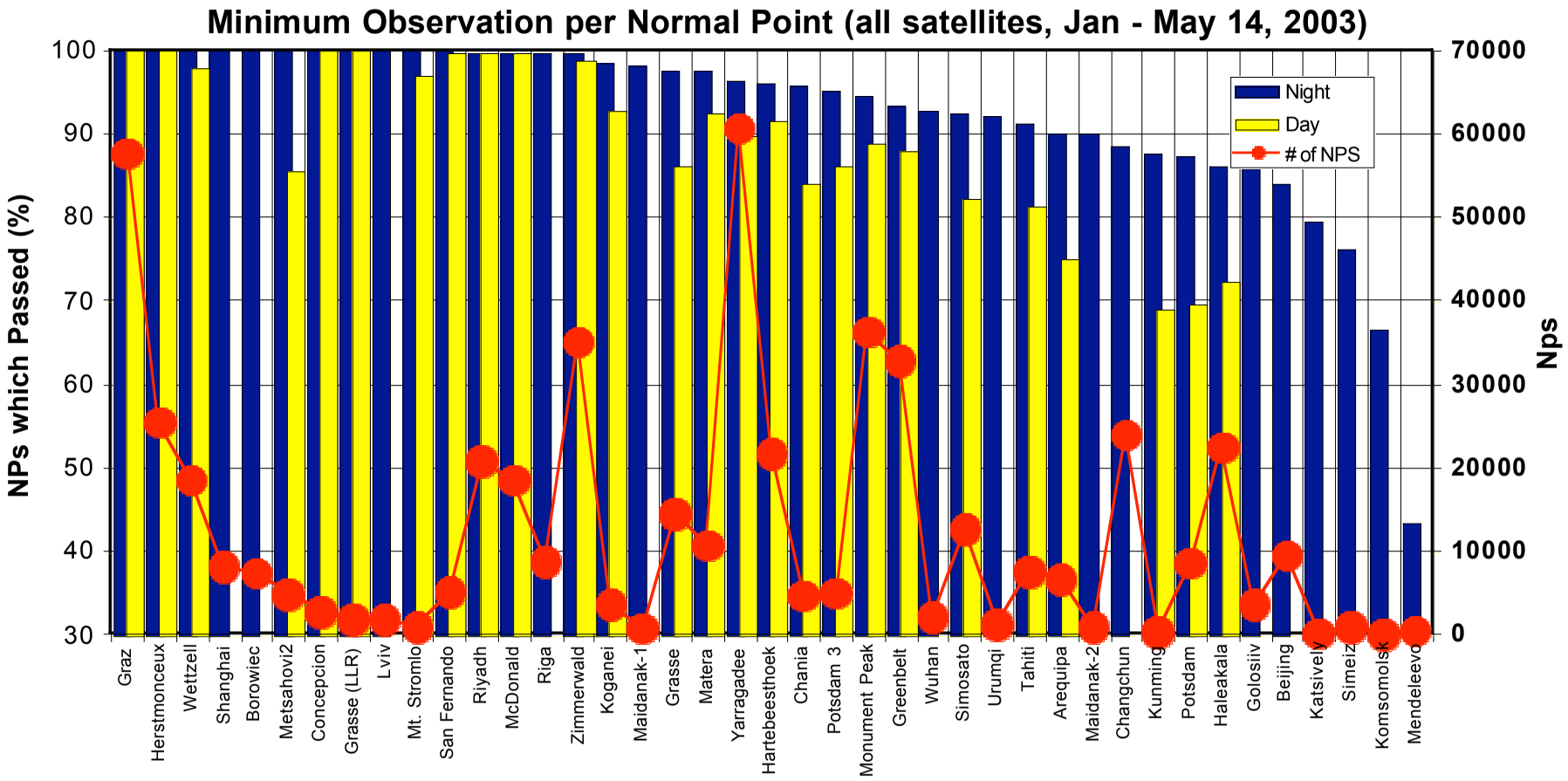

All Satellites except CHAMP and GRACE, Jan 1 - May 14, 2003					
Site	**Day NPs**	**Night NPs**	**Total NPs**	**Day %**	**Night %**
Graz	17831	39817	57648	100.0	100.0
Herstmonceux	9647	15774	25421	100.0	100.0
Wettzell	9111	9331	18442	98.1	100.0
Shanghai	0	8067	8067		100.0
Borowiec	0	7330	7330		100.0
Metsahovi2	21	4835	4856	85.7	100.0
Concepcion	18	2728	2746	100.0	100.0
Grasse (LLR)	469	1315	1784	100.0	100.0
Lviv	0	1780	1780		100.0
Mt. Stromlo	525	387	912	97.1	100.0
San Fernando	2196	2826	5022	99.9	100.0
Riyadh	11656	9079	20735	99.7	99.9
McDonald	8228	10259	18487	99.7	99.9
Riga	0	8750	8750		99.8
Zimmerwald	14267	20740	35007	98.9	99.8
Koganei	1610	1963	3573	92.9	98.4
Maidanak-1	0	721	721		98.2
Grasse	2366	12078	14444	86.1	97.8
Matera	3739	6961	10700	92.6	97.6
Yarragadee	26268	34320	60588	89.8	96.6
Hartebeesthoek	8581	13093	21674	91.6	96.2
Chania	1606	3012	4618	84.1	95.8
Potsdam 3	219	4788	5007	86.3	95.3
Monument Peak	15986	20181	36167	88.9	94.6
Greenbelt	13463	19263	32726	88.0	93.5
Wuhan	0	2029	2029		93.0
Simosato	4102	8447	12549	82.4	92.6
Urumqi	0	1242	1242		92.1
Tahiti	2639	4782	7421	81.5	91.5
Arequipa	3044	3591	6635	75.2	90.2
Maidanak-2	0	853	853		90.2
Changchun	0	23824	23824		88.6
Kunming	29	303	332	69.0	87.8
Potsdam	2009	6574	8583	69.7	87.5
Haleakala	9439	12917	22356	72.4	86.3
Golosiiv	0	3576	3576		86.0
Beijing	0	9500	9500		84.2
Katsively	0	98	98		79.6
Simeiz	0	937	937		76.3
Komsomolsk	0	6	6		66.7
Mendeleevo	0	379	379		43.5

Minimum Observation Per NP (LAGEOS only)

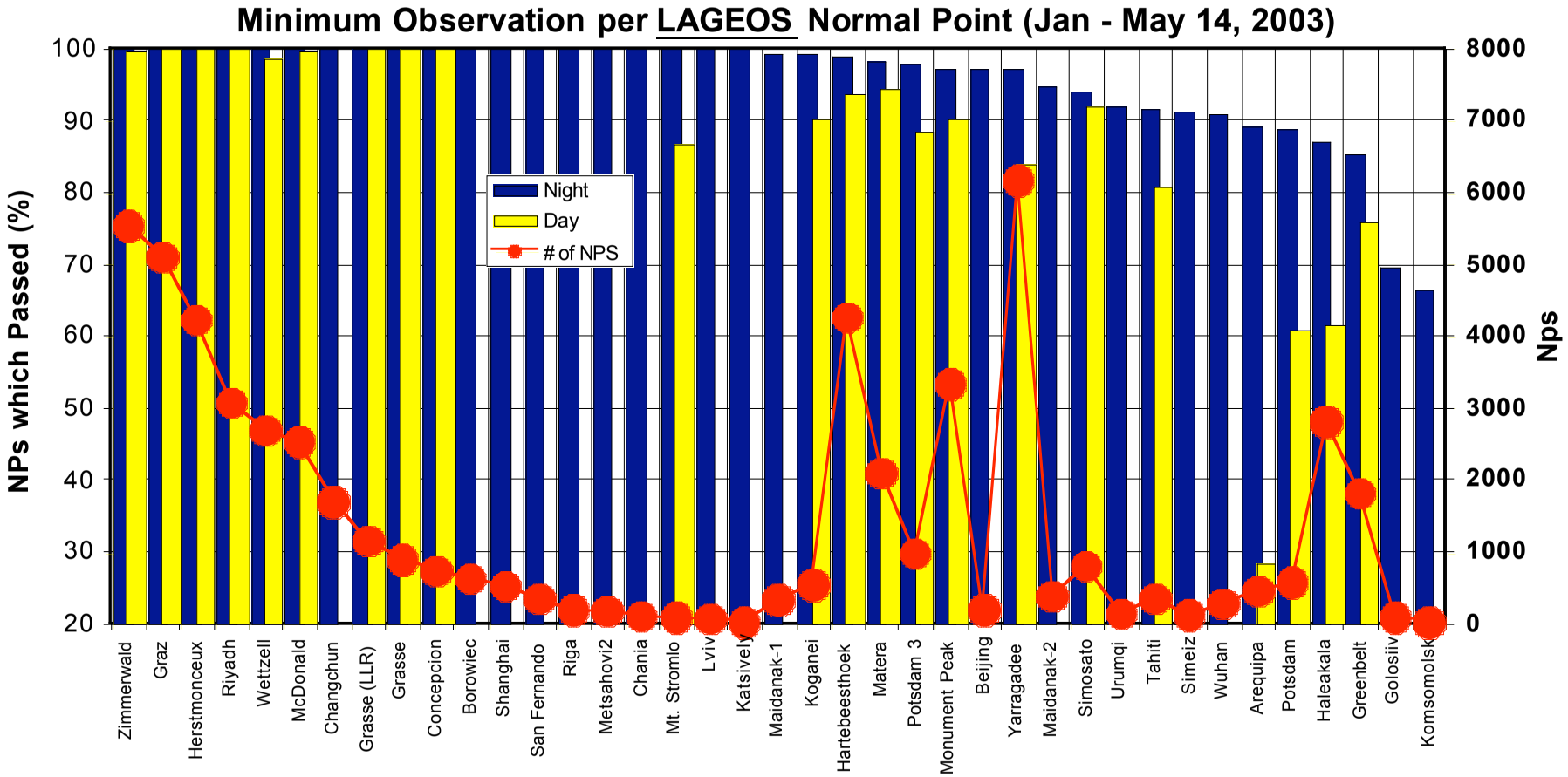

LAGEOS, Jan 1 - May 14, 2003					
Site	**Day NPs**	**Night NPs**	**Total NPs**	**Day %**	**Night %**
Zimmerwald	3022	2512	5534	99.7	100.0
Graz	2099	2984	5083	100.0	100.0
Herstmonceux	2069	2145	4214	100.0	100.0
Riyadh	1995	1061	3056	99.9	100.0
Wettzell	1580	1103	2683	98.8	100.0
McDonald	1321	1195	2516	99.9	100.0
Changchun	0	1685	1685		100.0
Grasse (LLR)	345	803	1148	100.0	100.0
Grasse	109	775	884	100.0	100.0
Concepcion	10	704	714	100.0	100.0
Borowiec	0	618	618		100.0
Shanghai	0	512	512		100.0
San Fernando	0	330	330		100.0
Riga	0	178	178		100.0
Metsahovi2	0	153	153		100.0
Chania	0	99	99		100.0
Mt. Stromlo	46	24	70	87.0	100.0
Lviv	0	53	53		100.0
Katsively	0	6	6		100.0
Maidanak-1	0	313	313		99.4
Koganei	221	312	533	90.5	99.4
Hartebeesthoek	1209	3051	4260	93.9	98.9
Matera	925	1157	2082	94.5	98.5
Potsdam 3	78	887	965	88.5	98.0
Monument Peak	1359	1969	3328	90.2	97.5
Beijing	0	187	187		97.3
Yarragadee	1260	4893	6153	84.1	97.2
Maidanak-2	0	366	366		94.8
Simosato	178	618	796	92.1	94.3
Urumqi	0	128	128		92.2
Tahiti	26	318	344	80.8	91.8
Simeiz	0	104	104		91.3
Wuhan	0	272	272		91.2
Arequipa	21	414	435	28.6	89.1
Potsdam	23	537	560	60.9	89.0
Haleakala	1128	1667	2795	61.5	87.2
Greenbelt	526	1284	1810	75.9	85.5
Golosiiv	0	79	79		69.6
Komsomolsk	0	6	6		66.7

SLR Quality Control Data Release Criteria

- NASA SLR Data are Quality Controlled to ensure the release of "Good Data" by the following Gross editing Criteria:
  - Satellite RMS > 1000 picoseconds OR

    Calibration RMS > 300 picoseconds OR

    (Calibration Shift < 600 picoseconds or > 200 picoseconds) AND Calibration RMS > 67 picoseconds OR

    System Delay = 0 picoseconds
  - NASA SLR Data is edited from the pre-released data set and stations are notified of errors
- The Global SLR Data Set is also Monitored and Edited for Gross Format and Integrity Compliance errors
  - HTSI performs four separate Data Format checks and nine separate Data Integrity Checks on all SLR Data before daily release to the Data Centers (CDDIS and EDC)
  - Data is edited from the pre-released data set and stations are notified of errors
  - A detailed description of all Data and Integrity Compliance Checks can be found at the ILRS Web Site at:

http://ilrs.gsfc.nasa.gov/products_formats_procedures/normal_point/format_and_data_integrity.html

Data Validation

- Verification of data integrity is both a station and operations center responsibility
- Checks to be performed
  - ILRS Normal Point format
    - Pass separation line (i.e., 99999)
    - Valid header and data records
    - Single pass per header record
  - Data integrity compliance
    - Header record contains valid satellite ID, date, and SOD
    - Data records contain valid laser firing time, surface pressure, surface temperature, humidity
    - Normal point bin size valid for satellite and bin formulation based from 0 hours UTC
- Any data failing these checks (with the exception of bin size criteria) are not released to the data centers
- Operations centers notify stations when failures occur

Session 6

How Shall We Handle Dynamic Priorities?

Mike Pearlman

Dynamic Priorities

Options Considered

- Elevate and depress satellite priorities based on data yield
- Set and post minimum pass criteria for network
- Post number of passes tracked and let the stations make decisions
- Set 3 to 4 categories of generally equal priorities and emphasize and deemphasize satellites within each category based on date yield

Dynamic Priorities

Strawman

Category 1	Category 2	Category 3
GRACE-A, -B	LAGEOS-1, -2	Etalon-1, -2
CHAMP	Ajisai	GLONASS-89, -87, -84
GFO-1	BE-C	GPS-35, -36
Envisat		
ERS-2		
Jason-1		
TOPEX/Poseidon		
Starlette		
Stella		
Meteor-3M		

Session 7

System Calibration

Ulrich Schreiber, Ivan Prochazka

Laser System Calibration

Ulrich Schreiber

Ivan Prochazka

Preamble

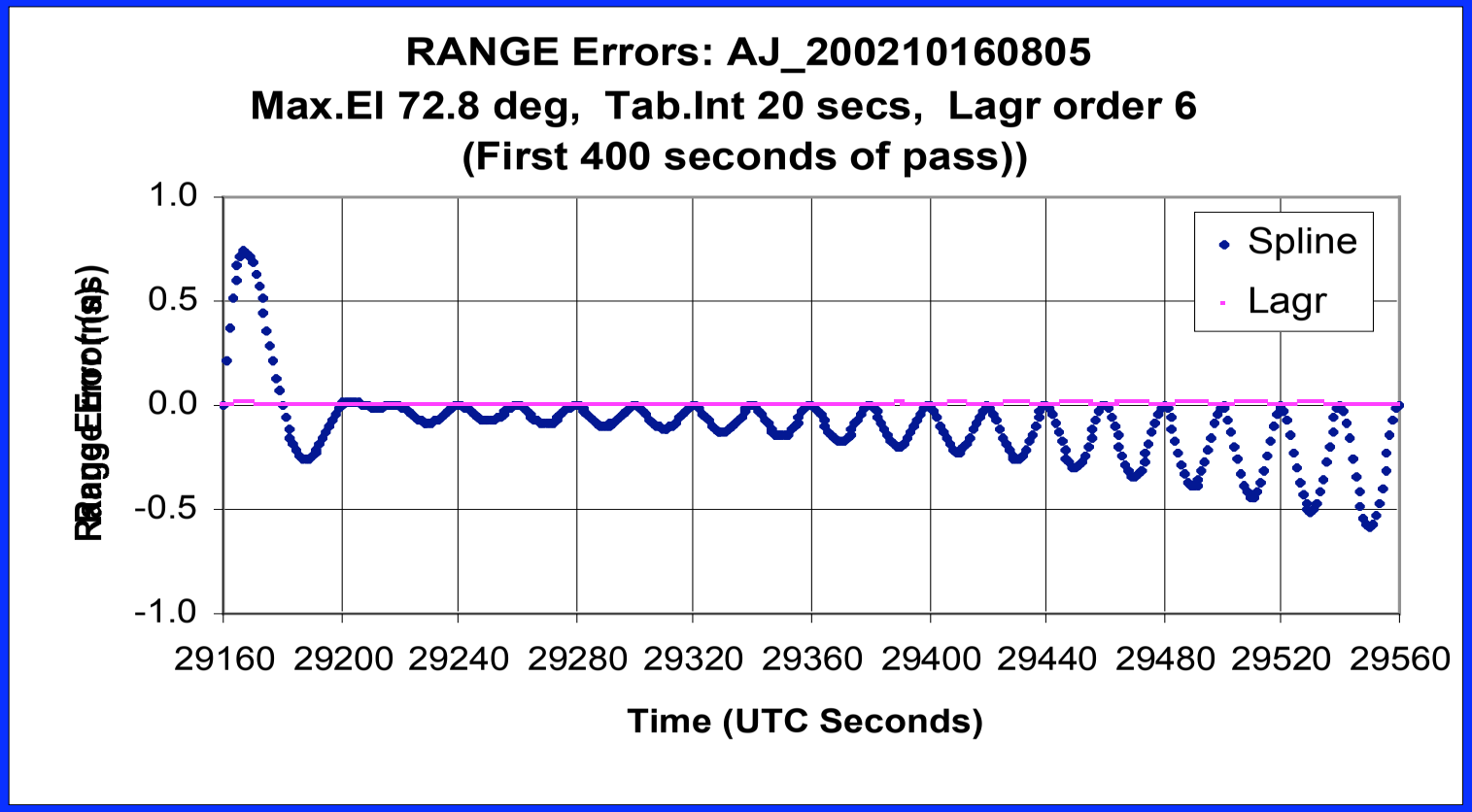

Warm regards from John Luck: The interpolation errors of the IRVs are propergating to the NP if things are not handled carefully

I. Geometrical Error Sources

Geometrical Error Sources

- Target structure (mechanical)
- Beam path through telescope (stability)

Example

Field of view is limiting the measurements to near axis ranges only

For a target 6m away from the focus it causes a sub-μm range offset

Conclusion

- These errors are typically small

II. Electronical Error Sources

Calibration Basics

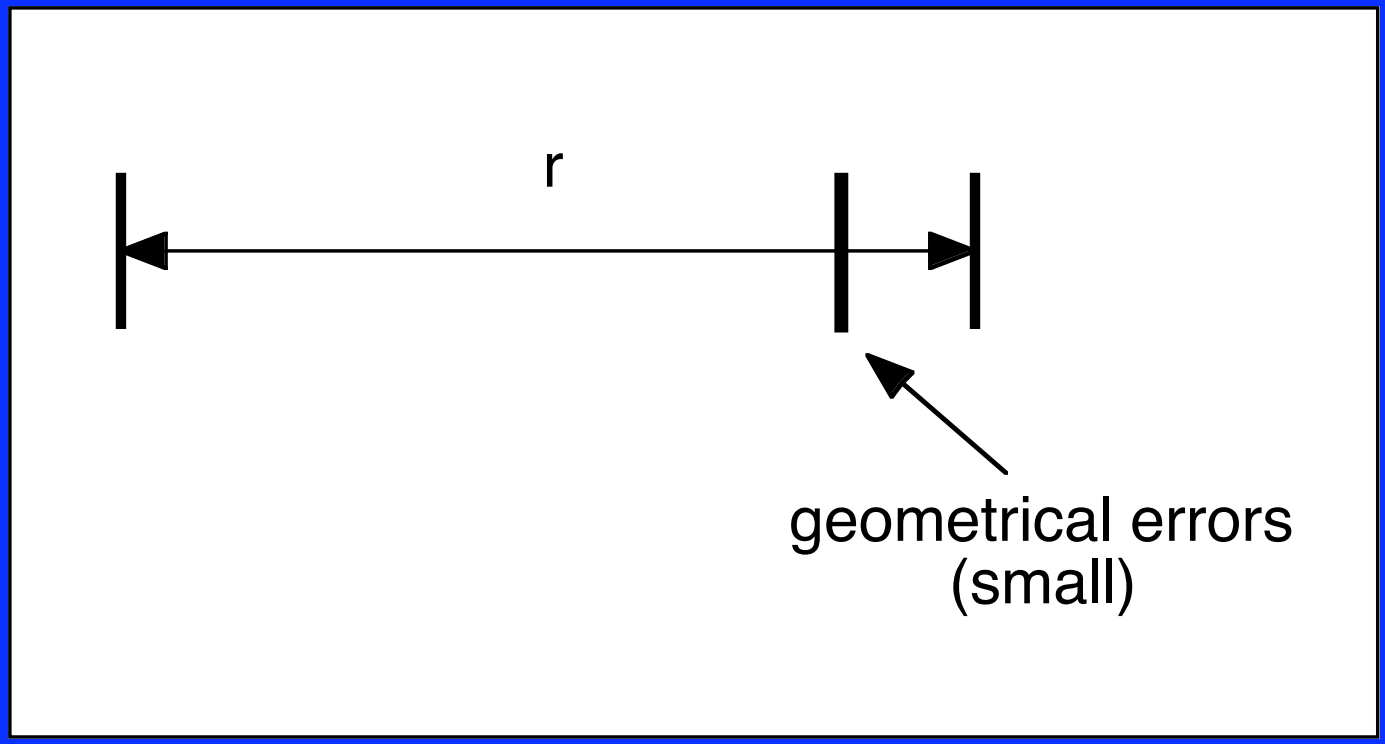

... as soon as we try to measure things they become more complicated

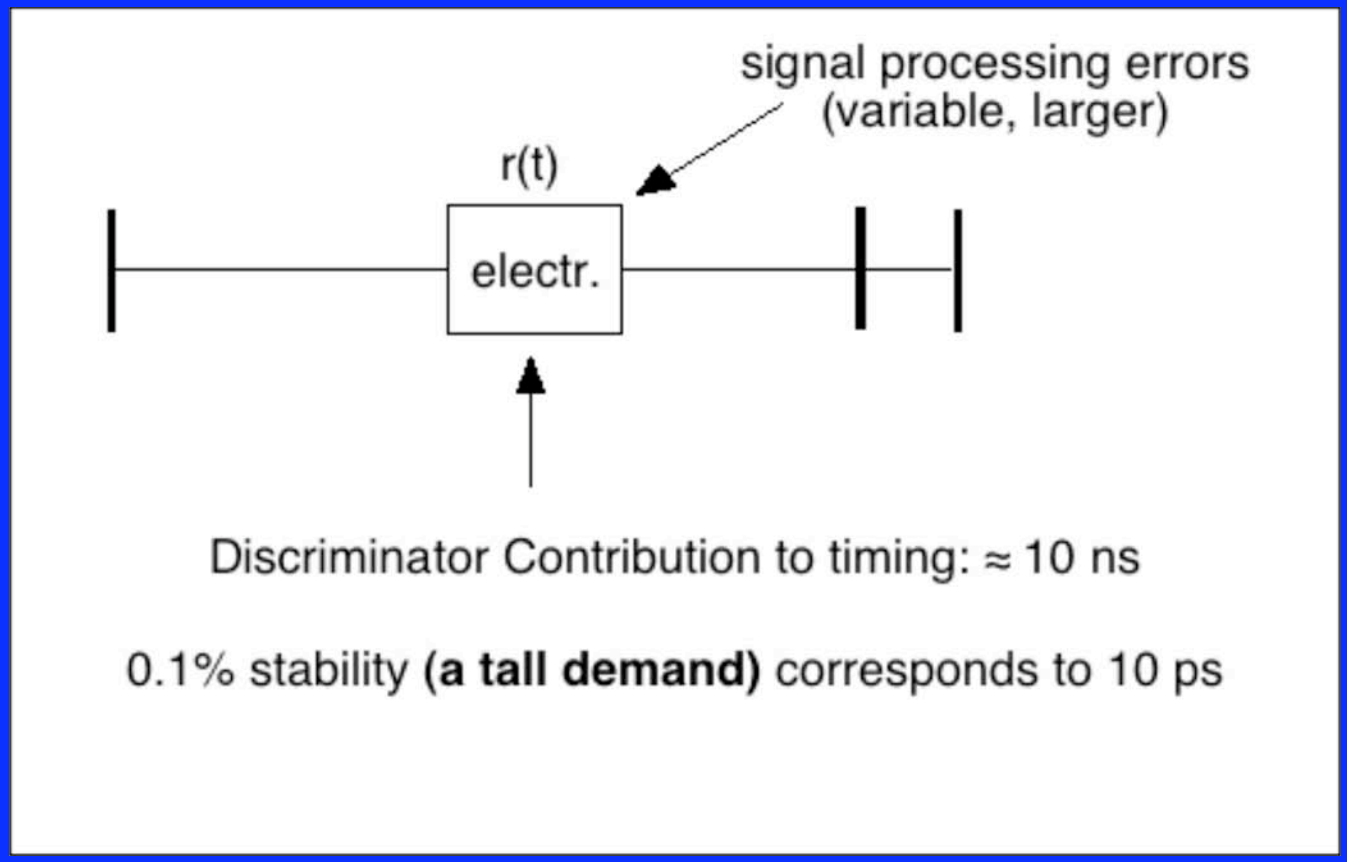

H-Maser Correction in VLBI

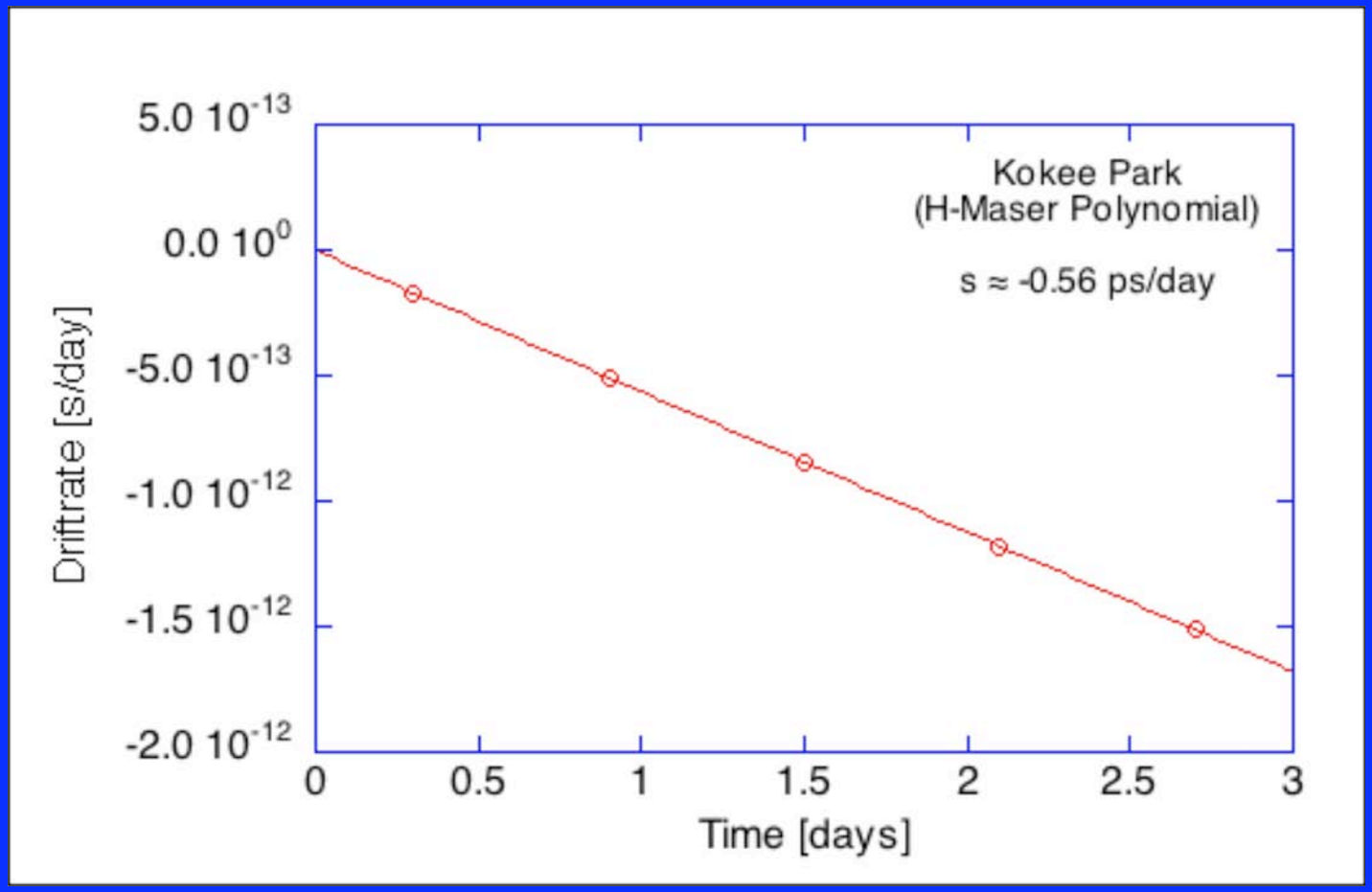

Interpretation

The intrinsic high clock accuracy is not accessible by the electronic hardware

Identification of Issues

- Electronic circuits cause time varying insertion delays
- Delays show temperature dependence
- Delays show bandwidth dependence
- Delays show impedance matching issues
- Delays show signal level related issues (supply voltage stability, ground reference)

Power Level Stability

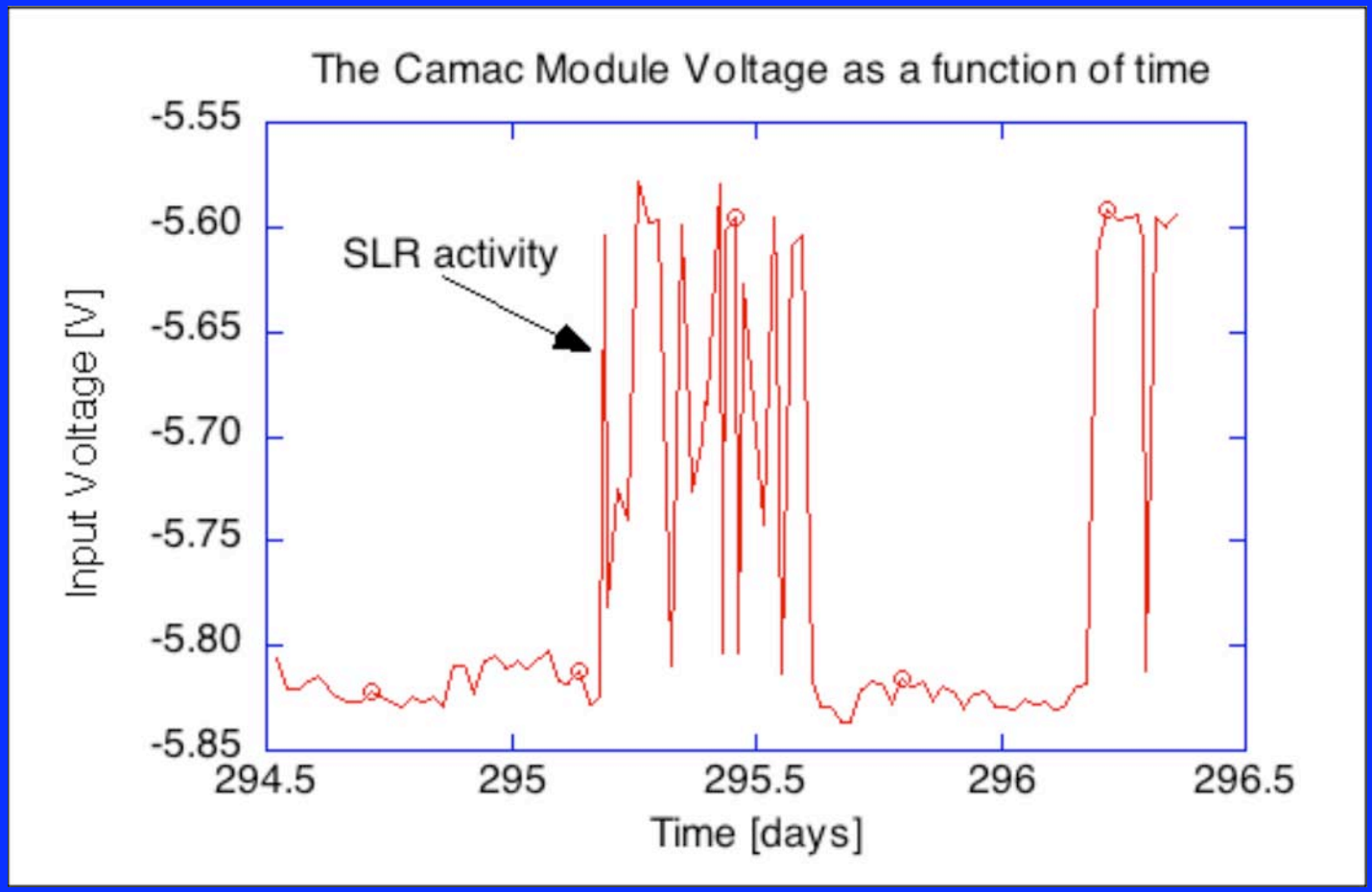

Trigger Threshold Stability

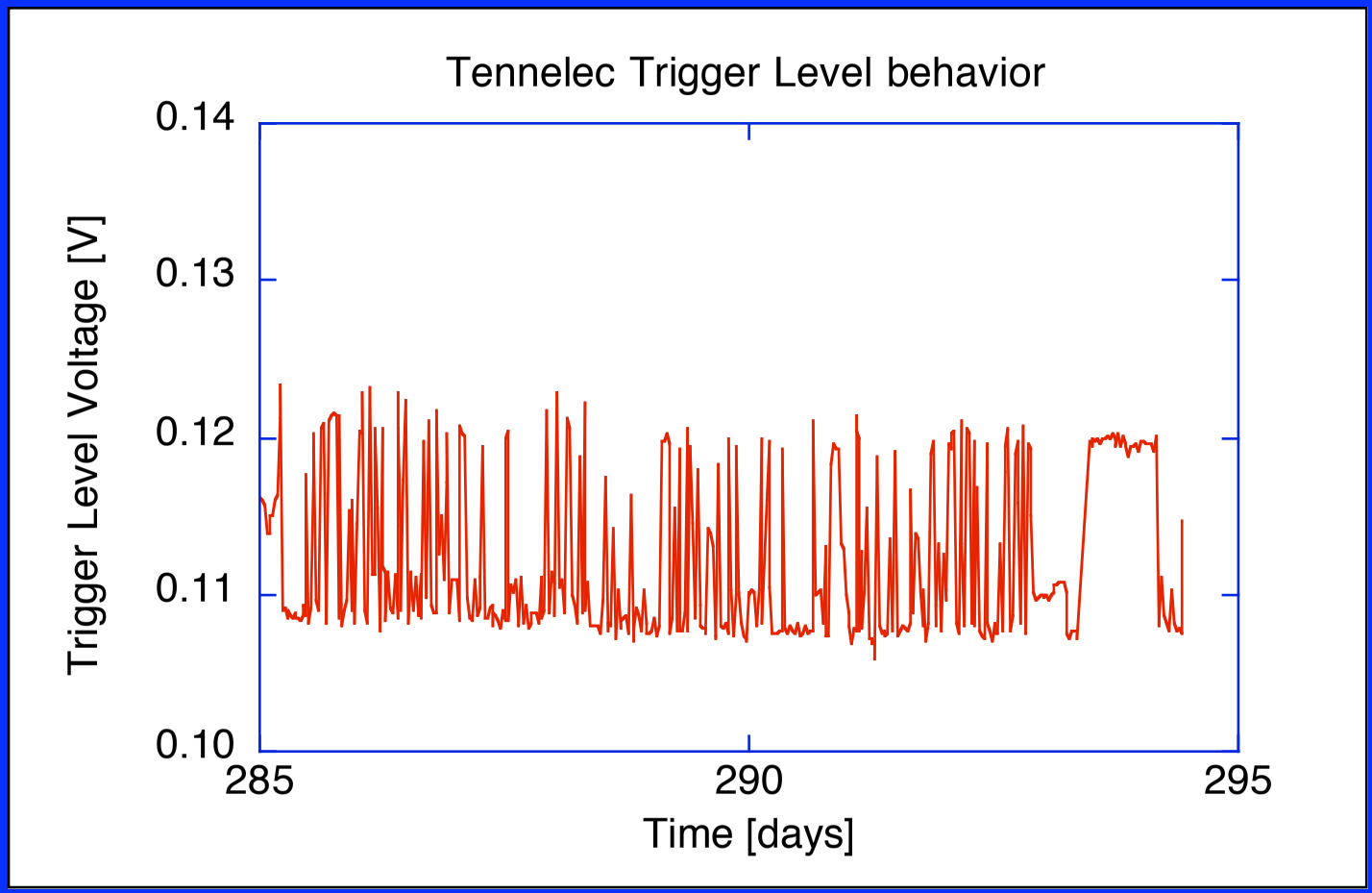

Impedance matching

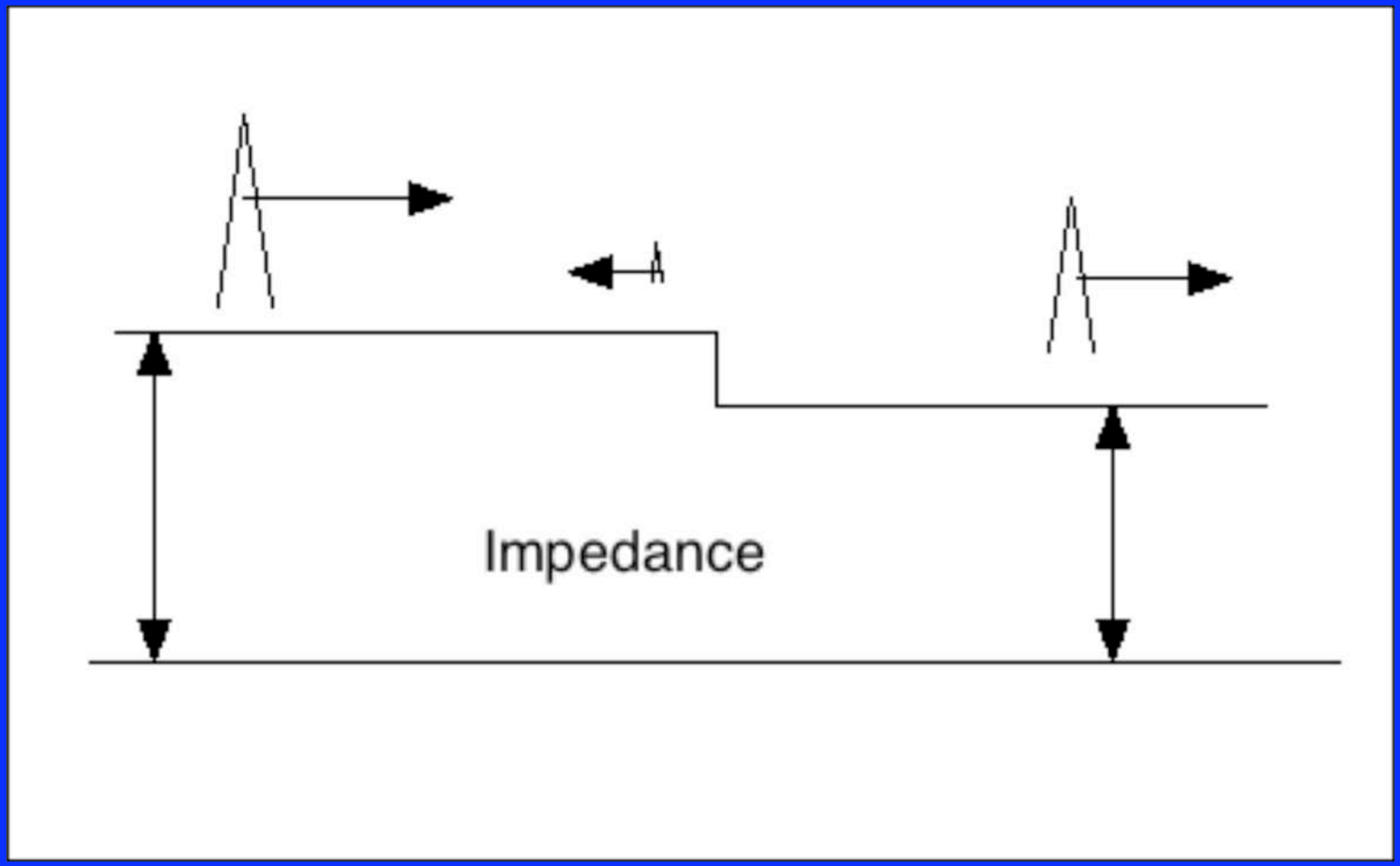

III. Optical Error Sources

Optical Error Sources

- Wavefront distortions
- Higher order spatial laser modes
- Laser backreflections and saturation effects (shared aperture)

IV. Solutions

System Design Symmetry

- use the same electronic components as much as possible or at least twin chips
- carefully adjust signal levels and pulse shapes for both calibration and ranging
- avoid timewalk

Redundancy!!!

- Co-Locations were used in the past (costly)
- Traveling barometer campaigns adjust the meteorology issues
- Several (electronic) subsystems are operated in parallel
- Counter Cluster (Graz) was the first step
- Portable Calibration Standard (flexible, cheap)

Access to a number of errors

- epoch and time interval timing
- time and frequency reference
- data aquisition, filtering and processing
- calibration scheme and ground survey
- operational procedures (habits)
- rf-interference, ground reference

Basic Concept

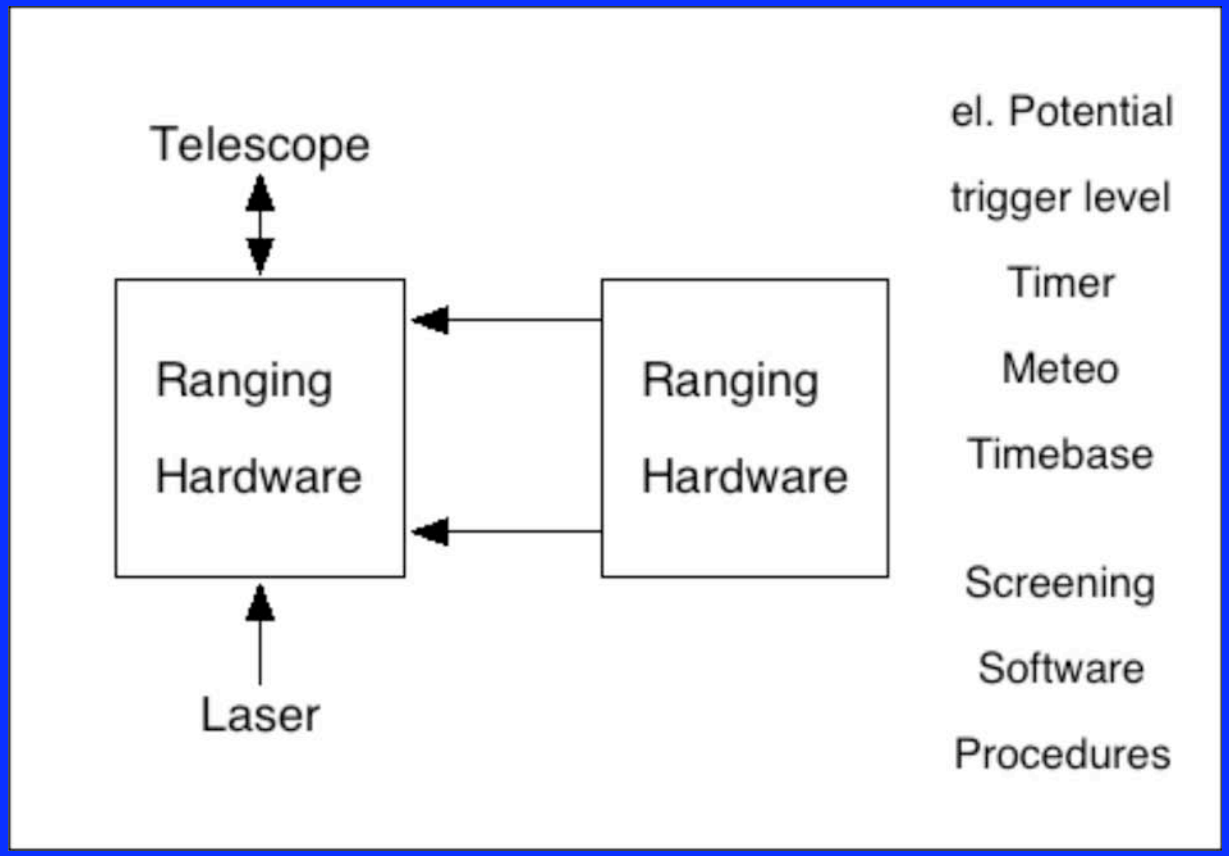

Inter-System Redundancy

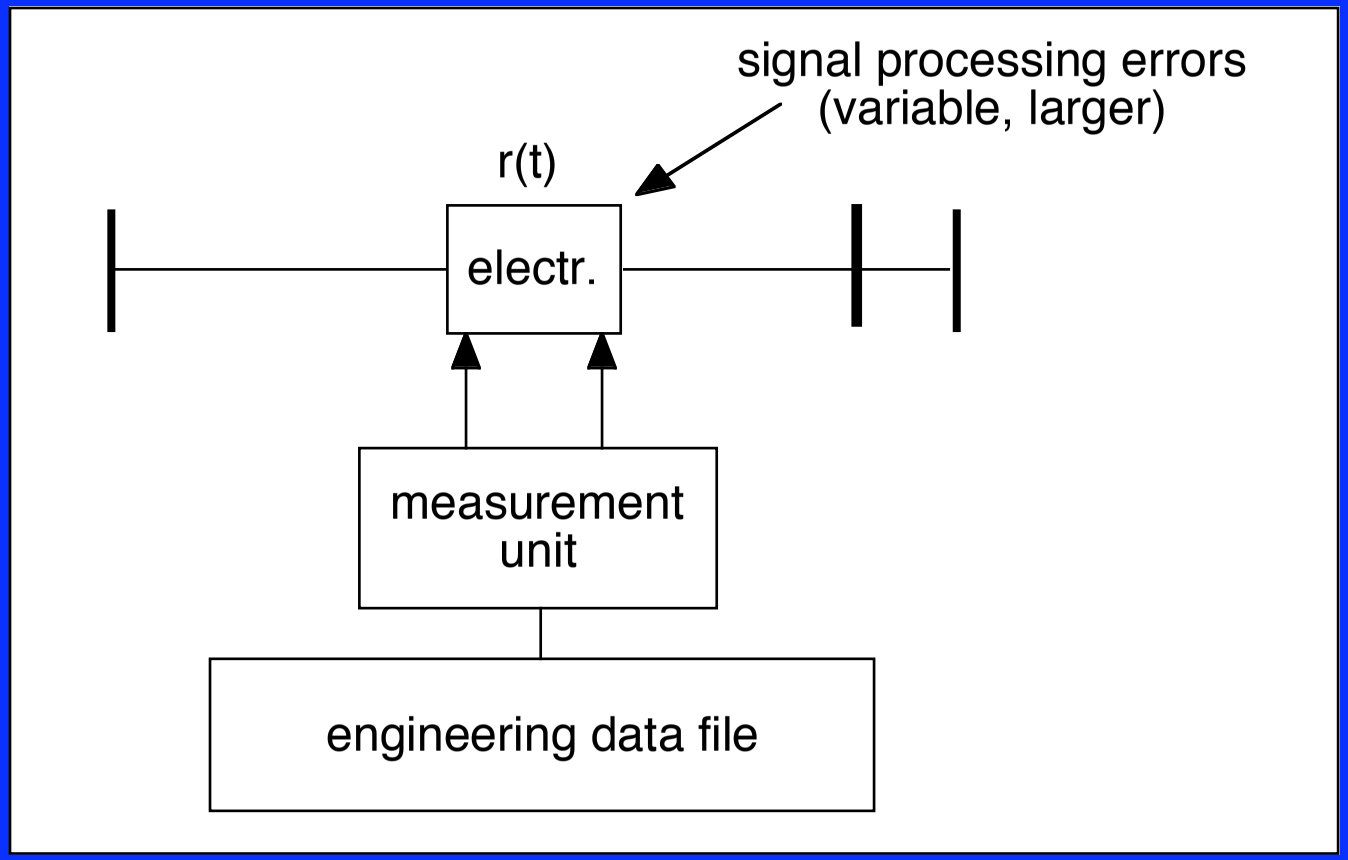

Satellite Laser Ranging Machine Bias Reduction Procedures

Toward Millimeter Accuracy
Vademecum

Karel Hamal, Ivan Prochazka
Czech Technical University, Prague, Czech Republic

SLR Machine Bias Reduction Procedure

Goals

- SLR systems bias reduction
- inter-comparison and standardization of SLR systems
- Portable Calibration Standard for Satellite Laser Ranging machine diagnostics
  identification of error sources due to :
  - epoch and time interval timing
  - epoch and frequency reference
  - data acquisition, filtering and processing
  - calibration scheme and ground survey
  - operational procedures
  - radio frequency interference
  - other sources

SLR Machine Bias Reduction Procedure

Portable Calibration Standard Philosophy

- high degree of **redundancy**
- based on top **quality and certified** hardware
- **independent** on SLR under test
  - signal processing and cabling
  - grounding, power line, RF shielding
  - timing (time interval, epoch)
  - calibration targets and ground survey
  - data acquisition and data processing
  - staff
- operated **in parallel to existing SLR**
- **easy to re-locate** (personal luggage)

SLR Machine Bias Reduction Procedure

PORTABLE CALIBRATION STANDARD

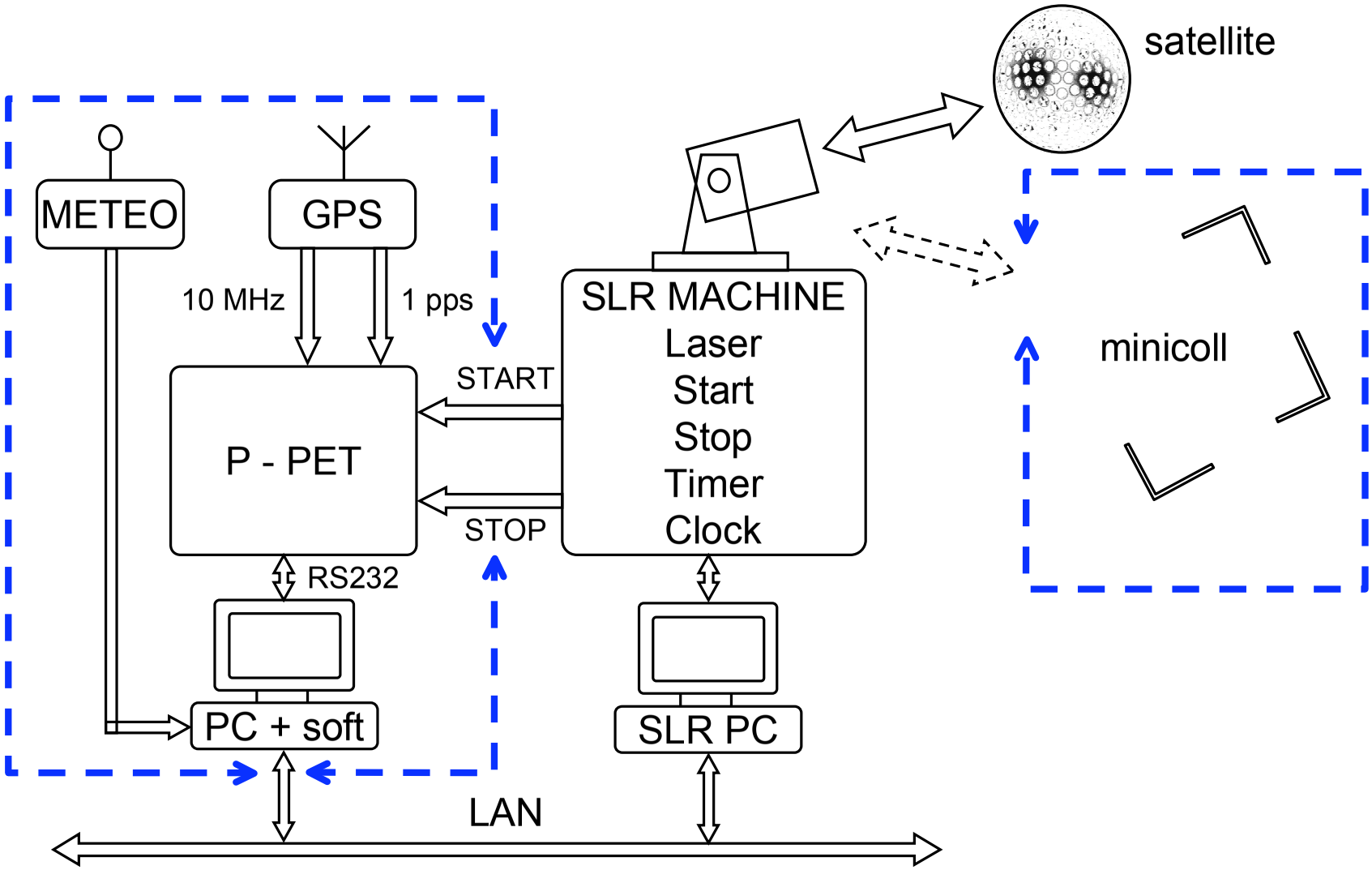

K. Hamal, I.Prochazka, Prague, May 2003

SLR Machine Bias Reduction Procedure

Portable - Picosecond Event Timer P-PET

BLOCK SCHEME

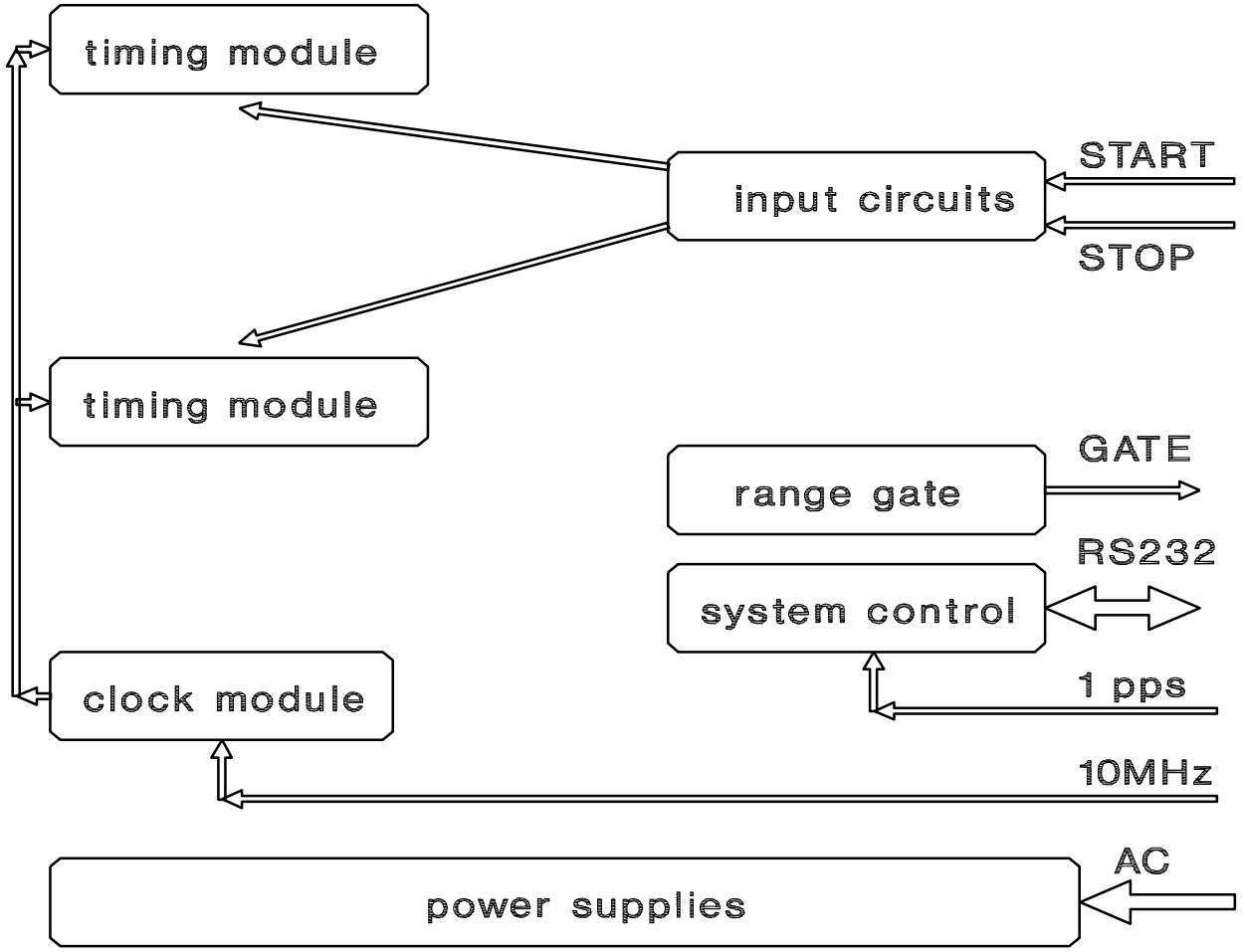

K.Hamal,I.Prochazka, EurOpto, London 1997

K. Hamal, I.Prochazka, Prague, May 2003

SLR Machine Bias Reduction Procedure

Pico Event Timer
Portable Calibration Standard

K. Hamal, I.Prochazka, Prague, May 2003

SLR Machine Bias Reduction Procedure

Ground Target Calibration

- “mini-coll” concept,
- use minimum 3 ground targets,
- distances < 100 meters,
  (difficulties to model horizontal atm. correction > 100m)
- different azimuths,
- “zero paralax” hollow retro reflectors (2D)
- targets reference points surveyed down to 1 mm accuracy 3 D
- the system internal delays evaluated by calibration ranging to different targets indicate the calibration accuracy and the calibration value confidence.
- the survey and calibration procedure has to be tuned until the internal delay consistency is on a mm level

SLR Machine Bias Reduction Procedure

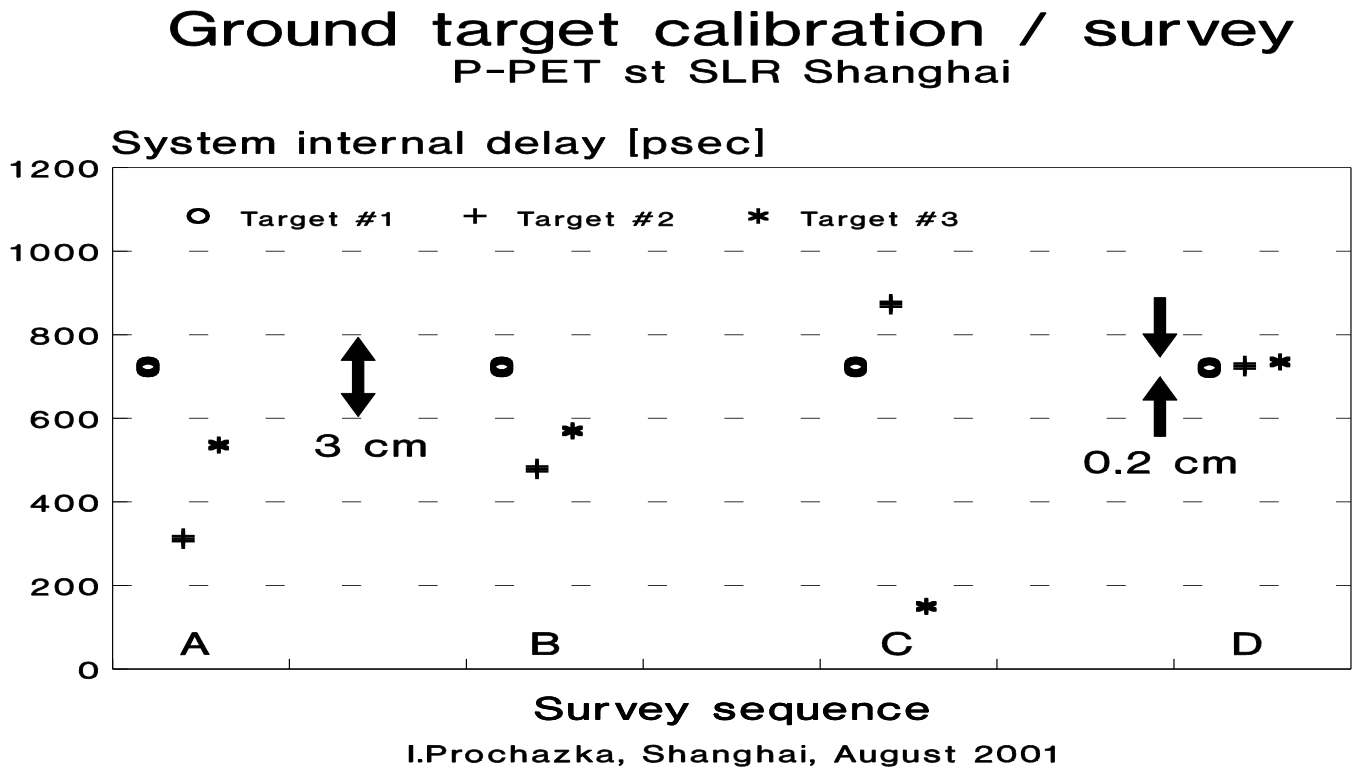

The 3 cal. targets /hollow 2D retros/ have been re-surveyed and the calibration procedure tuned until the the system internal delay value consistency of 2 mm has been achieved.
The 2mm level was a limit for the system at that time.

K. Hamal, I.Prochazka, Prague, May 2003

SLR Time Bias identification

- The PCS is operated in parallel to the SLR system under test,
- the corresponding pairs of SLR results are identified,
- the time bias is evaluated as a difference of corresponding epochs on a shot by shot basis,
- the time bias per pass is evaluated as a an arithmetic average,

SLR Machine Bias Reduction Procedure

Time Bias , PCS in Changchun

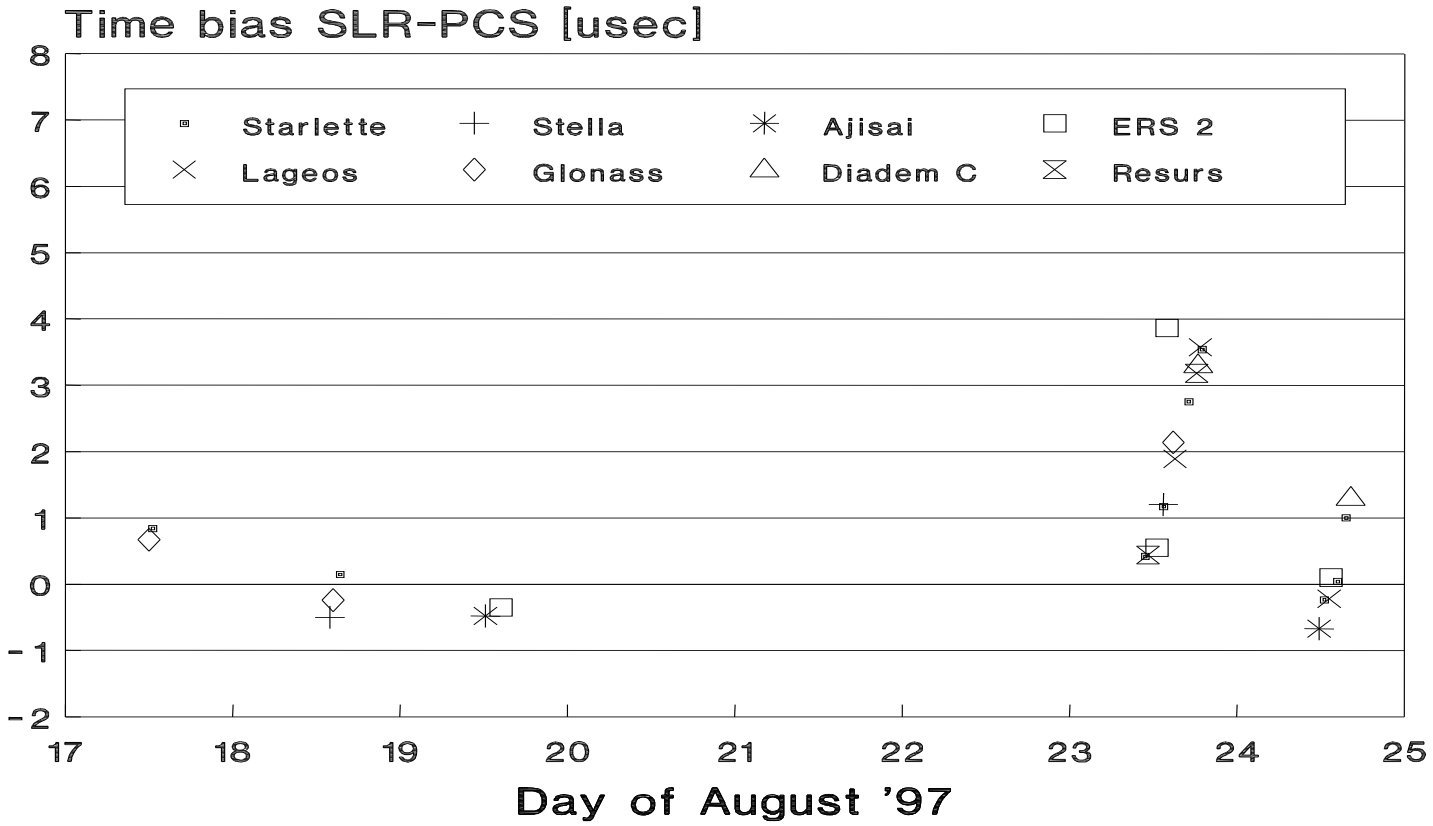

The SLR used a wrong frequency source (the slope),
the SLR time base has been synchronized only once per day
the time bias is target independent

K. Hamal, I.Prochazka, Prague, May 2003

SLR Range Bias Identification

- The PCS is operated in parallel to the SLR system under test,
- the corresponding pairs of SLR results are identified,
- the range bias is evaluated as a difference of corresponding range readings on a shot by shot basis,
- on a shot by shot basis, the range bias versus range identifies the time of flight linearity
- the range bias per pass is evaluated as a an arithmetic average, it characterizes the range bias of the SLR system vers. PCS

SLR Machine Bias Reduction Procedure

RANGING COUNTERS COMPARISON TO P-PET

P. Gibs, Herstmonceux, 2002

- Shown here is a summary plot of all the devices.

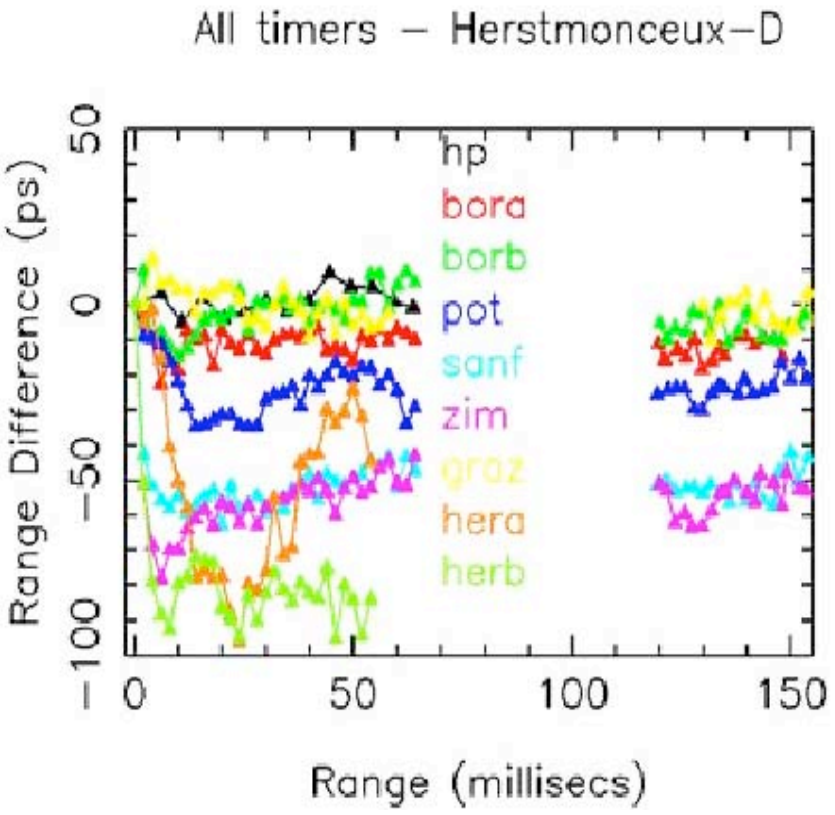

K. Hamal, I.Prochazka, Prague, May 2003

SLR Machine Bias Reduction Procedure

SR620 / P-PET Counter Linearity

Potsdam, 2001, LAGEOS pass

50 ps / div **Counter s/n 1014 (in routine use)**

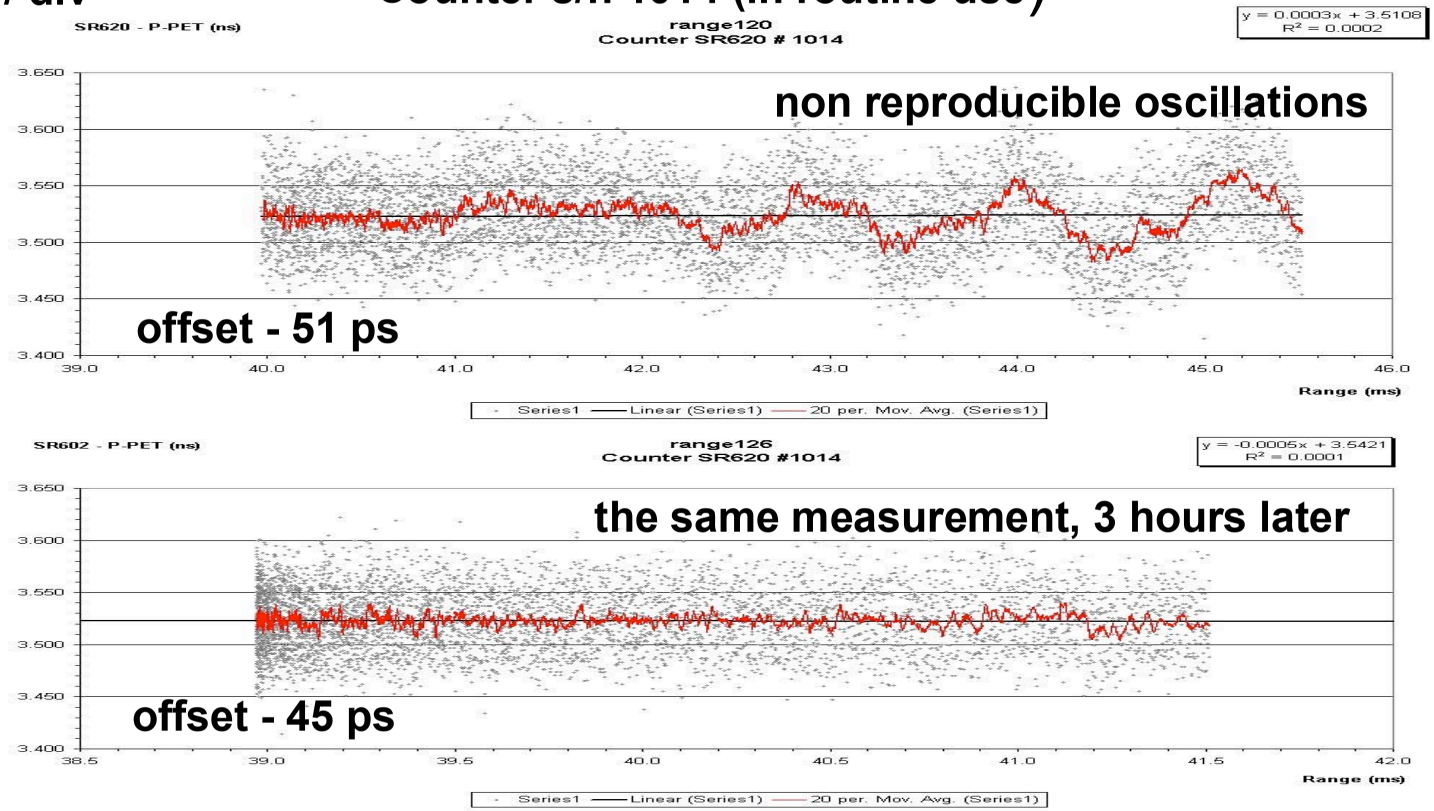

L. Grunwald, R.Neubert, H.Fischer, H.Pino, Potsdam, 2001

K. Hamal, I.Prochazka, Prague, May 2003

SLR Machine Bias Reduction Procedure

SR620 / P-PET Counter Linearity

Potsdam, 2001, Short times

Counter s/n 1014 (in routine use)

10 ps / div

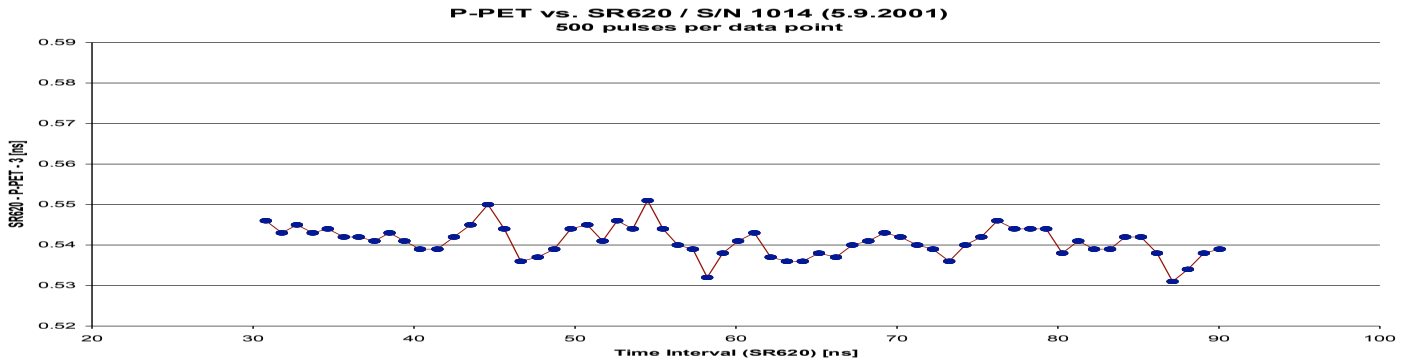

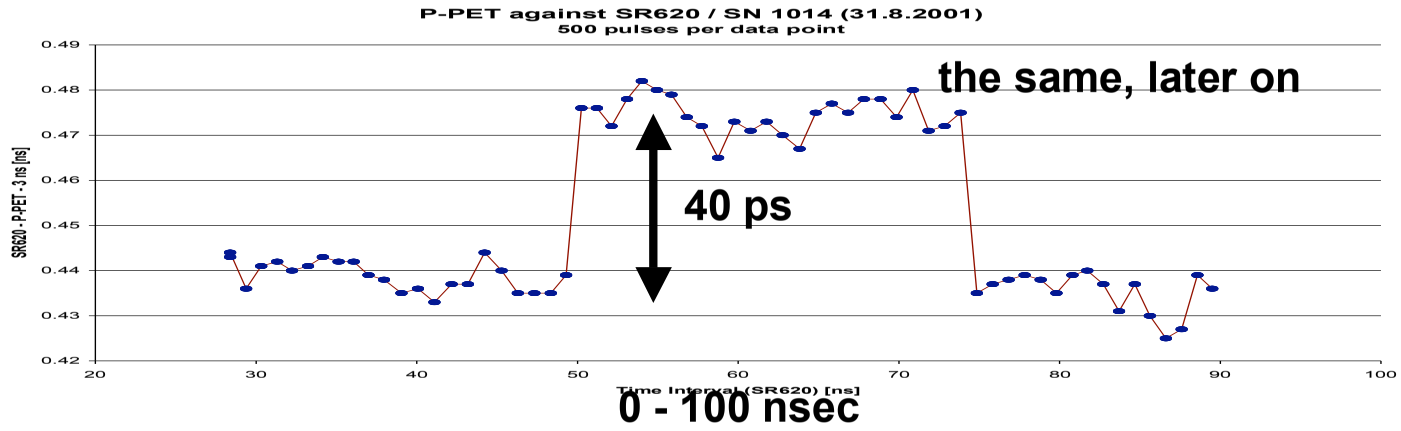

0 - 100 nsec

L. Grunwald, R.Neubert, H.Fischer, H.Pino, Potsdam, 2001

K. Hamal, I.Prochazka, Prague, May 2003

SLR Machine Bias Reduction Procedure

Range and Time Biases,Shanghai 2001

Satellite	T rms(mm)	SLR rms(mm)	Time bias(us)	Rng. bias(ns)	Sta

K. Hamal, I.Prochazka, Prague, May 2003

Time and Temperature Stability, SLR Graz

- The PCS was operated in parallel to the SLR system under test,
- the temporal and temperature drifts of the PCS are below 1 ps,
- the ground target calibration was repeatedly completed within one hour,
- the thick curve corresponds to the stability (+/- 1mm) of the SLR ranging chain excluding the time of flight instrument (counter cluster),
- the thin curve corresponds to the entire SLR system temporal stability (+/- 2 mm at that configuration)

SLR Machine Bias Reduction Procedure

P-PET in Graz, Calibration Stability

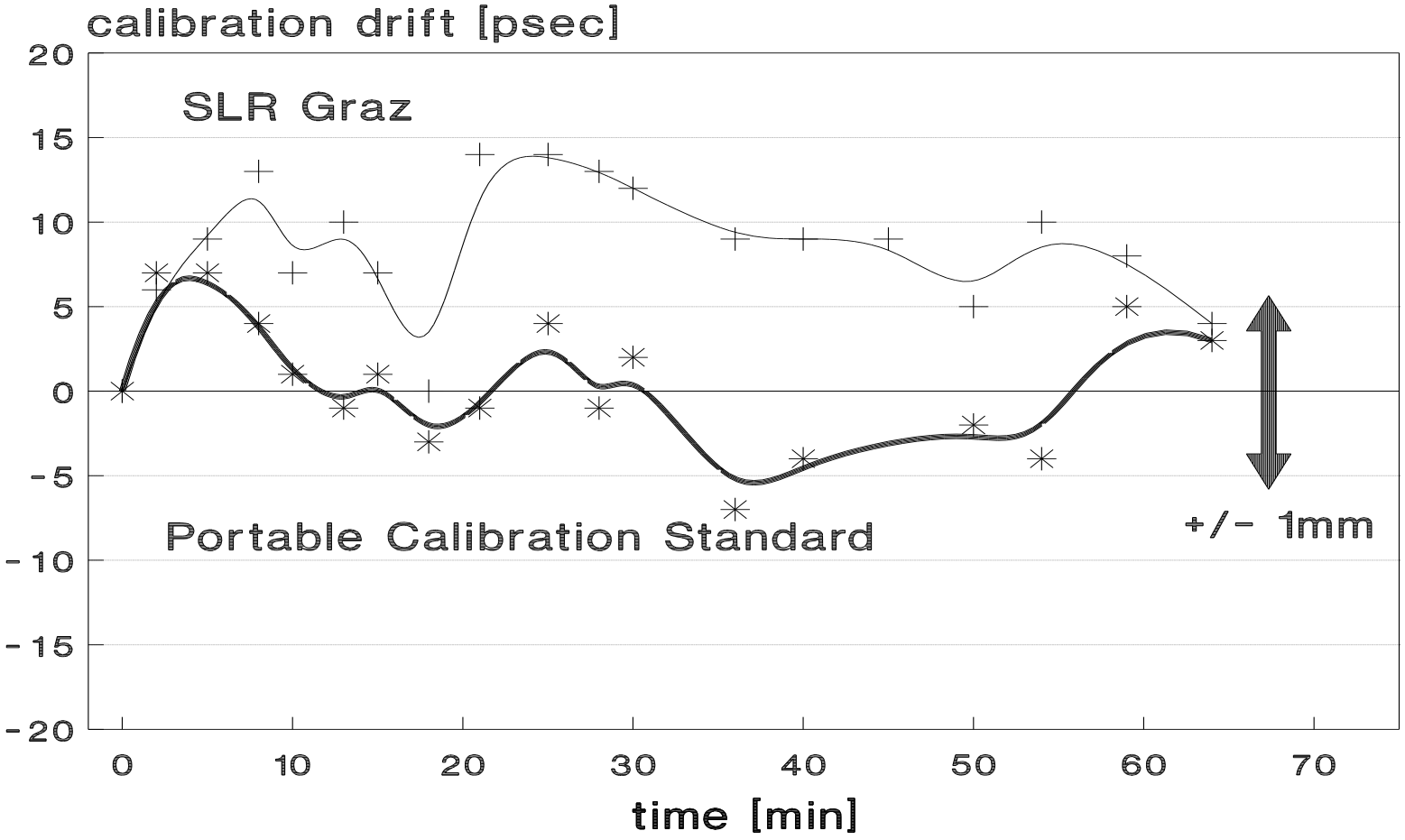

Kirchner,Koidl,Hamal,Prochazka,Graz 97

K. Hamal, I.Prochazka, Prague, May 2003

SLR Machine Bias Reduction Procedure

SLR Precision Increase

- operated **in parallel to existing SLR**
- high degree of **redundancy**
- **independent** on SLR under test
  - signal processing and cabling
  - grounding, power line, RF shielding
  - timing (time interval, epoch)
  - calibration targets and ground survey
  - data acquisition and data processing
  - operators and habits
- high quality instruments (P-PET, Meteo, Epoch & Freq.)
  - => high precision SLR data acquired on the PCS
  - => identification of “problem areas” and improvement os SLR

SLR Machine Bias Reduction Procedure

Zimmerwald, 24hour Mission,May 27-28,1998
Two wavelength ranging

Original station setup 150 psec

After system re-cabling and detectors tuning

SLR system	120 psec
P-PET timing	76 psec @ red
	58 psec @ blue

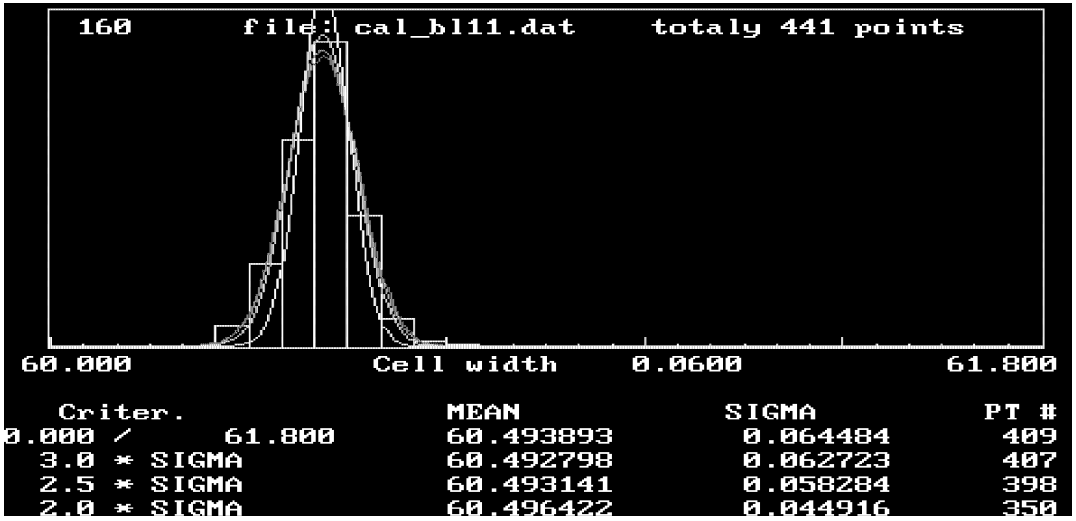

K. Hamal, I.Prochazka, Prague, May 2003

SLR Machine Bias Reduction Procedure

Shanghai SLR, Lageos, Aug. 19,2001

SLR timing 13.5 mm RMS

PCS-PET timing 7.0 mm RMS

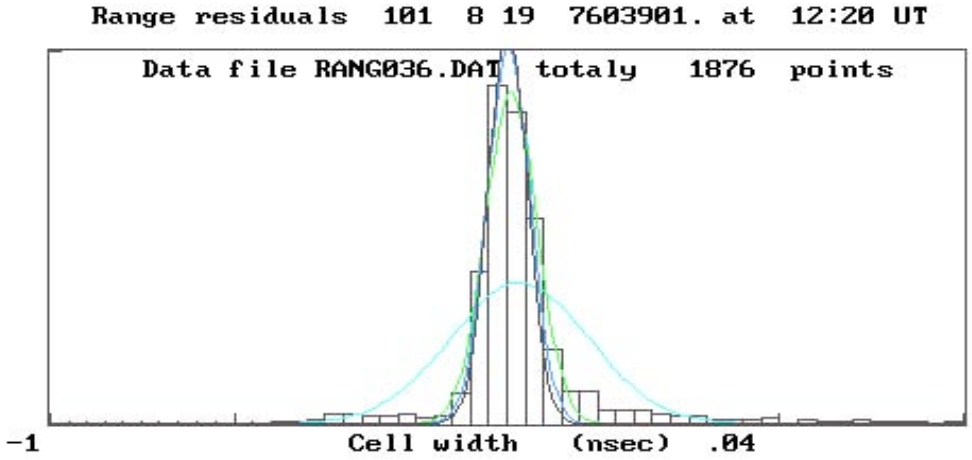

	Criter.		MEAN	SIGMA	PT #
Limits	-1.000 /	1.000	0.027430	0.151741	1315
	3 * SIGMA		0.007832	0.056696	1153
	2.5*SIGMA		0.002507	0.047051	1093
	2.2*SIGMA		0.000586	0.042044	1041

K. Hamal, I.Prochazka, Prague, May 2003

SLR Machine Bias Reduction Procedure

PCS-PET Mission, TIGO, 1998

Two wavelength ranging

4 x SR620

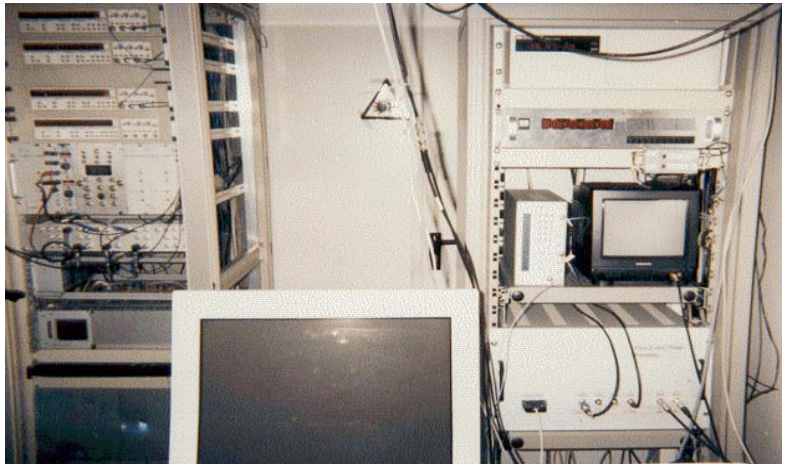

P-PET

SR620 timing	infrared	120 psec
	blue	95 psec
P-PET timing	infrared	75 psec
	blue	45 psec

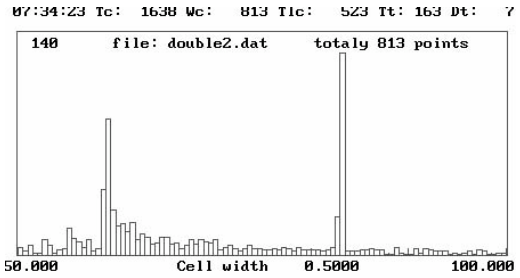

K. Hamal, I.Prochazka, Prague, May 2003

SLR Machine Bias Reduction Procedure

PCS Capabilities - Comparison

atic error source	collocation	Portable Calibration Standard	frequency and epoch	yes	yes	mount e

Conclusion

- Portable Calibration Standard based on a Pico Event Timer is a powerful tool to identify systematic error sources in the SLR “ranging machine” on the mm scale

- the entire system is compact, easy to transport fast to install and user friendly to operate,
  the calibration mission can be accomplished within one week time slot,

- P-PET mission to SLR sites did trigger several projects
  - WLRS (1998), TIGO(1999), Graz (2000)
    timing systems upgrade
  - European millimeter SLR joint activity (2002),
  - Herstmonceux Workshop (2002)

NASA SLR System Calibration Techniques

External Calibrations to Established, Stable and Formally Surveyed Ground Targets

- 90 minute maximum cycle time per tracking scenario – *(Offsetting potential diurnal effect and systematic drifts)*
- Calibration Target Ranges < 300M
- Calibration Pier design – concrete and metal reinforced for long term stability
- Optically calibrated corner cubes – optical transit path measured & accounted for in calibration range
- Pre & Post Calibrations to operational ground target ~ 1000 Shots
- Receive amplitudes maintained within dynamic range of the Constant Fraction Discriminator for Pre and Post Calibration AND operational satellite tracking
- Ground Test Calibrations to multiple targets also used as diagnostic tool

International Laser Ranging Service

Honeywell

NASA SLR System Calibration

Station	Target	Azimuth	Elevation Deg.	Range m
Monument Peak USA	**A**	**103.504**	**4.093**	**187.003**
	B	177.427	-1.089	1955.268
	C	198.854	-0.433	107.371
Yarragadee Australia	A	16.856	0.176	3116.742
	B	**14.778**	**-1.154**	**150.425**
	C	12.336	-1.376	100.419
Hartebeesthoek South Africa	A	3.76	0.467	150.246
	B	48.457	2.218	96.882
	C	126.752	1.86	100.642
	D	229.49	-0.86	131.15
	E	**278.626**	**-2.344**	**198.664**
	I	104.547	3.048	141.055
Greenbelt USA	A	65.189	-3.141	106.673
	B	95.515	-1.737	174.833
	C	**105.165**	**-1.671**	**170.526**

Station	Target	Azimuth	Elevation Deg.	Range m
Tahiti French Polynesia	A	42.845	6.55	171.262
	B	**138.854**	**4.424**	**263.234**
	C	332.272	-1.526	122.695
Arequipa Peru	A	10.23	-1.81	105.949
	B	**48.167**	**-1.265**	**105.978**
	C	132.063	0.818	423.29
	D	205.412	-3.029	51.438
	E	46.928	5.073	870
Mt. Haleakala Hawaii	**A**	**116.718**	**-8.732**	**39.129**
	B	114.999	-8.709	1109.635
	C	85.511	-1.316	602.099
	D	116.718	-8.732	39.129

** McDonald, USA – Performs internal Calibrations*

= *Operational Target*

Monument Peak Calibration RMS

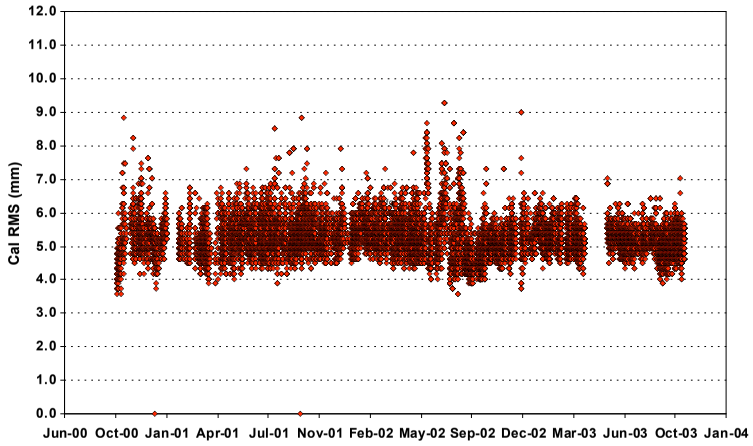

Nominal Combined Cal. RMS 4.0mm – 6.0mm

Monument Peak Calibration Shifts

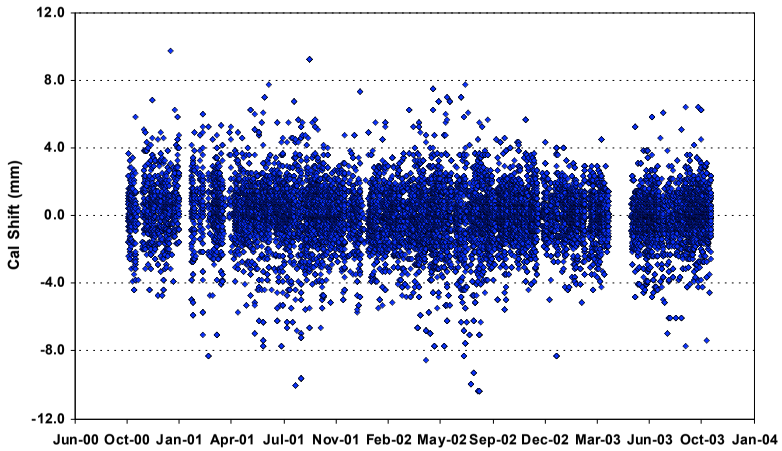

Nominal Pre to Post Calibration Shift <4.0mm

International Laser Ranging Service

Honeywell

Honeywell Technology Solutions Inc

Monument Peak (Moblas-4) Schedule for 10/22/03

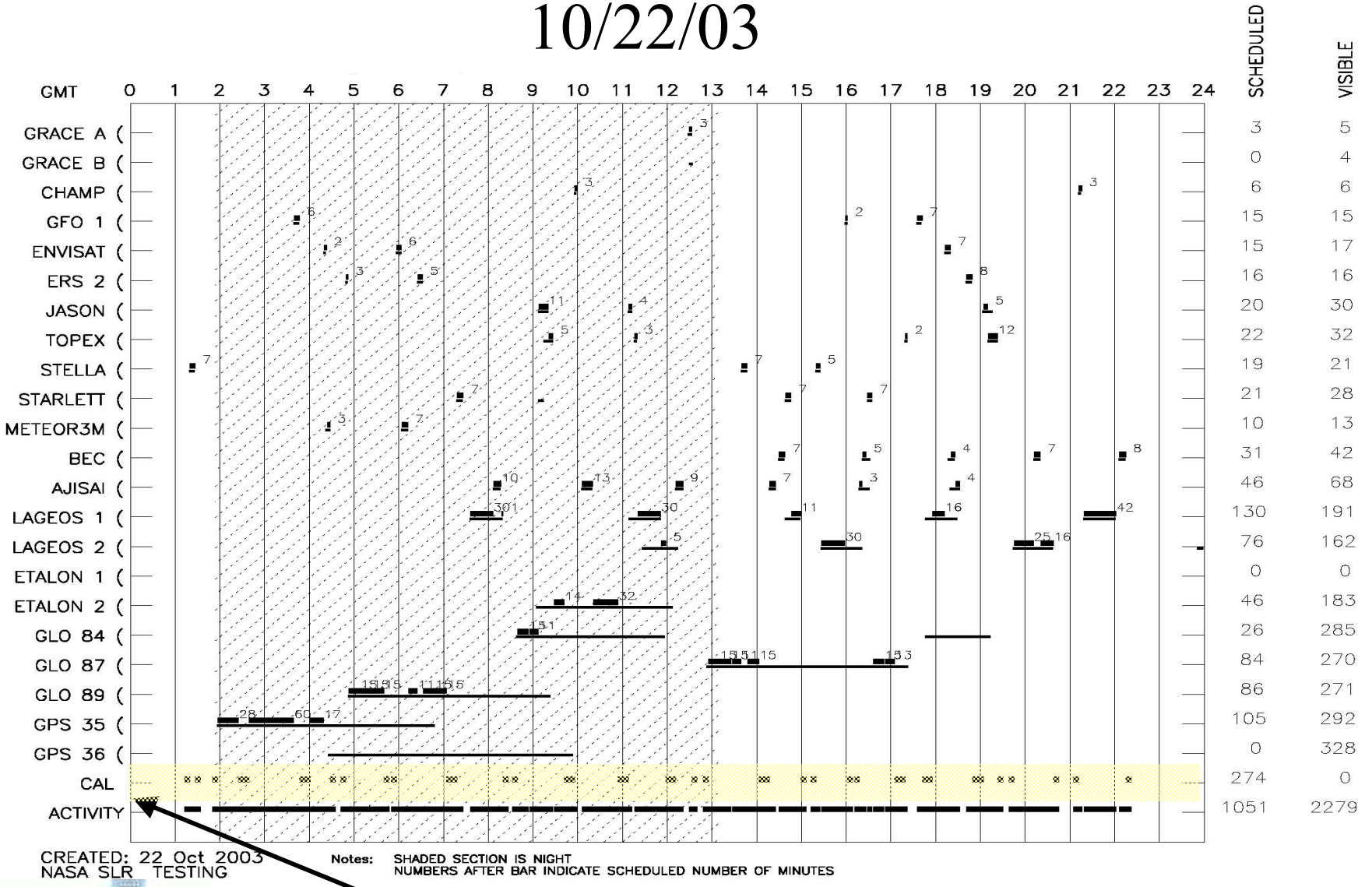

Scheduled Calibrations

International Laser Ranging Service

Honeywell

Honeywell Technology Solutions Inc

NASA SLR Meteorological Measurement Sensor (MET3) Calibration Technique

Pressure, Temperature, and Humidity Measurement

- Two Year Calibration Cycle:
  - ✓Station's unit replaced with a manufacturer calibrated sensor package
  - ✓Pre/Post installation calibration reports examined for anomalies
  - ✓Calibration reports will be maintained in a database
  - ✓NIST trace-ability maintained (Pressure Sensor)
- One Year Preventive Maintenance Cycle

Pressure – Accuracy: ± 0.08 mBar, Stability: < 0.1 mBar per year

Temperature – Accuracy: □ 0.5 Degree C, Stability: Better than 0.1 Degree C

Relative Humidity – Accuracy: ± 2% RH (@ 25 Degree C), Stability: Better than 1% per year

Future Improvements – MET3A, better performing pressure transducer, higher accuracy temperature readings, faster humidity saturation recovery time

International Laser Ranging Service

Honeywell

Honeywell Technology Solutions Inc

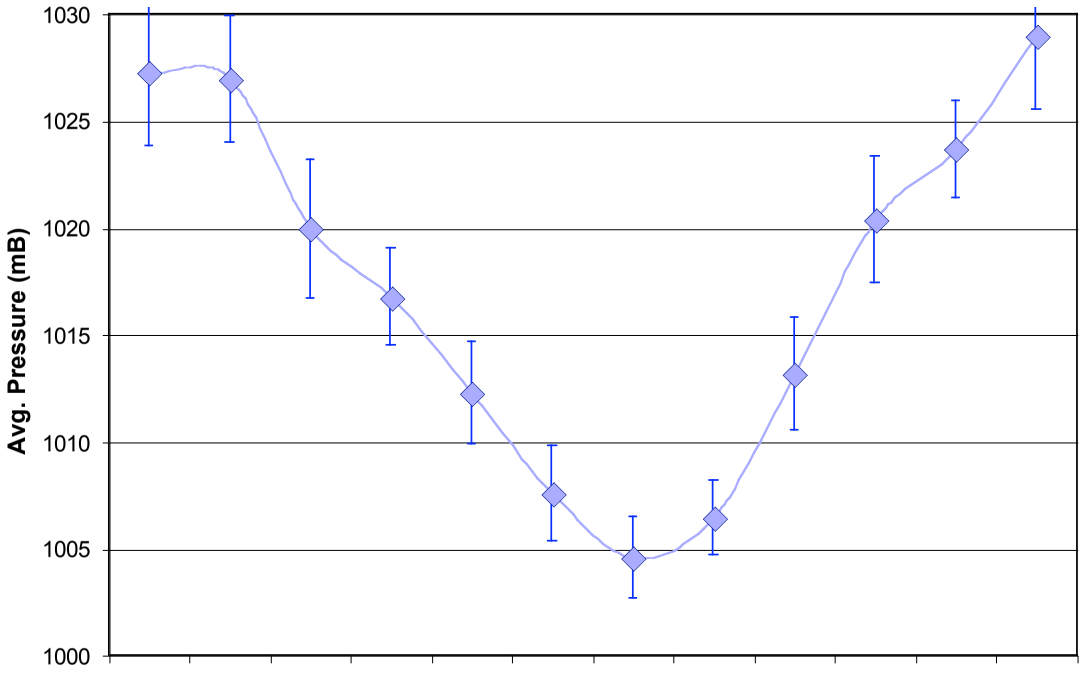

The effect of a barometer change or re-calibration

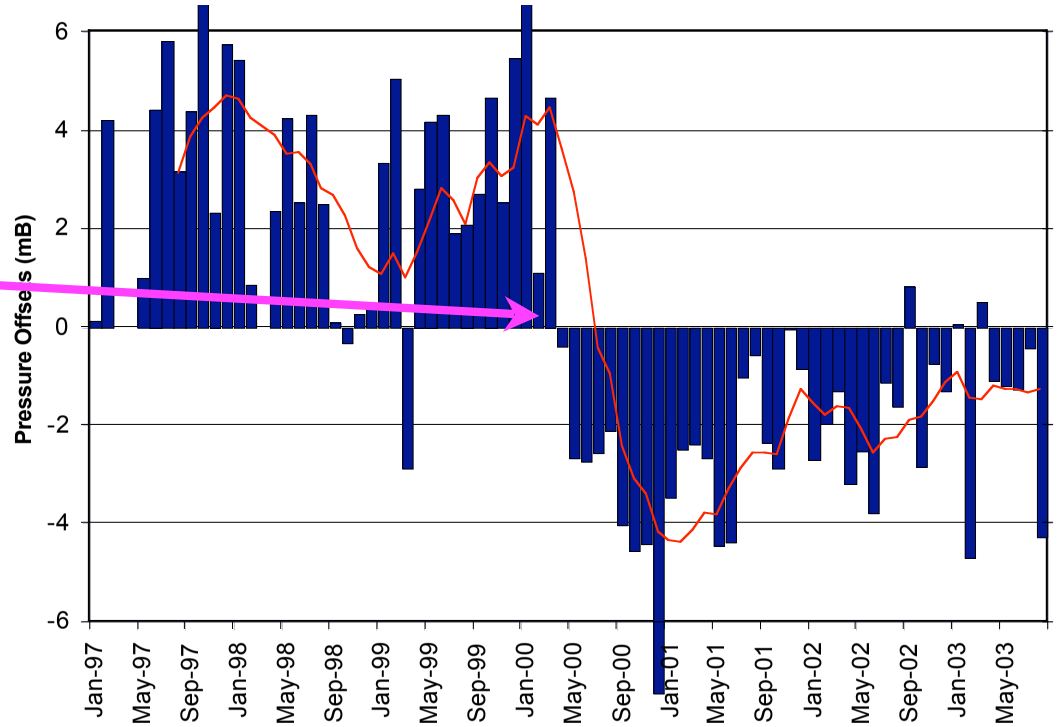

Session 8

Refraction Modeling

Stefan Riepl, Erricos Pavlis

Some remarks on refractivity, raytracing and numerical weather models

Rüdiger Haas[1] and Stefan Riepel[2]

(1) Onsala Rymdobservatorium, Chalmers Tekniska Högskola, Göteborg (Sweden)

(2) Observatorio Tigo, Universidad de Concepcion, Concepcion (Chile)

Background (1)

- Refractive effects impact space geodetic measurements (optical and radio regime).
- The usual approach is to estimate ”zenith wet path delays” from the observational data themselves.
- This approach uses apriori mapping functions and the apriori modelling of dry/wet delays.

Background (2)

- The approach is quite good, but still a source of uncertainty, e.g. due to:

  a) Atmospheric inhomogenities.

  b) The strong correlation between station height, GM and zenith delays in SLR.

- Thus, a new modeling of zenith path delays is needed and should be developed.

Questions – Ideas

- Could apriori path delays (dry, wet) be modeled via raytracing through dense atmospheric fields?
- Could numerical weather models be used for this approach?
- Could atmospheric gradients be handeled?
- Could we completely skip estimating path delays in case this approach works?

Existing raytracing programs (1)

1) RayTrace

- Authors: Jim Davis (CfA Harvard), Tom Herring (MIT), Arthur Niell (MIT).
- Frequencies up to 300 GHz.
- Performs raytracing through vertical profiles, e.g. radiosonde profiles or numerical weather models.

Existing raytracing programs (2)

2) EGOPS

- Authors: G. Kirchengast et al. (Uni Graz).
- Licensed sofware, Fortran, IDL.
- Frequencies up to 1 THz.
- Liebe models for all gases.
- Performs 3D raytracing through 3D fields, e.g. standard atmospheres or numerical weather models.

Numerical weather models (1)

1) ECWMF

- Restricted access, some free.
- Interpolation to desired area and grid resolution possible, flexible (MARS archive).
- Pressure, temperature, humidity at several layers with 6 h time resolution.

Numerical weather models (2)

2) NCAR/NCEP

- Free access.
- Fixed grid size.
- Pressure, temperature, humidity at several layers with 6 h time resolution.

Numerical weather models (3)

3) e.g. MM5, HILAM

- Usually restricted access.
- Meteorological agencies, e.g. SMHI, DWD.
- Flexible grid resolution.
- Several levels with pressure, temperature, humidity.

Outlook

- Translating radio refractivity profiles from radio raytrace programs to the optical frequencies?
- Supplement existing radio raytrace progams with code for optical frequencies?
- Developing a completely new optical raytrace program?

Low Elevation Data Analysis
Grasse (7845)

Erricos C. Pavlis

Magda Kuzmicz-Cieslak

JCET/UMBC - NASA/GSFC

2003 ILRS Workshop on Laser Ranging
October 28-31, 2003, Kötzting, Germany

Introduction

- Analyzed data span:
  - October 21, 2001 to December 15, 2002
  - January 12, 2003 to February 7, 2003
- Data come from a single site:
  - **Grasse, 7845**
- Data were deposited in the form of full rate data on the EDC archive, under a separate directory

Analysis

- The data were reduced using the orbital model fit to the standard weekly data sets
- A measurement bias for Grasse was simultaneously estimated since it was apparent that the data were biased at about the 2 cm level

Analysis (cont.)

- Atmospheric refraction corrections were applied in two different ways:
  - standard Marini - Murray model **[MM]**
  - a variation of Ciddor's ZD model by Mendes and the new FCUL (Mendes et al.) mapping function **[MC]**
- Residual differences examined for data below $\varepsilon < 10°$

Residual Differences vs. Elevation

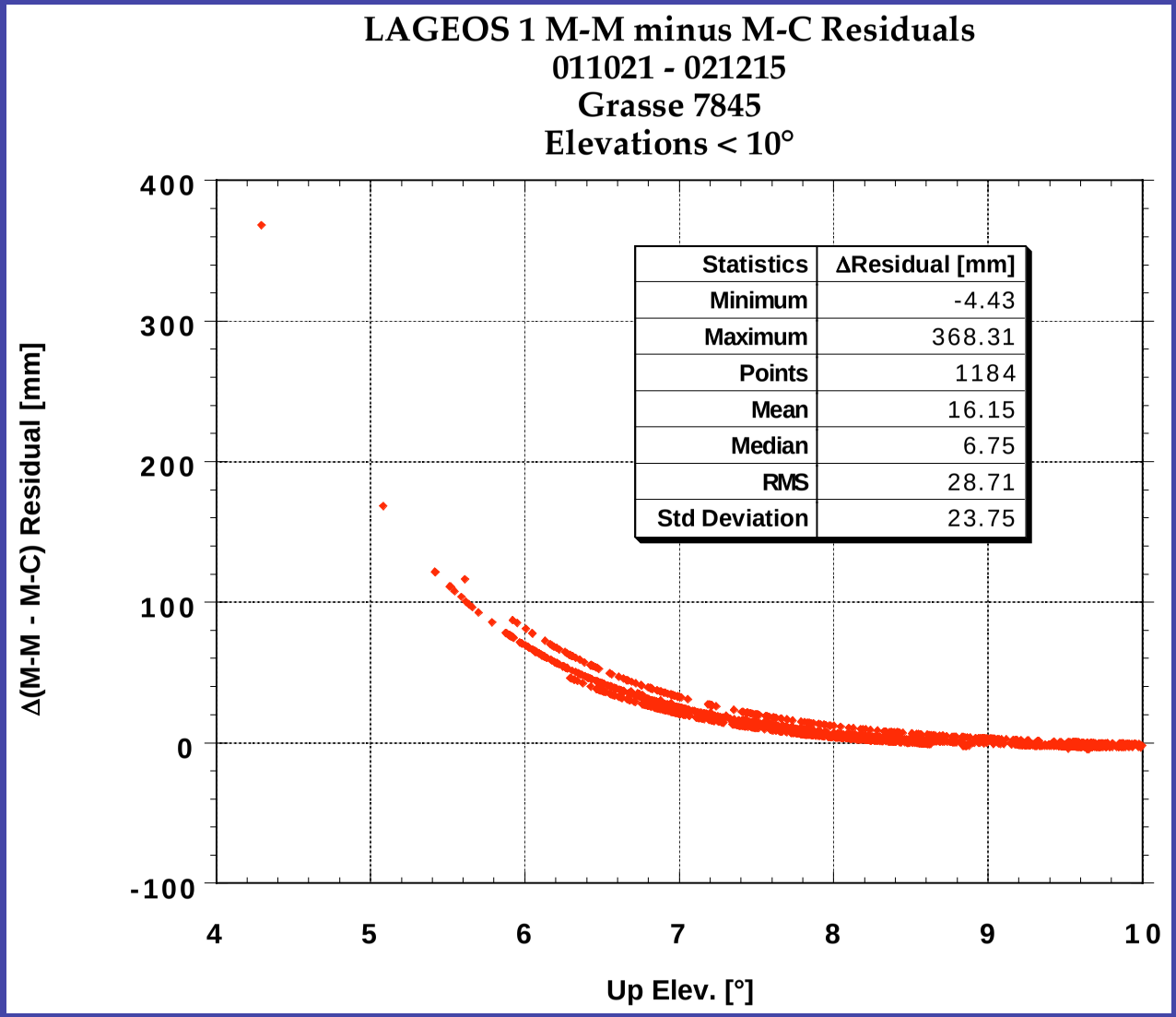

Residual Differences vs. Elevation

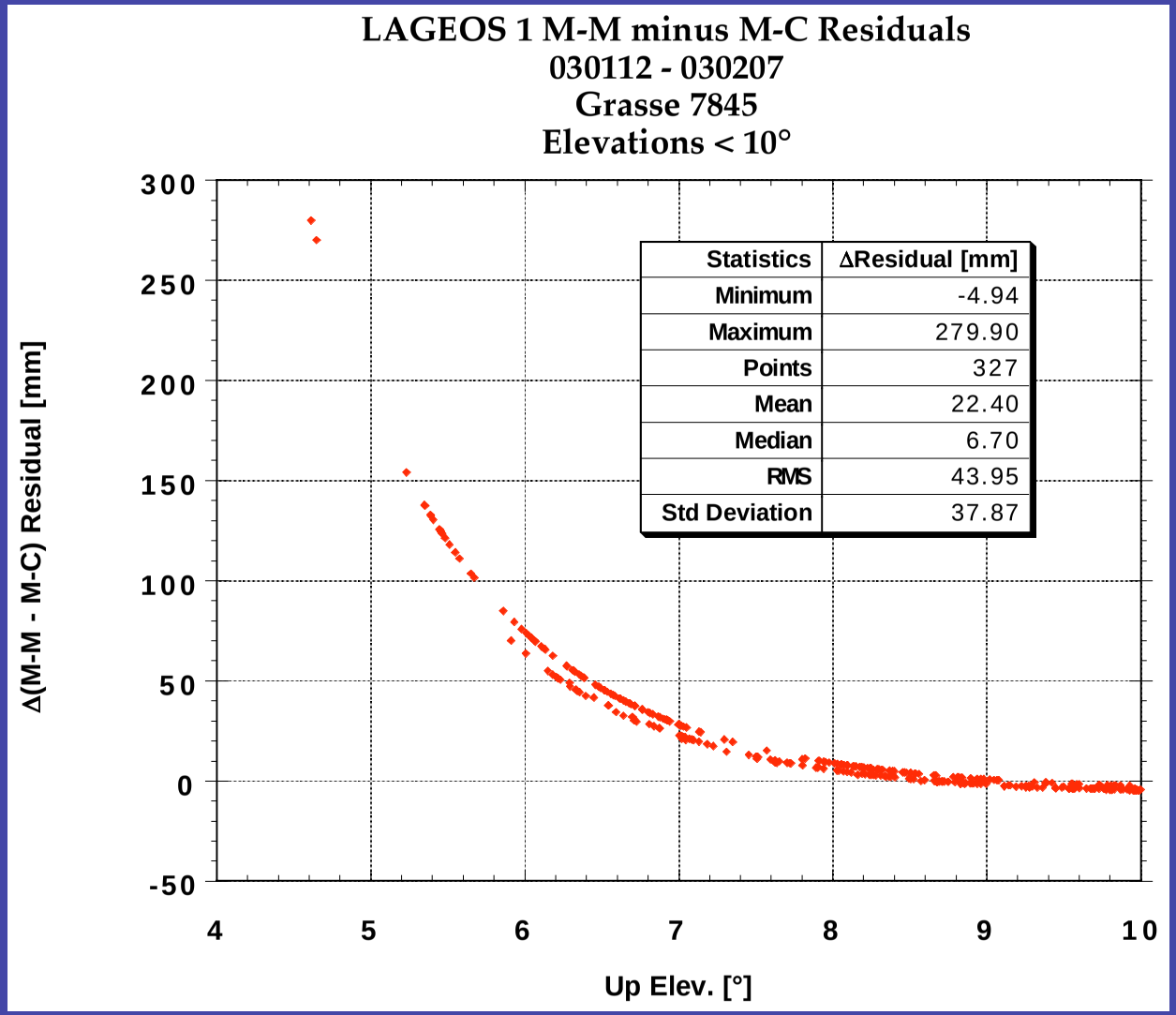

Residual Differences vs. Elevation

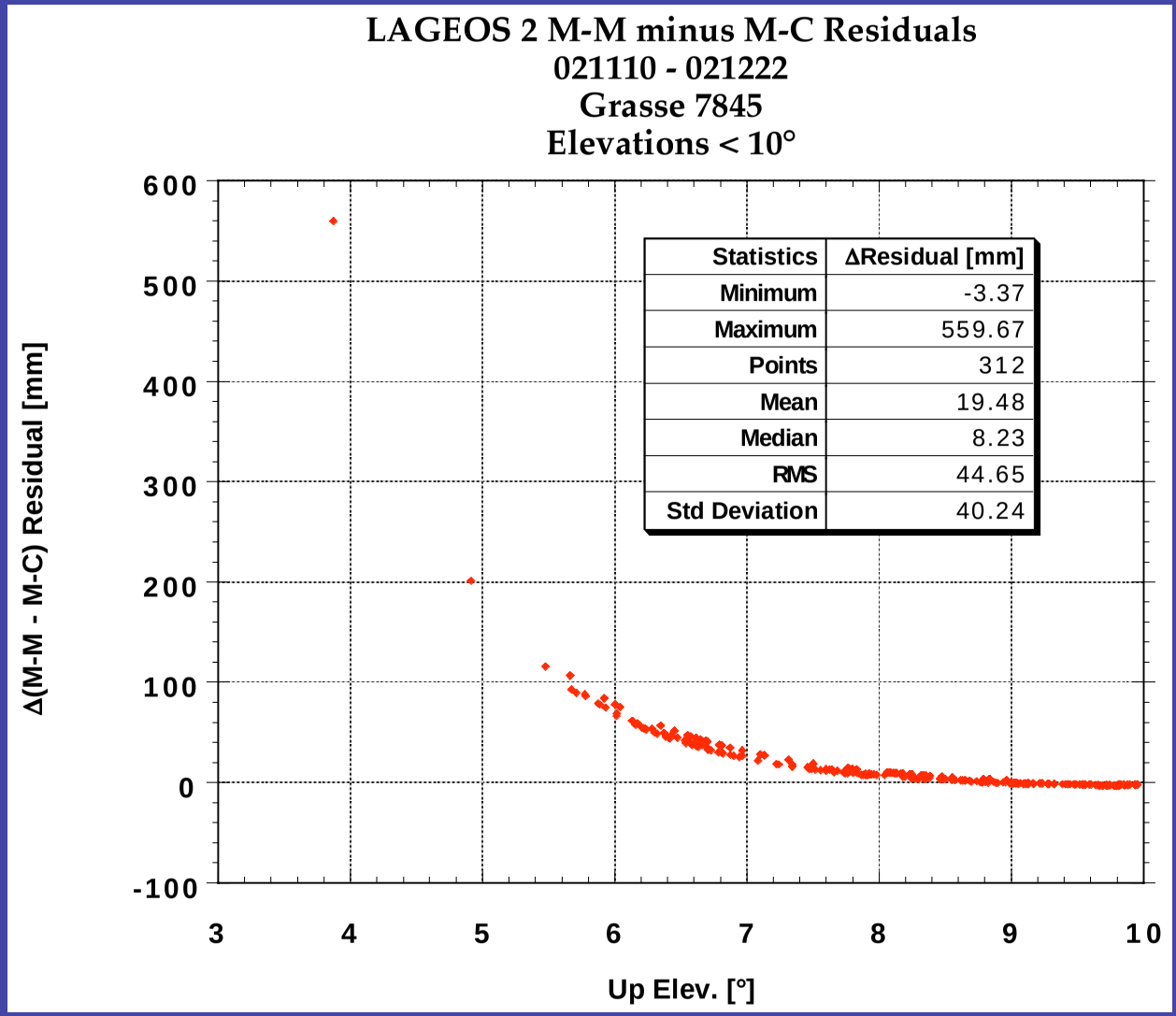

Residual Differences vs. Elevation

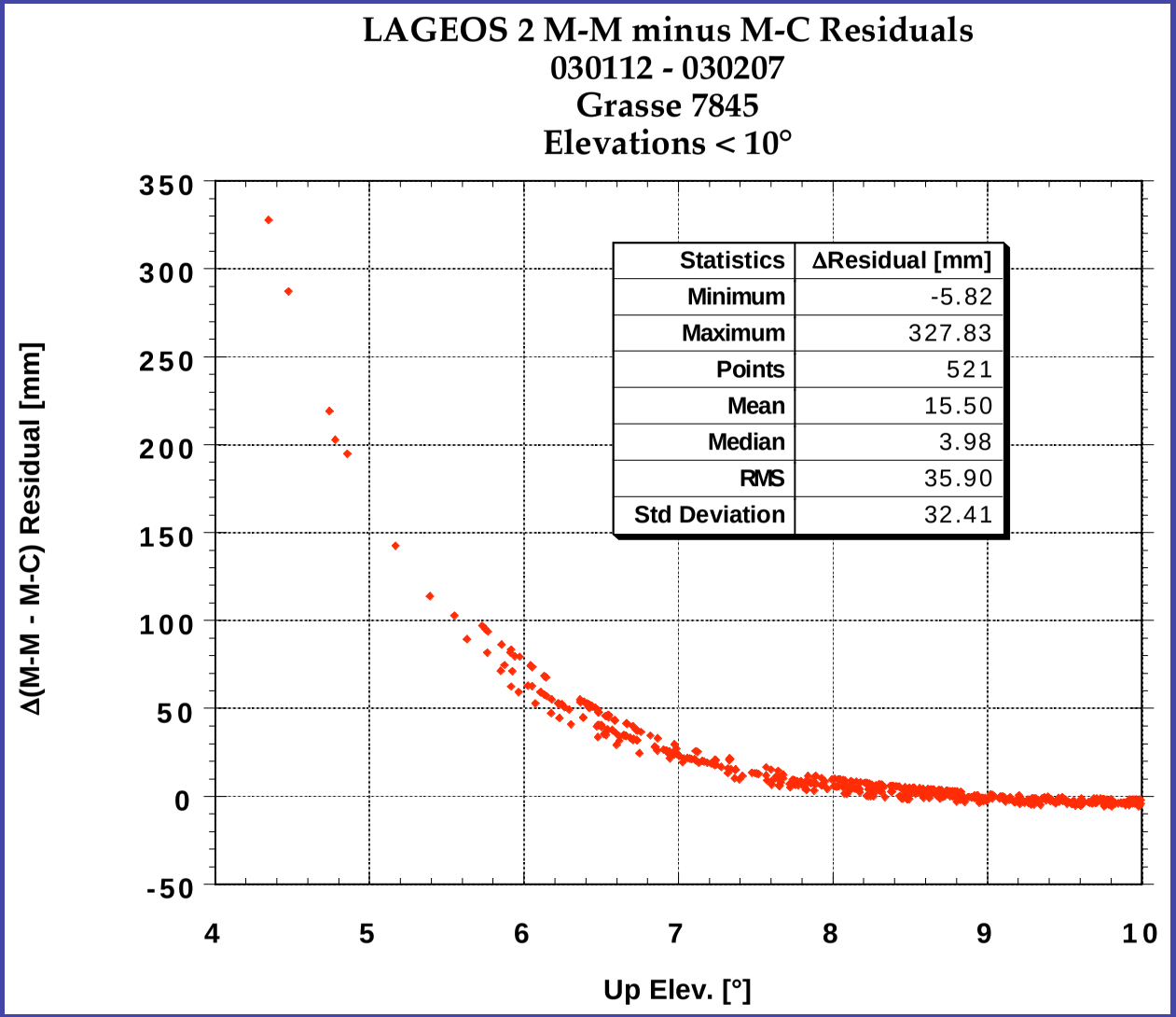

MM vs. MC

LAGEOS 1 & 2 Residual Statistics MM and MC Models

LAGEOS 1

Marini - Murray

	M-M Residual [m]
Minimum	-0.0537
Maximum	0.1872
Points	327
Mean	0.0504
Median	0.0402
RMS	0.0669
Std Deviation	0.0441

Mendes - Ciddor

	M-C Residual [m]
Minimum	-0.1266
Maximum	0.0965
Points	327
Mean	0.0280
Median	0.0276
RMS	0.0368
Std Deviation	0.0240

LAGEOS 2

	M-M Residual [m]
Minimum	-0.0666
Maximum	0.1607
Points	516
Mean	0.0345
Median	0.0333
RMS	0.0536
Std Deviation	0.0411

	M-C Residual [m]
Minimum	-0.1217
Maximum	0.1282
Points	516
Mean	0.0212
Median	0.0203
RMS	0.0442
Std Deviation	0.0388

Summary

- The system seems to deliver substantial data down to about 5° elevation
- The results indicate that applying M-M in the analysis for low elevation data ($5° < \varepsilon < 10°$) will introduce a mean bias of about 5 cm
- This will artificially increase the residual scatter for that site, but even worse, it will bias the recovered position of that site

Conclusions

- The system seems to deliver substantial data down to about 5° elevation
- Residual differences between reductions based on the M - M vs. those using the M - C increase exponentially with decreasing elevation, reaching several centimeters
- We need more low elevation data from many more systems, even if that data comes from lower (“clean”) geodetic targets (e.g. Starlette)

Atmospheric absorption lines and nonlinear refractivity of air effects.

Yury Galkin
Moscow State Forest University
(1, 1st Institutskaya St., Mytischi-5, Moscow reg., 141005, Russia,
tel. 7-095-786-1442, fax 7-095-586-9134, e-mail galkin@mgul.ac.ru)
and

Ruben Tatevyan
Central Scientific Research Institute
of Geodesy, Aerosurvey and Cartography
(26, Onezhskaya St., Moscow, 125413, Russia,
tel. 7-095-456-9321,)

Presented at the
International Laser Ranging Workshop
October 28-31, 2003
Koetzting, Germany

Introduction. The modern state of the art position.

It is known that the XXII General Assembly in 1999 recommended TWO formulas for the refractive index of the atmosphere suggested by the Ad-Hoc Working Group "Refractive indices of light, infrared and radio waves in the atmosphere" (Rueger (2002)). One of them (in Taylor's series form) is low accuracy (1 ppm), another (in Sellmeier's form) is more accuracy (better 1 ppm). State-of-the- art dispersion formulas are based on UV continium effect only. Usually exact formulas may be written, as follow

$$N \cdot 10^8 = (n - 1) \cdot 10^8 = A + \frac{B}{C - \sigma^2} + \frac{D}{E - \sigma^2}$$

where the coefficients A,B,C,D,E were suggested by different authors and the best of them is shown in table 1.

Table 1. The coefficients are suggested by different authors.

	A	B	C	D	E	
1.	Given as Taylor's series					Recommended by the XXII GA (1999)
2.	0	5792105	238,0185	167917	57,362	Recommended by the XXII GA (Ciddor96)
3.	8060,51	2480990	132,274	17455,7	39,329957	Peck&Reeder (1972) formula
4.	8342,13	2406030	130	15997	38,9	**Edlen's (1965) formula**
5.	8629,574	2323732,3	127,060012	12989,105	37,884361	**Galkin and Tatevyan (1997) formula**

The last experimental data were written by Peck and Reeder (1972) which have corrected some experimental data of Peck and Khanna (1962) (about $0.5 \bullet 10^{-8}$) and fitted new data to obtain new dispersion formula. Unfortunately anything special experimental data is absent and the XXII GA recommended two formulas (low precision and high precision) grounded by Peck and Reeder analysis and corrected on the temperature scale and CO2 content. Results of comparing are shown in the Table 2

Additionally there is shown optimized formula, which has the lowest RMS in last column.

Table 2. The differences of the formulas calculations minus the experimental data

—	**Wavelength □ micrometers**	**$N_{experim}$ x10E-8**	**Recommended as easy formula by the XXII GA (1999)**	**Recommended as exact formula by the XXII GA (Ciddor96)**	**Peck&Reeder (1972) formula**	**Edlen's (1965) formula**	**Galkin and Tatevyan (1997) formula**
1	1,694521	27314	4,1541956	1,5445055	0,2655215	0,7167135	0,2738517
2	1,530015	27326,41	4,0082396	1,3113552	0,0200432	0,4603064	0,0212895
3	1,529977	27326,1	4,3215394	1,6246317	0,3333165	0,7735767	0,3345609
4	1,529354	27326,56	3,9156752	1,2183842	-0,0729843	0,3672279	-0,0717708
5	1,47565	27331,28	4,1244603	1,3923415	0,0961548	0,532007	0,0945681
6	1,372233	27342,34	4,2468603	1,4362005	0,1293671	0,555395	0,1215256
7	1,372233	27342,52	4,0668603	1,2562005	-0,0506329	0,375395	-0,0584744
8	1,350788	27345,38	3,8548095	1,0256513	-0,2836459	0,1400694	-0,2929485
9	1,350788	27345,31	3,9248095	1,0956513	-0,2136459	0,2100694	-0,2229485
10	1,12905	27381,47	4,6740507	1,5913565	0,2499526	0,6419776	0,2210678
11	1,014257	27410,87	4,668668	1,3904036	0,026322	0,393831	-0,0171248
12	1,014257	27410,78	4,758668	1,4804036	0,116322	0,483831	0,0728752
13	0,966043	27426,28	4,8768434	1,49721	0,1220833	0,4768247	0,0712656
14	0,922703	27442,66	4,7030755	1,2202605	-0,1656118	0,1760694	-0,2238127
15	0,912547	27446,62	4,8828814	1,3740496	-0,0144528	0,323923	-0,0744967
16	0,912547	27446,43	5,0728814	1,5640496	0,1755472	0,513923	0,1155033
17	0,724716	27557,42	5,4666071	1,3171648	-0,1256837	0,1283708	-0,2289407
18	0,671829	27606,4	6,2493796	1,8564568	0,398697	0,6179052	0,2799573
19	0,644025	27638,2	5,7908657	1,2602317	-0,2042629	-0,0061245	-0,3315975

Table 2. The differences of the formulas calculations minus the experimental data

—	Wavelength □ micrometers	$N_{experim}$ x10E-8	Recommended as easy formula by the XXII GA (1999)	Recommended as exact formula by the XXII GA (Ciddor96)	Peck&Reeder (1972) formula	Edlen's (1965) formula	Galkin and Tatevyan (1997) formula
20	0,579226	27729,8	6,1029558	1,2464663	-0,2271617	-0,0869784	-0,3747713
21	0,57712	27733	6,4360516	1,5695381	0,0958489	0,2339169	-0,0523982
22	0,567747	27749,7	5,956003	1,0459983	-0,4277184	-0,2992559	-0,5787617
23	0,546227	27789,88	6,3382817	1,3382644	-0,1337797	-0,0285848	-0,2908928
24	0,501707	27891,53	6,4743271	1,3759449	-0,0822914	-0,0308325	-0,249099
25	0,49233	27916,71	6,4789896	1,3866325	-0,0663735	-0,0272043	-0,234421
26	0,491745	27918,7	6,1101503	1,0186167	-0,4340312	-0,3956395	-0,6021433
27	0,471446	27978,61	6,4204893	1,3982244	-0,0394525	-0,0288066	-0,2087149
28	0,467946	27989,85	6,401085	1,4002925	-0,0342683	-0,0285487	-0,2034821
29	0,447273	28062,08	6,1869999	1,391607	-0,0209681	-0,0450807	-0,1880079
30	0,435956	28106,3	6,0364431	1,4270908	0,0293266	-0,0115419	-0,1348728
31	0,435956	28106,5	5,8364431	1,2270908	-0,1706734	-0,2115419	-0,3348728
32	0,410933	28218,4	5,4107101	1,4926233	0,1349515	0,0566276	-0,0174304
33	0,404771	28249,54	5,1390278	1,4716239	0,1253279	0,0378494	-0,0227096
34	0,404771	28249,5	5,1790278	1,5116239	0,1653279	0,0778494	0,0172904
35	0,398509	28282,8	4,8201513	1,4501186	0,1159236	0,0192436	-0,0270109
36	0,388975	28336,79	4,2754431	1,4556653	0,140781	0,030398	0,0070821
37	0,380273	28390,5	3,1408789	0,9474014	-0,3492042	-0,4716177	-0,4727619
38	0,365587	28489,6	2,0698116	1,2815469	0,0159162	-0,1252089	-0,0863247
39	0,365119	28492,9	2,1040497	1,369229	0,104561	-0,0371174	0,0030936
40	0,356224	28559,5	1,5906434	1,9949496	0,7478589	0,5963095	0,6622768
41	0,354443	28574,4	0,5710811	1,2343384	-0,0094555	-0,1628165	-0,0915788
42	0,339168	28705,9	-1,9908321	1,4205045	0,1996018	0,0335988	0,1511246
43	0,29263	29264,3	-21,125423	1,5153873	0,1900421	0,0430504	0,2786222
44	0,289447	29314,4	-23,487773	1,5428644	0,1912606	0,0507216	0,2889381
45	0,285779	29374,8	-26,660677	1,3992657	0,0128765	-0,1190613	0,1202801
46	0,276059	29548,7	-36,385156	1,404872	-0,0984449	-0,2008539	0,0284199
47	0,27536	29562,1	-37,222981	1,377451	-0,1356618	-0,2355349	-0,0078913
48	0,267575	29719,8	-47,443707	1,4072727	-0,2259716	-0,2934173	-0,0947281
49	0,257711	29945,5	-64,119415	1,7180661	-0,0819116	-0,0959524	0,0284762
50	0,246482	30245,7	-90,652656	2,20108	0,2740376	0,3407201	0,3034355
51	0,244765	30297,3	-96,565969	1,3659913	-0,5614117	-0,480221	-0,5519836
52	0,237911	30514,4	-119,81141	1,6075054	-0,2099204	-0,0640882	-0,3062783
53	0,234617	30628,3	-133,49383	1,3558144	-0,3098704	-0,1286014	-0,4739523
54	0,230289	30787,6	-153,46746	1,5999116	0,2944622	0,5276015	0,0227756
55	0,214506	31496,8	-267,91322	-3,9468422	-0,2064336	0,3096475	-1,0080198
56	0,202605	32214,8	-423,92365	-17,189431	2,5912883	3,6500984	1,8825077
57	0,199052	32479,5	-497,03363	-31,113787	-1,0207661	0,3833109	-1,1874386
58	0,193585	32939,7	-637,244	-58,775678	-2,2454354	0,1255087	-0,1200724
59	0,186277	33697,4	-912,5541	-127,39999	5,2981688	11,109373	18,363192
60	0,185473	33805,5	-963,30413	-150,25495	-4,0859011	2,4234463	11,406945
			±124.499	**±9.199**	**±0.524**	**±0.554**	**±0.404**

In whole experimental data confirmed dispersion formula but however some experimental measurements (very high precision) gave more high magnitude for some wavelengths.

Table 3. Some experimental results after 1972

_	Authors	Range micrometers	Method	Data - Ed.65 in 10^{-8}
1	Schellekens et al (1986)	0.63	NPL	+6.0
2		0.63	PTB	+0.1
3		0.63	THE	+8.0
4		0.63	VSL	+3.0
5	Matsumoto (1988)	10	Michelson	+5.0
6	Birch and Downs (1993)	0.63	NPL	+5.9
7	Hou and Thalmann (1994)	0.63	OFMET	+1.4
8		0.63	BCR	+3.4

This situation and some former results (two color refractometer, IR EDM) gave the idea that special reasons may be here.

Influence of the atmospheric absorption lines.

It is known that there are a lot of (more 1000000 by the HITRAN electronoc basedata) resonances (absorption lines) from IR to RW. In generaly the resonances are combined by groups (absorption bands) including 100s or even 1000s separated absorption lines.
Usually a single absorption line near of the earth surface has the Lorentian form

$$\alpha(\nu) = \frac{S_i c}{2\pi_i} N \frac{g^2 \pi_i^2}{(\nu - \nu_i)^2 + g^2 \pi_i^2} = AN \frac{g^2 \pi_i^2}{(\nu - \nu_i)^2 + g^2 \pi_i^2}$$

Therefore change of the phase refractive index because of absorption may be written as

$$n(\nu) - 1 = ANg \frac{S_i(\nu_i - \nu)}{(\nu_i - \nu)^2 + \pi_i^2 g^2}$$

Symbolic graph shows resulting “unsmooth” curve.

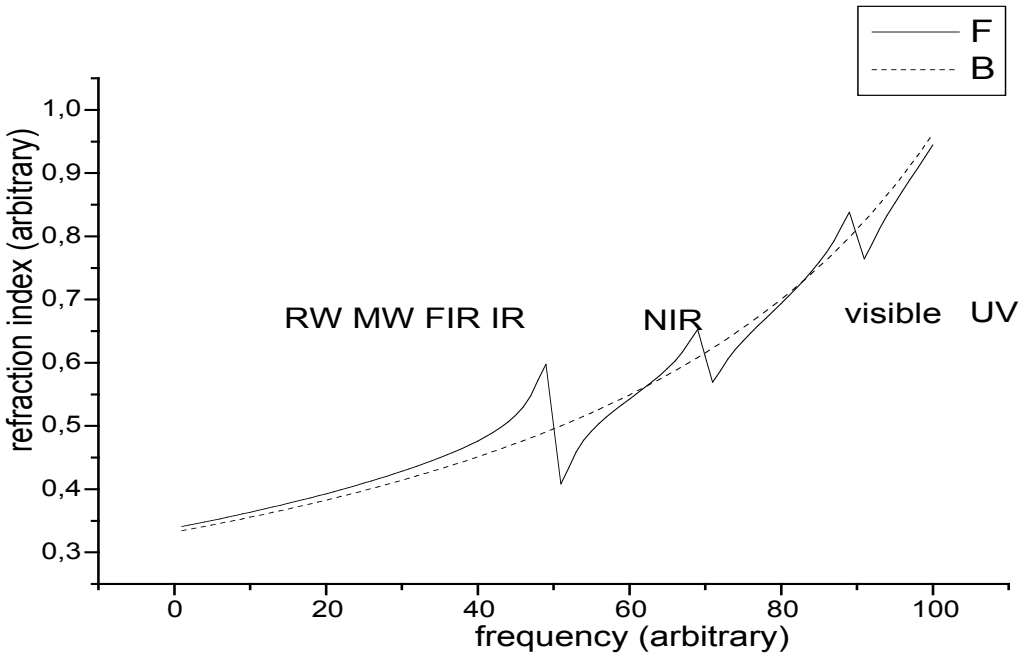

A single line has small effect 10^{-9}- 10^{-12} on the phase refractive index. This effect on short wave side aspires to zero, but (warning) one on long wave side aspires to a fixed terminal value. Therefore, the refractive index on long wave side of absorption band is above (sum of all lines effect) then the UV effect curve. We can acount important bands of the general atmospheric components (O_2, H_2O, CO_2 etc.) within visible, NIR, MIR, FIR and RW regions. The real refractive index of air is more complicated then the known formulas show.
More than that the group refractive index near absorption line may be written as

$$n_{gr}(\nu) - 1 = AN\gamma \frac{2(\nu_i - \nu)^3\gamma^2 + \gamma_i^2(\nu_i - \nu)^2 - \gamma_i^4\gamma^2}{\left[(\nu_i - \nu)^2 + \gamma_i^2\gamma^2\right]^2}$$

And if we take

$$x = \frac{\nu_i - \nu}{\gamma\gamma_i} \qquad \text{where} \quad \gamma\gamma_i \text{ is the halfwidth of the i-line}$$

we can easily estimate region of influence every line in number of the halfwidth of the line

$$\alpha(x) = AN\frac{1}{1+x^2} \qquad n(x) - 1 = AN\frac{x}{1+x^2} \qquad n_{gr}(x) - 1 = \frac{AN(x^2-1)}{\gamma(1+x^2)^2}$$

Usually AN is 10^{-9}-10^{-12} and g $\approx 10^{-6}$ for visible and IR regions therefore the single line effects on the group refractive index is million times more than on the phase index within spectral region from 0,5 nm to 50 nm around of a signal carrier frequency.
The phase refractive index is destroyed just when the signal spectrum and the absorption line are intersecting.
Since the SLR uses the group refractive index there are shown number of lines within of the ± 5 nm range around of the laser wavelengths used by SLR in Table 4.

Table 4. Absorption lines near SLR wavelengths.

No	Laser wavelength micrometer	O_2	CO_2	H_2O	The nearest line
1	0,353	Outside of database			
2	0,4235	0	0	0	0
3	0,435	0	0	0	0
4	0,46	0	0	0	0
5	0,532	0	0	32	0,5325
6	0,6329	85	0	117	0,632908
7	0,6942	124	0	218	0,69421
8	0,683	38	0	65	0,68304
9	0,847	0	0	105	0,847005
10	1,064	51	34	21	1,06402
11	1,57	17	232	36	1,570003

It is seen that in most cases the state of the art smooth dispersion formula is not enough for precision group refractive index of the air and real dispersion is not known and the special researches are required.
More than that, the oscillating form of the dispersion may be as reason of breach of correction of the group refractive index formula in whole.

Nonlinear refractivity effects.

The XXII General Assembly recommended to use the group refractive index calculated using the computer procedure suggested Ciddor and Hill (1999). This procedure assumes that the conditions are realized in air may be written as following

$$\square(\square_0) \square \square 0.5 \square(\square_0) \square^2$$

When the properties of medium (absorption and refractivity) may be written as the Taylor's series of the complex function

$$\square(\square_0)\square\square\square(\square_0)\square$$

$$k(\square) = k(\square_0) + k\square(\square_0)\square + 0.5k\square\square(\square_0)\square^2 + \ldots =$$
$$= \square(\square_0) + \square\square(\square_0)\square + 0.5\square\square\square(\square_0)\square^2 + \ldots$$
$$+ i\square(\square_0) + i\square\square(\square_0)\square + i0.5\square\square\square(\square_0)\square^2 + \ldots$$

where $k(\square)$ is a complex vector in a Taylor series in powers of $\square=(\square\square\square_0)$ for the absorption coefficient $\square(\square)$ and the phase delay $\square(\square)$

Unfortunately above-mentioned conditions may be not executed near absorption lines even for simple signals (AM-signal) (Galkin and Tatevyan (1997)). These conditions are destroyed even far away from absorption lines for the complicated signals, for example, such as the short laser pulse with the Gaussian envelope (width $\square$ at 50% power) (Galkin and Tatevyan (2002)). In this case using of the state of the art group refractive index gives an error in results because of the nonlinear refractivity gives the additional group delay

$$\square = \frac{2.78\square^2\square\square\$^2}{1+2.78\square^2\square\$}$$

and the shift received frequency relatively of transmitted optical frequency approximately as

$$\square\square = \square 2.78\square^2\square\$$$

where S is path through atmosphere, and the necessary derivatives can be calculated by Kramers-Kronig relations using known dispersion function (for the derivatives of absorption) or transparency function (for the derivatives of refraction).

The estimation of the additional group delay and the frequency shift for the state of the art dispersion equation and different laser wavelengths is shown on the Table 5. (Sensing to zenith. S=16,6 km)

Table 5. The additional group delay and the frequency shift for used lasers.

Wavelength micrometers	Pulse width 1 nsec		Wavelength micrometers	Pulse width 0,1 nsec	
	psec	$\times 10^{10}$		psec	$\times 10^{12}$
1,57	0,003	1,5	1,57	0,257	1,5
1,06	0,006	2,4	1,06	0,601	2,4
0,85	0,01	3,2	0,85	1,009	3,2
0,69	0,017	4,3	0,69	1,678	4,3
0,53	0,034	6,5	0,53	3,353	6,5
0,42	0,061	9,6	0,42	6,081	9,6
0,35	0,115	14	0,35	11,42	14

The additional group delay is the most important aspect for two color SLR. For two color measurements (Sperber and Riepl (2001)) the atmospheric correction may be obtained via the time delay Δt the pulses of different color (let $\lambda_1<\lambda_2$)

$$N_{gr}(\lambda_1)\, S = cN_{gr0}(\lambda_1)\, \Delta t\, (N_{gr0}(\lambda_2) - N_{gr0}(\lambda_1))^{-1}=cK\Delta t$$

where the components $N_{gr0}(\lambda_1)$ and $N_{gr0}(\lambda_2)$ are known and the factor K may be calculated, c is the light velocity in vacuum. According to this factor influence of the additional delay is increasing.

The resulting errors are calculated for a vertical ray path (double ray path through at sea level is assumed as 16.6 km) and a horizontal ray (path is equal 50 km) for different conditions. They are shown in Tables 6 – 9.

Table 6. Vertical ray path. Pulse width is 1.0 nsec.

$\lambda\lambda$(μm)	$\Delta\Delta$ (psec)	K	Error (mm)
1.064-0.532	0.027	22.6	0.18
0.532-0.355	0.077	14.06	0.32
1.064-0.355	0.10	8.44	0.26

Table 7. Vertical ray path. Pulse width is 0.1 nsec

$\lambda\lambda$(μm)	$\Delta\Delta$ (psec)	K	Error (mm)
1.064-0.532	2.72	22.6	18.44
0.532-0.355	7.68	14.06	33.64
1.064-0.355	10.4	8.44	26.33

Table 8. Horizontal ray path. Pulse width is 1.0 nsec.

□□(□m)	□□ (psec)	K	Error (mm)
1.064-0.532	0.30	22.6	2.02
0.532-0.355	0.69	14.06	2.91
1.064-0.355	0.99	8.44	2.50

Table 9. Horizontal ray path. Pulse width is 0.1 nsec

□□(□m)	□□ (psec)	K	Error (mm)
1.064-0.532	24.5	22.6	166.11
0.532-0.355	69.1	14.06	237.0
1.064-0.355	93.6	8.44	302.7

Conclusions

It is shown that the state of the art dispersion formulas particularly of the group refractive index is not enough to achieve millimeter accuracy of the SLR.
Taking into consideration a lot of the spectral lines of air it is necessary to research every used spectral region in detail by theoretic and experimental methods.
Worth while to pay attention on stated problems under exploitation of the existing SLR systems and development new perspective ones.

References.

Birch K.P., Downs M.J. (1993) Metrologia, v.30, p. 155.
Ciddor P.E. (1996) Applied Optics, Vol. 35, No. 9, 1566-1573.
Ciddor P.E., Hill R.J. (1999) Applied Optics, Vol. 38, No. 9, 1663-1667.
Edlen B. (1966) Metrologia, v.2, p. 71.
Galkin Yu.S., Zakharov D., Tatevian R.A. (1997) Geodesy and Cartography, No 11 (in Russian).
Galkin Yu.S., Tatevian R.A. (1997) Journal of Geodesy, No 71, 483-485.
Galkin Yu.S., Tatevian R.A. (2002) Presentation at the 13th ILRS, Washington D.C., USA.
Hou W., Thalmann R. (1994) Measurements, v.13, p. 307.
Mutsumoto H. et al. (1988) Metrologia, v. 25, p. 95.
Peck E.R., Khanna B.N. (1962) JOSA, v.52, p. 416
Peck E.R., Reeder K. (1972) JOSA, v.62, p. 958.
Rüeger J. M. (2002) UNISURV REPORT S-68, School of Surveying and Spatial Information Systems, University of New South Wales, Sydney, Australia.

Schellenkens P. et al. (1986) Metrologia, v.22, p. 279.
Sperber P., Riepl S. (2001) Proc. of the Int. conference “Mathematical and physical methods in ecology and environmental monitoring”, Moscow, Russia, 30-43.

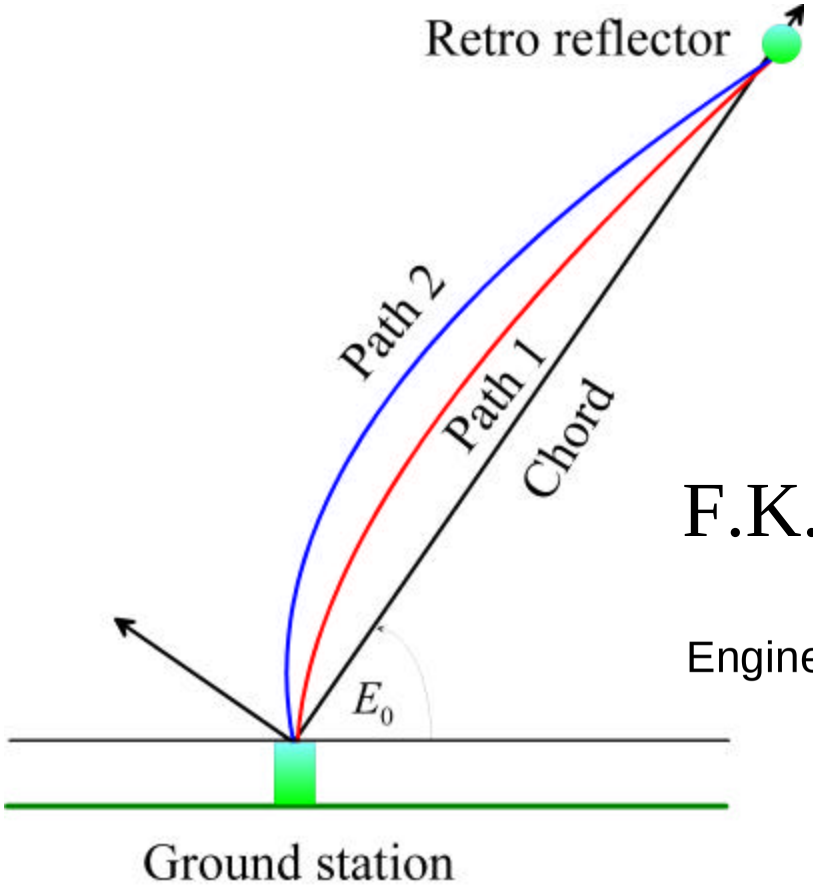

Modelling of dual-wavelength SLR measurements

F.K. Brunner and K.H. Gutjahr

Engineering Geodesy and Measurement Systems
Graz University of Technology

Motivation

Contribution to

Refraction Study Group (RSG) of ILRS

Goal was set to achieve

$$s_s \cong 1mm$$

Rigorous derivation of atmospheric effects in dual-wavelength SLR

Rigorous Derivation (1)

- Integration path determined by n_{ph}
- OPL = integration of n_{gr} along path yielding L_1 and L_2

$$L_1 = s + \int_{path1} \left[n_{gr}(l_1) - 1 \right] \cdot ds_1 + K_1$$

$$L_2 = s + \int_{path2} \left[n_{gr}(l_2) - 1 \right] \cdot ds_2 + K_2$$

$$L_2 = s + \int_{path1} \left[n_{gr}(l_2) - 1 \right] \cdot ds_1 + K_1 + P$$

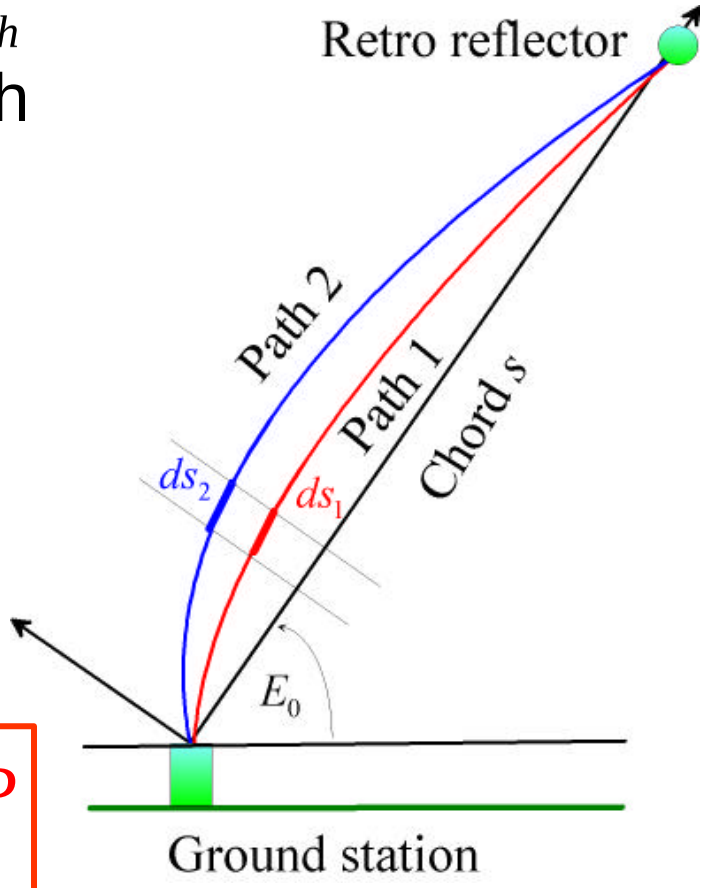

Rigorous Derivation (2)

- n_{gr} is expressed by dispersion factors and the associated densities of air

$$n_{gr} = 1 + D(l)\, r_{dry} + W(l)\, r_{wet}$$

- This leads to

$$L_1 = s + D(l_1) \int_{path1} r_{dry} \cdot ds_1 + W(l_1) \int_{path1} r_{wet} \cdot ds_1 + K_1$$

$$L_2 = s + D(l_2) \int_{path1} r_{dry} \cdot ds_1 + W(l_2) \int_{path1} r_{wet} \cdot ds_1 + K_1 + P$$

- Now $\int_{path1} r_{dry} \cdot ds_1$ can rigorously be eliminated

Rigorous Derivation (3)

$$s = L_1 - n\left(L_2 - L_1\right) + \left(nP - K_1\right) + W\left(l_1\right) H_{12} \int_{path1} r_{wet}\, ds_1$$

$$n \equiv \frac{D\left(l_1\right)}{D\left(l_2\right) - D\left(l_1\right)}$$ ... dispersive power

$$H_{12} \equiv \frac{W\left(l_2\right) - W\left(l_1\right)}{W\left(l_1\right)} - 1$$ ... humidity reduction factor

Raytracing

- Snell´s law
- Spherical layers of atmosphere of 1 m thickness
- 1976 Standard atmosphere values for temperature and pressure

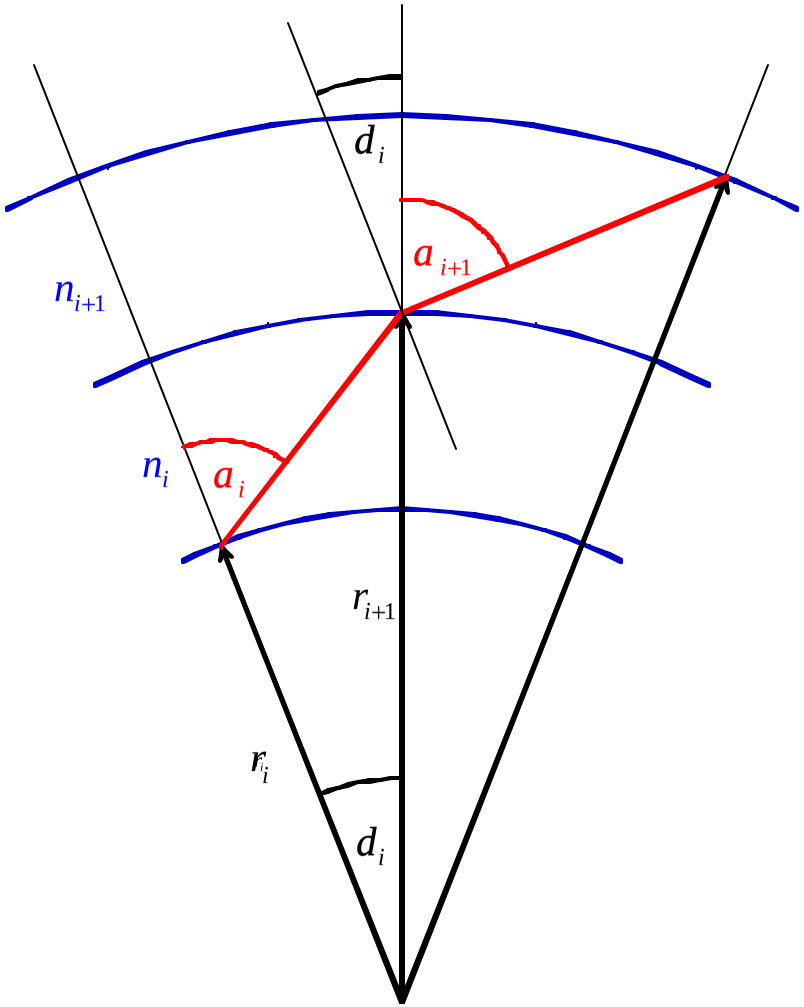

1976 Standard Atmosphere

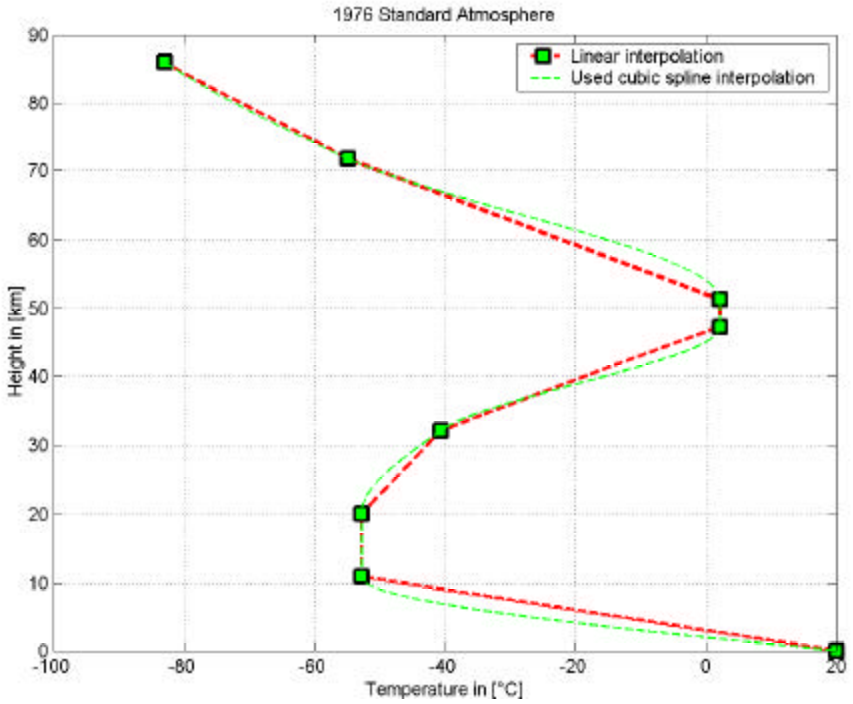

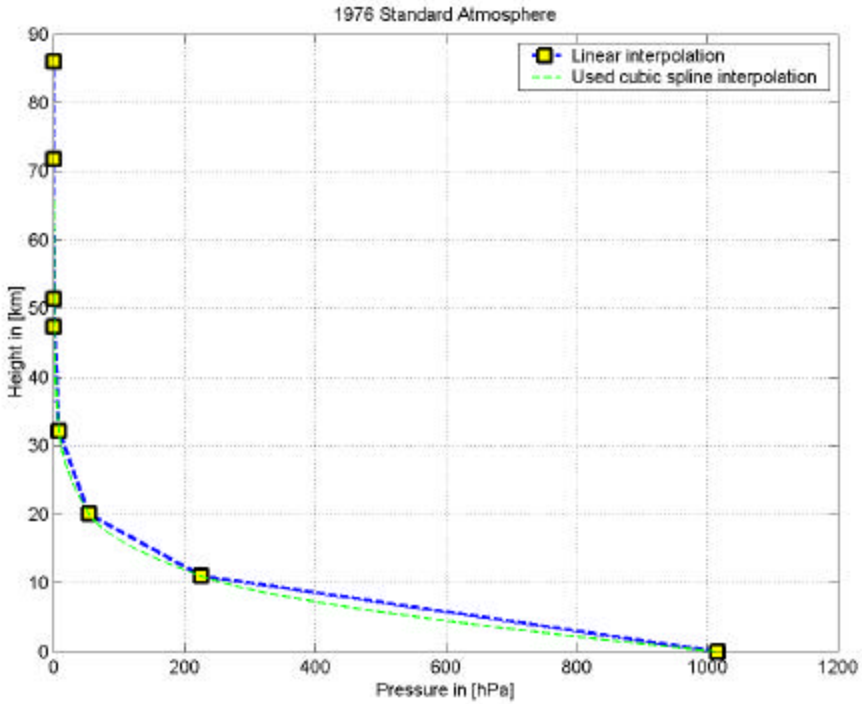

- Defined up to 86 km
- Start values at sea level: 20° C and 1016 hPa

Curvature and Propagation Effect

Curvature $$K_1 = \int_{path1} ds_1 - s$$

Propagation $$P = \int_{path2} n_{gr}(l_2) \cdot ds_2 - \int_{path1} n_{gr}(l_2) \cdot ds_1$$

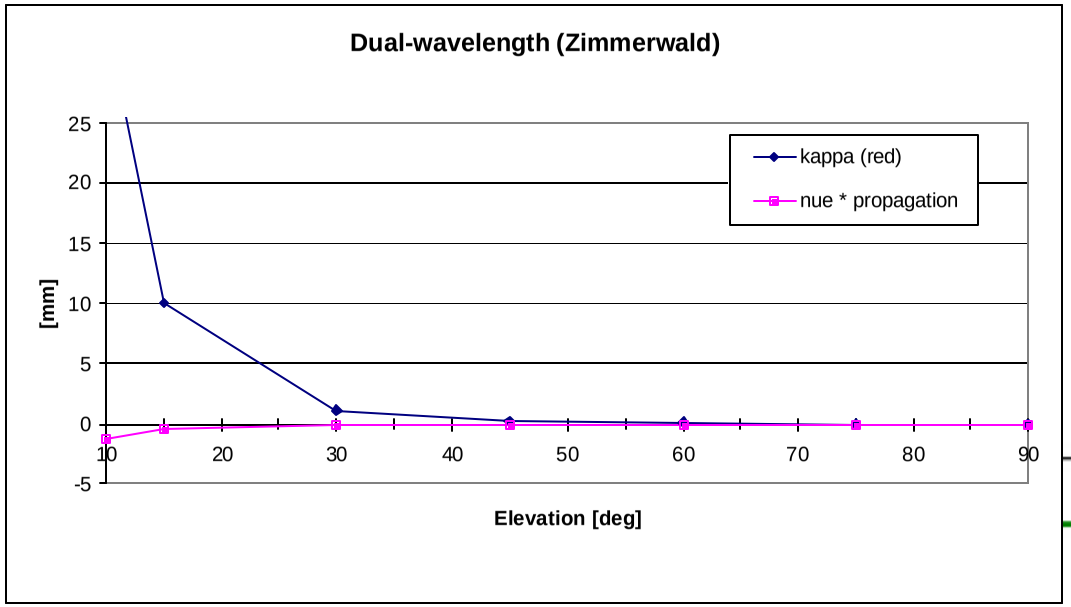

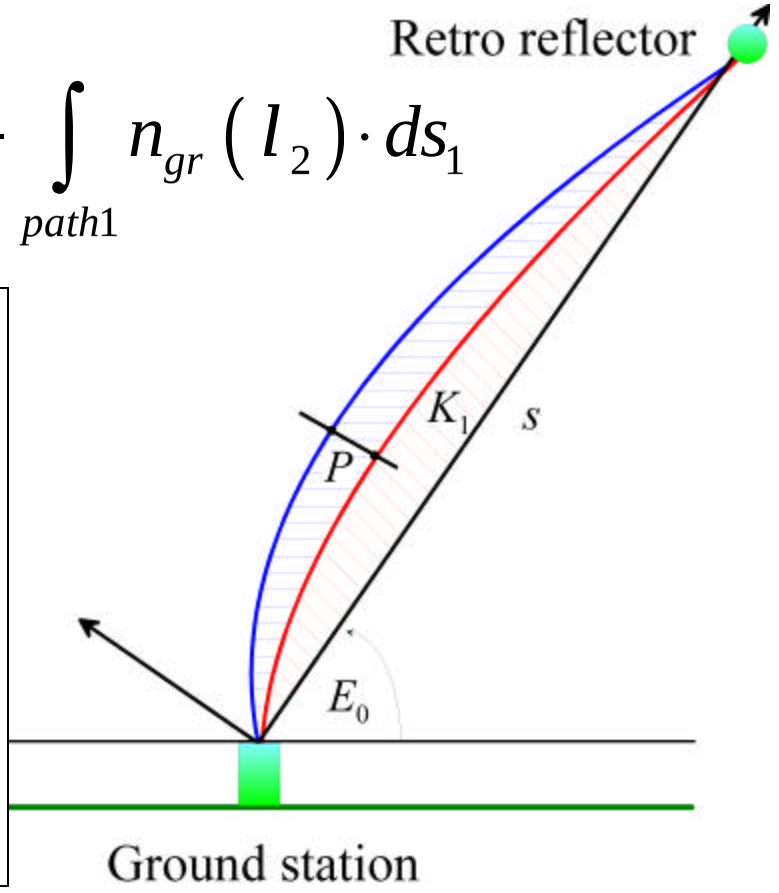

Water vapour range effect (1)

Integrated water vapour $IWV \equiv \int_{path} r_{wet} ds$

Single wavelength $R_w = W(l) \cdot IWV$

Dual-wavelength (Zimmerwald)

$\Delta_{12} R_w = W(l_1) H_{12} IWV$

$H_{12} = 0.42$

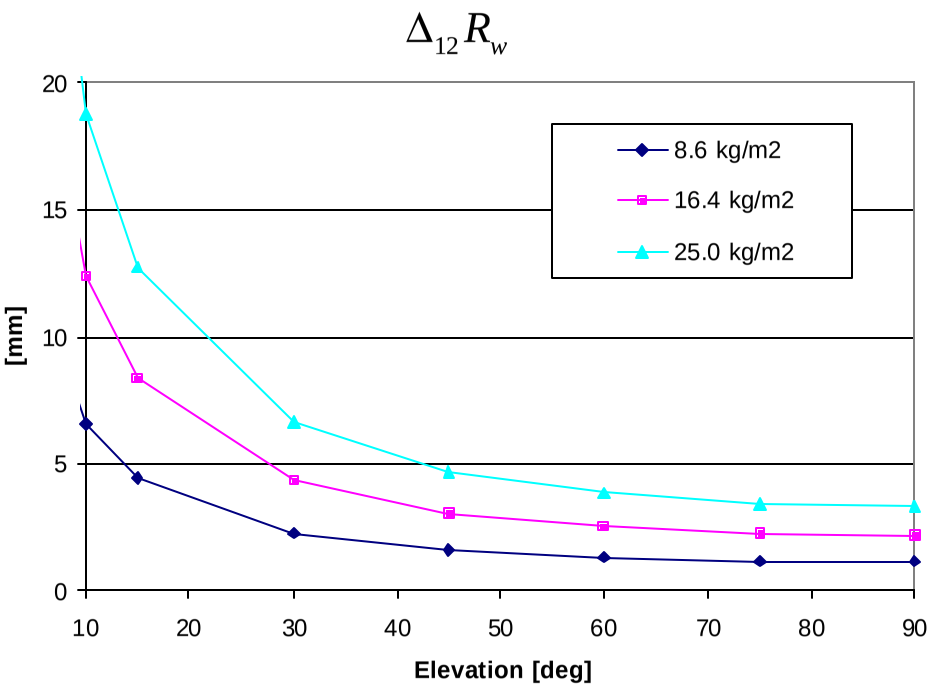

Water vapour range effect (2): Modelling of $\Delta_{12} R_w$

- *IWV* highly variable in position, azimuth and time

Example:
Potsdam
hourly *IWV* values
WVR and GPS

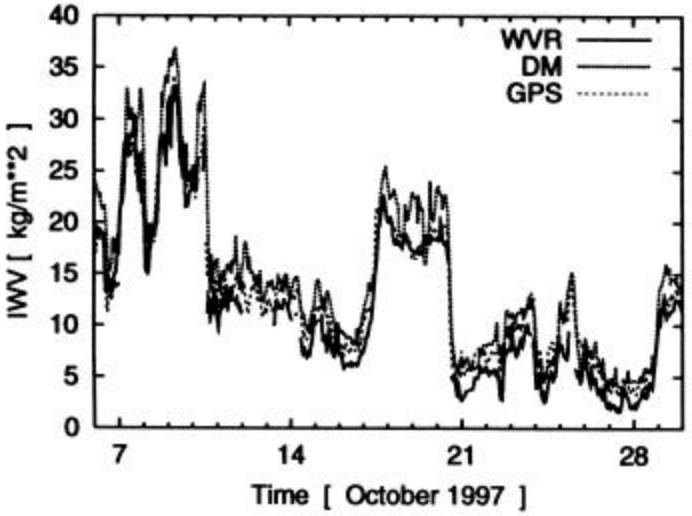

- GPS very useful and readily available technique (5-10% resolution of bias)
- Could be used to estimate the azimuth variation and thus $\int_{path1} r_{wet} \cdot ds_1$

Summary

- Rigorous derivation
- Horizontal gradients eliminated
  except for their effects on K_1 and IWV
- K_1 (10 mm for E_0=15°) can be modelled
- P <1 mm for E_0=15°
- IWV effect (11 mm for E_0 =15°) can be estimated using GPS (azimuthal sectors)

Problems

- Dual wavelength measurements:

  bias, precision, sampling?

  required precision $\simeq$ 0.04 mm
- Effect of turbulence
- Folded path?
- Dispersion precision: absorption bands for n_{gr}?

  required precision $\simeq 10^{-9}$
- Centre-of-mass correction
- Dispersion in glass retro-reflectors?

Using GPS-derived PWV to estimate tropospheric delay

A Combrink & L Combrinck

HartRAO Space Geodesy Programme

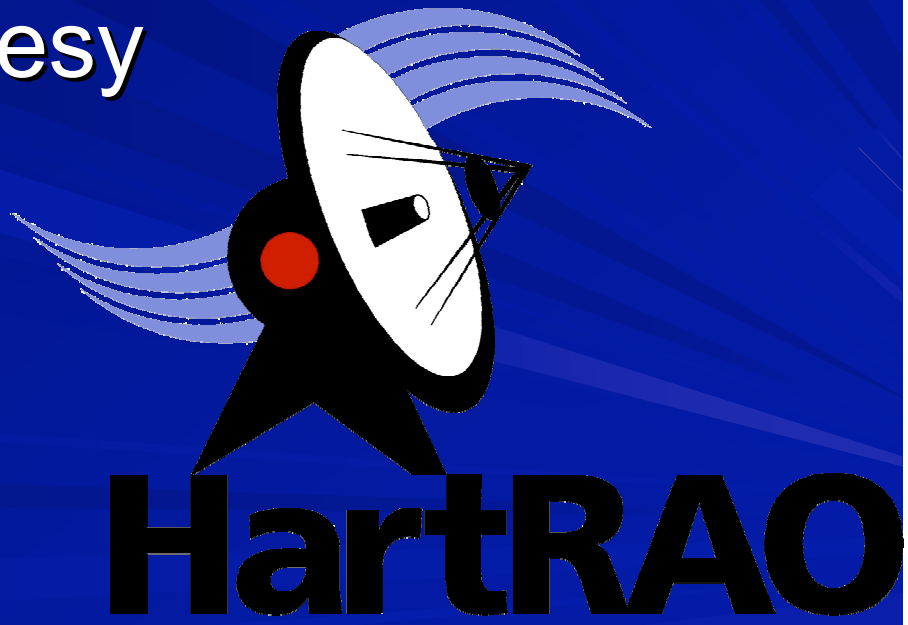

Assumptions

- Ground-measured Relative Humidity is uncorrelated with amount of water vapour in the troposphere.
- Tropospheric delay can be split up into wet and hydrostatic components (as for microwaves).
- Hydrostatic delay proportional to pressure, wet delay proportional to PWV.

Method used (for MOBLAS6)

- Obtain estimated zenith delay (microwave) for HRAO (collocated IGS station) from IGS final product.
- Fit 3rd order polynomial through points to determine zenith delay at SLR normal point observation time.
- Use pressure and temperature measurements with GPS zenith delay to determine (zenith) PWV.

Method used (continued)

- Multiply PWV by refractivity of water to get wet component of zenith delay.
- Use [Marini&Murray minus wet delay] as first approximation of hydrostatic component to obtain constant of proportionality $k(latitude, wavelength, height)$ ($HD = k \times P$)

Note: k should preferably be determined by radiosonde methods.

Method used (continued)

- Processed two years' data for Lageos 1 & 2 – which included 16100 normal points from MOBLAS6
- Used RGODYN (Appleby) which employs the Marini&Murray model.
- Used Marini&Murray model for all other stations.

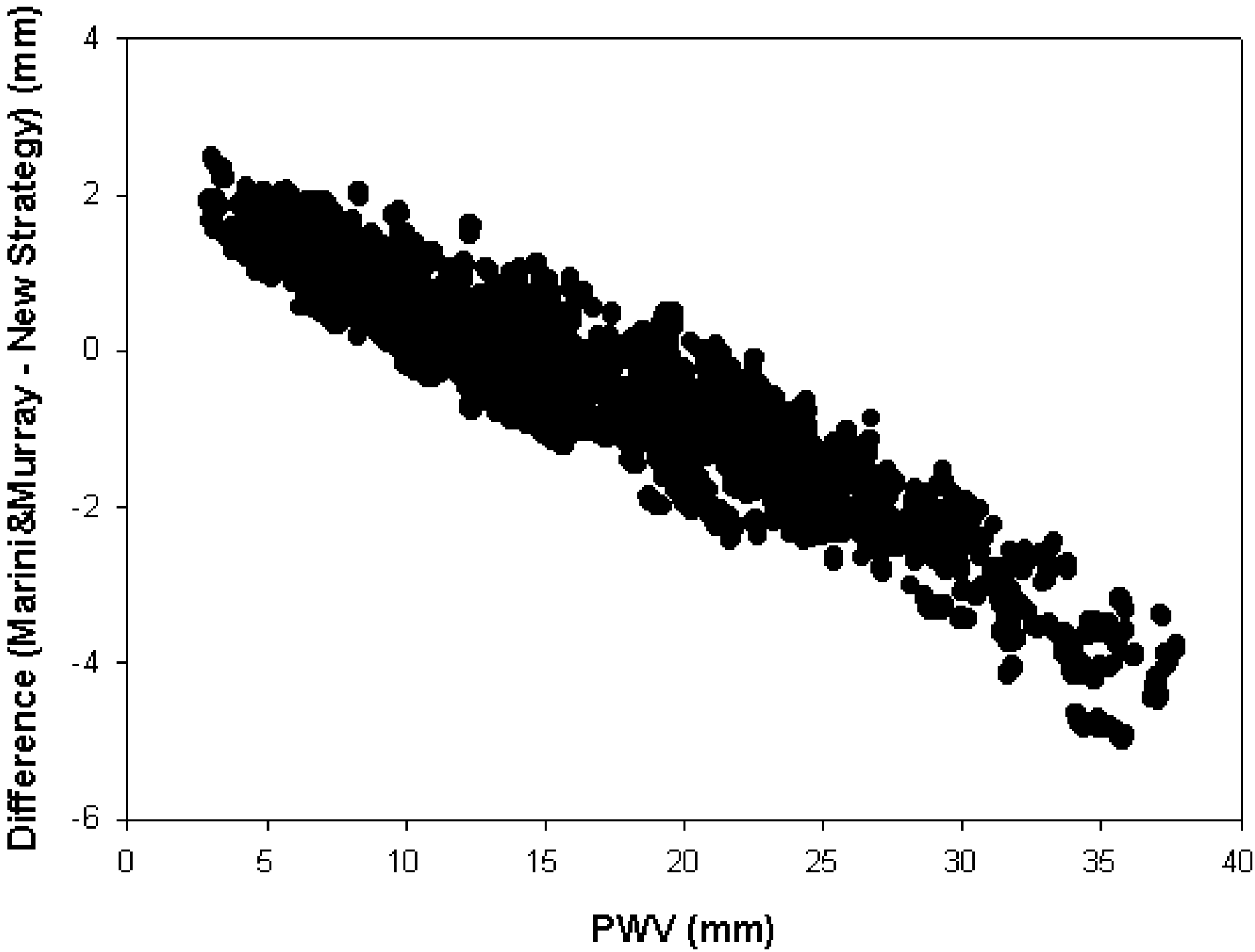
Difference (Marini&Murray - New Strategy) (mm)
4
2
0
-2
-4
-6
0
5
10
15
20
25
30
35
40
PWV (mm)

New Estimate

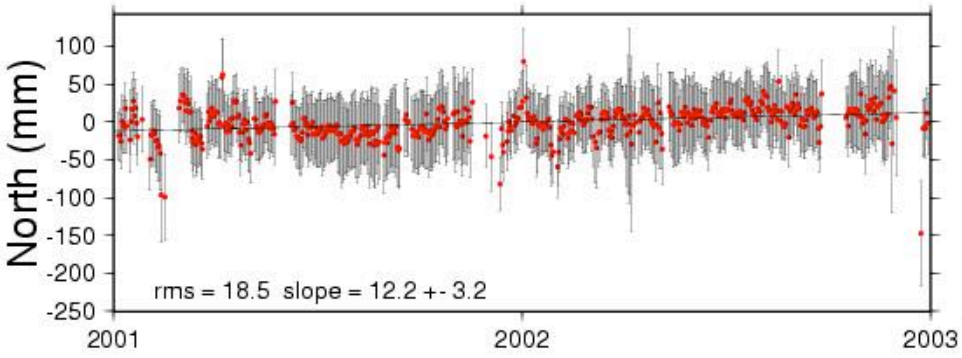

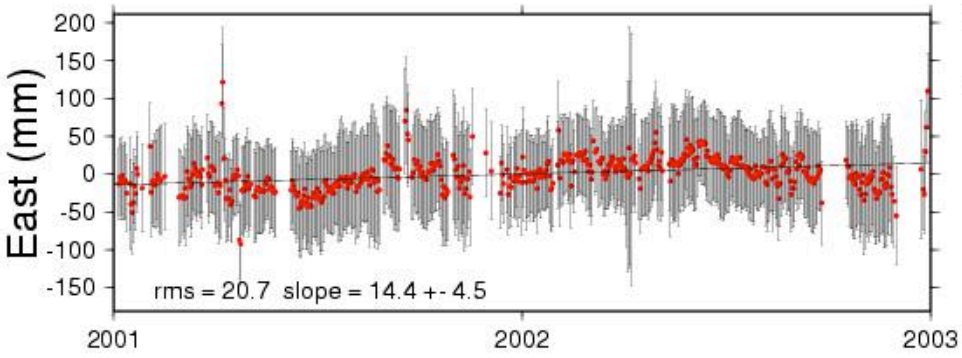

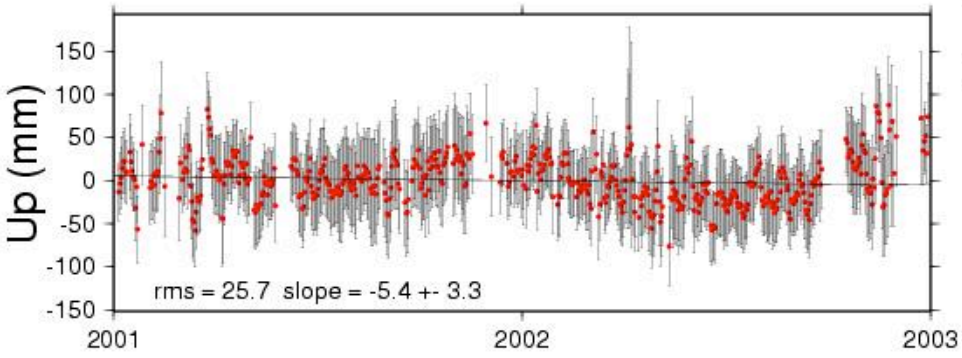

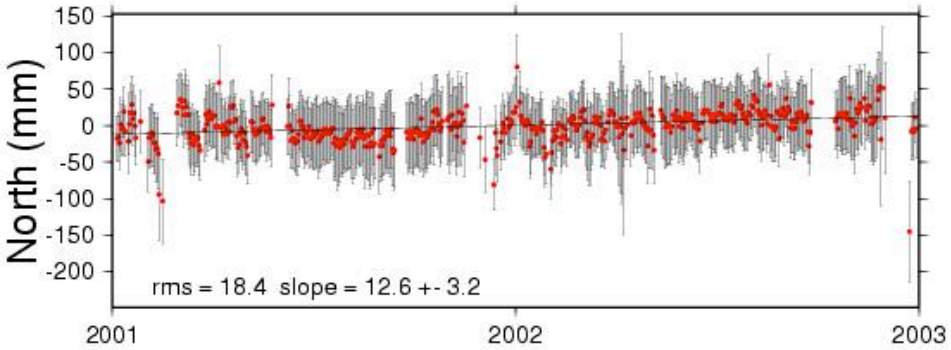

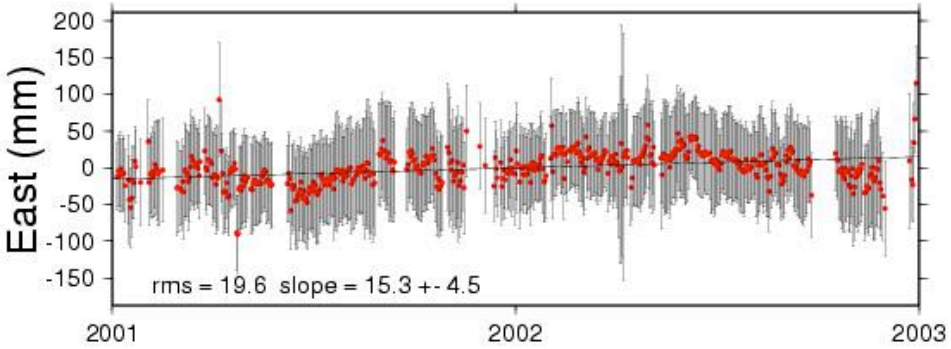

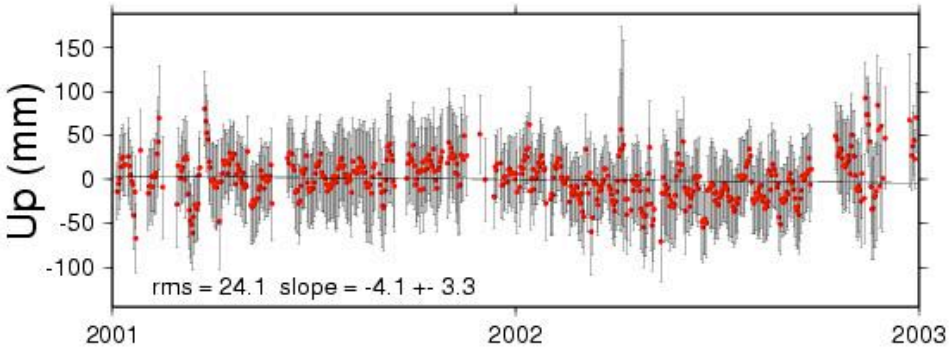

Marini & Murray

Results

- RMS of individual position estimates reduced by 0.5%, 5.3% and 6.2% in north, east and up directions respectively.
- Comparing time series with collocated VLBI: calculated station velocities improved by 10%, 70% and 23% in the north, east and up directions respectively.

Concluding remarks

- Including PWV in tropospheric delay estimation appears to improve results.
- To be done for more stations and over longer time span.
- Determine “constant” k from theory and radiosonde data instead of fitting data to Marini&Murray model (southern hemisphere?)
- Collocation of GPS, using other satellite techniques to estimate PWV at all sites (GPS results include gradients).

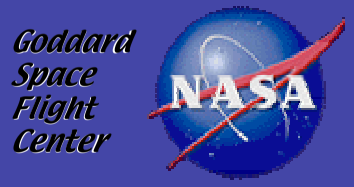

Refraction Modeling Studies in Support of ILRS Data Analysis

Erricos C. Pavlis

Glynn Hulley

JCET/UMBC - NASA/GSFC

2003 ILRS Workshop on Laser Ranging
October 28-31, 2003, Kötzting, Germany

Introduction

- UMBC/JCET is PI for AIRS instrument on NASA's AQUA spacecraft of EOS program
- When the mission is declared operational (real soon!!!), it will provide quick access to global fields of temperature, water vapor, and other geophysical environmental parameters daily in rapid mode
- Such data can be used for improved atmospheric delay modeling (e.g. gradients)

AIRS on AQUA

Illustration of the AIRS/AMSU Field-of-Regard (FOR)

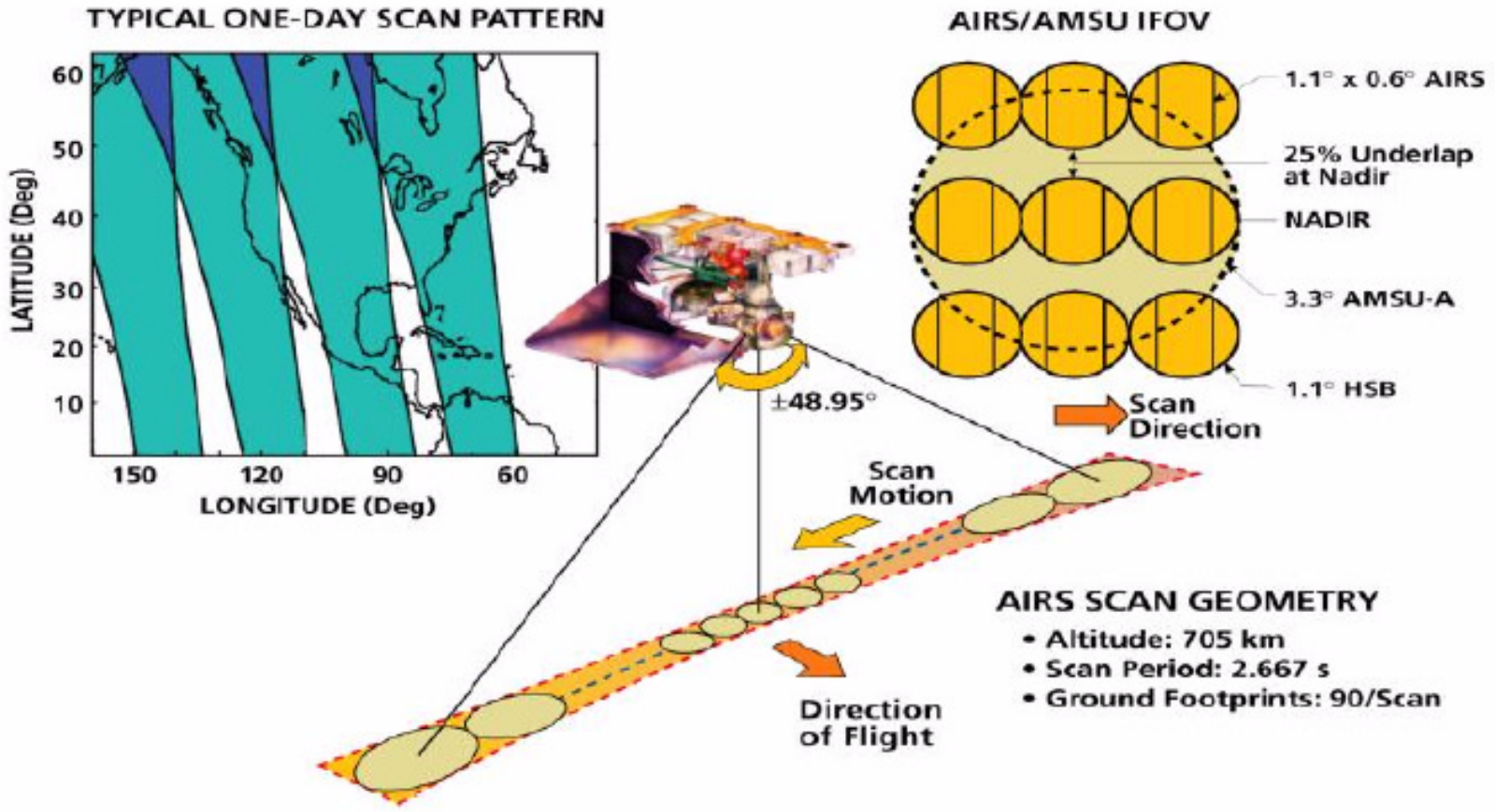

AIRS on AQUA

"First Light over the Med"

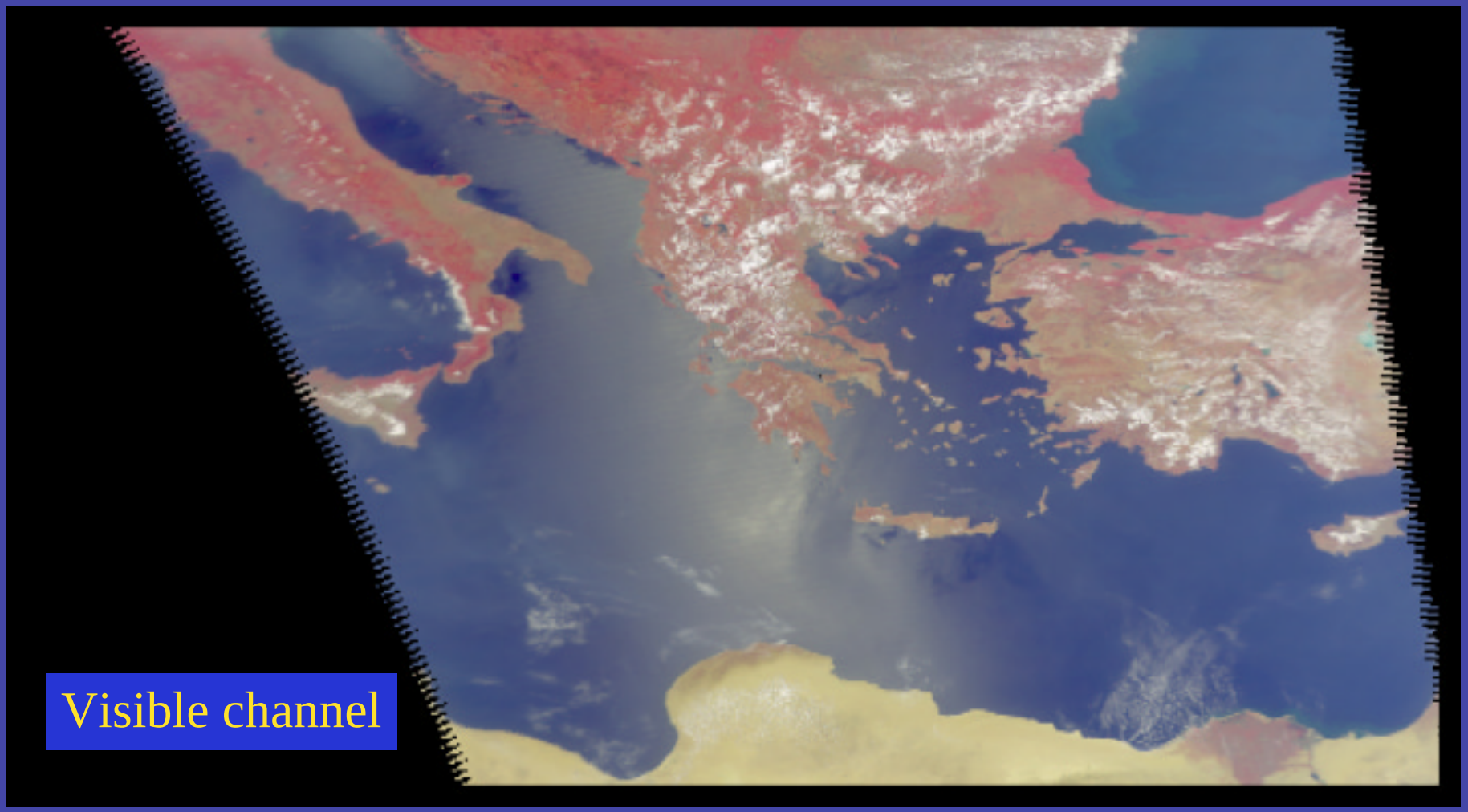

AIRS on AQUA

"First Light over the Med"

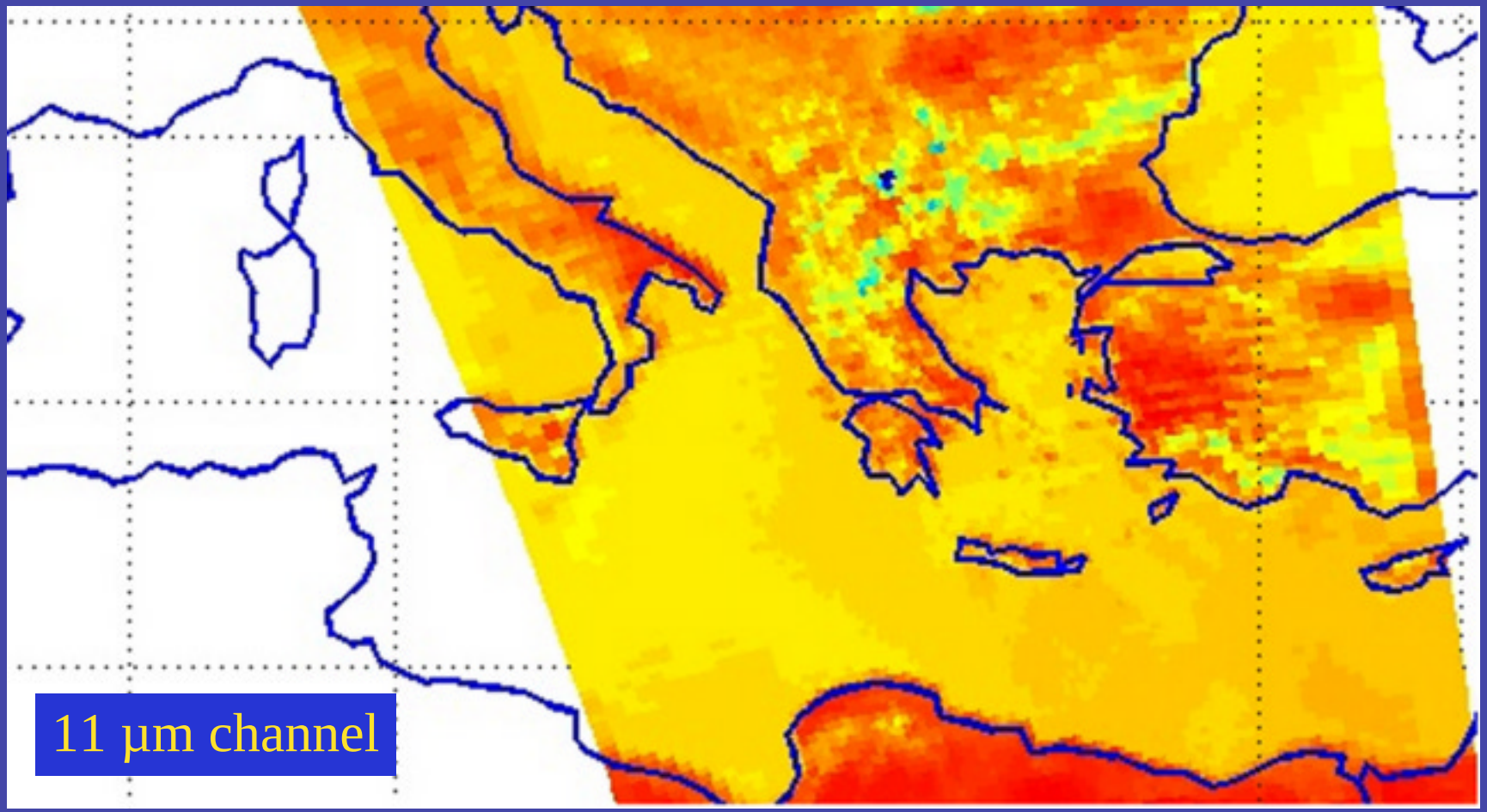

AIRS Products

Summary of Geophysical Products

$T(p)$	vertical temperature profile
$q(p)$	vertical water vapor profile ($\approx$ 8 g/kg @ surface)
$L(p)$	vertical liquid water profile (f/ AMSU/HSB)
$O_3(p)$	vertical ozone profile ($\approx$ 8 ppmv @ 6 mb)
T_s	surface temperature
$\epsilon(\nu)$	spectral surface emissivity, (*e.g.*, 0.95 @ 800 cm^{-1})
$\rho_\odot(\nu)$	spectral surface reflectivity of solar radiation
$P_{\rm cld}$	cloud top pressure for $\leq$ 2 cloud levels
$\alpha_{\rm cld,fov}$	cloud fraction for $\leq$ 2 cloud levels and 9 FOV's
CO_2	total column carbon dioxide ($\approx$ 363 ppmv)
$CH_4(p)$	methane profile ($\approx$ 1.65 ppmv)
$CO(p)$	carbon monoxide profile ($\approx$ 0.11 ppmv)

Ancillary Information Needed for Retrieval

P_s	surface pressure (f/ forecast)
θ	satellite zenith angle
$\theta_\odot$	solar zenith angle
$\epsilon_{\rm cld,\nu}$	spectral cloud emissivity for $\leq$ 2 cloud levels

AIRS Products - Coverage

October 10, 2003

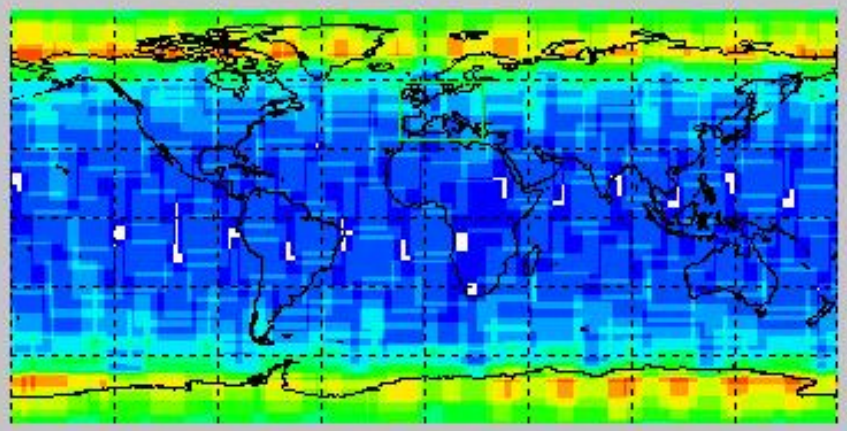

West Longitude	-11.0	South Latitude	34.0
East Longitude	25.0	North Latitude	59.0

ShiftMap

The total number of granules: 241

Color area

Number of granules per area 1 4 7 10 14

AIRS Products - Temperature

October 10, 2003

Goddard Space Flight Center

Channel: Retrieved Skin Surface Temperature

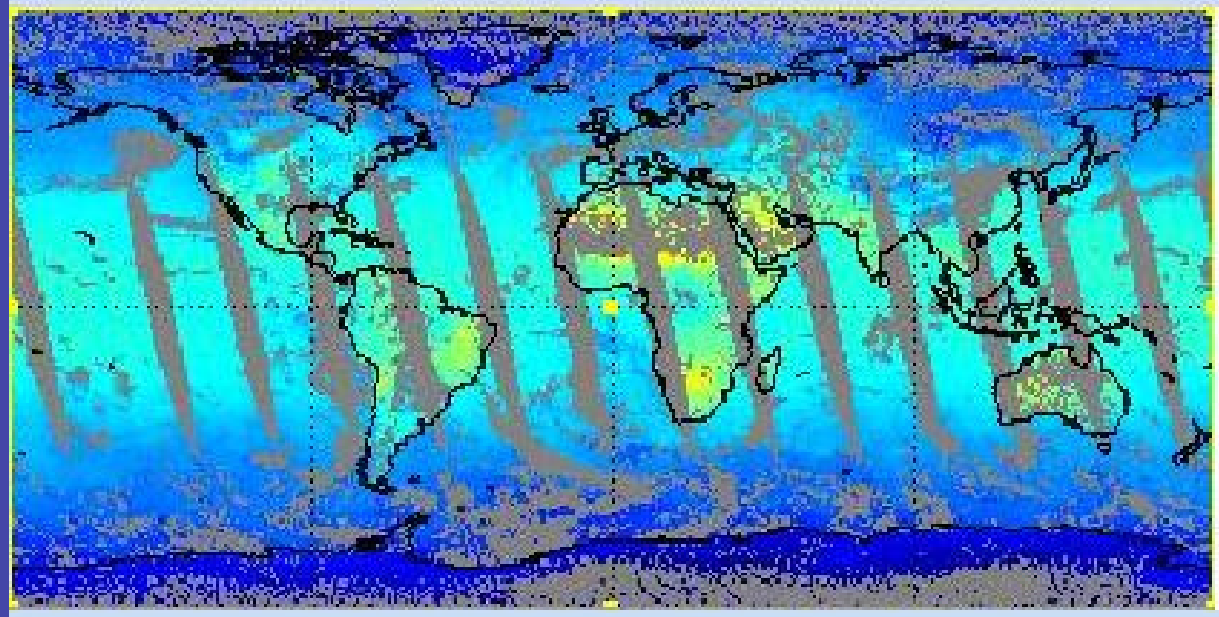

90.0 N

180.0 W 180.0 E

90.0 S

Zoom In Zoom Out

Kelvin

160.0 193.3 226.7 260.0 293.3 326.7 360.0

YEAR: 2003 MONTH: 10 DAY: 10

AIRS Products - Water Vapor

October 10, 2003

Goddard Space Flight Center

Channel: Total Water Vapor Burden

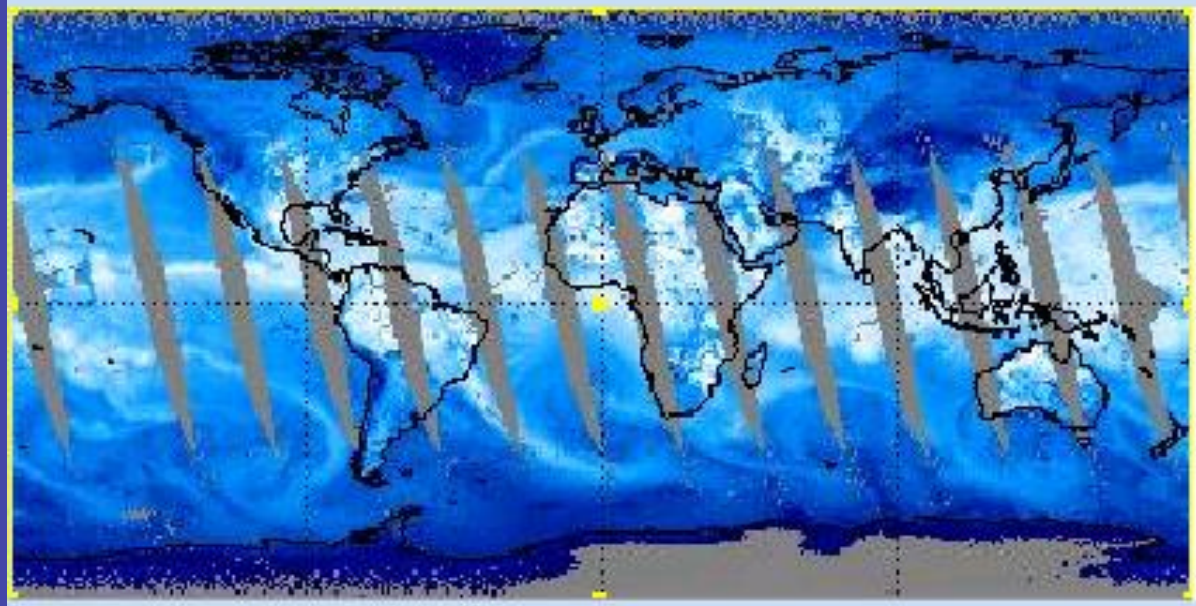

90.0 N

180.0 W 180.0 E

90.0 S

Zoom In Zoom Out

kg/m^2

0.05 16.71 33.37 50.03 66.68 83.34 100.00

YEAR: 2003 MONTH: 10 DAY: 10

H - Gradient Computation

- The system that we are developing in place retrieves the AIRS and ancillary data, several times a day around ILRS sites
- The data are preprocessed and converted to quantities useful in the derivation of the local gradients' functions (G_{NS} and G_{EW})
- The gradient formulation to be adopted is under investigation, including the possibility of an altogether brand new one.

H - Gradient Formulation

A possible model for adoption is one similar to what was used in prior studies with VLBI data:

$$\tau = m(\varepsilon)\cot(\varepsilon)[G_E \sin(\phi) + G_N \cos(\phi)]$$

according to [*Davis et al.*, 1993 and *MacMillan*, 1995]

but other approaches are being examined and in the computations we will adopt the [*Mendes et al.*] mapping function $m(\varepsilon)$, instead of the MTT one.

Summary

- Progress is hindered by incomplete and possibly incorrect data algorithms used in the temperature and WV retrievals and thereby a delay in releasing the data to the community

- JCET has access to a limited number of special (validated) data sets from NOAA, which will be used in the first step for developing, testing and validating this approach.

Atmospheric Refraction at Optical Wavelengths: Problems and Solutions

An update

V. B. Mendes
LATTEX and Departamento de Matemática
Faculdade de Ciências da Universidade de
Lisboa, Portugal (vmendes@fc.ul.pt)

Erricos C. Pavlis
JCET and NASA Goddard Space Flight Center
Univ. of Maryland Baltimore County
Baltimore, Maryland (epavlis@JCET.umbc.edu)

2003 Laser Ranging Workshop
October 28-31, 2003, Kötzting, Germany

Outline

- Background
- Zenith delay models
- Mapping Functions
- Wavelength dependence
- Conclusions

Atmospheric Delay

$$d_{atm} = \int_{ray} (n-1)\, ds + \left[\int_{ray} ds - \int_{vac} ds \right]$$

Propagation Delay

Ray Bending

Atmospheric Delay

$$d_{trop} = d_h^z \cdot m_h(\varepsilon) + d_w^z \cdot m_w(\varepsilon)$$

Hydrostatic Zenith Delay

Hydrostatic Mapping Function

Wet Zenith Delay

Wet Mapping Function

Atmospheric Delay

$$d_{atm} = d^{z}_{atm} \cdot m_t(\varepsilon)$$

Mapping Function

Zenith Total Delay

$$d^{z}_{atm} = 10^{-6} \int_{r_s}^{r_a} N \, dz$$

Zenith Delay Models

- Marini-Murray (1973)
- Saastamoinen (1973) – Hydrostatic and Wet
- Yan and Wang (1999) – Hydrostatic and Wet
- ***Revised version of Ciddor-Mendes – Hydrostatic & Wet***

	P	T	e (RH)	φ	H	λ
MM	✓	✓	✓	✓	✓	✓
SA	✓		✓	✓	✓	✓
YW	✓	✓	✓	✓	✓	✓
CM	✓	✓	✓	✓	✓	✓

Mapping Functions

- Marini-Murray * (1973) – Total **(includes ZD determination)**
- Saastamoinen * (1973) – Hydrostatic and Wet
- Yan and Wang* (1999) – Total
- FCULA (2002) * * – Total (uses surface Temperature)
- FCULB (2002) * * – Total (no meteorogical data)
- FCULZ (2002) * * – as FCULA, **(includes ZD determination with Saastamoinen model)**
  - * Wavelength dependent
  - ** Optimized for 532 nm

Ray-tracing

- Radiosonde data (1998) from a ~180 site global network
- Group refractivity computed according IAG resolutions
- Computer procedures described in Ciddor (1999) and Ciddor and Hill (1999)
- **Compressibility factors computed with full accuracy**
- Water vapor pressure computed using Davis (1992)
- Wavelengths: 355nm , 423nm, 532 nm, 847 nm, 1064 nm

New Zenith Delay Formulation

with Wavelength Dependence

$$d_{atm}^{z} = 10^{-6}\int_{r_s}^{r_a} N\, dz = \int_{r_s}^{r_a}(n-1)\, dz$$

$$d_{atm}^{z} = 10^{-6}\int_{r_s}^{r_a} N_h + 10^{-6}\int_{r_s}^{r_a} N_{nh}$$

Ciddor's 1996 formulation for the refractive index:

$$(n-1) = \left(\frac{\rho_a}{\rho_{axs}}\right)\left(n_{gaxs}-1\right) + \left(\frac{\rho_w}{\rho_{ws}}\right)\left(n_{gws}-1\right)$$

n_{gaxs} is the group refractive index for dry air component

n_{gws} is the group refractive index for water vapor component

New Zenith Delay Formulation

with Wavelength Dependence (cont.)

$$(n-1) = \left(\frac{\rho_a}{\rho_{axs}}\right)\left(n_{gaxs}-1\right) + \left(\frac{\rho_w}{\rho_{ws}}\right)\left(n_{gws}-1\right)$$

Dry air vs. Std. Dry air density ratio

WV vs. Std. pure WV density ratio

Ciddor's 1996 formulation for these ratios involves the use of the compressibility factor of moist air which in earlier implementation was ignored

New Zenith Delay Formulation

with Wavelength Dependence (cont.)

$$Z = 1 - \left(\frac{P}{T}\right)\left(a_0 + a_1 t + a_2 t^2 + \left(b_0 + b_1 t\right) x_w + \left(c_0 + c_1 t\right) x_w^2\right) + \left(\frac{P}{T}\right)^2 \left(d_0 + e_0 x_w^2\right)$$

Z enters the formulation for these ratios in a normalized form which is near unity, but not always:

$$\frac{\rho_a}{\rho_{axs}} = \left(\frac{T_d}{P_d}\right)\left(\frac{Z_d}{Z}\right)\left(\frac{P}{T}\right) - \left(\frac{T_d}{P_d}\right)\left(\frac{Z_d}{Z}\right)\left(\frac{e}{T}\right)$$

$$\frac{\rho_w}{\rho_{ws}} = \left(\frac{T_w}{P_w}\right)\left(\frac{Z_w}{Z}\right)\left(\frac{e}{T}\right)$$

Assessment of Wavelength Dependence of New Model

New Zenith Delay Formulation

ZD from older models vs. Ciddor-Mendes

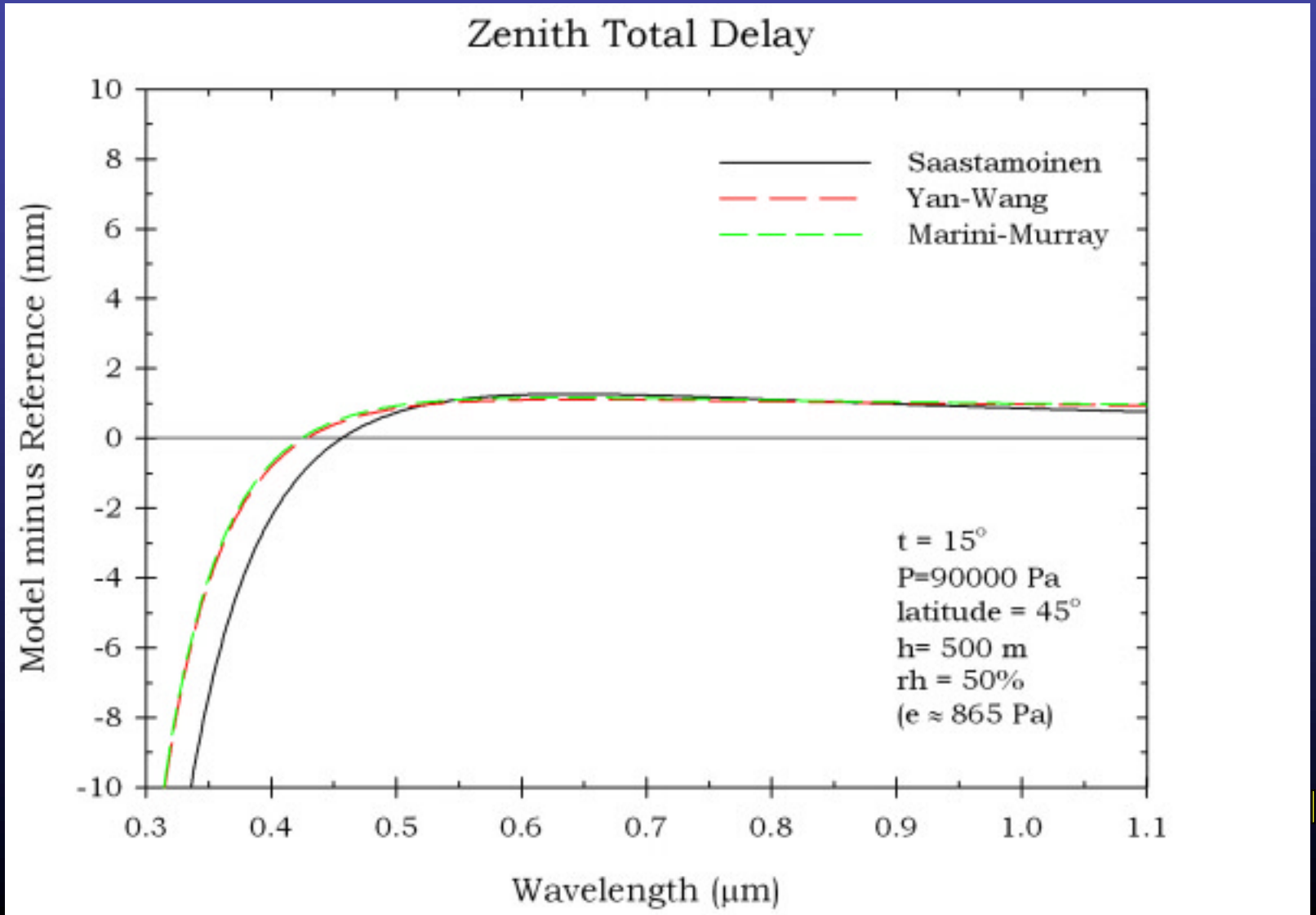

New Zenith Delay Formulation

ZD from older models vs. Ciddor-Mendes

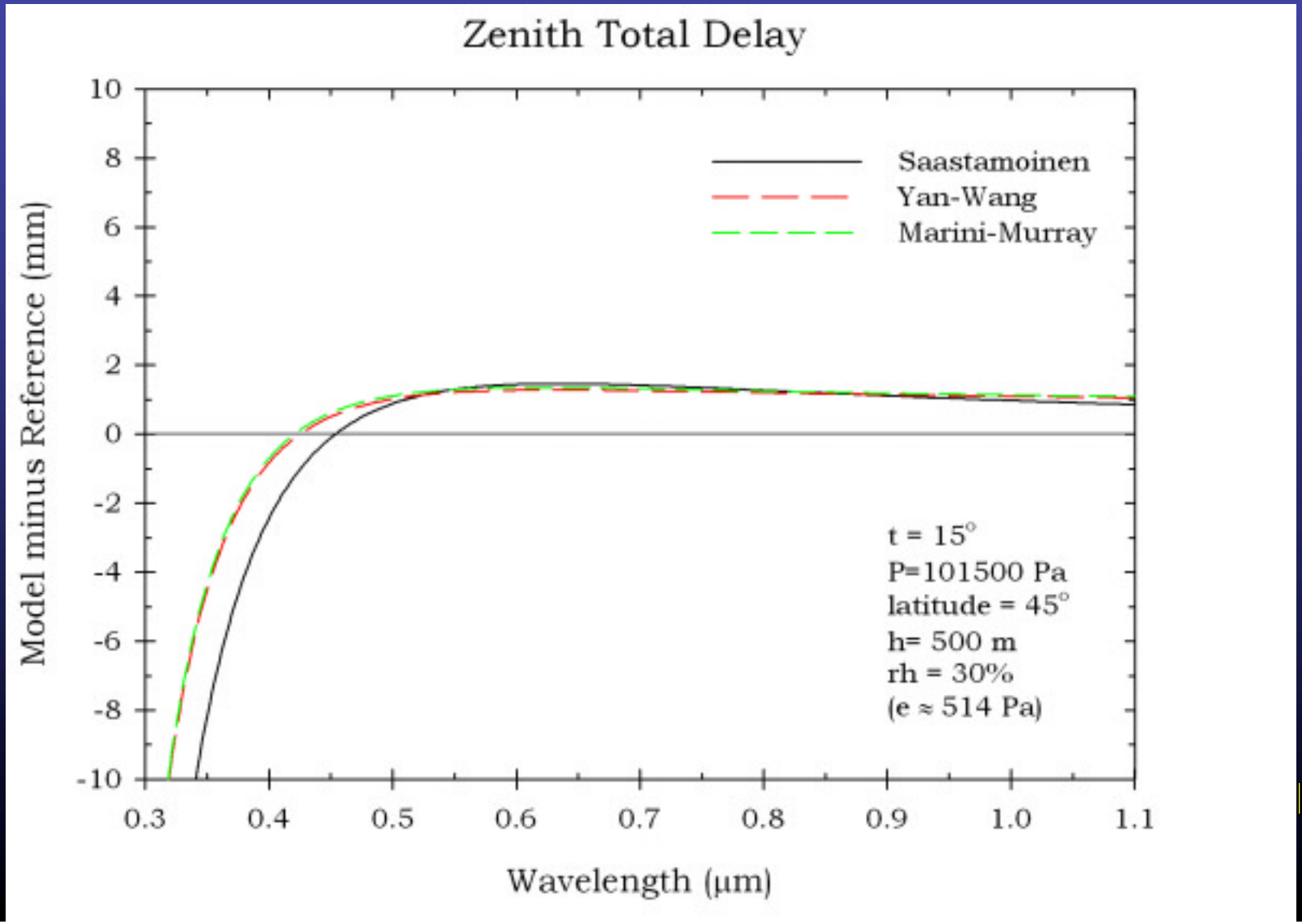

New Zenith Delay Formulation

ZD from older models vs. Ciddor-Mendes

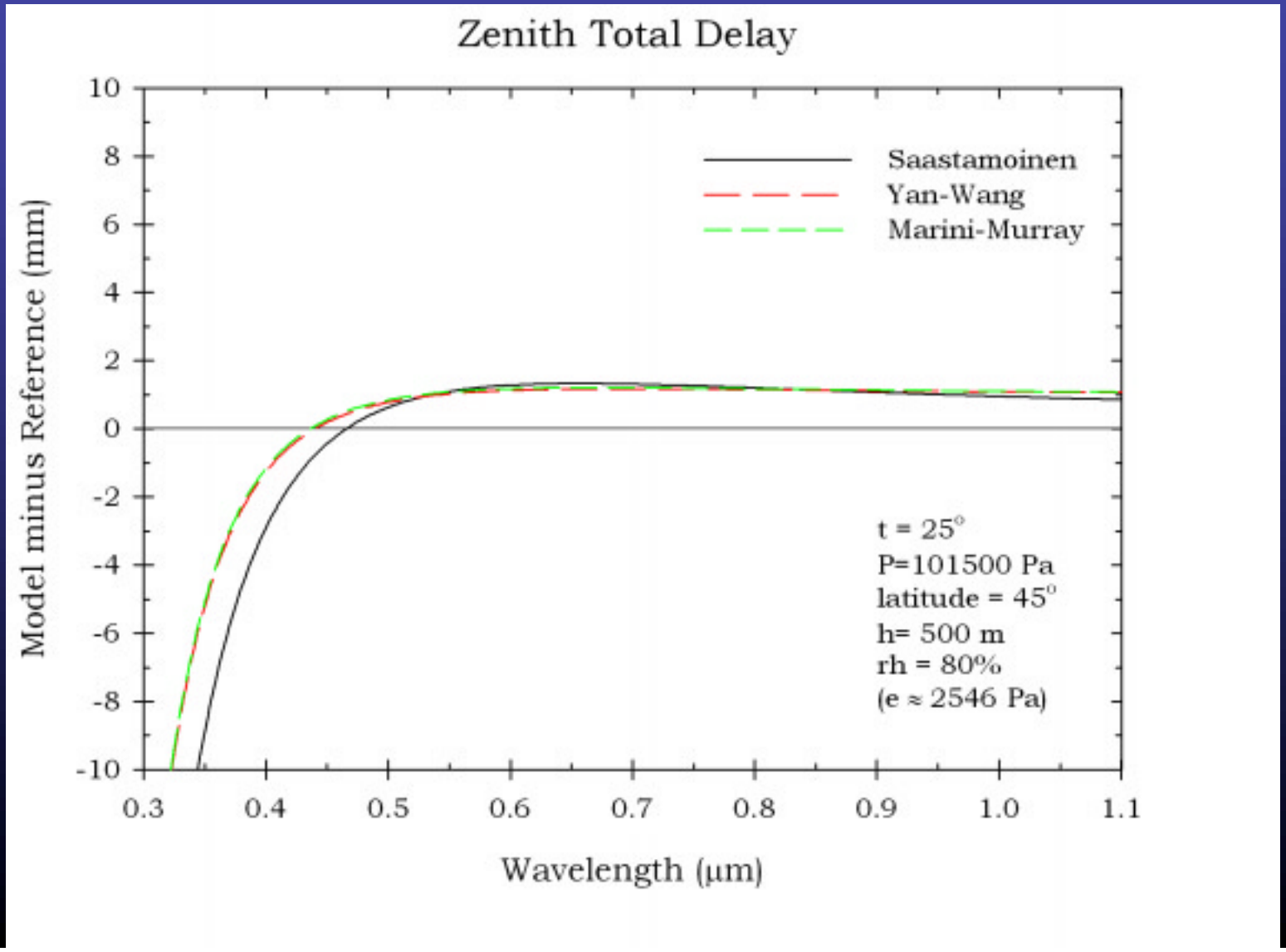

New Zenith Delay Formulation

Radiosonde Comparisons

Marini - Murray

532 nm

694 nm

423 nm

847 nm

355 nm

1064 nm

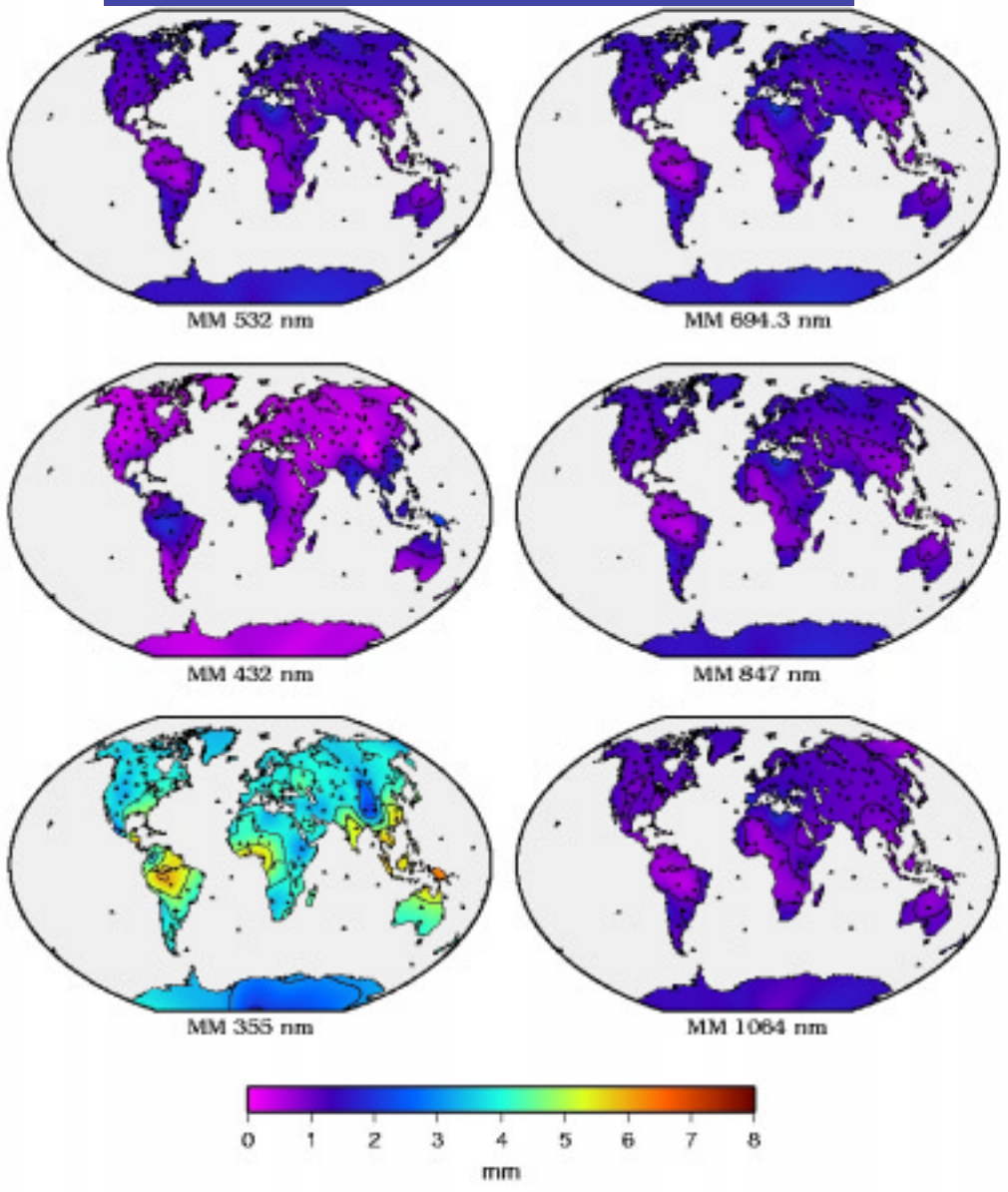

New Zenith Delay Formulation

Radiosonde Comparisons

Saastamoinen

532 nm

423 nm

355 nm

694 nm

847 nm

1064 nm

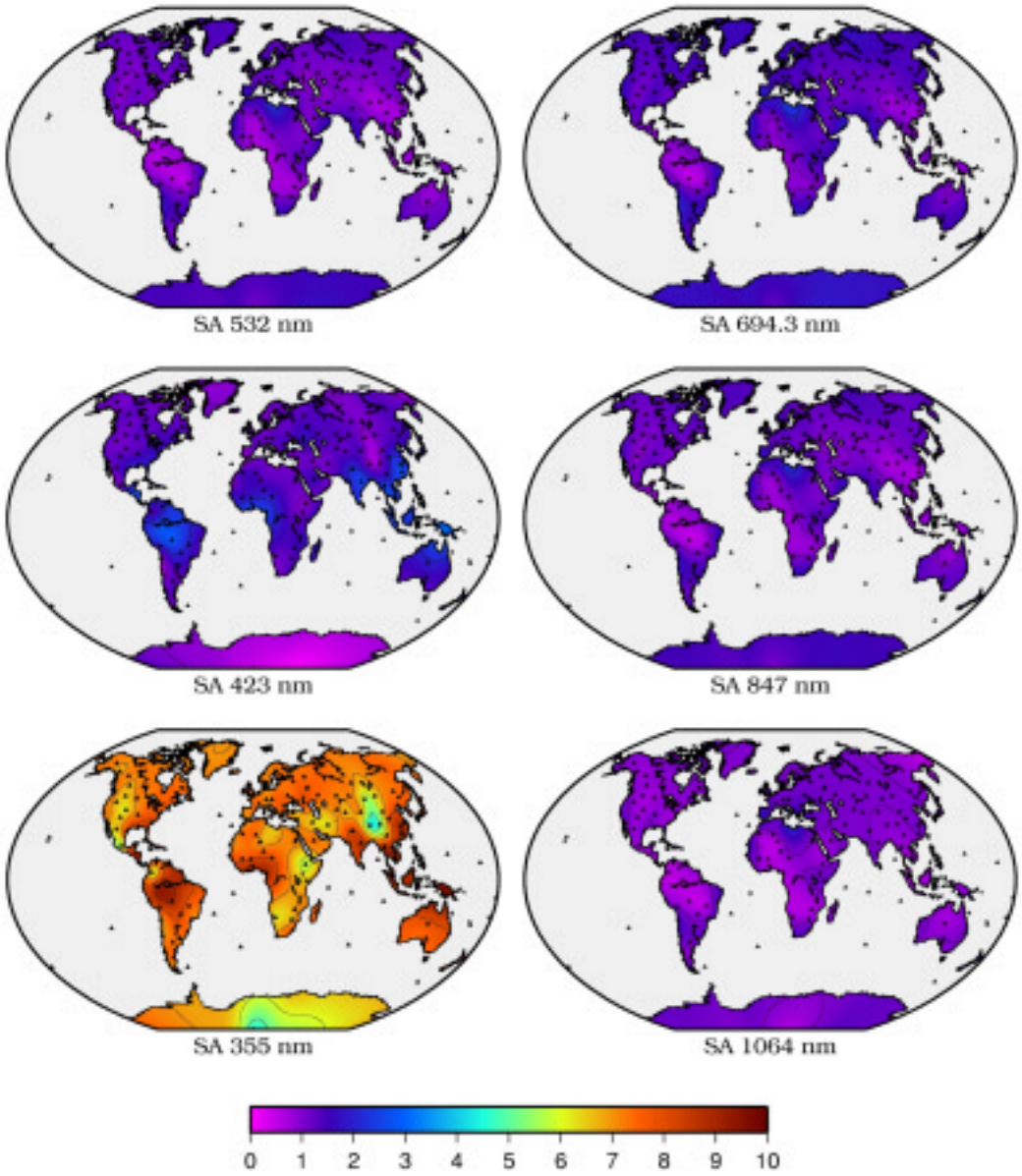

New Zenith Delay Formulation

Radiosonde Comparisons

Ciddor-Mendes

532 nm

423 nm

355 nm

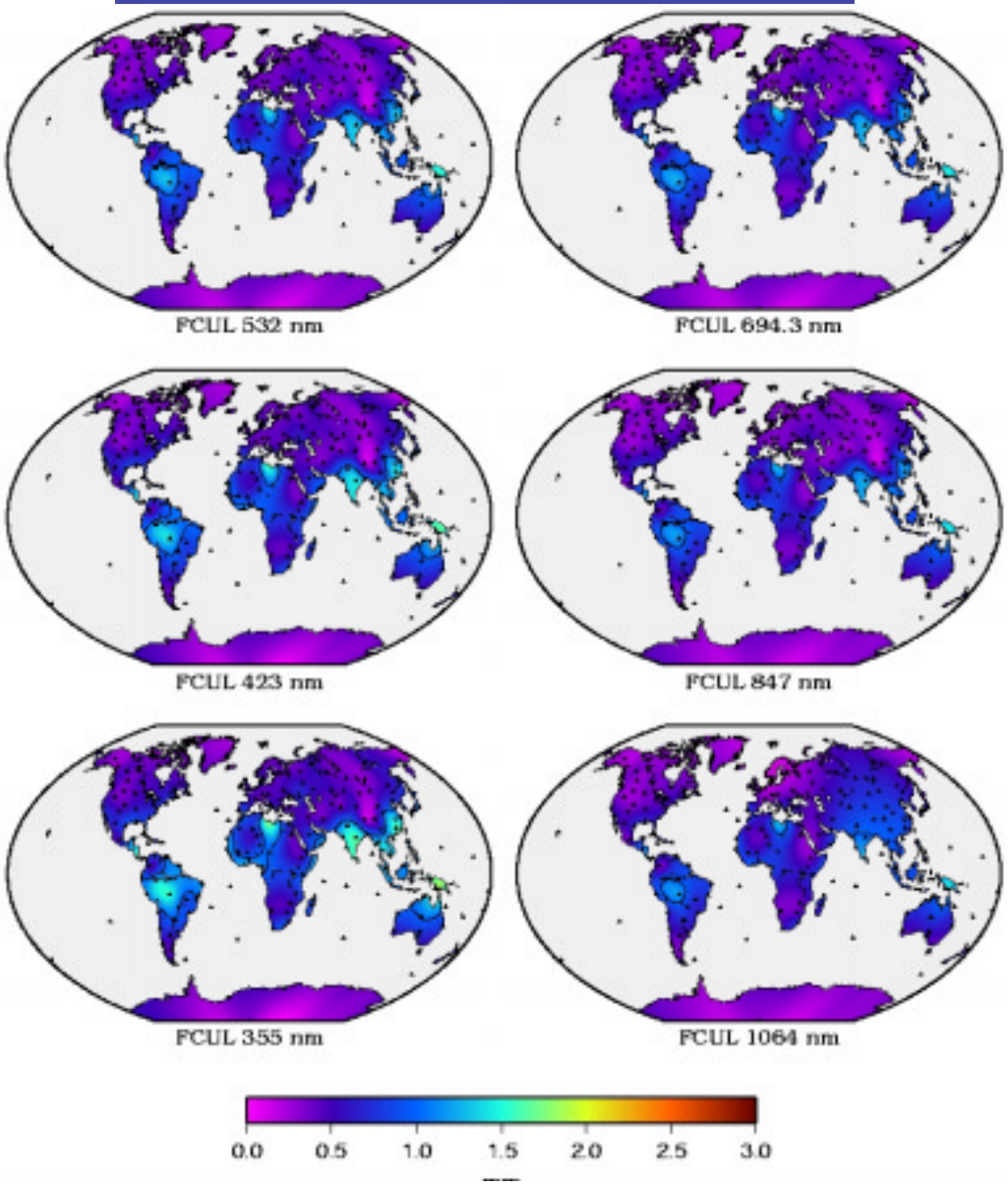

694 nm

847 nm

1064 nm

New Zenith Delay Formulation

Radiosonde Comparisons

Marini-Murray

Ciddor-Mendes

1064 nm

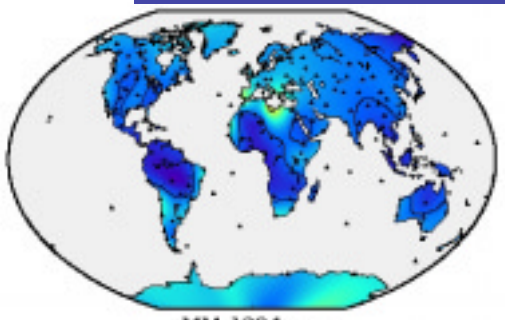

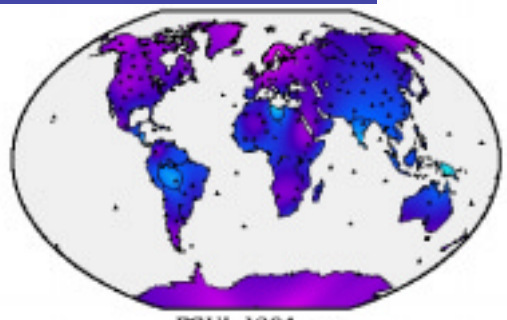

1064 nm

532 nm

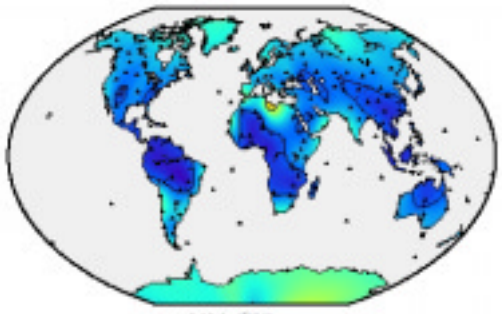

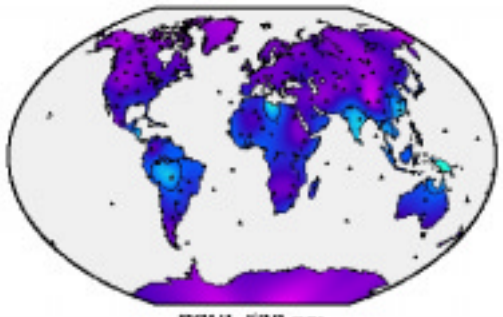

532 nm

423 nm

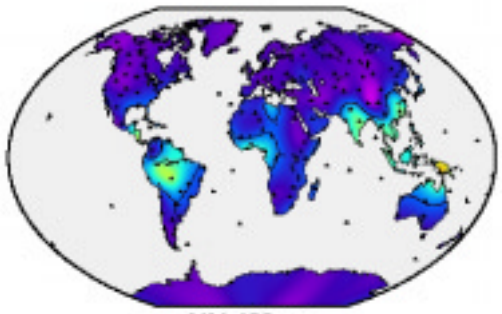

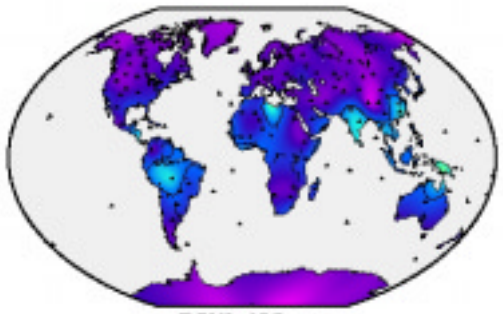

423 nm

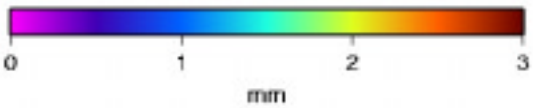

New Zenith Delay Formulation

Radiosonde Comparisons

Saastamoinen

1064 nm

532 nm

423 nm

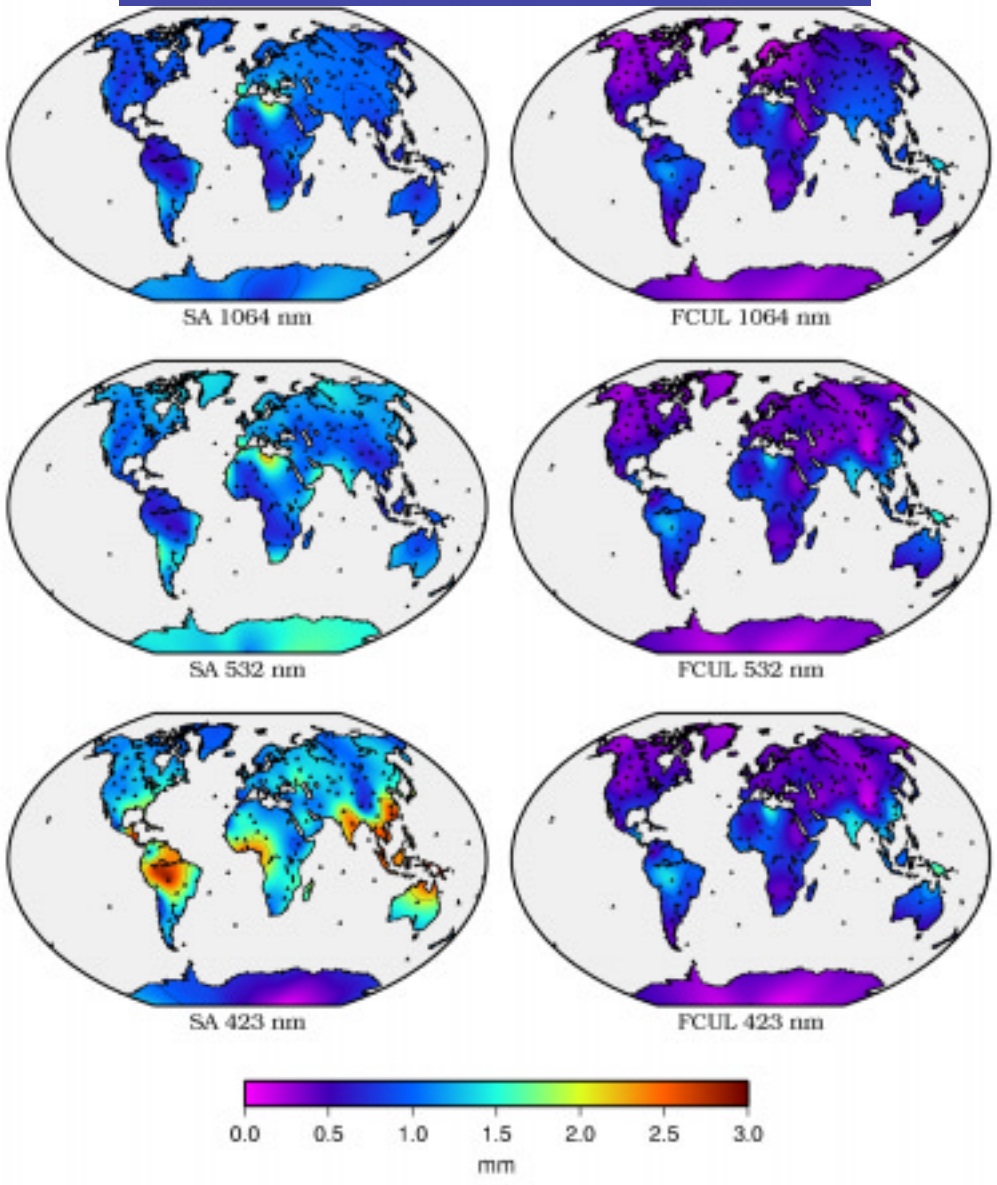

Ciddor-Mendes

1064 nm

532 nm

423 nm

Some concluding remarks ...

- Old zenith delay models exhibit a bias at the ~ 1 mm level for the wavelength interval 500 to 1100 nm (*WRT radiosondes*)
- For wavelengths < 500 nm, the bias changes exponentially, reaching the extreme value of ~10 mm at 355 nm
- The new and old models were compared to a global radiosonde data set (1 yr) and the conclusions are:
  - M-M shows a variable behavior, with best performance around the 423 nm wavelength, worst at 355 nm
  - **Saastamoinen is particularly poor at 355 nm, reaching 10 mm !**
  - C-M (**new**) shows a fairly uniform behavior across the specrum
  - With mapping function performance degrading with increasing zenith angles, these errors will be greatly enhanced in these cases
- SLR testing with low elevation data is in progress, but **PLEASE, observe LOW and release data you may have at wavelengths other than the green !!!**

Atmospheric contribution to the SLR jitter

I.Procházka, K.Hamal, L. Kral, J.Mulacova

Czech Technical University in Prague,

G.Kirchner, F.Koidl

Satellite Laser Station, Graz, Austria

presented at

International Laser Ranging Service Meeting, Koetzting, October 28-30, 2003

Goals:

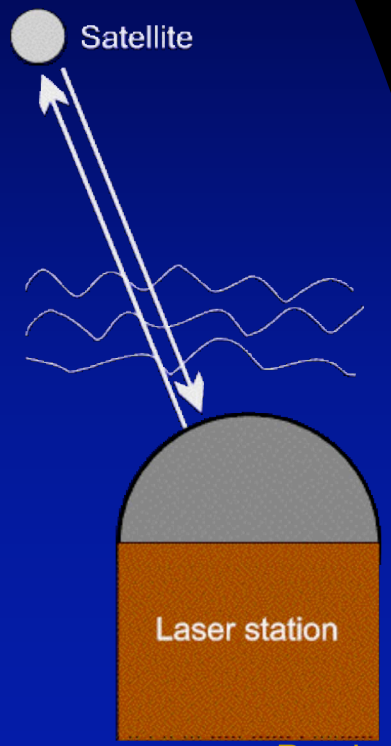

- Evaluate the contribution of the atmosphere fluctuations to the overall SLR jitter budget
- Create and test a model of propagation of a picosecond laser pulse through atmosphere in Satellite Laser Ranging (SLR)
- Verify the model on existing laser ranging data
- propose new laser ranging experiments to verify the model

Motivation

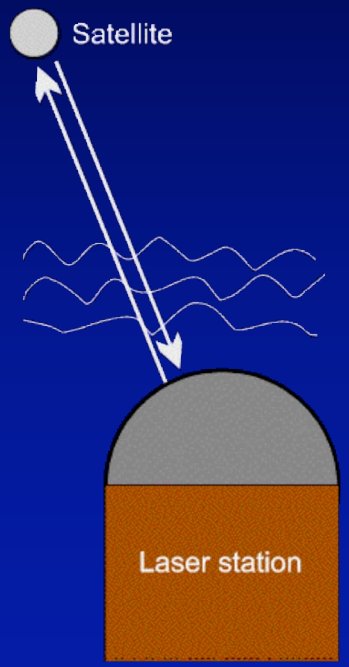

- The observed discrepancy in laser ranging precision (jitter) for different path length and geometry
- atmospheric fluctuation is one of the probable sources of random error contributors

Prochazka,Hamal, Kral,Mulacova,Kirchner, Koidl,ILRS, Koetzting, Oct.28-31, 2003

Geometrical Optics Approach

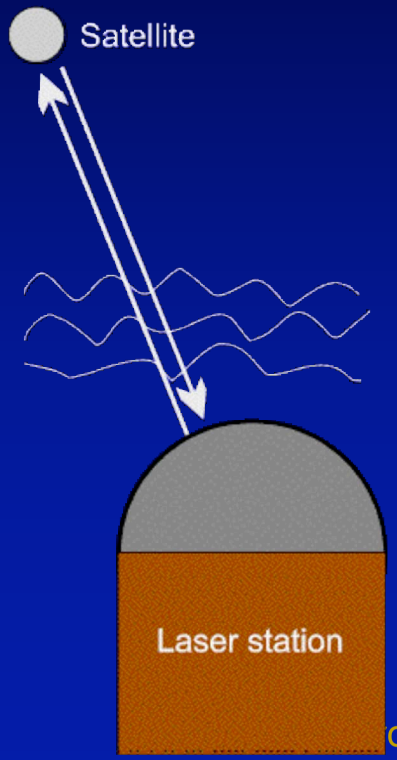

- C. Gardner [(1)] derived analytical formula for mean-square pathlength fluctuation (mm ..cm)

- $< \Delta L^2 > = 26.31\ C_n^2(0)\ L_o^{5/3}\ L_e$

  (Greenwood-Tarazano spectral model used)

- $C_n^2(0)$ ... initial value of refractive index structure constant (turbulence strength at start)
- new estimates of C_n^2 available since '76
- L_o ... outer scale of turbulence
  L_e ... effective pathlength (weighted by $C_n^2(\Delta)$)

(1) C. S. Gardner, Effects of random path fluctuations on the accuracy of laser ranging systems, Appl.Opt. Vol.15, No.10, pp.2539–2545, 1976

Geometrical Approach - Effective Pathlength

$$L_e = \frac{1}{C_n^2(0)} \int_0^L C_n^2(\xi) d\xi$$

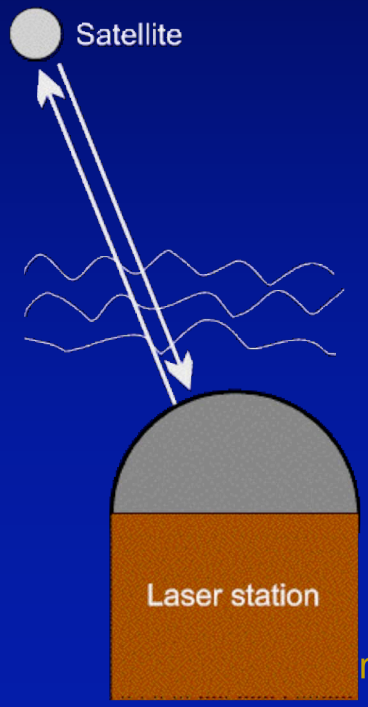

- L ... distance to target
- **Horizontal path:**
  C_n^2 constant ⇒ $L_e = L$
- **Slant path to space:**
  Hufnagel-Valley model of C_n^2 height dependence used to evaluate L_e

Geometrical Approach - Slant Path to Space

- atmospheric mass influence,
- ranging jitter dependence on the zenith distance and station elevation above the sea level

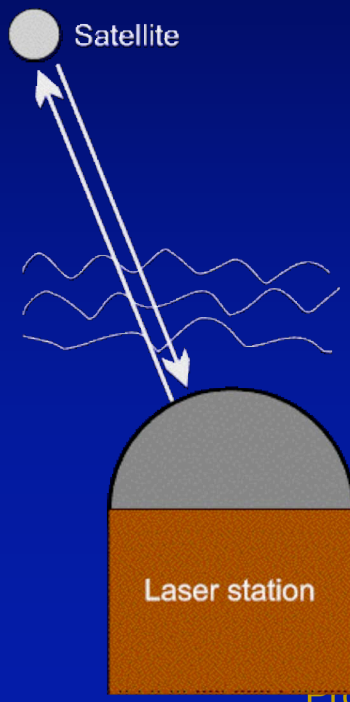

station at a sea level

elevation 2000 m above the sea level

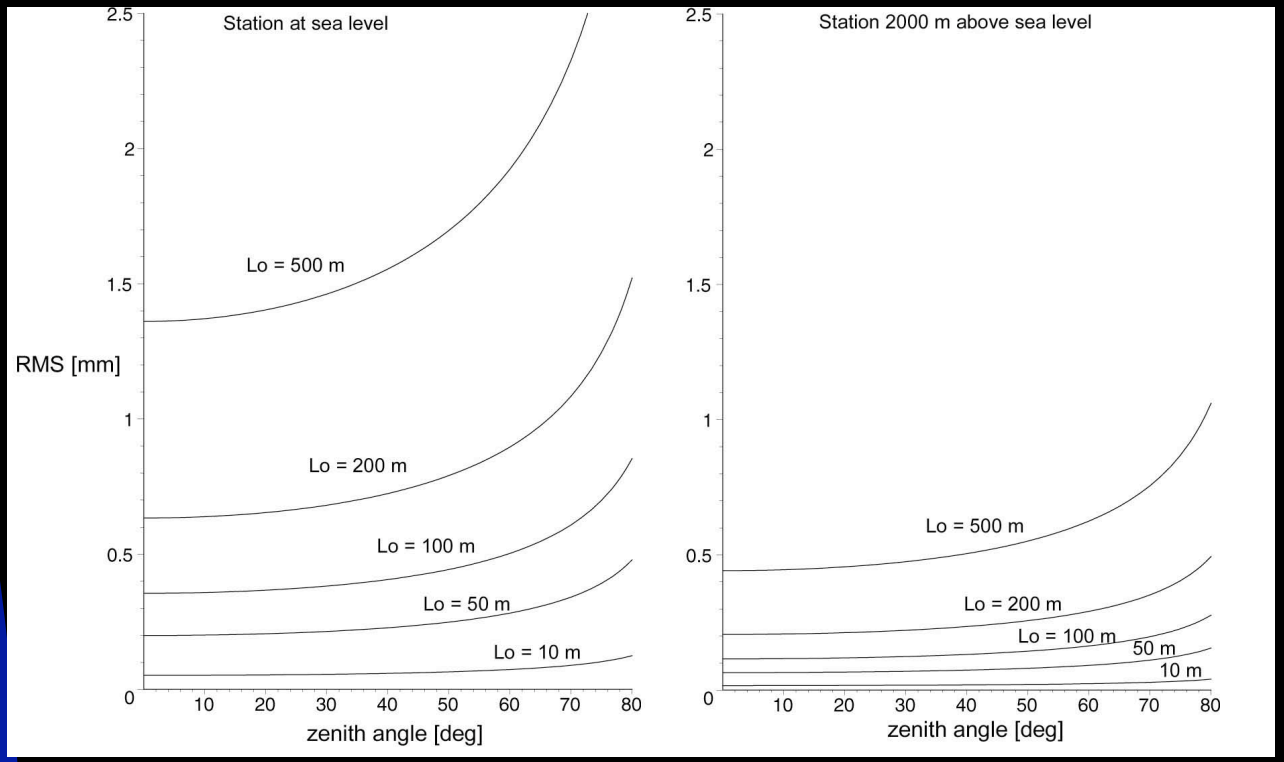

Experiments at SLR Graz

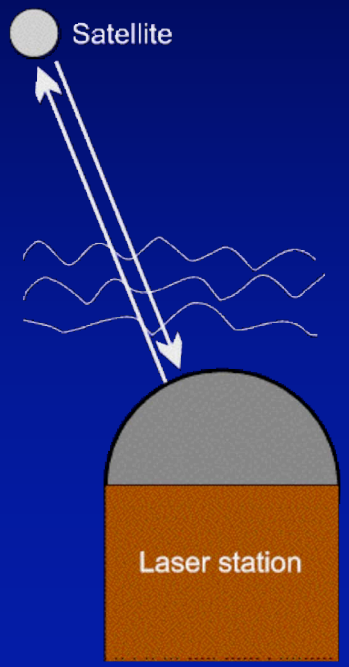

- horizontal path
  - laser ranging / 2 kHz reprate, 1 mm rms/
  - seeing measurements / via CCD, 30 msec time res./
- slant path
- SLR

Experiment - seeing versus ranging jitter

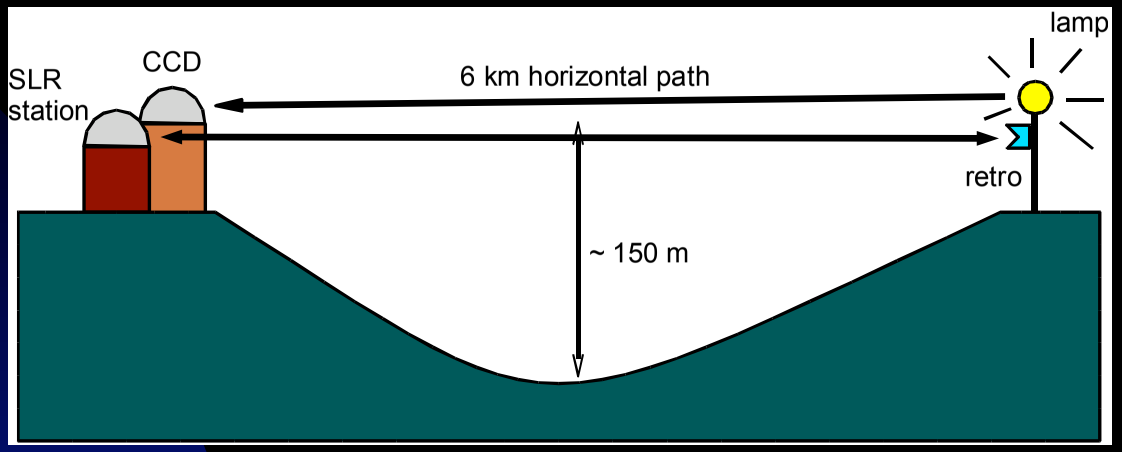

- MEAD 20” telescope
- CCD Star Tracker with image processing SW
- geometry resolution 0.8 ‘’ / pixel
- direction resolution 0.01 ‘’
- integration time 30 - 100 ms

Experiment - horizontal seeing results

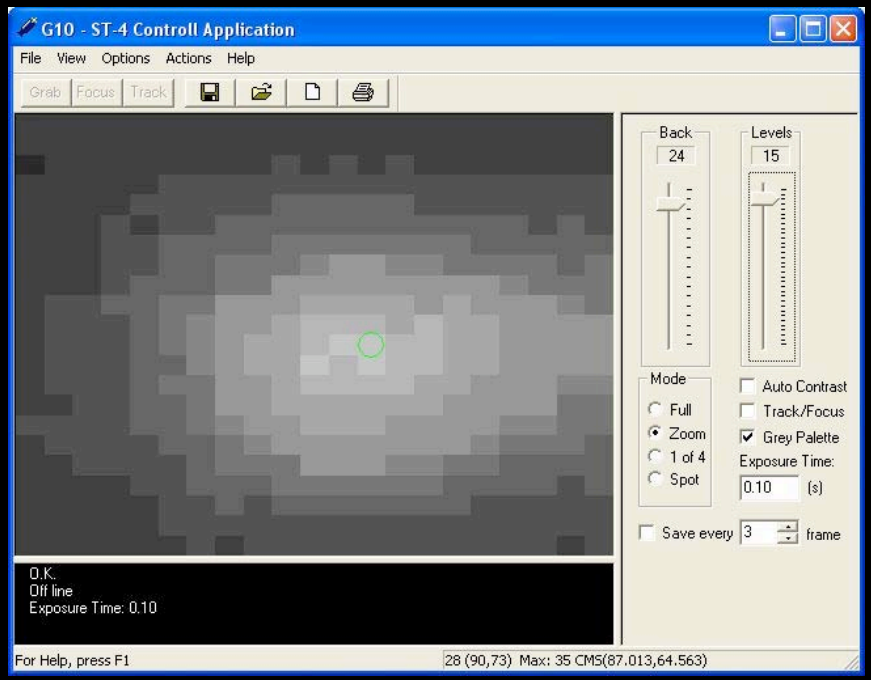

direction fluctuations

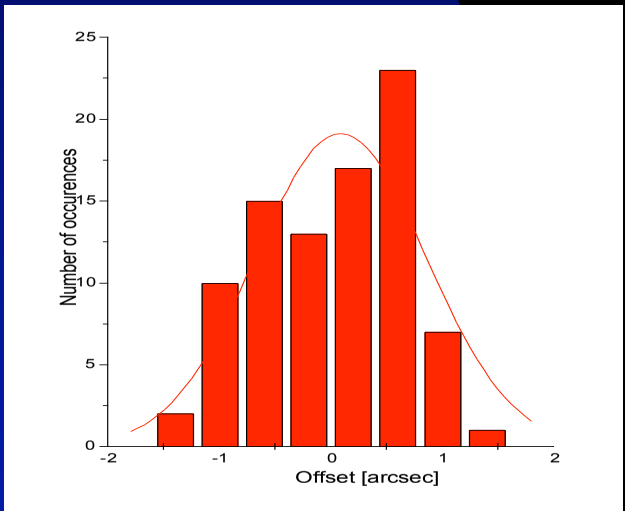

arc seconds

- FWHM = 1.9 arc sec
- equal for both 30 and 100 ms integration

Prochazka,Hamal, Kral,Mulacova,Kirchner, Koidl,ILRS, Koetzting, Oct.28-31, 2003

Horizontal path laser ranging

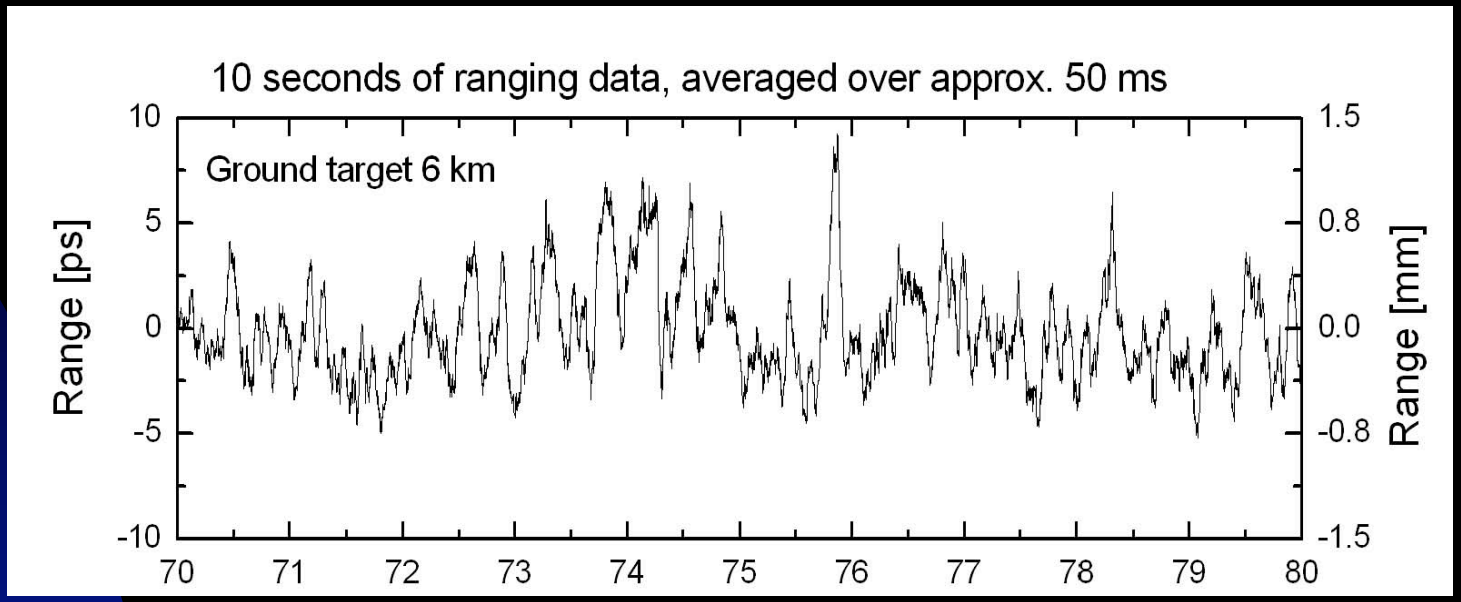

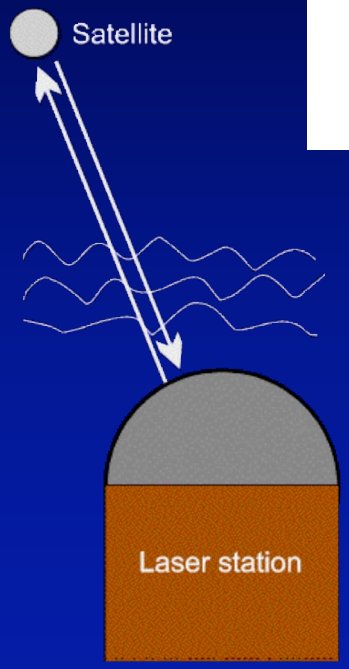

- single shot precision ~ 1 mm RMS
- displayed moving average /50 ms in time/
- main fluctuation time constant ~ 130 ms
- atmospheric fluctuation induced ranging jitter ~ 0.4 mm

- well correlates with the horizontal seeing data and model by Gardner

Prochazka,Hamal, Kral,Mulacova,Kirchner, Koidl,ILRS, Koetzting, Oct.28-31, 2003

Satellite laser ranging, ERS 2, Envisat

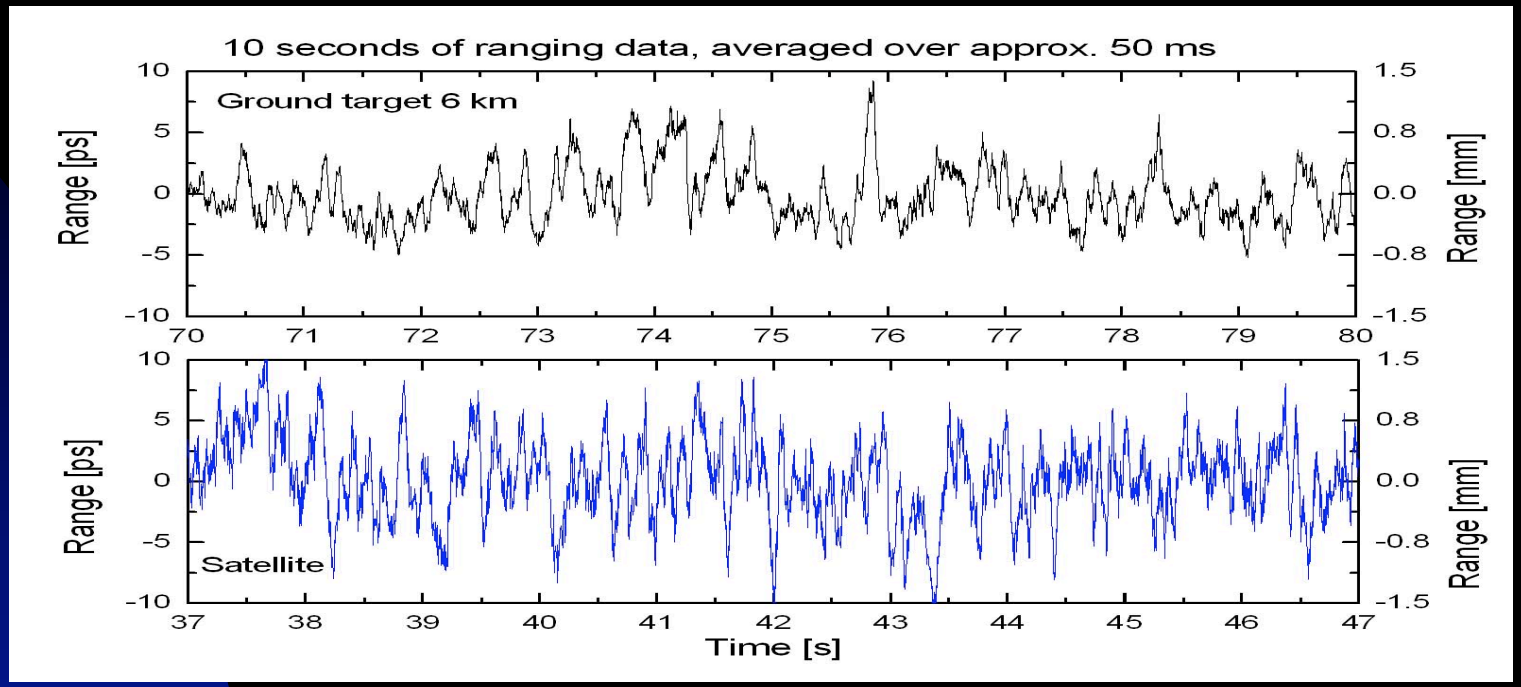

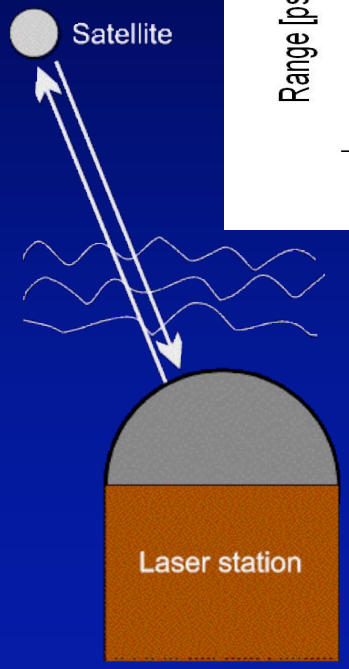

- single shot precision 2.8 mm RMS
- the time structure is less pronounced, 130 ms characteristic time may be identified
- the amplitude is similar to 6 km ground target

Prochazka,Hamal, Kral,Mulacova,Kirchner, Koidl,ILRS, Koetzting, Oct.28-31, 2003

Conclusion

Low Elevation Survey

Station	Limitation	Success	Comments
Arequipa	20	N/A	mountians mask at 6 degs + safety/security at 20 degs
Beijing	5	5	can go down to 5 degs (mountains at this elevation)
Borowiec	20	N/A	structural (az dep.), signal strength
Changchun	<10	??	can range down to 5 degrees assuming enough signal strength
Concepcion	18	11	have tracked LAGEOS down to 11 degs, safety limit is 18 degs
FTLRS	15	??	15 degs for LEO and 30 degs for LAGEOS
Golosiiv	15	??	can range down to 15 degs in certain azimuths
Grasse	5	5	**Closed**
Grasse (LLR)	5	5	can track LAGEOS and high sats. down to 5 degs
Graz	5	5	can range down to 5 degrees
Greenbelt	10	TBD	**approved for down to 10 degs, approval for other NASA sites pending**
Haleakala	20	N/A	structural interference from our dome at 20 degs
Hartebeesthoek	10	??	mountians mask as 10 degrees
Herstmonceux	30	N/A	only track down to 30 degrees for safety reasons
Katsively			**no response**
Koganei (CRL)	15	??	trees and buildings at 15 degrees
Komsomolsk			**no response**
Kunming	15	15	can track down to 15 degs
Lviv	20	N/A	structural limitations at 20-25 degs
Maidanak 2			**no response**
McDonald	20	N/A	need safety approval and HW/SW and structurl limitations
Metsahovi2	8	??	Some satellites to 8 deg., not Lageos or Jason
MLRO	20	N/A	safety and hardware/software issues below 20 deg
Monument Peak	20	N/A	safety, hardware/software
Mt. Stromlo2	15	??	site limit of 20 degs, perhaps can get approval at 15 degs
Potsdam	30	N/A	trees
Potsdam3	20	12	have gotten LAGEOS returns down to 12 deg, safety restrictions at 20 degs
Riga	15	??	can range down to 12 degs in the North, 18 degs other directions, 30 degs for LAGEOS
Riyadh	20	N/A	safety, hardware/software issues, system physical limit is 2 degs
San Fernando	0	??	no known physical or site mask limitations
Shanghai	25	N/A	25 degrees at current location
Shanghai, new site	0	N/A	can range to the horizon at new location
Simeiz	10	<15	can track down to 10 to 15 degs, but not LAGEOS
Simosato	15	15	can range down to 15 degrees, below 15 there are safety issues
Tahiti	20	N/A	safety, hardware/software
TROS-China	3	??	can range down to 3 degrees, signal strength limitations
Wettzell	10	N/A	safety limit is 20 deg, system capability is 10 degs
Wuhan			**no response**
Yarragadee	15	N/A	airspace current limit is 15 degs, can perhaps go lower
Zimmerwald	10	yes	horizon mask varies between 0 and 20 degs

Session 9

Developing and Implementing the New Consolidated Prediction Format

Cancelled

Session 10

LEO Data Submission - How Fast Is Fast Enough?

Graham Appleby, Rolf Koenig

Data Latency

- Fast turnaround required to support:
  - Very LEO Satellites Time Bias
- How fast is fast enough?
- Network and Computer problems can delay data for a few to many hours
- EOP and Station Positions are determined weekly each Monday morning using data through Sunday Night

Data Latency Chart (Median Latency)

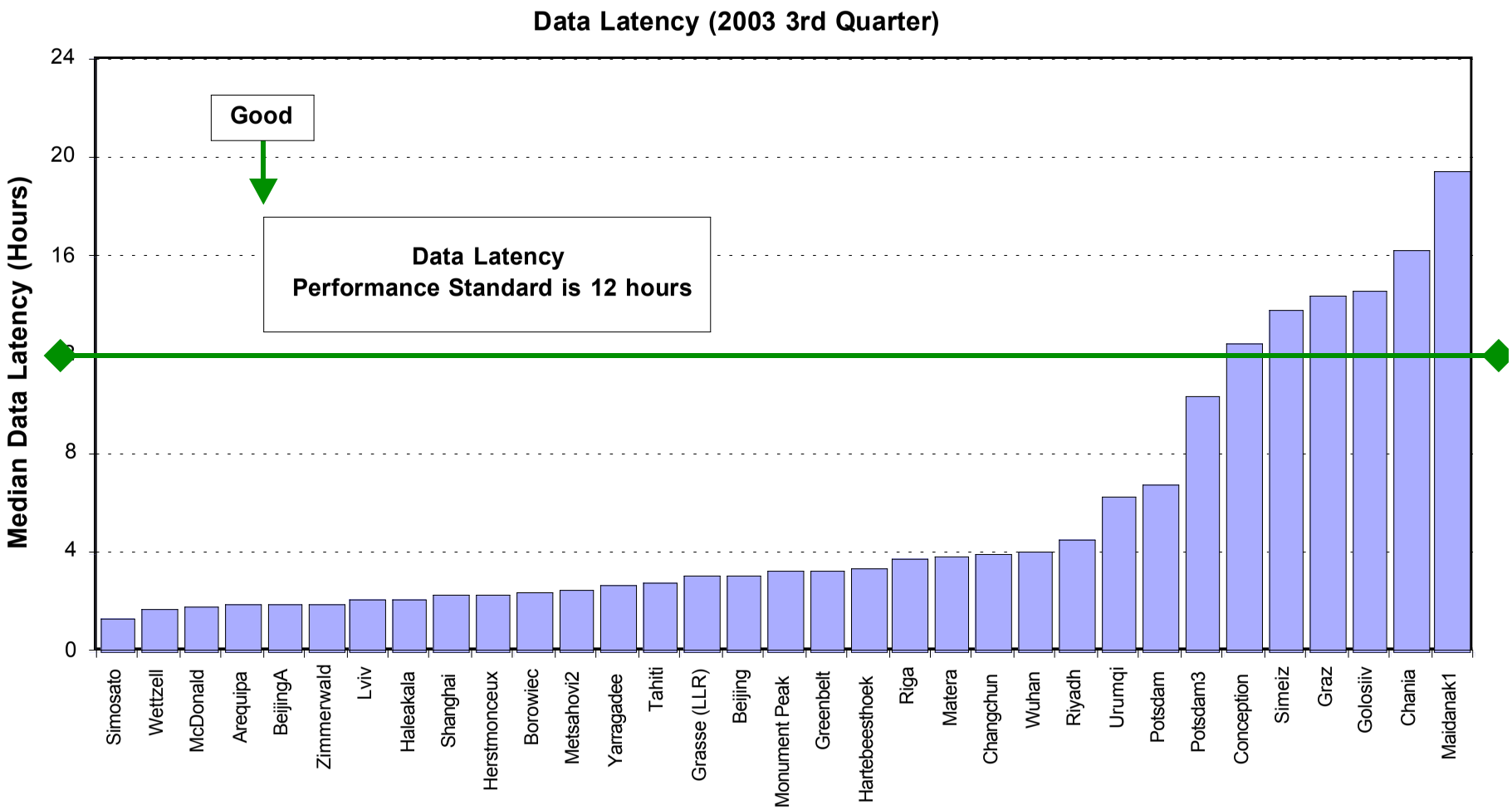

Data Latency Chart (Individual Passes)

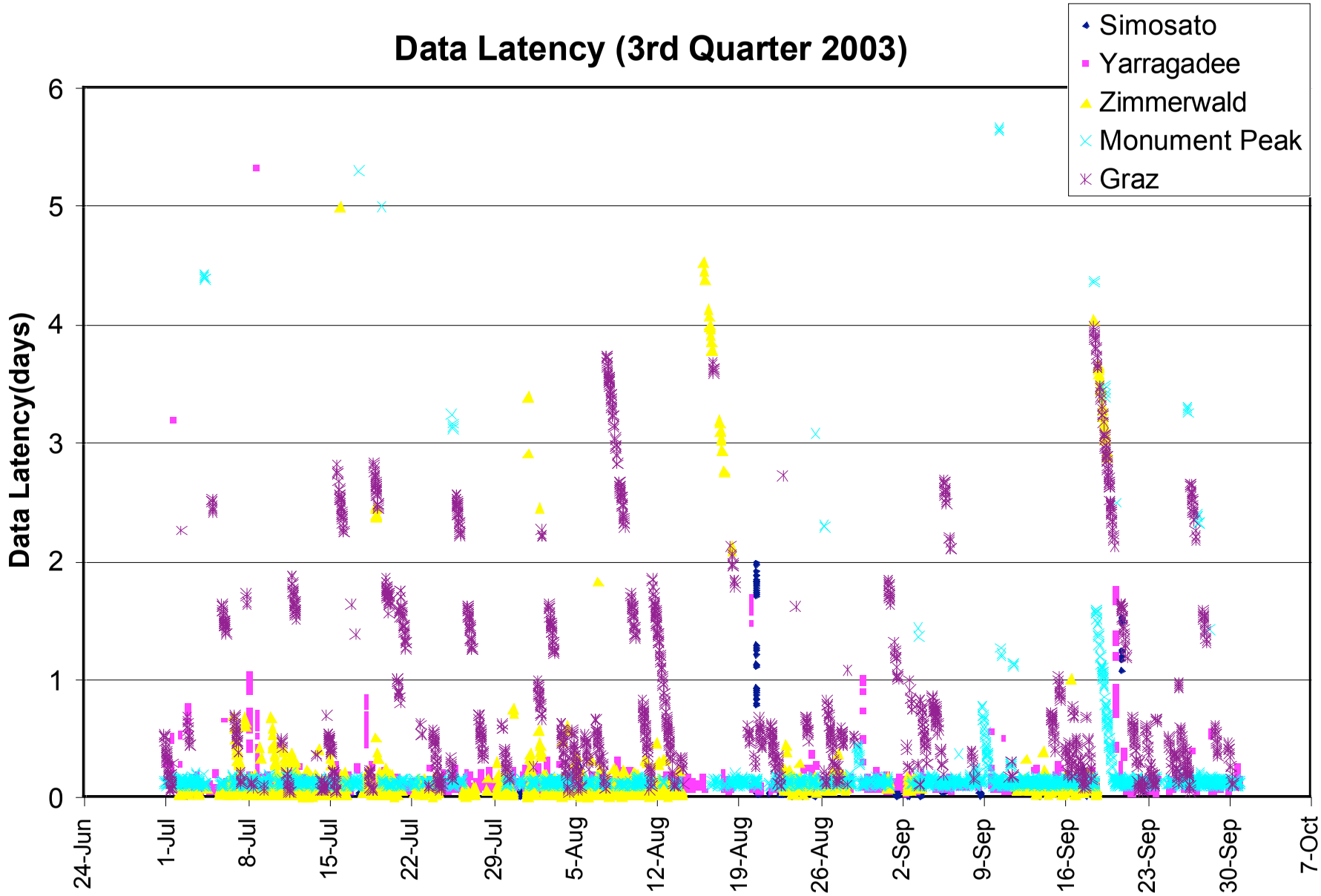

Session 11

Spacecraft Center-of-Mass Modeling

Graham Appleby, Toshi Otsubo

CoM Implementation Issues

Van Husson, HTSI
ILRS CB

Background

- In Nov 1996, SLR CSTG accepts Husson and Sinclair's proposal for reporting system configuration changes via configuration files and NP indicators
- Never got 100% participation
- ILRS Site Logs contain the same information as the configuration files, but have no pointers (i.e. no indexes) to the NP Flags

Configuration and Detector Flags

- Multi-Detector Systems
  - Herstmonceux (interchange SPAD and CSPAD)
  - Zimmerwald (blue-CSPAD, IR- PMT)
  - Wettzell (APD for LAGEOS and HEO, MCP for LEO and LAGEOS)
  - McDonald (MCP for LEO and LAGEOS, PMT for HEO and Lunar)
  - TIGO at Concepcion (CSPAD, APD, PMT)
  - Matera (MCP and streak camera/MCP)
- Systems one with detector, but different threshold levels (HSLR and non-HSLR)
  - NASA MOBLAS (Yarragadee, Greenbelt, Haleakala, Hartebeesthoek, Monument Peak, Tahiti)

Configuration Reporting Problems

- Configuration files are not current or missing and flags are inverted and/or mis-understood
  - EUROLAS
    - Herstmonceux, Zimmerwald, Wettzell, Concepcion, San Fernando, Matera, Potsdam3, Grasse (LLR), FTLRS
  - NASA
    - No problems
  - WPLTN
    - Beijing, BeijingA, Changchun

Network Data Screening Levels

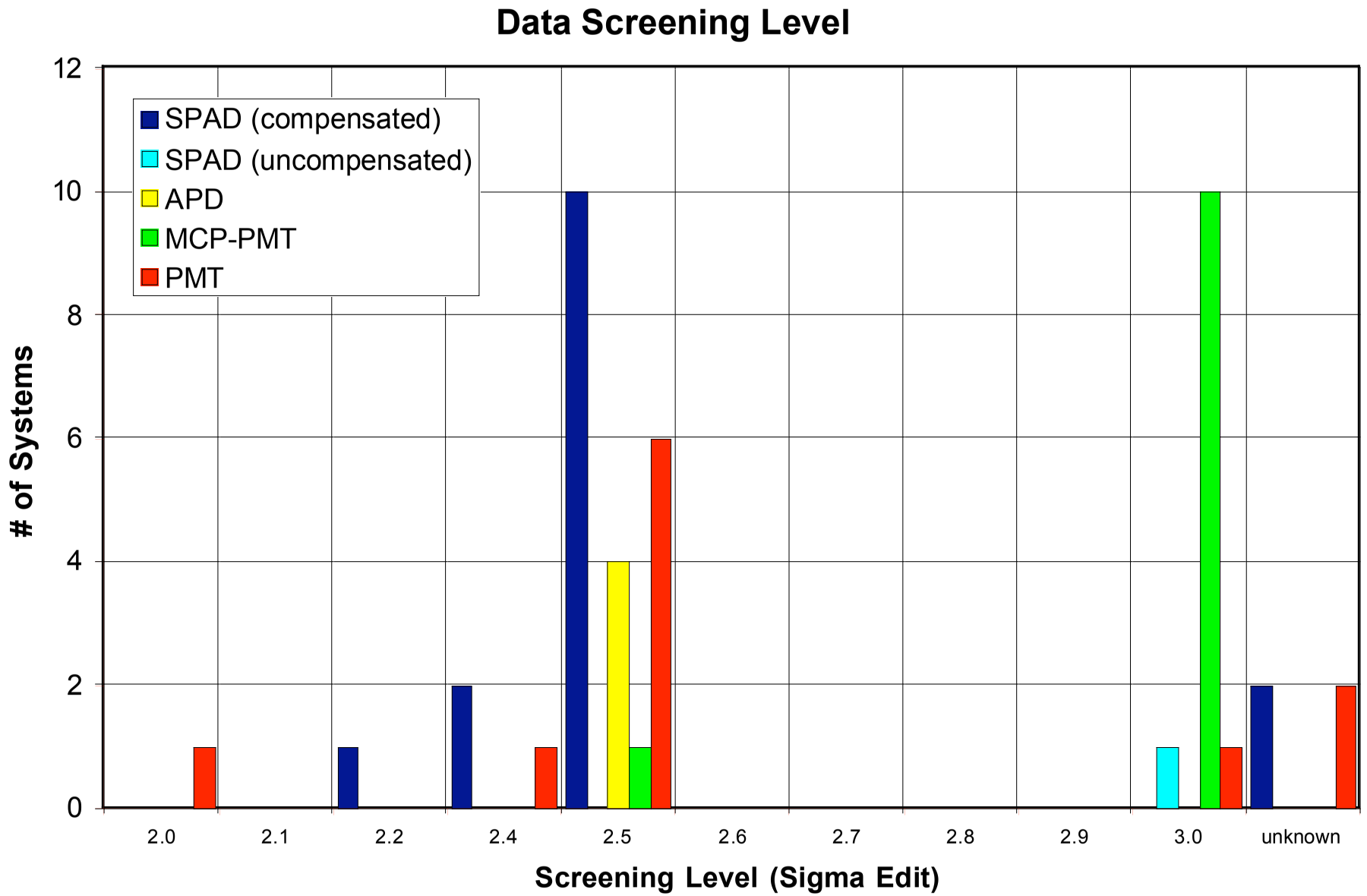

CoM Implementation Issues

- Proper use of system configuration indicators and the detector type in the NPs (header bytes 46 & 47, respectively).
- Variable data screening (e.g. 2.2, 2.5, 3.0, etc.) levels
- Need indicators for:
  - Signal Strength Indicator (SPAD and APD)
  - Discriminator Internal Cable Length (PMT systems)
  - Laser Polarization Type?
  - Laser Pulse-Width?

Strawman Recommendations

- The current names of header record bytes 46 and bytes 47 are very confusing
  - Byte 46: System Change Indicator – a flag to indicator major changes to the system.
  - Byte 47: System Configuration Indicator – a flag to indicator alternate modes of operation
- Recommend changing the names to:
  - Byte 46: System Configuration Indicator – a flag to indicate major changes to the system.
  - Byte 47: Detector Indicator – a flag to indicator the detector in use
- Bytes 44 (epoch time scale) and bytes 45 (system calibration method) have outgrown their real usefulness
  - Better use could be a indicator for data screening and discriminator cable length and/or laser polarization
  - For example, Byte 44:
    - 0 – 3.0 sigma edit
    - 1 – 2.5 sigma edit
    - 2 – 2.0 sigma edit

Strawman Recommendations

- NP data record bytes 48,49,50 are used for LLR, but not SLR (i.e. spare bytes)
- Currently the number of raw ranges compressed into the NP does not have enough bytes to support Khz lasers (bytes 44:47). Need at least 1 more byte.
- We need a flag to indicate average NP bin signal strength

Strawman Recommendations

- Standardize Detector Flags for the Network
  - For example, byte 47 is:
    - 1 – CSPAD (compensated channel)
    - 2 – SPAD (uncompensated channel)
    - 3 – MCP
    - 4 – PMT
    - 5 – APD
- Standardize the Screening Level for Each Detector Type (this would eliminate the need for a flag)
- Individual NPs contain Signal Strength info.
  - For example, in each NP reserve a byte for average energy level
    - 1 – single photon
    - 2 – few photons
    - 3 – 10 photons
    - 4 – 100 photons

Strawman Recommendations

- The Site Logs need pointers to the different configuration indicators contained in the normal points
- Data Formats and Procedures WG need to resolve these issues in close cooperation with the Networks and Engineering WG, the Signal Processing WG, and the Analysis WG

Engineering Verification of CoM Algorithms

- For a given SPAD station, take the full-rate and apply different screening levels and then compare the NPs from each set and note the difference in the NP OMCs.
- For systems with multi-detectors, take data in the same color simultaneously. Can this be done. It is like a 2-color experiment, except done in one color.

NATURAL ENVIRONMENT RESEARCH COUNCIL

CRL

Theoretical Centre-of-mass Corrections for LAGEOS, ETALON and AJISAI

See Otsubo and Appleby, JGR, 108, B4, 2201, Apr 200

Toshimichi OTSUBO

Communications Research Laboratory, Kashima, Japan

Graham M APPLEBY

Natural Environment Research Council, Monks Wood, UK

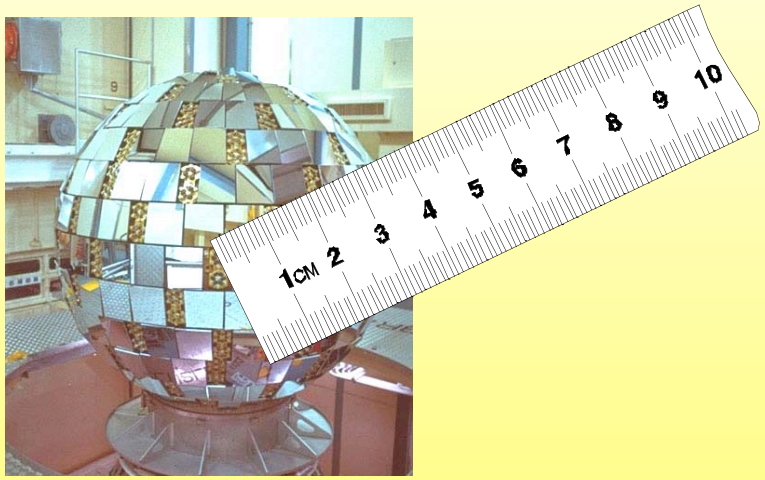

Laser Workshop 2003, Koetzting, 28-31 Oct 2003.

Satellite signature effect

- Multiple reflectors contributing to the satellite response.
- System-dependent detection timing
  - Single photon
  - C-SPAD
  - MCP-PMT

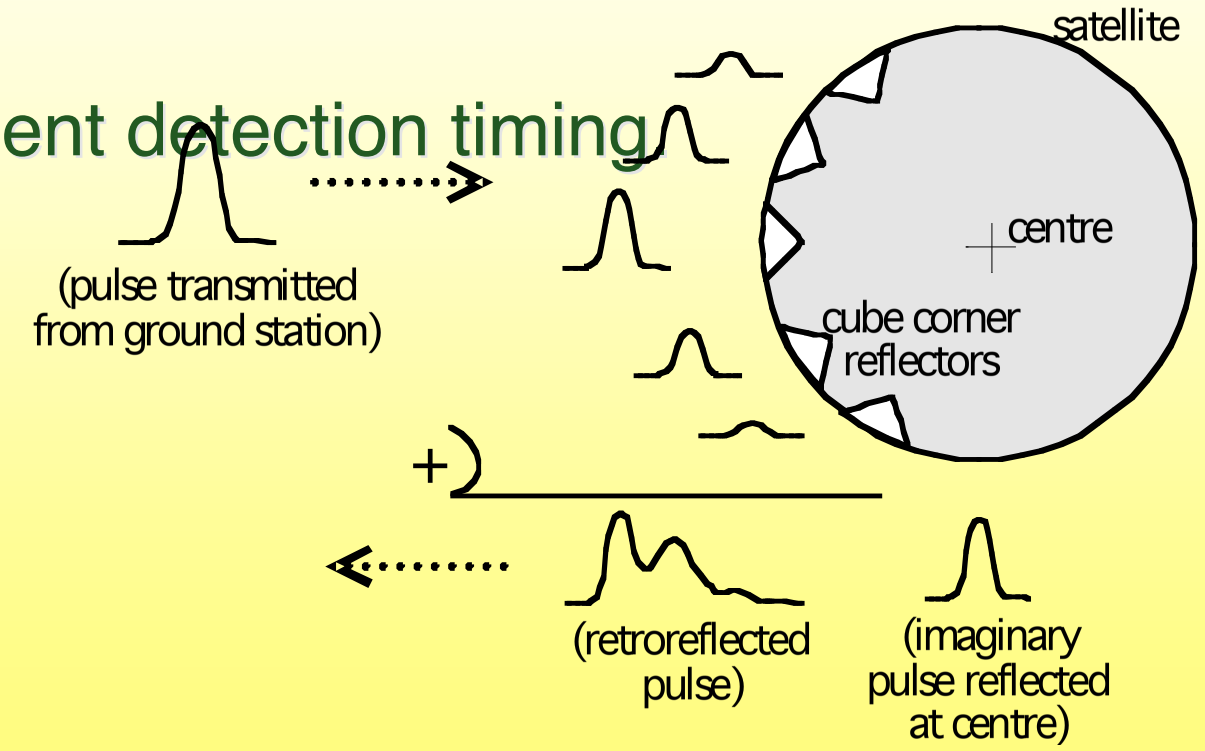

- Key error factor to achieve accurate GM and TRF

NATURAL ENVIRONMENT RESEARCH COUNCIL

CRL

LAGEOS(1&2)

US+Italy 1976, 92

Altitude 5900 km

Diameter 0.60 m

426 CCRs

AJISAI

Japan 1986

Altitude 1500 km

Diameter 2.15 m

1436 CCRs

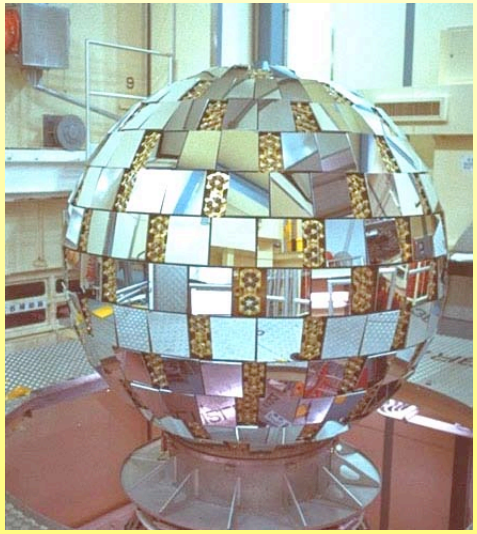

ETALON(1&2)

USSR 1989

Altitude 19000 km

Diameter 1.294 m

2134 CCRs

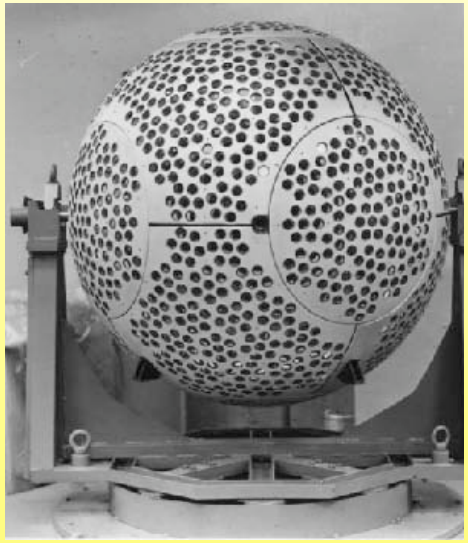

NATURAL ENVIRONMENT RESEARCH COUNCIL

CRL

Response from single reflector

- 3 factors to be considered.
  - –Effective reflection area (a)
  - –Reflectance (e)
  - –Diffraction
- How to compute the intensity.
  - $\propto ae$ … diffraction neglected.
  - $\propto a^2 e$ … simple diffraction model.

[Neubert, 1994; Otsubo, 1999]

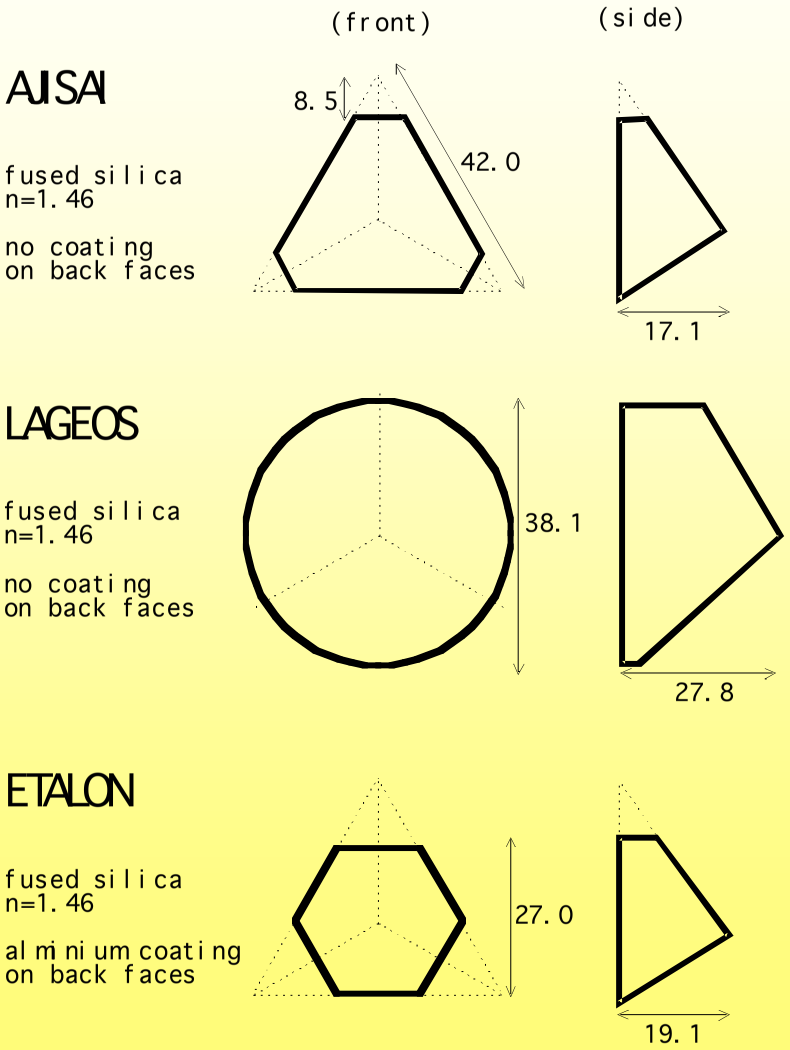

← Effective reflection area

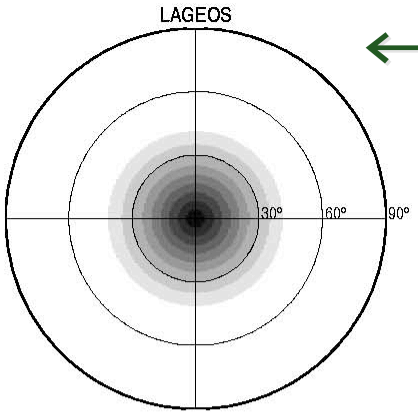

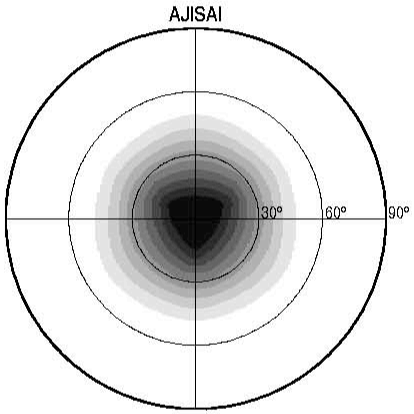

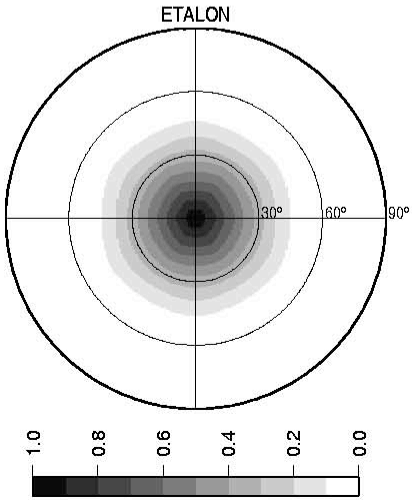

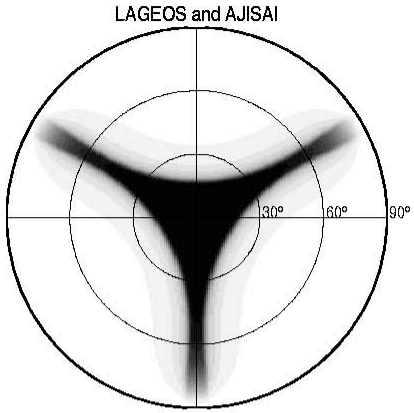

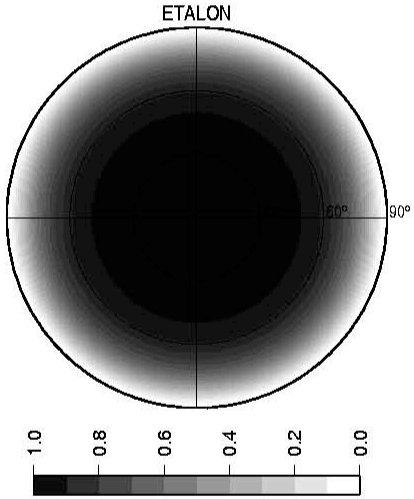

Reflectance

→

NATURAL ENVIRONMENT RESEARCH COUNCIL

Centre-of-mass correction

Extracted from Otsubo and Appleby, JGR, 108, B4, 2201, Apr

LAGEOS n=1.1

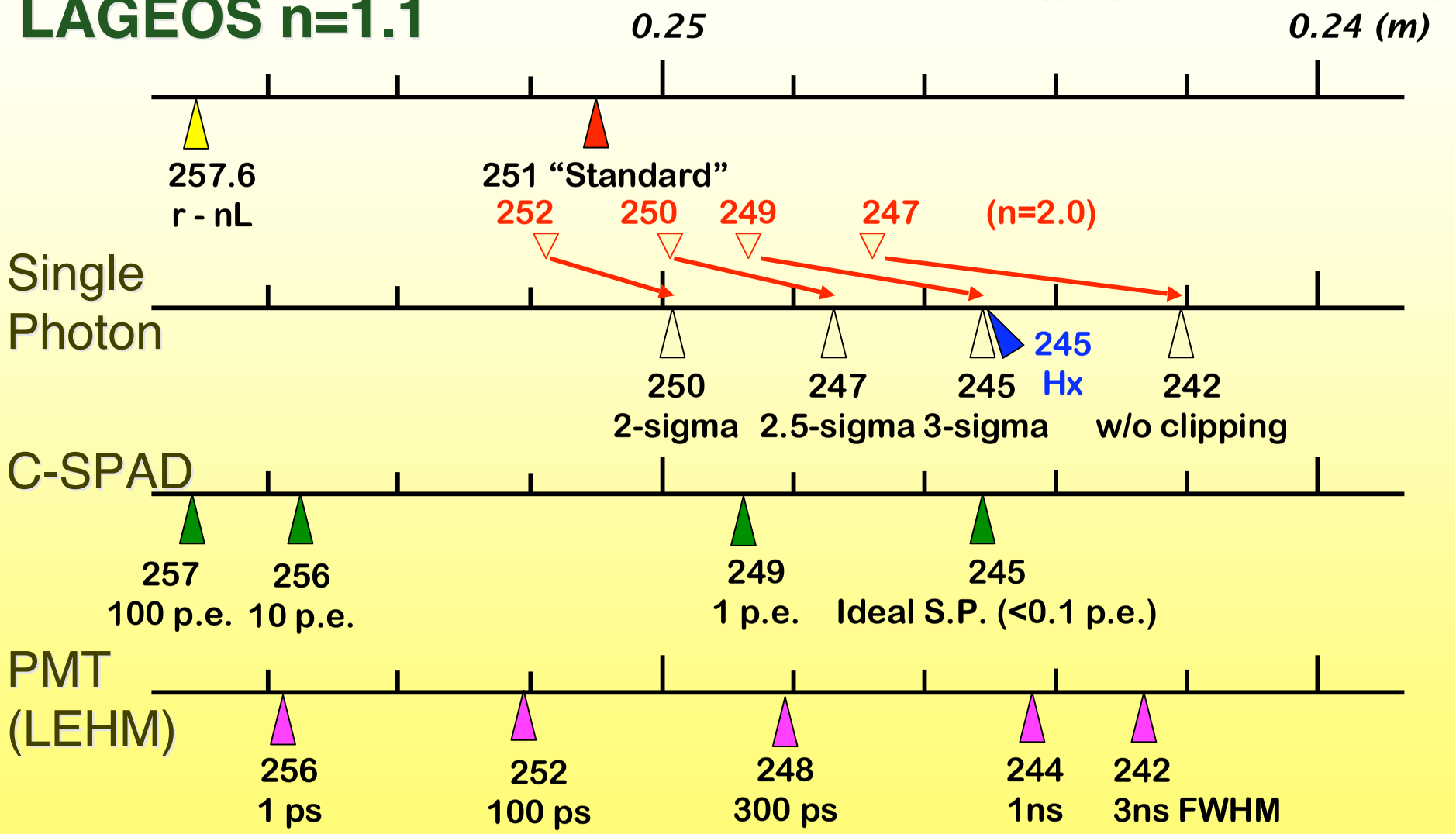

NATURAL ENVIRONMENT RESEARCH COUNCIL

Centre-of-mass correction

Extracted from Otsubo and Appleby, JGR, 108, B4, 2201, Apr

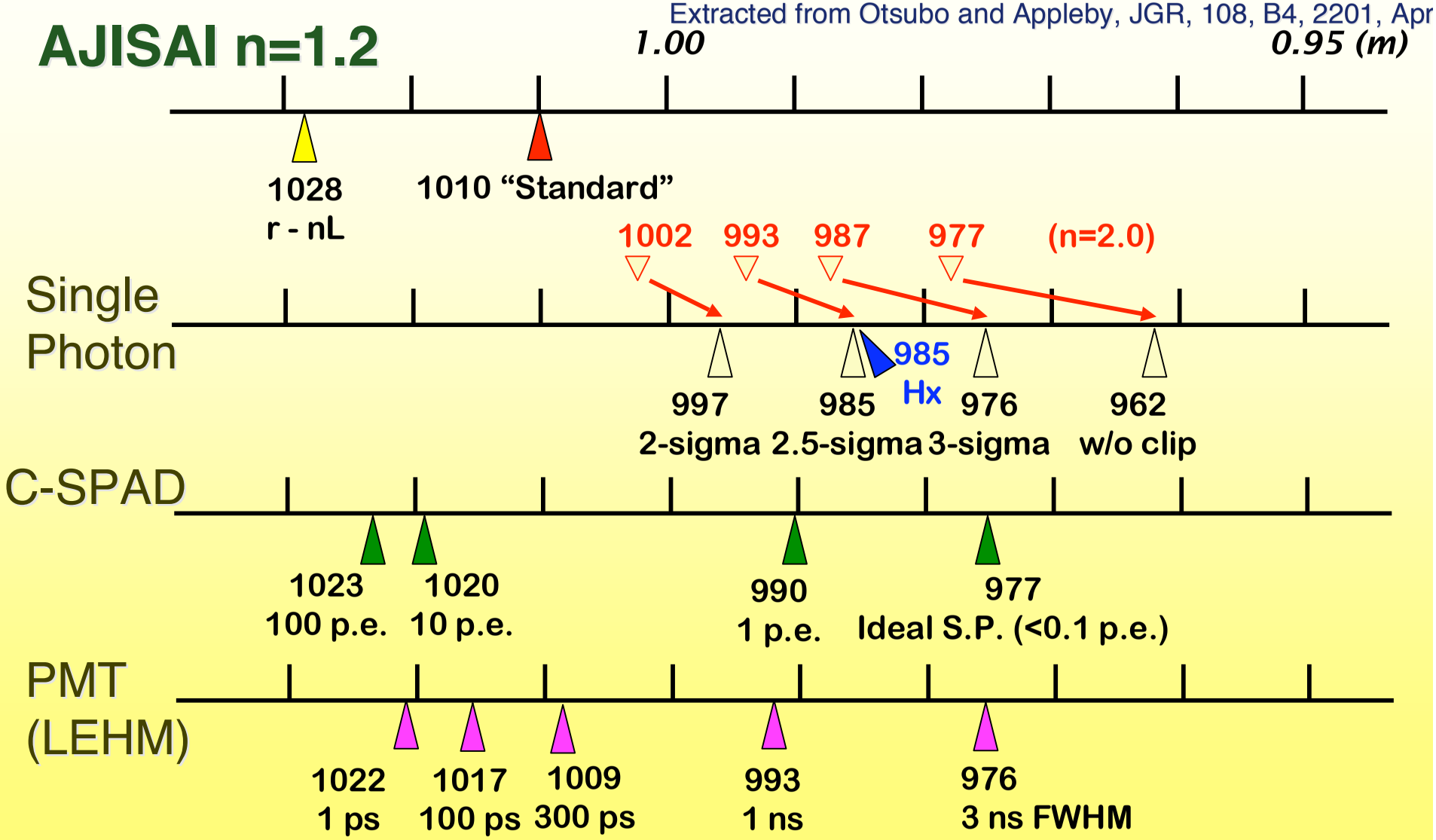

NATURAL ENVIRONMENT RESEARCH COUNCIL

Centre-of-mass correction

Extracted from Otsubo and Appleby, JGR, 108, B4, 2201, Apr

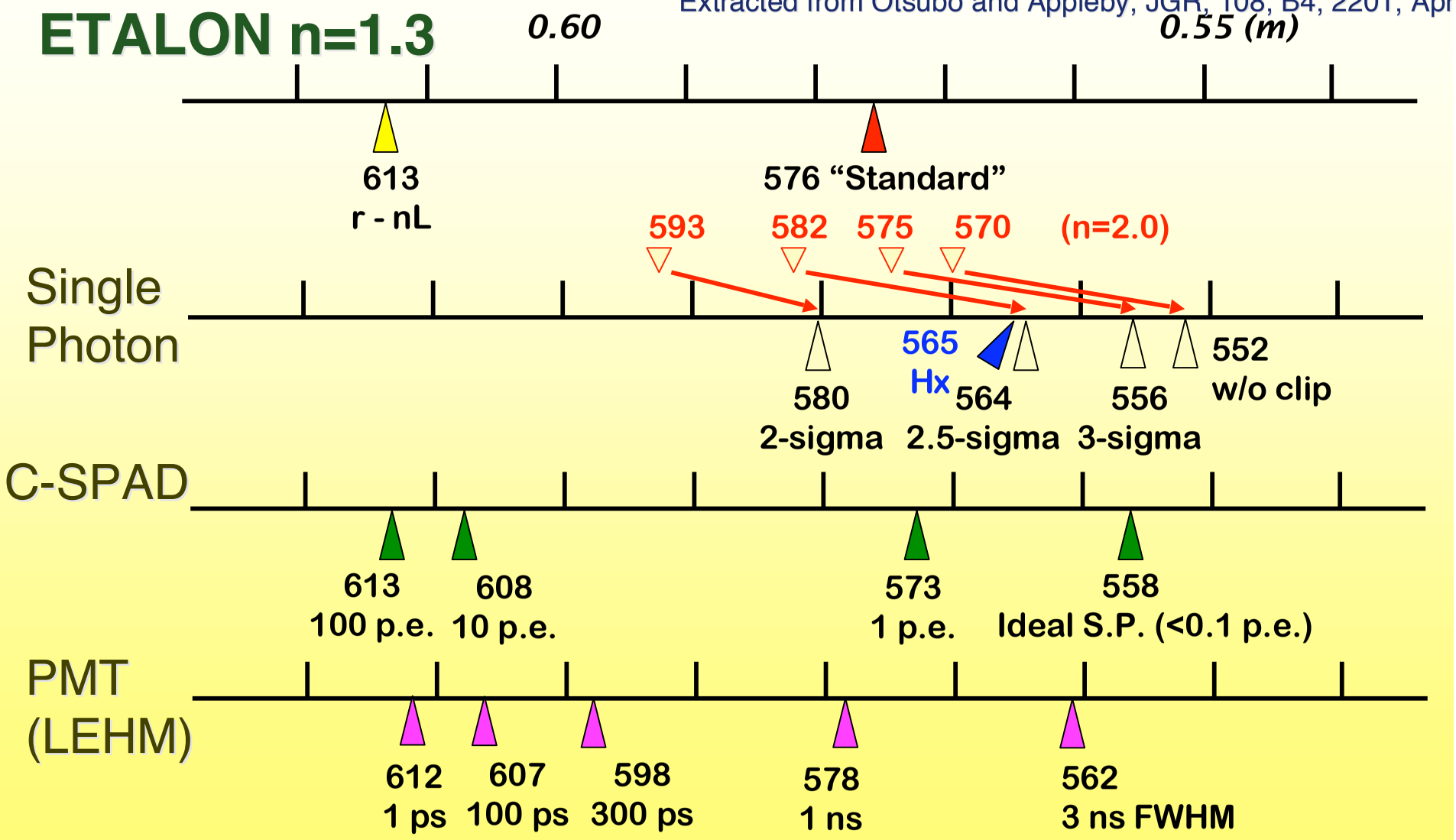

NATURAL ENVIRONMENT RESEARCH COUNCIL

CRL

Discussions (personal opinions) for mm ranging

- Avoid the intensity-dependent bias ON-SITE!
  - Likely to become the elevation-angle-dependent bias, which can significantly degrade the station height determination.
    - C-SPAD does NOT compensate the satellite returns. 1 cm for LAGEOS, 4-5 cm for AJISAI and ETALON.
    - MCP+CFD seems ok at 1-cm level, but not at 1-mm level.
  - Try the on-site shot-by-shot experiment.
  - kHz laser? Go for STRICT single photon!

Range residuals vs Intensity (Otsubo and Genba, DC Workshop, 2002)

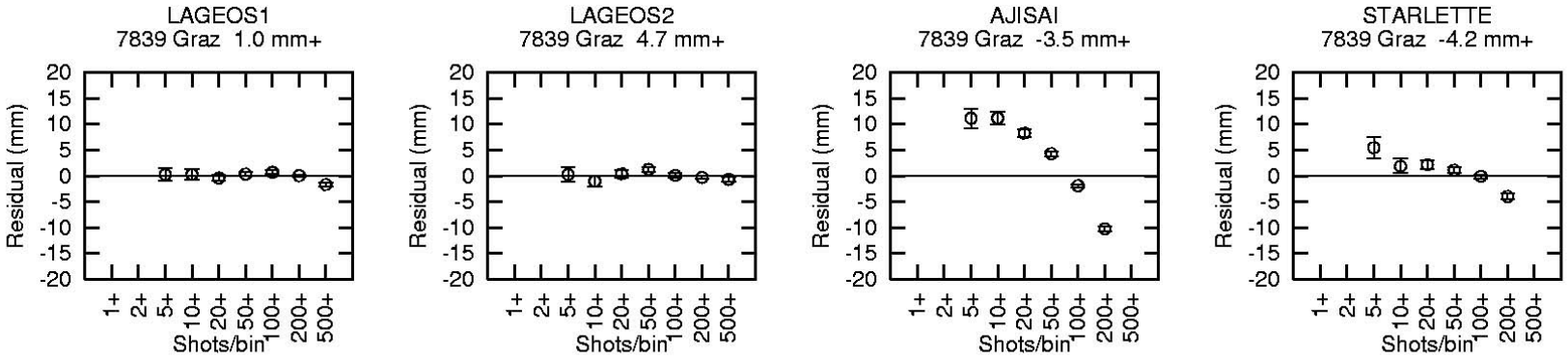

Range residuals vs Intensity (Otsubo and Genba, DC Workshop, 2002)

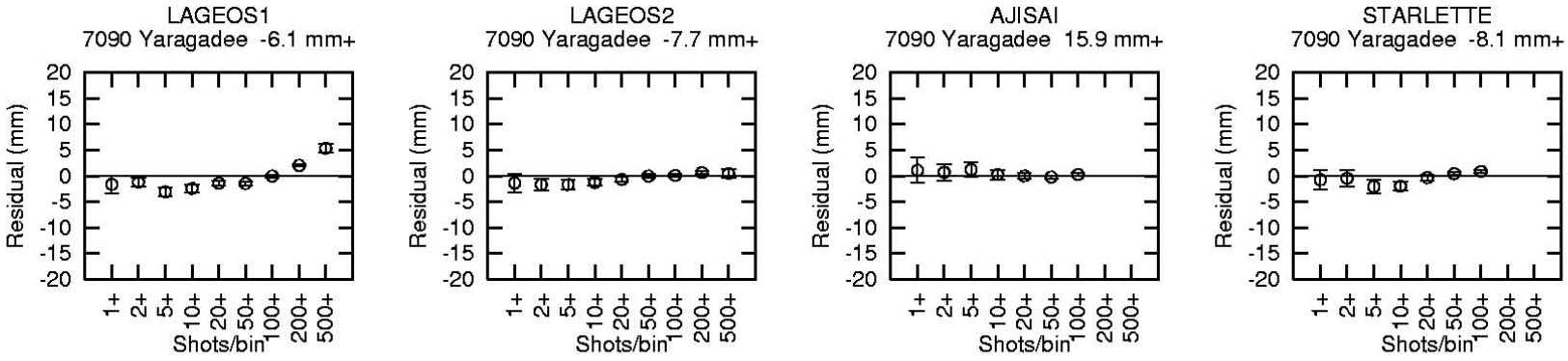

Range residuals vs Intensity (Otsubo and Genba, DC Workshop, 2002)

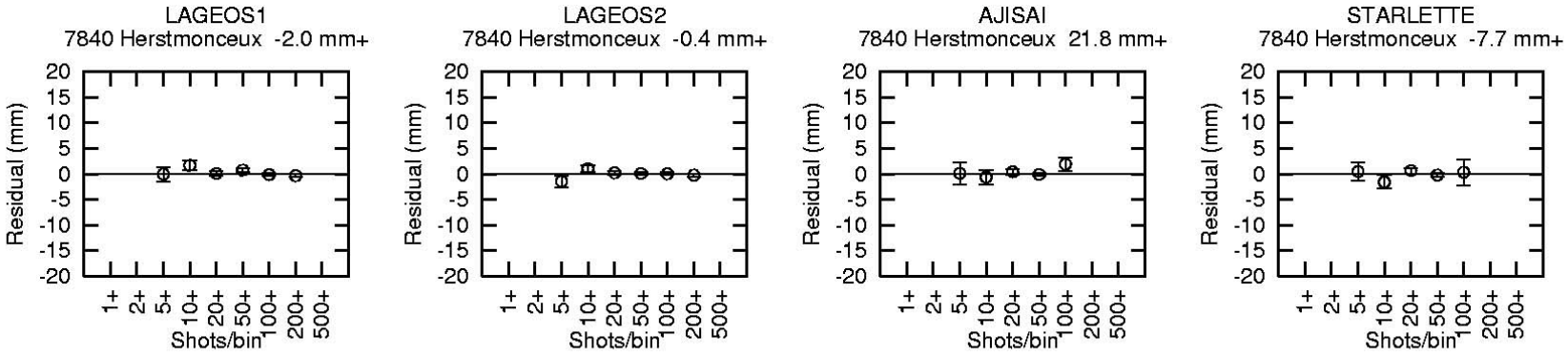

NATURAL ENVIRONMENT RESEARCH COUNCIL

CRL

Discussions (personal opinions) for mm analysis

- Better adjust the range bias for a while.
  - 1-mm accuracy is still a challenge.
    - Impossible to model the CoM correction for multi-photon (esp. MCP+CFD) systems at 1-mm accuracy.
    - Many other systematic error sources.
  - Accept a constant offset bias. Too risky to fix it to 0 mm.
  - Tight constraints can be applied if necessary.
  - A different story when all stations do the single photon.

NATURAL ENVIRONMENT RESEARCH COUNCIL

Summary

- Stations,
  - Eliminate any systematic range errors.
- Analysts,
  - Not assume zero range bias.
- English speakers,
  - Is the word “bias” appropriate? Probably negative impression to non-SLR people.

NATURAL ENVIRONMENT RESEARCH COUNCIL

CRL

Satellite Signature Effect in GLONASS SLR Data

Toshimichi OTSUBO

Communications Research Laboratory, Kashima, Japan

Graham M APPLEBY

Philip GIBBS

Natural Environment Research Council, Monks Wood, UK

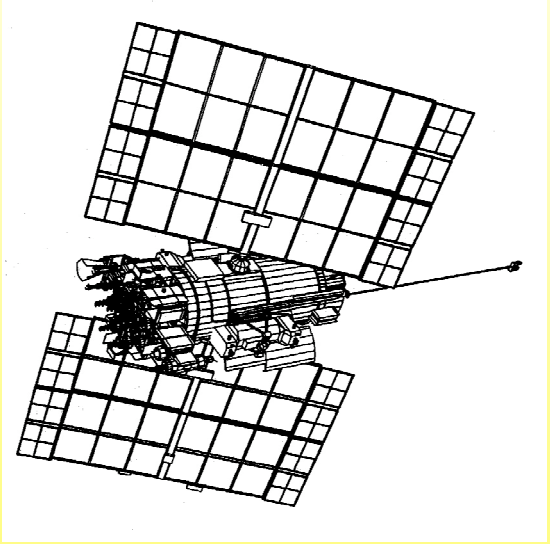

Laser Workshop 2003, Koetzting, 28-31 Oct 2003.

GLONASS CCR Array

Old type

- 396 CCRs.
- Until GLO-80.

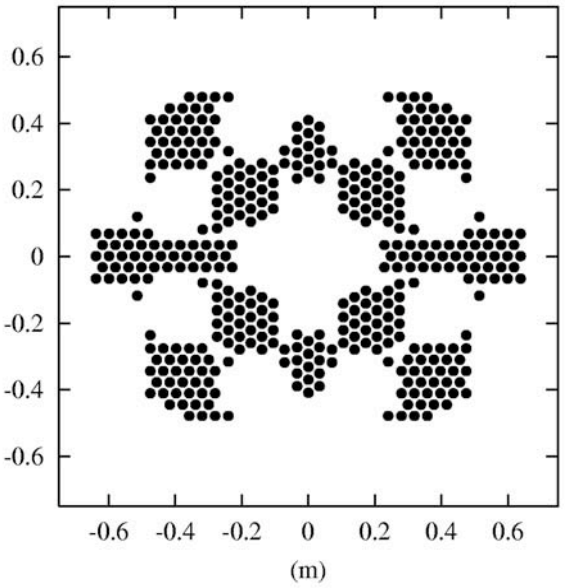

New type (except GLO-88)

- 132 CCRs.
- Since GLO-84.

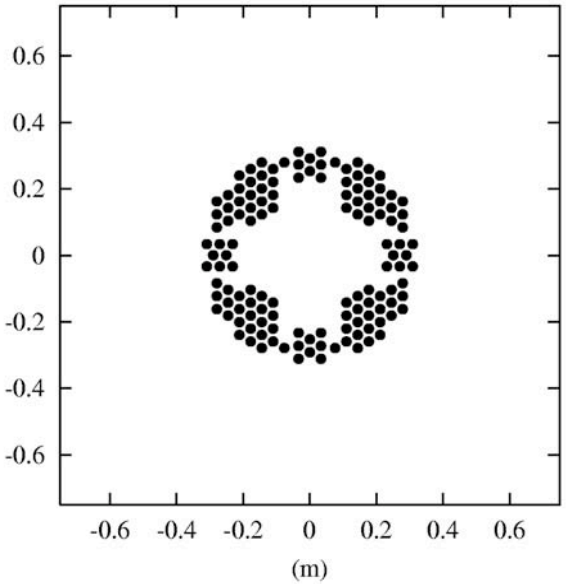

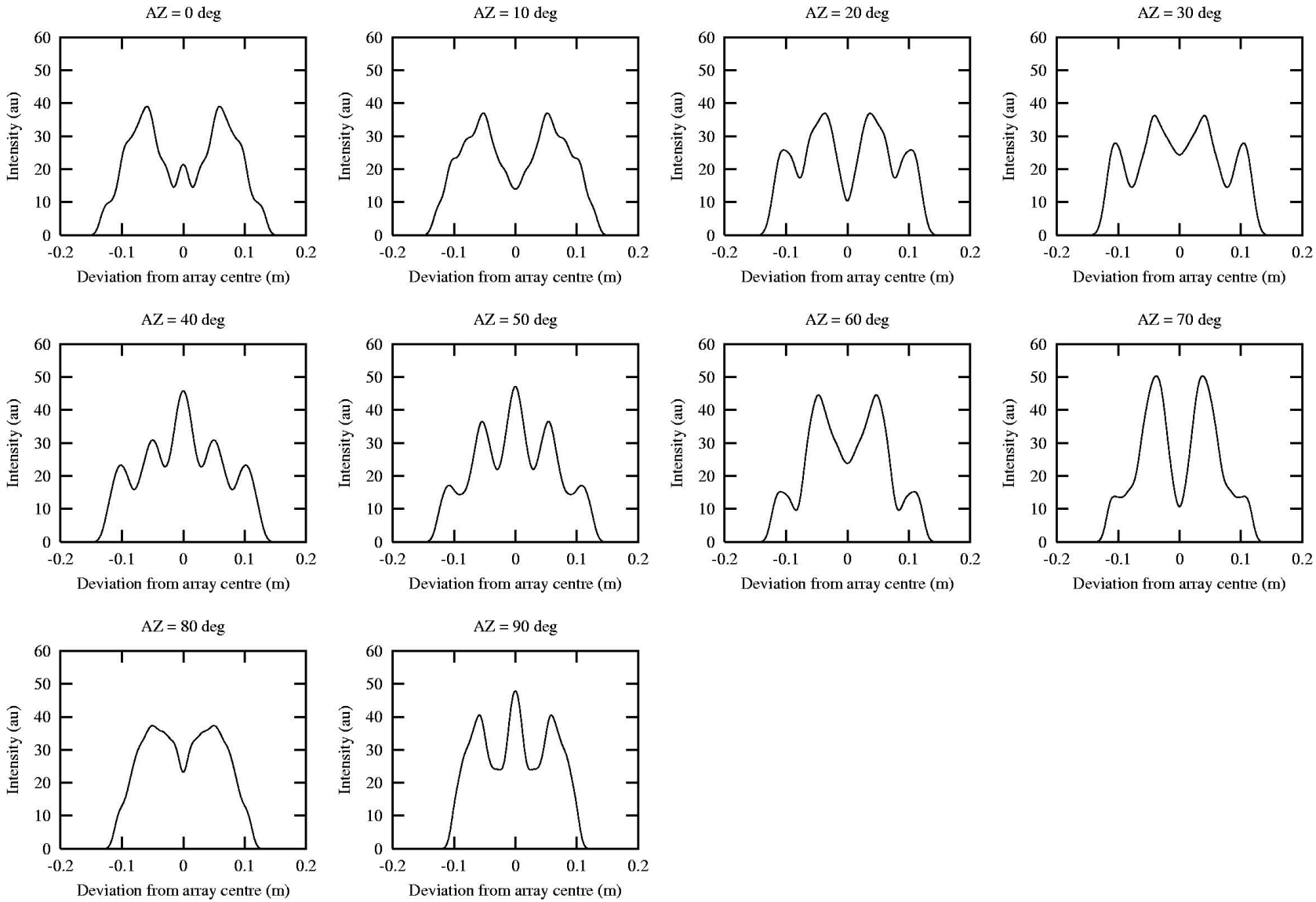
AZ = 0 deg
AZ = 10 deg
AZ = 20 deg
AZ = 30 deg
AZ = 40 deg
AZ = 50 deg
AZ = 60 deg
AZ = 70 deg
AZ = 80 deg
AZ = 90 deg
Intensity (au)
Deviation from array centre (m)
0
10
20
30
40
50
60
-0.2
-0.1
0
0.1
0.2

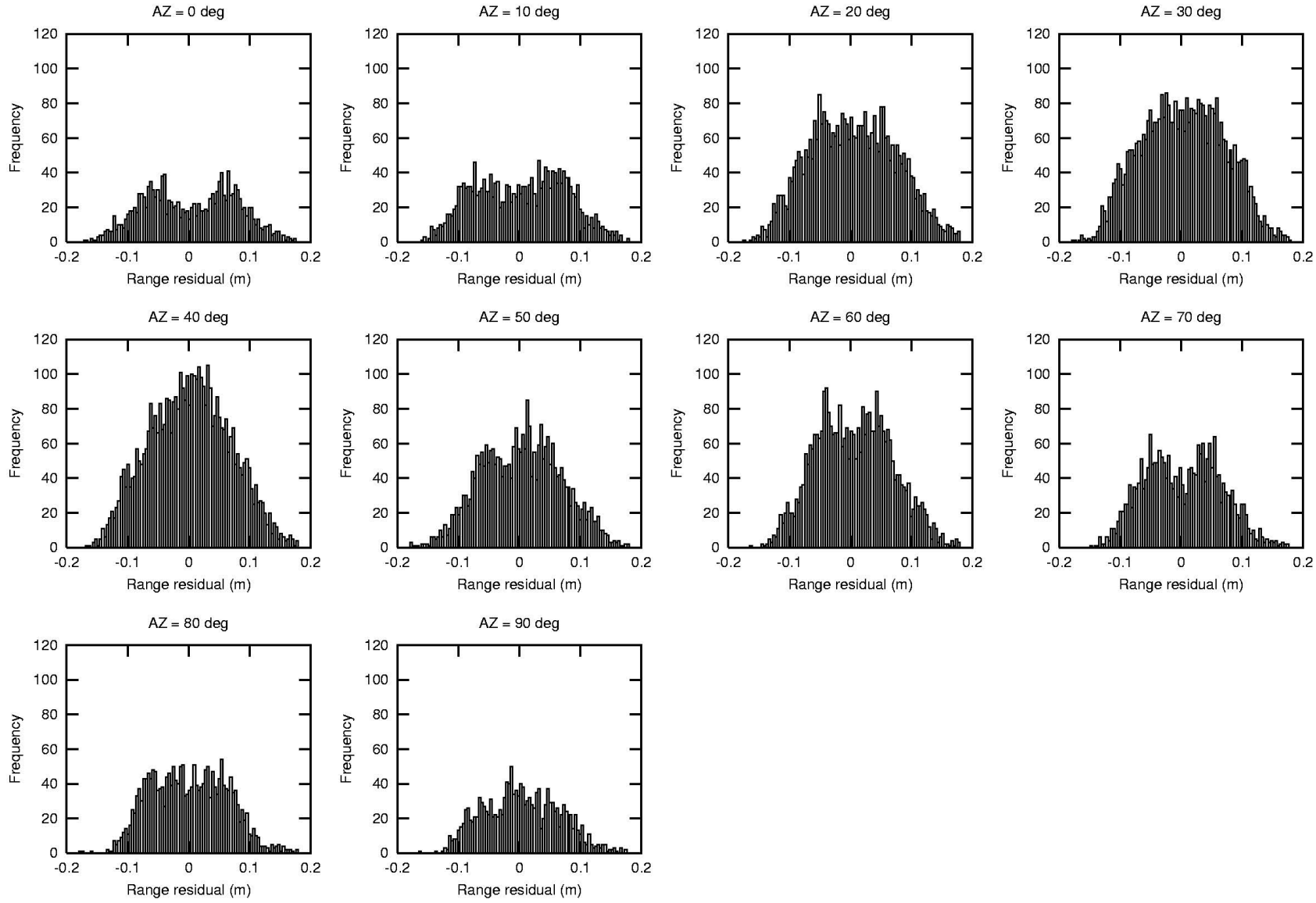
AZ = 0 deg
AZ = 10 deg
AZ = 20 deg
AZ = 30 deg
AZ = 40 deg
AZ = 50 deg
AZ = 60 deg
AZ = 70 deg
AZ = 80 deg
AZ = 90 deg
Frequency
Range residual (m)
0
20
40
60
80
100
120
-0.2
-0.1
0
0.1
0.2

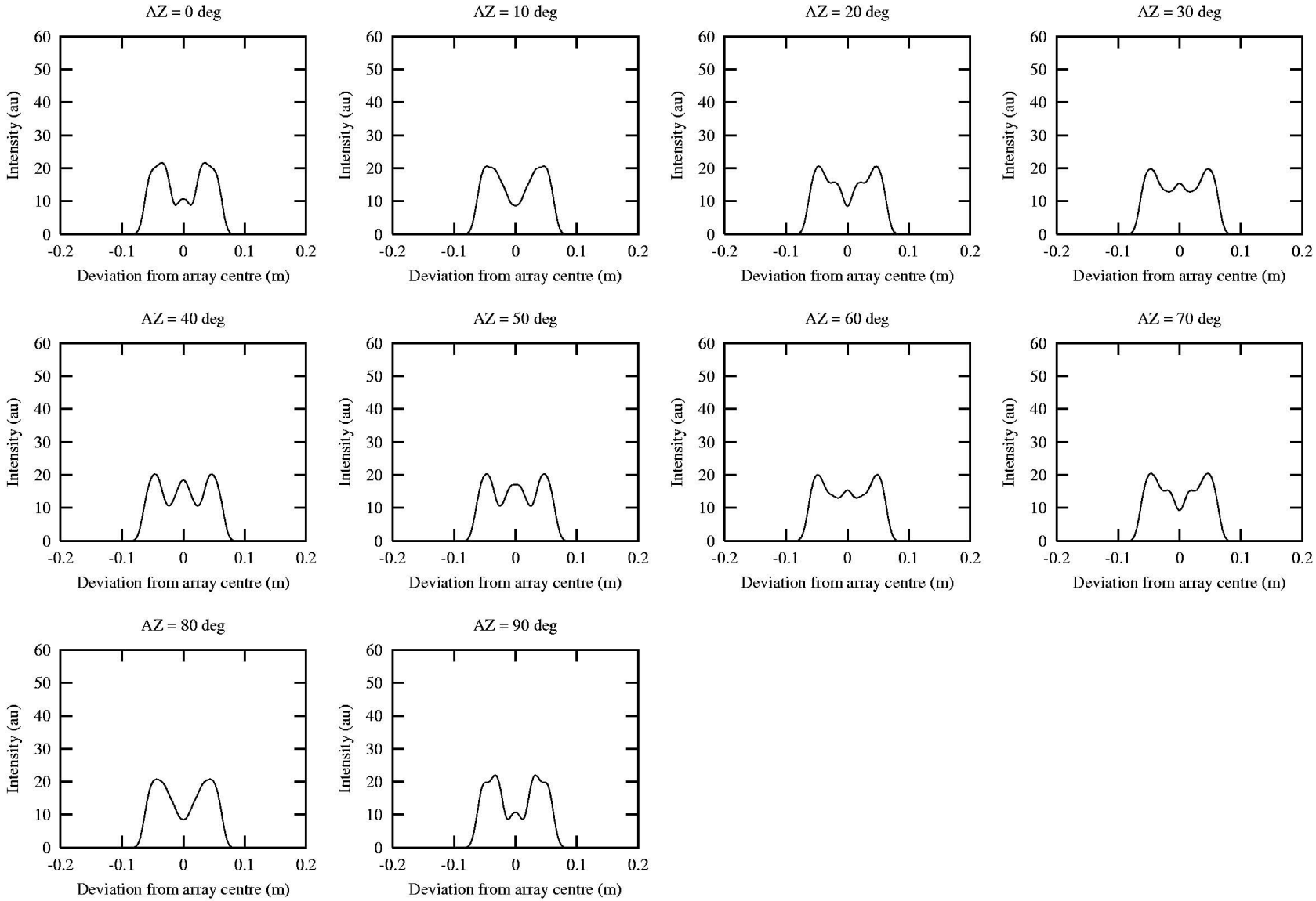
AZ = 0 deg
AZ = 10 deg
AZ = 20 deg
AZ = 30 deg
AZ = 40 deg
AZ = 50 deg
AZ = 60 deg
AZ = 70 deg
AZ = 80 deg
AZ = 90 deg
Intensity (au)
Deviation from array centre (m)
0
10
20
30
40
50
60
-0.2
-0.1
0
0.1
0.2

Effective array size estimation

- for 2001.
- estimated by concerto ver 3.
- bias

  elevation dependent

  average ～ (eff array size) x 0.15 .

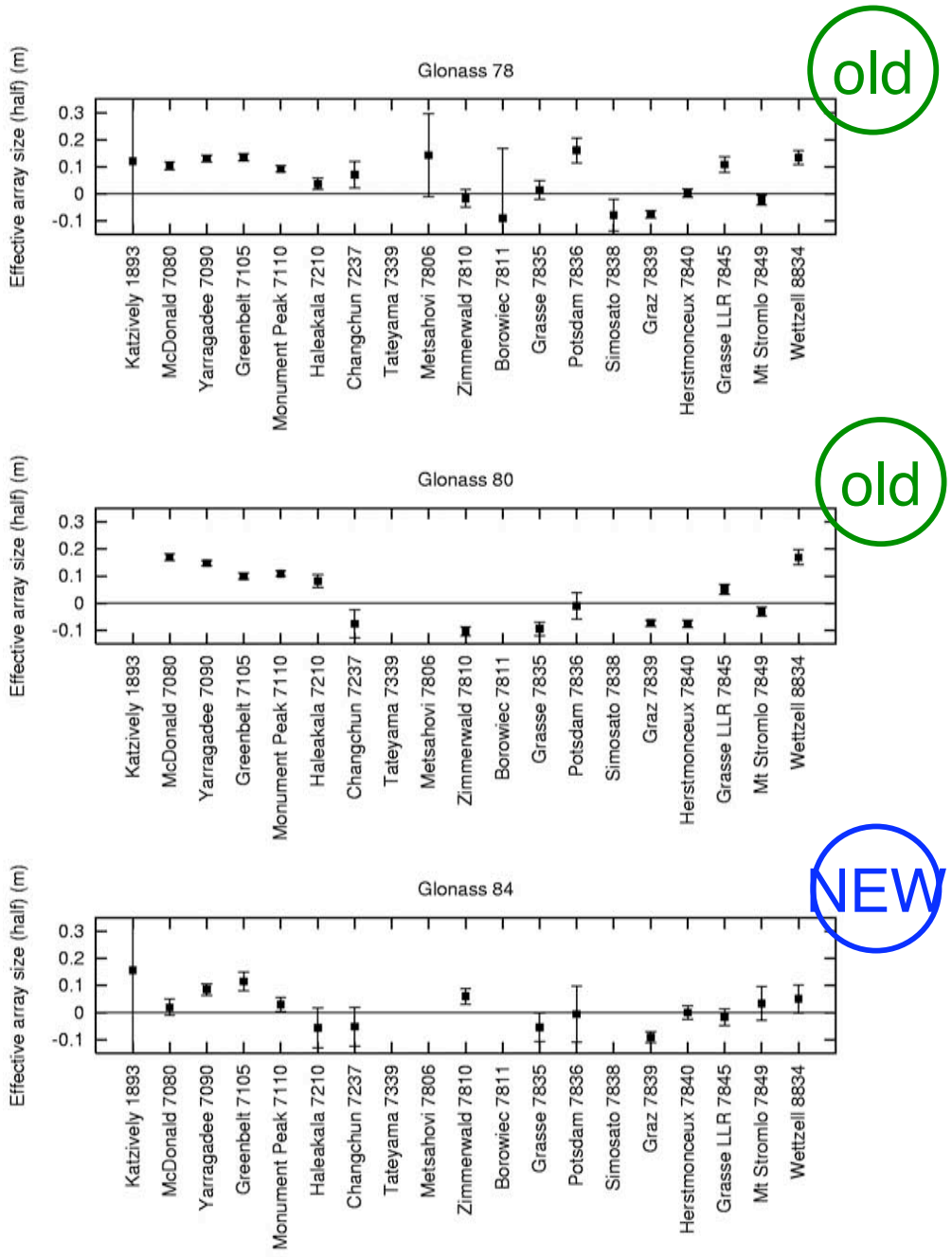

Effective array size estimation

- for 2002.

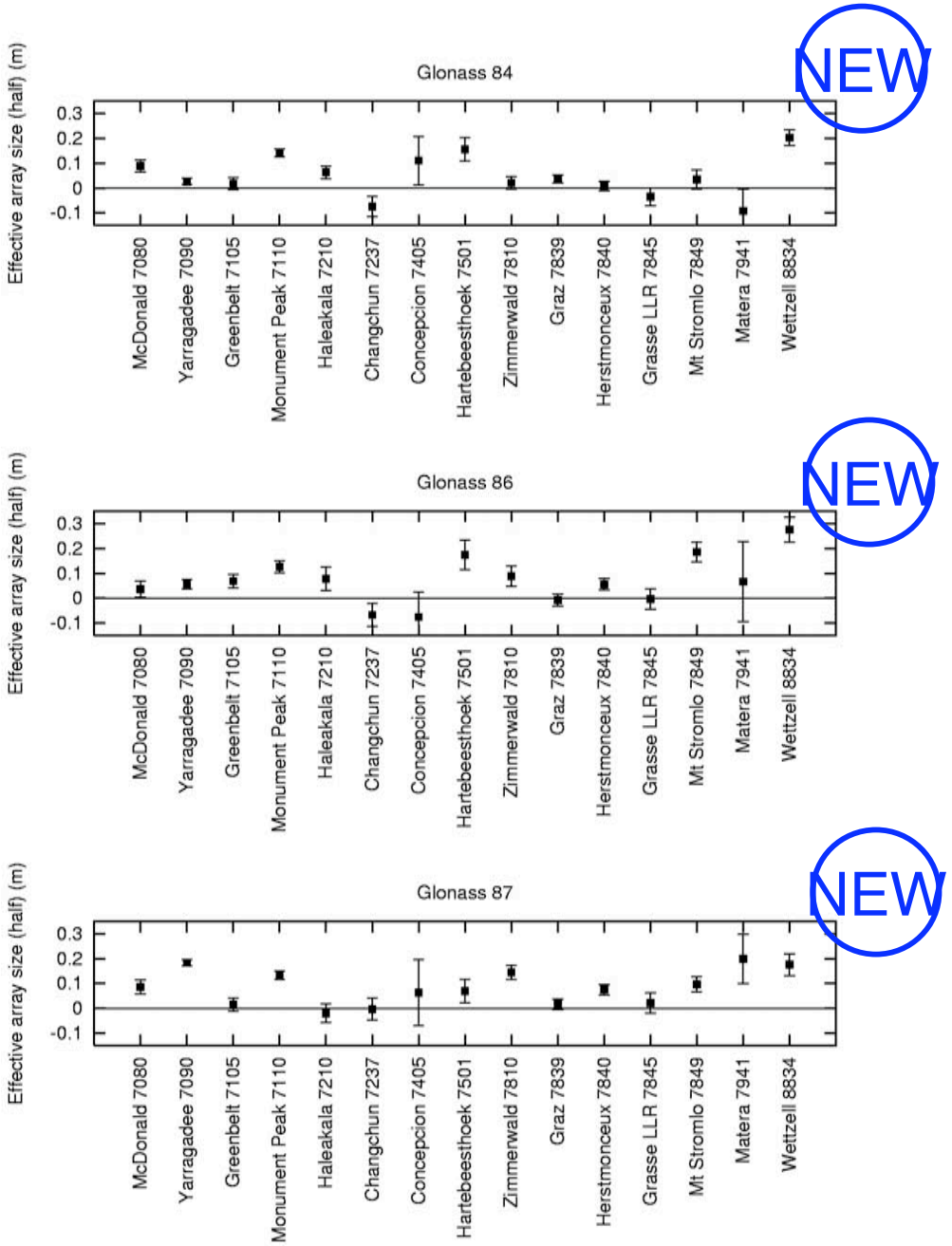

NATURAL ENVIRONMENT RESEARCH COUNCIL

CRL

Summary

- GLONASS CCR Design

  Large flat array is probably not the best idea. It causes the elevation-dependent range error. ~ 2 cm on average.

  New CCR array at least halved the signature effect. < 1 cm on ave.

- Return energy vs signature effect

  Difficult in observing new GLONASSes esp in daytime?

  What is the best array pattern for such high orbiters?

  How about in the GALILEO project?

CoM offset for ETALON 1 & 2 = ???

Erricos C. Pavlis
JCET/UMBC - NASA/Goddard/926

2003 ILRS Workshop
October 28 - 31, 2003, Kötzting, Germany

MM vs. MC

LAGEOS 1 & 2 Residual Statistics MM and MC Models

LAGEOS 1

Marini - Murray

	M-M Residual [m]
Minimum	-0.0537
Maximum	0.1872
Points	327
Mean	0.0504
Median	0.0402
RMS	0.0669
Std Deviation	0.0441

Mendes - Ciddor

	M-C Residual [m]
Minimum	-0.1266
Maximum	0.0965
Points	327
Mean	0.0280
Median	0.0276
RMS	0.0368
Std Deviation	0.0240

LAGEOS 2

	M-M Residual [m]
Minimum	-0.0666
Maximum	0.1607
Points	516
Mean	0.0345
Median	0.0333
RMS	0.0536
Std Deviation	0.0411

	M-C Residual [m]
Minimum	-0.1217
Maximum	0.1282
Points	516
Mean	0.0212
Median	0.0203
RMS	0.0442
Std Deviation	0.0388

A need for CoM offset for ETALON 1 & 2

- With an on-going campaign to intensively track the ETALON 1 & 2 spacecraft for Terrestrial Reference Frame improvement, the need for a credible CoM value valid for the variety of tracking systems surfaced in mid-2001
- After some "looking and asking around" we prompted an email response from Ron Noomen (June 2001)
- We initially adopted the values that were emailed by Ron Noomen, with the understanding that it was plausible that these values could and would change in the future, pending finalization of the responsible ILRS WG's results.

CoM offset for ETALON 1 & 2

- **CoM values adopted were emailed by Ron Noomen:**

From: Ron Noomen <Ron.Noomen@lr.tudelft.nl>
Subject: Etalon c.o.m.
To: ilrsac@cddisa.gsfc.nasa.gov (ILRS Analysis Centers),
ilrsaac@cddisa.gsfc.nasa.gov (ILRS Associate Analysis Centers),
ilrsawg@cddisa.gsfc.nasa.gov (ILRS Analysis Working Group)
Date: Thu, 14 Jun 2001 18:51:40 +0200 (MET)

…

Broadly:

- for strictly single-photon systems, use 560mm; e.g. Herstmonceux
- for CSPAD with higher-than-single photons, use 580mm; e.g. most of Europe;
- for MCP systems, use 610mm; e.g. the NASA systems.

Note:
The CoM value can vary by +/- 10mm according to (unknown) satellite orientation. Signal-strength variations are also potentially large.
Work to refine these values is ongoing.

…

Adopted CoM offset for ETALON 1 & 2 by site

- 18685901 -0.580

- 70802419 -0.610
- 70900513 -0.610
- 71050725 -0.610
- 71100411 -0.610
- 72102313 -0.610

- 72371901 -0.580
- 72496101 -0.580
- 73357201 -0.580
- 73397401 -0.580
- 73558401 -0.580

- 75010602 -0.610

- 78067601 -0.580
- 78106801 -0.580
- 78113802 -0.580
- 78208201 -0.580
- 78325501 -0.580
- 78353102 -0.580
- 78365801 -0.580
- 78372805 -0.580
- 78383602 -0.580
- 78393402 -0.580

- 78403501 -0.560

- 78457801 -0.580
- 78498001 -0.580
- 88341001 -0.580

- --other-- -0.580

E1 No Bias vs. ALL Adj. Bias

#Obs.	Mean	RMS	Site	# Obs.	Mean	RMS
252	0.0099	0.0186	MOBL7090	252	0.0000	0.0108
73	0.0000	0.0225	MTLR7501	73	0.0000	0.0148
41	0.0000	0.0137	WLRS8834	41	0.0000	0.0091
37	0.0158	0.0203	HALE7210	37	0.0000	0.0114
6	-0.0079	0.0248	MOBL7110	6	0.0000	0.0203
9	0.0227	0.0251	MLRS7080	9	0.0000	0.0126
42	-0.0030	0.0318	SALR7832	24	0.0000	0.0052
32	0.0129	0.0264	GRAS7845	32	0.0000	0.0120
11	-0.0032	0.0082	SWIS7810	11	0.0000	0.0186

E2 No Bias vs. ALL Adj. Bias

#Obs.	Mean	RMS	Site	# Obs.	Mean	RMS
30	0.0000	0.0150	WLRS8834	30	0.0000	0.0188
130	0.0045	0.0224	MOBL7090	130	0.0000	0.0187
23	0.0010	0.0061	CHAL7237	23	-0.0001	0.0059
94	0.0000	0.0157	MTLR7501	94	0.0000	0.0142
61	0.0050	0.0165	GRAZ7839	61	0.0000	0.0165
22	0.0043	0.0045	POT27841	22	0.0000	0.0007
60	0.0225	0.0307	HALE7210	60	0.0000	0.0189
141	-0.0078	0.0176	MOBL7110	141	0.0000	0.0159
21	-0.0158	0.0314	SWI.7810	21	0.0000	0.0225
28	-0.0117	0.0232	RGO_7840	28	0.0000	0.0178
18	0.0245	0.0346	MLRS7080	18	0.0000	0.0252
48	0.0000	0.0319	SALR7832	43	-0.0004	0.0071
3	0.0000	0.0000	KOM.1868	3	0.0000	0.0000
38	0.0075	0.0330	GRAS7845	38	0.0000	0.0296
12	0.0000	0.0000	MDN21864	12	0.0000	0.0000

ETALON 1 Estimated Biases

Units: mm

70802416	14.61	±4.81
70900512	28.87	±1.62
71100416	-10.61	±5.96
72102312	25.54	±3.51
75010600	58.72	±2.60
78106800	-38.44	±12.81
78325504	37.42	±10.49
78457800	14.26	±3.35
88341000	40.18	±3.11

ETALON 1 Estimated Biases

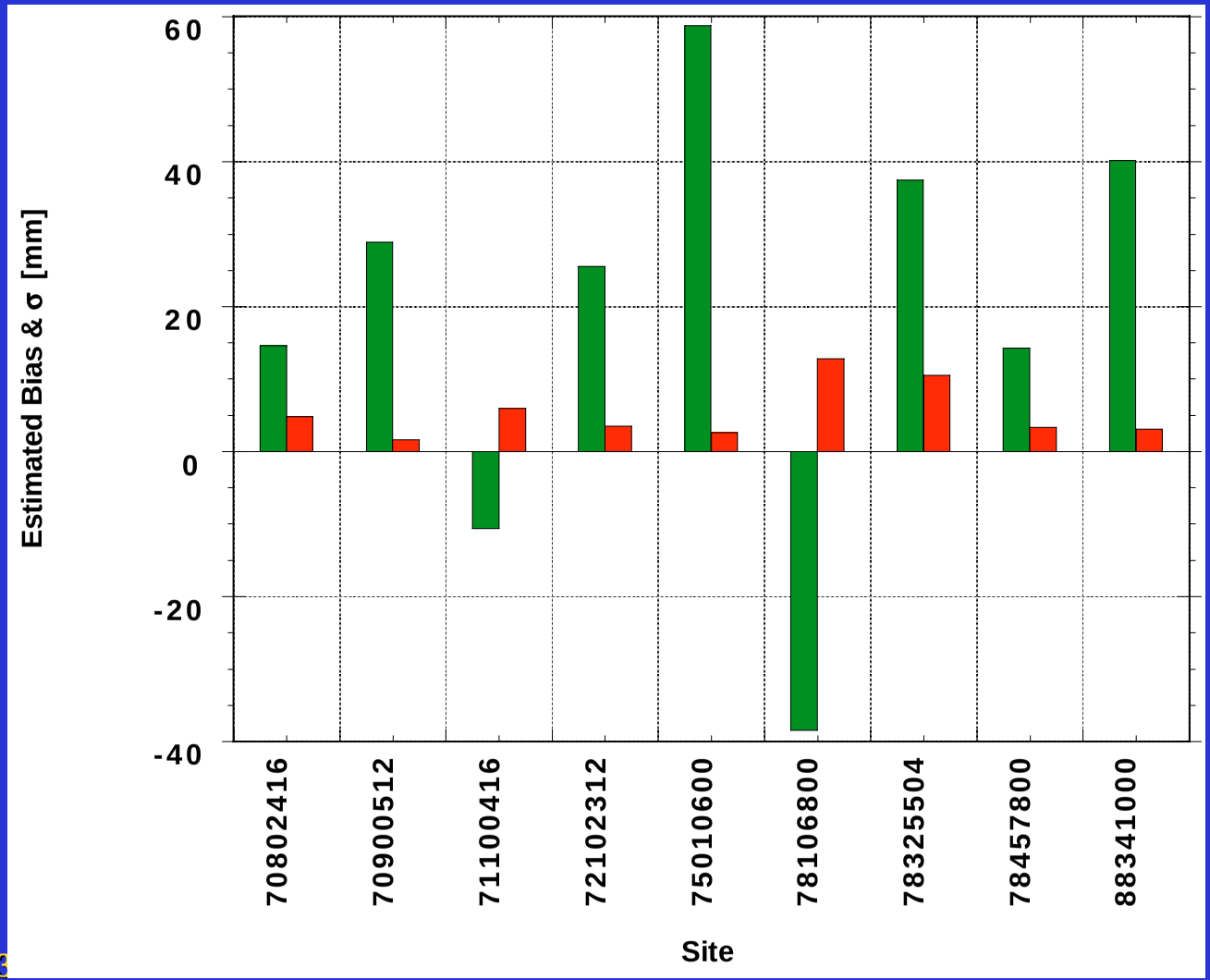

ETALON 2 Estimated Biases

Units: mm

70802419	21.22	±5.19
70900513	21.40	±3.07
71100412	-7.52	±2.36
72102313	28.51	±2.80
75010602	40.85	±3.33
78106801	-25.76	±4.67
78393402	0.03	±3.22
78403501	-19.49	±4.18
78418701	33.94	±39.20
78457801	7.26	±3.54
88341001	39.36	±4.35

ETALON 2 Estimated Biases

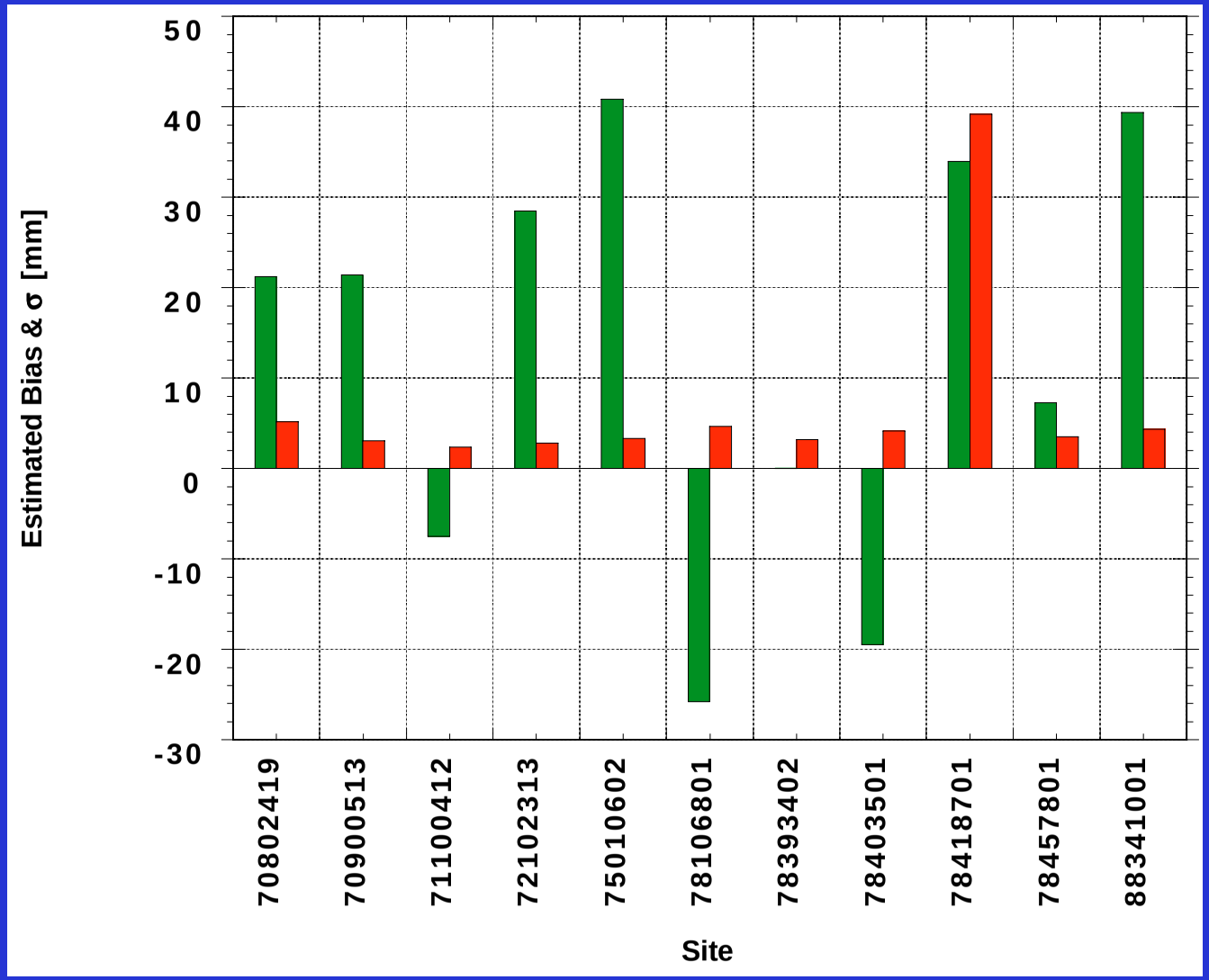

Summary

- Originally adopted CoM offsets (in disagreement with the recently published values), seem to imply that MCP systems (like NASA sites) should apply the revised offsets, closer to the newly published numbers
- Even with these changes taken into account, it seems that there is variation within "types" of receivers, depending on the mode of operation, as it is implied by the different (~ -1 cm) bias for the Monument Peak MOBLAS NASA system
- We need standard assignment of the most appropriate offset value for each site, preferably on a pass-by-pass basis, based on the responsible ILRS WG's results, and the operational regime appropriate for that pass.

Cross section of ILRS satellites

by

David Arnold - 94 Pierce Road, Watertown, MA 02472, 617-924-6812

1. Introduction

The cross section of the satellites tracked by ILRS has been computed using whatever information is available on the design of the arrays and the specifications of the cube corners. The cross section is not constant for any array. It is a function of incidence angle, velocity aberration, wavelength, and polarization if the cube corners are uncoated. The cross section is given by the intensity of the diffraction pattern of the array at the position of the receiver in the far field as determined by the velocity aberration. This report uses diffraction theory to calculate cross section matrices for the arrays at various incidence angles for wavelength 532 nanometers. The velocity aberration limits depend on the altitude of the satellite. The average cross section within the velocity aberration limits is computed at each incidence angle on the array. The average over all incidence angles is also computed and tabulated.

2. Cross section table.

Table 1 lists the current cross section for each satellite on the ILRS webpage and the revised cross section computed using diffraction theory. The minimum and maximum cross section as a function of velocity aberration and incidence angle are also listed for the satellites where there is enough information to do a diffraction calculation.

THEORETICAL CROSS SECTION
(Million sq m)

SATELLITE	ALTITUDE	CURRENT	REVISED		
			Minimum	Average	Maximum
Starlette	950	0.65	1.00	1.80	2.5
Lageos	6000	7.00	9.00	15.00	23.0
Etalon	19000	60.00	-	55.00	-
Topex	1300	2.00	6.00	33.00	83.0
BeaconC	940	3.60	0.00	13.00	35.0
Ajisai	1400	12.00	-	23.00	-
Gfo-1	800	2.00	.07	.50	1.1
Stella	950	0.65	1.00	1.80	2.5
Jason	1300	0.30	.20	.80	1.7
GPS	20000	40.00	-	19.00	-
Champ	500	1.80	.05	1.00	3.4
Westpac	835	0.03	0.00	.04	.4
ERS	800	0.30	.20	.85	1.6
Glonass396	20000	360.00	-	240.00	-
Glonass132	20000		-	80.00	-
Envisat	800	0.30	.20	.85	1.6
LRE	25000	1.25	-	2.00	-
SUNSAT	600	0.20	.04	.40	1.4

Table 1. Current and revised cross section for the ILRS satellites.

3. Diffraction model.

The diffraction calculations have been done using the theory given in SAO Special Report 382, "Method of Calculating Retroreflector Array Transfer Functions", David A. Arnold. The equations model coated or uncoated retroreflectors with a dihedral angle offset. The model does not include any manufacturing imperfections such as roughness or surface curvature. Manufacturing imperfections can result in a loss of cross section in the actual cube corners. These losses are probably a factor of 2 or more. Therefor the theoretical calculations should be considered as an upper limit to the actual cross section. There is no data on the actual "in-orbit' cross section in absolute units although relative measurements between some satellites have been done.

The cube corners on the Japanese satellites are in the shape of a triangle with the corners cut off. There is no model for the reflectivity of this design of cube corner. The Russian satellites are not manufactured to a particular specification. Therefor it is not possible to do an accurate theoretical calculation of the cross section. For satellites where no information is available on the dihedral angle offset, an angle optimized for the particular velocity aberration has been used. If the actual dihedral angle is not optimized, the cross section will probably be lower.

The Japanese satellites are spherical and use uncoated cube corners. Since the LAGEOS satellite is also spherical and uses uncoated cube corners, the cross section of the Japanese satellites is estimated by scaling the cross section of LAGEOS by the reflecting area.

4. Sample diffraction patterns.

Diffraction patterns of various satellites are shown in the report "Retroreflector Array Transfer Functions" available on the web at http://nercslr.nmt.ac.uk/sig/signature.html in PDF and WORD format (Reference 1). Some sample diffraction patterns for LAGEOS from that report are shown in Figure 1 for linear and circular polarization.

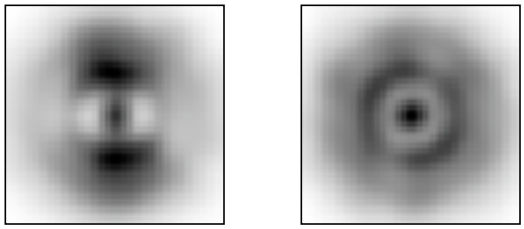

Figure 1. Cross section of LAGEOS for linear polarization (left) and circular polarization (right) at one orientation of the satellite. The axes are -50 to +50 microradians.

The diffraction pattern for linear polarization has a dumbbell shape with the axis of the dumbbell aligned with the polarization vector of the incident laser beam. The diffraction pattern for circular polarization has a more circular shape. The pattern for circular polarization is not perfectly circular because there are a limited number of cube corners that are active at a particular orientation of the satellite. The intensity of the diffraction pattern at the position of the receiver is the cross section of the satellite.

Figure 2 shows some sample diffraction patterns for TOPEX from Reference 1.

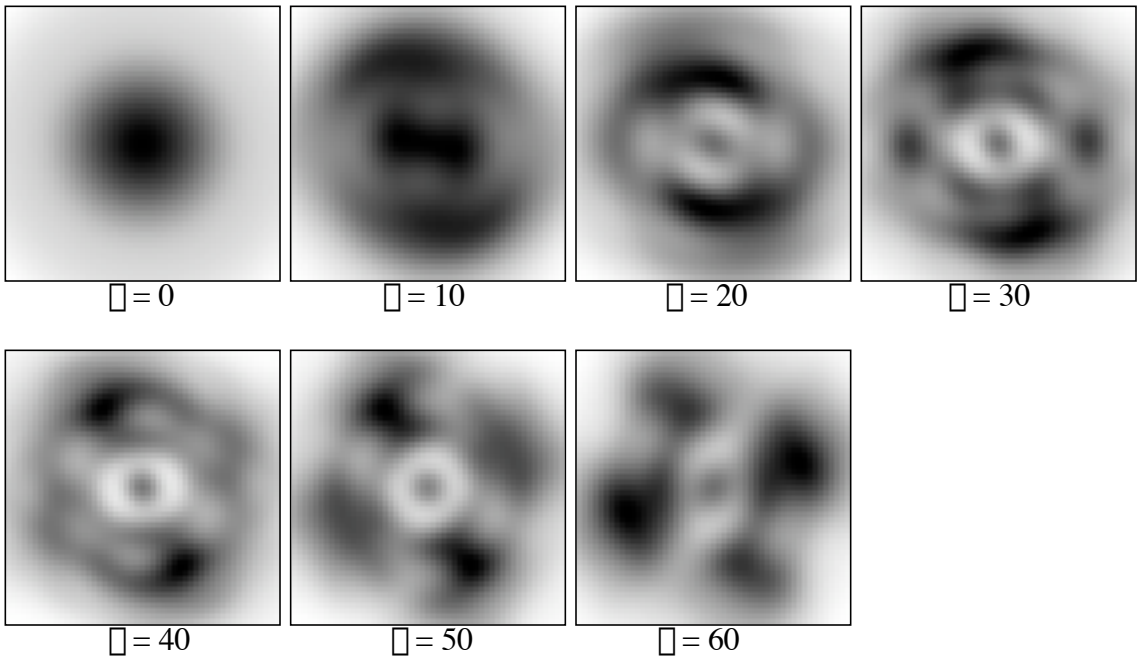

Figure 2. Diffraction patterns of the TOPEX retroreflector array for various incidence angles θ (deg) on the array.

5. Variation of the cross section with incidence angle.

A. TOPEX

As can be seen from figure 2 the cross section varies with incidence angle as well as with the position of the receiver in the far field pattern as determined by the magnitude and direction of the velocity aberration. Table 2 shows a summary of the cross section for TOPEX vs incidence angle on the array.

Cross section of TOPEX (million sq m)

Incidence Angle	Minimum	Average	Maximum	Active area
0	15	20	32	31
10	15	29	40	34
20	16	37	62	37
30	19	44	71	40
40	12	45	83	40
50	12	35	62	32
60	6	22	38	21

Table 2. Cross section statistics for TOPEX. The first column is the incidence angle in degrees, the second the minimum cross section, the third the average cross section between 25 and 50 microradians velocity aberration, the fourth the maximum cross section, and the fifth the total reflecting area in equivalent number of cube corners at normal incidence.

The average of the numbers in the third column is 33 million sq meters. The lowest cross section is 6 million at the bottom of column 2 and the highest cross section is 83 million in column 4 for 40 degrees incidence angle. This is the data that was used to generate the values in Table 1 for TOPEX.

B. SUNSAT

The Sunsat array has a ring of 8 cube corners tilted at 50 degrees with respect to the symmetry axis. There is no pole cube facing the earth such as on the ERS, JASON, GFO, and other similar satellites. The 9 cube arrays on these other satellites form an approximate hemisphere so that the cross section does not vary much with incidence angle. For the Sunsat array, the cross section at normal incidence on the array is very low because all the cube corners are being viewed at a 50 degree incidence angle. This is not far from the cutoff angle of about 57 degrees. The fact that the cross section is very low for normal incidence is not a problem because this only occurs at zenith where the range is shortest. In fact the absence of the pole cube can be an advantage in avoiding a large dynamic range in the signal. However, using a constant cross section in predicting signal strength would result in large errors since there is such a large variation in cross section. Figure 3 shows the variation of the cross section for Sunsat with incidence angle on the array.

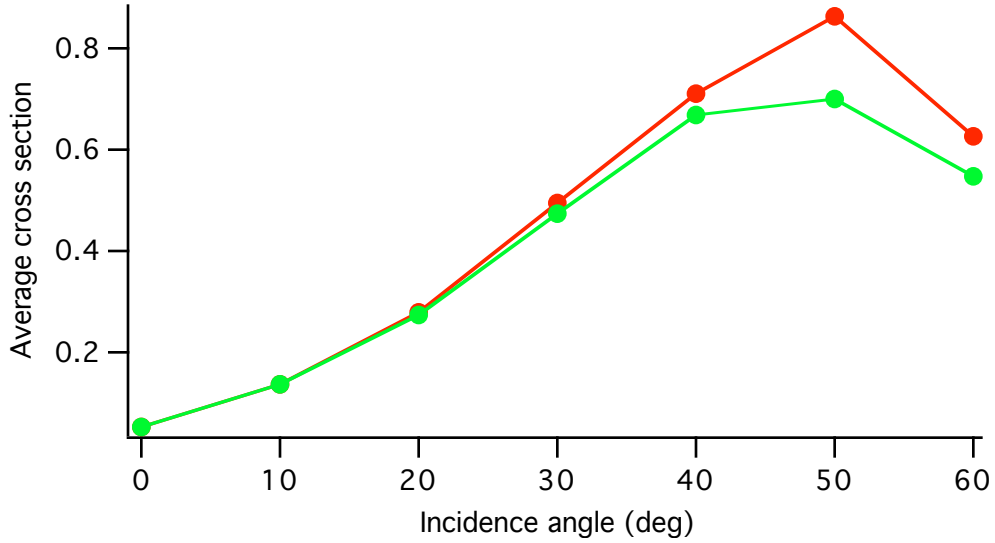

Figure 3. Cross section of Sunsat vs incidence angle (deg) on the array. The top curve (red) is for Theta = 0 deg and the bottom curve (green) is for Theta = 22.5 deg which is between the first two cube corners in the ring.

C. BEACON

Figure 4 shows a diagram of the BeaconC array. There is one panel at the top and 8 panels tilted at a 54 degree angle. The satellite is magnetically stabilized. Figure 5 shows the cross section vs incidence angle on the array. The green curve is between two panels so the cross section is lower. The cutoff angle is about 105 degrees. The cross section is reasonably constant up to about 70 degrees, but using a constant cross section would give a large error near the cutoff angle.

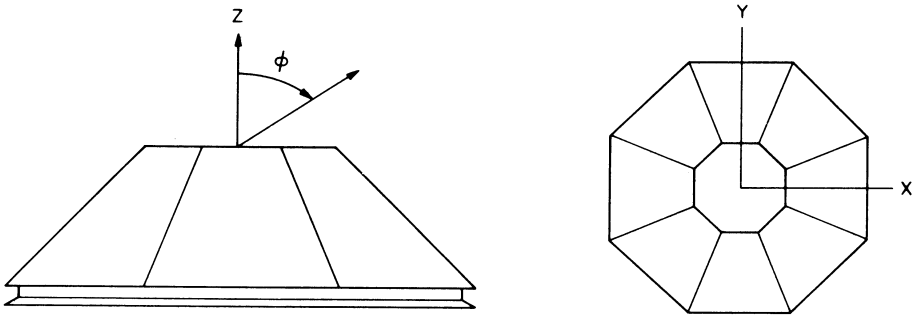

Figure 4. Diagram of the Beacon retroreflector array.

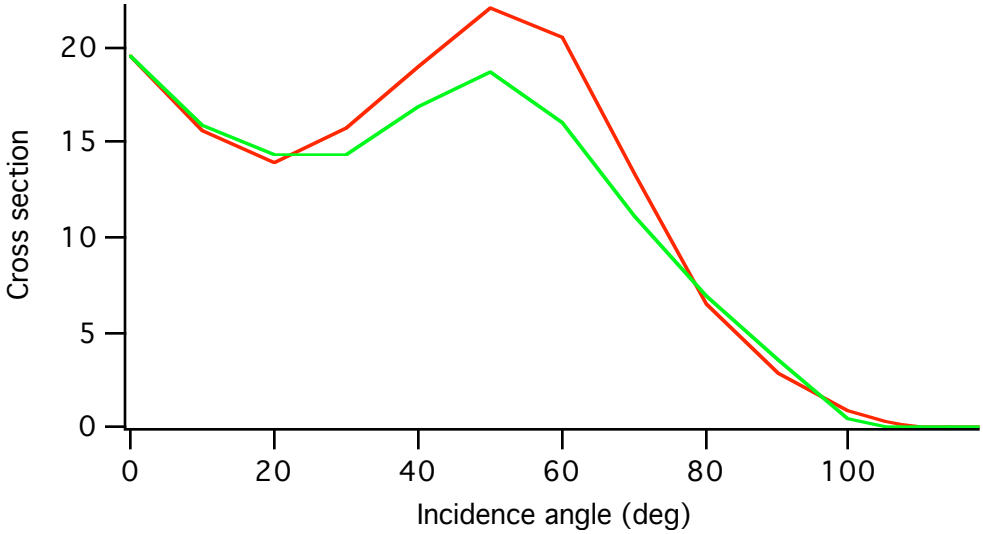

Figure 5. Cross section of the BeaconC array vs incidence angle. The top curve (red) is for Theta = 0 deg and the bottom curve (green) is for Theta = 22.5 deg.

D. CHAMP, GRACE

The cross section of CHAMP is fully documented in References 2 and 3. The array has 4 cubes on a 45 degree pyramid. Table 3 below summarizes the variations with incidence angle on a cube corner using the data in Reference 2. The cross section near zenith (about 40 deg incidence angle on a cube) is fairly low. However, the range is short so the design reduces the dynamic range of the signal strength. Using the cross section vs incidence angle on a cube would help to reduce the error in the predicted signal strength.

Incidence		Flux			Cross Sec.	
Angle	Minimum	Average	Maximum	Minimum	Average	Maximum
0	.0281	.0281	.0281	3.03	3.03	3.03
10	.0172	.0217	.0312	1.85	2.34	3.37
20	.00623	.0102	.0183	.67	1.10	1.98
30	.00216	.00356	.00680	.23	.38	.73
40	.00044	.00081	.00167	.047	.087	.180

Table 3. Cross section of CHAMP, and GRACE vs incidence angle on a cube corner. The cross section in million sq m is the flux times 108.

D. WESTPAC.

The WESTPAC array is designed so that only one cube corner is active at a time. This is done by recessing the cubes so that the cutoff angle is 13 degrees. This creates dead spaces where there is no signal between the cube corners. Table 4 shows the cross section as a function of incidence angle on a cube corner. The cross section is reasonably constant in the range 0 to 9 degrees and then drops off sharply.

Angle	Average	Max
0	.043	.121
1	.043	.202
2	.045	.284
3	.049	.348
4	.054	.380
5	.060	.373
6	.064	.332
7	.062	.266
8	.054	.188
9	.040	.114
10	.024	.055
11	.010	.018
12	.002	.002
13	.000	.000

Table 4. Average and maximum cross section as a function of incidence angle (deg).

E. Spherical, hemispherical, and planar arrays.

For spherical satellites such as LAGEOS, AJISAI, LRE, and ETALON, STARLETTE, and STELLA the cross section will vary some with velocity aberration but the average cross section is nearly independent of incidence angle.

Arrays that are approximately hemispherical such as ERS, ENVISAT, JASON, and GFO have cross section that do not vary much with incidence angle the same as the spherical satellites.

The high altitude satellites such as GLONASS, GPS have planar arrays. The cross section will vary some with incidence angle but the cross section is reasonably constant.

6. Cross section matrices.

The most accurate method of predicting the signal strength is to use the full cross section matrix to calculate the cross section as a function of the magnitude and direction of the velocity aberration. This procedure was used for the range correction on TOPEX. Because of the large size of the array the variations with velocity aberration were a few centimeters. Since signal strength predictions do not require the same accuracy as range corrections there is probably no need to do this for the cross section.

7. Summary.

The cross section of a retroreflector array may be relatively constant for some satellites and may have large variations for others. The cross section vs incidence angle or the full cross section matrix can be used to obtain more accurate signal strength predictions for satellites where there are large variations in the cross section.

8. References.

1. "Retroreflector array transfer functions", David A. Arnold, Proceedings of the 13th International Workshop on Laser Ranging, October, 2002, Washington, DC. Also available on the web at http://nercslr.nmt.ac.uk/sig/signature.html

2. Calculation of the Far field energy distribution of the CHAMP satellite retroreflector, Final report, prepared by: Jakob Neubert, IOF Jena, 1997, Fraunhofer Institut, Angewandte Optik und Feinmachanic.

3. "Investigation of the Effects of Aberration and Diffraction on the Performance of the Laser Reflector for the CHAMP Satellite", prepared by Reinhart Neubert GeoForschungsZentrum Potsdam, Dev.1: Kinematics and Dynamics of the Earth Telegrafenberg A17, D-14473 Potsdam, Germany
Tel.: (49)-331-288-1153, Fax.: (49)-331-288-1111, e-mail: neub@gfz-potsdam.de

4. Detailed data and reports for each satellite are available from the author, or Jan McGarry (NASA), or the Signal Processing Working Group (Graham Appleby).

Germanium flashes in LAGEOS-2 photometry data

by
David Arnold - 94 Pierce Road, Watertown, MA 02472, 617-924-6812
Graham Appleby, Robert Sherwood

1. Introduction

The rotation rate and spin axis of the LAGEOS-2 satellite have been determined by photometric observation of the solar flashes from the front face of the cube corners as the satellite rotates (Reference 1). However, since the flashes from the optical cubes are all the same, there is no way to determine the phase of the rotation using the flashes from the optical cubes.

There are 4 germanium cubes on LAGEOS-2 in holes 4N1, 4N16, 4S9 and 4S24. There are 31 holes in each row. The spacing between 4N1 and 4N16 is 15 holes. However, the spacing between 4N16 and 4N1, which could be considered to be in hole 4N32 if one were to continue the numbering past 31, is 16 holes. This lack of symmetry could be used to determine which germanium cube is being observed if there were a way to distinguish the germanium flashes from the optical flashes.

The flashes from the optical cubes are due to dielectric reflection from the front face. The reflection coefficient at normal incidence is about 4 percent. The germanium cubes are opaque at optical wavelengths and have a solar reflectivity of about 50 percent. The flashes from the germanium cubes should be much stronger than the flashes from the optical cubes because of the higher reflection coefficient.

2. Plots of photometry data

No evidence of stronger flashes from the germanium cubes has ever been reported in the photometry data. I asked Graham Appleby if it would be possible to look through the Herstmonceux data for the rows where the germanium cubes are located to see if there was any evidence of stronger flashes from the germanium cubes. An initial search did not turn up anything unusual.

The failure to find anything was rather perplexing since it seemed that the flashes should be there. I asked for a sample of the data to see if I could find any explanation for the apparent absence of any strong flashes. Robert Sherwood sent me an sample of data that contained a particularly long series of flashes from row 4S.

Figure 1 shows a plot of the data provided by Robert Sherwood. The strongest line in the data is a star. Stars can be distinguished from the flashes by the fact that they have a longer time duration. The flashes from the optical cubes can be seen throughout the plot. The dots above about 100 counts are from the laser which is firing during the first part of the plot. There does not seem to be anything in the plot to indicate the presence of germanium flashes.

The amplitude of the laser pulses is about 1600 counts which puts them off-scale in the plot which only goes up to 200 counts. The laser flashes are very short and are usually contained within one bin which is 1 millisecond long. Occasionally, the laser flash is split between two bins with any combination adding up to about 1600. For example, a laser pulse might be contained in 2 bins of amplitude 100 and 1500 totaling 1600 counts. This is what accounts for the points above 100 in the plot. The laser pulse rate is 10 pps and the optical flashes are at about 1 second intervals.

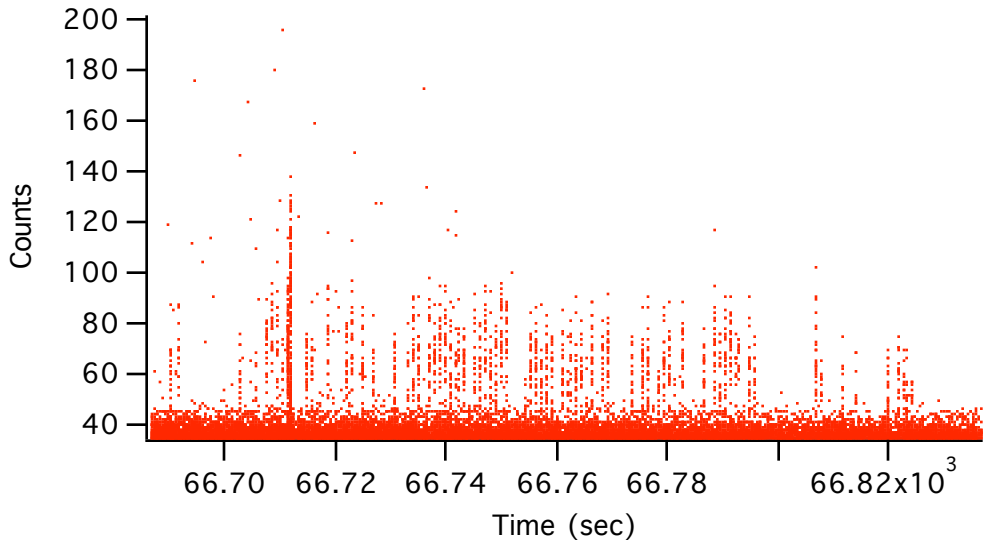

Figure 1. Plot of photometry data from row 4S of LAGEOS-2.

One possibility was that the germanium flashes might be hidden in the noise somehow. Since the laser flashes add noise to the data I decided to first filter out the laser pulses. The optical flashes cover a few tens of bins. This is more frequent than needed to define the shape of the flash. In order to get better signal to noise I averaged sets of 5 data points. With the laser pulses included, it is not possible to plot the data with lines connecting points since this would simply produce a box with amplitude of about 1600. However, lines between points should show the amplitudes more clearly if there were no laser pulses.

After filtering and smoothing the data, I plotted the results with lines connecting points. The results are shown in figure 2. There are 4 strong pulses immediately evident in the plot. The amplitude of the pulses is between about 400 and 550 counts.

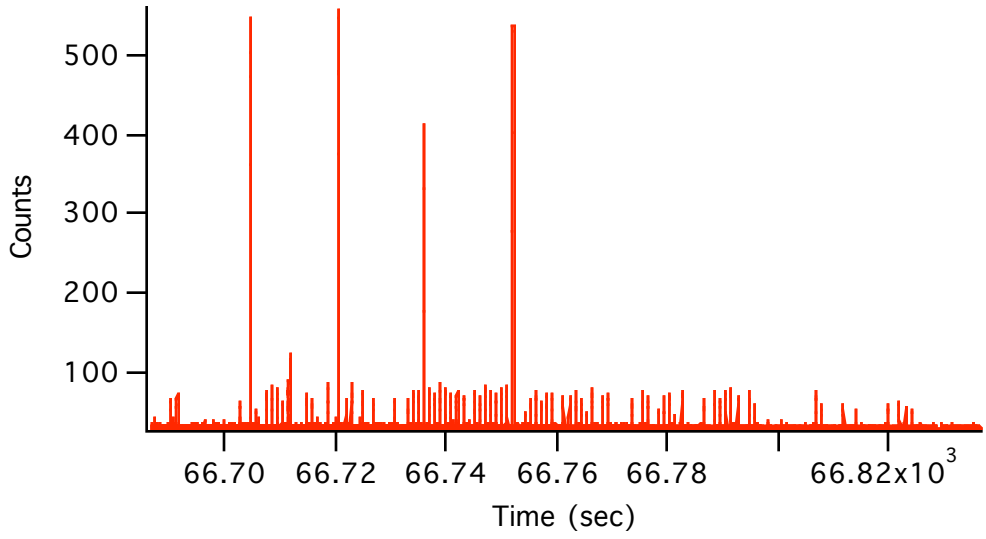

Figure 2. Plot of photometry data with laser pulses removed and sets of 5 points averaged.

Figure 3 shows a plot of the first part of the data with most of the background noise removed and a different filtering and smoothing algorithm. Although there is one optical flash missing, it is evident in the plot that there are 15 optical flashes between the third and fourth germanium flashes. Using the scale determined from this interval, one can determine that there are 14 optical flashes between the second and third germanium flashes and 15 optical flashes between the first and second germanium flashes. This is exactly the spacing one would expect from the positions of the germanium cubes.

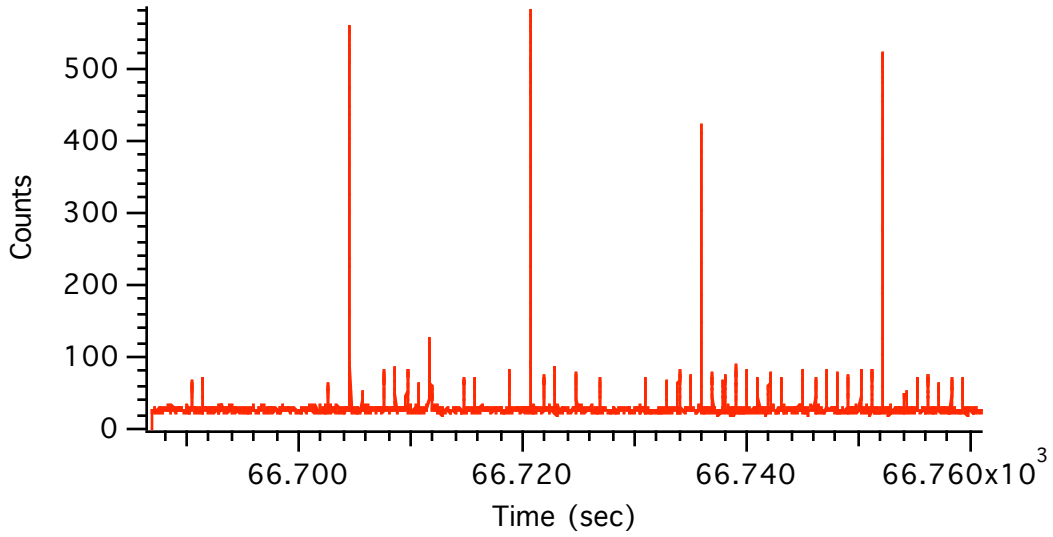

Figure 3. Plot of the first part of the photometry data with most background removed.

3. Interval between flashes.

Table 1 shows a computation of the timing and amplitude of each of the flashes. The columns are the interval between flashes, the average time of the flash, the begin time, end time, width, average amplitude, and peak amplitude. The germanium pulses are clearly evident in the next to the last column. The average amplitude of the germanium flashes ranges from 344 to 464 counts. They are easily distinguished from the optical flashes which range in amplitude from about 52 to 74 counts. The point at 66711 seconds with an amplitude of 78 counts is a star. Its width is .23 seconds which distinguishes it from the optical flashes which have a width of about .025 seconds.

Interval	Time	Begin	End	Width	Average	Peak
3.5736	66690.4136	66690.4036	66690.4236	0.0200	60.5	88.0
0.9971	66691.4086	66691.4007	66691.4165	0.0158	67.8	88.0
11.1499	66702.5586	66702.5506	66702.5666	0.0160	55.9	72.0
2.0279	66704.5925	66704.5785	66704.6065	0.0280	450.8	587.0
3.0320	66707.6226	66707.6105	66707.6346	0.0241	69.8	90.0
1.0091	66708.6310	66708.6196	66708.6425	0.0229	74.0	96.0
1.0179	66709.6480	66709.6375	66709.6585	0.0210	73.5	104.0
1.0100	66710.6530	66710.6475	66710.6586	0.0111	58.7	74.0
0.9301	66711.6956	66711.5776	66711.8135	0.2359	78.8	138.0
3.1240	66714.7141	66714.7016	66714.7265	0.0249	63.3	76.0
1.0220	66715.7326	66715.7236	66715.7415	0.0179	63.4	89.0
3.0319	66718.7665	66718.7555	66718.7775	0.0220	71.3	95.0
2.0121	66720.7811	66720.7676	66720.7945	0.0269	454.0	602.0
1.0340	66721.8141	66721.8016	66721.8266	0.0250	64.1	80.0
0.9950	66722.8086	66722.7966	66722.8206	0.0240	72.2	97.0
2.0339	66724.8430	66724.8305	66724.8555	0.0250	64.5	86.0

2.0391	66726.8771	66726.8696	66726.8846	0.0150	58.8	83.0
4.0449	66730.9260	66730.9145	66730.9375	0.0230	60.3	76.0
2.0201	66732.9390	66732.9346	66732.9435	0.0089	59.4	80.0
1.0120	66733.9596	66733.9466	66733.9726	0.0260	69.0	91.0
1.0060	66734.9651	66734.9526	66734.9776	0.0250	64.9	91.0
1.0339	66735.9930	66735.9865	66735.9996	0.0131	344.5	434.0
1.0061	66737.0056	66736.9926	66737.0186	0.0260	67.9	90.0
1.0039	66738.0075	66737.9965	66738.0185	0.0220	66.9	88.0
1.0160	66739.0235	66739.0125	66739.0346	0.0221	71.2	95.0
1.0061	66740.0311	66740.0186	66740.0436	0.0250	68.9	95.0
1.0170	66741.0481	66741.0356	66741.0605	0.0249	64.0	89.0
1.0040	66742.0531	66742.0396	66742.0666	0.0270	64.9	90.0
1.0229	66743.0750	66743.0625	66743.0876	0.0251	63.1	78.0
2.0270	66745.1006	66745.0895	66745.1116	0.0221	65.4	92.0
1.0160	66746.1150	66746.1055	66746.1246	0.0191	62.1	80.0
1.0141	66747.1321	66747.1196	66747.1446	0.0250	71.0	95.0
1.0130	66748.1436	66748.1326	66748.1546	0.0220	63.2	93.0
1.0119	66749.1535	66749.1445	66749.1625	0.0180	62.3	79.0
1.0090	66750.1665	66750.1535	66750.1796	0.0261	74.7	96.0
1.0211	66751.1851	66751.1746	66751.1956	0.0210	72.9	89.0
0.9950	66752.1815	66752.1696	66752.1935	0.0239	464.9	581.0
2.0380	66754.2105	66754.2076	66754.2135	0.0059	50.6	58.0
1.0107	66755.2288	66755.2183	66755.2394	0.0211	63.7	84.0
1.0142	66756.2445	66756.2325	66756.2565	0.0240	65.5	86.0
1.0271	66757.2671	66757.2596	66757.2746	0.0150	59.8	88.0
1.0057	66758.2774	66758.2653	66758.2895	0.0242	62.3	83.0
1.0150	66759.2894	66759.2803	66759.2984	0.0181	61.3	75.0
2.0061	66761.2980	66761.2864	66761.3095	0.0231	61.0	85.0
1.0291	66762.3264	66762.3155	66762.3374	0.0219	61.2	81.0
1.0160	66763.3440	66763.3315	66763.3565	0.0250	61.8	91.0
0.9969	66764.3395	66764.3284	66764.3506	0.0222	61.1	81.0
2.0252	66766.3671	66766.3536	66766.3805	0.0269	66.8	89.0
2.0438	66768.4064	66768.3974	66768.4154	0.0180	64.8	81.0
1.0011	66769.4095	66769.3985	66769.4205	0.0220	69.7	92.0
4.0489	66773.4554	66773.4474	66773.4634	0.0160	58.4	75.0
2.0260	66775.4855	66775.4734	66775.4975	0.0241	62.8	86.0
1.0150	66776.5014	66776.4884	66776.5144	0.0260	61.7	91.0
2.0440	66778.5354	66778.5324	66778.5385	0.0061	52.7	56.0
1.0000	66779.5425	66779.5324	66779.5525	0.0201	66.0	87.0
1.0080	66780.5524	66780.5404	66780.5644	0.0240	64.2	89.0
2.0320	66782.5850	66782.5724	66782.5975	0.0251	65.7	89.0
4.0441	66786.6260	66786.6165	66786.6355	0.0190	59.6	78.0
2.0369	66788.6659	66788.6534	66788.6784	0.0250	71.2	117.0
1.0172	66789.6790	66789.6706	66789.6874	0.0168	62.2	76.0
1.0060	66790.6895	66790.6766	66790.7024	0.0258	65.7	91.0
1.0078	66791.6958	66791.6844	66791.7073	0.0229	71.0	91.0
1.0022	66792.6996	66792.6866	66792.7126	0.0260	63.7	76.0
2.0468	66794.7438	66794.7334	66794.7543	0.0209	62.6	91.0
1.0021	66795.7416	66795.7355	66795.7476	0.0121	59.8	75.0
11.1410	66806.8875	66806.8765	66806.8984	0.0219	68.8	102.0
1.0199	66807.9024	66807.8964	66807.9085	0.0121	54.8	65.0
4.0591	66811.9590	66811.9555	66811.9624	0.0069	58.9	75.0
2.0310	66813.9890	66813.9865	66813.9915	0.0050	52.5	69.0
6.0760	66820.0690	66820.0625	66820.0755	0.0130	56.8	70.0
2.0199	66822.0920	66822.0824	66822.1015	0.0191	59.2	75.0
1.0039	66823.0984	66823.0863	66823.1104	0.0241	55.7	70.0

Table 1. Computation of the timing and amplitude of the flashes.

4. The amplitude problem

The germanium flashes are clearly visible in figures 2 and 3 but not in figure 1. One problem that is immediately obvious is that the amplitude of the germanium flashes is greater than the 200 counts. In figure 1 the plot scale is limited to 200 counts in order to eliminate the laser pulses which have amplitudes around 1600 and show the optical flashes which have an amplitude under 100 counts.

Figure 4 shows the same data as figure 1 plotted at full amplitude. The germanium flashes can be seen fairly easily in this plot. The concentration of points around 1600 is the laser firings. The laser stopped firing before the last germanium flash. The concentration of dots showing the germanium pulses is above the 200 count cutoff in figure 1. This is why they were not evident in the plot.

The third pulse in figure 4 might not be very obvious by itself against the background noise from the laser flashes. Figure 5 shows the same data as figure 4 but with the laser flashes removed. With the laser flashes removed there is no problem identifying the germanium flashes.

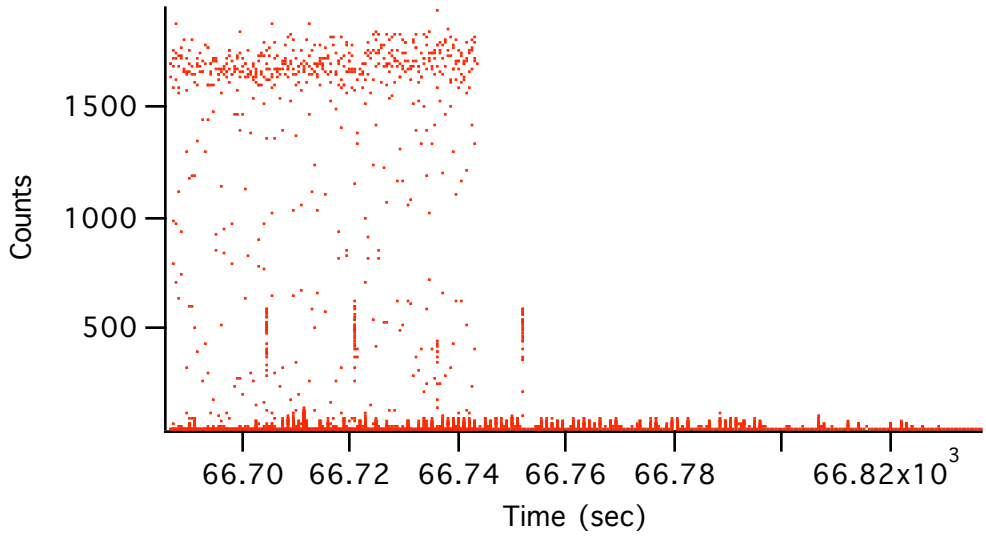

Figure 4. Plot of the complete data set at full amplitude.

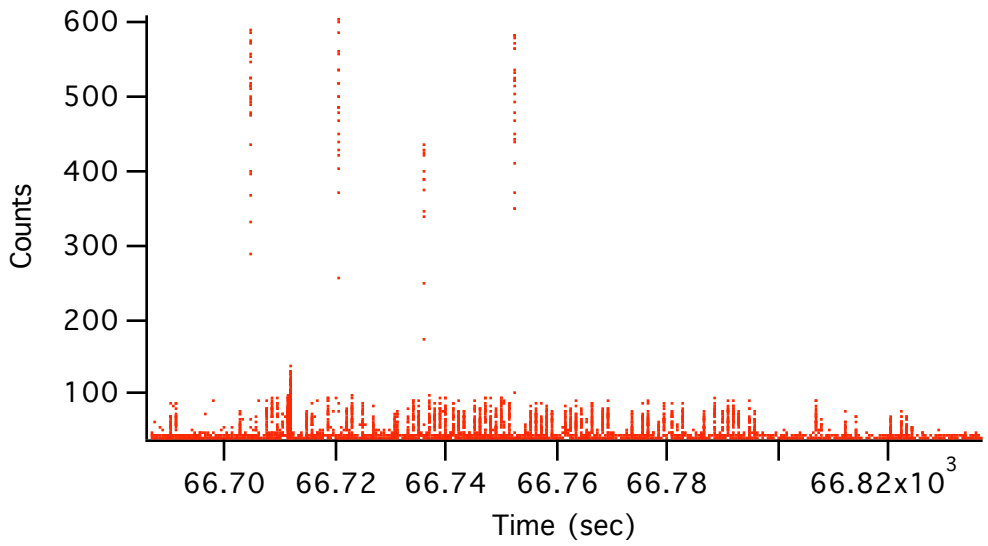

Figure 5. Plot of the data with the laser flashes removed.

5. Fixing the phase

The existence of the germanium flashes makes it possible in principle to determine the phase of the rotation of the satellite in addition to the spin rate and orientation of the spin axis. The extent to which this can be done depends on the density of the data and the stability of the spin rate. At the present time the available data is being cataloged to see what is available. Unfortunately, the spin rate is slowing down. Robert Sherwood has pointed out that as the rate slows there is less likelihood of geting enough data to include at least 2 germanium flashes. It might be possible to use a single flash if it is possible to interpolate the phase angle with sufficient accuracy between data sets having at least two germanium flashes. If there is a germanium flash missing the interval is always the same so that it is not possible to positively identify which cube is being observed.

The germanium cubes could be used in another way to determine the orientation of LAGEOS. The range to a germanium cube varies as the satellite spins. The amplitude of the variation depends on the angle between the line of sight and the spin axis. Range measurements to LAGEOS with a 10.6 micron laser would see only the germanium cubes. Such data could be used to determine the orientation of the satellite. This technique could be used for much slower rotation rates since the 4 germanium cubes with their high index of refraction provide coverage over all satellite orientations.

6. The range correction.

The accuracy goal for LAGEOS was 5 millimeters. The range correction fluctuates over a range of about +/- 5 millimeters as the satellite rotates. The rms error is on the order of 3 millimeters. The main factor limiting the accuracy of the range corrections for LAGEOS is that the orientation is unknown. If the orientation of the satellite were known, the range correction could be computed for that particular orientation. This would result in a significant increase in accuracy to perhaps 1 millimeter. The range correction is a function of polarization for LAGEOS because the cube corners are uncoated. In order to compute the range correction as a function of orientation and velocity aberration it would be necessary to know the polarization (linear or circular) and the angle of the polarization vector if linear polarization is used.

Spectral analysis of the range residuals for LAGEOS using data from the MLRO shows discrete spectral lines that are integral multiples of the rotation rate (Reference 2). This fact could be used as a test of whether range corrections computed as a function of orientation are being correctly applied. The spectral lines should disappear or be significantly reduced in amplitude after the corrections are applied.

7. Summary.

Photometry of sunlight reflected from the cube corners has been routinely used to determine the spin rate and orientation of LAGEOS-2 (Reference 1). Since the reflections from the optical cubes are all the same amplitude, they cannot be used to determine the phase of the rotation. Since the solar reflectivity of the germanium cubes is much greater then the reflectivity of the optical cubes, the phase angle can be determined whenever the viewing angle is such that reflections can be obtained from the rows containing the germanium cubes. Range data from the germanium cubes using a 10.6 micron laser might also be able to determine the complete orientation of LAGEOS. Knowing the complete orientation of LAGEOS would make it possible to apply a range correction as a function of the orientation in order to remove the variations in the range correction as the satellite spins.

8. References.

1. “LAGEOS-2 spin rate and orientation”, Robert Sherwood, Roger Wood, Toshimichi Otsubo, 13th International Workshop on Laser Ranging, October 7-11, 2002, Washington, DC.

2. “Measurement of LAGEOS-2 Rotation by SLR Observations”, G. Bianco, M. Chersich, R. Devoti, B. Luceri, M. Selden, Proceedings of the 12th International Workshop on Laser Ranging, Matera, Italy, 13-17 November, 2000.

Spectral Analysis of LAGEOS Range Data

by
David Arnold - 94 Pierce Road, Watertown, MA 02472, 617-924-6812
Giuseppe Bianco - Agenzia Spaziale Italiana, CGS - Matera

1. Introduction.

The paper "Measurement of LAGEOS-2 Rotation by SLR Observations", G. Bianco, et al. presented at the 12th International Workshop on Laser Ranging (Reference 1) shows that the range residuals from LAGEOS-2 contain discrete spectral lines which are integral multiples of the rotational rate. The lowest frequency is the spin rate. In this paper we show that simulated data for LAGEOS-2 contain the same spectral lines as the range data.

2. Simulation of the rotation of LAGEOS.

The paper "Retroreflector Array Transfer Functions", D. A. Arnold, presented at the 13th International Workshop on Laser Ranging (Reference 2, Figure 6) shows a simulation of the range correction as the LAGEOS satellite spins. The simulations were done using the method described in SAO Special Report 382, D. A. Arnold (Reference 3). Using the data from the simulation V. Luceri and R. Devoti have shown that the simulated data also contains spectral lines that are integral multiples of the spin rate as seen in Figure 1 below.

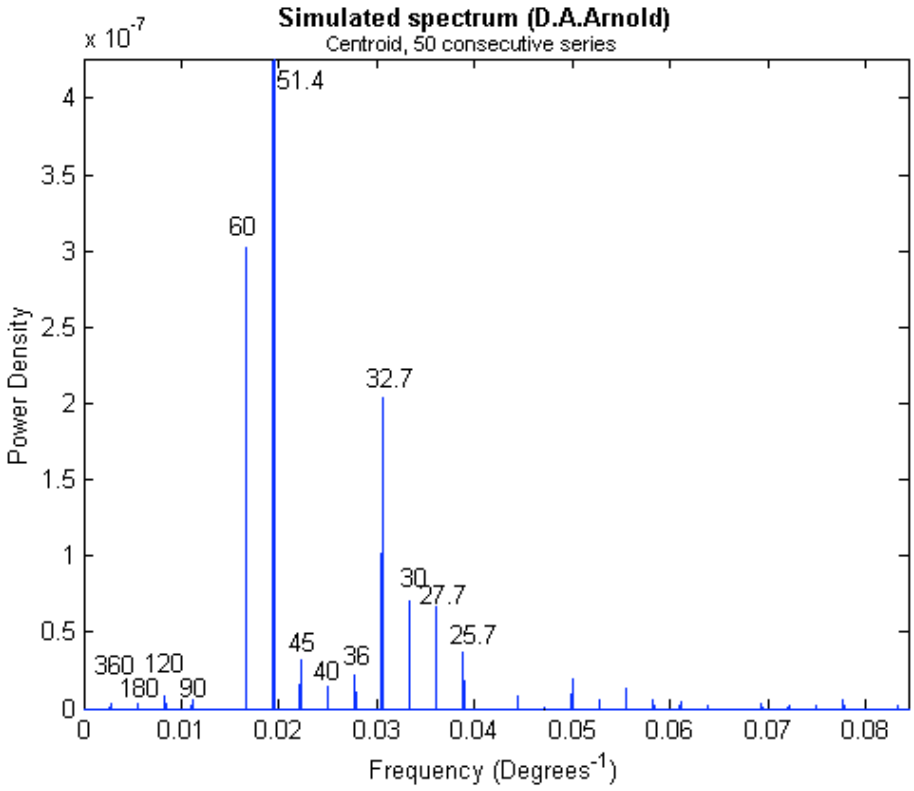

Fig. 1 Spectrum of simulated range residuals of 50 complete LAGEOS-2 rotations as viewed from the satellite's equatorial plane. The periods of the peaks are indicated in units of degrees.

3. Spectral analysis of actual ranging data.

Figure 2 shows a spectral analysis by V. Luceri and R. Devoti of range data from a pass on Oct. 15, 1998. The spectral lines are integral multiples of the rotation rate.

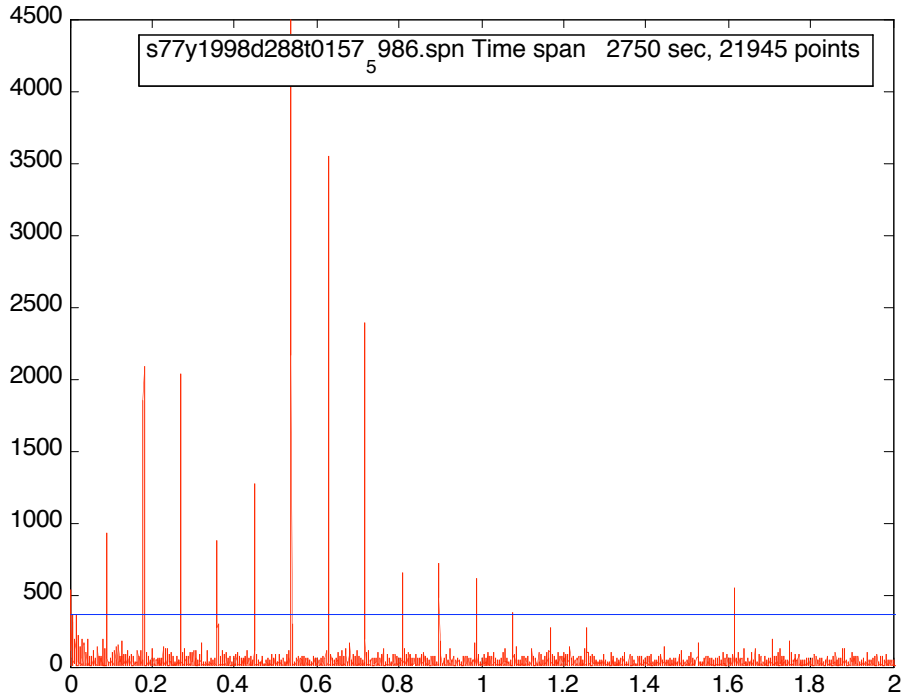

Fig. 2. Spectrum of observed range residuals (MLRO) from a real pass (Oct. 15, 1998), the fundamental period (first peak) is 10.9 sec, all the other peaks are exact harmonics of the fundamental frequency.

Figure 3 shows a second example of spectral analysis of real range data. This pass is from March 21, 2002. The amplitudes of the spectral lines are different but the spectral lines integral multiples of the spin rate. The period of the spin in Figure 2 is 10.9 seconds. In Figure 3 the period has increased to 55.4 seconds.

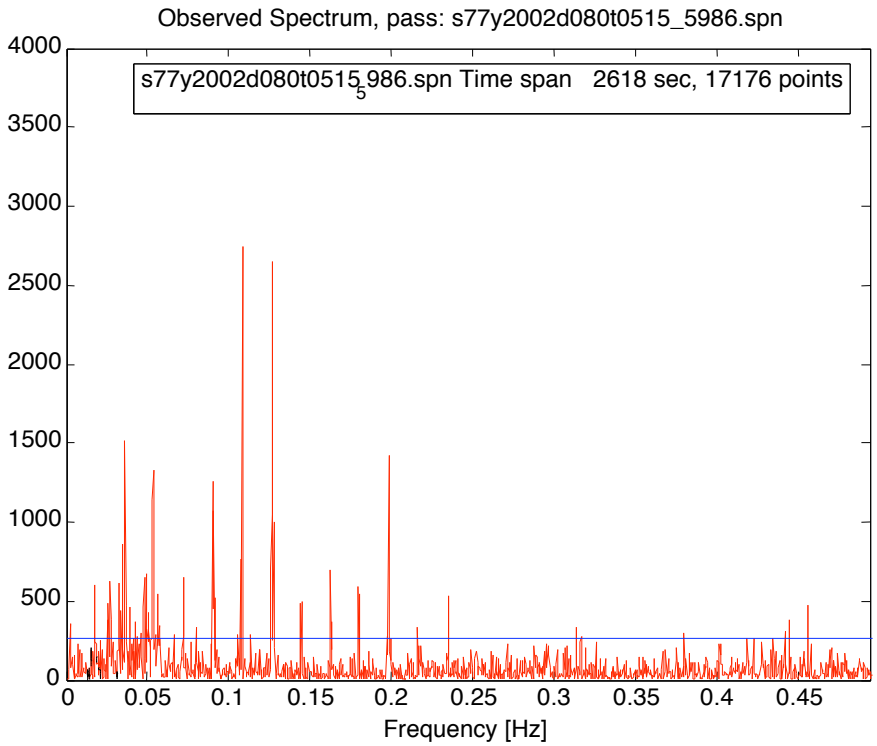

Fig. 3. Spectrum of observed range residuals (MLRO) from a real pass (March 21, 2002), the fundamental period (first peak) is 55.4 sec, all the other peaks are exact harmonics of the fundamental frequency.

4. Comparison of methods of spectral analysis.

The spectral analyses shown in Figures 1, 2, and 3 have been done using the Scargle algorithm for unequally spaced data analysis. The spectral analyses shown in Figures 1 and 3 have been repeated by D.A. Arnold using a different method. In this approach, the equation

$$R = A + B\sin(\omega t) + C\cos(\omega t) \qquad (1)$$

is used to do a least squares fit to the range R as a function of time. For range residuals from an orbital fit, the constant A would be approximately zero. For simulated range corrections, the constant A is about .243 meters. The coefficients B and C can be considered the imaginary and real part of a complex exponential containing the frequency and phase of the spectral component. The spectral analysis is done by varying the frequency ω from the spin rate to the highest spectral frequency. The power P in a spectral component is given by

$$P(\omega) = B^2 + C^2 \qquad (2)$$

Figure 4 shows the spectral analysis of the same data as Figure 1 done by D.A. Arnold using equation (1). The analysis includes only the first 20 spectral lines. Figure 5 shows the same data as Figure 3 analyzed with equation (1). The Scargle method and using equation (1) give essentially identical results.

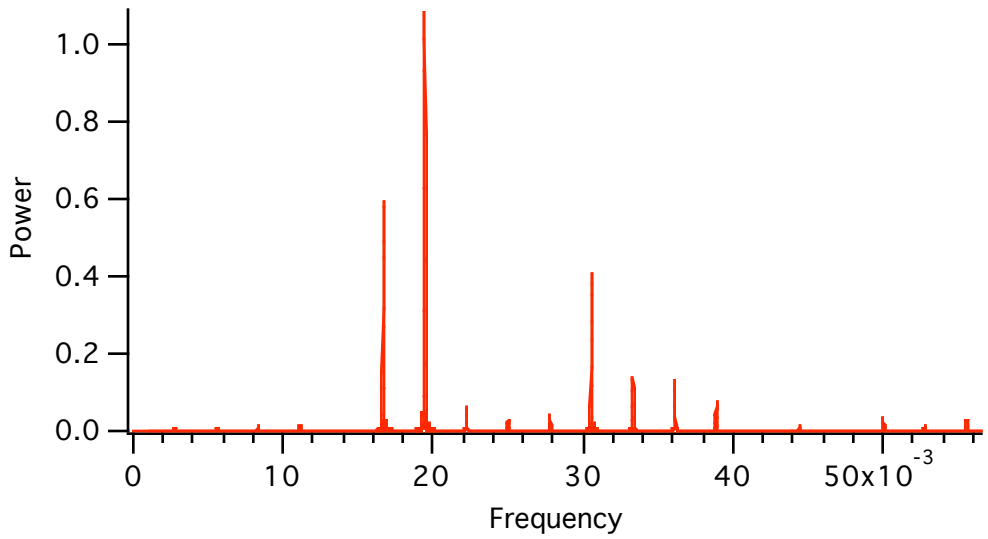

Figure 4. Spectrum of simulated range residuals of 50 complete LAGEOS-2 rotations as viewed from the satellite's equatorial plane. The frequency is in (1/deg).

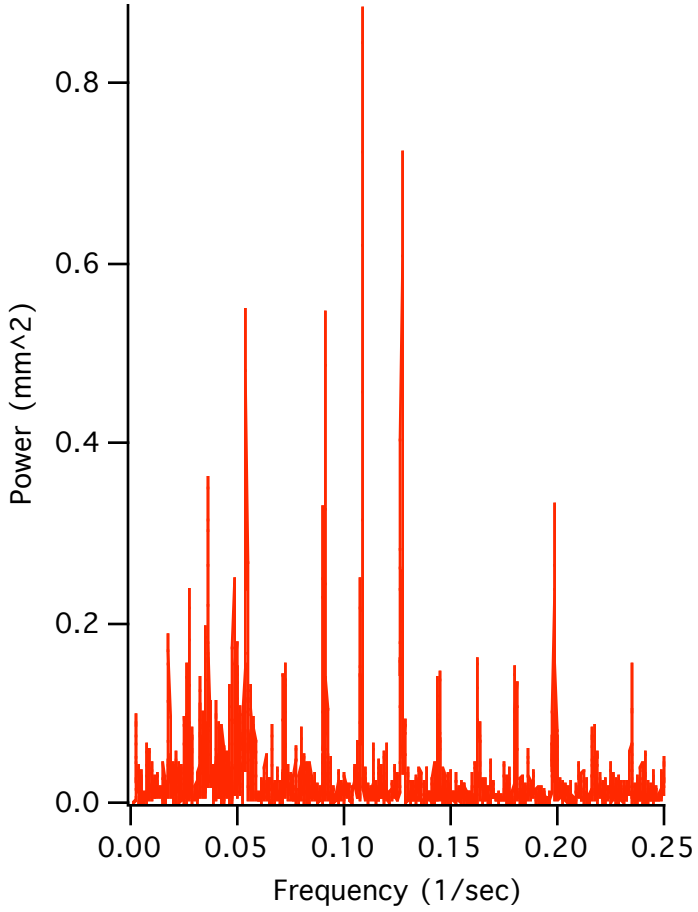

Figure 5. Spectrum of observed range residuals (MLRO) from a real pass (March 21, 2002), the fundamental period (first peak) is 55.4 sec.

5. Dependence on the angle from the spin axis.

In this section simulations are done at various angles from the spin axis of the satellite in order to show the variation in the amplitudes of the spectral lines. The angle between the line of sight and the spin axis is 90 degrees in Figures 1 and 4. In other words, the satellite is being observed from the equator. In Figure 6 the angle with respect to the spin axis is 30 degrees. In Figure 7 the angle is zero (looking directly at the pole).

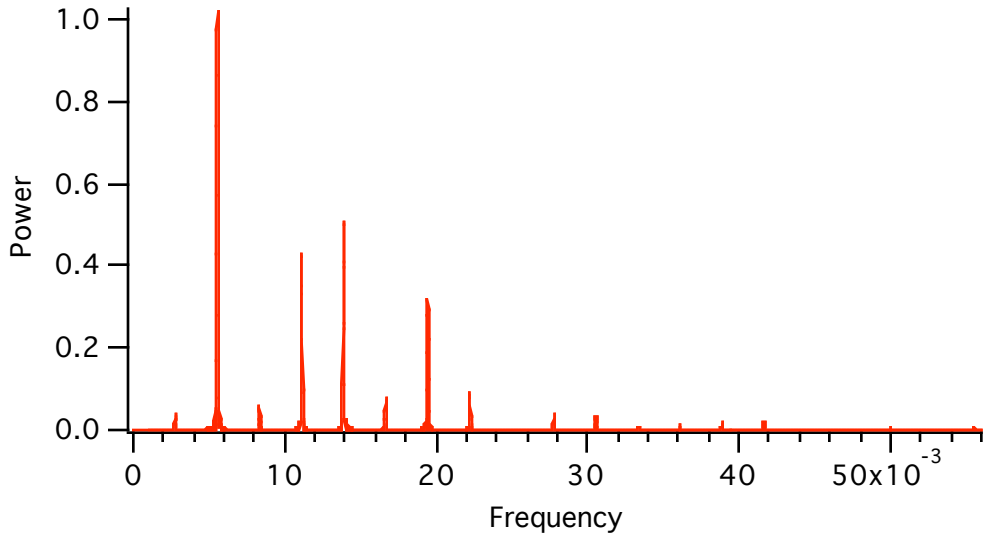

Figure 6. Spectrum with a 30 degree angle between the line of sight and the spin axis.

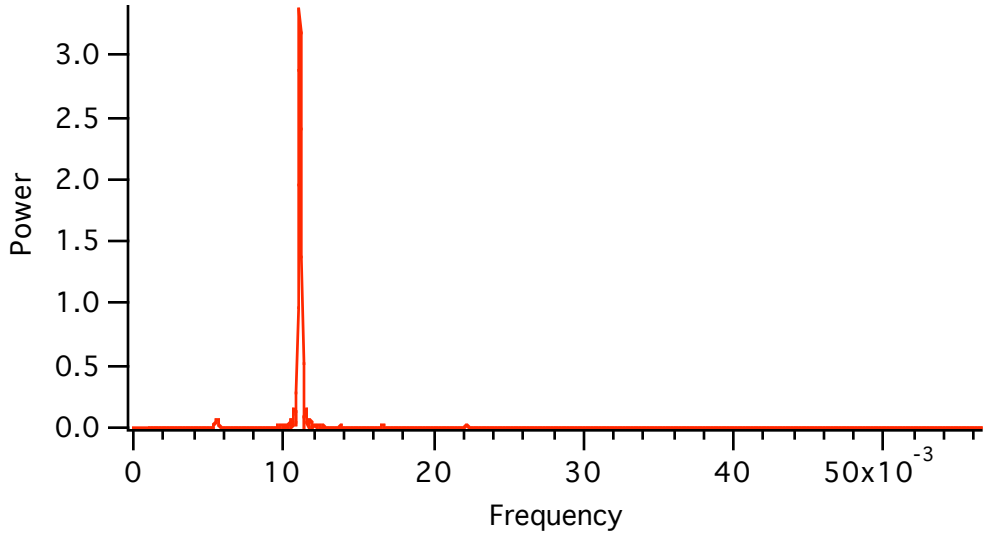

Figure 7. Spectrum looking at the spin axis.

Comparing Figures 4, 6, and 7 we see that the highest frequencies are when the satellite is viewed from the equator. At a 30 degree angle from the pole only the lower frequencies are visible. When looking at the pole there is only one major frequency which is 4 times the spin rate.

6. Phase plot.

Since it has been shown that the spectrum contains only discrete frequencies it is possible to do a spectral analysis with equation (1) using only the known frequencies. In order to obtain accurate results the data must contain an integral number of cycles of each frequency. Figures 8 shows a spectral analysis of the equatorial simulation using only integral multiples of the spin rate with data covering one complete revolution. Figure 9 is a phase plot of the spectral lines in figure 8.

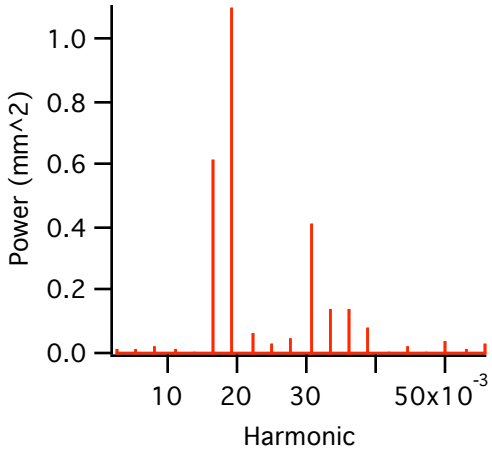

Figure 8. Spectral analysis of one revolution

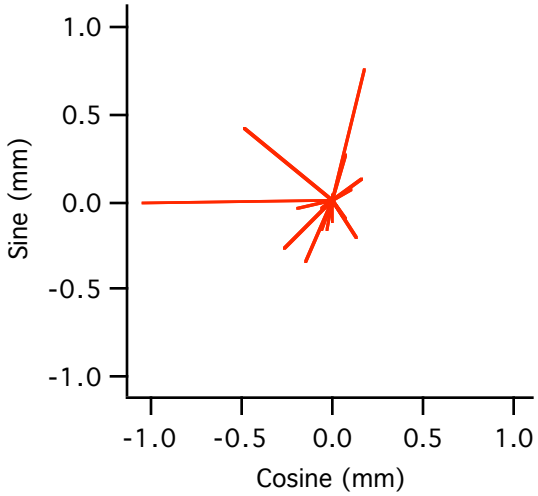

Figure 9. Phase plot of the harmonics

Tables 1 and 2 below shows the data used to plot Figures 8 and 9 respectively.

Period (deg)	Harmonic	Amplitude (mm)	Power (mm^2)	Frequency(1/deg)
360.000	1.000	0.077955	0.006077	0.002778
180.000	2.000	0.072774	0.005296	0.005556
120.000	3.000	0.126817	0.016083	0.008333
90.000	4.000	0.110108	0.012124	0.011111
72.000	5.000	0.032602	0.001063	0.013889
60.000	6.000	0.778751	0.606453	0.016667
51.430	7.000	1.045384	1.092827	0.019444
45.000	8.000	0.251219	0.063111	0.022222
40.000	9.000	0.168907	0.028530	0.025000
36.000	10.000	0.208311	0.043394	0.027778
32.730	10.999	0.638545	0.407740	0.030553
30.000	12.000	0.373327	0.139373	0.033333
27.690	13.001	0.369462	0.136502	0.036114
25.710	14.002	0.270873	0.073372	0.038895
24.000	15.000	0.019269	0.000371	0.041667
22.500	16.000	0.125351	0.015713	0.044444
21.176	17.000	0.025514	0.000651	0.047223
20.000	18.000	0.194486	0.037825	0.050000
18.947	19.000	0.107882	0.011639	0.052779
18.000	20.000	0.166709	0.027792	0.055556

Table 1. Data used to plot Figure 8.

Harmonic	Sine(mm)	Cosine(mm)	Amp(mm)	Power(mm^2)	Phase(deg)
1.0	-0.0017	-0.0779	0.0780	0.0061	181.24
2.0	-0.0363	-0.0631	0.0728	0.0053	209.89
3.0	0.0778	0.1002	0.1268	0.0161	37.82
4.0	-0.0856	0.0693	0.1101	0.0121	309.01
5.0	0.0326	-0.0015	0.0326	0.0011	92.63
6.0	0.7732	0.0932	0.7788	0.6065	83.12
7.0	-0.1402	-1.0359	1.0454	1.0928	187.71
8.0	-0.1900	0.1643	0.2512	0.0631	310.86
9.0	-0.1686	-0.0099	0.1689	0.0285	266.63
10.0	0.1578	0.1360	0.2083	0.0434	49.26
11.0	0.3116	-0.5573	0.6385	0.4077	150.79
12.0	-0.3666	-0.0708	0.3733	0.1394	259.07
13.0	-0.3115	-0.1987	0.3695	0.1365	237.46
14.0	0.2708	0.0075	0.2709	0.0734	88.42
15.0	-0.0191	-0.0023	0.0193	0.0004	263.08
16.0	-0.0808	0.0958	0.1254	0.0157	319.86
17.0	-0.0101	0.0235	0.0255	0.0007	336.80
18.0	-0.1013	-0.1660	0.1945	0.0378	211.40
19.0	-0.1012	0.0372	0.1079	0.0116	290.20
20.0	-0.1666	0.0054	0.1667	0.0278	271.86

Table 2. Data used to plot Figure 9.

7. Reconstructing the function from the spectral lines.

The Fourier coefficients computed for the simulated data can be used to reconstruct the function. The plot below shows the simulated data and the Fourier fit to the data using the spectral lines up to 20 shown in Table 2 above. The fit is not exact. Using a few more terms would probably improve the fit. Some rows of LAGEOS have 32 cubes.

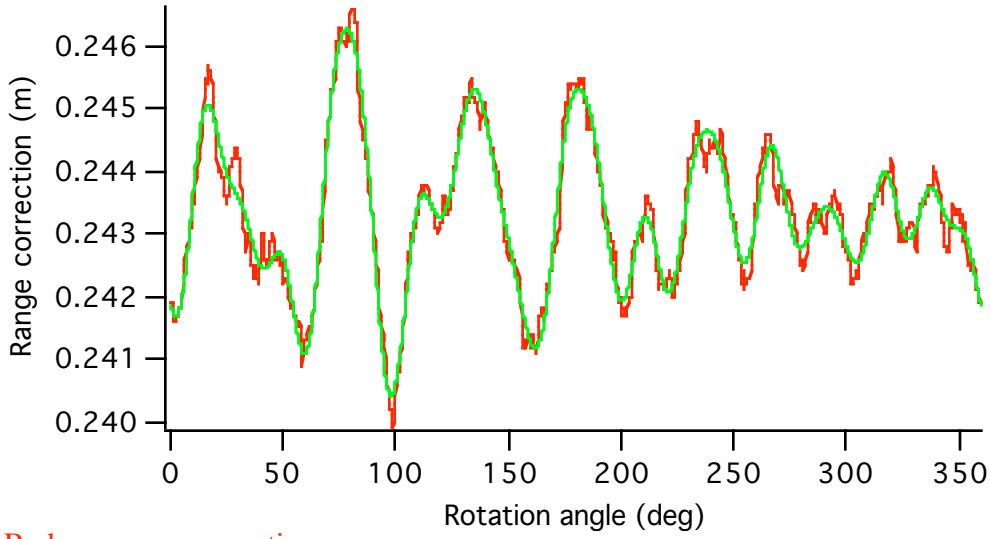

Red = range correction
Green = Fourier fit
Figure 10. Plot of the simulated data and the Fourier fit to the data using terms up to 20.

8. Dependence on the reflecting properties of the cube corners.

A LAGEOS cube corner can lose total internal reflection past about 17 degrees incidence angle depending on the orientation of the cube in its holder. One would expect that the variation of the range correction as the satellite spins would depend on the orientation of each cube in its holder. Figure 11 shows the spectrum looking at the equator with random orientations of the cubes.

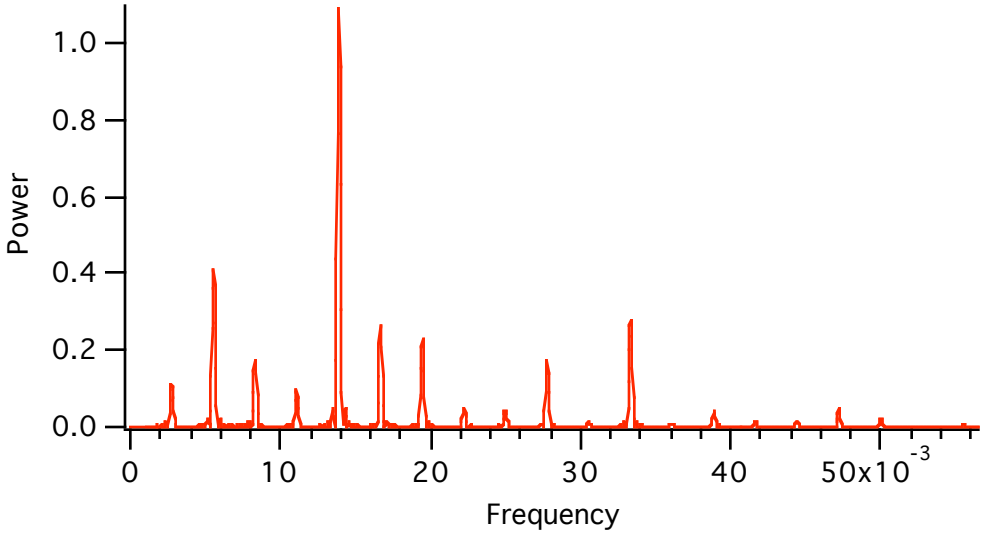

Figure 11. Spectrum looking at the equator with random orientations of the cubes.

Comparing Figure 11 with Figure 4 it is clear that the amplitudes of the spectral lines depend on the orientation of the cubes in their mountings.

9. Methods of computing the spectral lines.

The amplitudes of the spectral lines can be computed in two different ways:

A. If the spectrum of a set of data is unknown, it is necessary to try all frequencies in order to compute the spectral amplitudes. The analysis of the real Lageos data shows a certain amount of noise between the spectral lines. This is to be expected since there are various noise sources present in the data. The analysis of the simulated data shows much less noise between the lines.

B. The terms of a Fourier series are integral multiples of the fundamental frequency and form an orthogonal set of functions over one cycle of the fundamental. There are an integral number of cycles of each frequency in one revolution. Since the Lageos spectrum has been shown to be Fourier series with a finite number of terms it should be possible to solve for the known harmonics from one revolution or an integral number of revolutions by solving only for the known frequencies.

If an interval does not contain an integral number of cycles one will not get the correct amplitudes. Using a long data set with many cycles gives approximately the correct answer even though there may not be an integral number of cycles of each frequency. The error in determining the frequency is inversely proportional to the length of the time interval.

10. Variation of the spectral lines during a pass.

In principle, shorter periods of time could be used in the spectral analysis of real LAGEOS data if the spin rate were known, just as Figure 8 was computed using only one revolution and solving only for the known spectral lines.

Figure 12 below show a spectral analysis done on real data with the pass broken up into eight intervals. We see that the amplitudes of the spectral lines are different in each interval. This is what one would expect if the angle between the line of sight and the spin axis is changing during the pass. The green triangles show the position of the integral spectral lines. The width of the lines is broader and there is more noise between the lines.

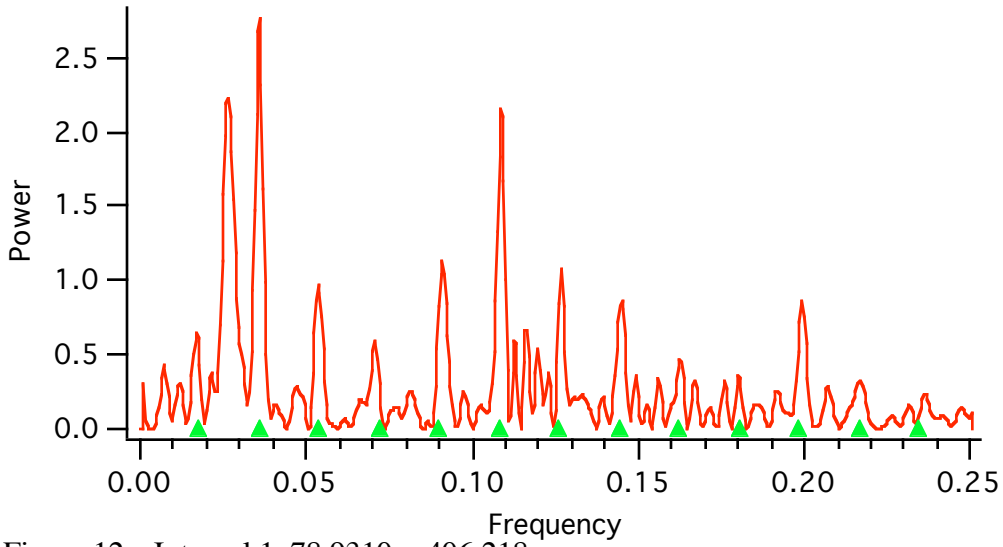

Figure 12a. Interval 1, 78.9310 - 406.218 sec

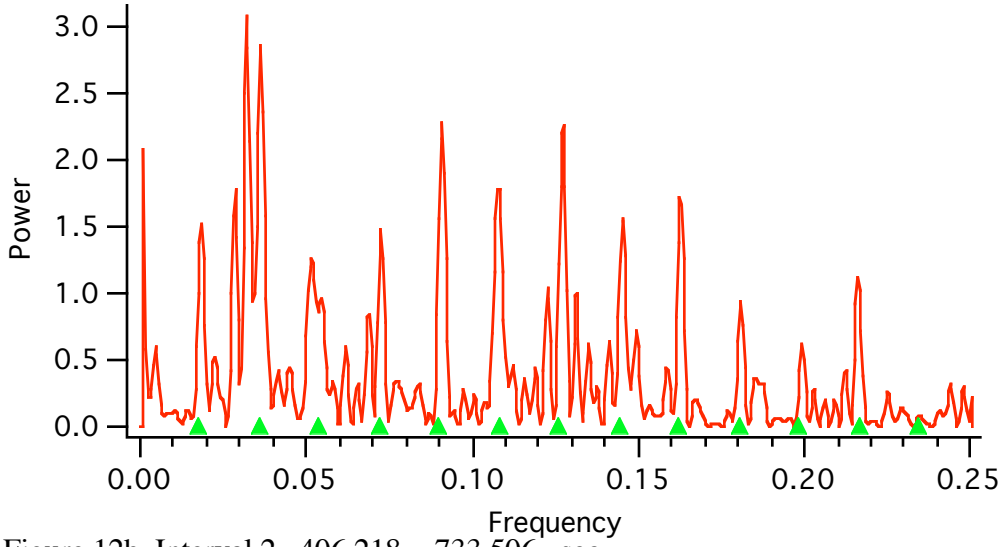

Figure 12b, Interval 2, 406.218 - 733.506 sec

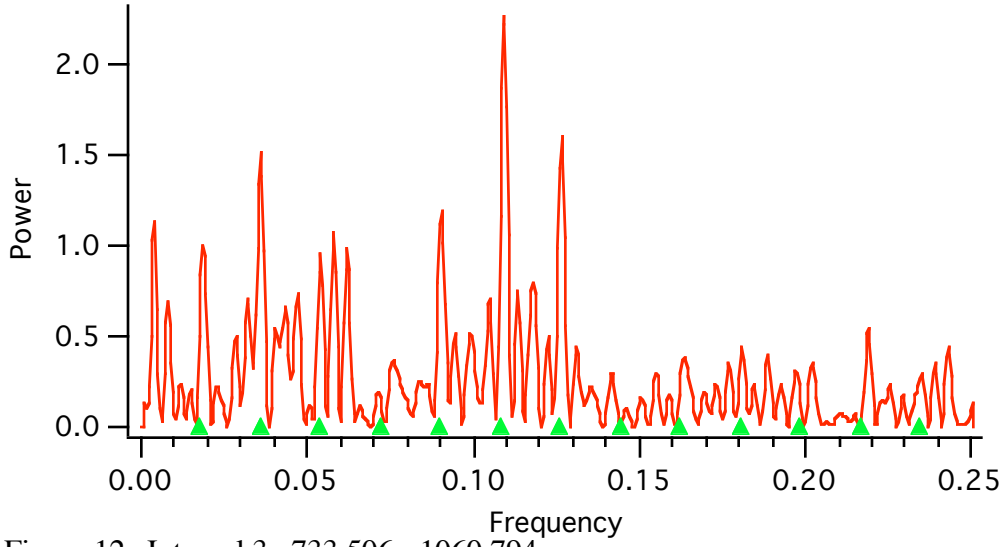

Figure 12c Interval 3, 733.506 - 1060.794 sec

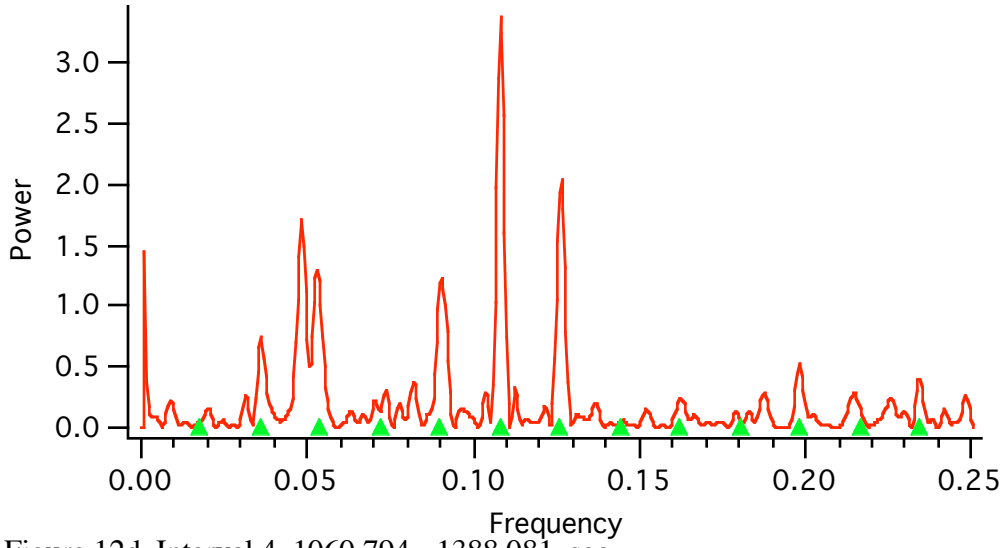

Figure 12d, Interval 4, 1060.794 - 1388.081 sec

The last 4 parts of Figure 12 are shown later in the paper.

11. Experimental verification of the dependence on the orientation of the spin axis.

The simulated data shows that higher frequencies are present when looking at the equator and lower frequencies dominate when looking at the pole. It should be possible to verify this experimentally. The paper "LAGEOS-2 spin rate and orientation", R. Sherwood (Reference 4) shows that the spin rate and orientation of the spin axis can be determined using photometry of the solar flashes from the front face of the cube corners. The spectrum of actual range data could be correlated with the angle between the observing direction and the orientation of the spin axis to see if the frequencies are lower near the pole. Since the angle with respect to the pole is constantly changing during a pass, one should use a short interval consisting of an integral number of revolutions in making the comparison.

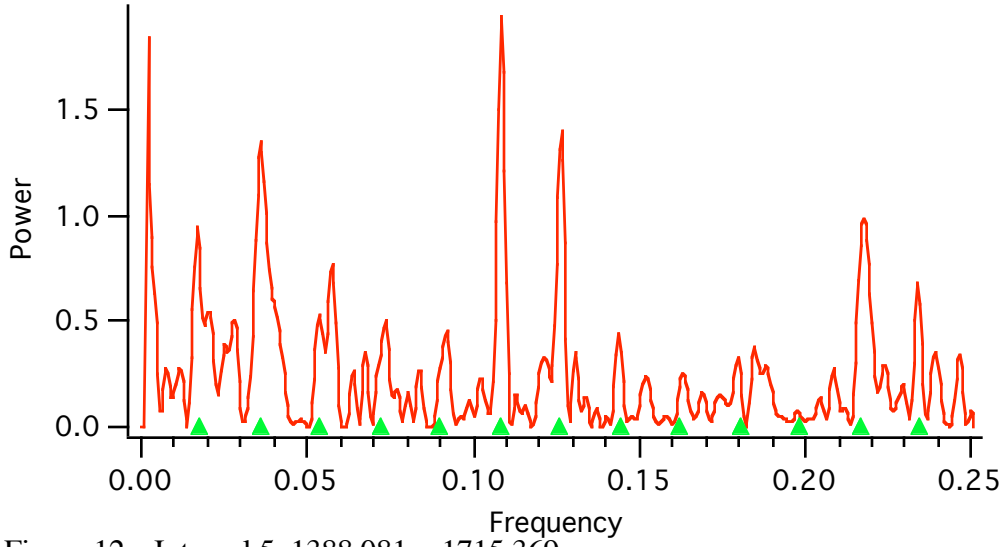

Figure 12e, Interval 5, 1388.081 - 1715.369 sec

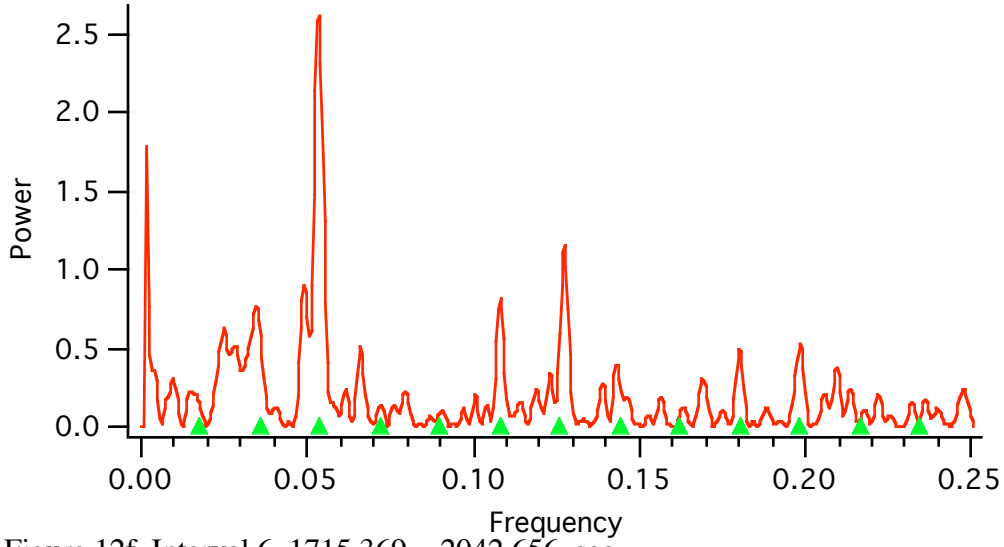

Figure 12f. Interval 6, 1715.369 - 2042.656 sec

12. Determination of the phase of the rotation using the range data.

Since the spin axis and orientation can be determined by photometry (Reference 4), it might be possible to determine the phase of the rotation using the range data. Since the frequencies of the spectral lines are known one could do a spectral analysis of an integral number of rotations. This can be used to reconstruct the range variations as a function of time as was done in Figure 10 of this report. The simulation program can be used to compute the predicted range variations for the time interval using an arbitrary starting phase of the rotation. The two curves could then be compared to try to match up the phase. A second approach suggested by G. Appleby is to vary the phase from 0 to 360 in the simulation and look for the phase angle that minimizes the rms difference between the simulation and the actual data. A third approach would be to add the phase angle to the orbital solution. This would require a starting value of the phase angle since the orbital solution is a non-linear least squares iteration.

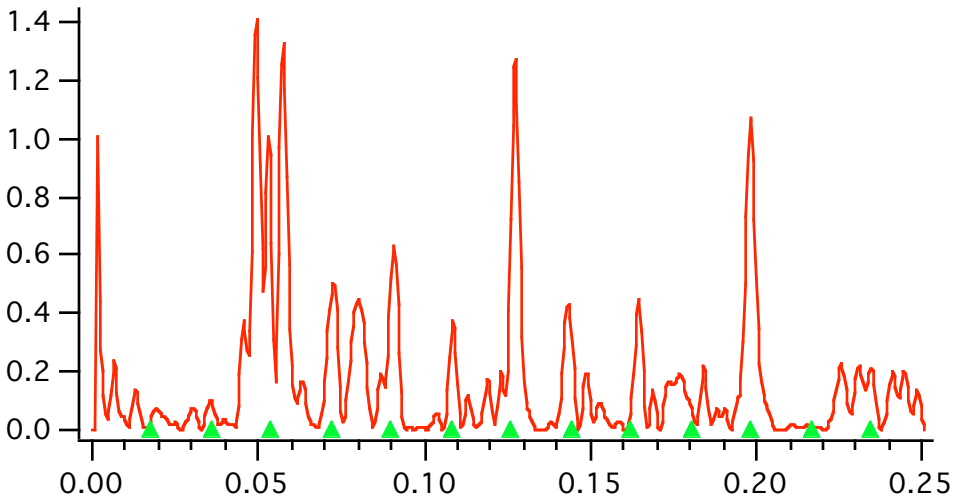

Figure 12g. Interval 7, 2042.656 - 2369.944 sec

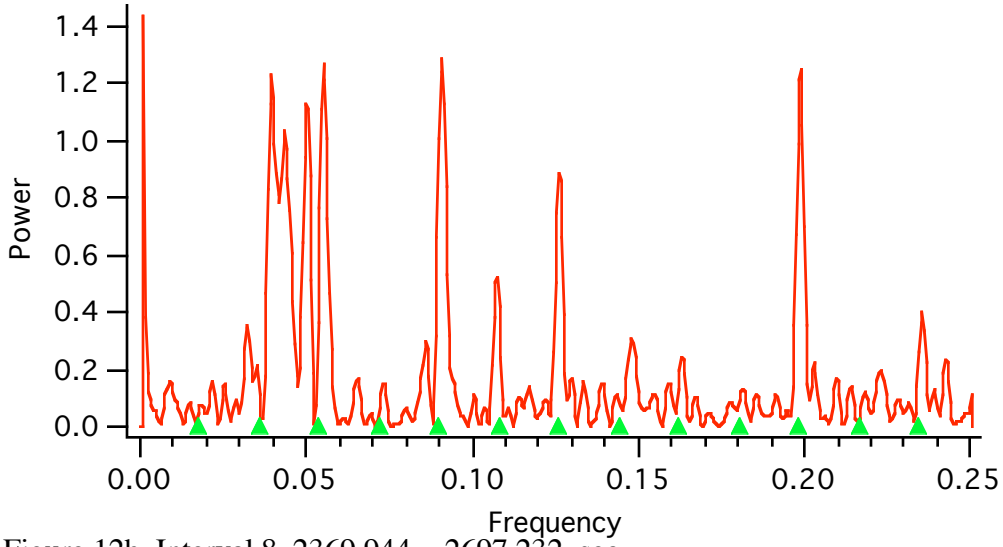

Figure 12h. Interval 8, 2369.944 - 2697.232 sec

13. Other methods of determinating the phase angle.

It has been shown recently that the phase of the rotation of LAGEOS can be determined by observation of the solar flashes from the germanium cubes (see "Germanium flashes in LAGEOS-2 photometry data", David A. Arnold, presented at this workshop). Since the amount of data on the germanium flashes is very limited it may be difficult to use this data to determine the phase throughout the whole period of the photometry. However, it could be used as a starting value for computing the phase in an orbital solution as described in Section 12.

The orientation of LAGEOS could, in principle, be determined by pulsed and CW infrared ranging to the germanium cube corners. This technique is discussed on Pages 187 and 188 of the report "Optical and infrared transfer function of the LAGEOS retroreflector array", D.A. Arnold (Reference 5).

14. Summary and conclusions.

Spectral analysis of simulated and actual LAGEOS range data shows spectral lines that are integral multiples of the spin rate. This seems reasonable since there are an integral number of cube corners in each row on the satellite. The amplitudes of the spectral lines depends on the reflecting properties of the cube corners and the angle of incidence with respect to the spin axis.

15. Acknowledgements

The authors wish to express their appreciation to V. Luceri and R. Devoti for their technical assistance in providing laser range data and doing the analyses shown in the Figures 1, 2, and 3 of this report.

16. References

1. “Measurement of LAGEOS-2 Rotation by SLR Observations”, G. Bianco, M. Chersich, R. Devoti, B. Luceri, M. Selden, Proceedings of the 12th International Workshop on Laser Ranging, Matera, Italy, 13-17 November, 2000.

2. “Retoreflector Array Transfer Functions”, David A. Arnold, Proceedings of the 13th International Workshop on Laser Ranging, Washington, DC, October 7-11, 2002. Also available on the website http://nercslr.nmt.ac.uk/sig/signature.html.

3. “Method of calculating retroreflector-array transfer functions”, David A. Arnold, Smithsonian Astrophysical Observatory SPECIAL REPORT 382.

4. “LAGEOS-2 spin rate and orientation”, Robert Sherwood, Roger Wood, Toshimichi Otsubo, 13th International Workshop on Laser Ranging, October 7-11, 2002, Washington, DC.

5. “Optical and infrared transfer function of the LAGEOS retroreflector array”, Grant NGR 09-015-002, David A. Arnold, May 1978, Smithsonian Astrophysical Observatory.

Session 12

Two-Wavelength Tracking

John Degnan, Cinzia Luceri

Zimmerwald Dual-Wavelength Operation

Werner Gurtner
Eugen Pop
Johannes Utzinger

Astronomical Institute
University of Bern

28-31 October 2003
Kötzting

Two-Wavelengths Design

- Receivers
  - Blue (423 nm)
    - CSPAD: Single shot rms: 50 ps
    - Hamamatsu PMT
  - IR (846 nm)
    - Hamamatsu PMT: Single shot rms: 150 ps
- Beam attenuation
  - Transmitting beams
    - Separate rotating polarizer for each color
  - Receiving paths
    - Circular adjustable ND filters
    - Neutral density filters inserted for calibration

Transmit Path

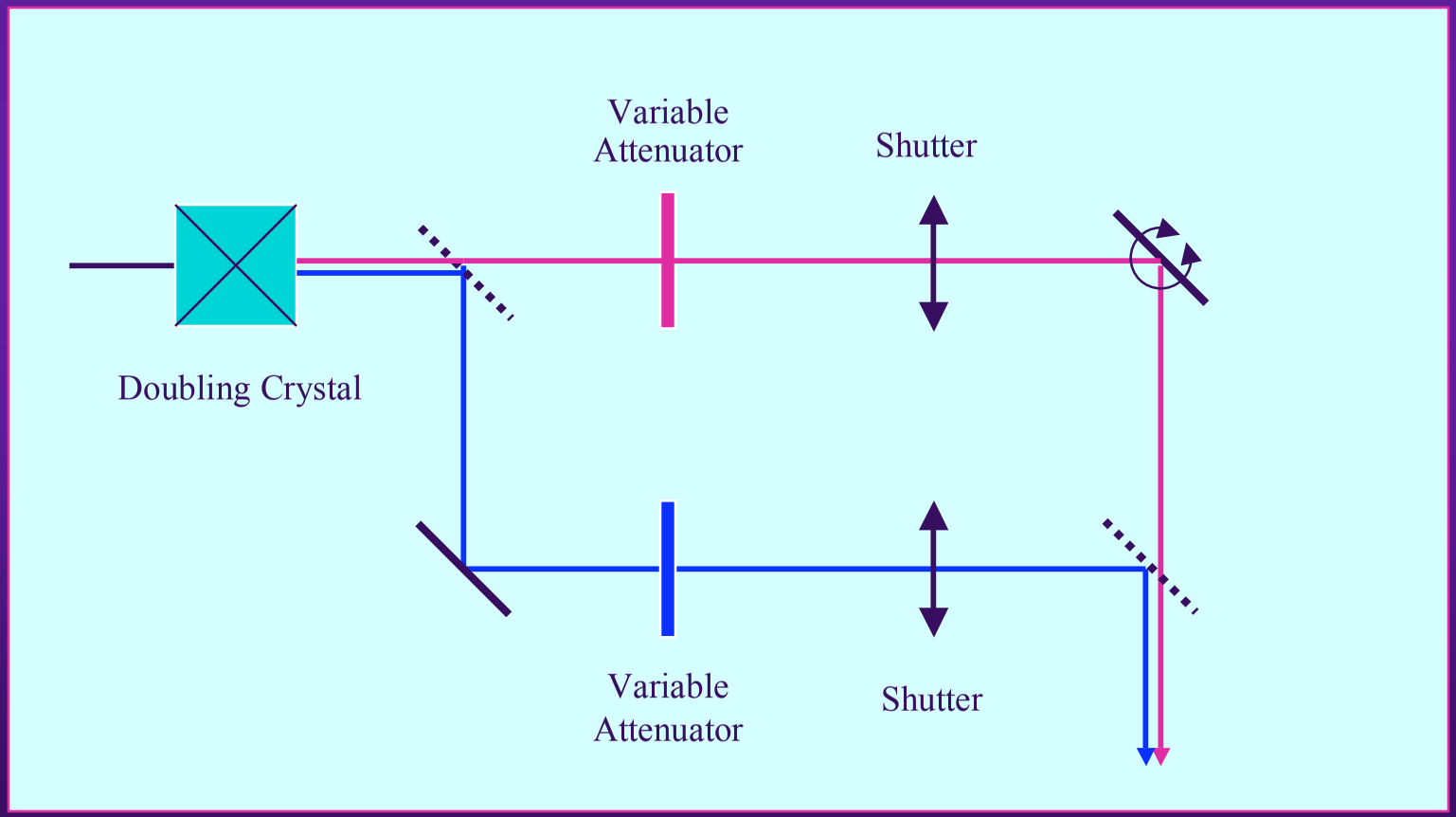

Receiving Path

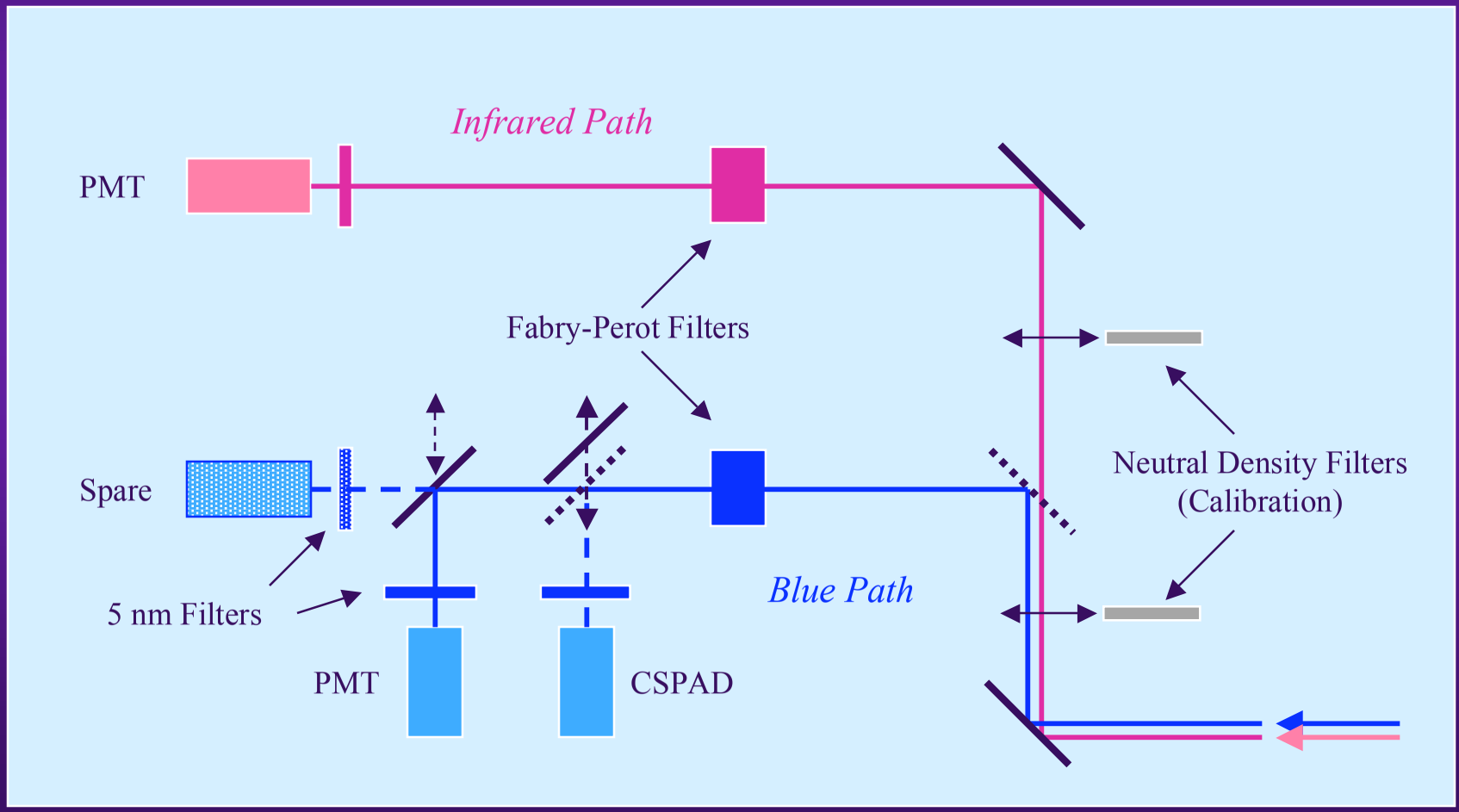

Example: Lageos-1 Pass
25 August 2002, 19:40-20:30 UT

Wavelength	Single shot observations	Single shot RMS	Calibration RMS	Number of

Lageos-1 Blue and IR Residuals (ns)

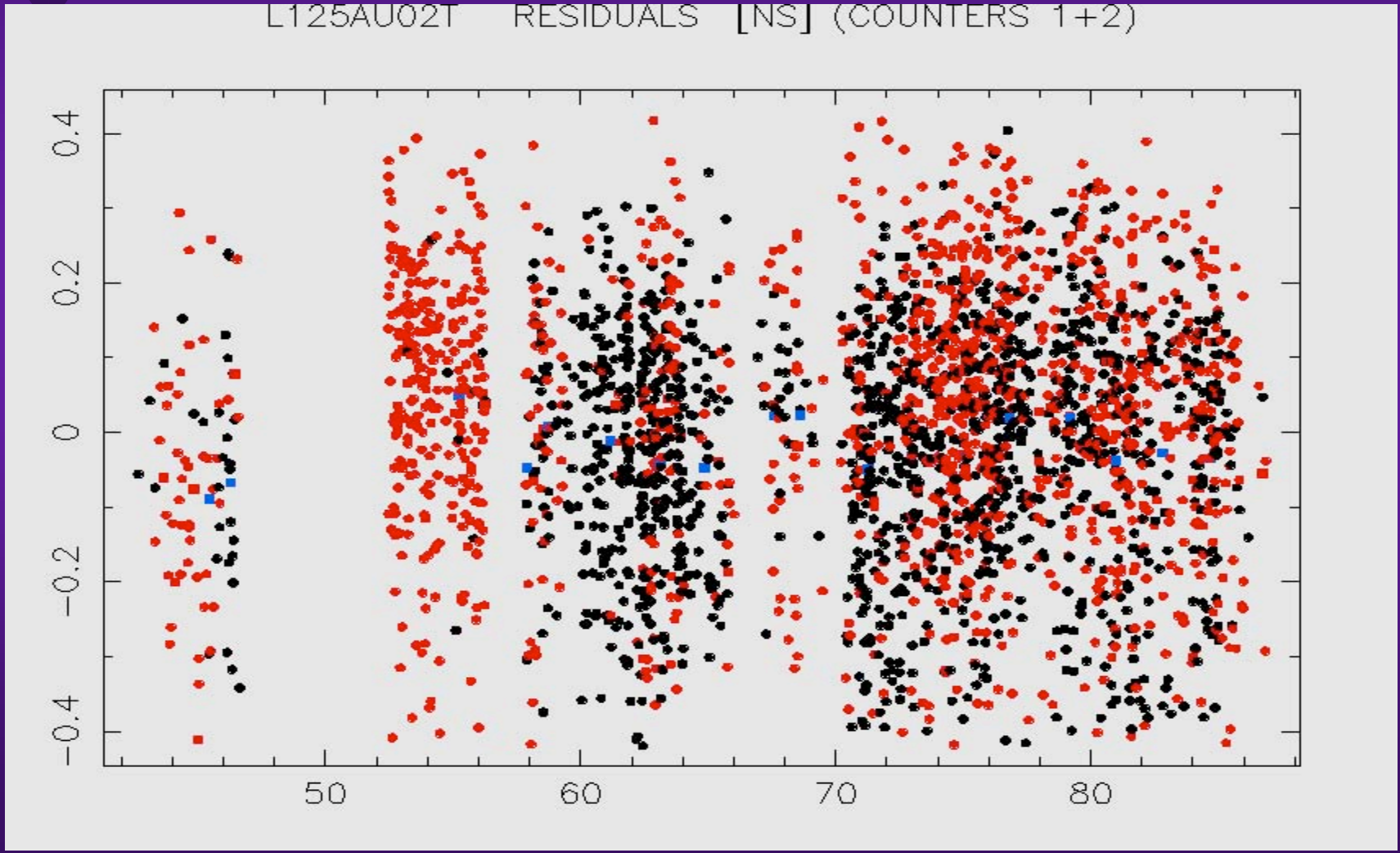

Experiences

- Beam alignment is rather critical
- Less noise in the infrared channel during daylight tracking
- Calibration RMS on IR larger by about 100 percents (180 ps vs. 90 ps)
- Average pass differences IR-blue (after M.M.-correction) < 0.08 ns

Conclusions

- Range biases between the two reception channels could still be in the system (a few millimeters?)
- Differences of the Marini-Murray refraction corrections at 423 and 846 nm obviously better than about 10 mm
- Is accuracy of the two wavelengths good enough for mapping function improvement?

Two-color Analysis Technique

(Slides by Van Husson)

- Zimmerwald: Robust 2-color dataset in July – August 2003
- Zimmerwald 2-color configuration
  - **Blue (423nm): CSPAD**, SR620 **#0236**, **2.5** sigma
  - **IR (846nm):** PMT, SR620 #2282, 2.5 sigma
- In simultaneous passes, difference range biases (RB) from each color [i.e. IR(RB) – Blue(RB)]
- Uses RB results from Delft and CRL weekly reports

Zimmerwald 2-Color RB Differences

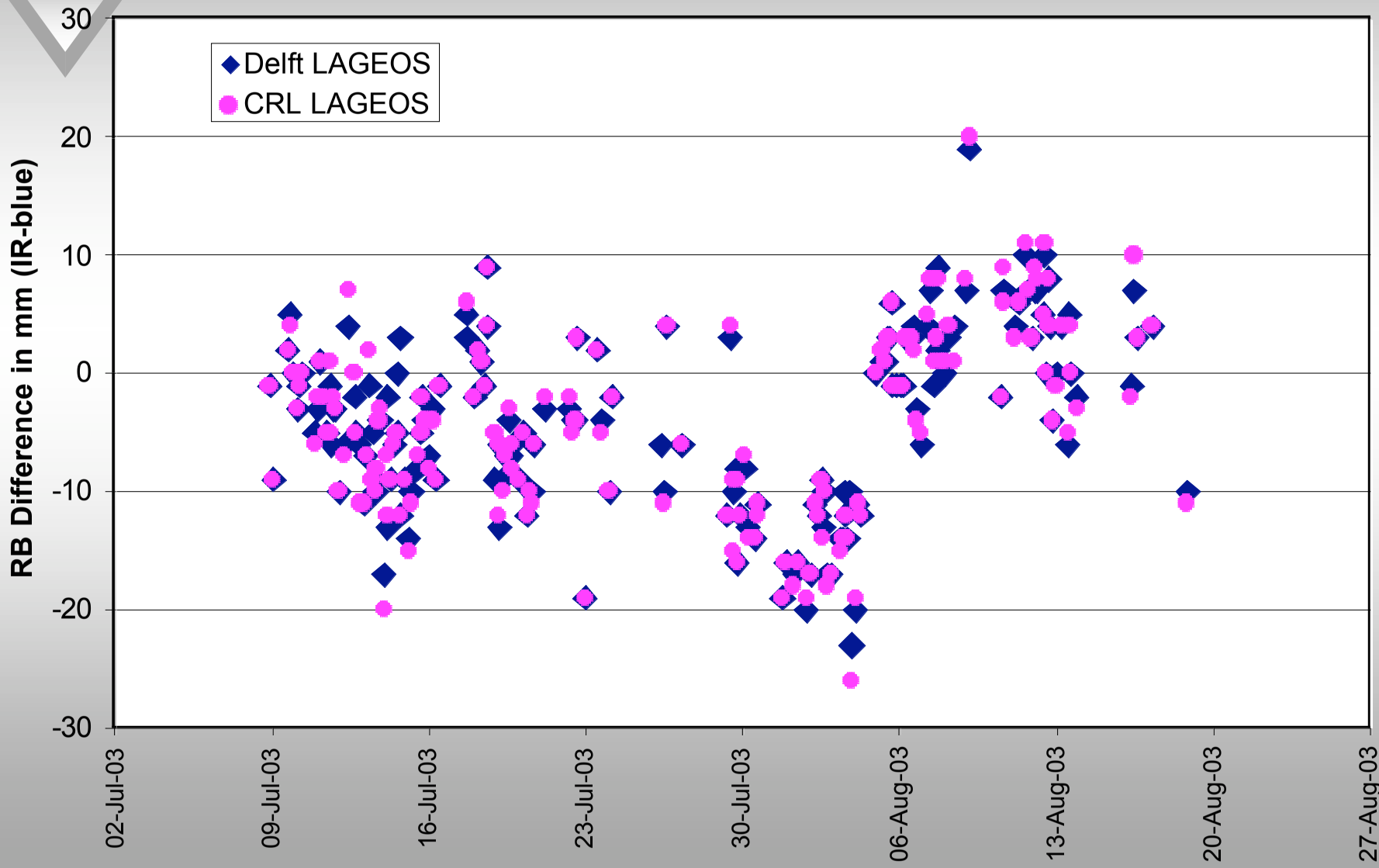

Zimmerwald 2-Color RB Differences

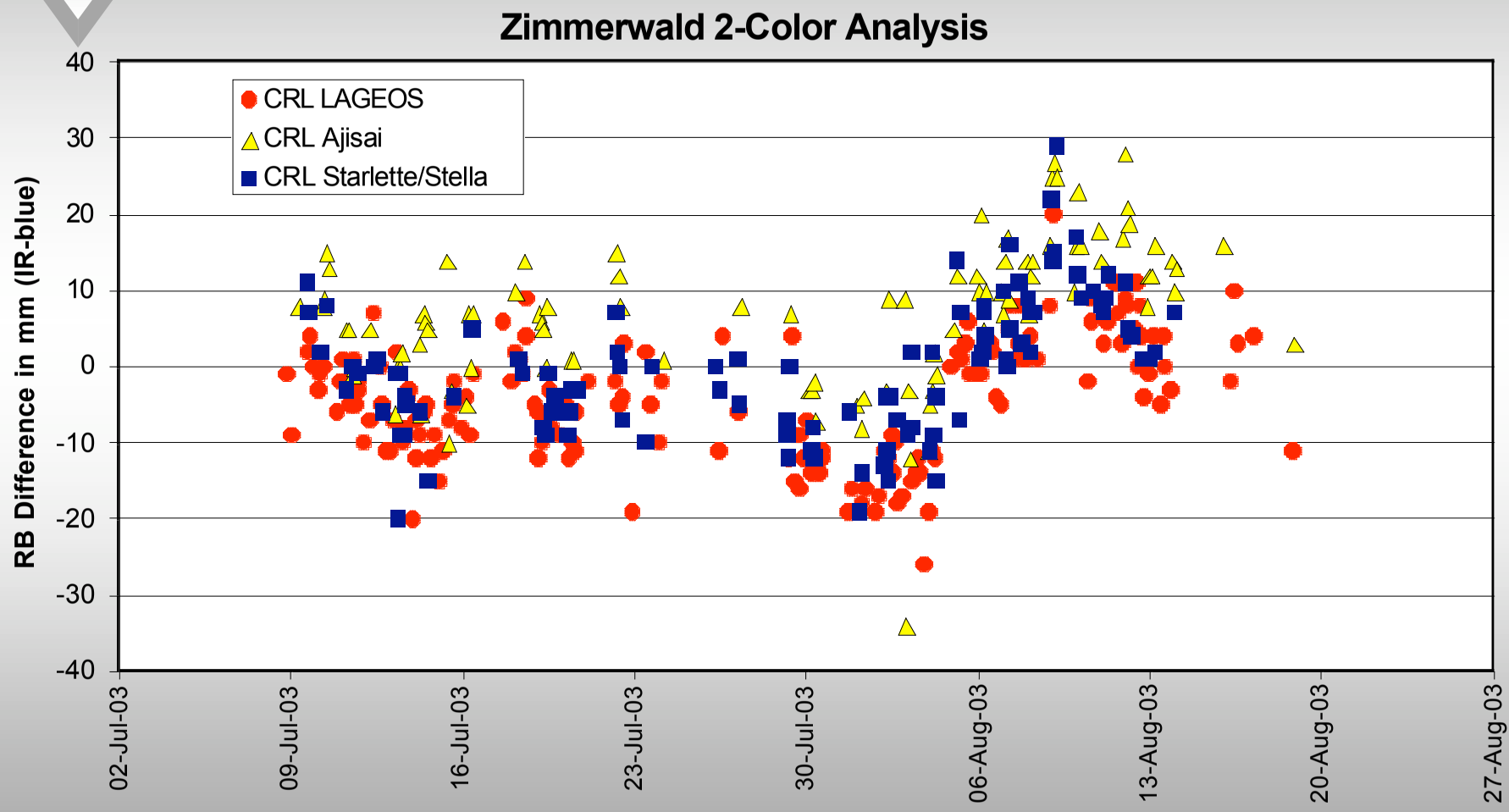

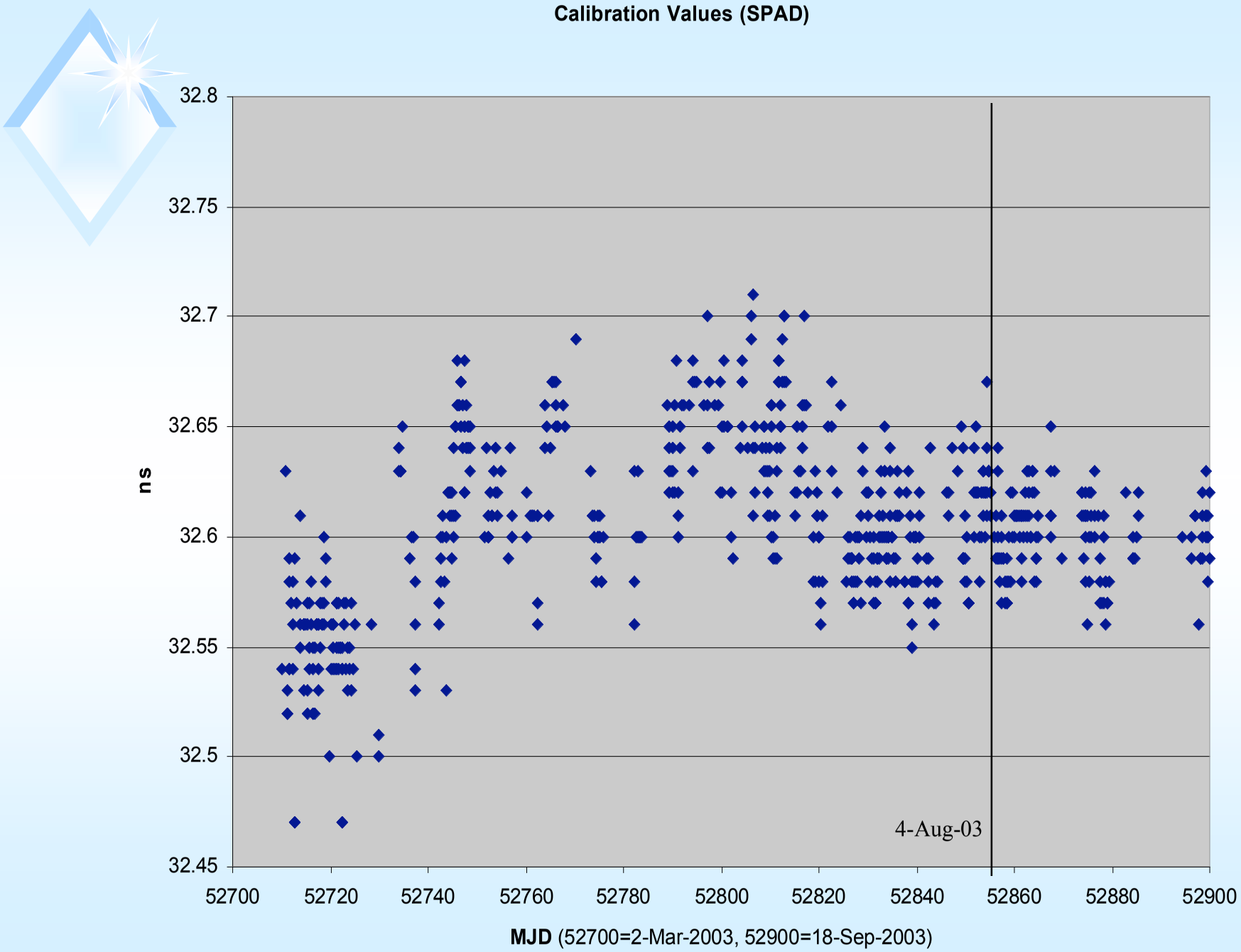
Calibration Values (SPAD)
32.8
32.75
32.7
32.65
32.6
32.55
32.5
32.45
ns
4-Aug-03
52700
52720
52740
52760
52780
52800
52820
52840
52860
52880
52900
MJD (52700=2-Mar-2003, 52900=18-Sep-2003)

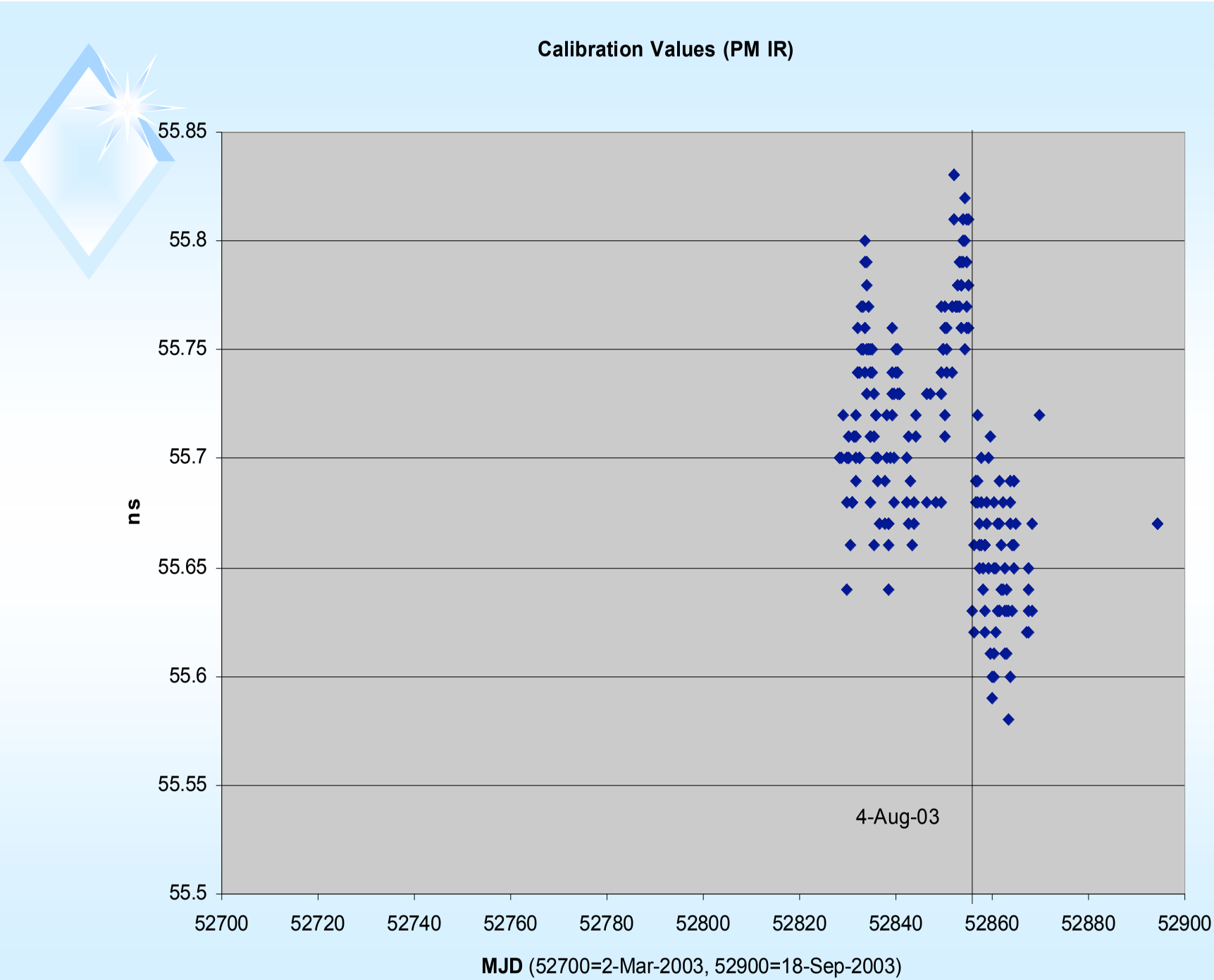
Calibration Values (PM IR)
55.85
55.8
55.75
55.7
55.65
55.6
55.55
55.5
ns
4-Aug-03
52700
52720
52740
52760
52780
52800
52820
52840
52860
52880
52900
MJD (52700=2-Mar-2003, 52900=18-Sep-2003)

Zimmerwald 2-Color Analysis

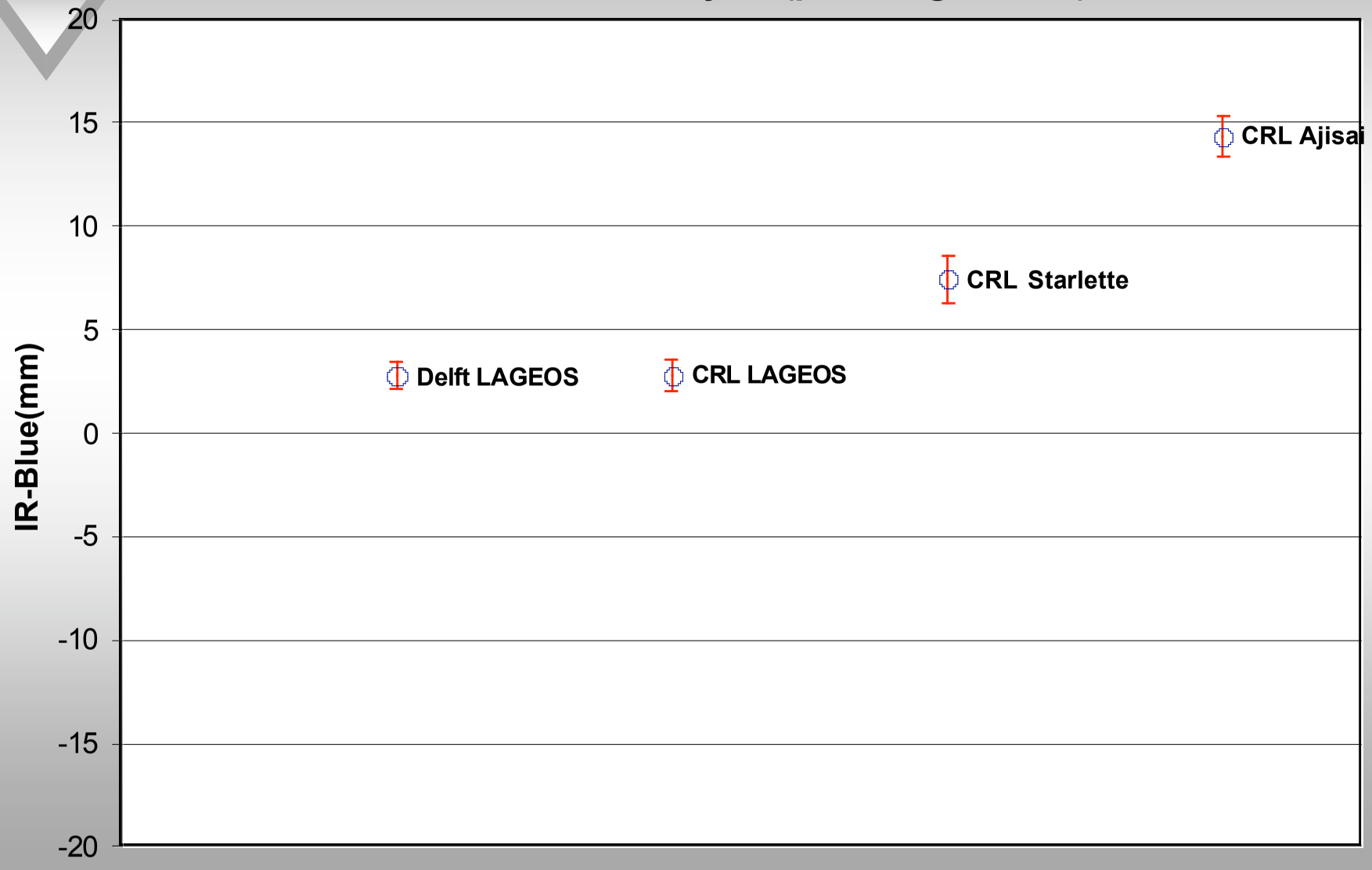

Possible Source of Differences

- Refraction Algorithm
- CoM Differences
  - Detectors (CSPAD vs PMT)
  - Dual Wavelengths
  - Signal Strength
  - Polarization?
- System Calibration
  - Different SR620 Counter linearities
  - Signal Strength
  - Optical Path Differences?

Dual Wavelength Data Analysis
423 & 846 nm

Erricos C. Pavlis
Magda Kuzmicz-Cieslak
Glynn Hulley
JCET/UMBC - NASA/GSFC

2003 ILRS Workshop on Laser Ranging
October 28-31, 2003, Kötzting, Germany

Description

- Analyzed data span 2001 to March 2003
- Data come from two sites:
  - **Zimmerwald (7810)** [PRIMARILY] , and
  - **Conception (TIGO)**
- Data are computed from already converged orbits and each wavelength is treated as an independent measurement at the same site

Description, (cont.)

- Atmospheric refraction corrections were applied in two different ways:
  - standard Marini - Murray model **[MM]**
  - a variation of Ciddor's ZD model by Mendes and the new FCUL (Mendes et al.) mapping function **[MC]**
- Residual differences examined for bias and scale differences

Description, (cont.)

- Residuals grouped by “sign”
  - Positive-residual differences:
    - **$MM^{+} - MC^{+}$**
  - Negative-residual differences
    - **$MM^{-} - MC^{-}$**
- Residuals grouped in 10° elevation bands and regressed to investigate scatter variation correlated with dependence on elevation

Residual wrt Elevation

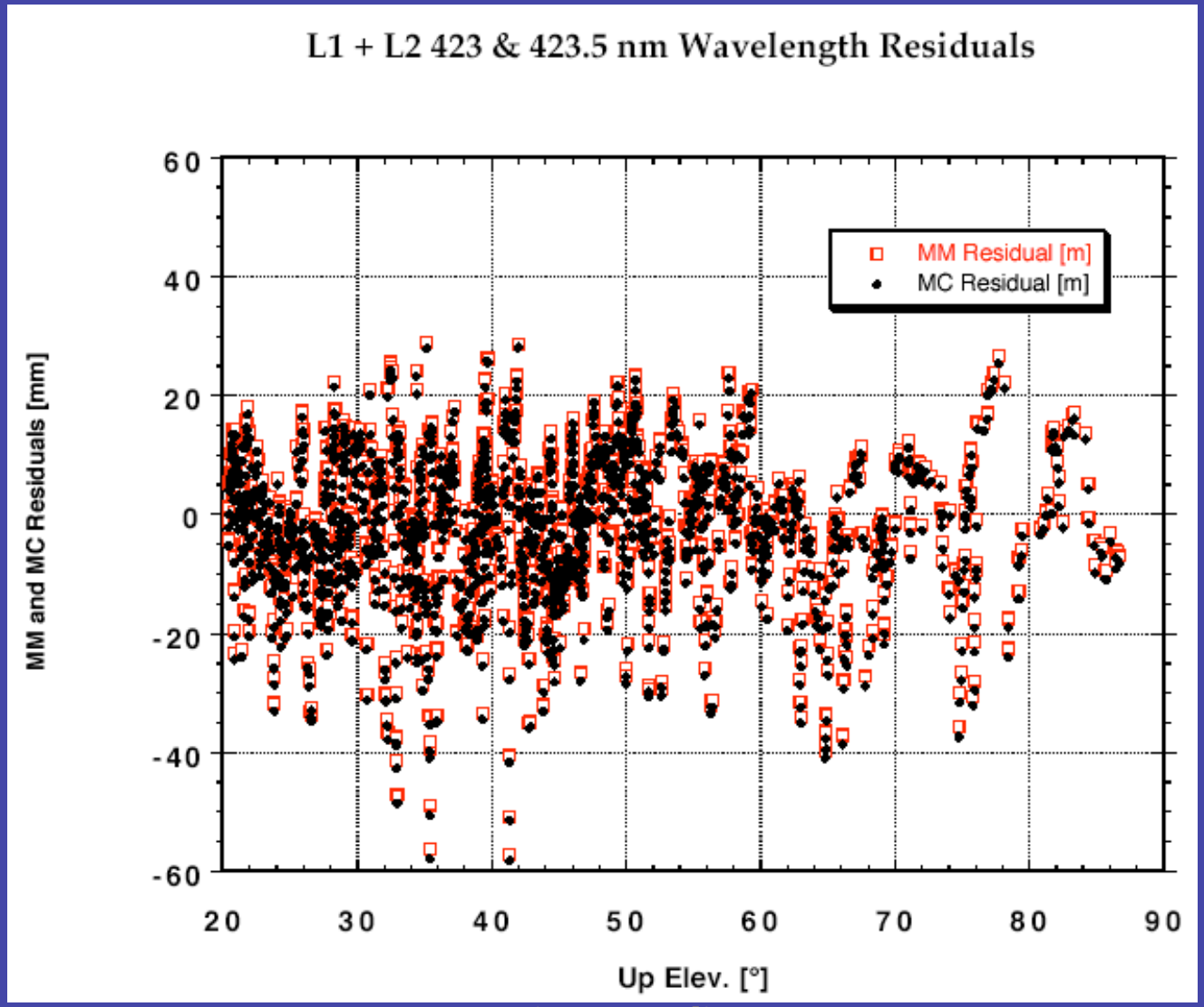

Residual Differences wrt Elevation

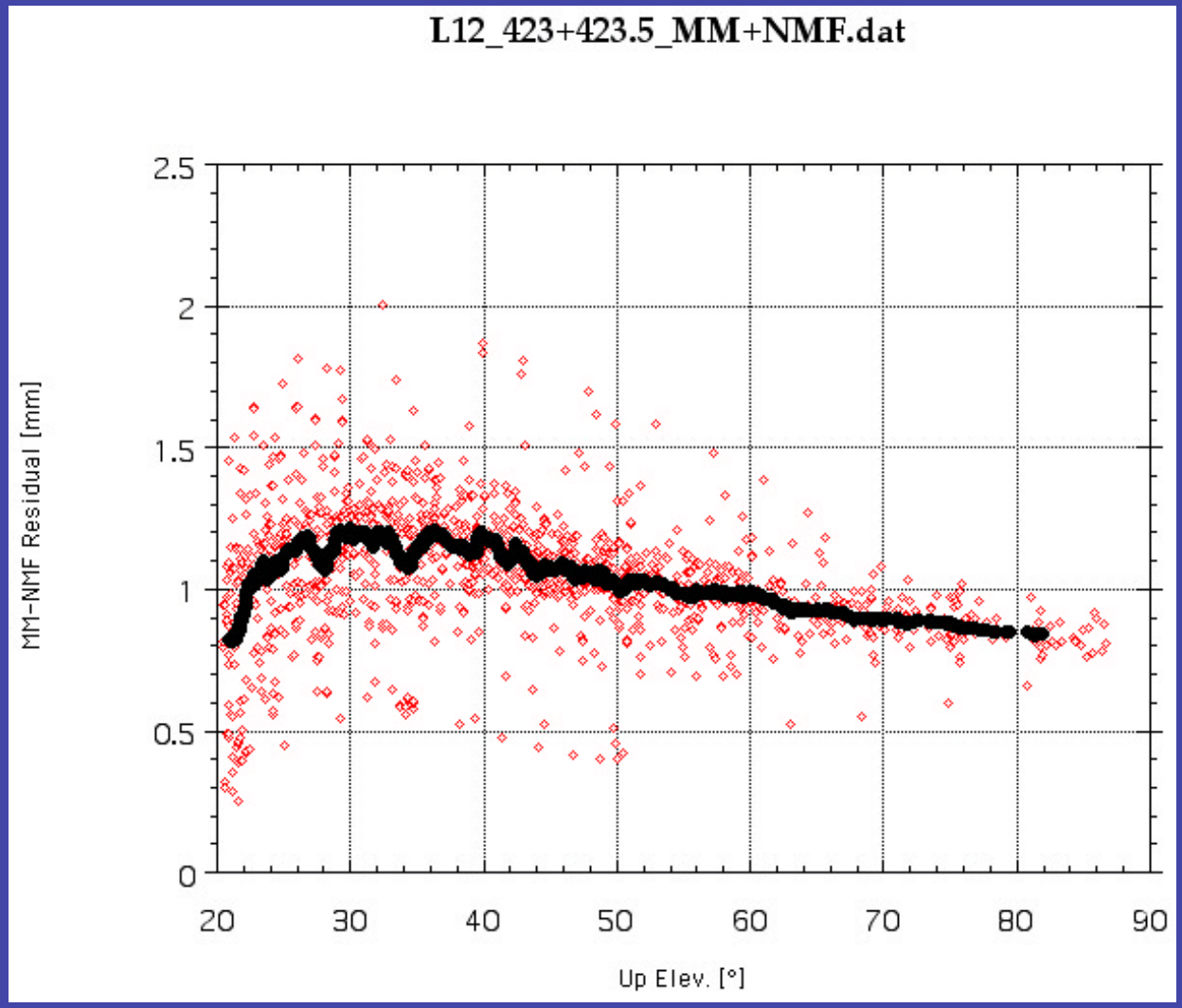

ZD Bias as a Function of Wavelength

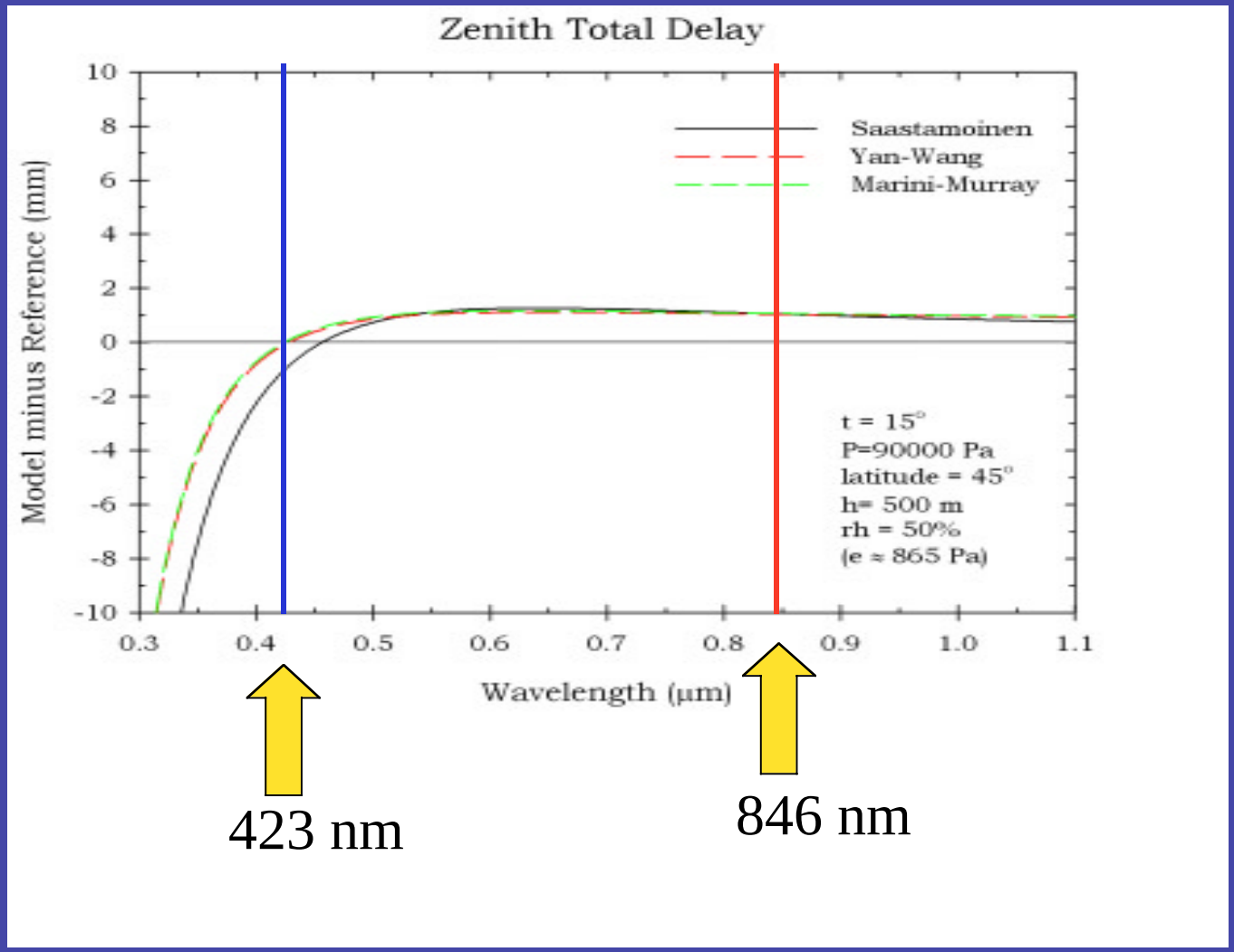

ZD Bias as a Function of Wavelength

1064 nm

532 nm

423 nm

Saastamoinen

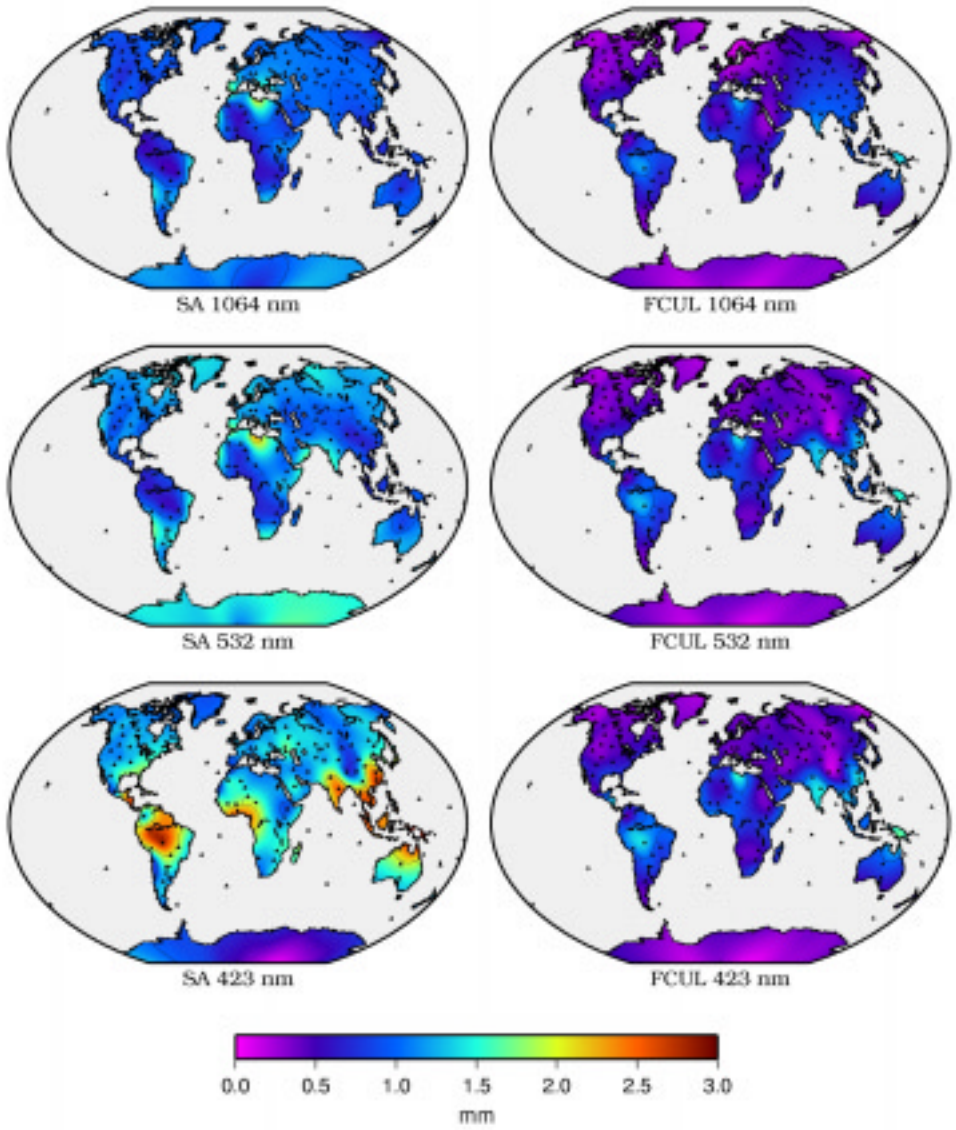

1064 nm

532 nm

423 nm

Ciddor-Mendes

Residual wrt Elevation

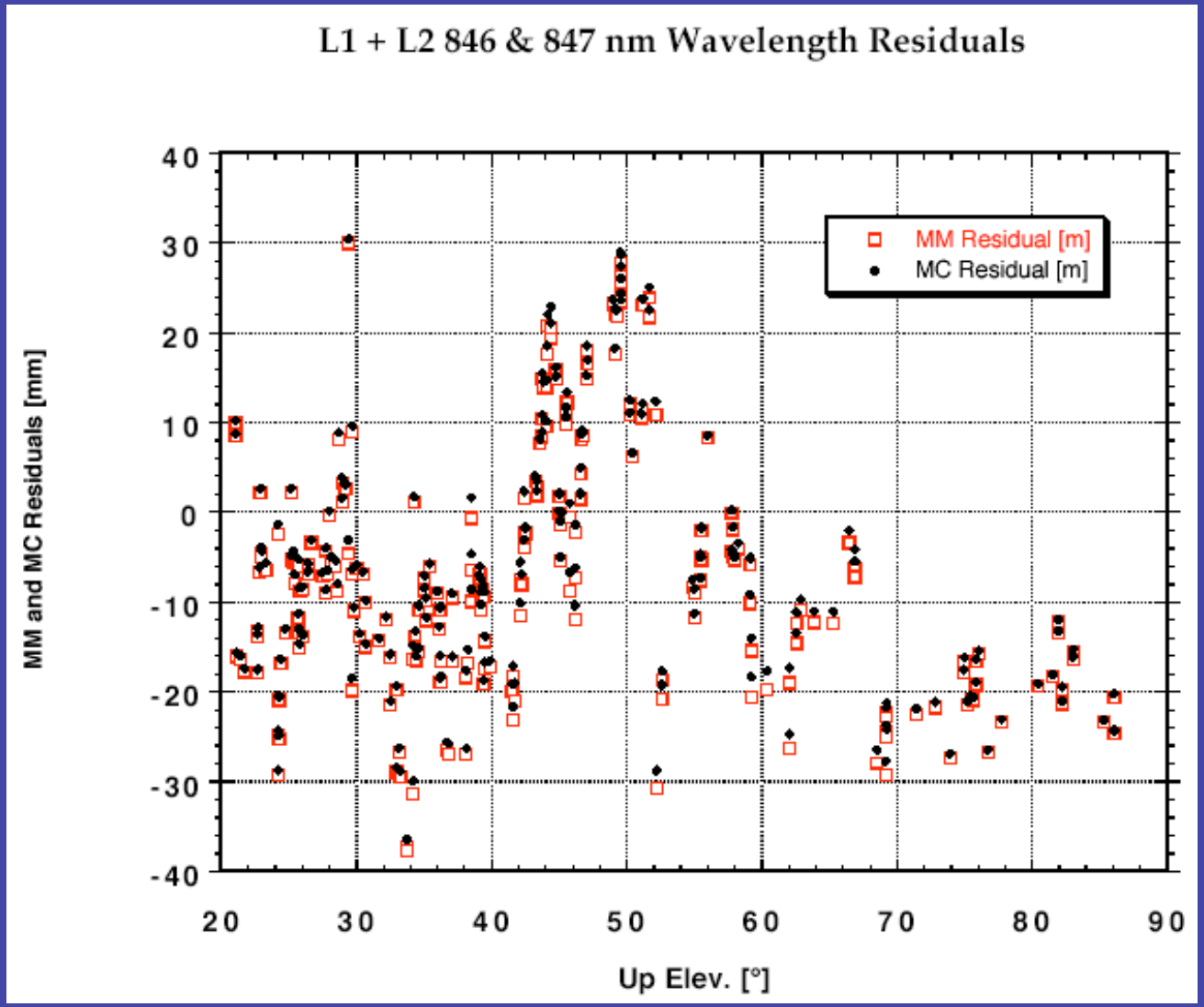

Residual Differences wrt Elevation

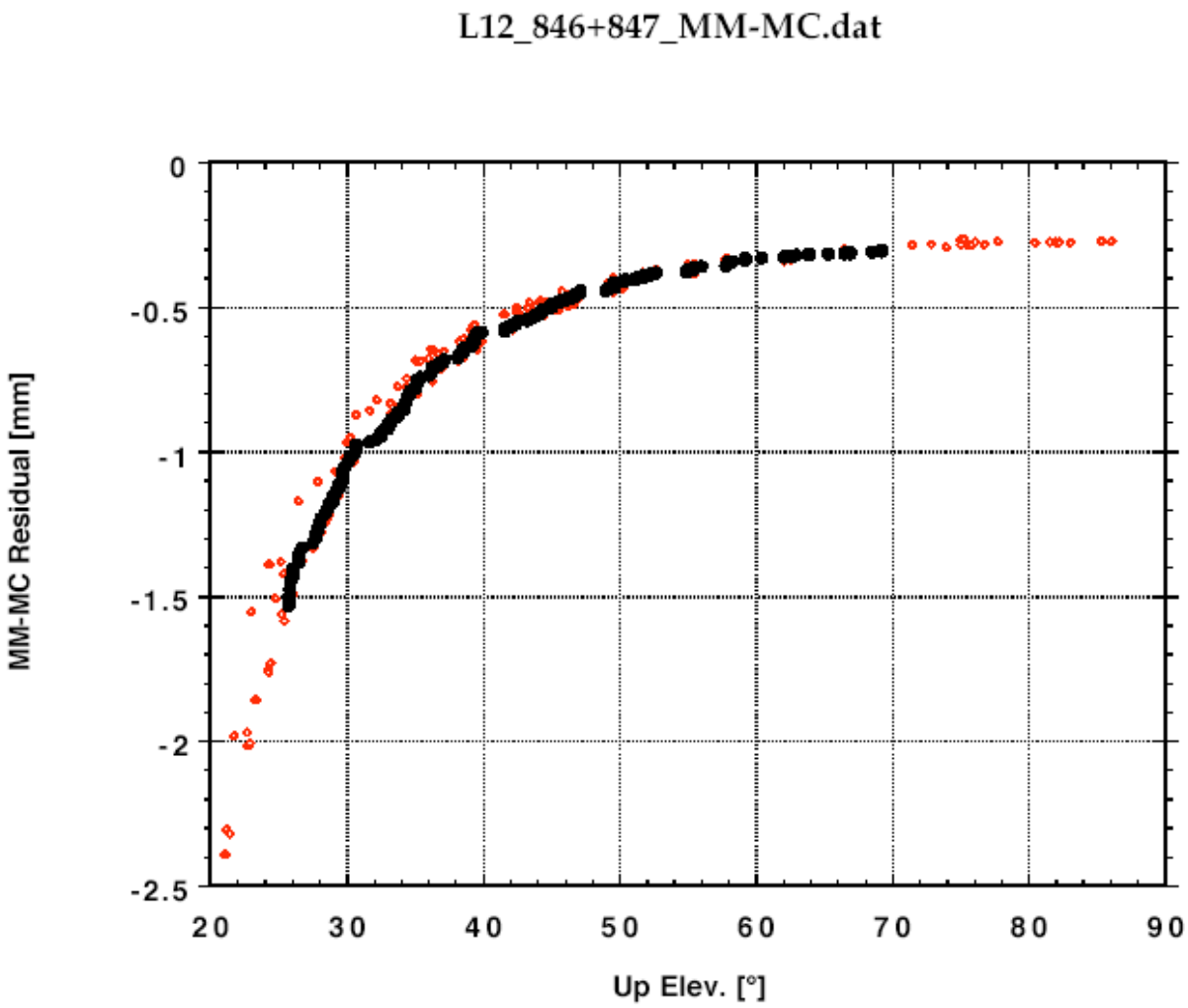

Residual Differences wrt Elevation

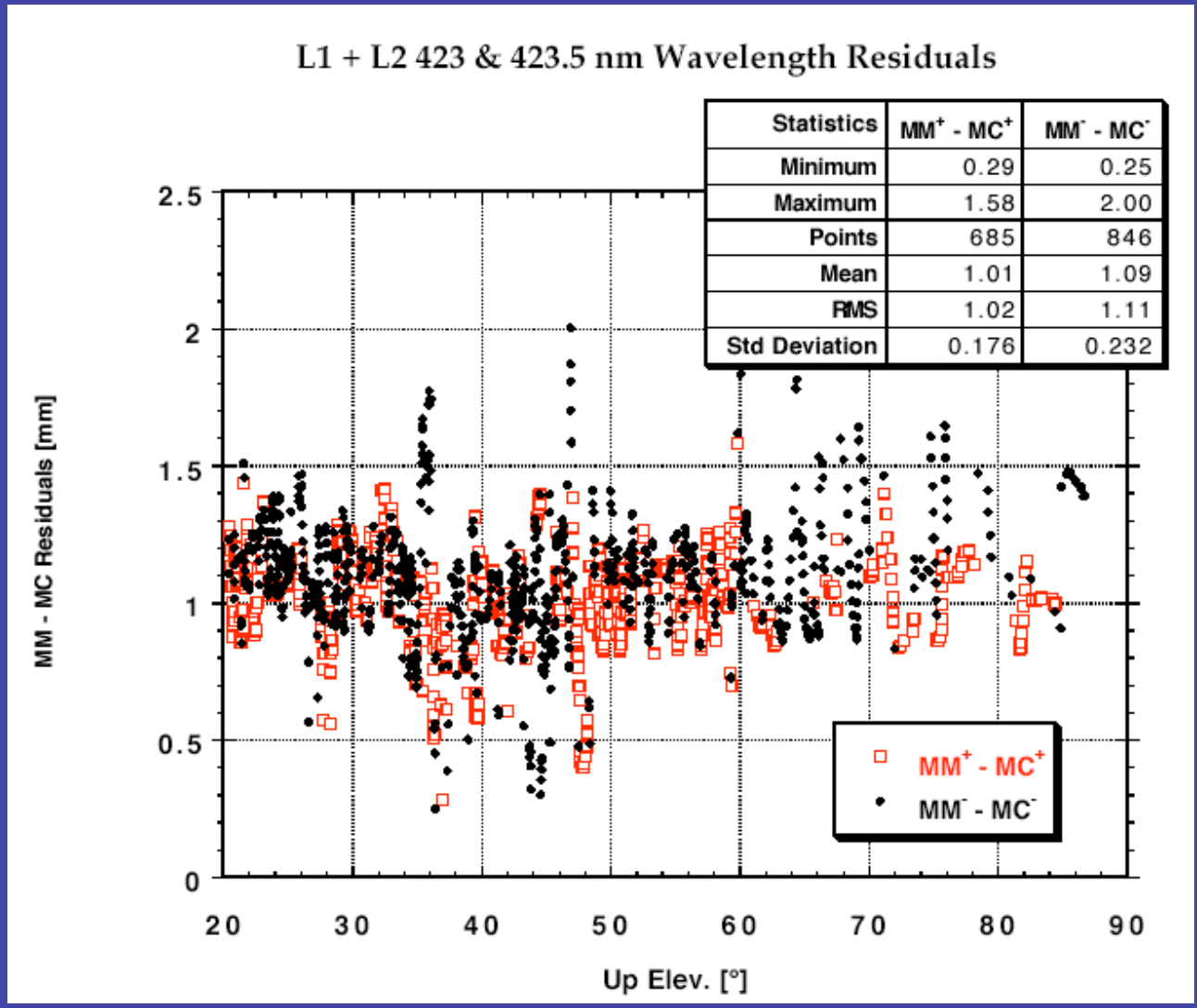

Residual Differences wrt Elevation

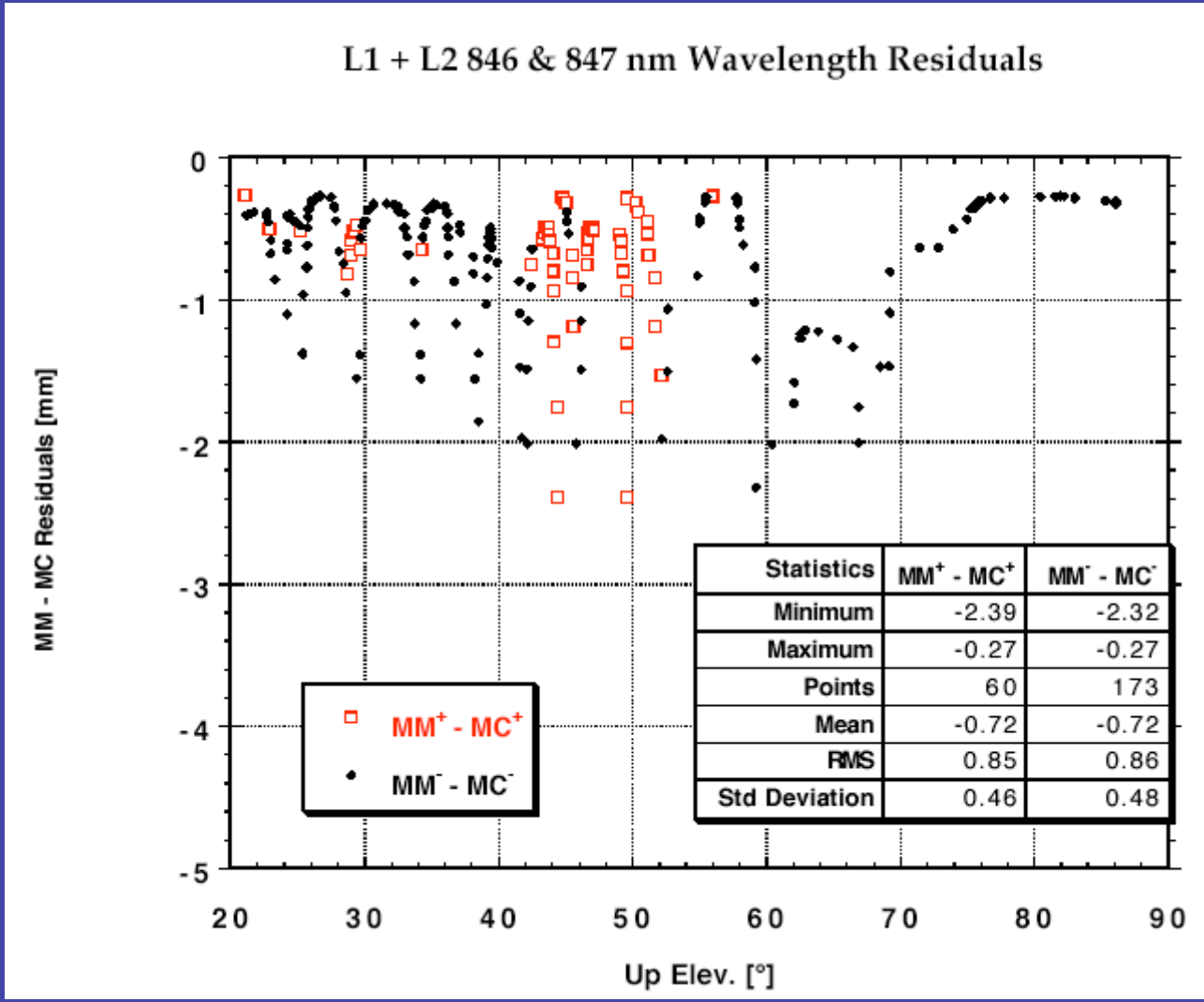

Residual Differences Regression
423 nm

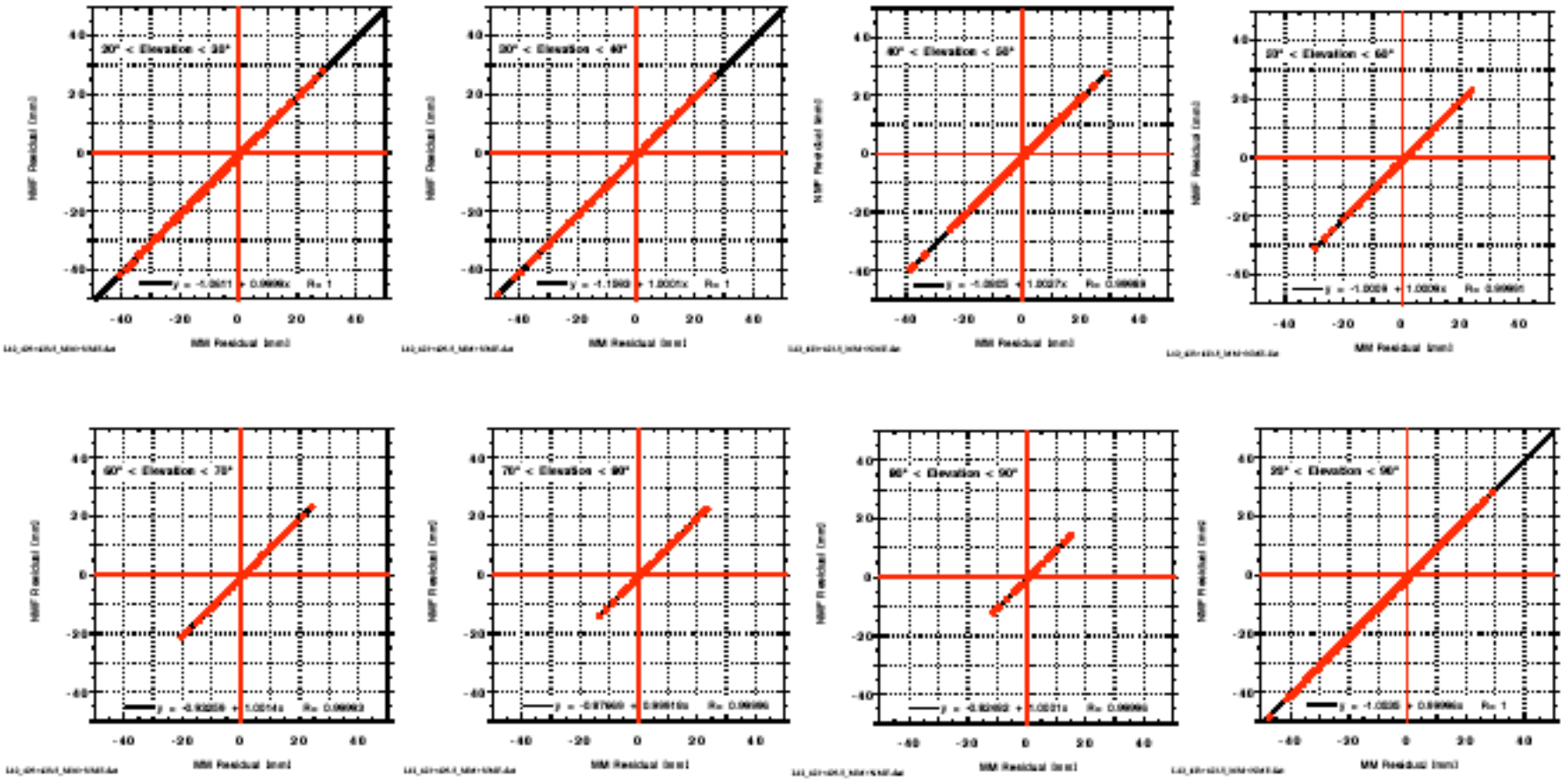

Residual Differences Regression 846 nm

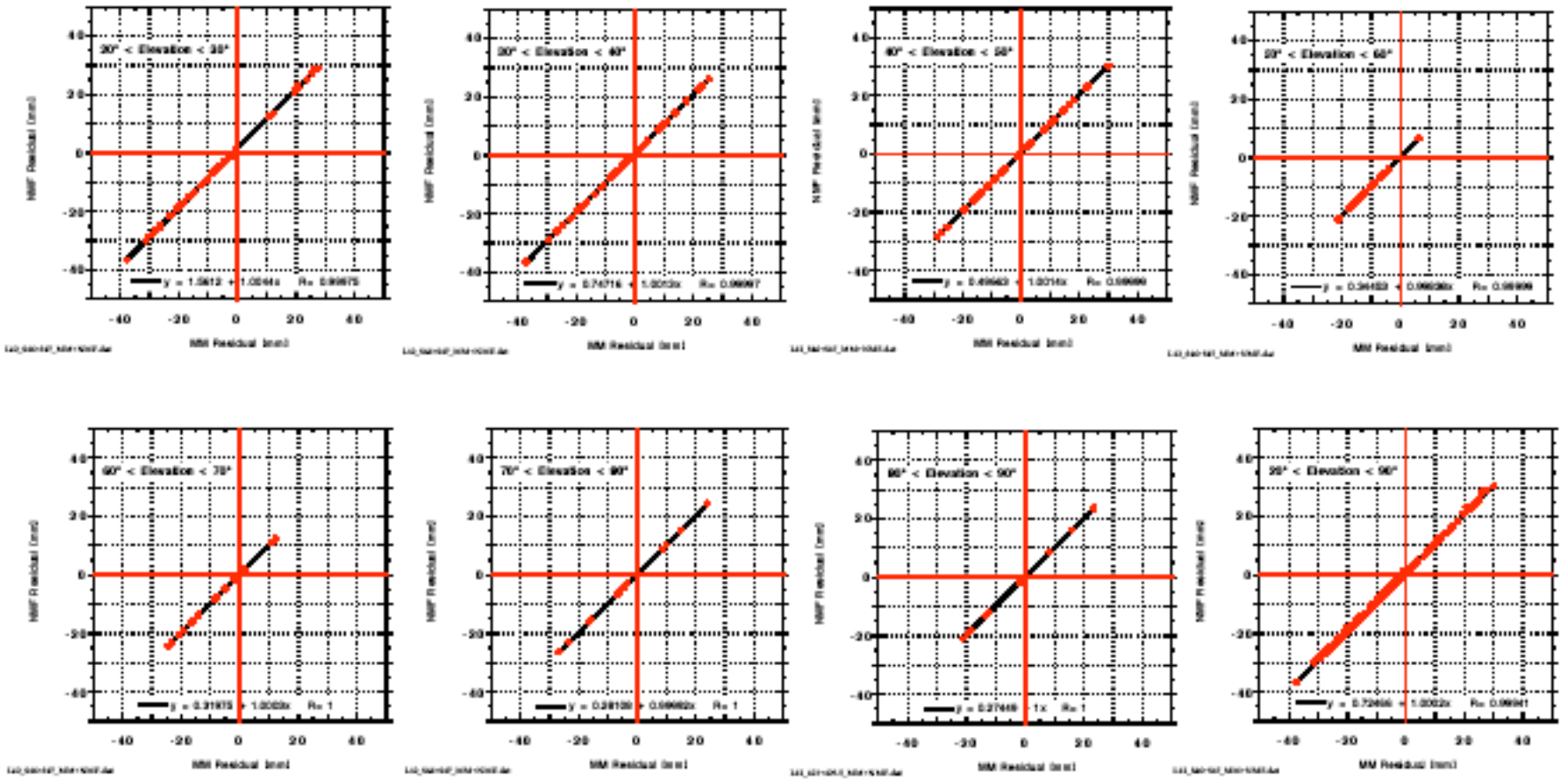

Residual Differences Regression 423 and 846 nm

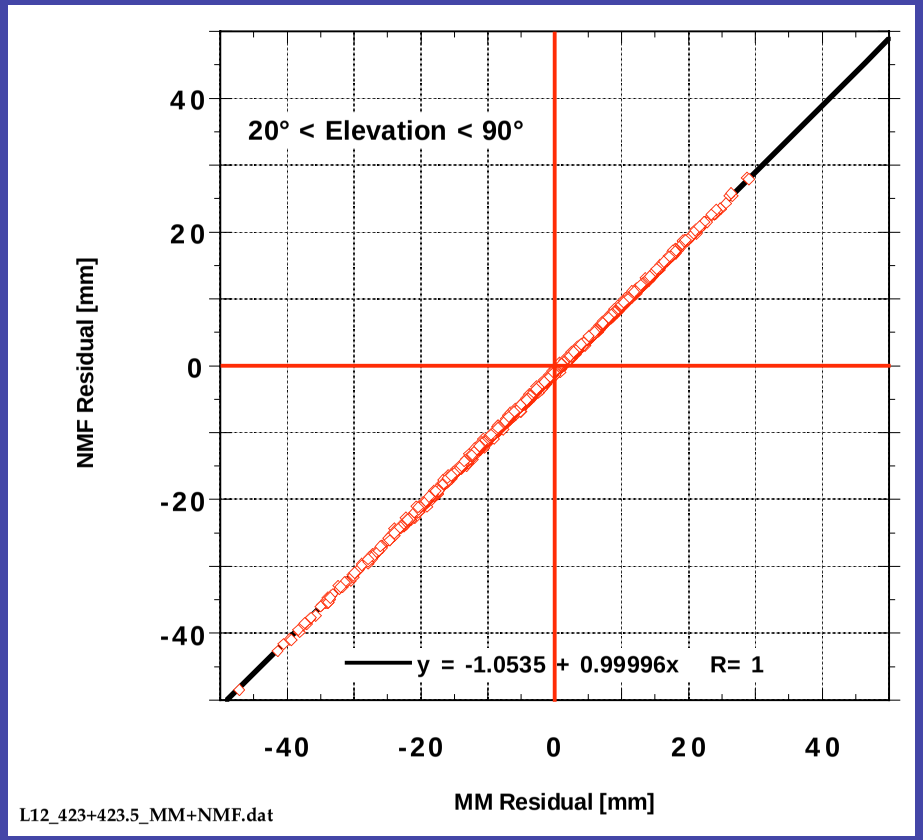

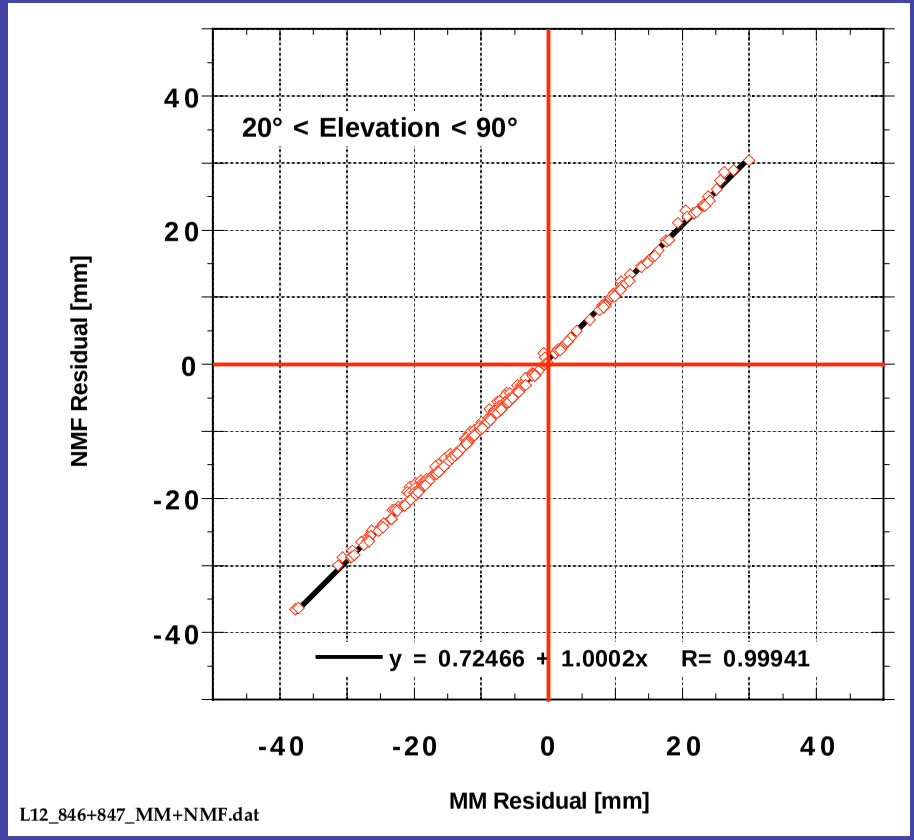

Summary & Conclusions

- The residuals for either atmospheric correction model exhibit very similar scatter for ~1800 NPs so far examined:
  - @ 423 nm 12.26 mm
  - @ 846 nm 12.31 mm

Summary & Conclusions (cont.)

- @ 423 nm :
  - Small bias (~ -1 mm) and a scale difference (0.99996) for M-M wrt Mendes - Ciddor
  - Current data set exhibits higher scatter at low elevation bands
  - Overall scatter about the mean is ~ 0.2 mm
  - The examined data set is small (~ 1500 NPs) so more robust conclusions can be obtained after the complete set of data is examined

Summary & Conclusions (cont.)

- @ 846 nm :
  - Small bias (~ +.7 mm) and a scale difference (1.0002) for M-M wrt Mendes - Ciddor
  - Most data are collected at elevations < 60° and exhibit lowest scatter at elevations:

    $50° < \varepsilon < 60°$

  - Overall scatter about the mean is ~ 0.5 mm
  - The examined data set is very small (~ 230 NPs) so we can not reach any conclusions until after the larger set of data is examined

Work in progress

- All of the data collected up to present (primarily from Zimmerwald) have now been processed and a more robust report will be compiled next month, with a simultaneous comparison of the data to atmospheric corrections derived from the revised Ciddor - Mendes model.

Preparing for Dual Wavelength SLR

- Once the differential delays become available routinely, we would like to compare them to model-derived delays:
  - The full precision formula of [Degnan, 93]
  - As well as the [Abshire and Gardner, 85] approximation

Comparison of the two approaches

- We have used the latest Mendes-Ciddor formulation for the group refractivity indices for each wavelength
- The *"laser frequency factors"* $f(\lambda)$ in the approximate [Abshire-Gardner] formula are obtained from the same formulation (i.e. Mendes-Ciddor), rather the suggested one used in Marini-Murray)
- We have used the LAGEOS data from the recent summer months to compare the two "γ" factors
- The examined data set indicates that we MUST use the full precision formula, if we want to maintain mm accuracy in our geodetic estimation problem

LAGEOS 1 July 10 - Aug. 21, 2003

Goddard Space Flight Center

Dual Wavelength Atmospheric Correction Computations

Full precision vs. Approximate

LAGEOS 1

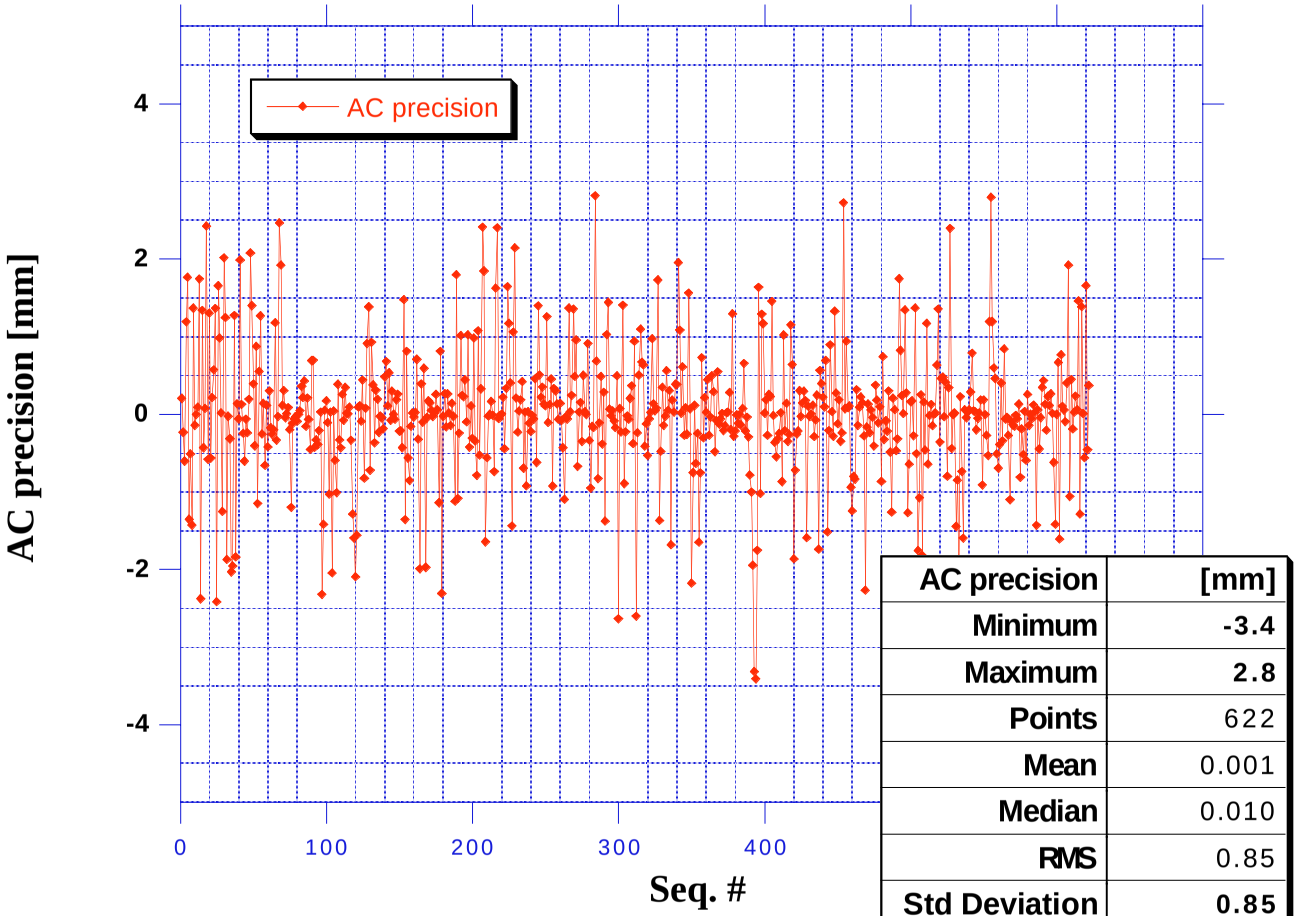

AC precision	[mm]
Minimum	-3.4
Maximum	2.8
Points	622
Mean	0.001
Median	0.010
RMS	0.85
Std Deviation	0.85

LAGEOS 2 July 10 - Aug. 21, 2003

Goddard Space Flight Center

Dual Wavelength Atmospheric Correction Computations

Full precision vs. Approximate

LAGEOS 2

AC precision	[mm]
Minimum	-2.598
Maximum	2.613
Points	420
Mean	0.025
Median	0.015
RMS	0.72
Std Deviation	0.72

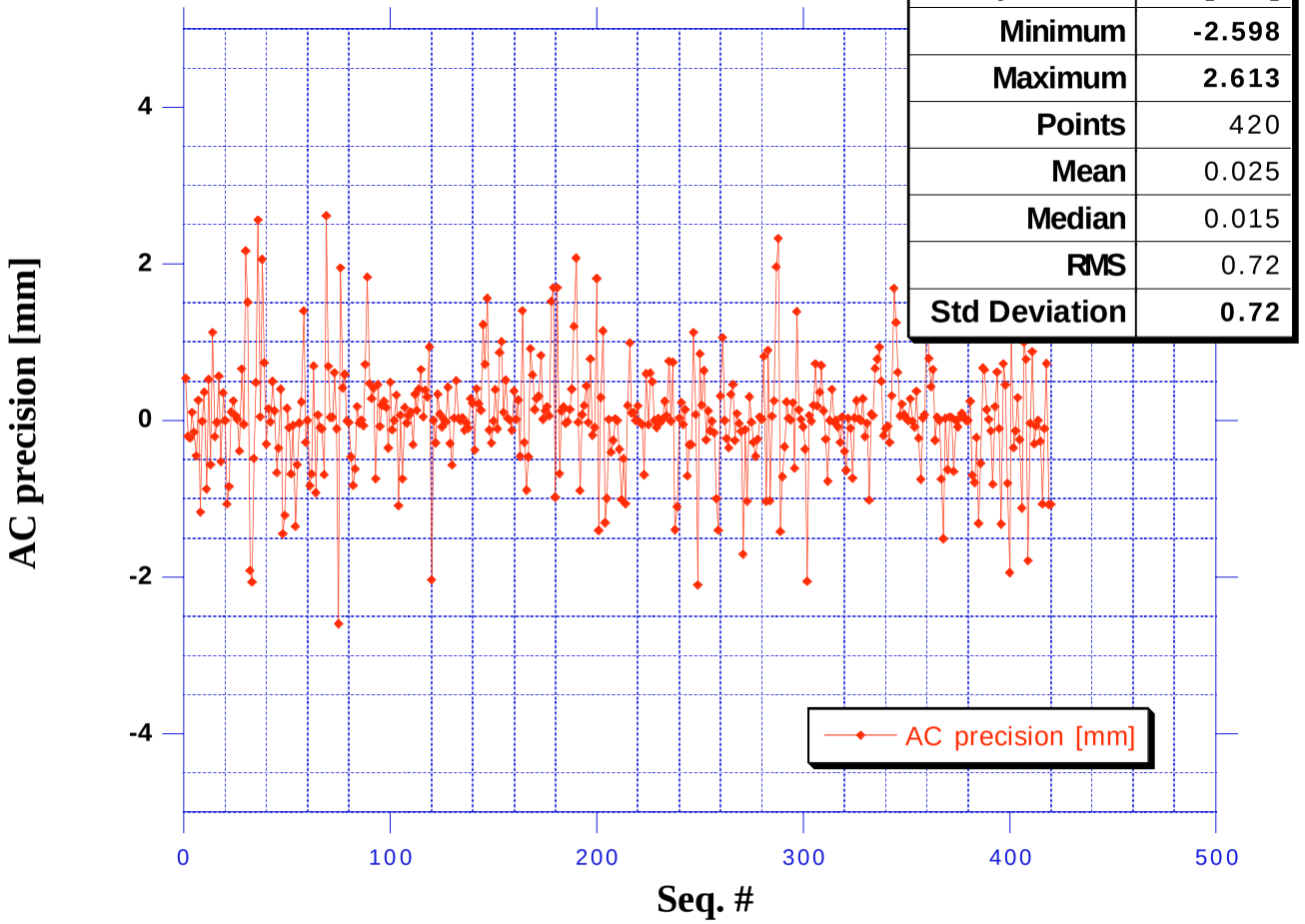

Two-color Analysis Technique

- Zimmerwald: robust 2-color dataset in July – August 2003
- Zimmerwald 2-color configuration
  - **Blue (423nm): CSPAD**, SR620 **#0236**, **2.5** sigma
  - **IR (846nm):** PMT, SR620 #2282, 2.0 sigma
- In Simultaneous passes, difference Range Biases (RB) from each color [i.e. IR(RB) – Blue(RB)]
- Uses RB results from Delft and CRL weekly reports

Zimmerwald 2-Color RB Differences

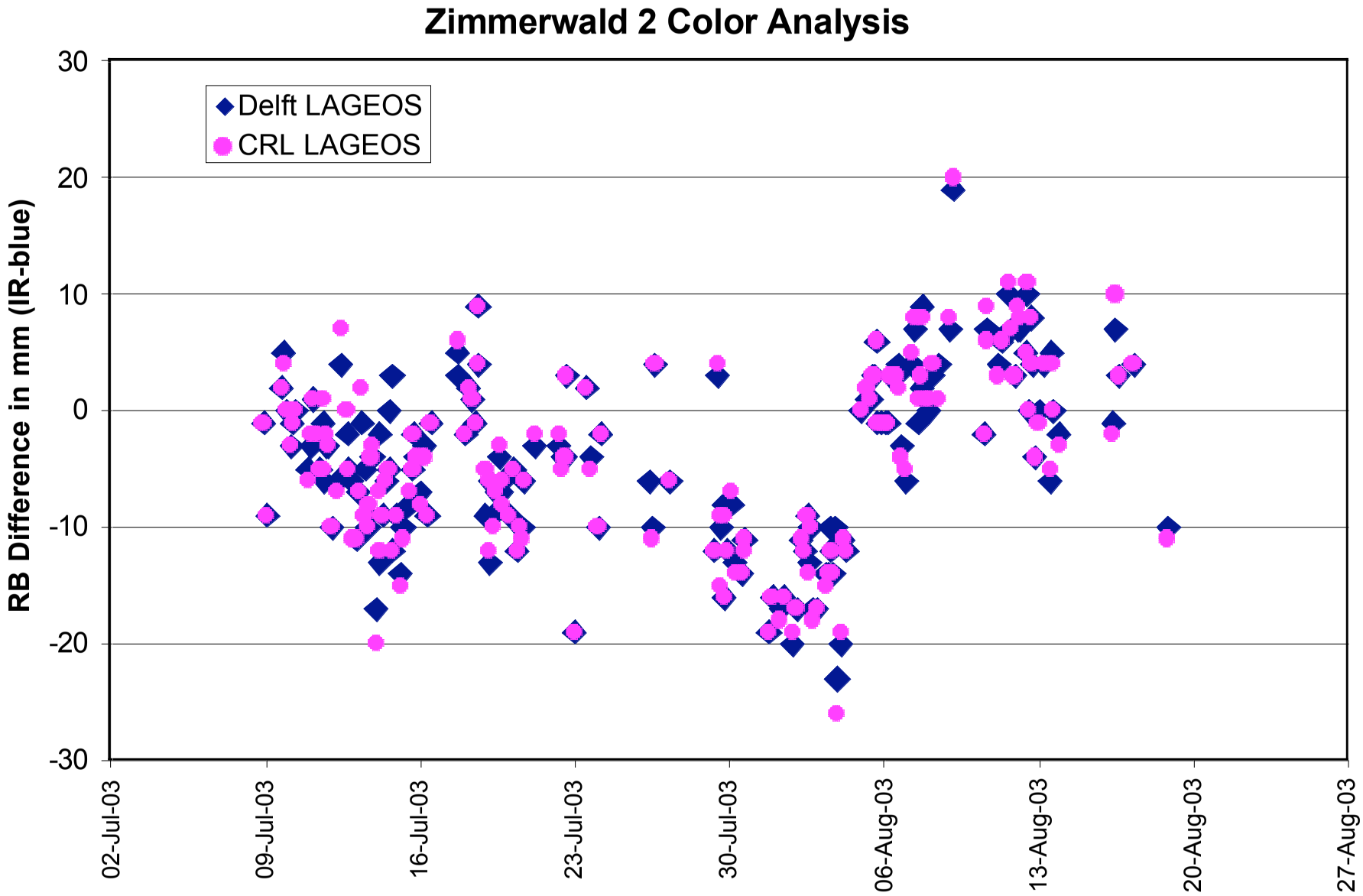

Zimmerwald 2-Color RB Differences

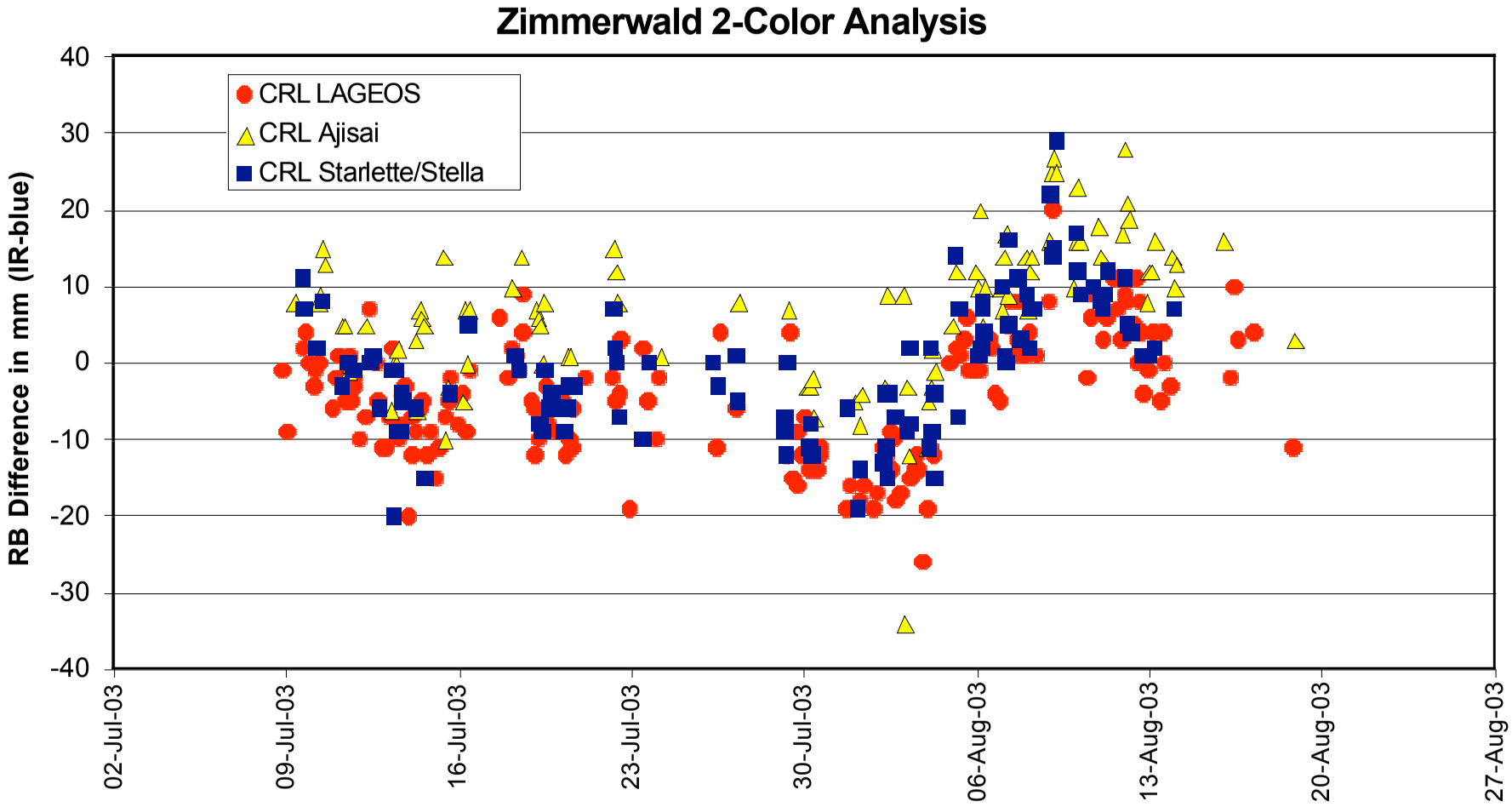

Zimmerwald 2-Color Analysis

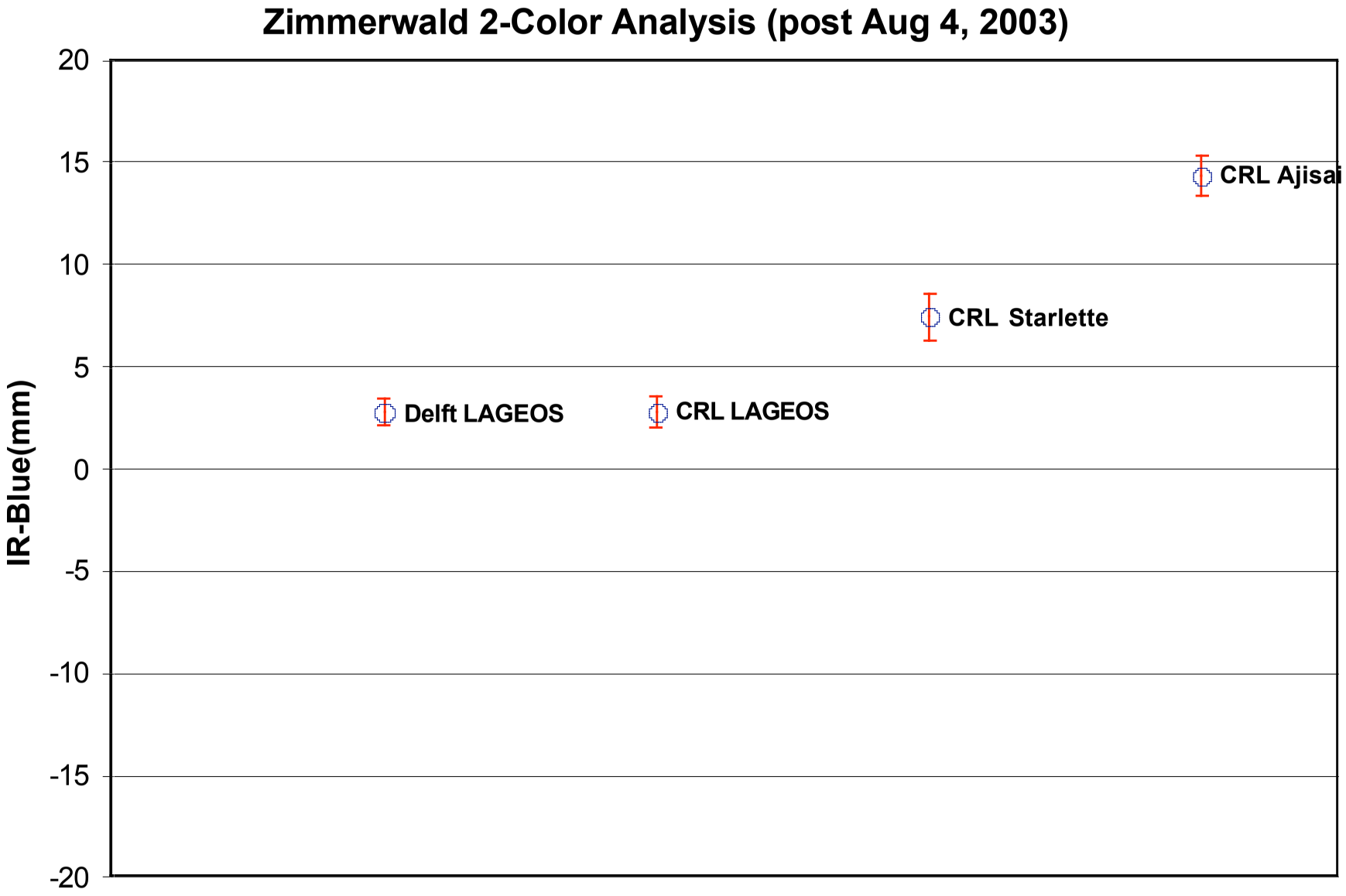

Possible Source of Differences

- Refraction Algorithm
- CoM Differences
  - Detectors (CSPAD vs PMT)
  - Dual Wavelengths
  - Signal Strength
  - Screening Levels (2.5 vs 2.0)
  - Polarization?
- System Calibration
  - Different SR620 Counter linearities
  - Signal Strength
  - Optical Path Differences?

Session 13

Pilot Projects

Graham Appleby, Mark Torrence

Harmonization of QC Results (Oct 2003)

Van Husson (HTSI)
ILRS Central Bureau

International Laser Ranging Service

QC Harmonization Goals

1. Determine absolute station biases and any changes

2. Quick communication of a problem

3. Develop a consolidated bias report

4. Communicate/document a system performance problem

Terms

- QC – quality control based on weekly LAGEOS reports
- RB – range bias
- TB – time bias
- EOP/POS – 28-day EOP and coordinate solutions

What's New

- Added CRL and Delft QC Results to Global Report Card
- CSR, MCC, Delft, and CRL QC results stored in Oracle database (90% automated)
  - Monthly averages computed
  - By year's end, publish RB & TB time-series for each site on **MyStationPerformance.COM**
- Two-color analysis results (e.g. Zimmerwald and TIGO)

Bias Determination

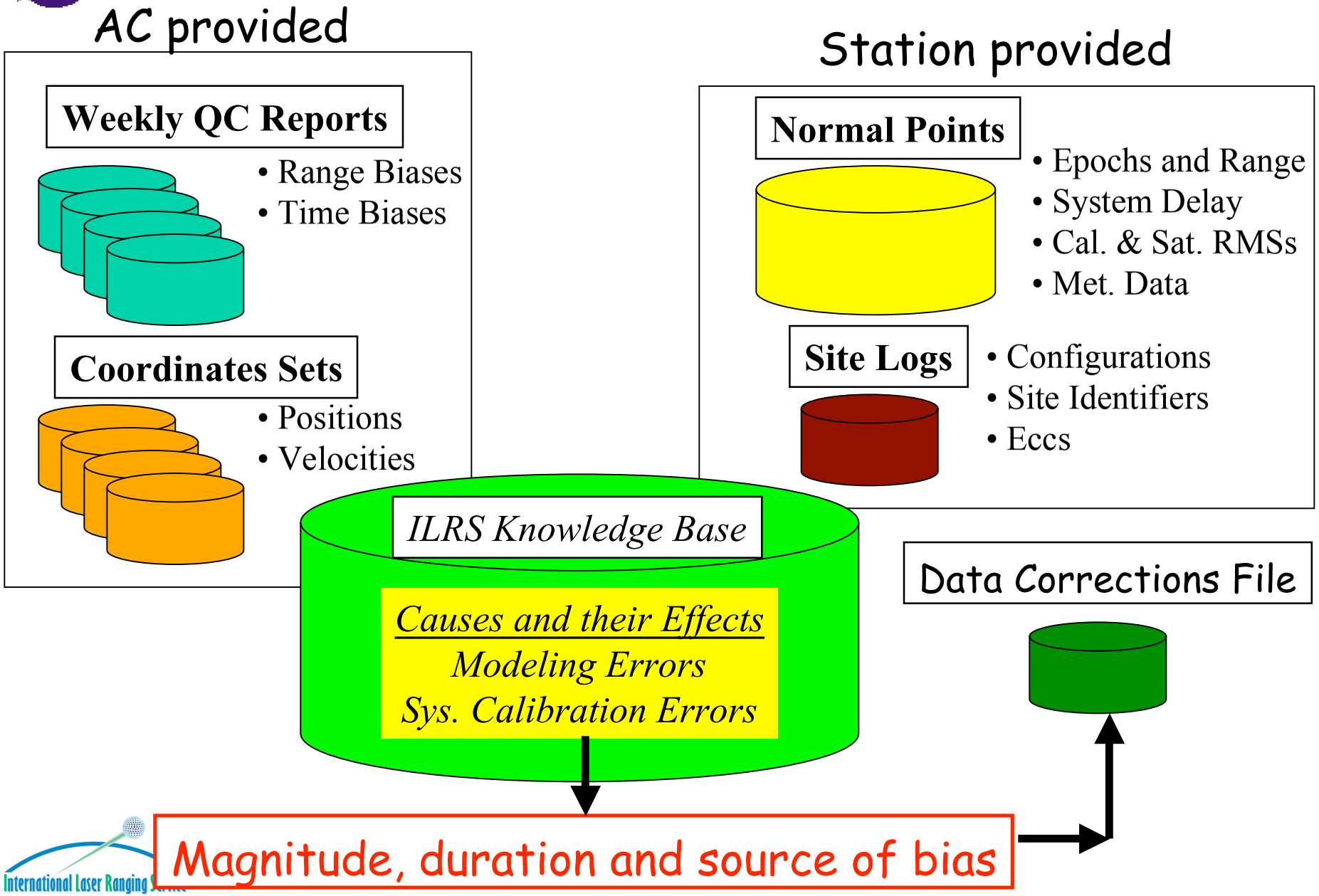

Modeling Limitations in absolute RB Determination

- Prime
  - Station Positions
- Secondary
  - Station Biases
  - Geocenter
  - Troposphere
  - Atmospheric Pressure Loading
  - Satellite CoM
  - GM
  - Temporal and Spatial Data Distribution

QC Results (Weekly Analysis)

Coordinate Systems

Analysis Center	Coordinates	Implementation
CRL	ITRF2000	2001
CSR	*CSR 95L01*	*1995*
Delft	ITRF2000	Jan 2002
MCC	MCC 00L01	March 2000

NP RMSs (3rd Quarter 2003)

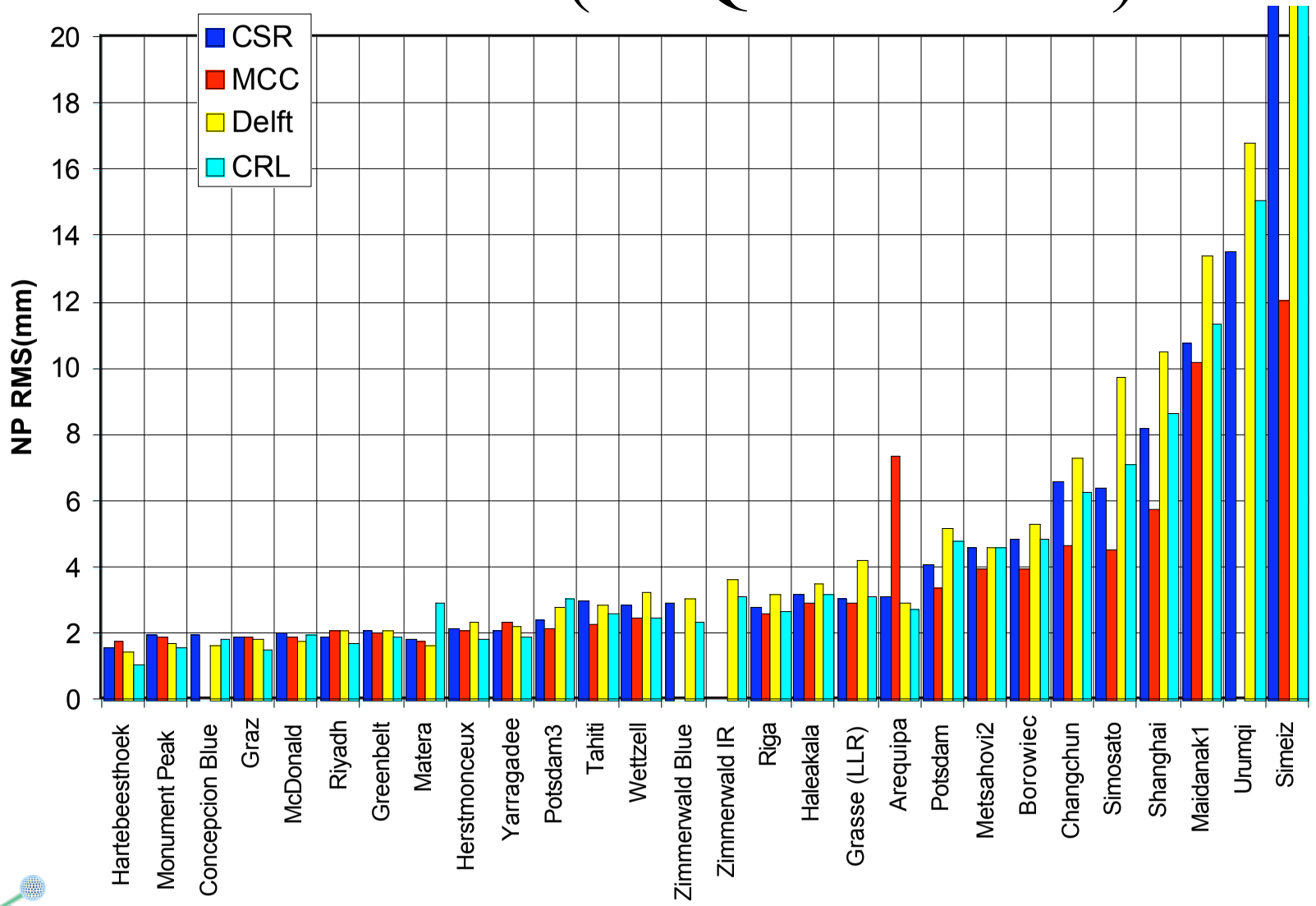

International Laser Ranging Service

2003 RB Stability

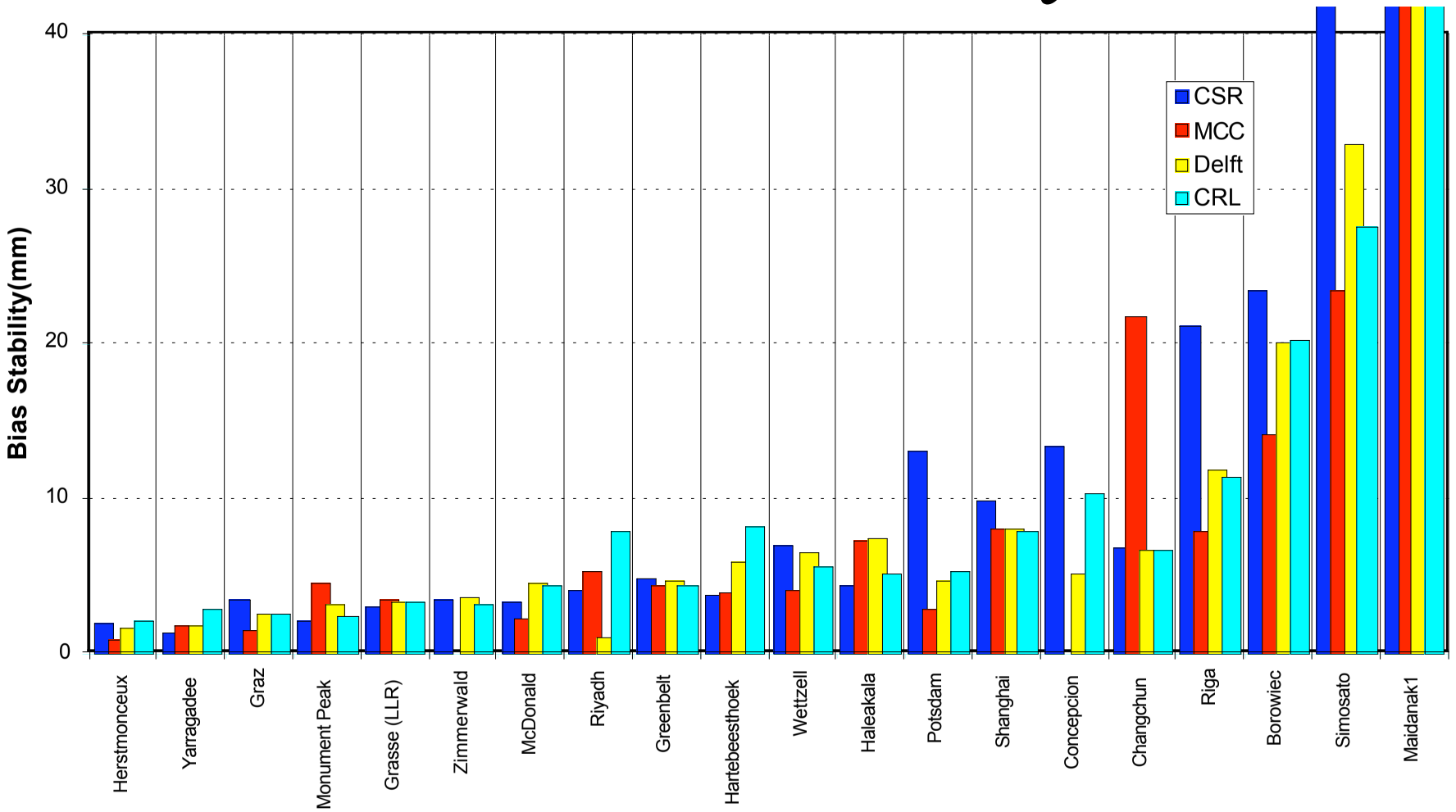

International Laser Ranging Service

2003 RB Estimates

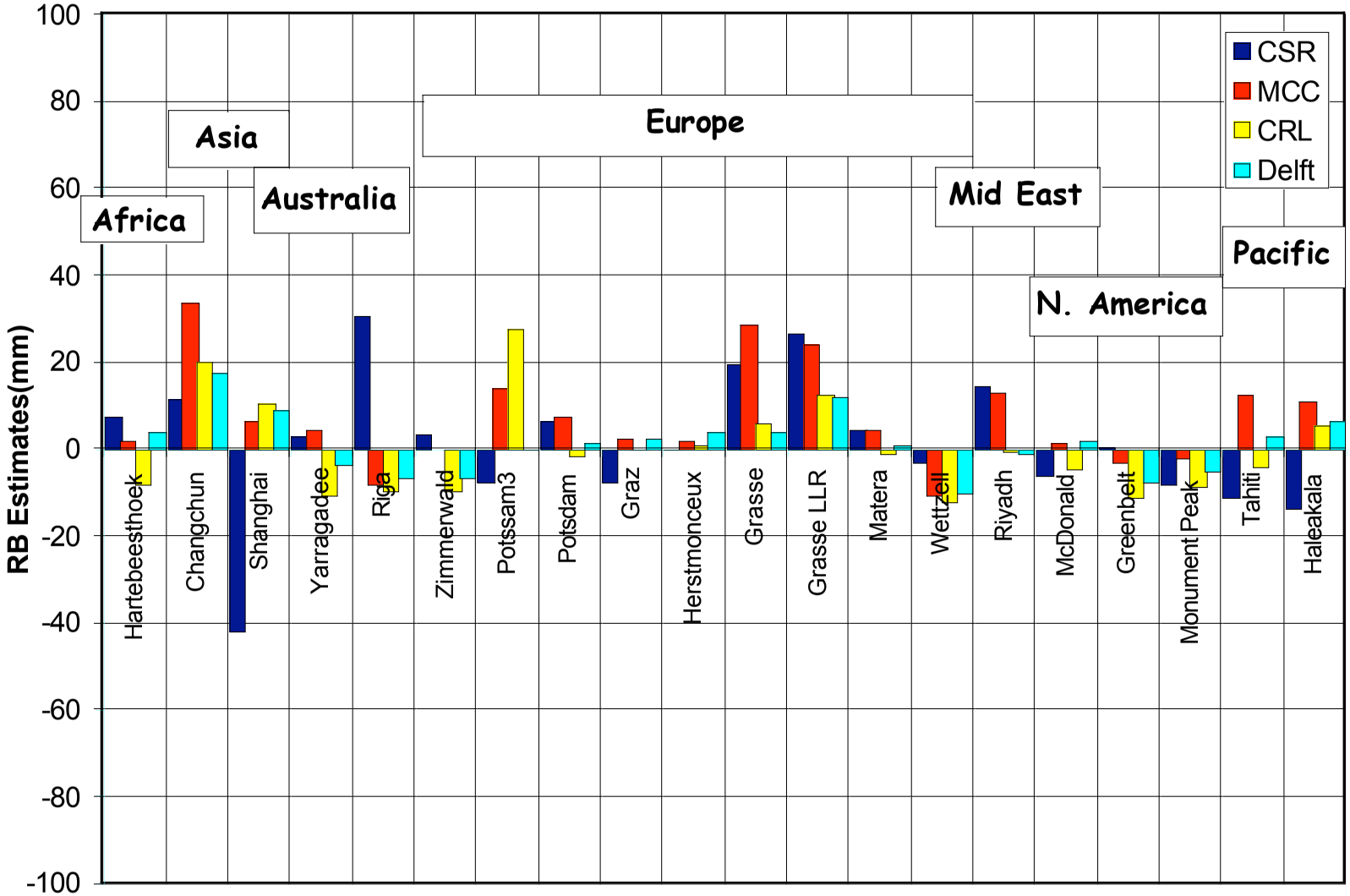

International Laser Ranging Service

Delft vs CRL RB Comparison

- Since 2002, Delft and CRL have been using ITRF2000 coordinates with a few exceptions
  - Notable exceptions are:
    - Riyadh 7832 (both use their own)
    - Shanghai 7837 (Delft uses their own)
    - Hartebeesthoek 7501 (CRL uses their own)

2003 (CRL – Delft) RBs

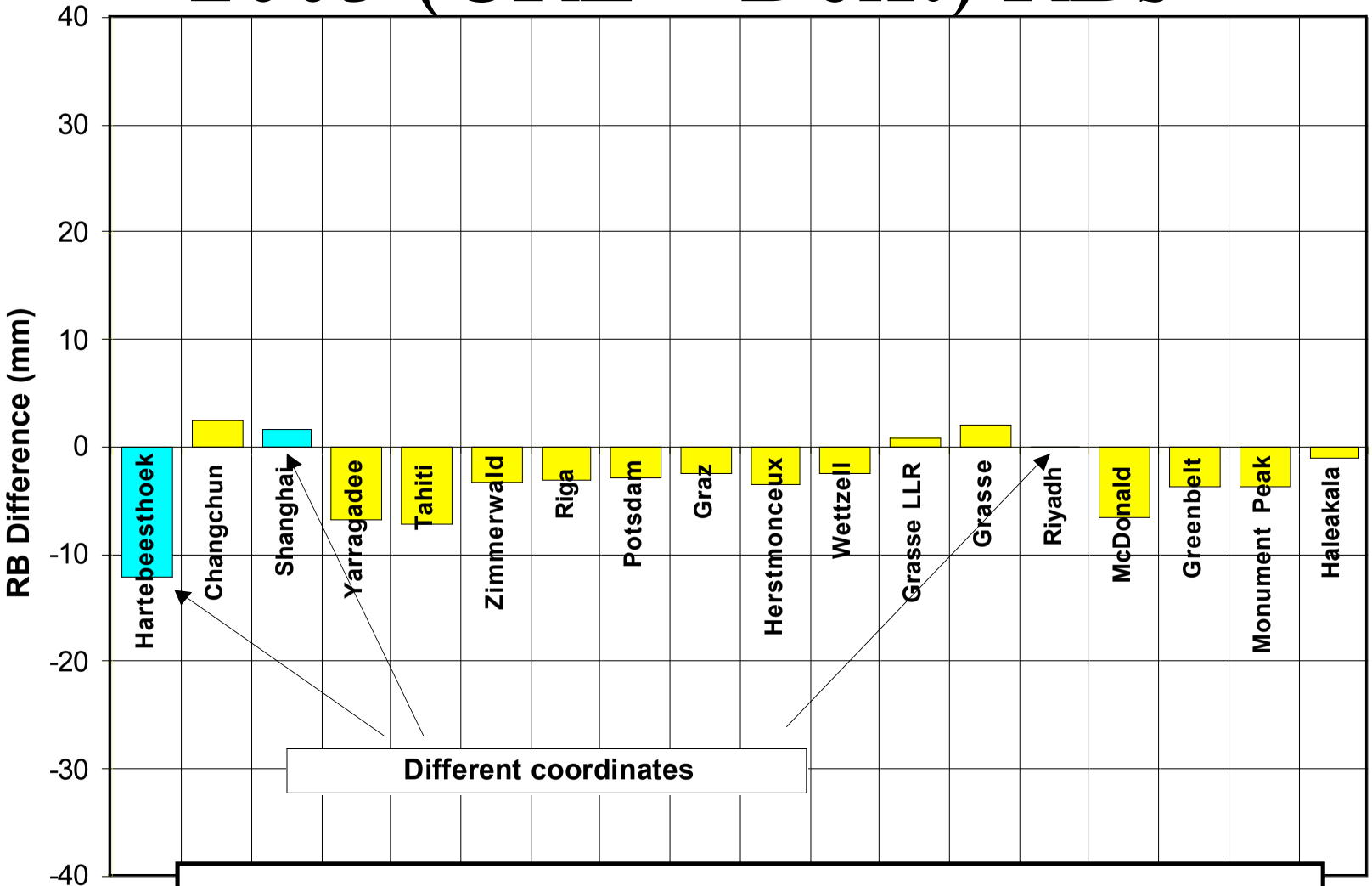

-2.7mm mean difference > Delft pressure truncation
some regional correlations in the differences

International Laser Ranging Service

QC Results

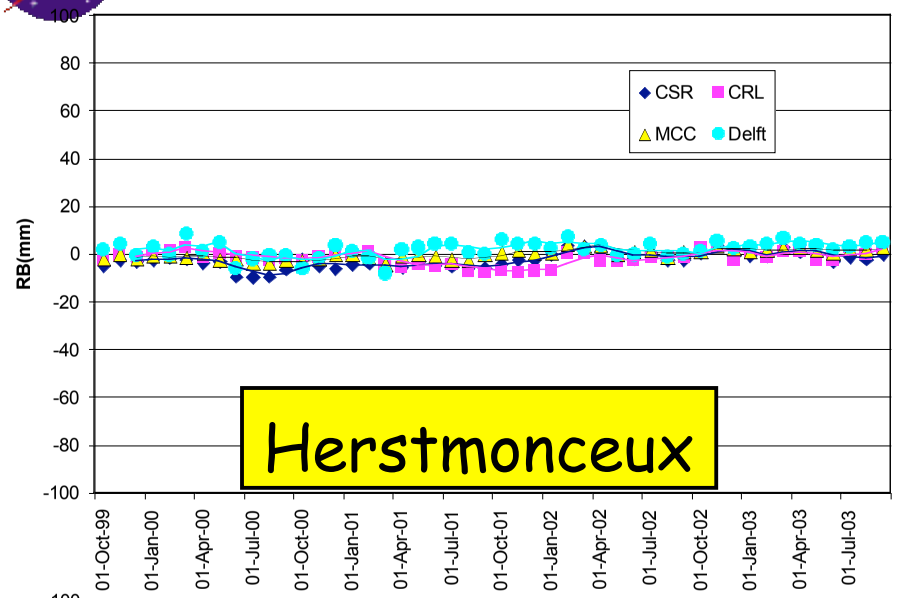

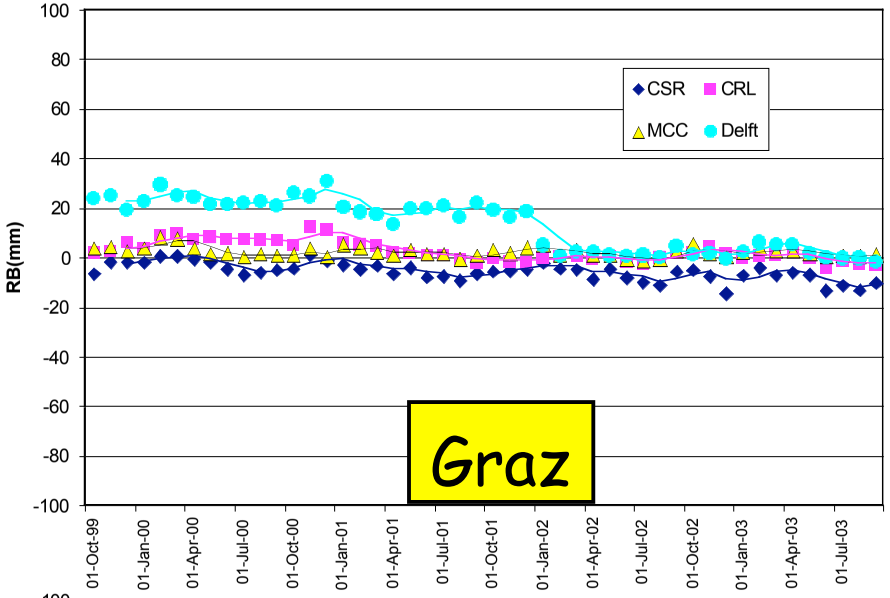

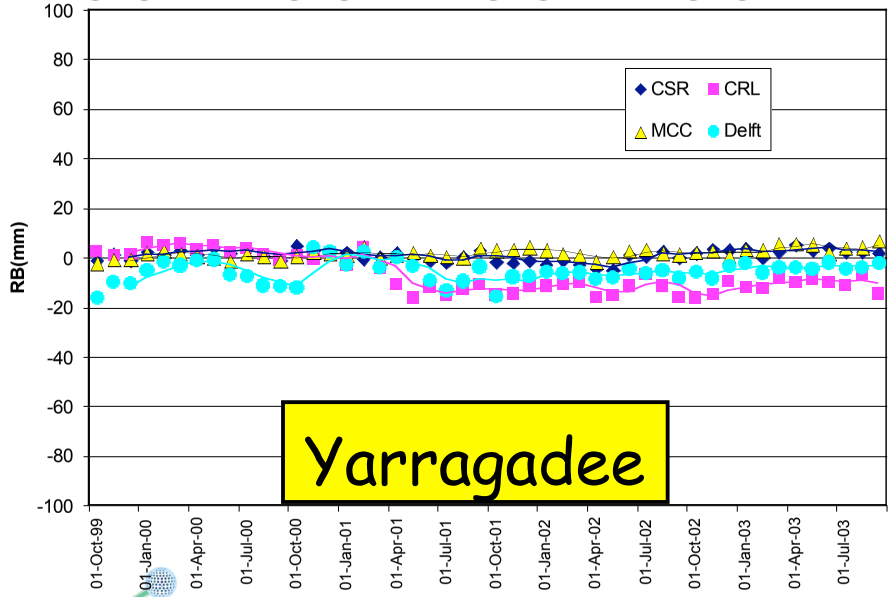

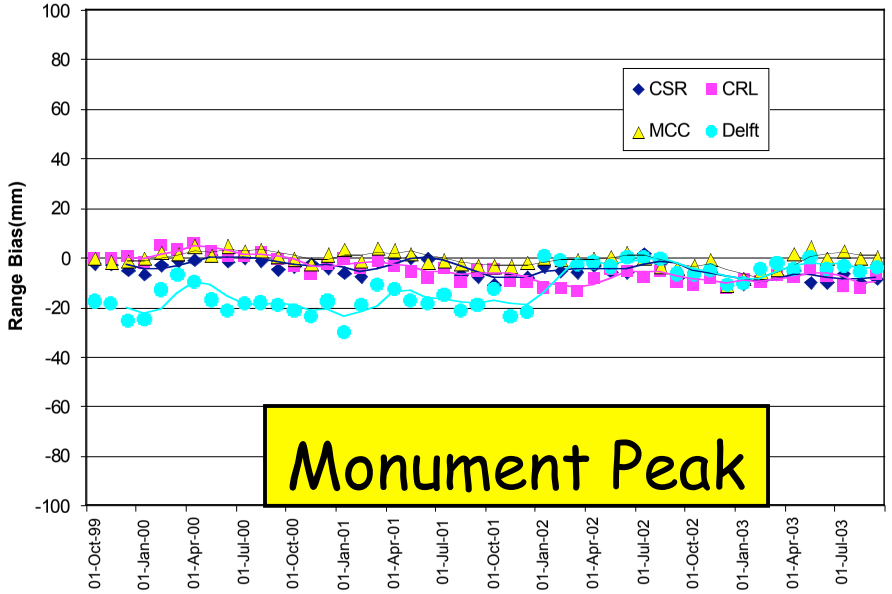

International Laser Ranging Service

QC Results

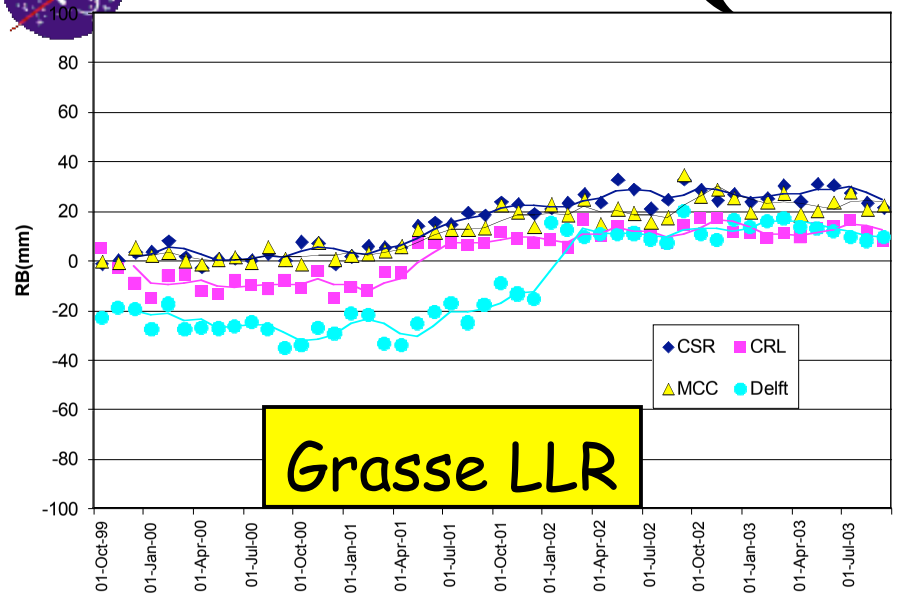

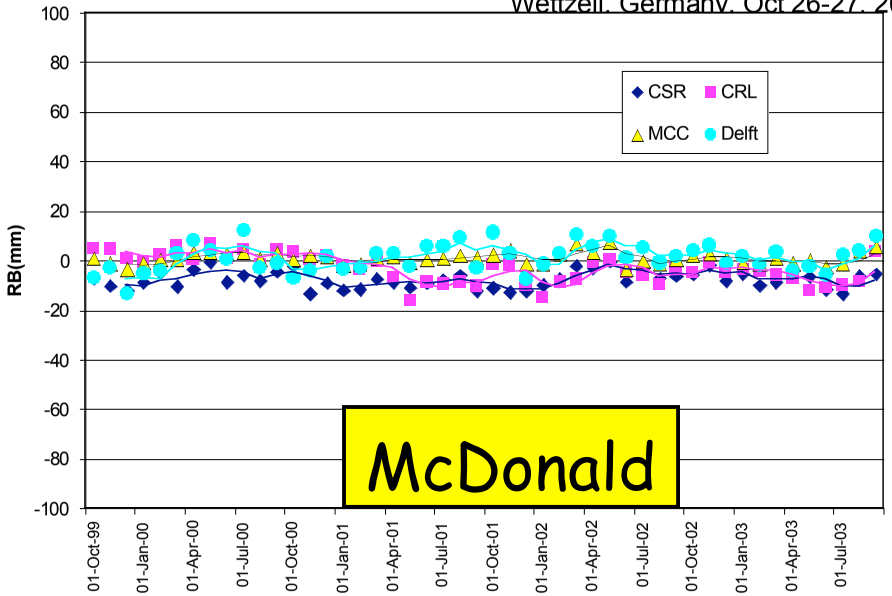

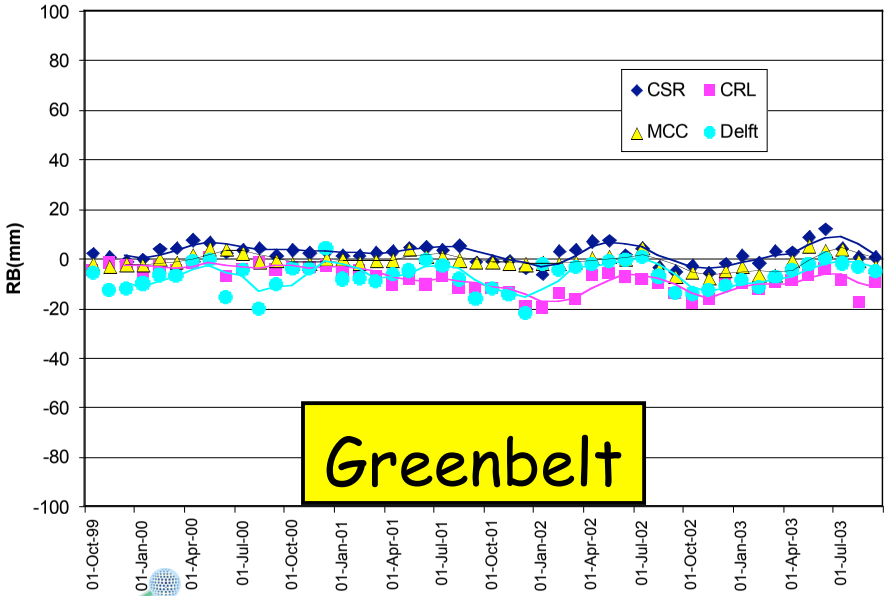

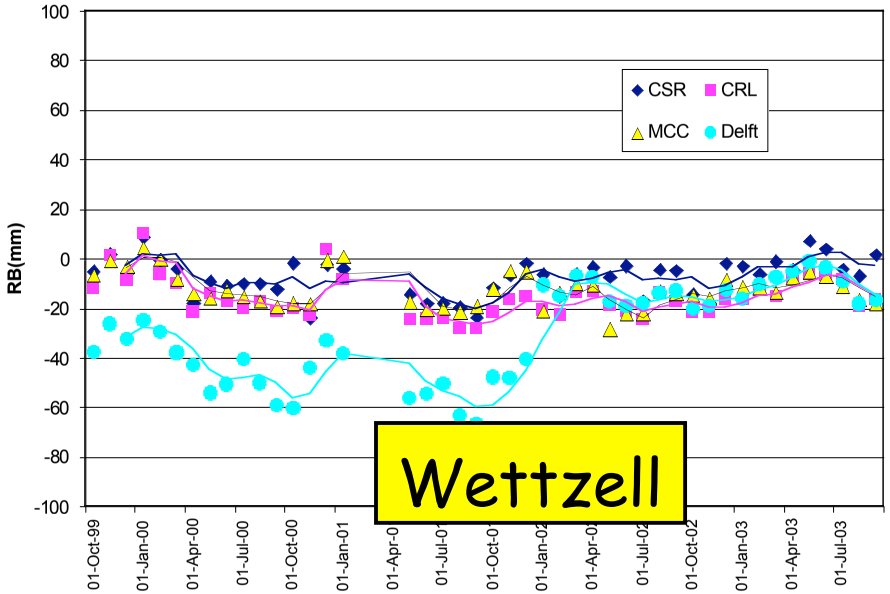

International Laser Ranging Service

10mm Seasonal Variations in RB Estimation

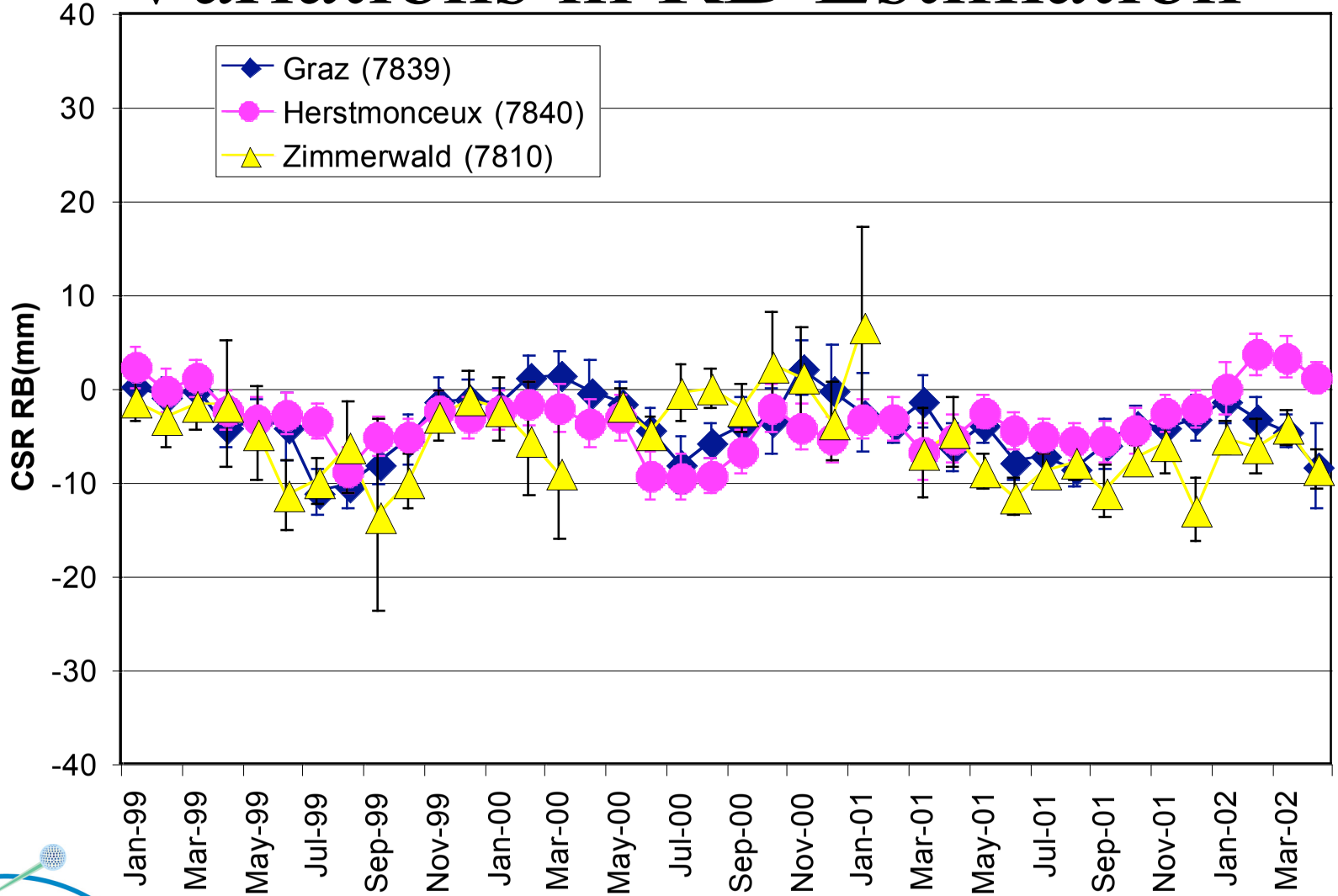

International Laser Ranging Service

EOP/POS Pilot Project 1999 Range Bias Estimation Results

1999 EOP/POS RB Estimates

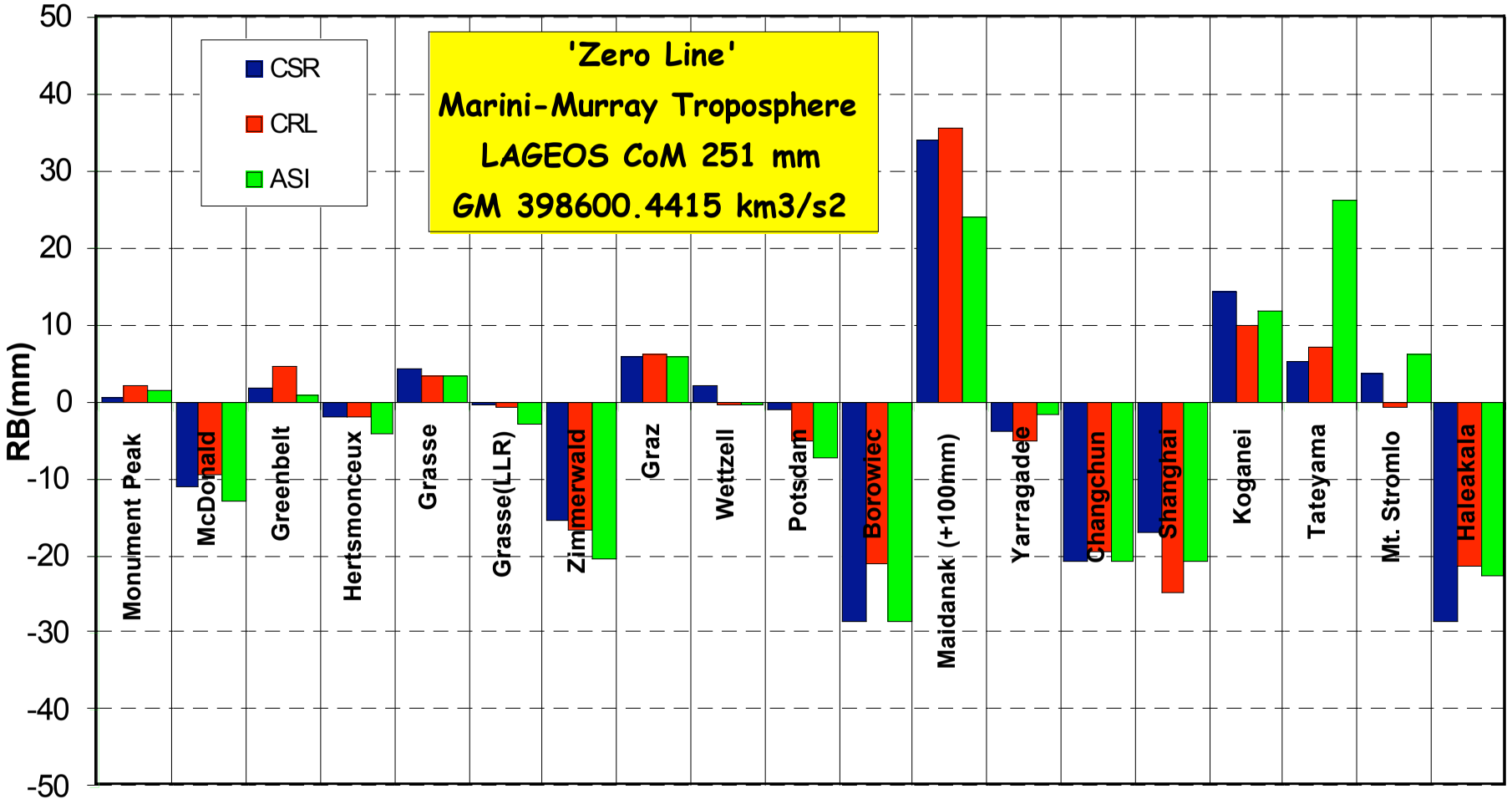

International Laser Ranging Service

1999 RBs Differences from EOP/POS

Honeywell
Honeywell Technology Solutions Inc
Harmonization of QC Results
Wettzell, Germany, Oct 26-27, 2003

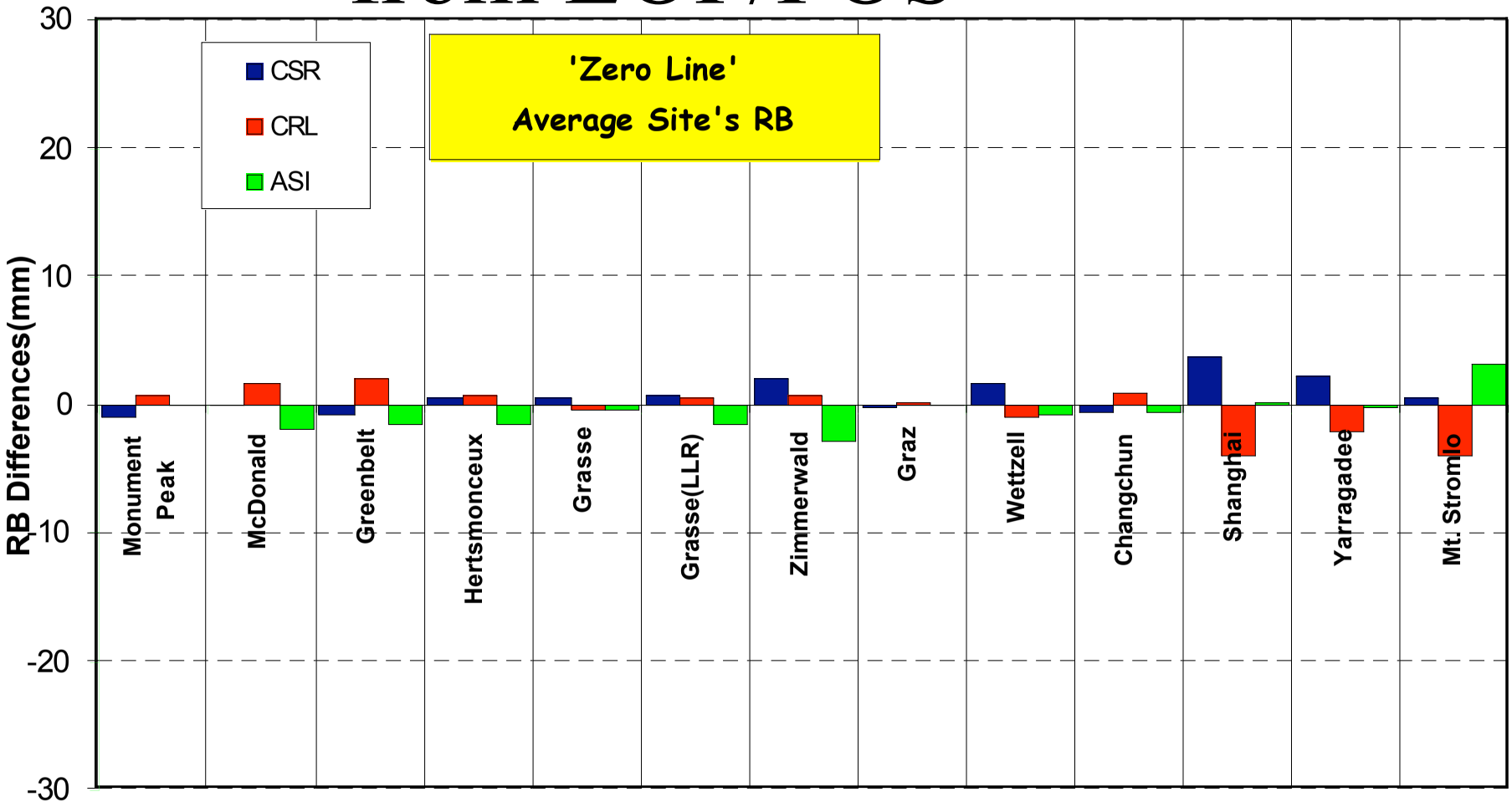

RB agreement to the few mm level.

QC Conclusions

- Action Items
  - Proper management of 2-color results
    - MCC (analysis and reporting)
    - CSR (add a wavelength flag)
    - Delft (reporting only, do not use FAKE CDP#)
  - Delft implement the new TDF program CSR's QC coordinates need to be refreshed
  - All centers need to document any updates in site coordinates
  - Investigate TB trends (Husson)
- Trend similarities are excellent
- Evidence of seasonal wiggles in the RBs
- Peak-to-peak variations have been minimized
  - Bias estimates since 2002 agree to better than 20mm

IERS/ILRS CRC Project Contribution

JCET/GSFC Report

Erricos C. Pavlis

2003 ILRS Workshop

October 28-31, 2003

CRC Contributions

- Four years of weekly ILRS SINEX files
- The files contain POS+EOP only
  - Modeling is similar to case D of ILRS PP
  - LAGEOS 1 & 2 ILRS NPs for 1999 - 2002 used
  - Caveats
    - The solutions were generated from linear shifting of the standard normal equations generated for our multi-year solutions, from the default epoch of 1997.0 to the middle of the week, using the *a priori*, ITRF2000 velocities
    - The "30 NPs or more" rule results in an average of ~23 sites per week
- Generated SINEX files are on the web (version 4.0)

Helmert Translation and Scale Results

Goddard Space Flight Center

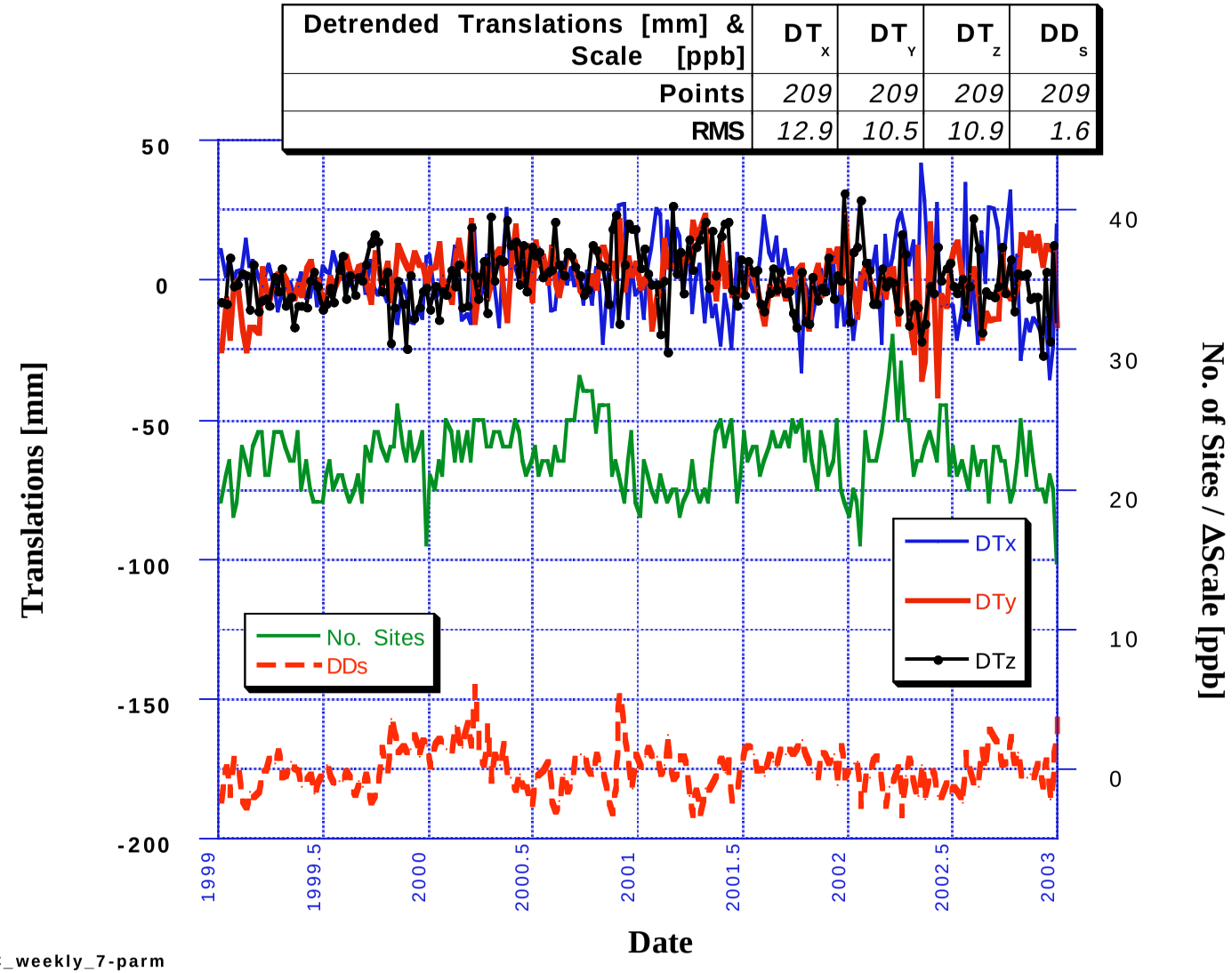

Helmert Rotation Results

Detrended Rotations	DR_X	DR_Y	DR_Z
Points	*209*	*209*	*209*
RMS [mas]	*0.381*	*0.398*	*0.327*

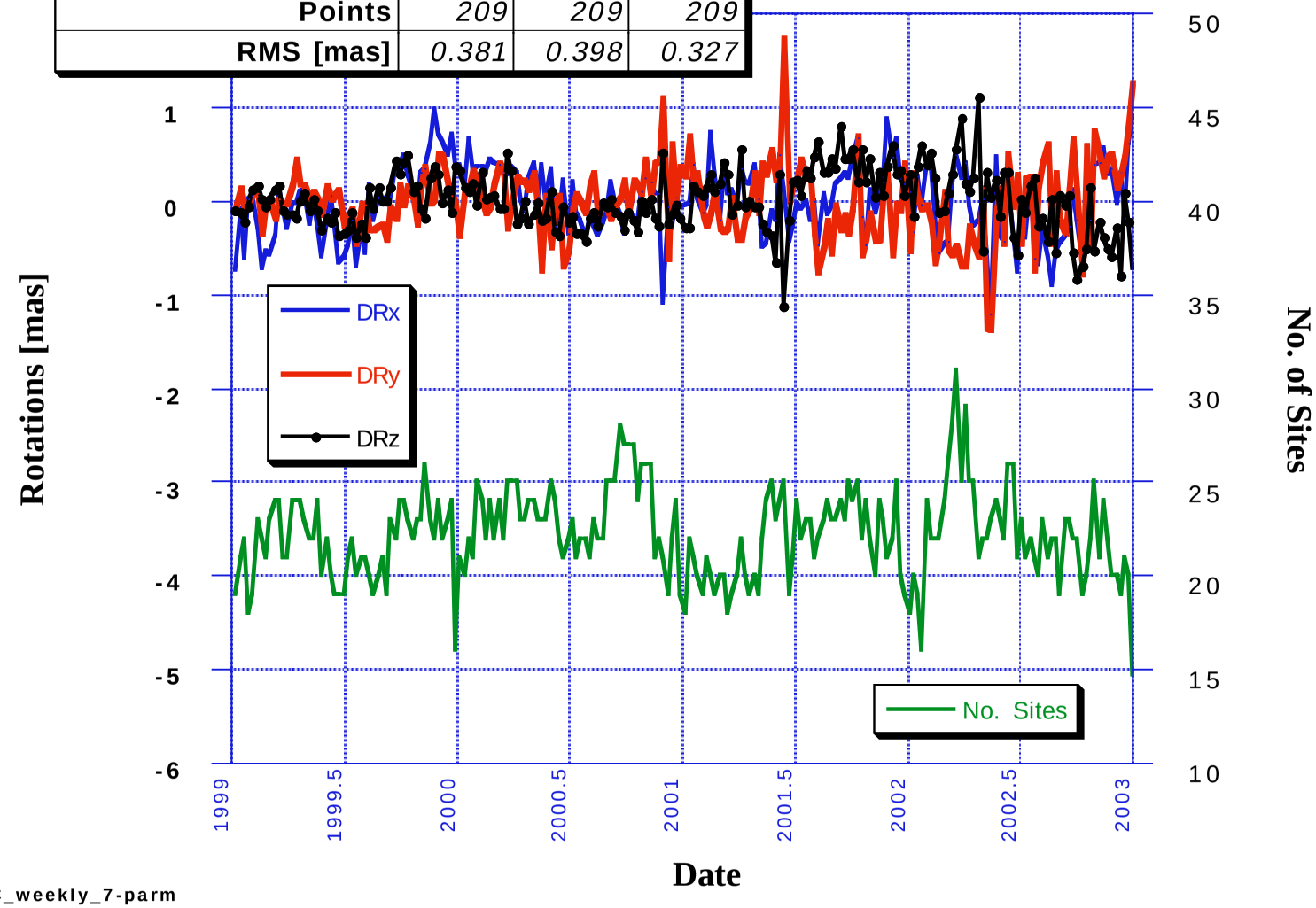

PPC_weekly_7-parm

JCET SLR Center of Mass Weekly Series
vs.
Atmosphere + Oceans + Hydrology
from Jianli Chen/CSR

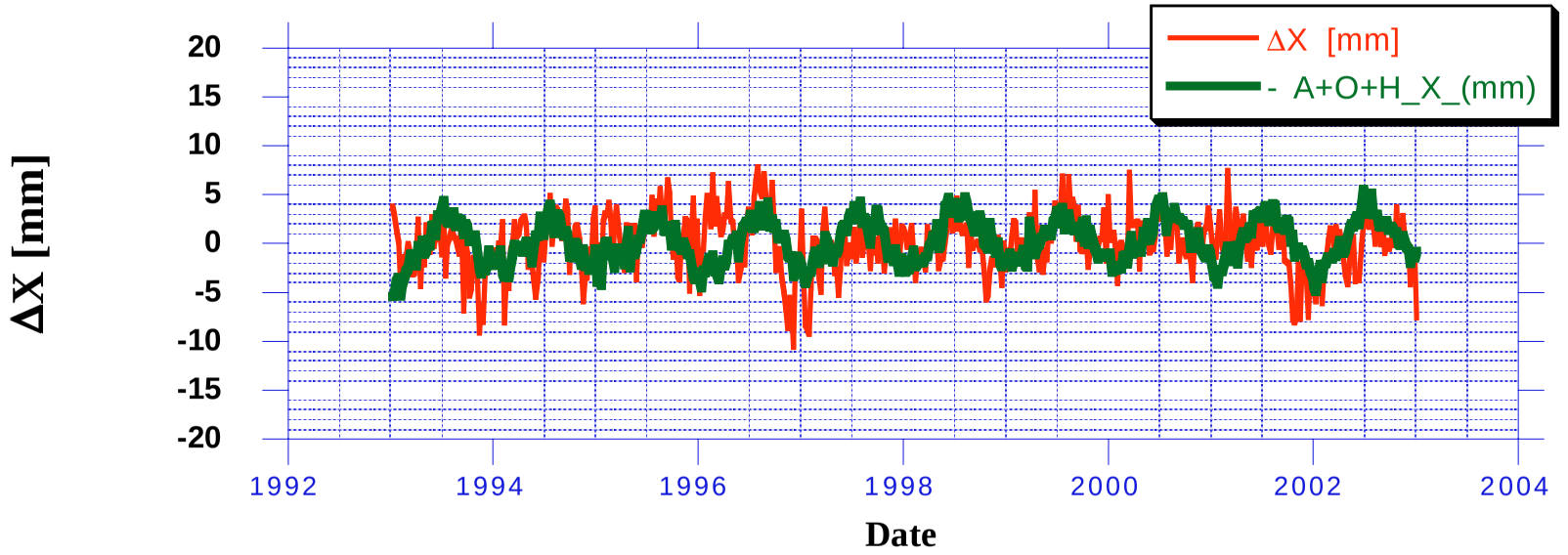

E. C. Pavlis / GSFC

JCET SLR Center of Mass Weekly Series
vs.
Atmosphere + Oceans + Hydrology
from Jianli Chen/CSR

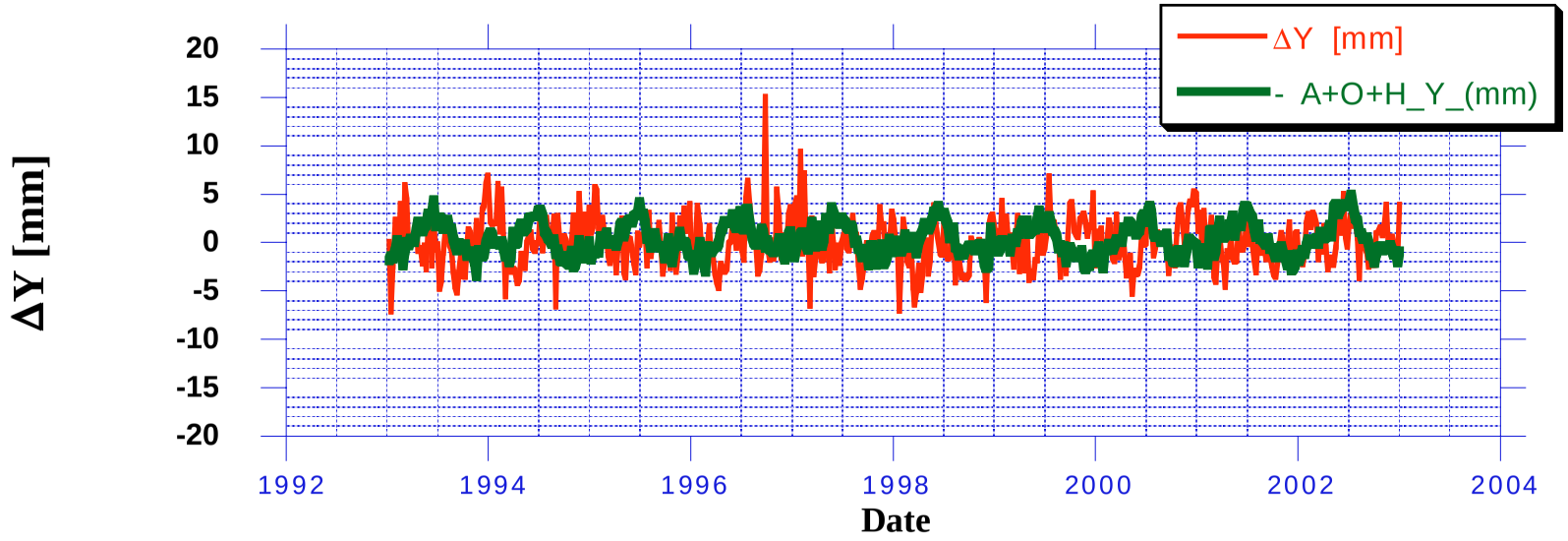

E. C. Pavlis / GSFC

JCET SLR Center of Mass Weekly Series
vs.
Atmosphere + Oceans + Hydrology
from Jianli Chen/CSR

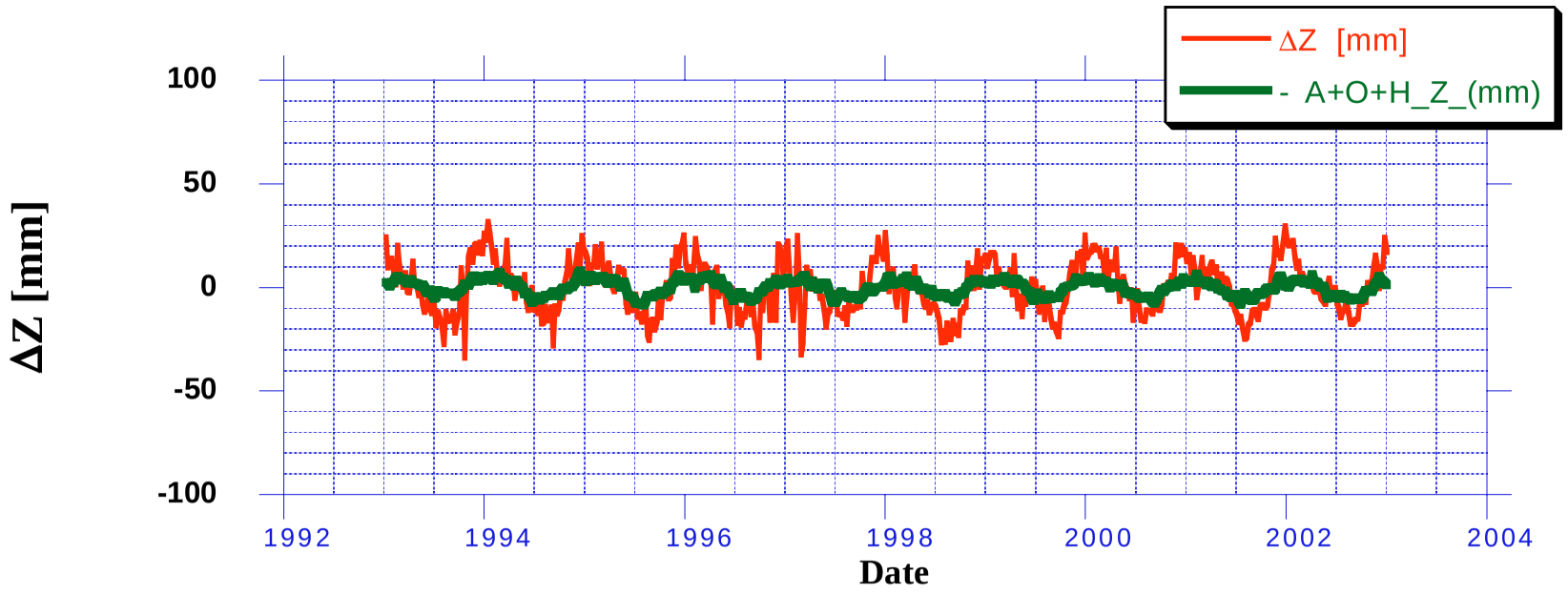

E. C. Pavlis / GSFC

Where to Download them From:

http://www.jcet.umbc.edu/~epavlis/interdisciplinary.html#SLR_SINEX

CRC Summary

- **Contributed *209 weekly SINEX* files from LAGEOS 1 & 2 for *1999 - 2002* to the IERS CRC PP**
- **Version 4.0 referenced to mid-week epoch, after it was originally generated with epoch *1997.0***
- **New version by early November (mid-week referenced)**
- **Optimal selection of sites, data thinning, and "loose" constraints for weekly solutions are still under investigation, along with the issue of EOP rates.**

Session 14

New Approaches

Erricos Pavlis, Mark Torrence

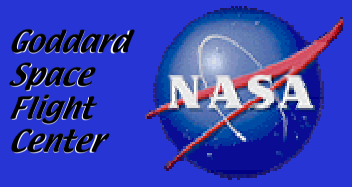

QL (Preliminary) System Positioning

The FTLRS @ Chania case

Erricos C. Pavlis
JCET/UMBC - NASA/Goddard/926

2003 ILRS Workshop
October 28 - 31, 2003, Kötzting, Germany

A need for quick positioning

- When an earthquake occurs in the region (e.g. Arequipa)
- When mobile systems relocate at a new site (e.g. FTLRS @ Chania)
- When a fixed system returns to operation after a re-build (Mt. Stromlo)
- When for any reason there is suspicion that there is “change” at a site

FTLRS @ Chania

GAVDOS MSL & Alt. Calibration Site

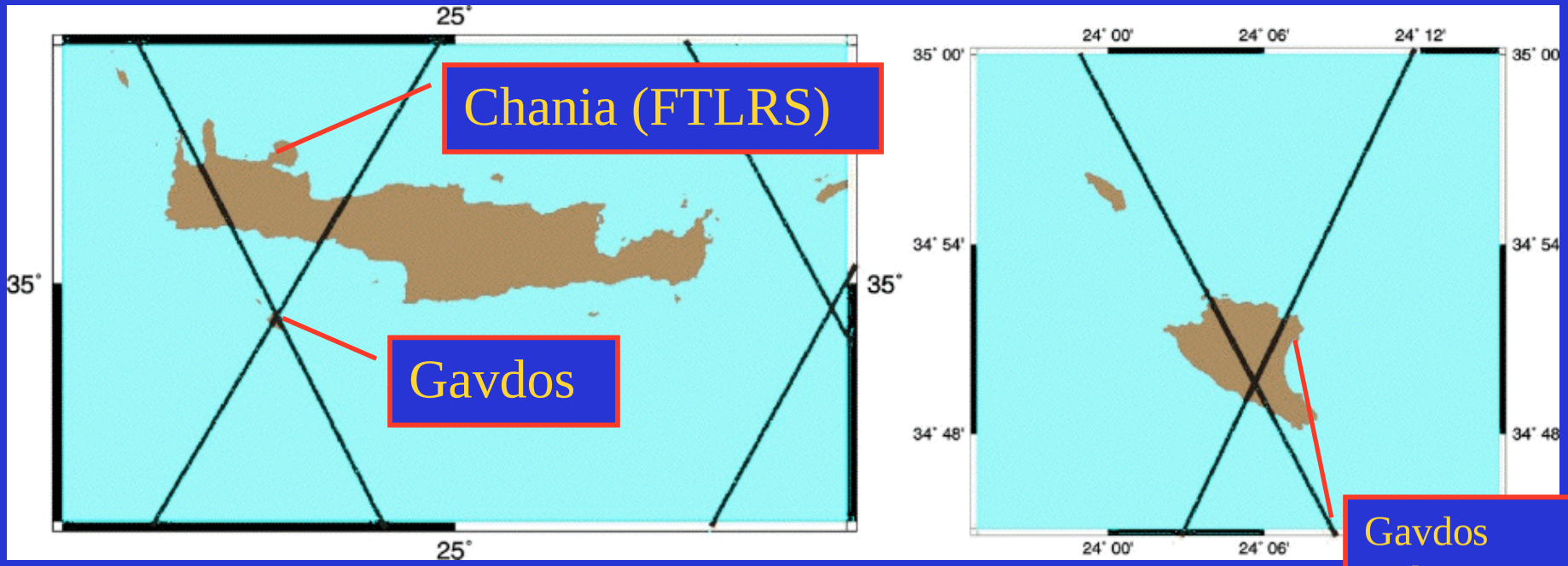

Starting GPS Position

GAMIT Results		
X [m]	Y [m]	Z [m]
4744552.5533	2119414.5451	3686245.1363
±1.0 [cm]	±1.0 [cm]	±1.0 [cm]
ϕ	λ	*h [m]*
35° 31' 58".95437	24° 04' 13".96631	161.0495
±1.25 [mas]	±1.40 [mas]	0.43 [cm]

Formal 1-σ uncertainties from data collected over 2003 DOY 71 - 81

SLR Data Distribution

	Passes	NPs
LAGEOS 1:	**15**	**89**
LAGEOS 2:	**28**	**232**

Week	LAGEOS 1	LAGEOS 2
2003.04.06	√	√
2003.04.20	√	√
2003.04.27	√	√
2003.05.11	√	√
2003.05.18	√	√
2003.05.25	edited	√
2003.06.01	-	√
2003.06.08	-	√
2003.06.15	-	√
2003.06.22	√	√

Measurement Bias Estimation

Arc week	Site ID	LAGEOS 1 bias [mm]	σ [mm]	LAGEOS 2 bias [mm]	σ [mm]
20030406	78306901	-2.1	38.0	-15.9	52.2
20030420	78306901	-8.6	53.1	-19.1	38.9
20030428	78306901	-4.8	32.7	-6.2	35.1
20030512	78306901	89.4	122.7	-12.6	57.8
20030518	78306901	-286.8	89.1	-17.2	41.7
20030524	78306901	0.0	0.0	-18.8	33.3
20030600	78306901	0.0	0.0	-16.4	29.7
20030608	78306901	0.0	0.0	-9.4	30.5
20030616	78306901	0.0	0.0	-4.1	34.2
20030622	78306901	17.4	90.2	9.7	35.9

	LAGEOS 1 Bias [mm]	σ [mm]	LAGEOS 2 Bias [mm]	σ [mm]
Minimum	-8.6	32.7	-19.1	29.7
Maximum	-2.1	53.1	9.7	57.8
Points	3	3	10	10
Mean	-5.17	41.2	-11.00	38.9
RMS	5.82	42.1	13.91	39.9

- Thin data set for LAGEOS 1
- Perhaps a ~ -10 ± 40 mm bias on LAGEOS 2

GEODYN Results		
Adopted	Velocity	Vector
V_X [m/y]	V_Y [m/y]	V_Z [m/y]
-0.0161	0.0190	0.0094
First Iteration		
X [m]	Y [m]	Z [m]
4744552.6490	2119414.4260	3686245.0800
±1.70 [cm]	±1.50 [cm]	±2.20 [cm]
ϕ	λ	*h [m]*
35° 31' 58".95210	24° 04' 13".96051	161.0482
±0.34 [mas]	±0.49 [mas]	±2.72 [cm]
Second Iteration		
X [m]	Y [m]	Z [m]
4744552.6650	2119414.4160	3686245.0860
±0.21 [cm]	±0.22 [cm]	±0.19 [cm]
ϕ	λ	*h [m]*
35° 31' 58".95208	24° 04' 13".95990	161.0602
±0.057 [mas]	±0.077 [mas]	±0.25 [cm]

Two Independent Results

JCET SLR0 Solution (1997.0):	... 552.665	... 414.416	... 245.086
+ Eccentricities (Husson) :	+1.351	+0.604	+1.057
JCET IAR Solution (1997.0):	... 554.016	... 415.020	... 246.143
*CSR CHANIA 7830	4744554.011	2119415.053	3686246.151
Δ(JCET - CSR) IAR	0.005	- 0.033	- 0.008

A second CSR solution, adopting the JCET velocity and making use of the eccentricitis, resulted in even closer agreement

* CSR/John Ries, Position Derived from JASON data

Summary & Conclusions

- SLR can produce ~2-3 cm positions with even sub-optimal data distribution and limited amount of data on LAGEOS-type satellites
- Independently derived (s/w, analyst, satellite) position from JASON, with significantly more data agrees to ~2-3 cm
- Perhaps it is the time to consider such tests in order to qualify targets for inclusion in our routine processing to improve EOP and TRF

Session 15

kHz Ranging and Its Impact

Georg Kirchner, John Degnan

kHz SLR in Graz

Now operational …

Georg Kirchner

Franz Koidl

Austrian Academy of Sciences

kHz SLR at Graz

kHz Laser Specs:

- Nd:Vanadate
  - Diode Pumped
  - Seed: SESAM
  - Regen. Amp
  - Post Amp
- 10 Hz – 2000 Hz
- <10 ps Pulse Width
- 0.4 mJ / Pulse @ 532 nm

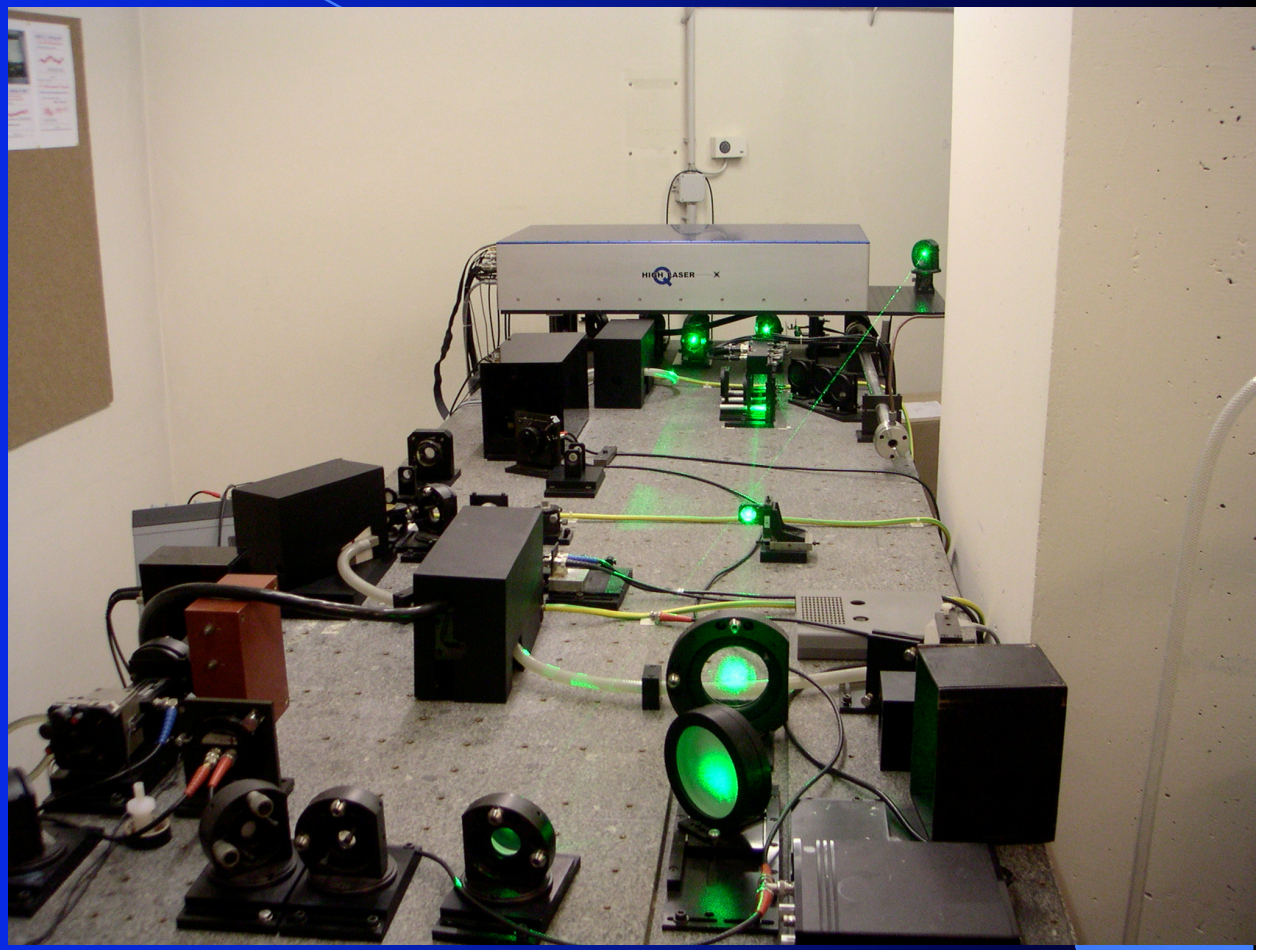

New kHz Laser on top of 10 Hz Quantel Laser ...

kHz SLR at Graz

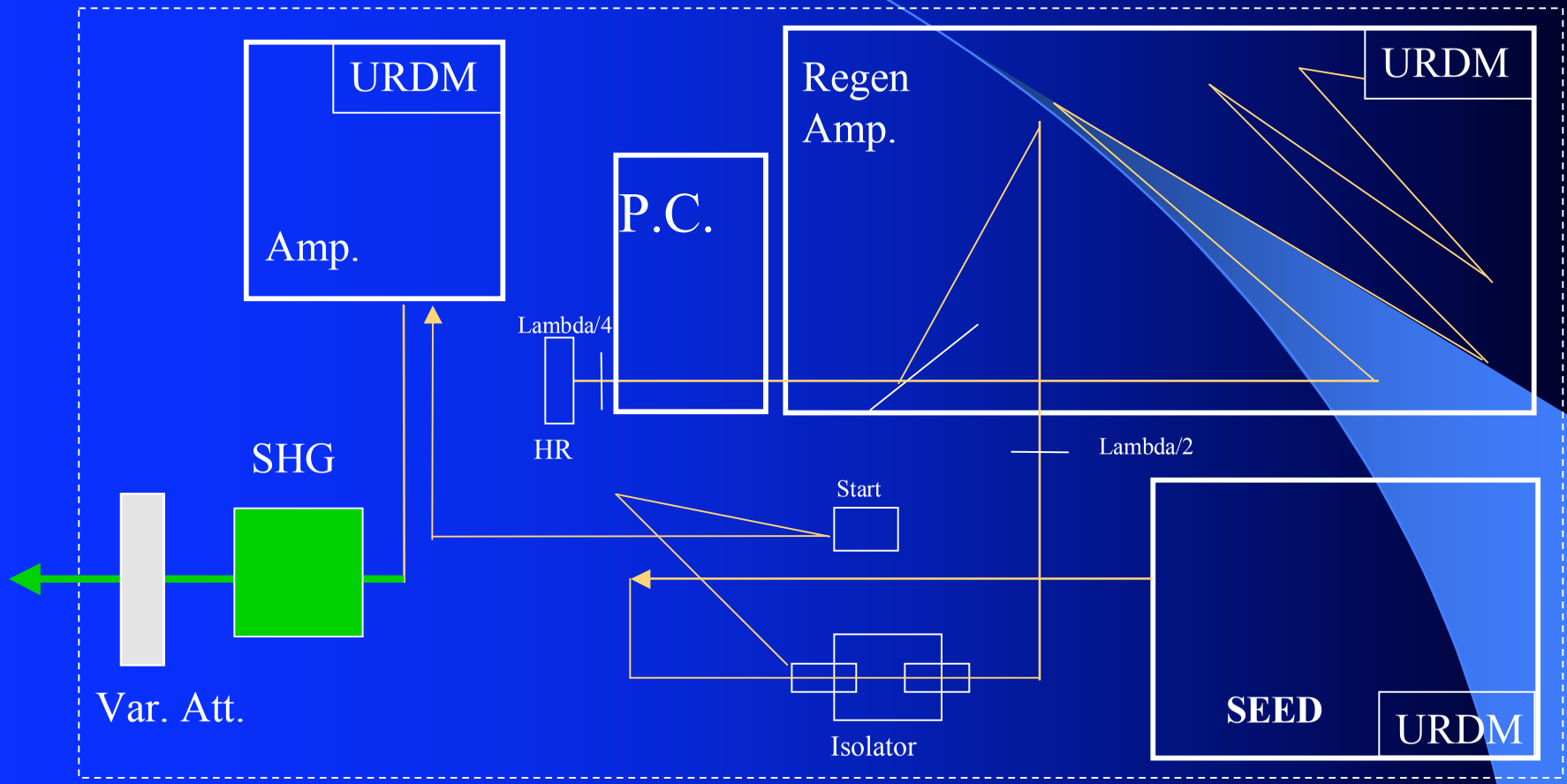

HIGH Q LASER

kHz SLR at Graz

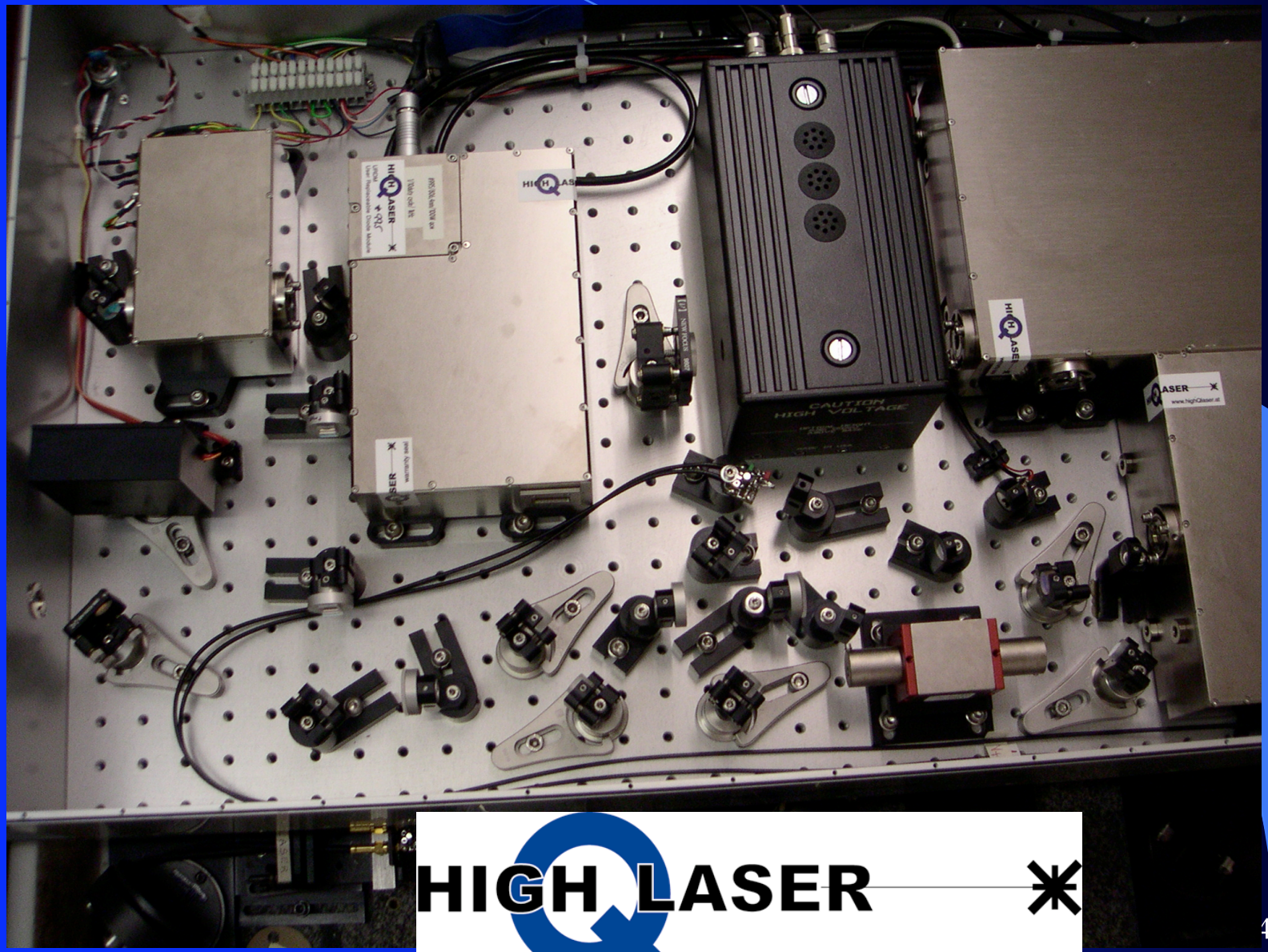

HIGH LASER

kHz SLR at Graz

New / adapted / necessary Items for kHz Laser Ranging:

- The kHz Laser itself;
- Event Timers: Graz E.T., using Dassault Modules;
- Range Gate Generator: FPGA Device, built in Graz; with < 500 ps Resolution
- 2.4 GHz PC as Real Time Controller;
- We use the „Stone-Age“ DOS (but it is fast ...)
- Software to handle everything within 500 □s cycles

kHz SLR at Graz

Statistics (2 weeks after start of kHz):

- 10 Hz Laser, first 279 days in 2003:
  - 6361 Passes, with 9.635.964 Returns
- kHz Laser, first 10 days after start (Day 281/2003):
  - 120 Passes, with 10.005.816 Returns

kHz SLR at Graz

Statistics (2 weeks after start of kHz):

- LAGEOS: Up to 200.000 Returns / Pass
- ENVISAT etc: Up to 350.000 Returns / Pass
- TOPEX: Up to 500.000 Returns / Pass
- AJISAI: > 1.000.000 Returns / Pass
- GPS 36: About 10.000 Returns / Hour ...

  (remember: 0.4 mJ/shot !)

kHz SLR at Graz

Statistics (2 weeks after start of kHz):

- LAGEOS: Up to 20.000 Returns / NP
- STARLETTE: Up to 38.000 Returns / NP
- AJISAI: Up to 45.000 Returns / NP

- In NP File: We state „9999“ if actual number exceeds that ....

kHz SLR at Graz

Statistics (2 weeks after start of kHz):

- We now submit only NPs with > 100 Pts / NP
- We might change that to > 600 Pts / NP for LEOs
  - This will increase NP stability again;
  - This eliminates NPs with „poor“ return rate;
- We will check also possible use of Single Photons only for specific / all satellites;
  - But presently everything points to MultiPhotons

kHz SLR at Graz

Additional Remarks:

- Day and Night: Similar Amount of Results
- Single Shot Accuracy: Similar as for the 10 Hz Laser:
  - Better due to < 10 ps pulses;
  - Better due to pulse uniformity of DPSSL;
  - Worse due to low return energy (IF Sat signature)
  - ERS-2, Envisat: 3 - 4 mm; GraceA/B: 2 - 4 mm

kHz SLR at Graz

G89 284 21:

- 311 k Pts
- 135 k Rets
- White: ID
- Yell.: Noise
- No other Noise stored

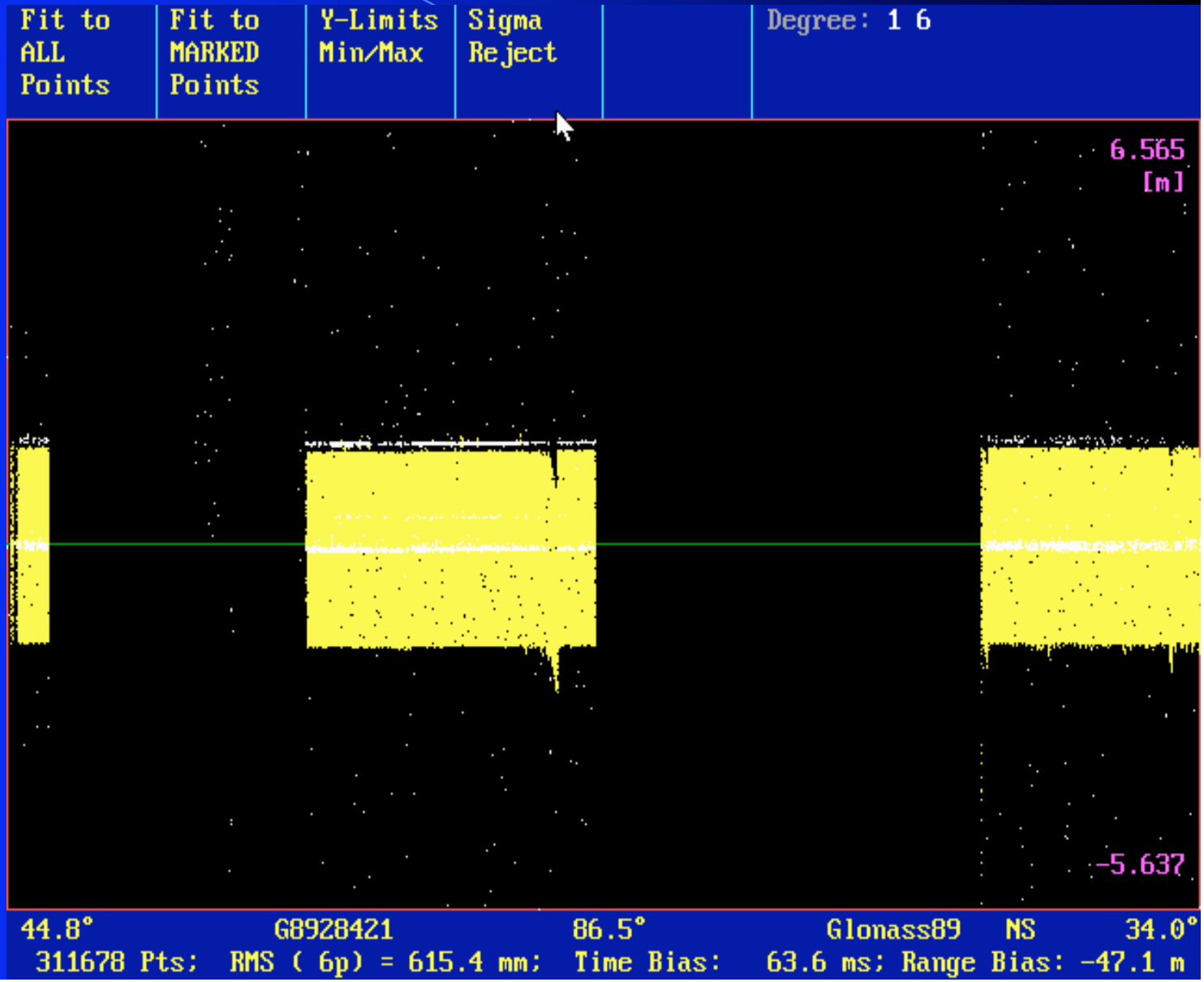

kHz SLR at Graz

G89 284 21:

- 311 k Pts
- 135 k Rets
- White: ID
- Yell.: Noise
- Shows Retro Panels

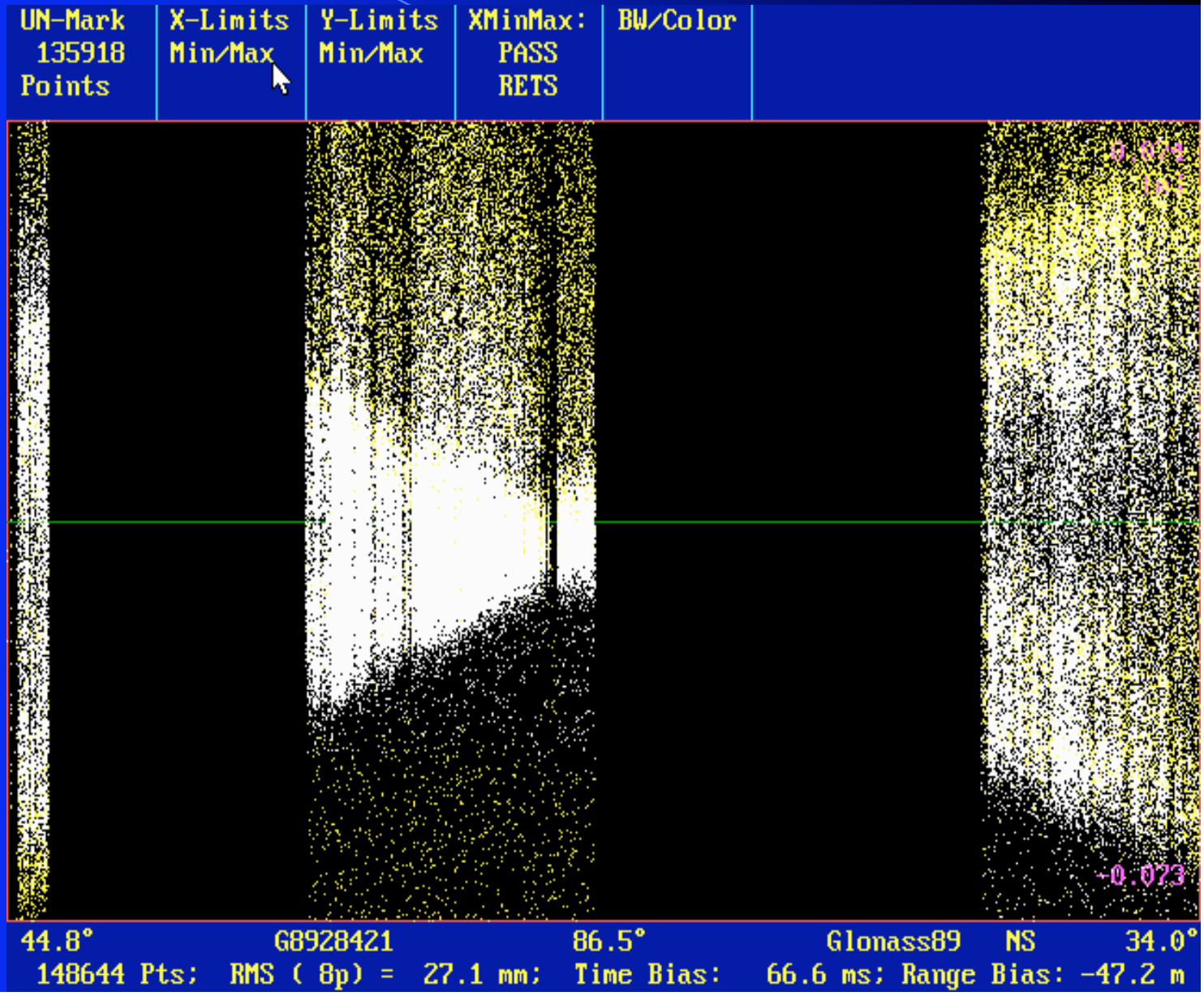

kHz SLR at Graz

ER2 282 20:

- 247 k Pts
- 179 k Rets
- Single Retros Visible ...
- Low Elev: < 8° with 0.4 mJ ...
- Only first track used

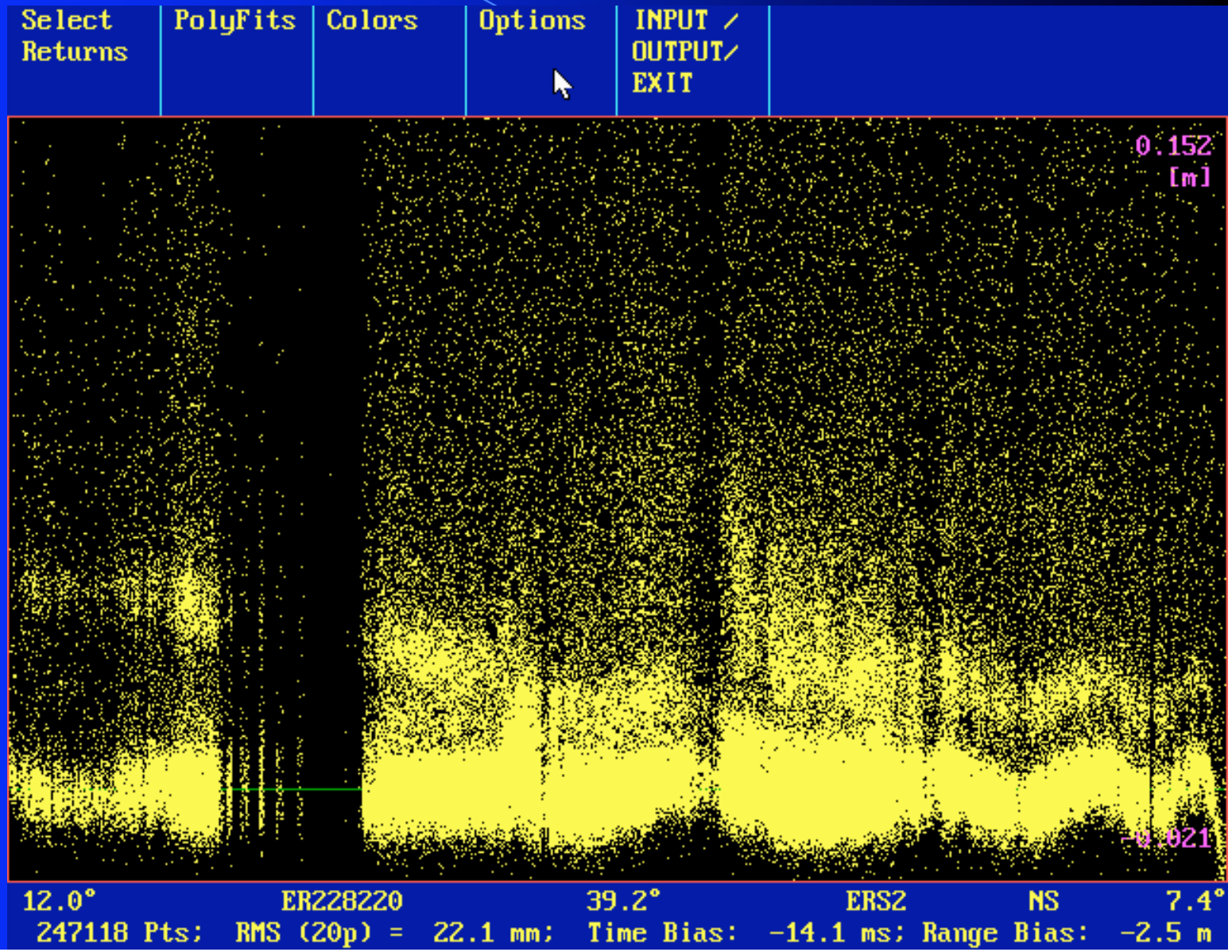

kHz SLR at Graz

G84 285 00:

Storage:

- Only ID Returns
- PLUS Pts around ID Returns
- 163 k Pts;
- 67 k Rets

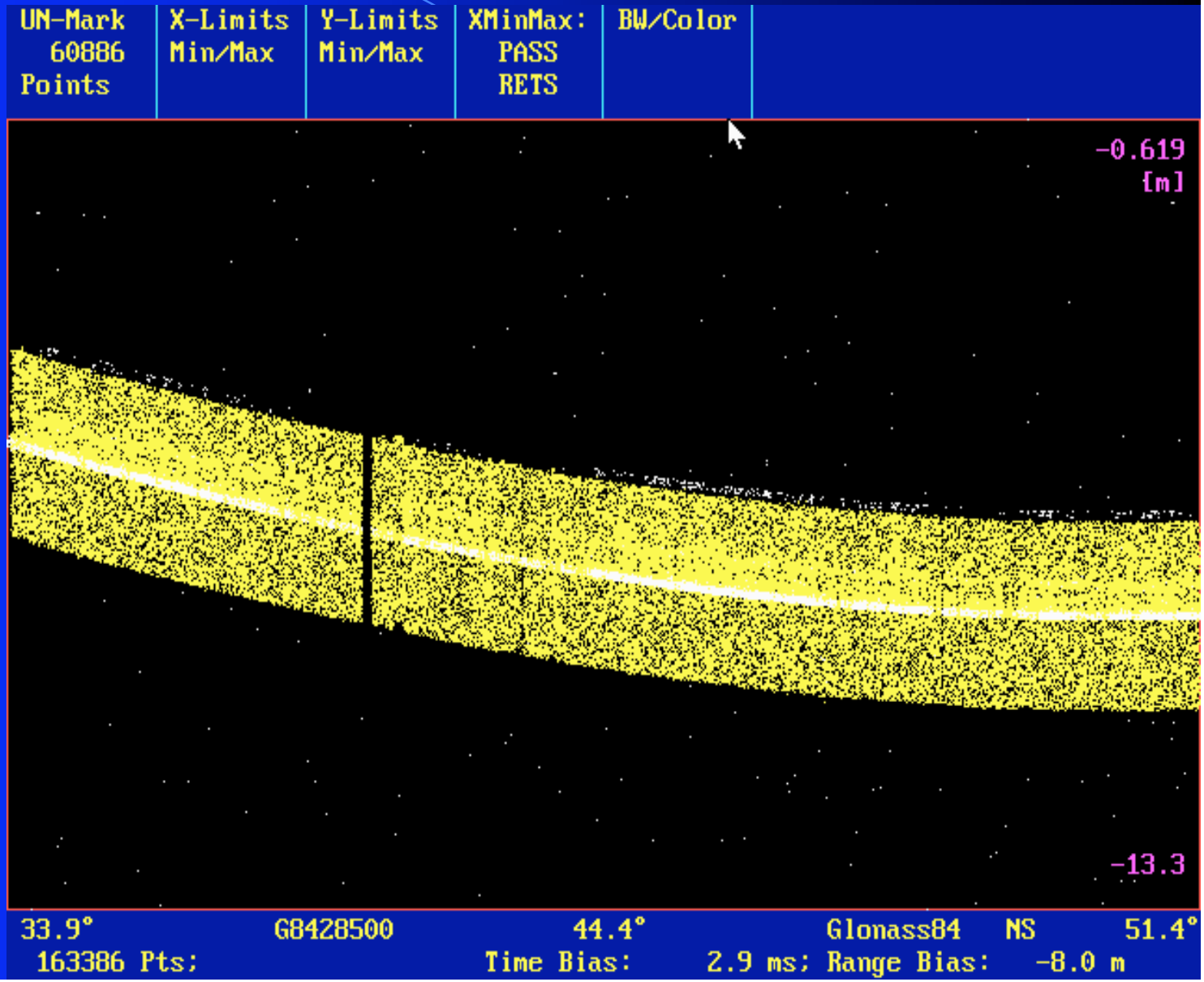

kHz SLR at Graz

Glonass 84 / Same Pass:

- Returns as identified in Real Time
- Various Retro Tracks
- About 67 k Returns;
- 35 mm RMS

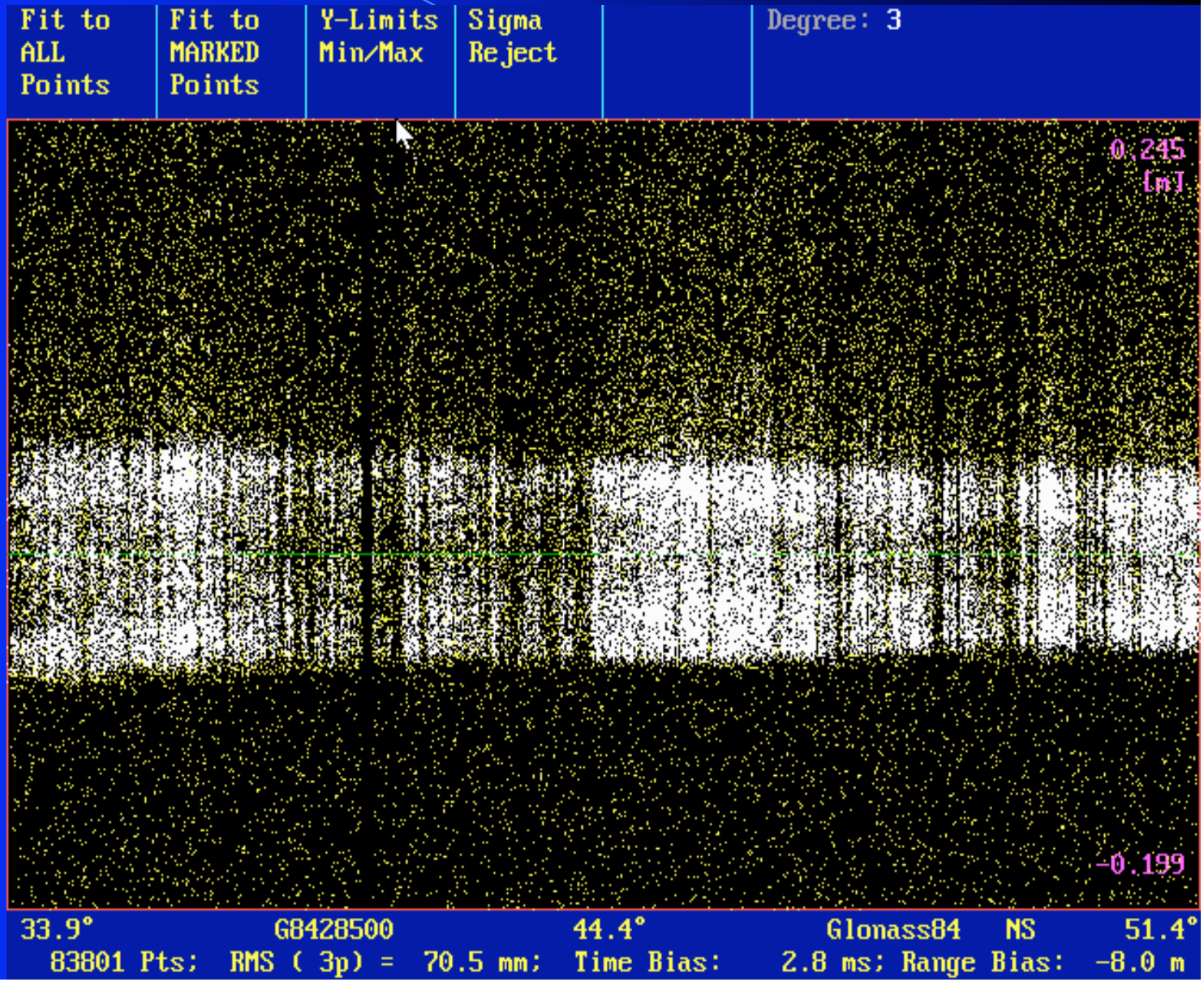

kHz SLR at Graz

TOP 290 01

- Elevation: Down to 10 °
- Post Tracks from Laser
- 778.400 Pts
- 501.000 Rets, 5.4 mm RMS

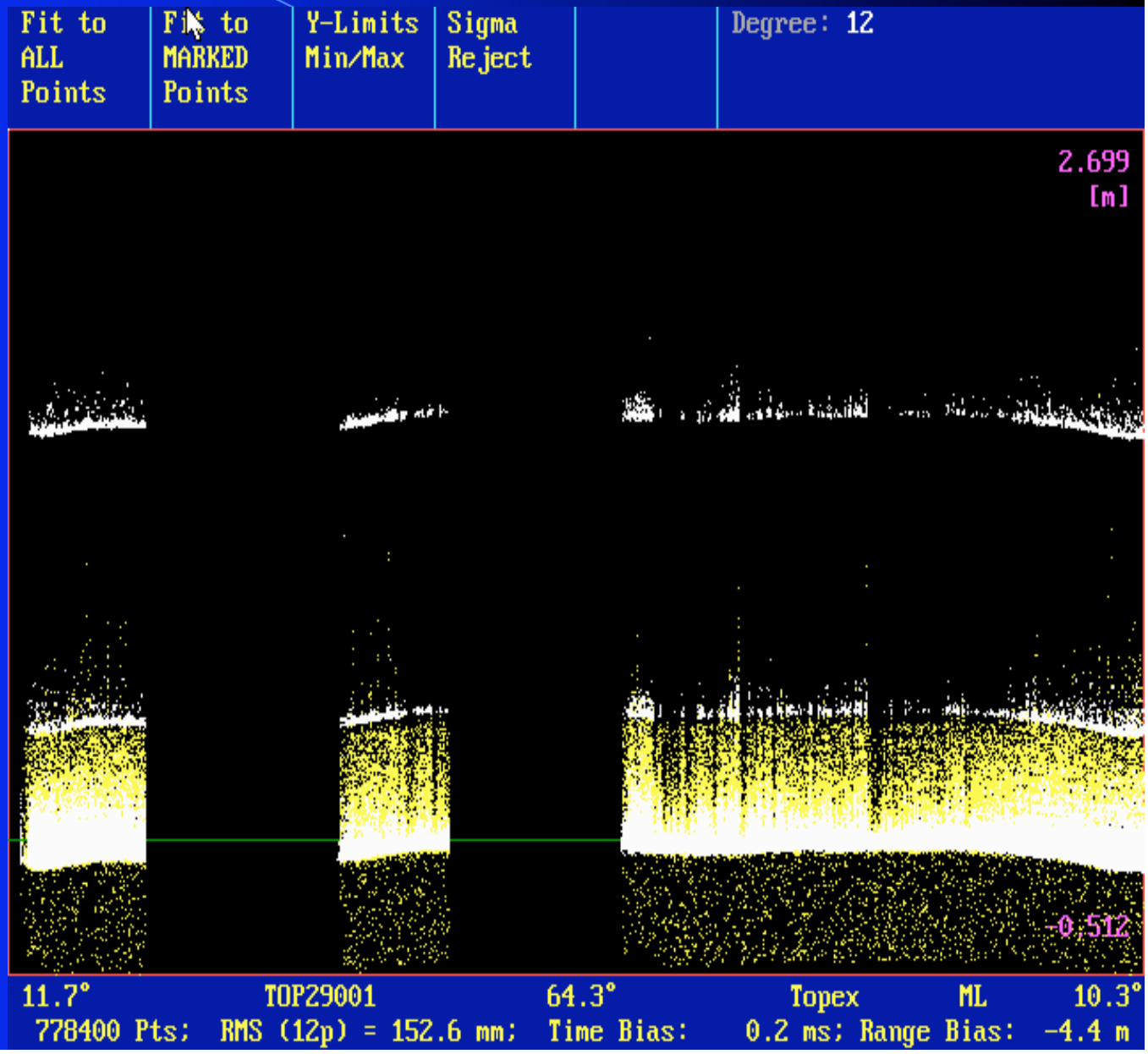

kHz SLR at Graz

TOP 275 11

- Full Daylight
- Low Elev.
  Down to 10°
- Retro Pattern

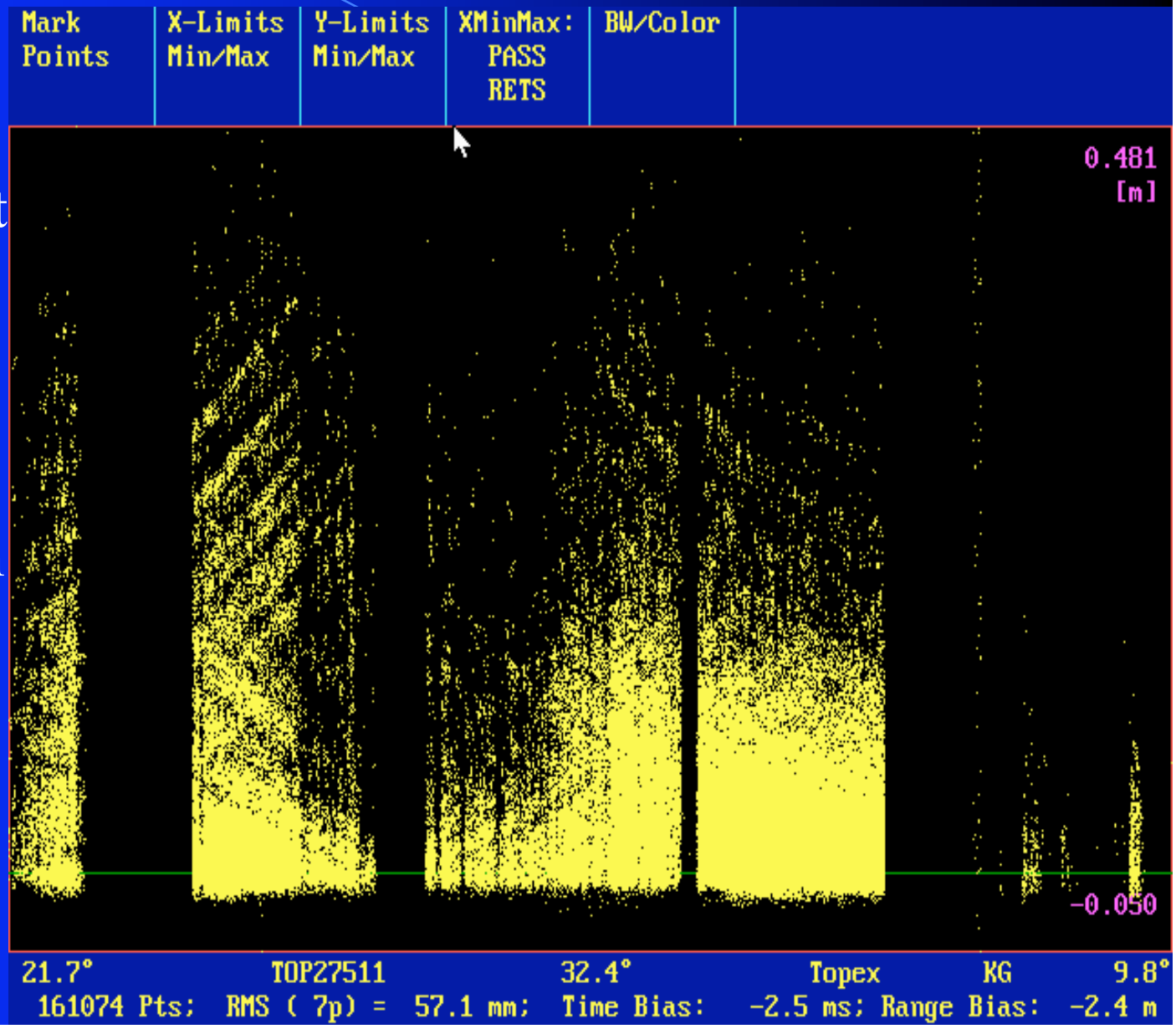

kHz SLR at Graz

TOP 261 18:

- NO Shift of Laser Firing;
- Periodically Noise Increase
- 600 k Pts recorded;
- 424 k Rets remaining

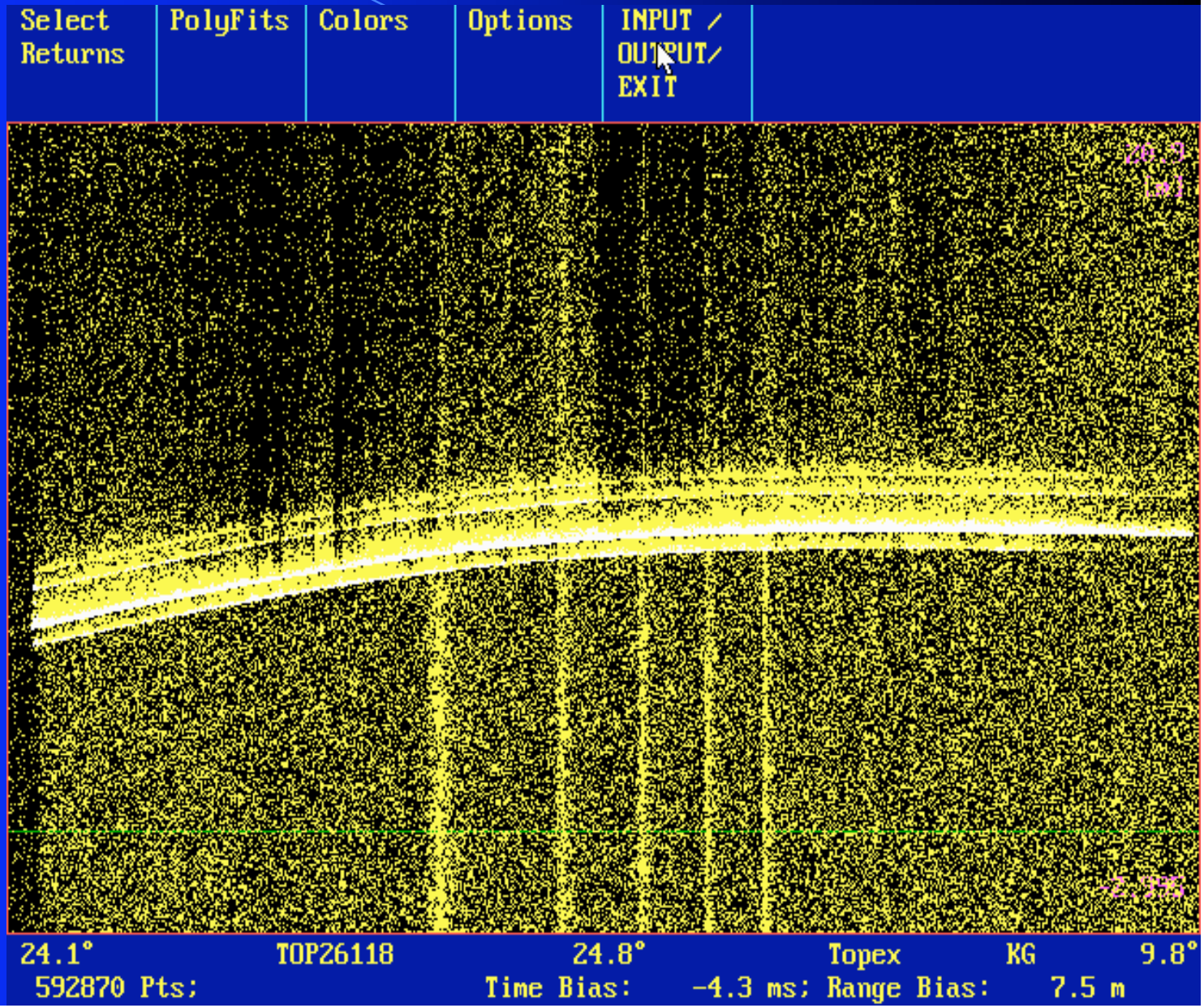

kHz SLR at Graz

TOP 261 18:

- 25° max El;
- Tracked to 10° elevation
- 424 k Rets remaing;
- Traces of Retros
- Only „First“ Track used for NPs

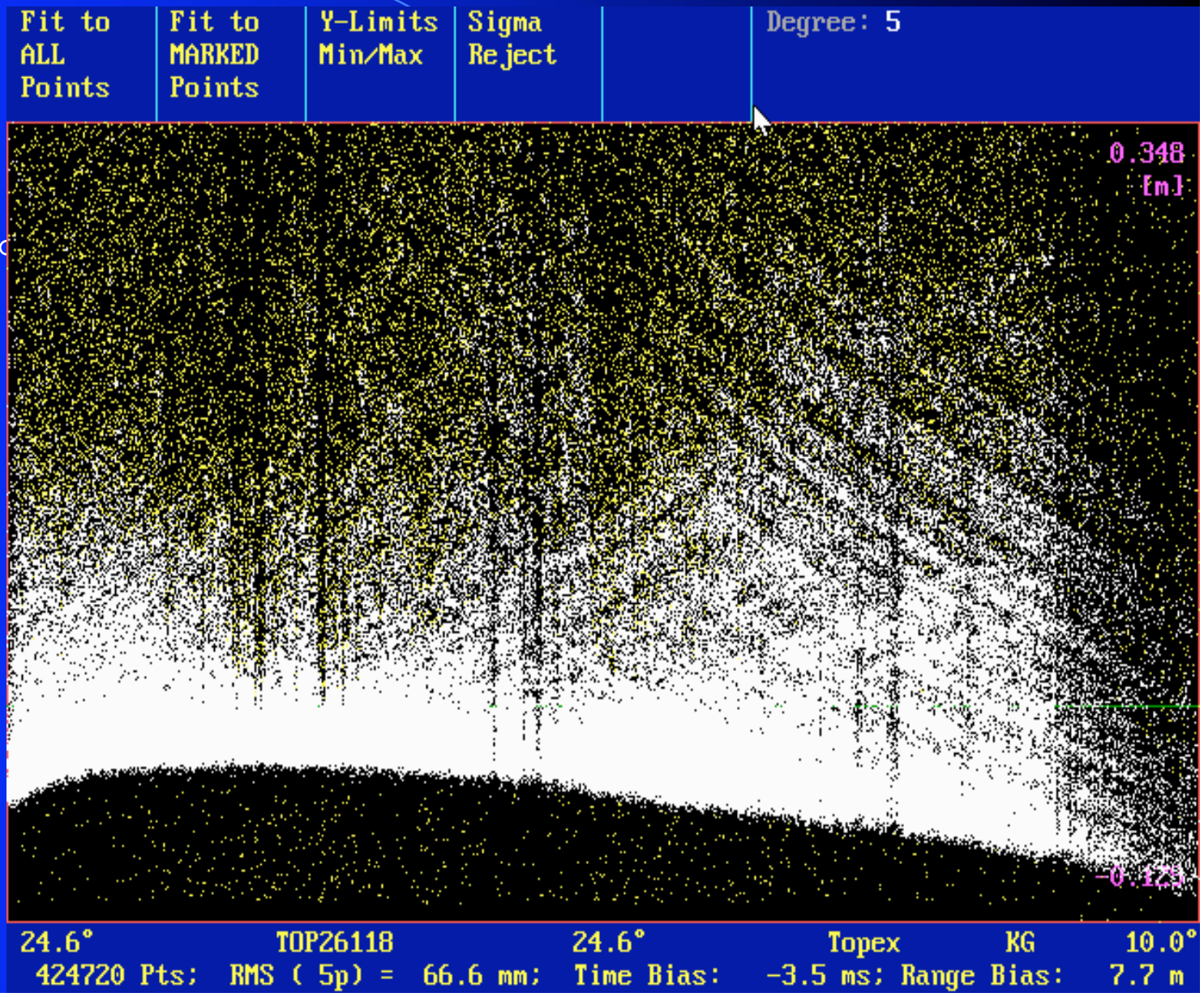

kHz SLR at Graz

kHz Advantages: *OPERATIONAL ITEMS:*

- Tracking and Acquisition: Much faster, easier;
- All Automatic Routines: Faster, better determined, more possibilities:
    - Auto Gate; Auto Track, Auto Time Bias, Auto Search etc.
- Difficult targets: Significantly easier to track !!!
    - GPS, Glonass, ETALONs: MORE Returns (even with 0.4 mJ);
    - Daylight tracking now easier !!!
- DPSSL: Much more stable, more uniform pulses, much less HF noise;
    - No more water leakage problems; no more flash lamp problems,
    - Easier alignments with kHz; etc.

kHz SLR at Graz

kHz Advantages: *Results:*

- NPs: Very High Data Density; from 25 to 5000 Pts/NP average (STA);
- Much higher stability / significantly less NP Jitter
  - Already seen in first LAGEOS passes;
- Accuracy: Single Shot => Similar to 10 Hz Laser; NPs: Much better ...
- Resolution: Does resolve single Retros;
- Calibrations: Much better RMS, better stability:
  - 10.000 returns for standard CAL, within 10 secs (50% Return Rate);
  - Allows fast and easy checks for Skew, Peak minus Mean etc.
  - RMS: 12-14 ps (2 mm)

kHz SLR at Graz

First Insights and Findings:

- Laser Pulse Shifting REQUIRED due to excessive noise in case of overlap with incoming returns;
- Satellite Signature becomes more important:
  - Single Retroreflectors visible on various satellites: TOPEX, ENVISAT, ERS-2, STARLETTE ....
- Inspite of low energy (< 0.4 mJ/Shot):
  - Huge Increase of Data for ALL satellites possible !

kHz SLR at Graz

First Insights and Findings (2):

- LAGEOS: Naturally MOST returns are in SP region; Maximum observed return rate up to now was about 25 %;
  - Even for these „High Return Rate“ Passes, the majority of returns will be Single Photon anyway;
- LEOs: Difficult to maintain SP region reliably;
  - For ERS-2 and similar: MultiPhotons seem to be the much better choice at the moment (low sat signature, no CoM problem, much better statistics etc.);

kHz SLR at Graz

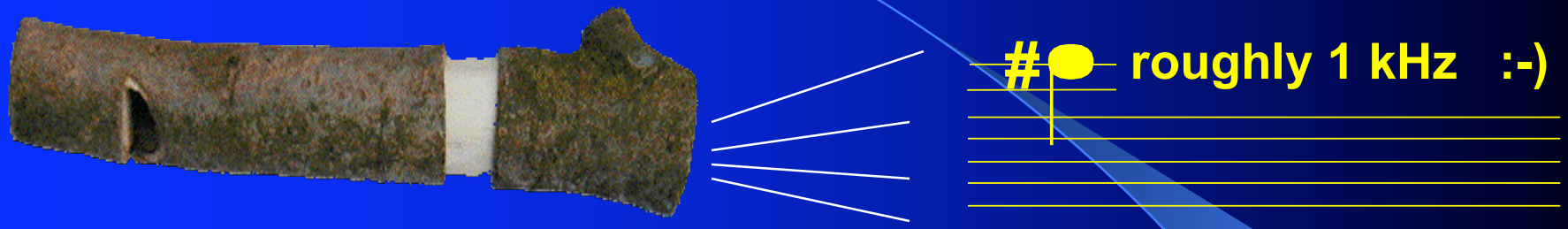

The Graz kHz Laser whistle has started ...

(Now even with 2 kHz ...)

IS kHz the **FUTURE OF SLR ???**

Multi kilo Hertz laser ranging for deep space missions

I.Procházka, K.Hamal, P. Jirousek, M.Kropik

Czech Technical University in Prague,

U. Schreiber

Technical University Munich

presented at

International Laser Ranging Service Meeting, Koetzting, October 28-30, 2003

GOALS

- multi kilo Hertz laser ranging
  for ESA deep space missions (Mercury..)
- laser ranging to non cooperative targets

- ranges 0 → > 1000 km
- range resolution < 1 m / shot (6 cm)
- /deep/ space qualified:
  radiation, heat flux, lifetime..
- photon counting concept
- high repetition rate microlasers

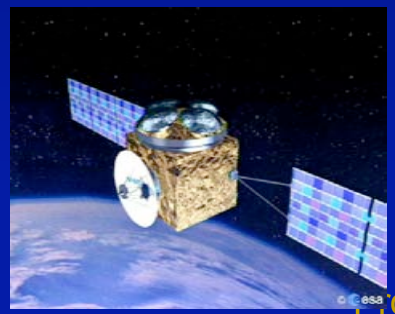

Technology demonstrator

Phase A (2003-2004)

- microlaser “NanoLas”
- 16 kHz , 1 uJ, < 1 ns, 532 nm
- Si SPAD , 40 um, CW
- Modular electronics
  - programmable gate arrays (100 MHz)

- optics - refractive
  - scaled to preserve
    - energy budget
    - high back ground count rate

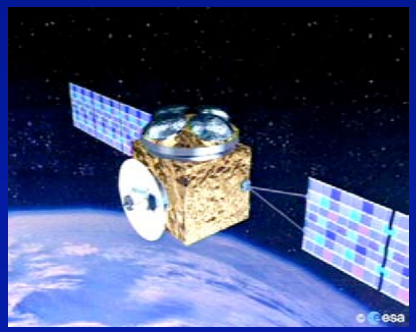

Technology demonstrator
Phase A (2003-2004)

- timing electronics
  - 100 nsec counter
  - 8 bit TDC -> 0.5 nsec resolution

- adaptive range gate
  - gate delay programmed via orbit parameters and terrain profile
  - gate strategy can be modified within the experiment

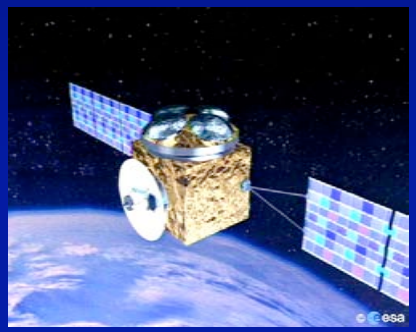

Technology demonstrator
Phase A (2003-2004)

- control electronics
  - Z80 based
  - real time & parallel processing OS
  - range gate position calculation
  - data flow control
  - data accumulation
  - echo signal identification

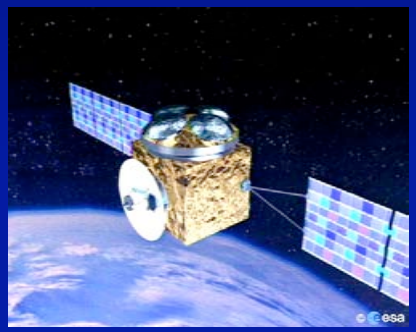

Technology demonstrator milestones

- concept design/decision — Oct. 2003
- budget collection — Oct. 2003
- laser, filter, SPAD — Dec. 2003
- mechanics & optics design — Jan. 2004
- breadboard electronics&control — Dec. 2003
- mechanics and optics — May 2004
- programming — Jan. June 2004
- first echoes — June 2004

Photon-Counting Kilohertz Laser Ranging

John Degnan

Sigma Space Corporation

Lanham, MD 20706 USA

2003 ILRS Workshop, Koetzting, Germany

October 28-31, 2003

Who is building kHz systems?

- **USA**
  - NASA SLR2000 system proposed at 1994 Canberra Workshop
  - Development begun in late 1997
  - Field testing of prototype underway. No satellite ranging attempts yet
  - 2 kHz, 300 psec, 130 μJ transmitter; microchip laser oscillator plus multipass amplifier
- Austria
  - Presented at 2002 Washington DC Workshop
  - Uses existing Graz SLR station
  - 1-2 kHz, 10 psec, 500 μJ transmitter planned; SESAM oscillator plus multiple amplifiers
  - Near 100% return rate from LEO's with 80 μJ at 125 Hz (computer-limited)
- Australia, Japan, and Russia are experimenting with 100 Hz systems

Advantages of kHz Systems

- **Can take advantage of microchip and SESAM laser technologies**
  - Simpler, more compact, and less expensive than modelocked lasers for picosecond pulse generation
  - Transmitter requires fewer amplifiers due to higher oscillator energies (up to tens of μJ for microchips vs nJ for modelocked lasers)
  - No electro-optic pulse selection or high voltages required
- **Increases number of range returns per normal point by about two orders of magnitude**
  - Can improve normal point precision by over an order of magnitude relative to current 5 or 10 Hz systems
  - May allow meaningful two color measurements of differential atmospheric delay using high speed PMT's or SPADS
- **Improves single photon ranging statistics**
  - higher repetition rate compensates for single pulse photon deficit
  - Allows single pulse output flux to be reduced to eyesafe levels thereby eliminating the need for safety observers or aircraft radars
  - Single photon range measurements are free of signal amplitude biases
  - Orbit range residuals can reproduce the impulse response of the overall system (laser, satellite,detector) within a single normal point period

Special requirements of kHz systems

- KHz gating circuits and range gate generators
- Use of event timers rather than time interval units due to multiple pulses in flight
- More sophisticated ranging software required to extract the signal from the background noise and to link the proper return signal to each start pulse and compute the pulse time of flight
- Faster interfaces between the ranging hardware and system CPU
- More aggressive background noise reduction and fast receiver recovery times in the case of photon-counting systems

Computation of normal points from kHz photon-counting data

1. Create station impulse response *h(t-t')* histogram using most recent single cube calibration target data where t is the independently measured roundtrip transit time to the target (tracks changes in system calibration)
2. Convolve cal data with theoretical averaged impulse response of target (relative to the satellite CofM) to form Poisson generating function for each station/satellite combination, i.e.,

$$g(t) = h(t) \quad s(t)$$

3. Maximize convolution integral with the normal point residuals *r(t)* from the nominal orbital fit to compute the displacement of the normal point relative to the fit, i.e.,

$$\Delta t_{opt} = \max\left[r(t) \quad g(t)\right]$$

4. **or** compute centroids for 2 and 3 using current normal point algorithms and difference the results to obtain the displacement.

Impact on ILRS Data System

- The computation of the normal point can be carried out at the stations or by the analysts (TBD)
- The proper satellite center-of-mass correction to be applied by the analysts is the distance between the computed ground system-dependent centroid of *g(t)* and the satellite center of mass plus Δt_{opt}.
- If N is the number of ranges per normal point, the RMS uncertainty in the normal point should be given by

$$RMS_N \approx \frac{RMS[g(t)]}{\sqrt{N}}$$

- To the analyst, normal points from kHz systems should look identical to those from lower rate systems, but we may want to redefine the normal point integration times for each satellite to better support atmospheric modeling studies and multi-wavelength systems.

Example: SLR2000 Ranging to LAGEOS

•There are 240,000 (120 sec x 2 kHz)ranging attempts in a two minute LAGEOS normal point.

• For standard clear atmosphere (visibility = 23 km) and no cloud cover, about 5,000 ranges per normal point (2% return) are expected during acquisition at 20^{o} elevation and rising to a maximum of about 60,000 ranges (25% return) near zenith

•Since RMS of LAGEOS impulse response is about 15 mm, the RMS precision of the centroid (normal point) would have a lower limit of 0.2 mm during acquisition and 0.05 mm near zenith.This calculation ignores any statistical broadening due to the system impulse response or the minimum timing resolution of the receiver.

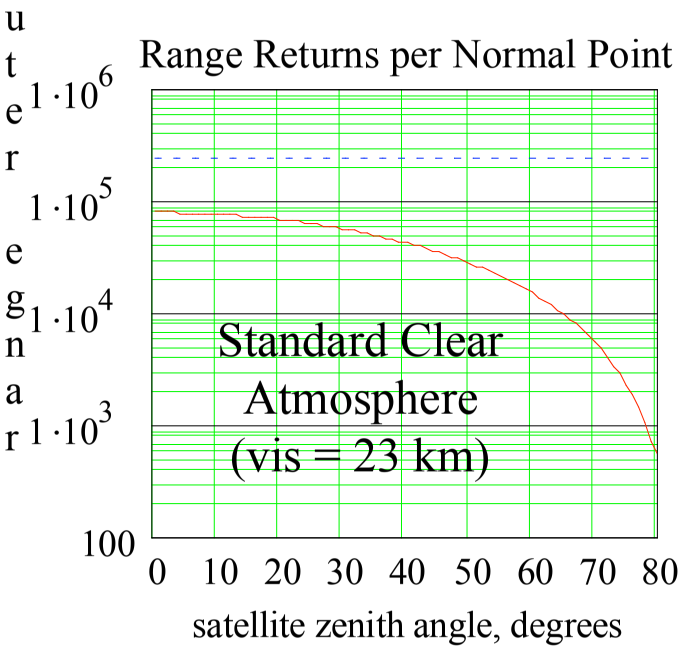

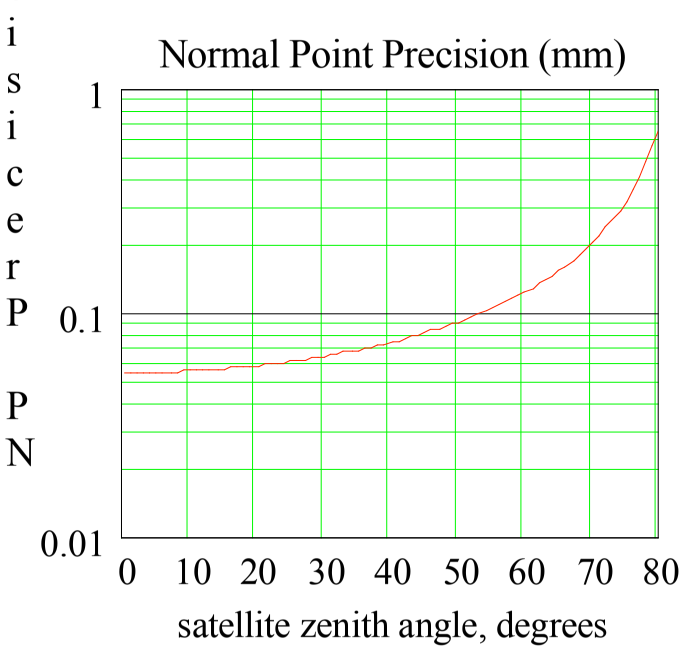

Session 16

SLR 2000

John Degnan

Session 17

Automation

Ben Greene, Werner Gurtner

Automation

Werner Gurtner

Ben Greene

ILRS Workshop
28-31 October 2003
Kötzting

Automation

- What does automation mean?
- What is our experience to date?
- What can we reasonably expect?
- How does this interface with remote control?

What does automation mean?

- Replace manual interaction/intervention by programmed actions (by hard- and software)
- **Prerequisite**: All necessary actions have to be performed either autonomously or under computer control
- Remote control can be first step to automation

Topics for Automation

- Prediction handling (e-mail, ftp, data base)
- Satellite passes (pass lists, ephemerides, observation and calibration schedule, sun interference, horizon mask)
- General power-up of station (e.g., laser)
- Start of tracking: Telescope, laser, dome, electronics, optical components, pass and calibration schedule
- Satellite acquisition (search, signal detection, time bias, range gate/window)
- Track keeping (time bias adjustment, fine tuning of pointing, signal level control)
- Pass interleaving (schedule, realtime adjustment of schedule)
- Stop tracking (telescope, laser, dome, electronics)
- Post-processing (data cleaning, reformating, data submission)
- General power-down of station

Critical Issues

- Weather conditions
  - General — Is it worth to power-up/start the system?
  - Special — Cloud distribution during tracking
  - Adverse — Rain showers during operation
- Satellite acquisition and track keeping
- System failures (hardware, software, power failures)
- Interferences with other on-site activities (maintenance, tests, secondary use of system, room cleaning personell, trespassing, …)
- Remote system checks (Internet, cellular phone)
- Alerts in case of problems (SMS, e-mail, phone calls)

What can we expect?
(Zimmerwald)

- Total of 2361 passes (blue) observed
  (from June to September 2003)
- Maximum of about 4 hours of unattended operation
- Onsite operated: 1840 = 78 %
  - Unknown percentage: Partly automated
  - ***Average number of returns: 516***
- Remotely controlled: 19 = 1 %
- Automated operation: 502 = 21 %
  - Unknown percentage: Remotely or locally supervised
  - ***Average number of returns: 563***

Plenary Session

Mike Pearlman, Werner Gurtner

Website Enhancements

- New navigation scheme with breadcrumbs
- Bulletin Board
- “Best Practices” for Timers and Met Devices
- Strawman template for Satellite CoM
- Website Statistics:
  - http://ilrs.gsfc.nasa.gov/awstats/
- Reorganization of Stations Section including:
  - Phase I of “MyStationPerformance.com”
  - Automatic conversion of site log into HTML
- Completion of the Washington D.C. Laser Workshop website:
  - http://cddisa.gsfc.nasa.gov/lw13/lw_proceedings.html

Future Enhancements

- Phase II of “MyStationPerformance.com”
  - Range and time bias analysis
- Redesign of the Satellite Missions pages
  - “MyMission.com”
    - Data volume by mission
  - Satellite Center of Mass Corrections
- Redesign of Web Forms
- Conformance with new NASA Web Site requirements for Look and Feel

Active ILRS Map

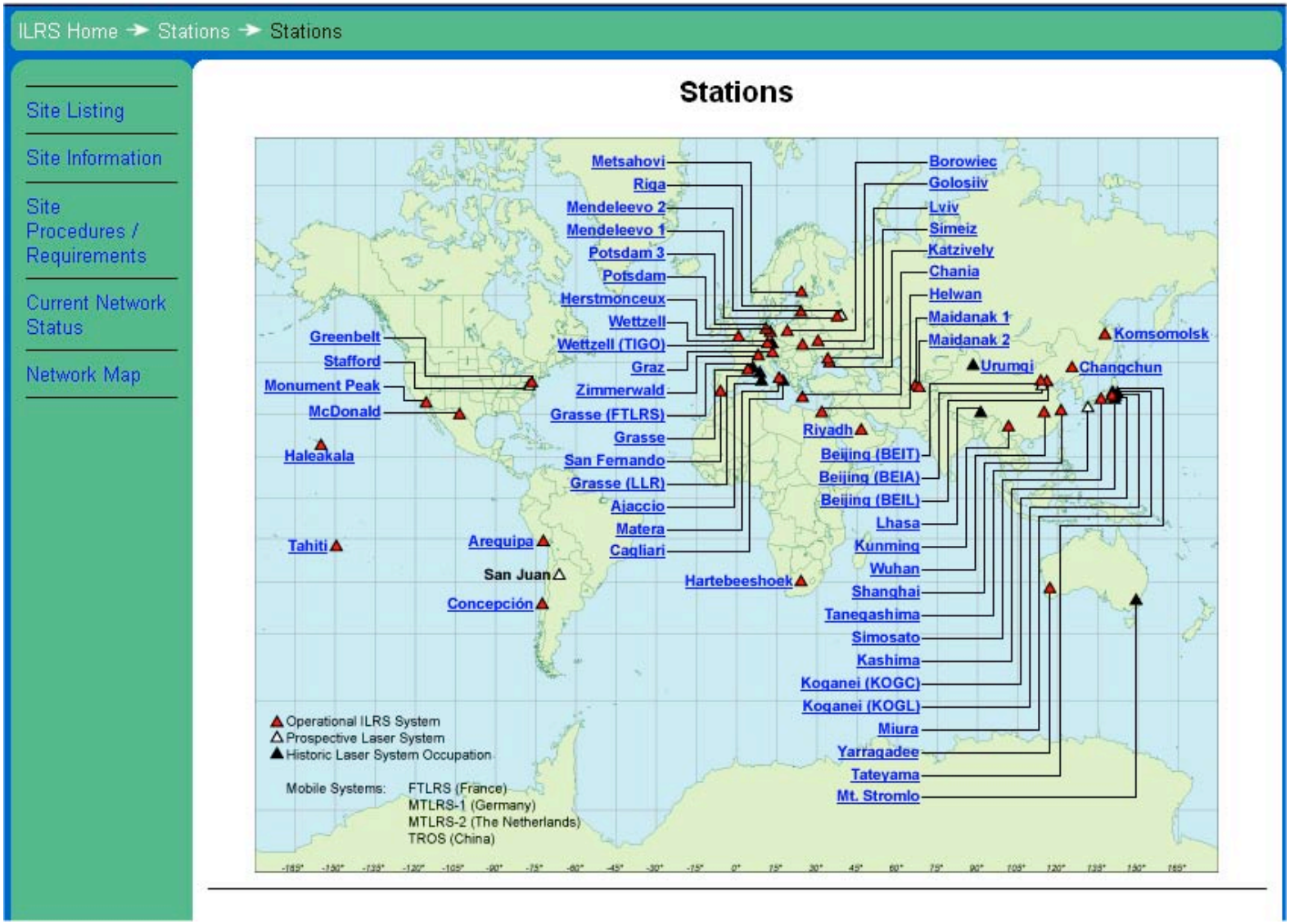

- The concept of “MyStationPerformance.com” was introduced in October, 2002
- Phase 1 was completed and deployed at: http://ilrs.gsfc.nasa.gov/stations/

Sample of a Typical Station's Page

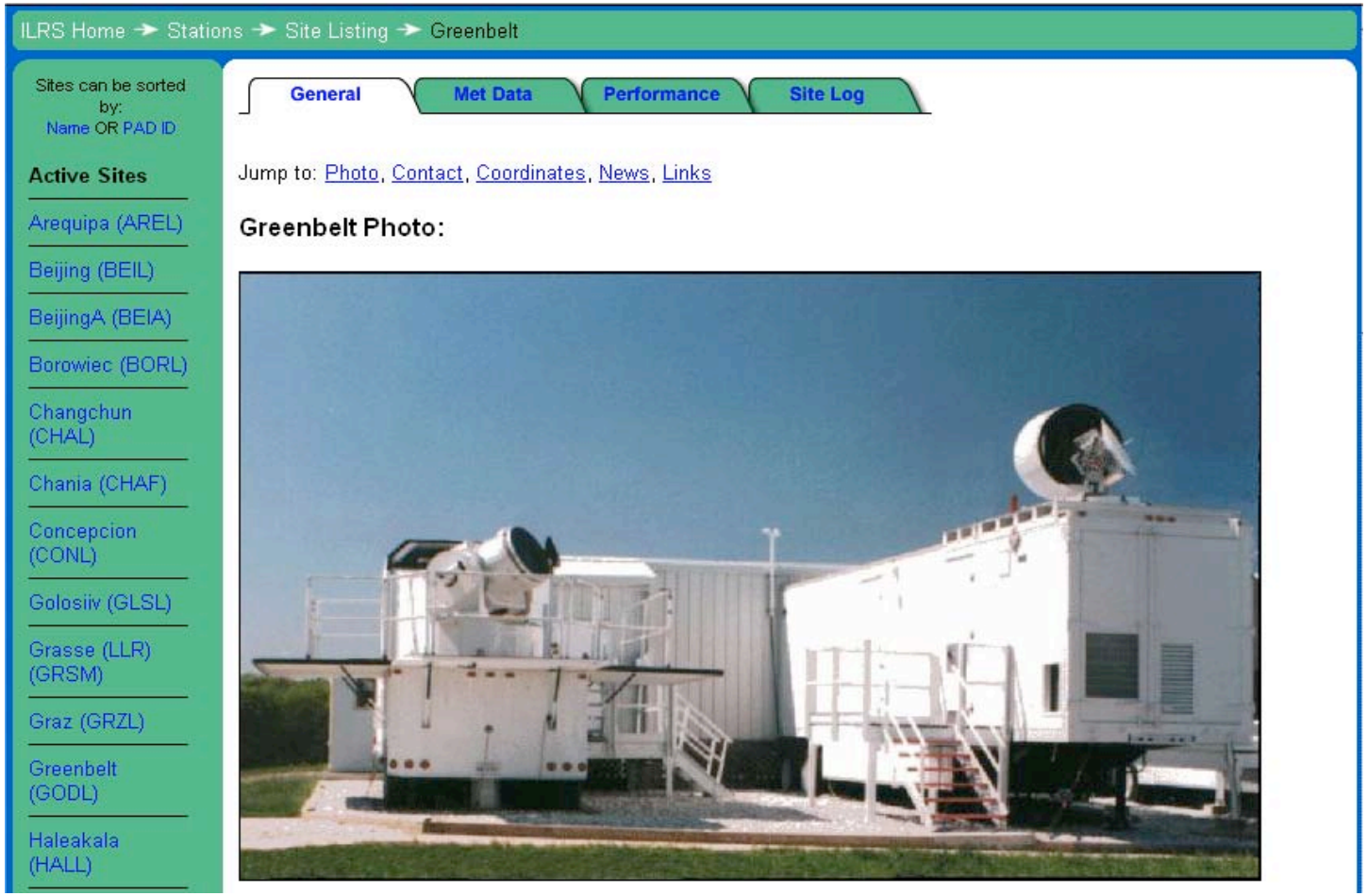

- Each station has its own page, the page has a tabulator navigation that will display various information about the site.
- The "General" tab displays information such as site contacts, news, approximate positions, photo. This information comes from the site log, so please keep your logs current.
- The left navigation will allow you to access other stations in the ILRS network. This navigation can be sorted by station name or PAD ID

Sample of a Typical Station Local Events

Mt. Stromlo News:

Local Events:

Date	2003-01-18
Event	Fire storm
Additional Information	SLR station destroyed along with GPS, Doris and Glonass monitoring equipment. Monuments STR0 and STR1 not detroyed but will require re-furbishment and re-survey once the site is re-established.
Date	2003-07-04
Event	Facility replacement begins
Additional Information	The Australian Government, through Geoscience Australia (formerly AUSLIG) signed a contract with EOS Space Systems Pty Limited (EOS) to rebuild the Stromlo SLR facility.
Date	2003-09-09
Event	Operation of facility
Additional Information	Another contract signed with EOS Space Systems Pty Limited (EOS) for the operation and maintenance of the Geoscience Australia facilty. The building is already completed awaiting the installation of the dome, telescope and laser. Engineering data is expected to be available in December 2003, with full operational status in early 2004.

- Station's News consists of Local Events taken from the site log as well as SLRMail messages.

Sample of a Typical SLRMail Messages as Station News

Zimmerwald:

SLRMail Messages:

Date	Subject
Thu Dec 19 16:00:02 MET 1996	New SLR System in Zimmerwald
Mon Jul 28 18:00:03 MET DST 1997	ZIMLAT range bias
Fri Sep 12 09:00:02 MET DST 1997	ZIMLAT 7810: Range and Time Biases
Tue Jul 21 13:00:03 MET DST 1998	Zimmerwald down
Thu Jan 21 18:00:01 MET 1999	1 ns range bias of Zimmerwald 7810
Thu Jan 21 19:00:02 MET 1999	Remark to SLRMAIL No.229
Thu Sep 28 01:20:00 CEST 2000	Zimmerwald Web Page
Wed Jan 10 16:20:00 CET 2001	Status of Zimmerwald SLR Station
Fri May 10 14:57:14 CEST 2002	ZIML 7810: Passes of April 25/26 replaced
Fri May 31 08:42:02 CEST 2002	Zimmerwald Range Bias Removed
Thu Aug 15 12:09:57 CEST 2002	Dual-wavelength data from Zimmerwald
Tue Sep 17 18:06:07 CEST 2002	Zimmerwald out of operation (mirror recoating)
Tue Nov 12 17:26:10 CET 2002	Zimmerwald: Operational again
Tue Mar 11 18:35:17 CET 2003	Zimmerwald: Switch to CSPAD
Mon May 5 14:27:07 CEST 2003	Zimmerwald: Change in Minimum Elevation
Mon May 5 14:27:07 CEST 2003	Zimmerwald Range Bias on 03 May 2003
Wed Jul 9 16:30:45 CEST 2003	Zimmerwald: Two-wavelengths observations restarted
Tue Sep 9 18:12:08 CEST 2003	7810 ZIML Range Bias 23/24-08-2003
Wed Oct 1 09:31:39 CEST 2003	7810 ZIML: System down: Laser damaged
Mon Oct 6 13:13:18 CEST 2003	7810 ZIML: Operation resumed, IR only

- On August 25, 2003, the ILRS adopted a standardized subject line for all station-related SLRMail messages.

Sample of a Typical Station's Meteorological Data

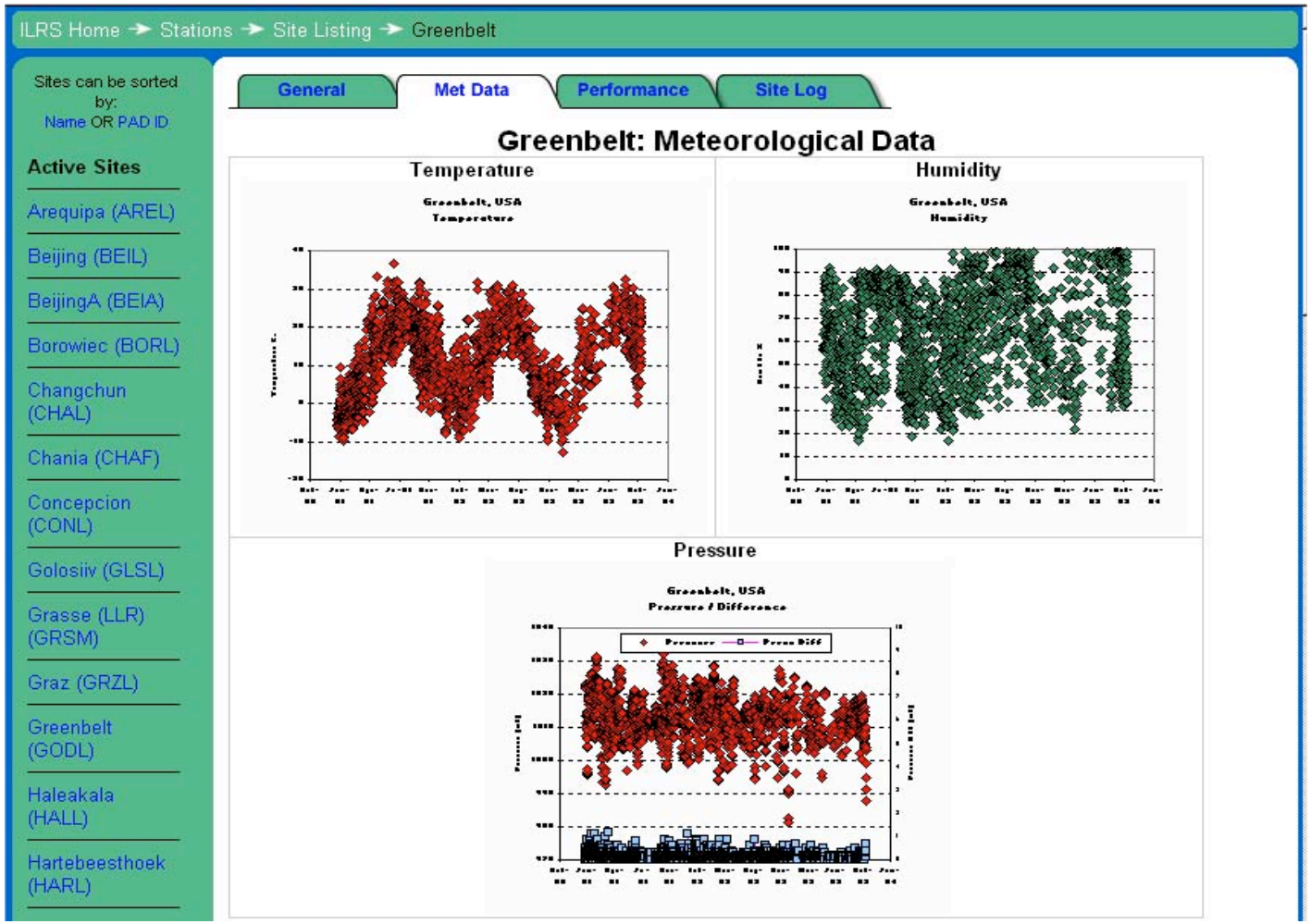

- The "Met Data" tab displays the temperature, humidity and pressure of the site.
- Click any one of these thumbnails, the actual chart will be displayed.

Sample of a Typical Station's Performance

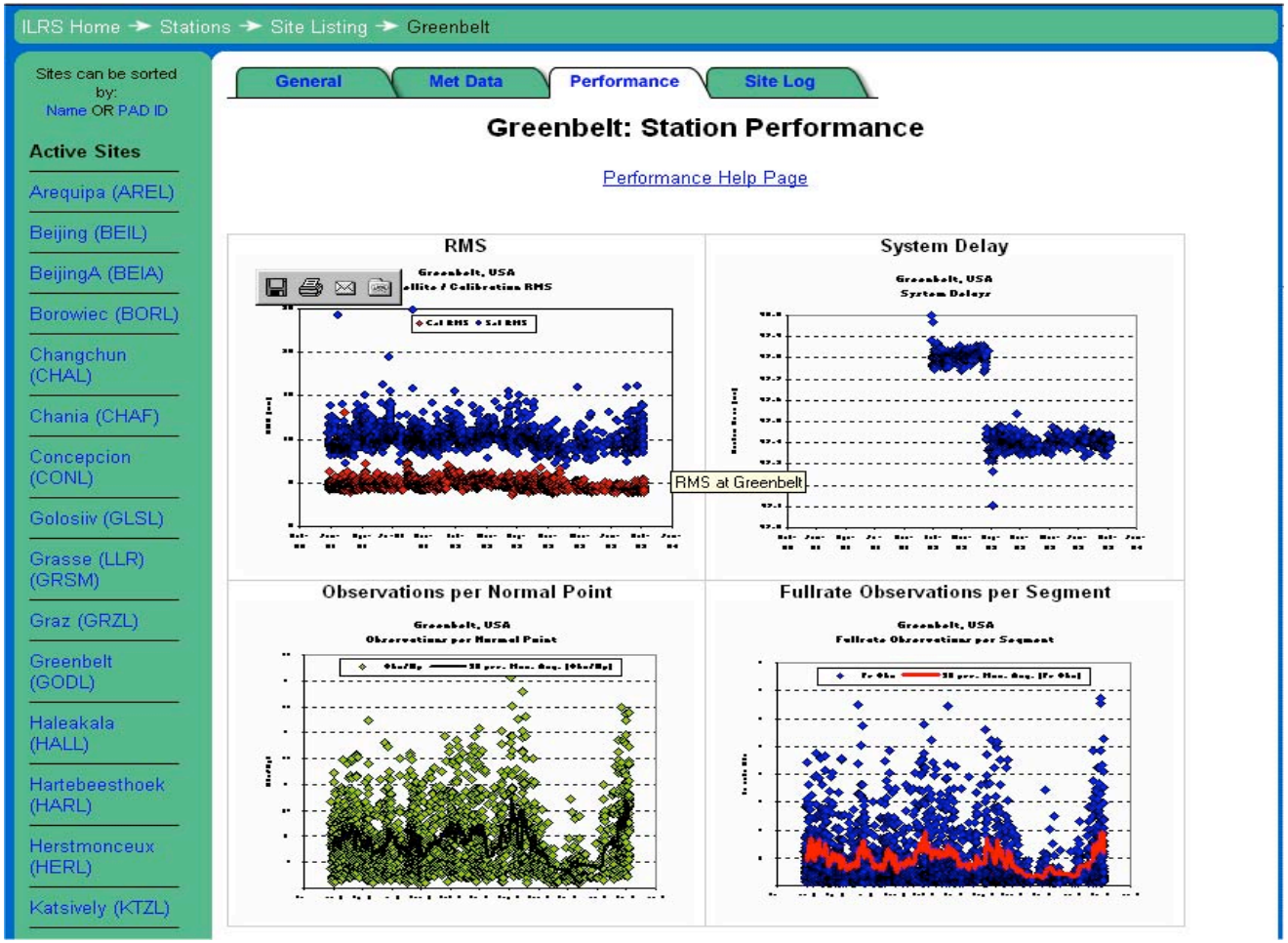

- The "Performance" tab displays the RMS, System Delay, Observation per Normal Point, Fullrate Observation per Segment.

Sample of a Typical Station's Site Log

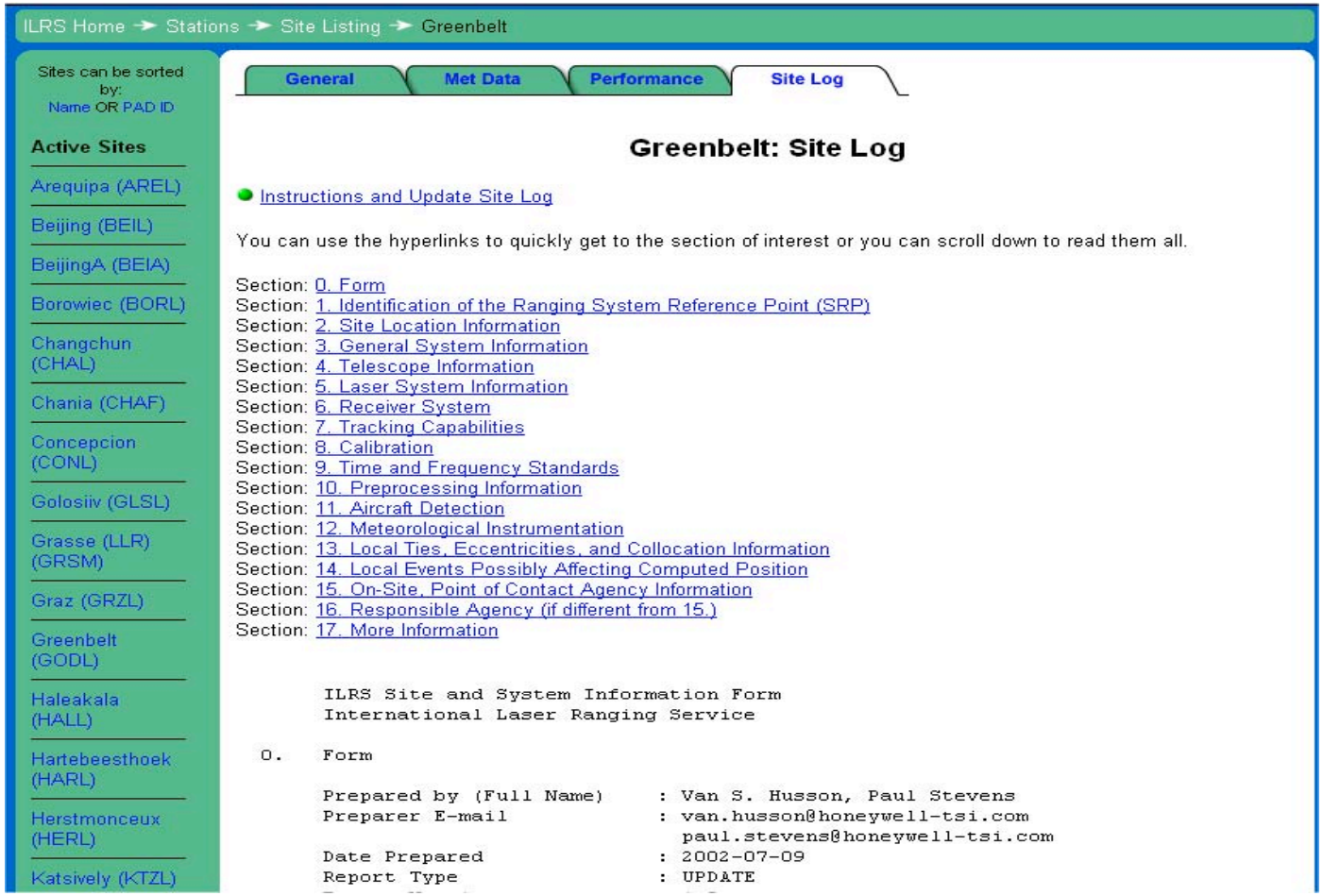

The "Site Log" tab displays the station's site log. The sections of the site log have been indexed for quick and easy access. Instructions on how to update the site log is also included.

Access Your Station's Page

To access your station's page, please bookmark the appropriate urls below:

http://ilrs.gsfc.nasa.gov/stations/sitelist/AJAF.html
http://ilrs.gsfc.nasa.gov/stations/sitelist/AREL.html
http://ilrs.gsfc.nasa.gov/stations/sitelist/BEIA.html
http://ilrs.gsfc.nasa.gov/stations/sitelist/BEIL.html
http://ilrs.gsfc.nasa.gov/stations/sitelist/BEIT.html
http://ilrs.gsfc.nasa.gov/stations/sitelist/BORL.html
http://ilrs.gsfc.nasa.gov/stations/sitelist/CGLL.html
http://ilrs.gsfc.nasa.gov/stations/sitelist/CHAF.html
http://ilrs.gsfc.nasa.gov/stations/sitelist/CHAL.html
http://ilrs.gsfc.nasa.gov/stations/sitelist/CONL.html
http://ilrs.gsfc.nasa.gov/stations/sitelist/GLSL.html
http://ilrs.gsfc.nasa.gov/stations/sitelist/GMSL.html
http://ilrs.gsfc.nasa.gov/stations/sitelist/GODG.html
http://ilrs.gsfc.nasa.gov/stations/sitelist/GODL.html
http://ilrs.gsfc.nasa.gov/stations/sitelist/GRSF.html
http://ilrs.gsfc.nasa.gov/stations/sitelist/GRSL.html
http://ilrs.gsfc.nasa.gov/stations/sitelist/GRSM.html
http://ilrs.gsfc.nasa.gov/stations/sitelist/GRZL.html
http://ilrs.gsfc.nasa.gov/stations/sitelist/HALL.html
http://ilrs.gsfc.nasa.gov/stations/sitelist/HARL.html
http://ilrs.gsfc.nasa.gov/stations/sitelist/HERL.html
http://ilrs.gsfc.nasa.gov/stations/sitelist/HLWL.html
http://ilrs.gsfc.nasa.gov/stations/sitelist/KASL.html
http://ilrs.gsfc.nasa.gov/stations/sitelist/KOGC.html
http://ilrs.gsfc.nasa.gov/stations/sitelist/KOGL.html
http://ilrs.gsfc.nasa.gov/stations/sitelist/KOML.html
http://ilrs.gsfc.nasa.gov/stations/sitelist/KTZL.html
http://ilrs.gsfc.nasa.gov/stations/sitelist/KUNL.html
http://ilrs.gsfc.nasa.gov/stations/sitelist/LHAL.html
http://ilrs.gsfc.nasa.gov/stations/sitelist/LVIL.html
http://ilrs.gsfc.nasa.gov/stations/sitelist/MAID.html
http://ilrs.gsfc.nasa.gov/stations/sitelist/MAIL.html
http://ilrs.gsfc.nasa.gov/stations/sitelist/MATL.html
http://ilrs.gsfc.nasa.gov/stations/sitelist/MATM.html
http://ilrs.gsfc.nasa.gov/stations/sitelist/MDOL.html
http://ilrs.gsfc.nasa.gov/stations/sitelist/MDVL.html
http://ilrs.gsfc.nasa.gov/stations/sitelist/MDVS.html
http://ilrs.gsfc.nasa.gov/stations/sitelist/METL.html
http://ilrs.gsfc.nasa.gov/stations/sitelist/MIUL.html
http://ilrs.gsfc.nasa.gov/stations/sitelist/MONL.html
http://ilrs.gsfc.nasa.gov/stations/sitelist/ORRL.html
http://ilrs.gsfc.nasa.gov/stations/sitelist/POT3.html
http://ilrs.gsfc.nasa.gov/stations/sitelist/POTL.html
http://ilrs.gsfc.nasa.gov/stations/sitelist/RIGL.html
http://ilrs.gsfc.nasa.gov/stations/sitelist/RIYL.html
http://ilrs.gsfc.nasa.gov/stations/sitelist/SFEL.html
http://ilrs.gsfc.nasa.gov/stations/sitelist/SHAL.html
http://ilrs.gsfc.nasa.gov/stations/sitelist/SIML.html
http://ilrs.gsfc.nasa.gov/stations/sitelist/SISL.html
http://ilrs.gsfc.nasa.gov/stations/sitelist/SNTL.html
http://ilrs.gsfc.nasa.gov/stations/sitelist/STAL.html
http://ilrs.gsfc.nasa.gov/stations/sitelist/STRL.html
http://ilrs.gsfc.nasa.gov/stations/sitelist/TATL.html
http://ilrs.gsfc.nasa.gov/stations/sitelist/THTL.html
http://ilrs.gsfc.nasa.gov/stations/sitelist/URUL.html
http://ilrs.gsfc.nasa.gov/stations/sitelist/WETL.html
http://ilrs.gsfc.nasa.gov/stations/sitelist/WETT.html
http://ilrs.gsfc.nasa.gov/stations/sitelist/WUH0.html
http://ilrs.gsfc.nasa.gov/stations/sitelist/WUHL.html
http://ilrs.gsfc.nasa.gov/stations/sitelist/YARL.html
http://ilrs.gsfc.nasa.gov/stations/sitelist/ZIML.html

Phase 2 of "MyStationPerformance.com"

Phase 2 requirements have been drafted. These requirements include:

1. Three new categories: Pass-by-Pass, Seasonal, and Aggregated – Seasonal will be added to the "Met Data" tab.
2. Five categories: Quantity, Precision, Accuracy, Latency, and Current Report Card will be added to the "Performance" tab.

We encourage to access your station's page and send us feedback and suggestions so that we can incorporate them in Phase 2.

Time of Flight Devices

SR620

HP5370B

Latvain Univ. A013a

Latvain Univ. A031

PESO Consulting PET

EOS MRCS

HTSI ET

TOF Devices Manufacture Specifications

Below is a table of TOF devices specifications, which are currently is use by the ILRS network (the most recent models in use are shown). The breakdown of TOF devices in the ILRS network as of October 2002, based on site log information, are presented in a pie chart. The specification below were taken from operation manuals or workshop papers (see references). For detailed specifications and best practices, please use the hyperlinks on the left.

Manufacturer	Current Model	Year	Approach	Resolution (ps)	Jitter (Ps)	Linearity (Ps)	Stability [Ps/K]	Stability [Ps/hour]	Max. repetition rate	Max. TOF (Secs)
SR	620	1988	Interval	4	22	50	5		100	1000
HP	5370B	1982	Interval	20	35	20			10	10
Latvian Univ.	A013a	2002	Interval	10	20	2		2	80	0.209
Ortec	TD811	<1980	Event	100			40			N.A.
PESO Cons.	PET4/TIGO	1999	Event	1.2	3.5	3	<0.3	<0.5	>100	NA
EOS	MRCS V.4	1998	Event	2	10	1		1	1000	NA
HTSI	MLRO	1998	Event	0.5	<2			0.5	2000	NA
Latvian Univ.	A031-ET	2003	Event	1	10.8	<1	0.1	0.5	1000	NA

Notes: HP spun-off its test, measurement and monitoring device business into Agilent Technologies. HTSI was formerly Allied Signal Technical Services (ATSC)

TOF Device Best Practices

Related links: SR620 best practices

Below are the BEST practices that are general and applicable to any time of flight device (time interval count or event timer) used for SLR/LLR applications:

1. **Signal integrity:**
    a. Use only high-quality cables and connectors.
    b. Take great care with shielding and grounding (earthing) in order to make sure that all noise sources are minimized.
2. **External frequency ("Clock source"):**
    a. Supply each timer with a separate, high quality 5 or 10 MHz sine wave;
    b. Make sure that the timer is set up to take an external "clock source"
3. **Power supply:**
    a. Never switch off. If the timer has been switched off for any reason, allow adequate warm up before any operational use. Please refer to the manufacturer's operations manual for more information.
    b. Use a stable mains voltage supply (for this and many other instruments it is useful to monitor the mains voltage regularly and warn when it falls).
    c. Use a transient suppressor to prevent voltage "spikes" reaching the timer.
4. **Environmental Control:**
    a. Maintain a stable working environment around the timer.
    b. Keeping the temperature constant is particularly important.
    c. Monitoring the temperatures of air at the timer air inlet and air outlet will give quick feedback of potential problems;
    d. Maintain a good airflow around and through the instrument.
    e. Be aware that nearby air-conditioning units, cycling on and off, can substantially alter the temperature of the air in the vicinity of the timer, even in a supposedly temperature stabilized room.
5. **Non-linearity/timer calibration:**
    a. For picosecond event timers perform optical calibration as recommended by the manufacturer.
    b. For time interval counters, either cluster the time interval units to help "average" non-linearities or calibrate each device versus a picosecond event timer and model any errors in data processing.
6. **Jitter**:
    a. Monitor the jitter of the timer at least monthly.

ILRS Bulletin Board

ILRS Home → ILRS Home

- What's New
- About the ILRS
- Contact ILRS
- Data & Products
- Engineering & Technology
- Links
- Links to Plug-ins
- Publications
- Satellite Missions
- Science & Analysis
- Search
- Stations
- Website Map
- Working Groups

Satellite laser ranging (brochure and animation) uses lasers to measure ranges from ground stations to satellite borne retro-reflectors to the millimeter level. The primary mission of the ILRS as stated in the organization's Terms of Reference is "*to support, through satellite and lunar laser tracking data and related products, geodetic and geophysical research activities.*"

If you have a suggestion or complaint about our service, please send an email to the ILRS CB Secretary.

ILRS Bulletins

Here is an alternate view of the ILRS Bulletins

3rd Quarter 2003 Performance Report Card is available on-line.

Center of Mass Correction Template

SLR SatelliteCventer-of-Mass Offset Information

SLR Satellite Center-of-Mass Offset Information

LRA Center-of-Mass Offset description

Satellite	Size of Array	Reflectors	spacecraft body fixed coordinates of the reflector center (mm)	spacecraft coordinate definition	CoM details
ADEOS-1	35.6 cm edge hollow cube	1	xx	yy	
ADEOS-2	16 cm diameter hemisphere	9	xx	yy	
AJISAI	214 cm diameter sphere	1,436	1010	sphere	details
ERS2	20 cm diameter hemisphere	9	(1000, -710, -1010)	X-axis direction of satellite pitch, Z-axis away from nadir	
ETALON 1 & 2	129.4 cm diameter sphere	2,134	576	sphere	details
GFO1	hemisphere	9	(-245, -764, -493)	Y axis anti-parallel with velocity	
GFZ1	20 cm diameter sphere	60	58.5	sphere	details tbd
GLONASS	120x120 cm square array	396	151	yy	
GPS 35 and 36	23.9x19.4 cm square array	32	220	yy	
LAGEOS-1	60 cm diameter sphere	426	251	sphere	details
LAGEOS-2	60 cm diameter sphere	426	251	sphere	details
TOPEX/Poseidon	150 cm diameter annulus	192	(1064, 419, 825)*	X-axis in direction of velocity, Z-axis nadir	function of s/c station geometry

Washington DC Laser Ranging Workshop Website

13th International Workshop on Laser Ranging
"Toward Millimeter Accuracy"

Instructions for preparations of papers for the proceedings from the Thirteenth International Workshop on Laser Ranging are available. **Reminder:** Papers for these proceedings were due **DECEMBER 31, 2002.**

The workshop proceedings are sorted by session:

- Scientific Achievements, Applications, and Future Requirements
- Laser Technology Development
- Improved or Upgraded Systems - Poster Session
- Timing Devices
- Detectors and Optical Chain Components
- Automation and Control Systems
- Lunar Laser Ranging
- Station Performance Evaluation
- System Calibration Techniques
- Station Operational Issues
- Target Design, Signatures, and Biases
- Atmospheric Correction and Multiwavelength Ranging
- Advanced Systems and Techniques
- Surveying Primer (splinter session presentation by Jim Long)

Phase II: Met. Data

Chart Set#1	Chart Set#2	Chart Set#3
Phase I	Phase II	Phase II
(Current)	(New)	(New & Default)
Pass-by-Pass	**Seasonal**	**Aggregate OMCs**
Pressure	Pressure	Pressure
Temperature	Temperature	Temperature
Humidity	Humidity	Humidity

New Met. Charts for Phase II

Seasonal

Aggregate OMCs

Pressure

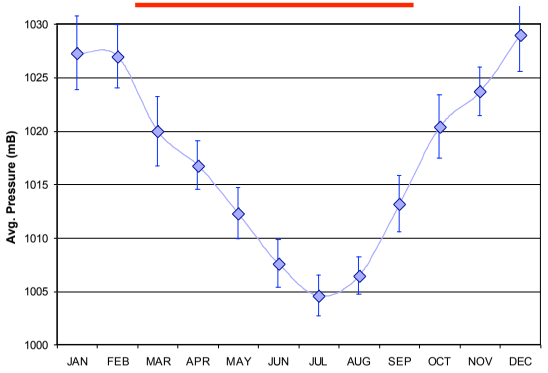

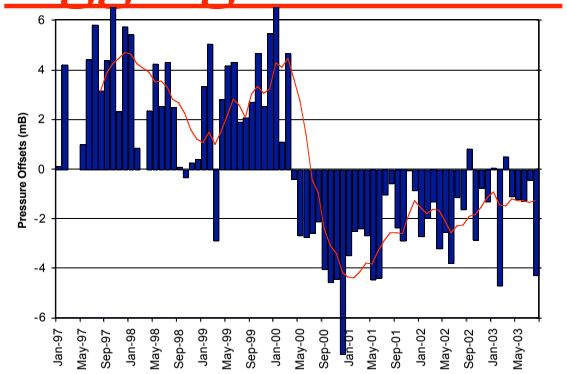

Temperature

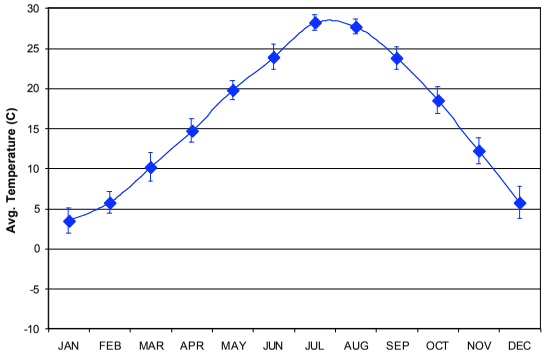

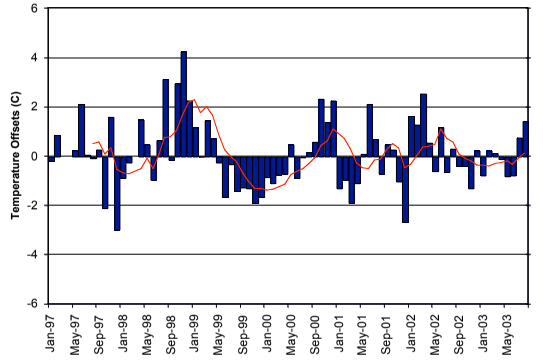

Humidity

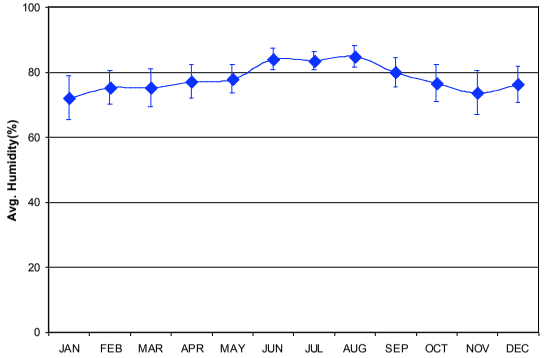

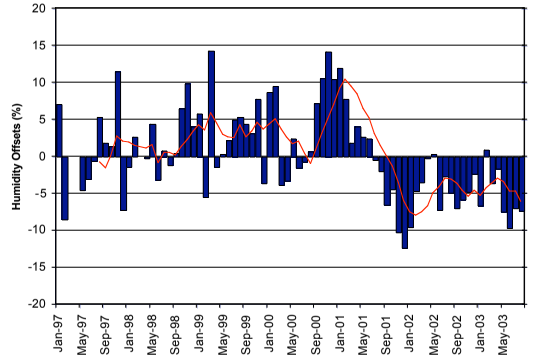

New Data Quantity Performance Charts for Phase II

LAGEOS Passes

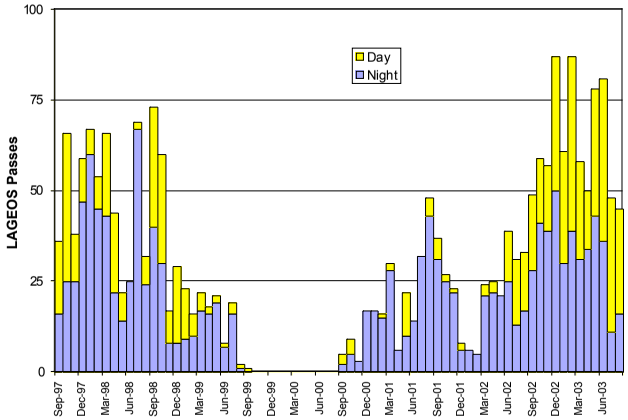

LAGEOS Return Rate

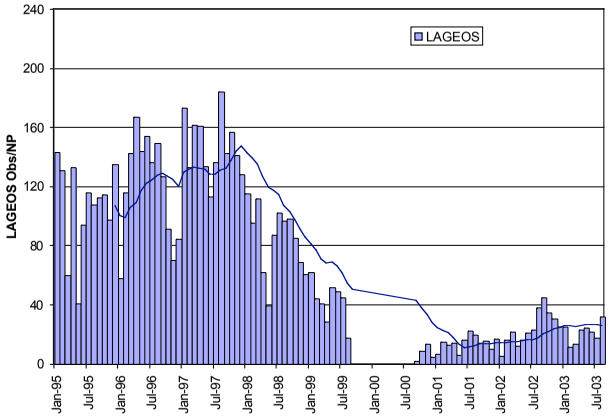

Total NPs

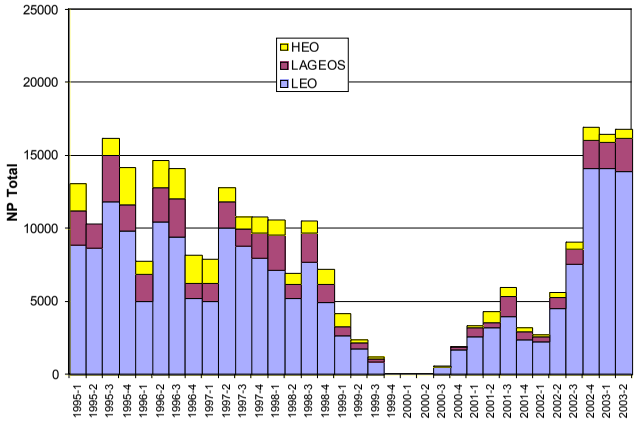

Ajisai Return Rate

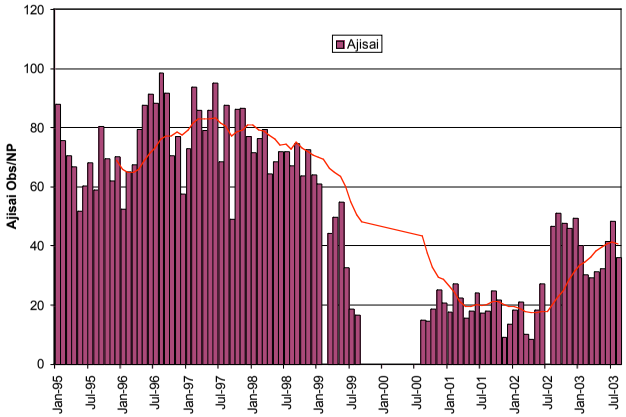

Critical ILRS Site Log Developments

All Global Site Logs Now Available from ILRS Web Site

- All System Site Logs now easily downloadable for review & updates.
- Available and accessed through individual station's ILRS URL.
  - http://ilrs.gsfc.nasa.gov/stations/
- Condensed instructions to facilitate understanding and rapid completion.

Increasing expectations from the ILRS CB to have accurate and current Site Logs available for use.

Responsibilities to maintain and update Site Logs when configurations and environments dictate, is that of each participating ILRS Station.

International Laser Ranging Service

ILRS Data Analysis Survey

ILRS Central Bureau
NASA GSFC, Greenbelt, MD USA
cb@ilrs.gsfc.nasa.gov

2003 ILRS Data Analysis Survey

1. What general areas of study are underway at your center that rely on laser ranging data?
2. Which targets are you currently using in your analysis work?
3. What are your applications for each target?
   - Artificial Satellites
     - Earth Orientation (EOP)
     - Reference Frame (GM, Earth center of mass)
     - Gravity Field (static and time varying)
     - Tides
     - Comparison with other techniques
     - Improved orbit development
     - Station position/motion
     - POD (mission specific)
     - Q/C of stations
     - Spacecraft models
     - Gravitational physics tests, relativity
     - Other
   - Lunar Reflectors
     - Lunar rotation
     - Lunar composition
     - Lunar Love numbers
     - Excitation of librations
     - Precise solar system ephemerides
     - Other
4. Are you receiving sufficient data volume?
5. Are you receiving sufficient data coverage?
6. Are the data of sufficient accuracy for your applications?
7. What other satellites do you plan to use in the future?
8. What do you need that you are not getting?
9. How do you access the data (CDDIS, EDC, etc)? Is it easy?
10. What other comments or suggestions do you have regarding the ILRS data?

Analysis Center Responses

- Sent to Analysis and Associate Analysis Center in July 2003
- Received 21 responses (total of 28 ACs and AACs)
- SLR Analysis Centers
  - DUT/DEOS (Netherlands)
  - U. Texas/CSR (USA)
- SLR Associate Analysis Centers
  - ASI (ITALY)
  - BKG (Germany)
  - CLG/BAS (Poland)
  - CODE (Switzerland)
  - CRL (Japan)
  - DGFI (Germany)
  - ESA/ESOC (Germany)
  - FFI (Finland)
  - GA (Australia)
  - GFZ (Germany)
  - GSFC/RITSS (USA)
  - IPA (Russia)
  - NASDA (Japan)
  - NERC (UK)
  - Newcastle (UK)
  - OCA/CERGA (France)
  - Shanghai (China)
- LLR Analysis Centers
  - IfE/FESG (Germany)
  - JPL (USA)
- No Responses
  - GAOUA (Russia)
  - Graz (Austria)
  - IA (Russia)
  - IMVP (Russia)
  - MCC (Russia)
  - Paris LLR (France)
  - U. Texas LLR (USA)

Areas of Investigation

Artificial Satellites

- Science
  - Reference Frame (GM, Earth CoM)
  - Earth Orientation Parameters (EOP)
  - Gravity Field (static and time varying)
  - Tides
  - Station position/motion and deformation
  - Gravitational physics tests, relativity
  - Atmospheric density
  - Time transfer
- Orbit
  - Improved orbit modeling
  - Mission-specific POD
  - Calibration/validation of altimetry
- Engineering
  - Q/C of stations
  - Comparison with other techniques
  - Spacecraft models
  - Refraction models

Areas of Investigation

Lunar Reflectors

- Lunar rotation
- Lunar composition, properties of core
- Lunar tides: Love numbers and tidal Qs
- Precise solar system ephemerides
- Excitation of free librations
- Lunar reference frame and reflector positions
- Lunar moments of inertial and gravitational harmonics
- Gravitational physics tests: relativity, equivalence principle, dG/dt
- Astronomical constants: obliquity, GM (Earth+moon)
- Tidal dissipation

Areas of Investigation

Artificial Satellites

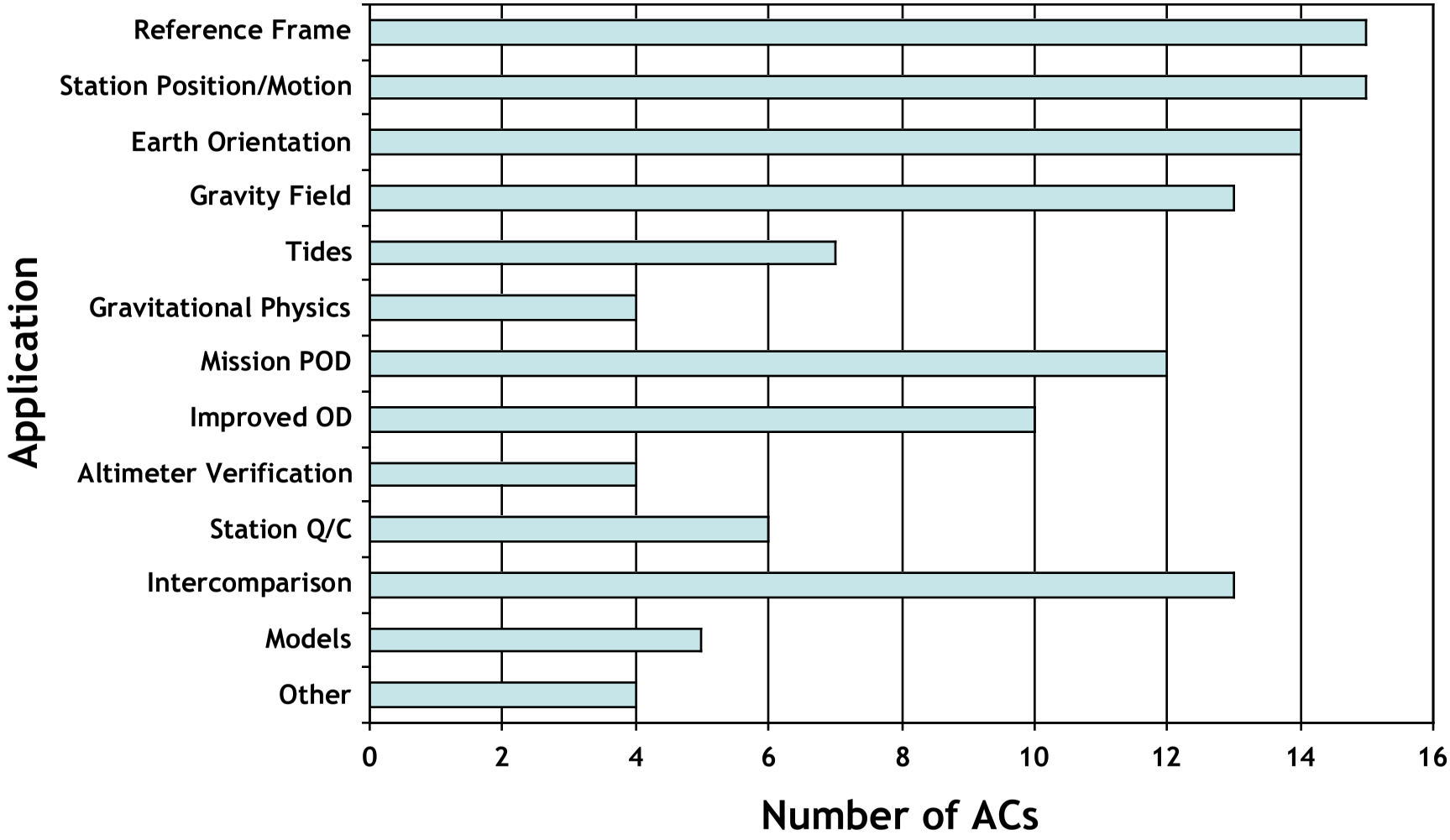

Other includes atmospheric density, global deformations of Earth's crust, time evolution of EOP, relativity.

Areas of Investigation

Lunar Reflectors

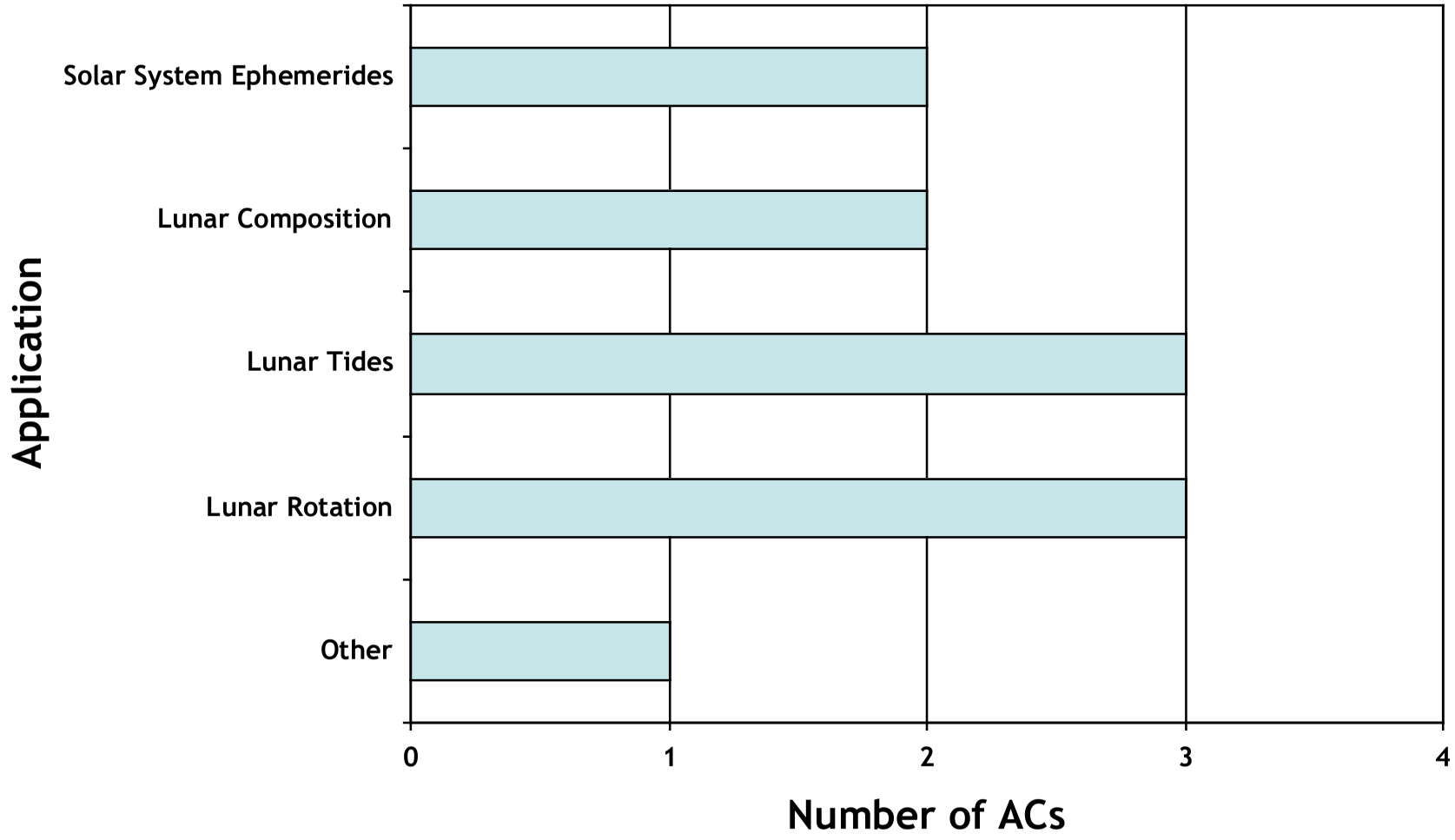

Other includes lunar reference frame and reflector positions, lunar moments of inertial and gravitational harmonics, gravitational physics tests, astronomical constants, tidal dissipation

Satellite Usage

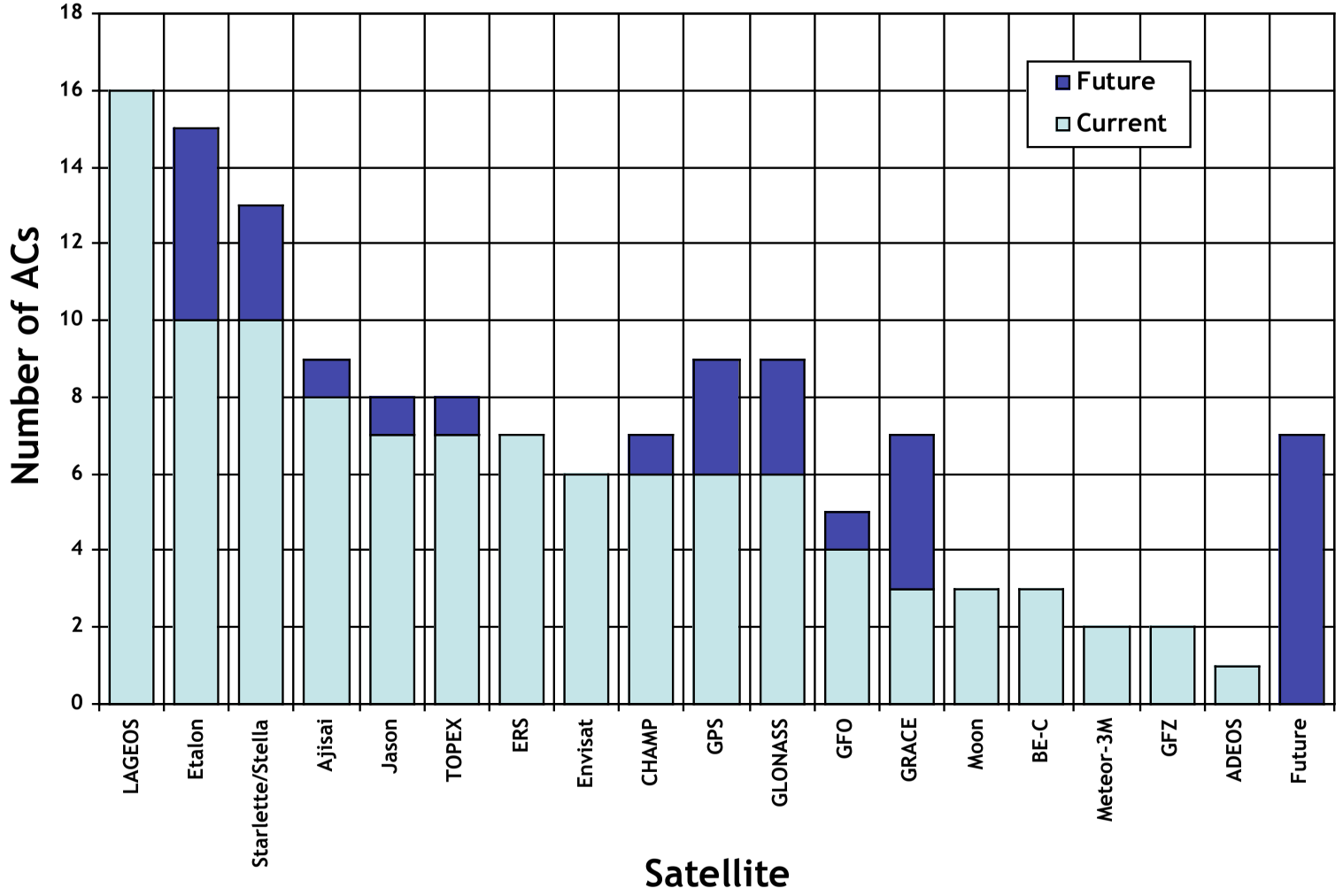

Questionnaire Responses
(SLR)

- Data volume
  - Generally, sufficient data (but could always be larger)
  - Dependent on satellite and region
  - Adequate LAGEOS
  - Need more tracking on Jason-1, GRACE, Etalon
  - Too much ERS tracking
  - Data volume sufficient for long-term analysis but not for short-term resolution of EOP
- Data coverage
  - Generally, sufficient (but could always be better)
  - Need more SLR stations colocated with VLBI
  - Pacific and Southern Hemisphere coverage not sufficient; more data from Arequipa; more data from inland areas (e.g., Maidanak)
  - Use mobile systems to increase coverage

Other Questionnaire Responses

(SLR, continued)

- Data accuracy
  - Generally, sufficient (but could always be better)
  - Quality of data from core stations is sufficient; other stations are downweighted
- New requirements
  - Site coordinates (in ITRF2000) and eccentricities need to be updated and distributed
  - Accurate site ties to VLBI and/or GPS
  - Regular submission of SINEX files by Acs (more complete info)
  - Access to historical info on range and timing bias by station
  - Better data distribution in space and time
  - Special issues of scientific journals on SLR (e.g., JGR, etc.)
- Data access
  - Access through CDDIS or EDC works fine
  - DCs should use same directory structure and post data with same file naming conventions

Other Questionnaire Responses

(SLR, continued)

- Suggestions and comments
  - Generate summaries of logfiles on a daily basis
  - Edited NPT data
  - CoM correction information and instruction on use
  - Modify NPT format to accommodate CoM, station parameters
  - Consistent file naming through the years
  - Create yearly NPT data files
  - Proper SINEX formats from ACs
  - Clarify corrected data in data files vs. use of data corrections file
  - Faster data delivery to data centers/users
  - Don't modify SLR format unless VERY necessary
  - Create new working group on use of mobile systems
  - Identify SLR R&D issues of the future
  - New applications of SLR for calibration of time transfer from Earth to space
  - ILRS is doing a good job!

Questionnaire Responses
(LLR)

- Data volume
  - Insufficient data on small lunar reflectors
- Data coverage
  - Insufficient LLR data and from small lunar reflectors in particular
  - Need more LLR-capable stations in the southern hemisphere
- Suggestions and comments
  - Push LLR as well as SLR analysis

ILRS E-Mail Exploders

- Currently:
  - In August 2003, excessive spam and virus-infected messages forced suspension of ILRS e-mail exploders at CDDIS
  - ILRS e-mail exploders (with the exception of *ilrspred* and *urgent*) continue to be operated through host ilrs.gsfc.nasa.gov (i.e., CDDIS)
  - CB personnel review all incoming e-mail prior to distribution (except for predictions and urgent email)
  - Only legitimate e-mail is distributed to ILRS associates
  - New procedure prevents the distribution of spam
  - *ilrspred* and *urgent* are operated (and not "moderated") through EDC
- Future Plans:
  - Investigate alternatives to moderated email:
    - majordomo or listserv software at CDDIS
    - Filtering software (e.g., Challenge/Response Spam Filtering)
  - Any modifications must wait for new CDDIS Linux server operations (mid-2004)

SLR Data Resupply Policy

- Data can be resupplied by stations within 30 days of the date of the data
- Data centers will replace these data in the on-line archive
- Replacement data older than 30 days should not be forwarded to operations centers
- E-mail should be issued about data older than 30 days detailing the problem and supplying the correction information
- Problem data older than 30 days will NOT be removed from the archives
- CB will maintain webpages with data problem/correction information
- Stations must ensure the release flag in the normal point data is updated if data are resupplied
- Should there be a mechanism for deleting bad data?

14th International Workshop on Laser Ranging

- San Fernando, Spain
- June, 7-11, 2004
- AWG meeting to be held before workshop
- ILRS General Assembly and Working Group Meetings to be held during week of workshop
- Preliminary Organizing Committee formed:
  - Jose Martin Davila, Jorge Garate, John Degnan, Michael Pearlman, Carey Noll, Peter Shelus (?), Francis Pierron, Stanislaw Schillak, Ulli Schreiber, Yang Fumin, Ben Greene (?)

14th International Workshop on Laser Ranging
Prelminary Agenda

- Monday
  - Scientific Achievements, Applications, and Future Requirements
- Tuesday
  - Laser Technology Development
  - Improved or Upgraded Systems
  - Timing Devices
  - Detectors and Optical Chain Components
  - Automation and Control Systems
- Wednesday
  - Lunar Laser Ranging
  - Station Performance Evaluation
  - System Calibration Techniques
  - Station Operational Issues
- Thursday
  - Target Design, Signatures, and Biases
  - Atmospheric Correction and Multiwavelength Ranging
  - Advanced Systems and Techniques
- Friday
  - ILRS General Assembly
  - Workshop Summary/Resolutions/Closure

Information on ALOS: Dynamic Priorities for satellite with time-restricted observation:

- ADEOS-II ceased operation at the end of October, because of a malfunction in power-system.
- ALOS (Advanced Land Observing Satellite) will be launched next June.
- As with ADEOS-II, ALOS has sensitive sensors to be protected from optical damage
  Differences from ADEOS-II
  - Small interference area (its duration is from 5 to 10 seconds) => we need precise prediction
  - Plural interference area => station is required to perform a complex operation (see slides in appendix)
- The operational procedure for the safety of the satellite is based on ADEOS-II and was proposed by JAXA.
- Station operates based on the time table which lists permitted period, distributed by JAXA and reported to JAXA actual operation time (laser start and stop time) and/or full-rate data.
- GB requests that JAXA organize a preparatory experiment for station qualification where before the campaign starts stations shall track a current satellite (such as Ajisai) with time-restricted operation as proposed by JAXA.

ALOS Overview

ALOS carries two optical sensors, PRISM and AVNIR-2.

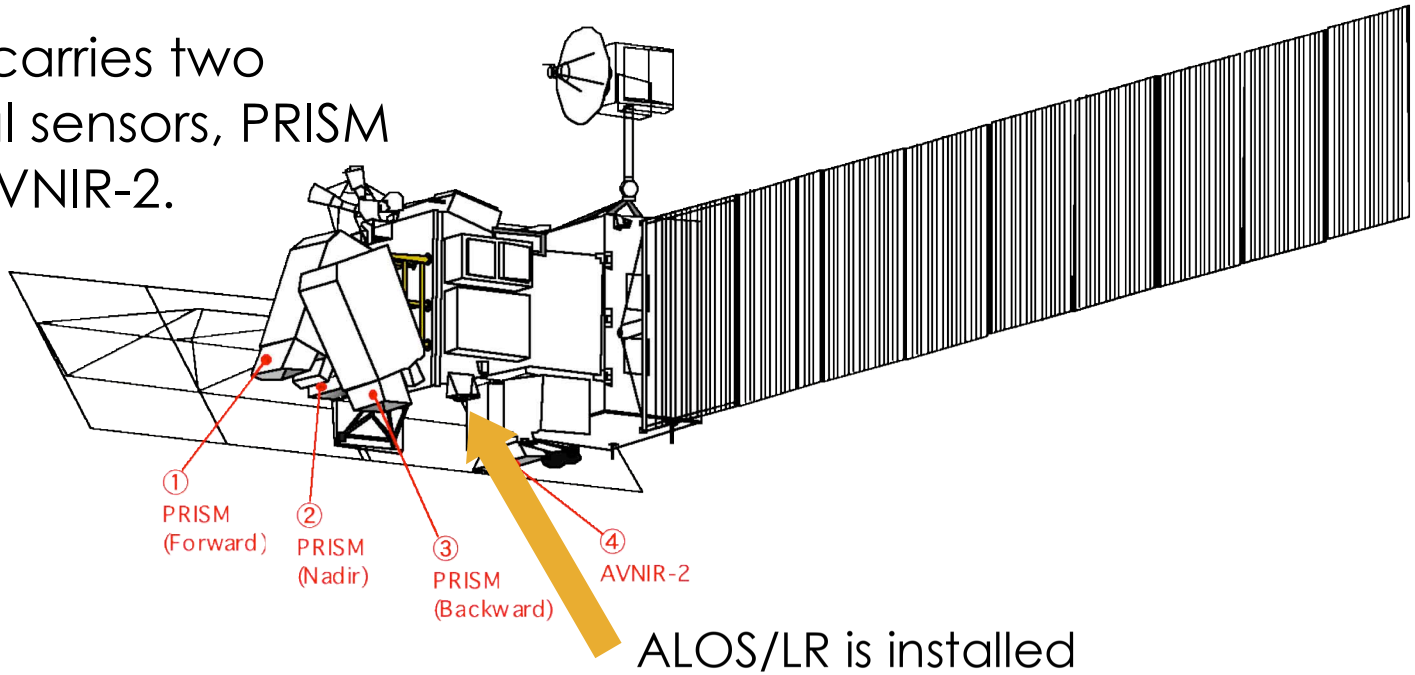

ALOS/LR is installed

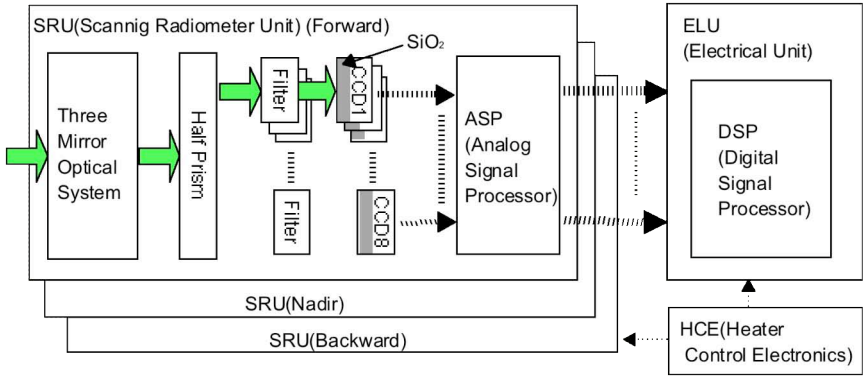

PRISM Block diagram

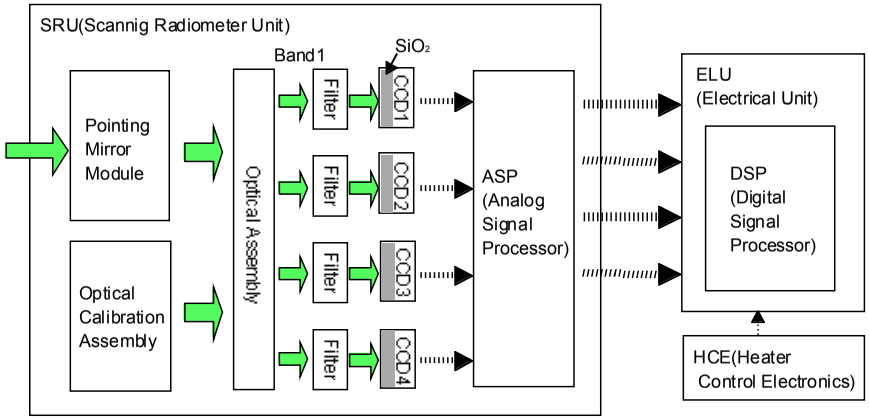

AVNIR-2 Block diagram

Restricted Area of ALOS

The characteristic of restricted area
- The view restriction domain is narrow than ADEOS-II
- Plural areas are existing

---> We need precise restriction information for ALOS operation.
---> It was required complicated conditions to SLR operation for SLR

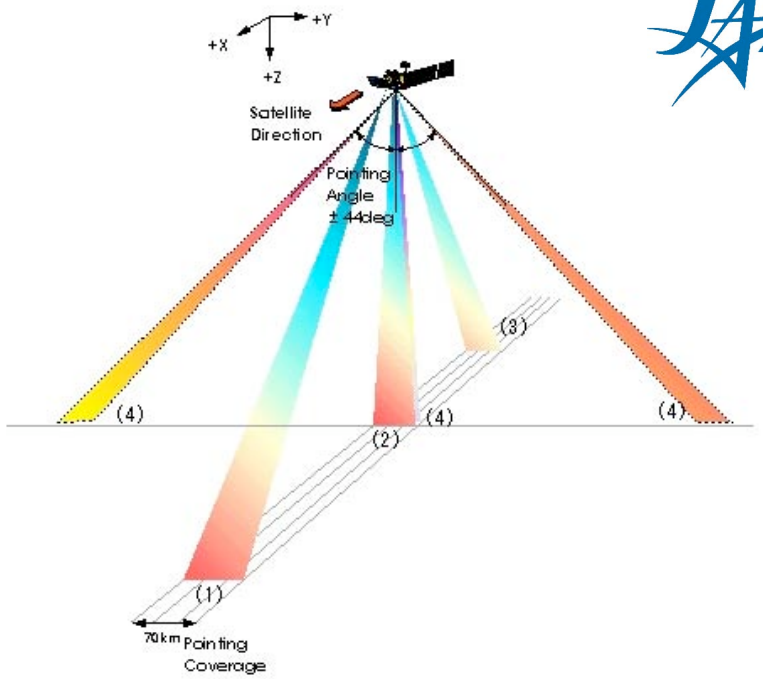

Each number indicated in Figure equivalent to meet restrictions of each sensor.
(1),(2) and (3) shows the transmitting restriction area by PRISM sensor and (4) is a transmitting restriction area by AVNIR-2. PRISM sensor consists of three components in order to acquire 3D geometric information. Therefore, the restriction area has separated into three. On the other hand, AVNIR-2 carries out its observation with +/- 44 degrees scan width. Above of a figure is +X axis as an advance satellite direction.
Therefore, SLR station must be controlled its Laser transmission precisely in order to satisfy this conditions.

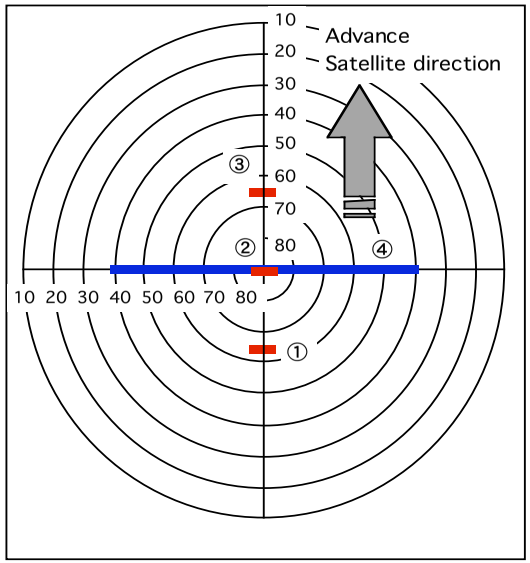

The influence on SLR Operation

The summary of passes about ALOS during 46 days recurrent cycle at Herstmonceux (HERL/7840) is shown on this table(example).

- It will not pass through a SLR restriction area when the elevation angle of observation is 32 degrees or less.
- It will surely pass through a SLR restriction area at one time from 32 to 80 degrees elevation.
- It will surely pass through a SLR restriction area second or three times exceeds 80 degrees elevation.

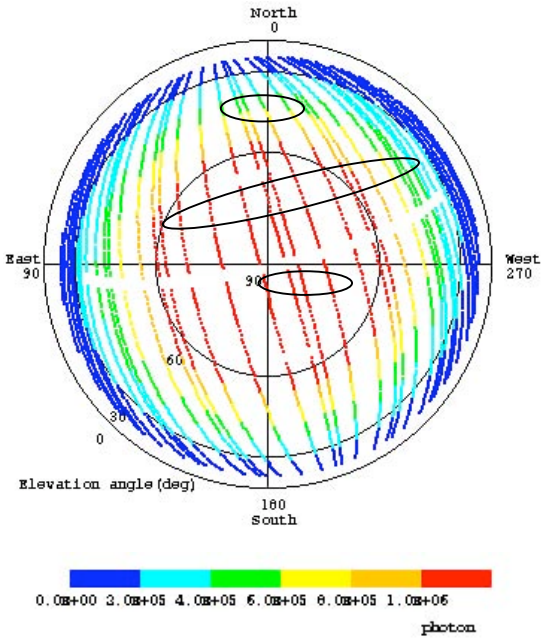

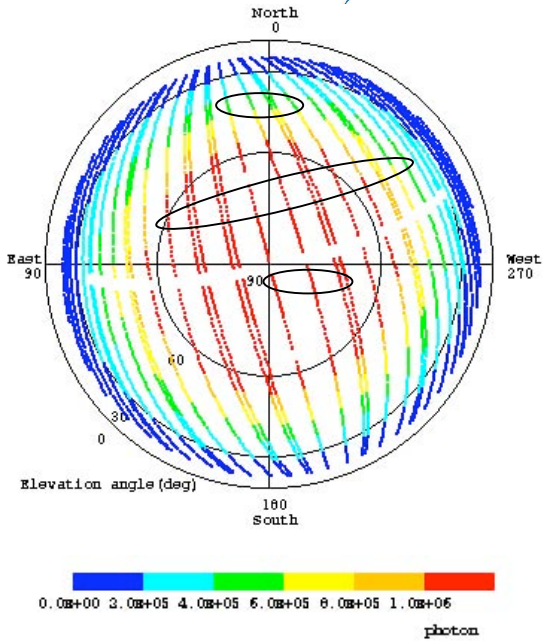

The number of times which crosses SLR restriction area per pass	The number of pass which is exceeding 20 degrees elevation(%)	Max elevation of zone at SLR station (degrees)
NONE	53(35.1)	<32.4
1	90(59.6)	32.4<81.8
2	2(1.3)	81.8<83.4
3	6(4.0)	83.4<
Total	151(100)	-

	Minimum	Maximum	Average
Crossing time of SLR restriction area (seconds)	5	10	7.7

Operation procedure(PROPOSAL)

It is required of the SLR stations support to ALOS to allow the operation procedure to keep the safety of satellite sensor.
This procedure is based on the actual operation result for ADEOS-II.

- IRV will deliver to the station directory
- keep SLR permitted period based on SLRSUP information which is generated by JAXA
- Inform to JAXA about your tracking plan before the SLR tracking
- After the tracking ALOS, inform to JAXA about tracking result (actual laser start/stop time)
- QLNP will send to JAXA directory